

Debris Impact on Emergency Coolant Recirculation

Workshop Proceedings
Albuquerque, NM, USA
25-27 February 2004



A Joint Report by
the NEA Committee on Safety of Nuclear Installations (CSNI)
and the US Nuclear Regulatory Commission (NRC)

Debris Impact on Emergency Coolant Recirculation

**Workshop Proceedings
Albuquerque, NM, United States
25-27 February 2004**

© OECD 2004
NEA No 5468

NUCLEAR ENERGY AGENCY
ORGANISATION FOR ECONOMIC CO-OPERATION AND DEVELOPMENT

ORGANISATION FOR ECONOMIC CO-OPERATION AND DEVELOPMENT

Pursuant to Article 1 of the Convention signed in Paris on 14th December 1960, and which came into force on 30th September 1961, the Organisation for Economic Co-operation and Development (OECD) shall promote policies designed:

- to achieve the highest sustainable economic growth and employment and a rising standard of living in member countries, while maintaining financial stability, and thus to contribute to the development of the world economy;
- to contribute to sound economic expansion in member as well as non-member countries in the process of economic development; and
- to contribute to the expansion of world trade on a multilateral, non-discriminatory basis in accordance with international obligations.

The original member countries of the OECD are Austria, Belgium, Canada, Denmark, France, Germany, Greece, Iceland, Ireland, Italy, Luxembourg, the Netherlands, Norway, Portugal, Spain, Sweden, Switzerland, Turkey, the United Kingdom and the United States. The following countries became members subsequently through accession at the dates indicated hereafter: Japan (28th April 1964), Finland (28th January 1969), Australia (7th June 1971), New Zealand (29th May 1973), Mexico (18th May 1994), the Czech Republic (21st December 1995), Hungary (7th May 1996), Poland (22nd November 1996), Korea (12th December 1996) and the Slovak Republic (14th December 2000). The Commission of the European Communities takes part in the work of the OECD (Article 13 of the OECD Convention).

NUCLEAR ENERGY AGENCY

The OECD Nuclear Energy Agency (NEA) was established on 1st February 1958 under the name of the OEEC European Nuclear Energy Agency. It received its present designation on 20th April 1972, when Japan became its first non-European full member. NEA membership today consists of 28 OECD member countries: Australia, Austria, Belgium, Canada, the Czech Republic, Denmark, Finland, France, Germany, Greece, Hungary, Iceland, Ireland, Italy, Japan, Luxembourg, Mexico, the Netherlands, Norway, Portugal, Republic of Korea, the Slovak Republic, Spain, Sweden, Switzerland, Turkey, the United Kingdom and the United States. The Commission of the European Communities also takes part in the work of the Agency.

The mission of the NEA is:

- to assist its member countries in maintaining and further developing, through international co-operation, the scientific, technological and legal bases required for a safe, environmentally friendly and economical use of nuclear energy for peaceful purposes, as well as
- to provide authoritative assessments and to forge common understandings on key issues, as input to government decisions on nuclear energy policy and to broader OECD policy analyses in areas such as energy and sustainable development.

Specific areas of competence of the NEA include safety and regulation of nuclear activities, radioactive waste management, radiological protection, nuclear science, economic and technical analyses of the nuclear fuel cycle, nuclear law and liability, and public information. The NEA Data Bank provides nuclear data and computer program services for participating countries.

In these and related tasks, the NEA works in close collaboration with the International Atomic Energy Agency in Vienna, with which it has a Co-operation Agreement, as well as with other international organisations in the nuclear field.

© OECD 2004

Permission to reproduce a portion of this work for non-commercial purposes or classroom use should be obtained through the Centre français d'exploitation du droit de copie (CCF), 20, rue des Grands-Augustins, 75006 Paris, France, Tel. (33-1) 44 07 47 70, Fax (33-1) 46 34 67 19, for every country except the United States. In the United States permission should be obtained through the Copyright Clearance Center, Customer Service, (508)750-8400, 222 Rosewood Drive, Danvers, MA 01923, USA, or CCC Online: <http://www.copyright.com/>. All other applications for permission to reproduce or translate all or part of this book should be made to OECD Publications, 2, rue André-Pascal, 75775 Paris Cedex 16, France.

FOREWORD

The Workshop on Debris Impact on Emergency Coolant Recirculation was held on 25-27 February 2004 in Albuquerque, NM (USA). It was organised under the auspices of the Committee on the Safety of Nuclear Installations (CSNI) of the OECD Nuclear Energy Agency (NEA), in collaboration with the US Nuclear Regulatory Commission (NRC).

On 28 July 1992, a steam line loss-of-coolant accident (LOCA) occurred when a safety relief valve inadvertently opened in the Barsebäck-2 nuclear power plant in Sweden. The steam jet stripped fibrous insulation from adjacent pipework. Part of that insulation debris was transported to the wetwell pool and clogged the intake strainers for the drywell spray system after about one hour. Although the incident in itself was not very serious, it revealed a weakness in the defense-in-depth concept which under other circumstances could have led to the emergency core cooling system (ECCS) failing to provide water to the reactor core.

The Barsebäck incident spurred immediate action on the part of regulators and utilities alike in several OECD member countries. Research and development efforts of varying degrees of intensity were launched in many countries and in several cases resulted in findings that earlier strainer clogging data were incorrect because of previously unrecognised essential parameters and physical phenomena. Such efforts also resulted in substantial backfittings being carried out for boiling water reactors (BWRs) and some pressurised water reactors (PWRs) in several OECD countries. These and later backfittings, and the situation in fifteen countries at the end of 2001, are described in the report “Knowledge Base for Strainer Clogging – Modifications Performed in Different Countries Since 1992” [NEA/CSNI/R(2002)6].

An international workshop organised in Stockholm in 1994 under CSNI auspices revealed a confusing picture of the available knowledge base. Workshop participants found examples of conflicting information and a wide range of interpretation of guidance for strainers in PWRs contained in US NRC Regulatory Guide 1.82. An international working group was set up by the CSNI to establish an internationally agreed knowledge base for assessing the reliability of ECC water recirculation systems. The working group's report was published in 1996 under the title “Knowledge Base for Emergency Core Cooling System Recirculation Reliability” [NEA/CSNI/R(95)11].

The overall purpose of the February 2004 workshop was to discuss the impact of new information made available since 1996, and to promote consensus among NEA member countries on the remaining technical issues important for safety and possible paths for their resolution.

The specific purposes of the workshop were:

- to review the knowledge base which has been developed since the report NEA/CSNI/R(95)11 was published – in particular the information developed since 1999 – and to consider the validity of the conclusions drawn;

- to exchange information on the current status of research related to debris generation, debris transportation, and sump strainer clogging and penetration phenomena (in particular for PWRs), and to assess uncertainties – in particular, to critically review and then consolidate and expand the current, still incomplete and partially ambiguous, knowledge base;
- to exchange and disseminate information on recent and current activities and practices in these areas;
- to identify and discuss differences between approaches relevant to reactor safety;
- to identify technical issues and programmes of interest for international collaborative research and develop an action plan outlining activities that the CSNI should undertake in the area of strainer clogging over the next few years.

Some 130 experts attended the workshop. They came from Belgium, Canada, the Czech Republic, Finland, France, Germany, Japan, Mexico, the Netherlands, the Slovak Republic, Slovenia, Spain, Sweden, Switzerland, the United States and the OECD/NEA.

TABLE OF CONTENTS

FOREWORD	3
EXECUTIVE SUMMARY	9
SESSION I: SAFETY ASSESSMENT AND REGULATORY REQUIREMENTS	13
<i>Chairpersons: Dr. J.M. Mattei and Mr. J.N. Hannon</i>	
<i>Y. Armand and J.M. Mattei</i>	
Assessment on the Risk of Sump Plugging Issue on French PWR	17
<i>B. Tombuyses, P. De Gelder and A. Vandewalle</i>	
The Sump Screen Clogging Issue in Belgium from the Standpoint of the Authorized Inspection Organisation (AIO).....	29
<i>J. Huber</i>	
Conclusions Drawn from the Investigation of LOCA-Induced Insulation Debris Generation and its Impact on Emergency Core Cooling (ECC) at German NPPs – Approach Taken by/Perspective of the German TSO (TÜV)	41
<i>C. Harwood, V.Q. Tang, J. Khosla, D. Rhodes and A. Eyvindson</i>	
Uncertainties in the ECC Strainer Knowledge Base – The Canadian Regulatory Perspective	53
<i>J.N. Hannon</i>	
NRC Approach to PWR Sump Performance Resolution	63
<i>A. Hsia</i>	
Overview of US Research Related to PWR Sump Clogging	67
<i>M. Henriksson</i>	
Results of Tests with Large Sacrificial and Self-cleaning Strainers and the Installation at Ringhals 2	73
<i>Y. Armand and J.M. Mattei</i>	
Sump Plugging Risk	113
SESSION 2: EXPERIMENTAL WORK	125
<i>Chairpersons: Dr. Y. Armand and Dr. B. Letellier</i>	
<i>Y. Armand, J.M. Mattei, J. Batalik, B. Gubco, J. Murani, I. Vicena, V.N. Blinkov, M. Davydov and O.I. Melikhov</i>	
Risk of Sump Plugging – Experimental Program.....	127

<i>A. Eyvindson, D. Rhodes, P. Carson and G. Makdessi</i> Emergency Core Cooling Strainers – The CANDU Experience.....	149
<i>M. Ding, A. Abdel-Fattah, B. Letellier, P. Reimus, S. Fischer and T.Y. Chang</i> Characterisation of Latent Debris from Pressurised Water Reactor Containment Buildings.....	163
<i>C.J Shaffer, M.T. Leonard, A.K. Maji, A. Ghosh, B.C. Letellier and T.Y. Chang</i> Debris Accumulation and Head-loss Data for Evaluating the Performance of Vertical Pressurised Water Reactor Recirculation Sump Screens.....	177
<i>S. Alt, R. Hampel, W. Kaestner and A. Seeliger</i> Experimental Investigations for Fragmentation and Insulation Particle Transport Phenomena in Water Flow	193
<i>K. Howe, A.K. Maji, A. Ghosh, B.C. Letellier, R. Johns and T.Y. Chang</i> Effects of Debris Generated by Chemical Reactions on Head Loss Through Emergency Core Cooling System Strainers	209
<i>U. Waas and G.-J. Seeberger</i> Results of the Latest Large-scale Realistic Experiments Investigating the Post-LOCA Behaviour of Mineral Wool Debris in PWRs.....	217
SESSION 3: ANALYTICAL WORK	261
<i>Chairpersons: Dr. M. Maqua and Dr. T.Y. Chang</i>	
<i>J.U. Klügel</i> Simple Evaluation Model for Long Term Debris Transport Velocity in the Torus of a Mark I Containment	263
<i>E. Krepper and A. Grahn</i> Numerical Investigations for Insulation Debris Transport Phenomena in Water Flow.....	271
<i>F.W. Sciacca and D.V. Rao</i> Reassessment of Debris-Ingestion Effects on Emergency Core Cooling System Pump Performance	281
<i>A.K. Maji, D.V. Rao, B.C. Letellier, L. Bartlein, K. Ross and C.J. Shaffer</i> Separate Effects Tests to Quantify Debris Transport to the Sump Screen	301
<i>T.S. Andreychek, B.F. Maurer, D.C. Bhomick, J.F. Petsche, J. Ghergurovich, D.J. Ayres, A. Nana and J.C. Butler</i> Break Characteristic Modelling for Debris Generation Following a Design Basis Loss of Coolant Accident.....	307
<i>T.S. Andreychek and D.J. McDermott</i> Containment Sump Channel Flow Modelling	329

SESSION 4: INDUSTRY SOLUTIONS	339
<i>Chairpersons: Mr. A. Vandewalle, Mr. J. Butler</i>	
<i>J.-C. Delalleau, C. Delveau, G. Du Bois d'Enghien, L. Vandermeeren and J. Pirson</i>	
Actions Taken in the Belgian Nuclear Power Plants for the Resolution of the GSI-191	341
<i>J.U. Klügel</i>	
Safety Analysis Performed in Switzerland for the Resolution of the Strainer Clogging Issue	353
<i>J.R. Cavallo and A. Griffin</i>	
Original Equipment Manufacturers' (OEM) Protective Coating Design Basis Accident Testing ..	367
<i>J.W. Walker and H.L. Williams</i>	
Overview of Site Specific Blockage Solutions at US PWRs	373
<i>G. Zigler, G. Hart and J. Cavallo</i>	
LOCA Induced Debris Characteristics for Use in ECCS Sump Screen Debris Bed Pressure Drop Calculations	389
List of participants	399

EXECUTIVE SUMMARY

1. Sponsorship

The Workshop on Debris Impact on Emergency Coolant Recirculation was held from 25 to 27 February 2004 in Albuquerque, NM (USA). It was organised under the auspices of the Committee on the Safety of Nuclear Installations (CSNI) of the OECD Nuclear Energy Agency (NEA), in collaboration with the US Nuclear Regulatory Commission (NRC).

2. Background of the Workshop

On 28 July 1992, a steam line safety relief valve inadvertently opened in the Barsebäck-2 nuclear power plant in Sweden. The steam jet stripped fibrous insulation from adjacent piping system. Part of that insulation debris was transported to the wetwell pool and clogged the intake strainers for the drywell spray system after about one hour. Although the incident in itself was not very serious, it revealed a weakness in the defense-in-depth concept which under other circumstances could have led to the emergency core cooling system (ECCS) failing to provide recirculation water to the core.

The Barsebäck incident spurred immediate action on the part of regulators and utilities alike in several OECD countries. Research and development efforts of varying degrees of intensity were launched in many countries and in several cases resulted in findings that earlier strainer clogging data were incorrect because essential parameters and physical phenomena had not been recognized previously. Such efforts resulted in substantial backfittings being carried out for BWRs and some PWRs in several OECD countries.

An international workshop organised in Stockholm in 1994 under the auspices of CSNI revealed a rather confusing picture of the available knowledge base, examples of conflicting information and a wide range of interpretation of guidance for assessing BWR strainers and PWR sump screen performance contained in US NRC Regulatory Guide 1.82. An International Working Group was set up by the CSNI to establish an internationally agreed-upon knowledge base for assessing the reliability of ECC water recirculation systems. The report of the International Working Group was published in 1996 with the title “Knowledge Base for Emergency Core Cooling System Recirculation Reliability” [NEA/CSNI/R(95)].

An initiative was taken by the CSNI in 1998 to revisit the subject. The general objective was to make an update of the knowledge base for strainer clogging. The specific objective was to review the knowledge base developed since the former CSNI report in 1996, to review the latest phenomena for PWRs and to provide a survey of actions taken in member countries. Workshops were held in 1999 and 2000. The backfittings made with respect to strainer clogging, and the situation in fifteen countries at the end of 2001, were described in report NEA/CSNI/R(2002)6, “Knowledge Base for Strainer Clogging – Modifications Performed in Different Countries Since 1992”.

New information contained in NUREG/CR-6771 indicated that the core damage frequency could increase by one to two orders of magnitude because of strainer clogging. Consequently, the CSNI decided to continue its previous efforts in the area. In addition, the CSNI decided to ask its working groups GAMA and WGOE to develop a plan outlining activities that CSNI should undertake in the area of strainer clogging during the next few years.

3. Purpose of the Workshop

The overall purpose of the Workshop was to discuss the impact of new information made available since 1996 and to promote consensus among member countries on identification of remaining technical issues important to safety, and on possible paths for their resolution.

The specific purposes of the Workshop were:

1. To review the knowledge base which has been developed since report NEA/CSNI/R(95)11, was issued, and in particular information developed after 1999, and to consider the validity of the conclusions drawn.
2. To exchange information on the current status of research related to debris generation, debris transportation, and sump strainer clogging and penetration phenomena, in particular for PWRs, and to assess uncertainties. In particular, to critically review and then consolidate and expand the current, still incomplete and partially ambiguous, knowledge base.
3. To exchange and disseminate information on recent and current activities and practices in these areas.
4. To identify and discuss differences between approaches relevant to reactor safety.
5. To identify technical issues and programs of interest for international collaborative research and develop an Action Plan outlining activities that CSNI should undertake in the area of strainer or sump screen clogging during the next few years.

4. Scope and technical content of the Workshop

Since 1992 and again after the completion of report NEA/CSNI/R(95)11, a number of efforts have been carried out, new insights have been gained, and safety improvements, essentially larger strainers and exchange of insulation, have been implemented. Although several of the sump strainer clogging phenomena are similar for BWRs and PWRs, the report NEA/CSNI/R(95)11 focused on BWR phenomena. There could be differences in, for example, transportation and clogging characteristics of insulation debris and characteristics of failed coating which could warrant separate analyses for PWRs. There was, therefore, a need to consider clogging phenomena that are common to BWRs and PWRs, and also such phenomena that are unique for PWRs and VVERs. All sizes of breaks (small, medium, and large) were to be considered, as well as short and long term effects on the emergency coolant recirculation.

5. Workshop attendance

Over 130 experts attended the Workshop. They came from Belgium, Canada, the Czech Republic, Finland, France, Germany, Japan, Mexico, The Netherlands, the Slovak Republic, Slovenia, Spain, Sweden, Switzerland, and the USA.

6. Summary of the main findings

1. The safety significance of the sump strainer clogging depends on the plant design (e.g. sump strainer, ECCS) and backfitting measures performed.
2. The following are examples of PWR design features that could influence the debris impact on the ECCS sump performance:
 - Type of insulation (material, combination of materials, protection).
 - Break size to be postulated.
 - Transport in containment with or without containment spray system (CSS).
 - Degree of turbulence and flow velocities in the sump influenced by CSS, water level, break flow location and sump geometry.
 - Redundancy of sumps and residual heat removal system (RHRS).
 - Strainer design (area, mesh size).
 - Positioning of recirculation pumps and vortex protection.
 - Amount of latent debris (e.g. use of qualified coatings, size of unprotected ferritic surfaces, cleanliness regime after outages).
 - Chemical effects due to NaOH.
3. Sump strainer clogging may substantially increase the total core damage frequency. This statement depends strongly on the design features mentioned above and the assumption made to estimate the amount of insulation material reaching the sump strainer and the resulting pressure loss. Presently, different assumptions are used in different countries regarding debris generation and transport.
4. Timely resolution of the sump strainer clogging issue is essential. Some participants presented solutions to the problem based on:
 - new strainer designs;
 - reduction of insulation material generation;
 - development of strainer cleaning procedures e.g. back-flushing.
5. Timely solutions to the sump strainer clogging problem are plant design specific and debris specific.
6. Assessment methods should continue to be enhanced. However, some countries have developed solutions or implemented compensatory measures.
7. Chemical effects have to be taken into account.
8. Latent debris continues to be of concern.
9. Thin bed effect is one of the major concerns impacting strainer head loss and core cooling.

7. Conclusions and recommendations

A plenary session was conducted which included a presentation of the IRSN proposal on an experimental program, a summary of the open issues based on the input of the participants, and a

discussion on recommendations for issue resolution and perspective for future actions. These were input to the draft CSNI action plan in the area of strainer and sump screen clogging.

Following are highlights of preliminary recommendations collected from workshop attendees during the Plenary Session.

Debris generation assessment method considerations

Conical or spherical model can be applied with L/D validated for specific plant design and insulation types. Other robust conservative assumptions can also be used.

Head loss

Head loss should be assessed by conducting plant specific and material specific tests. For most plants, the thin bed effect may occur and should either be avoided or accommodated.

Chemical effects

Chemical effects need to be taken into account for potential impact on pressure drop across sump screens.

Emergency procedures

Emergency procedures need to be enhanced or developed to handle potential debris blockage events.

Downstream effects

In seeking solutions to this issue, utilities need to find a balance between screen grid size, total screen area, and debris approach velocity. Downstream pumps, throttle valves, heat exchangers, diaphragms, containment spray nozzles and fuel elements should be considered in the assessment.

Plant cleanliness

It is highly recommended that utilities keep the plant, particularly the containment, clean. The foreign material exclusion program needs to be enhanced and enforced.

SESSION 1

SAFETY ASSESSMENT AND REGULATORY REQUIREMENTS

Chairpersons: Dr. J.M. Mattei (IRSN) and Mr. J. Hannon (USNRC)

HIGHLIGHTS

Seven papers were presented in Session 1.

Taking benefit of the lessons from the Barsebäck accident, many countries have improved their units since 1992. In Sweden, new strainers were developed for PWR installations which included large sacrificial strainers and self-cleaning “wing-strainer” to provide robust debris handling.

The Canadian Nuclear Safety Commission (CNSC) and Canadian industry worked closely together to solve the strainer issue. AECL performed extensive tests and developed finned strainers to provide added strainer areas.

Despite the issue of an official recommendation in 1998, German technical support organisations and utilities performed further experiments to demonstrate the function of the sump suction after LOCAs. These works are still ongoing and will result in a modified recommendation in near future.

As for France, IRSN has conducted an experimental program since 2000, and concluded that sump screen blockage is a potential problem for the 58 existing PWR units. At present, DGSNR and EDF agree that there is a need to assess the sump screen blockage issue and to implement improvements on all French PWR units. In addition, an experimental program was proposed by IRSN to resolve two problems considered by the French to be still pending – debris generation and the water chemical effects.

While conducting technical assessment regarding the debris impact on sump performance, the present objective is to confirm or to define approved safety requirements to solve this safety issue for existing reactors and also for future reactors. A universal description of the LOCA progression and corresponding debris generation and behavior is not easy due to variability of plant designs and their respective safety requirements.

During the panel discussion at the end of the session, main topics covered were summarised as follows.

1. Debris generation and distribution

The key parameters were the following:

- Location of the break.
- Size of the break:
 - influence of break preclusion concept;
 - duration of the jet;

- insulation material;
- other potential debris (paints, concrete);
- coating qualifications.

2. Other latent debris

Quantity of latent debris in the containment depends mainly on the cleanliness of the containment. In addition, a good evaluation of dust (quantity, granulometry) is needed.

As conclusion, a good cleanliness of the containment is required.

3. Vertical transport and horizontal transport

The French paper presented debris transport tests results from IVANA and VITRA loops. The German paper emphasised the results of their new large scale and plant specific transport experiments. As conclusion, beyond differences due to different plant designs, some uncertainties remained in the assessment methods for debris transport. These uncertainties could be reduced using qualified CFD models (if available) or using well scaled tests appropriate for the respective plant design.

4. Chemical effects on the fiber bed

Taking into account the results obtained from experiments realized, several participants emphasised the risk of potential increased head loss across the fixed fiber bed on the screens considering possible chemical effects and creation of gelatinous material. For the creation of the gelatinous material, the main parameters are the temperature of the water containing boron and NaOH, the insulation material, and latent debris (e.g. dust, concrete, paints).

As conclusion, chemical effects on the fiber bed should be considered as part of the assessment of debris impact on sump performance.

5. Compensatory measures including emergency procedures

The USNRC emphasised the need for compensatory measures to minimize the potential for sump failure in the time period before final corrective actions are implemented.

As conclusion, depending on the plant's configurations, the efficiency of compensatory measures has to be thoroughly analysed, because some countries' experiences have shown that the risk of strainer clogging may not be lowered substantially.

6. Effects on components downstream from the filters

Investigations on downstream component effects have already been performed in different countries. These effects may occur, if the strainer mesh size is comparatively large (e.g. 9 mm x 9 mm).

As conclusion, the following downstream effects have to be considered:

- The mesh size of the filters and their total area (potential adverse effect of ingestion of debris and particulates can occur if the area is too large).
- The critical components are: pumps, valves, exchangers, diaphragms, spray nozzles and the fuel assemblies.

8. Future reactors

Future reactor vendors are required to address severe accidents (core melt) as part of design certification. In case of core melt, the parameters to be considered can be different, in particular the primary temperature due to hot gas circulation and consequently the total amount of debris generated after spray system activation during core melt progression may differ compared to design basis accidents.

Consequently, the main question is related to the respective safety requirements to be used to design the ECCS system for design basis accidents to prevent core melt, the Containment Heat Removal System used for severe accident mitigation, and passive systems.

As conclusion, regulatory requirements for future reactor designs dealing with debris impact on recirculation cooling have to be developed and plant vendors should consider the effects of debris generation for severe accident analyses.

ASSESSMENT OF THE RISK OF SUMP PLUGGING ISSUE ON FRENCH PWR

Yves Armand and Jean Marie Mattei
IRSN, France

1. Introduction

This report presents an assessment of the operational characteristics of the filtration function used during the recirculation phase of safety injection system (SI) and containment spray system (SS) in the event of a break of the primary system in the containment for the French pressurised reactors (58 reactors), which have been designed according with the Regulatory Guide 1.82 (revision 1) published in 1985.

In spite of the lessons learned from the Barsebäck accident occurred in 1992 and the corresponding questioning about the appropriate character of the requirements of this Regulatory Guide, Électricité de France has always proclaimed the compliance of the French plants with revision 1 of the Regulatory Guide 1.82 and has refused to review this position.

Consequently, the “Institut de radioprotection et de sûreté nucléaire” (IRSN) has decided to perform its own assessment. A general overview of the literature has been conducted between October 1999 and November 2000, questioning the capability of the safeguards systems to operate during recirculation phase which resulted in defining an approach methodology and writing technical specifications related to the French design reactors.

After this general overview, the “Institut de radioprotection et de sûreté nucléaire” has decided to perform a detailed study on the risk of sump plugging for the French reactors.

2. IRSN study

The IRSN study has been carried for the CPY series, 900 MWe pressurised water reactors (28 reactors) for the different sizes of primary breaks: large, median and small LOCA. The characteristics of the CPY sumps are the following:

- water height: 1.5 m;
- three pre-filters:
 - mesh size: 20 x 20 mm (wire diameter: 7 mm);
 - area: 12 m² (2 x 2, 2 x 1.5 + 3 x 1.5).
- four filters – 1 per train (SS, ECCS) with three sets of filtration:
 - passage area: 4 x 10 m²;

- anti-vortex protection: minimum level: 0.4 m;
- flow of ECCS train: 650 m³/h;
- flow of SS train: 1 100 m³/h.
- three grids:
 - 11.8 x 11.8 mm (wire diameter: 2 mm);
 - 4.53 x 4.53 mm (wire diameter: 1.5 mm);
 - 2.5 x 2.5 mm (wire diameter: 1.2 mm).

On the CPY 900 Mwe units, the sumps are located at the bottom of the containment at the level -3,5 m.

For each size of break, located on the welding between SG and the hot leg (3 locations), different characteristics of generated debris, flows of ECCS and SS systems have been defined.

Table 1. The following table gives a summary of the flow-rates sucked for each size of break by the ECCS (LPSI) and SS pumps from the sumps (figure)

Flow rate (m ³ /h)	28" > Diam > 6"	6" > Diam > 4.5"	4.5" > Diam > 2"	2" > Diam > 3/8"
ECCS – A	1 020/650	1 020/650	900/550	430/265
ECCS – B	0/650	0/650	0/550	0/265
SS – A	1 100	1 100	0	0
SS – B	1 100	1 100	0	0

To estimate the risk involved in each case, the following points were studied:

- inventory of debris generated of the following types:
 - glass wool thermal insulation fibers;
 - paints and particulates;
 - oxides.
- dusts present in the containment, in suspension or on the walls;
- vertical transfer of different debris;
- structural modification of debris in the containment;
- horizontal transfer of debris at the bottom of the containment;
- filtration efficiency under realistic conditions (temperature, pH, quality of the water, effects of different particulates);
- modification of sump hydraulics/air and debris ingestion;
- operation of SI and SS circuit equipment with mud and air present.

The subjects giving rise to important questions have been collected.

For some of them, assumptions have been taken.

Insulation debris generation

On the typical parameter used to define debris generation (L/D), great uncertainties exist. An experimental approach has been set up to define it. It appears that the tests have only been performed to estimate the pressure wave under questionable conditions for break size, pressure, fluid. Jet effects, shock wave, whipping, reflection have not been considered. As said in the ACRS letter 30 September 2003, a large panel of values exists from 7 (NUREG 6224) to 35 (MARVIKEN test).

For IRSN study, a spherical model of degradation has been adopted for double-ended break (NUREG 6762) with a ratio of $L/D = 12$. This value is coming from the USNRC-ONTARIO test realised under the following conditions: break size: 50 mm, pressure: 100 bar of steam/water jet. A semi-spherical model of degradation has been used for lower sizes of breaks.

Insulation debris repartition

Insulation debris repartition has been established on the basis of KASHIRA test results. The following data has been taken:

- individual fibers: 20%;
- small debris: 40%;
- large debris: 40%.

For the other ones, an experimental approach was chosen in order to answer:

- IVANA loop (VUEZ/SLOVAKIA): grinding of fibrous debris on the grating system (mechanical action of falling water).
- VITRA loop (EREC/RUSSIA): settling, taking off speed, horizontal transfer speed of different debris at the bottom of the reactor building.
- MANON loop (VUEZ/SLOVAKIA): pressure drop and air and debris ingestion at the sump filters. Using the results of the tests, methodology of event trees has been used to define the initial conditions of test: characteristics of the debris and their arrival point at the bottom of the containment.
- ELISA loop (VUEZ/SLOVAKIA): breakdown of fibrous debris so-called efflorescence, behaviour of the fiber bed under chemical action of water, effect of temperature and establishment of different correlations.

3. Lessons

The information gathered is:

1. The mechanical degradation speeds of insulation materials under the effect of water falling from 4.6 m are relatively high (up to 90%) and the insulation materials under the overflow are “pushed” and “cut up” within a few minutes, regardless of the flow rate.
2. The approach used to characterise horizontal transfer of debris was based on a statistical study of the behaviour of each type of debris involved, using appropriate video recordings. In the case of insulation materials, the fluid speed required to set 95% of debris in motion is

4 cm.s⁻¹, and around 3 cm.s⁻¹ for 50% of the debris. For paints, the fluid speed required to set 95% of debris in motion is 14 cm.s⁻¹, and around 11 cm.s⁻¹ for 50% of the debris.

3. In the MANON loop, it emerges that for debris made up of a mixture of small debris and large debris (clusters of 20/30 mm), pre-filter clogging produces a lowering of the water level around the filtering boxes. A large transient appears if the boxes stay uncovered and the air gets inside. The current tests will make it possible to define the quantity of insulation materials needed to cause SS function failure.
4. The closing of one suction line leads to an increase of the speed of plugging of the neighbouring filter.
5. From 40°C, there is a considerable degrading of thermal insulation fibers under the effect of water with a pH of 9, regardless of the flow rate considered. Temperature therefore has an extremely important influence on reaction kinetics. The degradation products are more often small-sized particles than fibers. If they agglomerate on the filters, the resulting pressure drops are much greater than those obtained with an equivalent quantity of fibers or clusters.
6. Different correlations have been established to link the head loss obtained on the MANON loop with the parameters as pH, quality of water, velocity or temperature. This correlation is established on the ELISA loop.
7. The water quality has an extremely important influence on reaction kinetics and consequently on the head loss of the filters due to behaviour of the fiber bed.

The preliminary gathered has been confirmed by additional tests carried out in 2003. The results of this additional program are summarised in Appendix A.

They have demonstrated:

- The negative effect of the pre-filters. Three levels are created:
 - the first one before the pre-filters;
 - the second one around the filtering grids;
 - the third one inside the filtering grids.
- The criterion linked with air ingestion (anti-vortex plate on low level) is reached for small sizes of primary breaks when pre-filters are considered.
- A benefit due to removal of the pre-filters but not sufficient to cope with all the breaks considered in the design.
- The negligible effect of initial settling of the debris: 3% are always settled at the end.
- The important influence of the particles (depending of their sizes and instant of arrival).
- The important influence of the characteristics of the water (Ca, Mg, ...) on the behaviour of the fiber bed and consequently on the increase of its head loss during long term.
- Test results assessment leads to estimate different critical break sizes depending on configurations and major factors:
 - critical break size with pre-filter due only to insulation plugging: *4 inches*;
 - critical break size without pre-filter due only to insulation plugging: *12 inches*;

- critical break size without pre-filter due to insulation and particulates plugging (simultaneous injection with initial settling): *8 inches*;
- critical break size without pre-filter due to insulation and particulates plugging (insulation injected firstly with initial settling): *6 inches*;
- critical break size without pre-filter due to insulation and particulates plugging (insulation injected firstly with initial settling) and with chemical effects during long term: *4 inches (estimation)*.

On the basis of the results of its study, IRSN has estimated that, for a large spectrum of primary breaks, ECCS and CSS were not able to perform recirculation phase. This conclusion was extended to all the French units of the different series [900 MWe (CP0, CPY), 1 300 MWe (P4, P'4), 1 450 MWe (N4)] after examination of their differences with CPY Series.

Status of sump filter clogging issue

The results of this programme have led IRSN to debate the significant impact of the existing filters on the plants safety and to discuss with Électricité de France the opportunity to improve the situation of the plants. The corresponding results have been presented by IRSN to the French standing group for reactor, a group of experts that advises the safety authority.

On the 12 June 2003, the standing group endorses the strong concern of IRSN that Électricité de France has to assess the question of the efficiency of the filters of all the plants.

At the end of October (30 October 2003), French nuclear safety authority (DGSNR) has told Électricité de France to accelerate the study of the risk of sump strainer clogging in all 58 of its PWRs and to report by the end of the year on whether the measures, including backfits and temporary compensatory measures are needed to reduce that risk (Appendix B).

The Électricité de France position has been presented at the end of 2003. Électricité de France considers that improvements are needed for all the French series to cope with primary breaks higher than 4" and the first improvements will be installed from 2005. The corresponding DGSNR position is presented in Appendix C.

A report [1] on the strainer clogging issue including open items has been published by IRSN on October 2003. The corresponding appendix consists of:

- Assessment of risk of plugging for non nuclear installations.
- Assessment of the different types of insulation.
- Application to French Units of the reports related to "Sump Screen Clogging Issue" (28 reports, GSI 191, USNRC rules):
 - assessment of the ECCS and SS flow-rates for different sizes of primary breaks (900 MWe);
 - assessment of the quantity of damaged insulation closed to a primary break for different sizes of break (900 MWe);
 - test reports (IVANA, VITRA, ELISA and MANON loops) [2-7];

- assessment of transported quantity of insulation debris to the bottom of the containment for different sizes of primary breaks and different locations of the break (900 MWe);
- results and assessment of representative tests on MANON loop;
- assessment of the feasibility of a test to define and to characterise debris in case of LLOCA, MLOCA or SLOCA (EREC/RUSSIA);
- first study of the evolution of the head loss of a fiber bed due to characteristics of the water (TRENCHIN Academia/SLOVAKIA).

Conclusion

On 28 July 1992, the Barsebäck-2 nuclear power plant loss-of-coolant accident has led to the ECCS failure due to the plugging of its sump screens. To cope with this problem, the international community assessments firstly focused on the BWR units and modifications were implemented till 1996, based on the existing knowledge at that time. Then, assessments on PWR units have been conducted or are in progress worldwide.

For French nuclear power plants, IRSN has performed an experimental program, from 2000 until now, concluding on the potential sump screens plugging for the 58 existing French units. A lot of experimental data have already been obtained and conclusions drawn on this issue [9]. At the present time, an agreement exists between EDF, DGSNR and IRSN on the need to consider the problem and to implement improvements on all the French units.

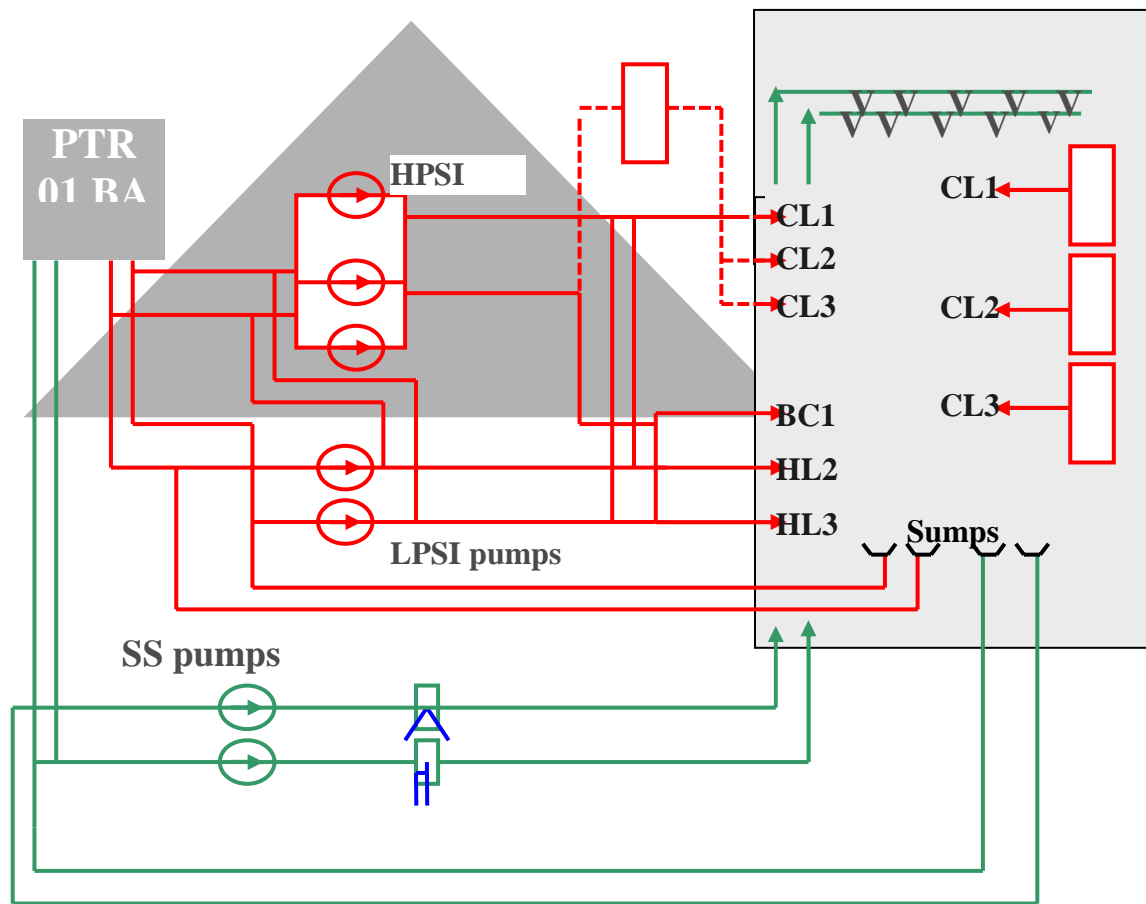
The knowledge evolution gained by IRSN could be internationally used. Moreover, IRSN considers the current knowledge is not enough substantiated about a few main fields needed to precise design requirements to assess globally this issue. The pending problems are related to the debris generation and the water chemical effects on the fiber bed fixed on the filters [8].

An experimental program is proposed by IRSN to solve these two open questions in a short term. This program could be of interest for a great number of countries. It will be presented during the Plenary Session [10].

REFERENCES

- [1] Synthesis report IRSN/DES/SERS/400, 14 October 2003.
- [2] IVANA report, VUEZ SA – TS-OTS-1318, May 2002.
- [3] VITRA report, EREC – MT DA 118 1.091-02, 2002.
- [4] MANON report, VUEZ SA – TS-OTS-1336, December 2002.
- [5] MANON report, VUEZ SA – TS-OTS-1398, October 2003.
- [6] ELISA report, VUEZ SA – ZZ-OTS-1331, August 2002.
- [7] ELISA report, VUEZ SA – TS-OTS-1397, October 2003.
- [8] Albuquerque Workshop (2004), Opened questions – Y. Armand, J.M. Mattei, IRSN, France.
- [9] Albuquerque Workshop (2004), Experimental programme, Y. Armand, J.M. Mattei, IRSN France.
- [10] Albuquerque Workshop (2004), Action plan proposal, Y. Armand, J.M. Mattei, IRSN, France.

Figure



Appendix A

MANON test results

Tests/ Results	Pre-filter	SG	LB	SB	SI	SS	Particules	Criterion	Needed quantity (kg)	Correlated quantity (m³) (T, pH)	Critical break size
Test 1	WITH	2	X		1 300 2 files	2 200	WITHOUT	Low level of AV plate on 2 files SS	43.8	2.3	4" or 3" if part.
Test 2 (/1)	WITH	2	X		1 020 1 file	2 200	WITHOUT	Low level of AV plate on 1 IS	36.5	1.9	3" or 2" if part.
Test 3 (/1)	WITHOUT	2	X		1 300 2 files	2 200	WITHOUT	Delta P max (1.5 m) on 2 files SS	204	10.7	12" or 8" if part.
Test 4 (/1)	WITH	3	X		1 300 2 files	2 200	WITHOUT	Low level of AV plate on 2 IS	58	3.1	5" or 3.5" if part.
Test 5	WITH	2		X	900 1 file	0	WITHOUT	Not reached with pure insulation			
Test 6	WITH	2		X	430 1 file	0	WITHOUT	Not reached with pure insulation			
Test 7 (/3) (with initial settling)	WITHOUT	2	X		1 300 2 files	2 200 2 files	WITHOUT	Delta P max (1.5 m) on 2 SS files	160 + 15 (1 st SS loss) + 35 (2 nd SS loss) = 210	11 (5.8 kg remain settled at the end of the test)	12"
Test 8 (/3) (with initial settling)	WITHOUT	2	X		1 300 2 files	2 200 2 files	WITH (injection of insulation and of particulates is realised simultaneously)	Delta P max (1.5 m) on 2 SS files	135 (insulation) + 135 (particulates)	7.1	8"
Test 9 (/1/2)	WITH	2	X		1 020 1 file	1 100 1 file	WITHOUT	Low level of AV plate on IS and SS	58.4	3.1	5" or 3.5" if part.
Test 10 (/3)	WITHOUT	2	X		1 020 1 file	1 100 1 file	WITHOUT	Delta P max (1.5 m) on SS file	94.9	5	7" or 5" if part.
Test 11 (/8) (with initial settling of insulation)	WITHOUT	2	X		1 300	2 200	WITH (particulate injection is realised after fiber bed creation)	Delta P max (1.5 m) on SS files	70 (insulation) + 20 (particulates)	5	6"

Appendix B

DGSNR position Potential anomaly on the water recirculation circuit of EDF nuclear power plants

Studies undertaken at the international level and research work recently carried out in France by IRSN raise interrogations on the possibility of filter clogging in the water recirculation sumps, located at the bottom of the reactor building. This clogging could compromise reactor cooling during some accidents.

These sumps collect water in the event of important leakage from the primary circuit during an accidental situation, in order to return it in the safety injection circuit and ensure reactor cooling.

In the current state of knowledge this clogging phenomenon, which might be a concern for all pressurised water reactors in the world, has yet to be confirmed. This is explained by the difficulty of modelling it and the multiplicity of parameters involved. If the clogging possibility was confirmed, the resulting event would be classified level 2 on the international nuclear event scale (INES).

Taking into account the potential impact that this phenomenon could have for safety, the nuclear safety authority, in its letter dated 9 October 2003, published on its website, required EDF to address this question as a priority for all types of French reactors and to give its conclusions before the end of the year 2003 on the possibility sump filter clogging and, if needed, the means to counter it.

An information notice (*in French*) on this subject is available on the website of the French nuclear safety authority (www.asn.gouv.fr).

Appendix C

DGSNR position Potential anomaly on the water recirculation circuit of EDF nuclear power plants

Électricité de France a confirmé à l'Autorité de sûreté nucléaire (ASN) la possibilité, dans certaines situations accidentelles, d'un colmatage des filtres des puisards du circuit de recirculation de l'ensemble de ses réacteurs nucléaires à eau sous pression.

Ces puisards, situés au fond du bâtiment réacteur, ont pour fonction de collecter l'eau qui s'échapperait en cas de fuite importante du circuit primaire, afin notamment de la renvoyer dans le circuit d'injection de sécurité et d'assurer le refroidissement du réacteur. De récents travaux de recherche, menés en France et à l'étranger, avaient conduit l'ASN à demander le 9 octobre 2003 à EDF de prendre position, avant fin décembre 2003, sur la possibilité de colmatage des filtres des puisards et, le cas échéant, sur les moyens d'y remédier.

Dans sa réponse, EDF indique que, dans certaines situations accidentelles très improbables (rupture complète d'une tuyauterie du circuit primaire), le colmatage des filtres des puisards ne peut être exclu, mais qu'il peut être écarté pour des brèches moins importantes. EDF précise que des modifications matérielles des installations sont en cours d'étude afin de remédier à l'anomalie et seront présentées à l'ASN avant la fin du mois d'avril 2004 pour une mise en œuvre à partir de 2005. En parallèle, EDF analyse différentes mesures visant à limiter, en attendant la mise en œuvre des modifications, l'impact de l'anomalie en situation accidentelle.

L'ASN examinera, avec l'appui de l'IRSN, les différentes propositions de l'exploitant.

Compte tenu de son impact potentiel sur la sûreté des installations, l'ASN a classé au **niveau 2 de l'échelle INES** cet incident générique.

**THE SUMP SCREEN CLOGGING ISSUE IN BELGIUM
FROM THE STANDPOINT OF THE AUTHORISED INSPECTION ORGANIZATION (AIO)**

B. Tombuyses

Association Vinçotte Nuclear (AVN), Belgium

P. De Gelder

Association Vinçotte Nuclear (AVN), Belgium

A. Vandewalle

Association Vinçotte Nuclear (AVN), Belgium

Abstract

All Belgian NPPs are PWRs. These PWRs have different containment designs and different sump designs. The four most recent units (Doel 3 & 4 and Tihange 2 & 3) took RG 1.82 rev. 0 into account for the recirculation sump design. Several improvements were made in the framework of the first Periodic Safety Review to the oldest units (Doel 1 & 2 and Tihange 1) such as enlargement of the sumps strainer in 1985, taking into account the requirements of RG 1.82 rev. 0.

The problem of recirculation sump screen clogging due to the accumulation of insulation debris after an accident was also identified as a safety issue in the first Periodic Safety Review for Doel 3 and Tihange 2 and the second Periodic Safety Review for Doel 1 & 2 and Tihange 1, that started in the nineties. One of the purposes of the Periodic Safety Review being the justification of the safety level of the power plants with regard to the **most recent** safety rules and practices, the licensee was asked to review the characteristics of the sump strainers according to the revision 1 of the RG 1.82 (which referred to Nureg 0897 rev. 1).

Later on, the Barsebäck incident and the events leading to the NRC IN 93-34 showed that the conclusions of Nureg 0897 could underestimate the potential for loss of NPSH of the ECCS- and CSS-pumps. The issue was further examined and the AIO asked the licensee to continue efforts to recollect information.

After issuance of the results from the parametric evaluation for pressurised water reactor recirculation sump performance (GSI-191) performed by LANL¹ under NRC contract, the AIO asked the Belgian licensee in August 2002 to increase its efforts to investigate and to solve this issue.

The requirements to the Licensee and the corresponding action plan as approved by the AIO are presented. Some significant lessons learned from the implementation of this action plan are discussed.

1. NUREG/CR-6762.

Belgian situation – Application of the USNRC rules in Belgium

The Belgian nuclear fleet consists of 7 PWR units with a Westinghouse or Framatome NSSS design, commissioned from February 1975 (Doel 1) till September 1985 (Tihange 3). These PWRs have different containment designs and different sump designs. The plants were in general designed following the US practice. Since the Belgian regulation does not include very detailed requirements on nuclear safety, it was decided to use the regulations (and associated document) issued by the USNRC as an acceptable basis for the licensing of the last four units. From a more formal point of view, they have followed the USNRC rules existing at the moment of the NSSS purchase order (the so-called Applicable Rules). Later NRC rules are not directly applied but are examined jointly by the Architect Engineer and the Authorized Inspection Organization during the Periodic Safety Review (which occurs every 10 years, as a Licence condition). They may then be taken into account, either fully or with specific amendments. There is also the possibility to use the recent rule as a source of inspiration only (reference rule as opposed to applicable rule).

The potential problems related to the risk of sump strainer clogging during the recirculation operation were identified and examined in the framework of the Periodic Safety Reviews.

Application of RG 1.82 rev. 0

Units build before RG 1.82 rev. 0

The oldest units (Doel 1/2 and Tihange 1) were designed before the publication of Regulatory Guide 1.82 rev. 0.

For Doel 1/2 (two loops units) there was a single sump with two distinct suction lines, each protected by two small cylindrical strainers with an approximate diameter of 50 cm.

Tihange 1 (three loops units with two ECCS trains) has six suction lines associated with two safety injection trains, two internal and two external spray trains. Each strainer is constituted by 4 filtration surface. The total filtration surface was approximately 13 m².

The first periodic safety review includes a re-evaluation of the ECCS with regard to various problems (NPSH of pumps, redundancy ...). By the publication of the RG 1.82 rev.0 a new subchapter was added at the first periodic safety review of those units to handle this issue. A re-evaluation was performed for the three units that lead to the enlargement of the strainers. For the three units the studies and the modifications were completed by 1987.

For Doel 1 and Doel 2, a new common strainer was build, like a cage, corresponding to a filtration surface of approximate 4 m², multiplying at least by four the filtration surface. The old strainers were left in the new common “cage”.

For Tihange 1, the new strainers replaced the old ones. A common cage was build above the safety injection and the external spray suction lines of each train. The two strainers of the internal spray trains were also enlarged. The total filtration surface with these four strainers is now approximately 60 m².

Units build after RG 1.82 rev. 0

The four most recent units (all three-loops-units) took RG 1.82 rev. 0 into account for the recirculation sump design. For Doel 3 and Doel 4 there is a common suction line for the safety injection and spray pumps per train. The total filtration surface is approximately 70 m². Tihange 2 and Tihange 3 have separate suction lines and separate sumps for the spray and the safety injection lines. The total filtration surface associated to the six strainers is approximately 50 m² (Tihange 2) and 65 m² (Tihange 3).

Application of RG 1.82 rev. 1

The impact of the new revision of the RG 1.82 has been examined in the next periodic safety review of the units, i.e. the second one for the oldest units and the first one for the latest units.

The estimation of the debris susceptible to reach the sumps was performed on a rather conservative way (in particular, 100% of the small created debris were assumed to reach the sumps). The debris considered at that time were supposed to be generated by destroyed isolation material. Then the head losses on the strainers were computed and the margin with regard to the NPSH was evaluated.

These assessments demonstrated that, even after the first strainer surface enlargement, the situation was still not in conformance with the applicable regulation (RG 1.82 rev. 1) for Doel 1 and 2. A new strainers enlargement was done in 1994, corresponding to an approximate filtration surface of 16 m². This new surface was nevertheless not yet sufficient according to the criteria proposed by the RG 1.82 and a reduction of the SI-recirculation flowrate was imposed at the same time. A third enlargement, bringing the filtration surface up to 24-26 m², allowed to return to the original recirculation flowrate while being in accordance with the acceptance criteria.

The situation was just acceptable for Tihange 1, with a very limited margin, and there was some margin for the other units.

Barsebäck and RG 1.82 rev. 2

Later on, the Barsebäck incident and the events leading to the NRC IN 93-34 showed that the conclusions of Nureg 0897 might underestimate the potential for loss of NPSH of the ECCS- and CSS-pumps.

The studies, which were under development, took into account some of the phenomena discovered during the Barsebäck incident or the experiments performed abroad, but in an incomplete and unsatisfactory way.

Nevertheless AVN agreed that the new phenomena were not enough quantified by the experiments already performed and – at that time – foreign regulators as well as licensees did not seem to pay a lot of attention to potential sump screen clogging in PWRs. It was concluded that the available NPSH was acceptable with regard to the **applicable** regulation (RG 1.82 rev. 1).

The issue was closed in the frame of the Periodic Safety Review and a new **generic issue** (for all power plants) was set up: the licensees had to continue efforts to recollect information. Afterwards the licensee and the AIO (AVN) had to agree on the estimation of the influence of the different

phenomena on the pressure drop over the strainers, and a new evaluation of safety margins with regard to the needed NPSH had to be performed.

GSI-191 “Technical assessment: parametric evaluations for pressurised water reactors recirculation sumps performance”² – actions taken

The Licensee examined the results provided by the assessment performed by the Los Alamos National Laboratory under the auspices of the USNRC and considered that this study was very alarming. Taking into account the critics expressed by the US Licensees they concluded that no specific actions had to be taken except further follow-up of the international activities on this issue.

AVN was convinced that the assessment made by the LANL had to be taken seriously into consideration for the Belgian nuclear power plants and that the issues deserved appropriate attention to be paid. One concern was that the technical assessments performed during the periodic safety issues were far from being considering all potentially negative parameters of the strainer clogging. It was also considered that the issue was not limited to large break LOCA and that the potential common cause failure of the recirculation was to be considered as likely, even in case of a small break of the reactor coolant system.

Probabilistic safety assessment made to evaluate the influence of an increased probability of sump blockage showed that, considering a total failure probability of 0.1 of the recirculation mode, the probability of core melt was multiplied by about a factor 100.

Consequently, the licensee was requested to give an answer to different questions such as:

- How to prevent the sump strainers to be clogged by debris?
- How to identify the clogging of the sump strainers?
- How to prevent damages to the ECCS due to loss of flow rate?
- How to keep sufficient core cooling and/or to restore it in due time?

Contacts with foreign regulatory authorities

In parallel to the discussions with the Belgian Licensee on the strainer clogging issue, representatives from AVN get in touch with foreign colleagues in order to share their experience in solving or assessing the issue. A delegation was sent to Finland, Sweden, and France to gain information from the corresponding regulatory authorities.

In particular, the experiments performed at that time by the French IRSN were discussed and the first partial results gained at that time were discussed.

2. NUREG/CR-6762.

Actions plan

General

After discussions, the AIO approved the action plan proposed by the licensee. This action plan was covering the following issues:

- walk-downs in the reactor building of the different Belgian units;
- support to the operators related to the potential loss of recirculation;
- evaluation of modifications performed in foreign countries;
- evaluation of the applicability of the technical assessment performed by LANL to the Belgian NPPs;
- follow-up of research activities and experimental work related to the strainer clogging issue.

Walk-downs in reactor buildings

The methodology used to perform the walk-downs was mainly based on the document issued by NEI³. The complete methodology was not applied given the Licensee argued that reliable information on insulation material was available. The main objective of these walk-downs was to collect the information necessary to perform further evaluations on the potential clogging of sump strainers as follows:

- configuration of sumps;
- strainers;
- critical characteristics of the ECCS components (NPSH, flow rate, acceptable debris, ...);
- compartments inside the containment;
- paints and other coatings;
- isolation materials;
- all fibrous material or other type of material that could significantly impair the operation of the recirculation;
- additional attention to ageing phenomena that could affect the performances of the strainers.

Support to the operators

These studies are intended to develop tools and guidelines in order to:

- assist the operator in identifying the clogging of the strainers;
- propose alternatives or corrective measures to be taken when it occurs;
- examine possible modification of existing procedures in order to delay the switch over in recirculation mode.

3. NEI 02-01 "Condition Assessment Guidelines: Debris Source Inside Containments".

Lessons learned

Walk-downs

Although not yet completed the walk-downs performed in the different containment buildings revealed a lot of relevant information. Up to recently, all studies related to the strainer clogging were performed on a theoretical base only. As already mentioned, only debris from isolation material were taken into account in these studies. The investigations were performed by the licensee. In addition, the AIO performed independent limited inspections.

It was observed during these inspections that materials that were never considered in the theoretical studies could have a significant impact on the clogging of the strainers. Examples of these findings are:

- presence of foreign material downstream the strainers (boron crystals, rags) – see Figure 1;
- presence of types of isolation material not taken in to account in the studies – see Figure 2;
- fibrous material containing SiCa used for fire separation – see Figure 3;
- blow out panels in synthetic foam – see Figure 4;
- tags used for several purposes: exit ways, fire hoses, location indication, maps – see Figure 5;
- protective plastic foils – see Figure 6;
- protective synthetic foam for personnel protection fixed with tape – see Figure 7;
- inadequate maintenance of paints and coatings – see Figure 8;
- shortcomings in the foreign material exclusion policy – see Figure 9;
- openings through the strainers, e.g. for pipe penetrations.

Corrective measures were taken as far as possible in order to improve the situation.

Support to the operators

The emergency response procedures are revisited in order to improve the surveillance of the proper operation of the recirculation function. In some cases, the Licensee considered that no significant modifications were needed. In other, specific guidelines will be established to allow the operator to monitor the recirculation function.

Future activities

Although improvements can already be noticed due to the actions taken, a lot of work has still to be performed to satisfactorily prevent and/or remedy to the strainer clogging issue.

Potential areas for improvements are to be considered in the following domains:

- paints and coatings;
- foreign material exclusion policy;

- behaviour of materials inside the containment not qualified to withstand to post-accidental environmental conditions;
- countermeasures taken by the operators to:
 - prevent strainer clogging;
 - identify a potential loss of recirculation;
 - restore adequate core cooling.
- characteristics of strainers (filtering area, type, ...);
- maintenance and periodic inspection of strainers;
- components downwards the strainers (pumps, fuel assemblies protective grids, ...).

Conclusions

Despite of measures taken in the past, recent information and insights have learned that further action is needed to ensure the operability of the recirculation function of ECCS and CSS after a loss of coolant accident.

Investigations are on-going for the Belgian NPPs to examine whether further modifications to the sump strainers are needed and whether additional aids for the operators to diagnose and manage a loss of recirculation can be provided.

An intensive actions plan is being undertaken in close collaboration between the licensee, the architect-engineer and the AIO (AVN).

Figure 1. Boron crystals downwards the strainer



Figure 2. Other types of insulation material



Figure 3. Fibrous material for fire separation



Figure 4. Blow out panels

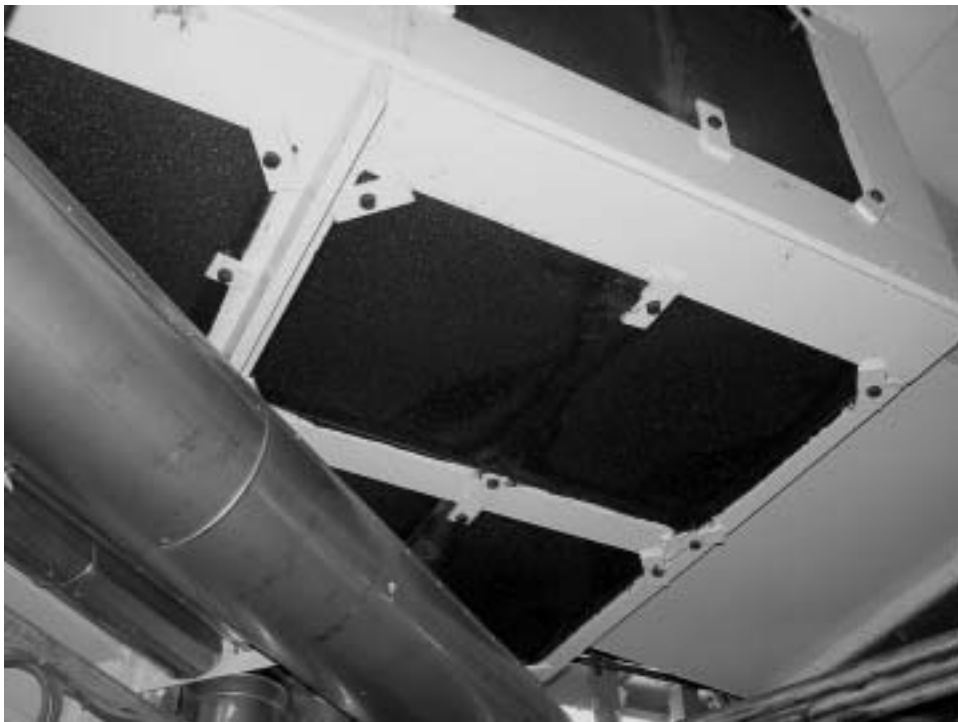


Figure 5. Tags and other tapes



Figure 6. Plastic foils



Figure 7. Personnel protection



Figure 8. Paints & coatings



Figure 9. Foreign material exclusion



**CONCLUSIONS DRAWN FROM THE INVESTIGATION OF LOCA-INDUCED
INSULATION DEBRIS GENERATION AND ITS IMPACT ON EMERGENCY CORE
COOLING AT GERMAN NPPS – APPROACH TAKEN BY/PERSPECTIVE OF THE
GERMAN TSO (TÜV)**

Josef Huber
TÜV Süddeutschland, Germany

1. Preface/Introduction

ÜV Süddeutschland, located in Munich/Bavaria in the southern part of Germany, is a technical support organisation (TSO) in conventional and nuclear technology in Germany. It is an organisation of independent experts. The nuclear division of this organisation supports the Bavarian and Hessian state authorities in charge of nuclear facilities. The task of the TÜV's nuclear division is to deliver expert's opinions on licensing and supervisory procedures. To fulfill this task corresponding to up to date knowledge (so called "state of science and technology" within the German framework of rules and standards) it is necessary to examine new experiences, like the Barsebäck incident, in its consequences to the safety of nuclear power plants.

The following plants are supervised by TÜV Süddeutschland:

Plant	Electric performance	Start of operation
PWR:		
NPP Biblis unit B (KWB-B)	1 300 MW	1977
NPP Grafenrheinfeld (KKG)	1 345 MW	1982
NPP Isar 2 (KKI 2)	1 475 MW	1988
BWR:		
NPP Isar 1 (KKI 1)	912 MW	1979
NPP Gundremmingen (KRB II):		
Unit B	1 344 MW	1984
Unit C	1 344 MW	1985

2. Initiation and basis of the new investigations of LOCA-induced insulation debris generation and its impact on emergency core cooling of German PWRs

Initiated by the Barsebäck incident in 1992 and the following activities related to the LOCA-induced insulation debris generation and its impact on emergency core cooling, investigations on the German PWRs and BWRs were carried out. These investigations were performed on the basis of:

- the new knowledge of LOCA-induced insulation debris generation and its impact on strainer plugging learned by the Barsebäck incident and further investigations of the relevant parameters and phenomena;

- the OECD report issued by the International Working Group in 1996;¹
- recent experiments in Germany concerning insulation debris generation and the transport mechanism in the containment sump towards and through the sump strainers.

In contrast to the German PWRs the investigations on the German BWRs were carried out in detail immediately after the Barsebäck incident in the years 1992 through 1994. As result of these BWR specific investigations backfitting measurements were performed in these years to improve the protection of the German BWRs against the impact of the LOCA-induced insulation debris generation on the emergency core cooling. The impact on the German PWRs was appraised to be not very important at that time. That is why detailed investigations on the German PWRs only started after the issue of the OECD report in 1996. Therefore the investigations on the impact of LOCA-induced insulation debris generation on strainer plugging carried out in Germany in the last years were focused mainly on the German PWRs.

3. Relevant parameters and phenomena investigated by the PWR plant owners in 1997 through 1999 and results

In the framework of these recent investigations concerning the LOCA-induced insulation debris generation and its impact on emergency core cooling, the following relevant parameters and phenomena were investigated in detail by the plant owners:

- size of leak cross sections for debris generation and core cooling calculations;
- debris generation (NUREG cone model);
- debris transport (containment, sump);
- pressure drop at the strainers due to the settled insulation debris and the resulting effects on the strainer structure and on the ECCS-pumps (NPSH);
- effects on the core cooling due to the insulation debris passing through the strainers and settling in the reactor core at the fuel elements;
- related effects such as dislodging of concrete, painting, coatings, etc.

These parameters and phenomena were investigated by the plant owners in the years 1997 through 1999. The results were summarised in reports for each plant and led to a prevailing opinion by the plant owners that backfitting in German PWRs was not needed to guarantee emergency core cooling following a LOCA with insulation debris generation. The reasons for this conclusion are given in the following chapters.

3.1 Size of leak cross sections for debris generation and core cooling calculations

In Germany the “break preclusion concept” (BPC) and the assumptions concerning the size of leak cross sections for the investigation of local effects caused by jet forces and core cooling calculations are mainly based on the following assumptions: “basic safety” and “independent redundancies” in compliance with the RSK-Guidelines (Guidelines of the German Reactor Safety Commission) and the KTA-Rules (Rules for the nuclear technology in Germany).

1. “Knowledge Base for Emergency Core Cooling System Recirculation Reliability”, February 1996, NEA/CSNI/R(95)11.

The basic safety of plant components depends on:

- high quality material characteristics, in particular toughness;
- a conservative restriction of stress;
- the prevention of peak stresses through optimal design;
- the assurance of the application of optimised manufacturing and testing technologies (e.g. in respect to welding);
- the knowledge and assessment of possible defect conditions;
- consideration of time dependent influences during operation (e.g. in respect to corrosion).

The Independent Redundancies concept comprises in-service inspection, load monitoring and leak detection systems in connection with leak-before-break-behaviour.

Applying the above described criteria, the following assumptions are made concerning the leak cross sections in the primary coolant piping and connecting austenitic piping with a diameter larger than 200 mm:

- for the calculation of local effects: a leakage with the size of 0.1 A (A = cross-sectional area of the piping) which is approximately equal to the rupture area of the connecting surge line;
- for the core cooling calculations: a leakage with the size up to 2 A in the primary coolant piping.

For these assumptions to be valid it has to be considered that not all German NPPs are designed on the basis of the “basic safety concept”. Originally these potential leak cross sections could only be assumed for the newer so-called “Konvoi”-plants whose design includes the “basic safety concept” (plants with the “break preclusion concept”). For the older plants investigations were performed with the objective to show that the design of these plants is equivalent to the “basic safety concept”. Therefore, according to the “break preclusion concept”, more independent redundancies (e.g. service inspections) have to be taken into account if the requirements of “basic safety” cannot be totally met. In case of positive results of these investigations, the above described assumptions for leak cross sections can also be applied to these plants (confirmed “basic safety” respectively “break preclusion”). As of today, these investigations are not completed for all older plants.

In the course of the new investigations about the LOCA-induced insulation debris generation and its impact on emergency core cooling, caused by the Barsebäck incident, the RSK decided at the 320th meeting in 1998 that for the investigations of the insulation debris generation a leakage with the size of 0.1 A has to be assumed for plants with confirmed “basic safety” whereas for the remaining plants pipe breaks with the size of 2 A have to be assumed. The investigations of the impact of the LOCA-induced insulation debris generation for the German NPPs were done on the basis of these recommendations.

3.2 Debris generation (NUREG cone model)

For the investigation of the debris generated by the LOCA-forces the NUREG cone model² was used. This model (90° circular cone for the region of destruction, originating at the postulated pipe

2. US Nuclear Regulatory Commission, “Sumps for Emergency Core Cooling Systems”, Regulatory Guide 1.82, Revision 1, 1985.

break) was transferred to the insulation conditions in the German plants by the following assumption to the debris generation (generally mineral wool, no glass wool insulation is used in German NPPs):

Region	Distance from leak (L = Distance from break to target, D = Diameter of broken pipe)	Destruction	Material (type of insulation)
Region I	$L/D \leq 3$	Total (100%)	All insulation material
Region II	$L/D > 3$ to $L/D \leq 7$	Total (100%)	“conventional” insulation type, (i.e. mineral wool, covered with a thin metal sheet)
Region II	$L/D > 3$ to $L/D \leq 7$	Partial (50%)	cassette insulation type, (mineral wool or other insulation enclosed in a so called “metal cassette”, consisting of a stainless steel-clad mineral wool panel)
Region III	$L/D > 7$ to $L/D \leq 30$	Total (100%)	“conventional” insulation type
Region III	$L/D > 7$ to $L/D \leq 30$	No destruction (0%)	cassette insulation type

The conservativeness of these assumptions especially was based on experiments of the Battelle Ingenieurtechnik (so called “Battelle/KAEFER tests”³).

Further assumptions for the application of the model are:

Concerning the application of the model it is assumed that in case of a 0.1 A leakage, the leak has a circular shape with the tip of the cone touching the surface of the pipe. The location of the 0.1 cross-sectional area leaks are assumed to be at each point of the circumference of the welding seams of the primary coolant piping. In the case of 2 A cross-section area ruptures the breaks are assumed to be located at each circular welding seam of the loop lines. Basing on these assumptions the estimation of the generated mass of insulation material was done on the base of special calculating rules.

Typical results of the investigation of the debris generation were:

- approximately 1 m³ to 2.2 m³ generated insulation material for 0.1 A leakage (for the “Konvoi”-plants conservatively covered by the break of the surge line);
- approximately 4 m³ to 7 m³ generated insulation material for 2 A breaks, depending on the location of the pipe break (for the older plants of the 1300 MW_{el}-class without “break preclusion”).

The investigations show that the generation of other materials beside insulation material, such as painting or concrete coats, is not relevant for the further analyses.

3.3 Debris transport (containment, sump)

The main transport mechanism for the debris distribution in the containment is the blow down phase of the LOCA accident. In this phase the debris (fine fragmented mineral wool) will be distributed with the steam flow to all regions of the containment and sticks on all structure surfaces. These mechanisms are verified by former experiments and incidents occurring in the past and also

3. Test Report of the Battelle Ingenieurtechnik GmbH B.I.G. V-68.262, June 1995, “Blow-down-Untersuchungen zum Verhalten von Isoliersystemen – unter Berücksichtigung von Regulatory Guide 1.82”, Final Report for KAEFER Isoliertechnik GmbH & Co. KG Bremen.

described in the OECD report.¹ As a conservative covering value it was assumed that 50% of the generated debris reaches the containment sump.

For debris transport in the containment sump it is relevant, that the residual heat removal system (RHRS) is not in sump operation mode during the blow-down phase. It was assumed that in this phase most of the debris in the sump settles onto the ground before the RHRS switches into the sump cooling mode. Only the suspended part of the fine fibers of the debris in the sump during the sump cooling mode of the RHRS can be effective for the plugging of the sump strainers. Due to results of experiments executed in Germany in 1998⁴, it was assumed that the amount of particles that remain suspended in the coolant depends on the location of the pipe leak or break. Further results of these experiments showed that only leak locations where a water jet directly into the sump pool during the sump cooling operation occur, generates a relevant amount of particles remaining suspended in the sump. Considering this fact, it was concluded from these experiments that in the case of a leak above the sump pool approximately 5% of the insulation particles generated by the LOCA-forces remain in suspension whereas other leak positions generate only 2.5% in suspension. This suspended material can settle on the strainers or pass through the sump strainers.

Regarding the further effects, the German experiments⁴ also show that for the mostly used sump strainers in German PWRs with a grid mesh width of 9 x 9 mm, most of the suspended fine fibers in the sump penetrates the strainers (80%, i.e. a maximum of 4% of the insulation particles generated by the LOCA-forces), and only a small part settles on the sump strainers (20%, i.e. a maximum of 1% of the insulation particles generated by the LOCA-forces).

3.4 Pressure drop at the strainers due to the settled insulation debris and the resulting effects on the strainer structure and the ECCS-pumps (NPSH)

The experiments of 1998⁴ were also the basis of the calculations of the pressure drop (head loss) at the strainers due to the settled insulation debris. At these experiments the head loss at the strainers was determined as a function of the velocity in front of the strainers and the mass of the insulation settled on the strainers. The experiments were carried out for different strainer geometries, for which the part of insulation material settled on the strainer were measured dependant on the mesh size of the grid. The dependence on the temperature of the coolant had been determined in previous experiments and confirmed with these new experiments to be a function of the cinematic viscosity of the medium, i.e. lower temperatures result in a higher pressure drop. Depending on these parameters, the results showed head losses at the sump strainers of lower than 0.1 bar (9 x 9 mm grid with 20% of the suspended material deposited on the strainers).

Further calculations show that the pressure drop at the strainer caused by the settled insulation debris will not impose problems for the strainer structure due to the pressure drop forces. The influence on the required suction head of the ECCS-pumps was also calculated to be not inadmissible.

Concerning the long-term-behaviour of the deposited insulation material (mineral wool) experiments were performed in Germany in 1989. These experiments showed that for mineral wool insulation material that is widely used in Germany for about four weeks no significant change of the material characteristics and no increase in the presser drop occurred under realistic simulated long term accident conditions.

4. KKB Reports: TTR/15/1998 dated from 17 February 1998; TTR/79/1998 dated from 7 December 1998.

3.5 Effects on the core cooling due to the insulation debris passing through the strainers and settling in the reactor core within the fuel elements

For the estimation of the effects of the insulation material it was assumed that all of the suspended fine fibers in the sump penetrating the strainers (80% of the suspended Material) reach the fuel elements in the reactor core. There the material settles on the debris filters at the feet of the fuel elements or between the fuel rods on the spacers within the fuel elements. Because of this deposition the pressure drop in the core increases and the heat transfer decreases. This effect was calculated by the computer code S-RELAP5. In these calculations the increase of the pressure drop coefficient for the calculation of the coolant flow through the reactor core was estimated from the results of experiments⁴ and included into the code input. Assumptions for the calculations were homogenous distributions or heterogeneous distribution of the insulation material at the core inlet or outlet respectively. The results of these calculations showed that up to 20 kg of insulation material that was assumed to be deposited in the core causes no inadmissible influence on the core cooling (conservatively, it was assumed that steam production in the core is not allowed during this cooling phase). Due to this result, it has been the opinion of the plant owners in 1998/1999 that core cooling of the German PWRs is not inadmissibly affected by the insulation debris generated by pipe breaks.

3.6 Related effects such as dislodging of concrete, painting, coatings, etc.

The following related effects were investigated by the plant owners:

- effects on the cooling systems;
- leakage at the cover of the reactor pressure vessel;
- effects on concrete, painting or coatings;
- effects of common soiling and corrosion products;
- the investigations led to the following results.

Due to the fact that only fine fibers of the insulation material can pass the sump strainers and reach the cooling systems (RHRS and fuel pool cooling system), an inadmissible impact on the cooling system is not expected to occur. The dominant reasons are the large cross-sectional areas of the flow path in the affected components, compared with the length of the fibers, and the large velocity of the flow. Thus no relevant deposition of fibers is possible.

Leakage at the cover of the reactor pressure vessel with generation of insulation debris can not lead to a clogging of the pipeline between the reactor pool to the containment sump because of the large diameter of the pipes without strainers.

The coatings and paintings used in the containment are specified to resist the loads prevailing at LOCA conditions. However, the water/steam jet hitting a wall may lead to a dislodging of concrete at the target area. Because of the higher density of the concrete in comparison with the density of the water, this case is not relevant due to the good settling behaviour of the dislodged material. Effects of common soiling and corrosion products are not relevant because of administrative measures against soiling in the containment during a plant outage, and the exclusive use of austenitic material that contacts with the coolant. Austenitic material is required for prevention of relevant amounts of corrosion products to occur.

Because of these reasons the plant owners came to the conclusion that the related effects do not lead to inadmissible consequences.

Summarising the results of all of the relevant parameters and phenomena investigated, the plant owners did not accept the requirement for backfitting in German PWRs as necessary.

4. Results of the examination of the TSO (TÜV Süddeutschland)

As the technical support organisation for the Bavarian and Hessian state authority, the TÜV Süddeutschland was called upon to examine the investigations initiated by the Barsebäck incident and the conclusions drawn by the owners for the NPP listed in Chapter 1. We considered each of the parameters and phenomena investigated by the plant owners, applying the state of knowledge contained in the OECD report,¹ as well as the results of more recent experiments of the NPP owners and additional calculations. We prepared a detailed expert's opinion for the NPP KWB unit B, which was issued to the Hessian state authority in May 1999.

The results of our examination confirmed that the investigations of the plant owners were generally correct, especially regarding the completeness of the investigated relevant parameters and phenomena, but we stated also, that due to existing uncertainties, further investigations are necessary to validate the results. The reasons for this conclusion are the following.

4.1 *Size of leak cross sections for debris generation and core cooling calculations*

The investigations of the plant owners followed the RSK recommendations described in Chapter 3.1. Thus, regarding the assumptions of the size of the investigated leak cross sections, no further need of investigation was seemed necessary in 1998/1999.

Now, as a result of further investigations in 2003, changes of the PWR sump strainers are planned in Germany. Therefore a renewed discussion about the assumptions for the size of leak cross sections for debris generation and for the calculations of the effects on core cooling takes place. The final decision has not been made yet, but it is expected that the assumptions for the debris generation defined in 1998 are accepted for further investigations as well (0.1 A- leak cross sections for plants with "break preclusion"). The calculations of the effects on core cooling remain to be done for leakages covering leak sizes up to 2 A in the primary coolant piping.

4.2 *Debris generation (NUREG cone model)*

To verify the conservativeness of the transfer assumptions of the NUREG cone model, applied to the insulation conditions in the German plants, we examined the experiments performed by the Battelle Ingenieurtechnik³ institute. The result of our examination was that uncertainties do exist in application of the model. However, the assumptions of the cone model for the insulation conditions in the German plants, described in Chapter 3.2, are valid if defined additional conservative assumptions and special calculating rules are applied. The conservatism could be proved by experiments performed in 2001 at the Siemens large scale valve test facility (GAP at Siemens Karlstein, Germany). We think that under these conditions the NUREG cone model can also be used for the new investigations as a conservative generation model.

4.3 Debris transport (containment, sump)

Our examination in 1999 proved the assumption to be conservative that 50% of the generated debris reaches the containment sump. This opinion corresponds with the new NUREG report.⁵ Therefore the value of 50% can also be used for the new investigations as a very conservative estimation for the containment conditions in German NPPs.

But we demanded in our expert's opinion that additional investigations had to be performed to verify that no inadmissible load of the sump strainers can occur during the blow-down phase. To meet this demand, additional analyses of the forces resulting by the flow of the steam-water mixture through the strainers in this accident phase were done. The results proved that no inadmissible load of the sump strainers occurs during the blow down phase (2 A primary coolant pipe rupture).

Our examination confirmed as plausible that the amount of particles that remain suspended in the containment sump depends on the location of the pipe break, where during the sump cooling operation a water jet directly into the sump pool occurs. This fact has generally been proved by the German experiments.⁴ Thus we had no argument against the proceeding of the plant owners to make different assumptions between leaks above the sump pool and other leak positions. We also concluded that the factor two between the leak positions above the pool versus leaks above the surrounding concrete is a good assumption for quantification of these effects. However, due to further experiments done in the NPP KKG we could not agree that in case of a leak above the sump pool with influence of the leak water jet on the part of the suspended material in the pool only 5% of the insulation generated by the LOCA-forces remains in suspension in the sump pool. To meet this demand, the plant owners installed a working group for planning and performing newer, more realistic large-scale experiments (see Chapter 5).

4.4 Pressure drop at the strainers due to the settled insulation debris and the resulting effects on the strainer structure and the ECCS-pumps (NPSH)

In contrast to the plant owners we concluded from the German experiments in 1998,⁴ that much more than 20% of the suspended material in the sump pool can be deposited on the strainers (mesh width 9 x 9 mm). Consequently, the new, more realistic large-scale experiments were designed to investigate this aspect too (see Chapter 5). In addition, the above described demand to investigate the influence of the water jet on the amount of the suspended material in the pool also can lead to more insulation material that deposits at the strainers and the head loss at the strainer arises.

4.5 Effects on the core cooling due to the insulation debris passing through the strainers and settling in the reactor core within the fuel elements

Due to our assumption, that in case of a leak above the sump pool, the part of the suspended material in the pool could be higher than the plant owners had calculated, also more insulation material could get into the reactor core. The results of our calculations to estimate the effects on the core cooling under these conditions showed, that up to 30 kg of insulation material that was assumed to be deposited in the core, causes no inadmissible influence on the core cooling. But due to the identified uncertainties, the amount of insulation material settling in the reactor core had to be

5. US Nuclear Regulatory Commission: NUREG/CR-6808, LA-UR-03-6880, "Knowledge Base for the Effect of Debris on Pressurized Water Reactor Emergency Core Cooling Sump Performance", Los Alamos National Laboratory, February 2003.

validated by further investigations. The new, more realistic large-scale experiments were designed to take into account this aspect as well (see Chapter 5).

4.6 Related effects such as dislodging of concrete, painting, coatings, etc.

Our examination in 1999 resulted in no need for further investigation to these aspects. We agree with the opinion of the plant owners that the related effects do not lead to inadmissible consequences.

Summarising the results of all the relevant parameters and phenomena investigated, we came to the conclusion in 1999 that further investigations are needed to validate the results.

5. Specification of new, more realistic large-scale sump-experiments with water jet and additional experiments for strainers and fuel elements

As mentioned above, the owners of the NPPs in Germany installed a working group for planning and performing newer, more realistic large-scale experiments (scaling factor 1:4) to investigate the transport mechanism of the insulation material within the containment sump, the head loss at the strainers and to estimate the amount of insulation material passing through the strainers. The important effect simulated by the experiments that had been demanded by our expert opinion, was the realistic simulation of the water jet during the sump operation mode of the RHRS. The approach to these more realistic conditions was to specify the new sump experiments to include this water jet. A pipe was used to simulate the opening of the break. This break opening was positioned at a realistic height above the basin of the experimental installation, representing the sump pool. The impact on the basin structure during recirculation of the water with a recirculation pump, simulating the cooling procedure with the RHRS, was recorded. We assumed that this effect – which was not realistically considered in the experiments conducted by the plant owners in 1998 – causes less insulation material settling onto the ground so that the amount of suspended debris would increase. Additional experiments were performed to investigate the behaviour of the insulation material passing through the strainers and settling in the fuel elements.

The experiment installation was specified on the base of realistic and conservative conditions that were to be representative for all German PWRs. By variation of relevant parameters the gained results of the experiments should be transferable to the real conditions in the different plants. Because of the normal mesh size of 9 x 9 mm in German NPPs until 2001 the large-scale experiments were done with 9 x 9 mm strainers. Additional experiments were performed to investigate the behaviour of different mesh sizes.

The insulation debris used during these transport experiments had previously been produced by another experiment using a realistic blow-down jet impact on a thermal insulation structure (altered mineral wool of a plant from 1982). This experiment took place at the large scale valve test facility Siemens Karlstein, Germany in 2001. The transport experiments in the sump pool and the fuel element experiments were performed in 2001 in Geesthacht, Germany by the GKSS.⁶

6. GKSS; DWR-Transportversuche für Isolationsmaterial, Test Report TZL0910 from 2 January 2002; Rev. a, 14 June 2002, GKSS, DWR-Brennelementversuche mit Isoliermaterial, Report TZL0702, 6 March 2002.

6. Aims, results and consequences of the new experiments

The aims of the experiments were:

- generation of fine fibers of insulation material for representing the effects of a LOCA incident as realistically as possible, as a precondition for realistic transport experiments;
- as realistically as possible estimation of the settling of the insulation material on the ground of the sump pool and on the sump strainers and the part of material passing through the strainers;
- application of generic correlations for the amount of material settling on the strainers and passing through the strainers depending on the area of the strainers;
- application of generic correlations for the head loss of the strainers depending on the area of the strainers, type and amount of the settled material, velocity at the strainers, the medium (demineralised water, concentration of boron acid) and the medium temperature;
- variation of relevant parameters so that the gained results of the experiments can be transferred to the real conditions of the different plants.

The results of these new transport experiments showed that under the new boundary conditions the behaviour of the insulation debris within the containment sump was much more disadvantageous than shown in the experiments conducted by the plant owners in 1998 (higher percentage of debris that does not settle in the sump pool). The following correlations were derived (approximate values, corresponding to the material transported into the sump pool):

- Part of the settled material on the strainer (9 x 9 mm): 2.5% for 2 x 22 m² to 10% for 6 m² strainer area (these values are to be compared with the values used in 1998 of generally 2% of the material transported into the containment sump in the case of a leak above the sump pool).
- Pressure loss for mineral wool ISOVER MD2 (1982), 10 cm/s, 25°C: 100 mbar for a deposition of 1 kg/m² insulation material (linear dependence from the velocity and the deposited material).
- Part of the material passing through the strainer (9 x 9 mm): 17% for 2 x 22 m² to 13% for 6 m² strainer area (these values are to be compared with the values used in 1998 of generally 8% of the material transported into the containment sump pool in the case of a leak above the sump pool).
- Suspended insulation material in the sump pool (sum of the parts of the insulation material settled on the 9 x 9 mm strainer and the material passing through the strainers): 19.5% for 2 x 22 m² to 23% for 6 m² strainer area (these values are to be compared with the values used in 1998 of generally 8% of the material transported into the containment sump pool in the case of a leak above the sump pool).
- Factor for the pressure loss depending from the type of insulation material: 1.0 for ISOVER MD2 to 2.4 for ROCKWOOL RTD2 (Materials, both produced in Germany in 1983 by two different manufacturer; tests of the different insulation materials show, that the manufacturer and the production year is very important; in 1998 no distinction was known between the behaviour of the different mineral wool materials).
- Combination of mineral wool with MINILEIT (particulate insulation of a silicate base) on a strainer (2 x 2 mm): This can lead to a clogging of the strainer (possible disadvantageous behaviour against the knowledge of 1998).

- Factor for the pressure loss depending on the medium (demineralised water, concentration of boron acid): Factor of < 1.1 for 2 400 ppm boron acid in opposite to demineralised water may be possible.
- Factor for the pressure loss depending on the medium temperature: 1.0 for 25°C (temperature of the experiments) to 0.28 for 100°C, corresponding with the cinematic viscosity of the medium).
- the assumptions of the head loss in the fuel elements for the core cooling calculations were verified to be conservative; the head loss of an element with a fuel foot with debris filter is generally lower.

After these experiments a few uncertainties remained (they are going to be investigated in this year):

- the influence of mixtures of various types of mineral wool (MD2 and RTD2) (to clear whether the assumption of linear dependence is correct);
- the influence of mixtures of mineral wool with MINILEIT (to clear whether there is a non linear influence);
- the influence of the mesh size of the strainers (to clear the behaviour of the different insulation materials by use of 3 x 3 mm strainers instead of 9 x 9 mm strainers, used for the large-scale experiments);
- the settling behaviour of the mineral wool type RTD2 (to clear whether there is a difference to the behaviour of ISOVER MD2 which was used for the new large-scale experiments).

As a consequence of the results of the new large-scale experiments, the plant owners now review their investigations for the German PWRs. This is likely to result in new investigations to be done for estimation of the head loss at the strainers and the corresponding effects as well as for the core cooling calculations. Because of the important influence of the insulation material the types of insulation materials used in the plants had to be determined before these calculations could begin. Depending on the new results, changes of the sump strainers, e.g. enlarging the sump strainers with smaller mesh width or exchanging of the insulation materials (installation of insulation material covered in solid cassettes or removal of insulation materials to avoid disadvantageous mixtures of materials with extremely high head loss at the strainers or in the fuel elements) could be necessary. These activities are currently being performed. Perhaps new experiments are necessary to verify the measures. Changes of the sump strainers could be performed during the next plant outages.

7. Summary

Initiated by the Barsebäck incident in 1992 and the following activities related to the LOCA-induced insulation debris generation and its impact on emergency core cooling, investigations on German PWRs and BWRs were performed in these areas. The investigations on the German BWRs were carried out in detail immediately after the Barsebäck incident in the years 1992 through 1994. Detailed investigations on the German PWRs started after the issue of the OECD report in 1996. Therefore the investigations on the impact of LOCA-induced insulation debris generation on strainer plugging carried out in Germany in the last years were focused mainly on the German PWRs.

In the framework of these investigations of the German PWRs, the relevant parameters and phenomena were investigated in detail by the plant owners in the years from 1997 through 1999. The results were summarised in reports for each plant. The main results of the investigations conducted by

the plant owners were that the plant owners considered backfitting in German PWRs is not necessary to guarantee emergency core cooling following a LOCA with insulation debris generation.

As the technical support organisation for the German Bavarian and Hessian state authority, the TÜV Süddeutschland was called upon to examine these investigations and the conclusions drawn by the plant owners. We compared each of the parameters and phenomena against the state of knowledge. The results of our examination in 1999 showed that the investigations of the plant owners were generally correct, but we stated also, that due to existing uncertainties, further investigations are necessary to validate the results.

To meet these demands, the plant owners installed a working group for planning and performing newer, more realistic large-scale experiments (scaling factor 1:4) to investigate the transport mechanism of the insulation material within the containment sump, the head loss at the strainers and to estimate the amount of insulation material passing through the strainers. The important effect simulated by the experiments that had been demanded by our expert's opinion was the realistic simulation of the water jet during the sump recirculation phase.

The results of these new transport experiments, performed in 2001, showed that under the new boundary conditions the behaviour of the insulation debris within the containment sump was much more disadvantageous than shown in the experiments of the plant owners in 1998 (higher debris percentage that does not settle in the sump pool). After these experiments a few uncertainties remained.

As a consequence of the results of the new experiments, the plant owners now review their investigations for the German PWRs. Depending on the results of these investigations, changes of the sump strainers e.g. enlarging the sump strainers with smaller mesh width or exchanging of the insulation materials could be necessary.

UNCERTAINTIES IN THE ECC STRAINER KNOWLEDGE BASE – THE CANADIAN REGULATORY PERSPECTIVE

C. Harwood and Vinh Q. Tang

Canadian Nuclear Safety Commission (CNSC), Canada

J. Khosla

Nutech Safety Assessment Inc., Canada

D. Rhodes and A. Eyvindson

Atomic Energy of Canada Limited (AECL), Canada

1. Introduction

When the Canadian Nuclear Safety Commission (CNSC) became aware of concerns relating to the collection of debris at suction strainers for emergency core cooling (ECC) systems following the incident in Barsebäck, Sweden, it issued a notice to Canadian utilities requiring them to review their ECC strainer capability in view of the potential increase in pressure drop, and address any deficiencies. During this review period, a number of uncertainties were identified as needing resolution, principally those items directly related to the head loss across the strainer (both in the short and long term), as well as a few secondary issues such as the likelihood of air ingestion. Canadian utilities contracted Atomic Energy of Canada Limited (AECL), through the CANDU owners group (COG), to perform extensive fundamental testing to establish the important parameters governing ECC strainer performance. AECL expanded upon this knowledge base with additional tests to confirm proposed designs for specific applications. As a result of all the testing, a substantial body of knowledge was produced and has been used by the utilities to support their final ECC strainer design solutions in their submissions to the regulator.

This paper discusses these uncertainties and their resolution. It also identifies the remaining uncertainties in the ECC strainer knowledge base, as it applies to CANDU stations, and how various conservatisms were used to offset these uncertainties.

2. Background

A loss of coolant accident (LOCA) in a CANDU station involves the leakage of primary coolant, D₂O, from the main heat transport system (HTS). This immediately triggers a shut-down of the reactor, but coolant flow through the reactor must be maintained for at least 90 days to remove decay heat. This is the function of the ECC system. For CANDU 6 stations, the ECC system has three main stages. First, high pressure injection of water into the reactor building is triggered by the LOCA. This is followed by medium-pressure injection, from water in the dousing tank located at a high elevation in the reactor building. Finally, during the low-pressure stage, the water in the reactor

UNCERTAINTIES IN THE ECC STRAINER KNOWLEDGE BASE – THE CANADIAN REGULATORY PERSPECTIVE

C. Harwood and Vinh Q. Tang

Canadian Nuclear Safety Commission (CNSC), Canada

J. Khosla

Nutech Safety Assessment Inc., Canada

D. Rhodes and A. Eyvindson

Atomic Energy of Canada Limited (AECL), Canada

1. Introduction

When the Canadian Nuclear Safety Commission (CNSC) became aware of concerns relating to the collection of debris at suction strainers for emergency core cooling (ECC) systems following the incident in Barsebäck, Sweden, it issued a notice to Canadian utilities requiring them to review their ECC strainer capability in view of the potential increase in pressure drop, and address any deficiencies. During this review period, a number of uncertainties were identified as needing resolution, principally those items directly related to the head loss across the strainer (both in the short and long term), as well as a few secondary issues such as the likelihood of air ingestion. Canadian utilities contracted Atomic Energy of Canada Limited (AECL), through the CANDU owners group (COG), to perform extensive fundamental testing to establish the important parameters governing ECC strainer performance. AECL expanded upon this knowledge base with additional tests to confirm proposed designs for specific applications. As a result of all the testing, a substantial body of knowledge was produced and has been used by the utilities to support their final ECC strainer design solutions in their submissions to the regulator.

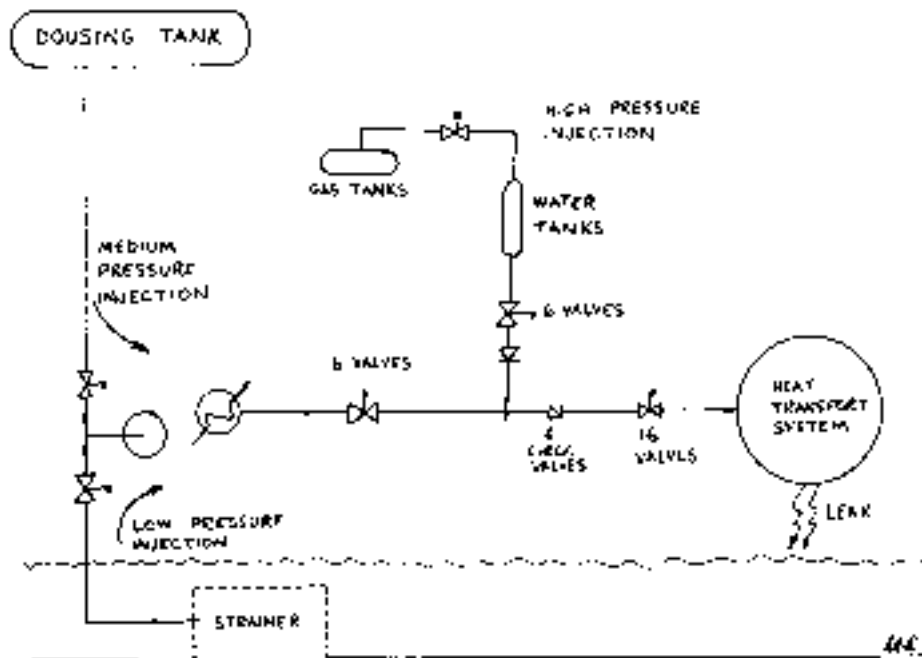
This paper discusses these uncertainties and their resolution. It also identifies the remaining uncertainties in the ECC strainer knowledge base, as it applies to CANDU stations, and how various conservatisms were used to offset these uncertainties.

2. Background

A loss of coolant accident (LOCA) in a CANDU station involves the leakage of primary coolant, D₂O, from the main heat transport system (HTS). This immediately triggers a shut-down of the reactor, but coolant flow through the reactor must be maintained for at least 90 days to remove decay heat. This is the function of the ECC system. For CANDU 6 stations, the ECC system has three main stages. First, high pressure injection of water into the reactor building is triggered by the LOCA. This is followed by medium-pressure injection, from water in the dousing tank located at a high elevation in the reactor building. Finally, during the low-pressure stage, the water in the reactor

building sump is pumped through the core to cool the reactor. The mission period for this stage is typically 90 days. Figure 1 shows the three phases for a CANDU 6 station.

Figure 1. CANDU 6 ECC System



The water in the sump may contain debris of various sizes and types from a number of sources. The function of the strainers in the reactor building basement or sump is to filter this water before it is pumped through the reactor. The strainer must have a surface area large enough to accommodate all the postulated debris without causing excessive pressure drop that could lead to pump cavitation or collapse of the strainer, and must also be able to prevent small debris from passing through and clogging downstream components.

Multiple unit CANDU stations use a vacuum building arrangement and the details of the high and medium pressure ECC injections are somewhat different. However, the design of the low pressure injection phase and the challenges to the ECC strainer are very similar to those described above.

The existing strainers for most CANDU stations at the time of the Barsebäck incident had surface areas varying from 4 to 95 m². The adequacy of these strainers was evaluated and a number of uncertainties were identified.

3. Uncertainties – debris

One of the prime uncertainties identified early in the Canadian strainer evaluation process was the type and quantity of debris that could reach the strainer during the accident and post-accident period. The debris in the sump was considered to be generated in one of three ways – dislodgement of insulation and other material due to direct impingement by the jet of reactor coolant from the failed piping, transportation of pre-existing debris from on or near the floor in the flow path from the break discharge to the strainer, or peeling of coatings from walls, floors or equipment, which could be carried by the flow of the condensate to the sump. Most of the insulation used in CANDU reactors in

Canada is fibrous in nature, but a small amount of particulate insulation also exists in some reactors. The nuclear industry carried out an extensive programme to identify the types of insulation or other materials which may potentially be dislodged and to develop data for the pressure drop through the debris bed on the strainer. During this programme, it was recognised that fine particulates significantly increase the pressure drop; hence the impact of dirt, paint chips and other fine particulate was investigated in considerable detail.

3.1 *Jet impingement*

In CANDU reactors, a high proportion of the large primary heat transport piping is inside the feeder cabinet, which is a large insulated box. This was identified to be an area with the potential for dislodgement of large amounts of debris. The amount of debris generated due to jet impingement was calculated using a spherical zone of influence (ZOI) model. This model predicts the volume of space in which material will be broken down by a jet. According to the model, the volume is a function of the pipe diameter cubed, the break geometry (e.g. restrained or unrestrained), break discharge medium (steam or water) and the resistance of the material impacted.

The ZOI model used by the CANDU industry includes numerous uncertainties. First, the destruction pressure of materials is not precisely known, and was estimated for CANDU-relevant materials based on the available information, with a low value selected for conservatism (a lower destruction pressure results in a larger ZOI and therefore more debris generation). All material of a given type was assumed to have the same destruction pressure. Second, the model itself is an approximation. Third, the model assumes that all material within the ZOI is destroyed (and none outside the ZOI); however, this does not account for the thickness of the material or its orientation relative to the jet (direct, oblique angle, etc.).

Despite the uncertainties in the ZOI model, the distance from the break to the insulation was estimated conservatively to give the largest possible amount of debris generated. In addition, the destruction pressure used in the model was the lowest value of all the materials tested in the reference documents [1]. These two factors combined were expected to give a conservative value for debris generated from the break. The nuclear industry also did some confirmatory tests on typical insulation materials, as well as on some materials for which data did not exist.

3.2 *Floor debris*

Outside the ZOI, debris on or near the floor that is in the flow path can be transported to the strainer. The amount and type of this debris is difficult to quantify. It can include transient articles, such as garbage cans and their contents, which will vary almost daily. The debris also includes floor dirt, which is also variable both in terms of amount and type.

The quantity of floor debris to be used for the strainer performance evaluation was estimated based on plant walkdowns and a review of foreign materials exclusion (FME) programmes. Floor swipes were used to estimate the quantity of rust, dust or dirt particulate per unit area; this was then multiplied over the entire area of interest to give an overall estimate. Larger debris such as plastic gloves, rubber boots, garbage cans and their contents were assumed to be removed as part of plant FME programmes.

Despite the walkdowns and floor swipes, it is clearly not possible to obtain a precise measurement of the amount of floor debris that could exist at the time of an accident. Some conservatism was applied to account for these uncertainties.

First, the amount of rust, dust and dirt in the entire area of interest was calculated based on the upper range of measured debris per unit area (as determined by the floor swipes), rather than on the mean value. Second, all this debris was assumed to be transported to the strainer; no credit was allowed for any debris that might fall out of suspension along the way or get caught in stagnant areas. Third, although FME programmes were assumed to prevent large debris such as rubber boots or gloves from reaching the strainer, some testing was performed to confirm the ability of the strainer to withstand limited quantities of this type of debris.

3.3 *Coatings*

The coatings on various surfaces and equipment inside the reactor building could peel off due to high radiation fields and exposure to the water in the sump. To estimate the amount of coating debris that could be generated, the licensees typically calculated the volume of coating in the area of interest by estimating the coating thickness and the surface area. A safety margin was then applied to account for uncertainties in these values. Then, estimates of the fraction of this coating that could delaminate, and the fraction that would be transported to the strainer, were made. This resulted in a final estimate of the amount of coating debris that could reach the strainer.

Because of the uncertainties in the above assessments, AECL also performed tests to investigate the three main issues that could impact the amount of coating debris reaching the strainer. These were:

- the ability of the coating to remain attached to the substrate when exposed to accident and post-accident conditions;
- transport of coating debris in the water flow towards the strainer; and
- the impact on strainer head loss for a given quantity of coating debris.

The first item was addressed by coating concrete and steel substrates with various undercoats and topcoats, then exposing these to lifetime radiation doses, accident conditions and post-accident conditions. Adhesion tests were performed at predetermined points to determine how well the coatings adhered to the substrate. This information was then available to the stations to refine estimates of paint quantities, or to demonstrate conservatism in the original estimates.

Transport tests were performed in which coating samples were placed in moving water to determine the effects of water velocity, material type and geometry on transport. These tests also included placing small obstructions in the flow path to observe whether the materials would be stopped or not. In head loss tests, the tendency of the chips to settle naturally to the floor of the test facility rather than reaching the strainer was observed.

Many head loss tests were performed with coating as part of the total debris. Different sizes of flakes were tested, and the effect of adding the coating after the debris bed had been deposited was compared to the result when the coating was mixed in with the rest of the debris. The tendency of the chips to settle out before reaching the strainer was overcome by stirring the test mixture to prevent debris from settling on the floor.

Despite the coating tests, some uncertainties still remain. These have been addressed through various methods.

1. The testing could not include all possible paint types in use at the stations (in some stations, the exact type of paint used could not be confirmed; in other cases, it was no longer available on the market). Thus the performance of the specific coating in a given station could not be explicitly determined. However, generic types were covered, including epoxy, urethane and alkyd (including coatings not qualified for use in nuclear facilities), on both steel and concrete substrates. How this information was used in submissions to the regulator depended on the station. For instance, a factor of safety could be used to account for uncertainties in the coating type; the results of the unqualified coating could be applied to qualified coatings to provide a degree of conservatism; or the coating used in the station could be assumed to be reasonably represented by the coating types tested.
2. It was not possible to expose the paint samples to all possible simulated accident scenarios. Instead, the worst-case accident condition enveloping all stations was used as the standard. Therefore, the performance of the coating to any given accident scenario could only be surmised by estimating how much less severe the given scenario was compared to the worst-case scenario. Using the results of the worst-case conditions provides conservative results.
3. Despite the evidence indicating that some coating chips would tend to deposit on the floor prior to reaching the strainer, qualification tests for strainers were performed with coating as part of the debris mix and the mixture was stirred continuously in the tank to ensure that the coatings did not drop to the floor, but instead deposited in the debris bed on the strainer. This resulted in a conservative test result.

4. Uncertainties – head loss

Short term head loss tests were performed in two different types of facilities. These were a medium scale facility, shown in Figure 2, and a large scale facility, shown in Figure 3.

The medium scale facility consists of a Jacuzzi-sized tank with a strainer screen. An external pump is used to draw the water through the screen, past a heat exchanger and filter bag (both of which can be valved in or out of the piping system) and inject it back into the tank. A stirring mechanism is used to keep the debris in suspension before it deposits on the screen. The water temperature can be controlled, and temperature, flow and pressure drop across the screen are measured continuously.

The large scale facility has similar functions to the medium scale facility, but is large enough to hold approximately 15 m² of strainer surface area. It consists of a large lined tank (approximately 1.5 m deep, 2.5 m wide and 5 m long) connected to a large piping system. Flow rates up to 240 L/s and temperatures from 20°C to 55°C can be tested. Temperatures, pressures, test duration and flow rate were monitored during testing.

Figure 2. Medium scale facility



Figure 3. Large scale test facility

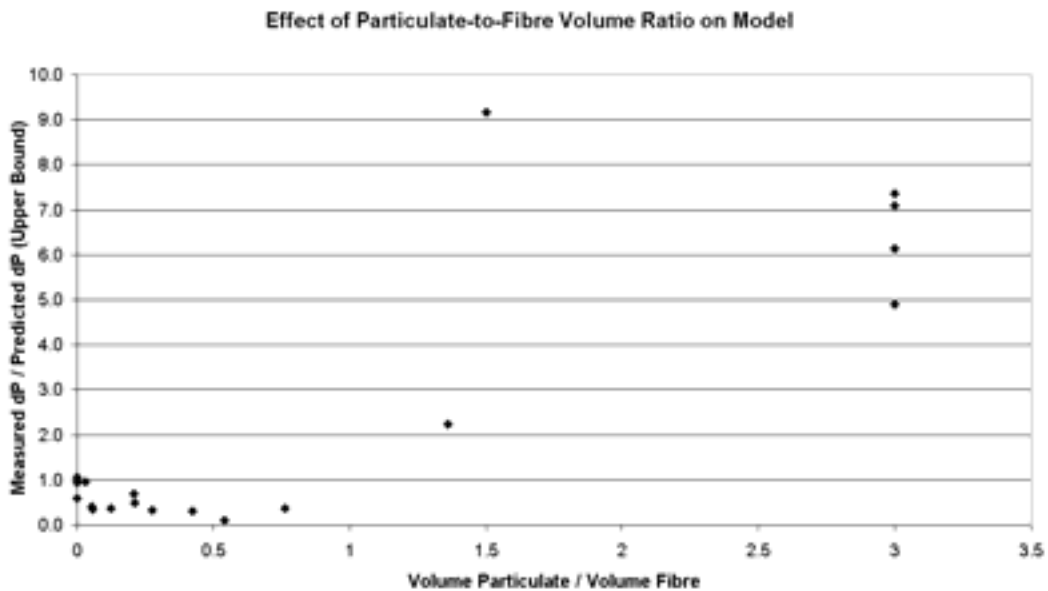


4.1 Head loss model – short term

A large number of tests were performed for durations of up to ten days. These were performed using a variety of debris types and combinations, flow rates and temperatures. The method of debris fabrication (e.g. shredding, grinding) was varied to determine its effect on the head loss. As the database expanded, the test results were compared to the values predicted using a published head loss correlation, and significant discrepancies between the measured and predicted values were noted. Based on this, a new CANDU-specific correlation was developed. This correlation was used to predict the short term (2 day) head loss across a strainer for a given approach velocity (velocity of the water at the strainer screen), water temperature, material volume and type. However, even the new correlation was found to be limited in its range of applicability. It was developed from tests with approach velocities from 0.006 m/s to 0.01 m/s, so its use is limited to this range. In addition, when the volume

ratio of particulate debris to fibrous debris exceeds approximately 1.5, the model is unsuitable, as it under-predicts head loss by a significant amount.

Figure 4. Effect of Particulate-to-Fibre volume ratio on short term head loss model



The uncertainties in the short term head loss correlation were addressed in one of the following ways. First, a large number of tests were performed, so most of the conditions of interest were tested one or more times. Sometimes small changes were made between tests to determine the sensitivity of head loss to a particular parameter. The large number of tests increases the confidence level on the results. Second, a safety factor was added to the head loss correlation. This factor results in an over-prediction of head loss for all cases used to develop the correlation, thus providing a safety margin to give added assurance that the predicted result will be conservative.

Head loss model – long term

Although a 90-day mission period is the typical requirement for the low-pressure CANDU ECC system, most head loss tests were performed for a much shorter duration (typically up to ten days). This permitted more exploration into the effects of different debris types, quantities, flow rates and other parameters. However, a small number of long term tests, of durations ranging from 20 to 90 days, were performed to confirm that the short term test results could (in some cases) be extrapolated to a longer period. Due to time and budget restraints, not all possible test conditions could be tested over the long term. Therefore, long term tests were performed using conditions relevant to postulated station conditions.

The uncertainties in the long term head loss were addressed in two ways. Long-term tests to verify the effectiveness of planned strainer modifications in a specific station were performed at conditions matching those in the station as closely as possible. In addition, an extra margin on capacity was added to all new strainers to account for uncertainty in the long term head loss. (This margin covered many potential uncertainties, such as debris quantities, water temperature, and extrapolation

of test data out to 90 days.) The predicted head loss for the new strainer at the design conditions was typically one half to one quarter of the allowable head loss.

5. Uncertainties – air ingestion

The possibility of ingesting air into the ECC system through the strainer was identified early on as a concern, due to its potential harmful effect on the ECC pumping capability. This was evaluated during tests by several means. In one set of tests, the submersion of the strainer (i.e. the vertical distance from the water surface to the uppermost straining surface) was varied for a given flow rate and debris loading until vortices were observed. In another set of tests, the flow rate was varied while other parameters were held constant. Different debris loading conditions were also evaluated. From the tests, the minimum acceptable strainer submersion level for the conditions relevant to each station could be determined.

Conservatism was applied to the results of these tests when identifying strainer requirements for the stations by using the minimum possible water level when specifying the maximum strainer elevation.

6. Current state of affairs

The Canadian nuclear industry has made significant advancements in its ECC strainer knowledge base over the past several years. Nevertheless, a number of unknowns still exist. Despite these uncertainties, based on this knowledge, all the licensees have implemented design changes in their ECC systems and in other relevant areas, such as impeding debris transportation by water flow. The regulator has accepted the solutions presented by the licensees on the basis of the low probability of the accident event, the constraints on the strainer area that could be installed as a back-fit, the risk reduction due to the timely implementation of the design change, the conservatism applied to the test results, the defence-in-depth principle of CANDU stations, and the station-specific testing performed. Although some outstanding items remain to be resolved, the overall performance of the ECC systems in Canada now is much improved. The regulator and industry have been working together on the remaining items to bring this issue to a close.

7. Summary

An extensive series of tests have been performed in Canada to address strainer issues relevant to CANDU stations. These tests resolved many of the previous uncertainties regarding strainer performance and debris quantities. Although minor uncertainties remain, these have been addressed by applying conservatism to the test results. The Canadian regulator has remained fully informed of the testing and has accepted the ECC system changes proposed by Canadian utilities. These changes are either completed or nearing completion at Canadian facilities and have resulted in a significant improvement in safety at the CANDU stations.

References

- [1] Continuum Dynamics Report 96-06, “Air Jet Impact Testing of Fibrous and Reflective Metallic Insulation”, rev. A, September, 1996.

NRC APPROACH TO PWR SUMP PERFORMANCE RESOLUTION

John N. Hannon

Branch Chief, Plant Systems Branch (SPLB)
Office of Nuclear Reactor Regulation (NRR)
US Nuclear Regulatory Commission (USNRC)

Regulatory requirements and background

NRC regulations in the US *Code of Federal Regulations* require that the emergency core cooling systems in a nuclear power plant must provide the capability for long-term cooling of the reactor core. As set forth in 10 CFR 50.46(b)(5), the emergency core cooling systems must have the capability to remove decay heat so that the core temperature is maintained at an acceptably low value for the extended period of time required by the long-lived radioactivity remaining in the core. For US plants that are licensed to the General Design Criteria in Appendix A to 10 CFR Part 50, General Design Criterion 35 specifies additional emergency core cooling system requirements, such as fuel and clad damage that could interfere with continued effective core cooling. Similarly, for plants licensed to the General Design Criteria, General Design Criterion 38 provides requirements for containment heat removal systems, and General Design Criterion 41 provides requirements for containment atmosphere cleanup. Many licensees credit a containment spray system, at least in part, with performing the safety functions to satisfy these requirements, and plants that are not licensed to the General Design Criteria may credit a containment spray system to satisfy similar plant-specific licensing basis requirements. In addition, licensees may credit a containment spray system with reducing the accident source term to meet other regulations.

The pressurised water reactor sump performance issue deals with the possibility that debris may impede recirculation after a loss of coolant accident. Proper recirculation of water during and after a loss of coolant accident would be restricted if the sump pumps are not able to suction enough water. The concern is that debris caused by the loss of coolant accident would lodge in the sump screens surrounding the pump, creating a filter effect whereby flow through the screen would be substantially decreased. This increase of head loss could potentially cause cavitation and failure of the pumps, or may prevent water from getting to the pumps.

The event at Barsebäck in 1992 caused the NRC to focus on the resolution of strainer performance at US boiling water reactors, which is a similar issue to the sump performance at US pressurised water reactors. The NRC conducted a research program from 1992 through 1995 that addressed the boiling water reactor concern. The NRC issued Bulletin 96-03, and, as a result, the boiling water reactor licensees installed suction strainers with much larger surface areas in response to this Bulletin. However, additional research was needed before a final conclusion could be reached regarding the potential clogging of sumps at pressurised water reactors. To address this issue at pressurised water reactors, the NRC opened Generic Safety Issue 191, "Assessment of Debris Accumulation on PWR Sump Performance".

Research

The NRC then sponsored a research program and completed its technical assessment of this issue in September 2001. The assessment, which is documented in NUREG/CR-6762, "GSI-191: Parametric Evaluations for Pressurized Water Reactor Recirculation Sump Performance", used a combination of plant-specific and generic information to model sump performance. This assessment concluded that sump clogging was a plausible generic concern for pressurised water reactors and that regulatory action may be warranted. The results of this research pointed out the need to conduct plant-specific analyses to determine if sump performance could potentially be degraded. The research did not account for specific design features at some plants that might improve sump performance, such as specific operator actions that can reduce the likelihood of sump failure recognising the limitations of the generic studies that formed the technical basis for this concern, NRC sponsored a study to evaluate the potential risk and another follow-on study to examine how much recovery actions lessened the potential for sump clogging. This second study demonstrated that effective recovery actions could significantly reduce the potential risk of sump clogging.

Regulatory action

This new information prompted the NRC to issue Bulletin 2003-01. In the Bulletin, the NRC informed pressurised water reactor licensees of the results of the research program and asked the licensees to either confirm their compliance with existing regulatory requirements, or describe interim risk reduction measures they would put in place to reduce potential risks associated with sump blockage. If, while taking appropriate risk-reduction measures, a licensee discovers that they are not in compliance with our regulations, they are required to take prompt corrective action. The underlying purpose of the Bulletin is to ensure licensees implement near-term compensatory measures that reduce the risk associated with sump failure.

The NRC is currently in the process of evaluating the responses to the Bulletin. Licensees of all 69 pressurised water reactors have submitted responses and 68 of the pressurised water reactors chose to pursue interim risk reduction measures. The Bulletin describes interim compensatory measures that licensees were encouraged to implement where appropriate. These measures included the following:

- training operators on sump clogging;
- modifying procedures to delay recirculation via containment sumps (e.g. shutting down redundant pumps);
- providing alternate water sources to refill reactor water storage tank or to inject into containment and core;
- maintaining more aggressive containment cleaning and foreign materials controls;
- ensuring containment drainage paths are unblocked;
- ensuring sump screens are free of gaps or breaches.

Based on the follow-on report, certain of these measures have a demonstrated risk benefit. If operator actions are taken to restore flow despite loss of net positive suction head, or reduce flow to decrease net positive suction head; and an alternate source of borated cooling water is available and aligned to either refill the reactor water storage tank or directly inject into containment and the core, then the risk of core damage decreases by an order of magnitude. In the bulletin, the NRC also encouraged licensees to propose other compensatory measures not specifically listed.

In addition to NRC technical staff reviewing the Bulletin responses, regional NRC staff are performing inspections to verify licensees have effectively implemented the compensatory measures according to their Bulletin responses.

As part of the resolution, the NRC is preparing a generic letter that will request licensees to provide an evaluation of their sump performance, take appropriate corrective actions, if necessary, and perform plant modifications, if necessary. The NRC plans to audit plants on a sampling basis to verify a licensee's evaluation, corrective actions, and/or plant modifications. For the selection of which plants to audit, the NRC will select a diverse group of plants with different sump configurations and different generic letter responses. This audit review is very similar to the process used to review the licensee evaluations and modifications for the boiling water reactor strainer issue.

To support the assessment of sump performance, the NRC has issued Regulatory Guide 1.82, Rev. 3, "Water Sources for Long-term Recirculation Cooling following a Loss of Coolant Accident". This Regulatory Guide provides the industry with guidance on evaluating and maintaining sump availability and long-term cooling. It will be used to review the licensee's own assessment of their sump performance.

Summary

The NRC is following a well-established regulatory process to resolve a complex safety issue. The two-pronged approach first evaluates near-term compensatory measures designed to reduce risk, and second ensures that a thorough analysis of the condition has been made and that any necessary modifications have been taken to resolve the issue. This regulatory framework achieves the goals of maintaining safety.

OVERVIEW OF US RESEARCH RELATED TO PWR SUMP CLOGGING

Dr. Anthony Hsia
Office of Nuclear Regulatory Research
US Nuclear Regulatory Commission

Outline

- History of GSI-191.
- Research to date:
 - Technical assessment.
 - Regulatory guide and evaluation guidance.
 - Model validation.
- Current and planned tests:
 - Chemical effect and calcium silicate tests.
 - Latent debris and downstream effect tests.
 - Integrated chemical effect tests.
 - EPRI coatings study.

History of GSI-191: Assessment of debris accumulation on PWR sump performance

- USI A-43, “Containment Emergency Sump Performance” resolved in 1985:
 - Tests showed air ingestion from vortex is less severe than previously expected.
 - Insulation debris transport tests showed that debris can readily be transported at low velocities (0.2 to 0.5 ft/s).
 - Small debris that can pass through screens should not impair long-term performance of pumps.
 - 19 NPPs surveyed to identify insulation types/quantities/distribution, sump designs/locations, etc.
 - Effects of debris clogging on NPSH margin should be assessed on a plant-specific basis.

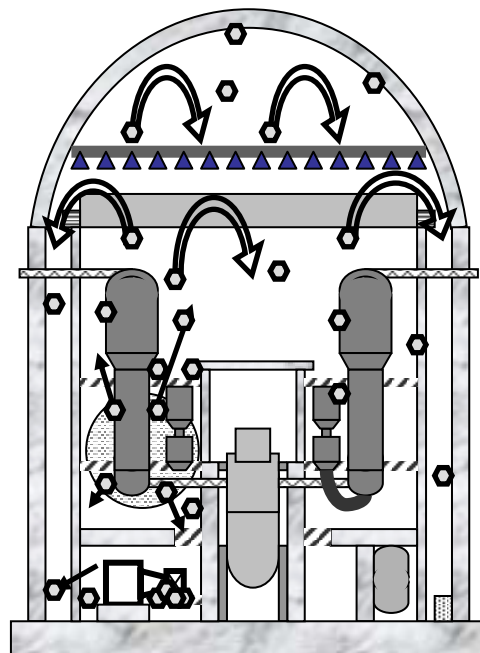
- ECCS strainer clogging events at Barsebäck and some US BWR plants in early to mid-1990s prompted revisit of USI A-43.
- BWR strainer issue resolved by industry actions according to BWR URG, in response to NRC Bulletin 96-03.
- GSI-191 established in 1996 to determine if further action was needed beyond the original resolution of USI A-43.

Research to date

Technical assessment

- NRC/RES conducted technical assessment to determine whether sump failure is a plausible generic concern for PWRs.
- Assessment used plant-specific and generic information.
- Sources of information used were from industry responses to: (1) NEI survey; (2) NRC GL 97-04 (for assurance of NPSH margin in ECCS pumps).
- NRC sponsored assessments considered:
 - debris sources and generation;
 - debris transport;
 - sump screen head loss.

Figure. Debris Sources



- Sump failure defined as:
 - loss of NPSH margin, i.e. cavitation (submerged sump screens);
 - cavitation or starvation (partially submerged sump screens).

Regulatory guide and evaluation guidance

- RG 1.82, Rev. 3 issued (November 2003):
 - Provides guidance and acceptable methods for evaluating PWR sump performance.
 - Considers dominant debris sources.
 - Based on realistic selection of break sizes/locations with potential for debris generation causing head loss across sump screens, i.e. break-to-clogging.
 - Using analytical models benchmarked by test data.
- Draft NEI evaluation guidance issued October 2003.

Model validation

- Debris generation tests:
 - BWROG air-jet impact tests;
 - HDR 2-phase jet, etc.
- CAD code with data from a representative plant.
- Debris transport – using plant specific sump and screen info:
 - separate-effects tests;
 - integrated-effects tests, etc.
- Head loss tests:
 - tests for different types of debris.

Current and planned tests

Chemical effect and calcium silicate tests

- Small scale chemical effect tests completed and LANL report issued in November 2003. Key findings are that if gelatinous material is formed, head loss across the sump screen can be much higher than created by fiber glass alone. (ACRS concern raised in February 2003).
- Calcium Silicate (CalSil) insulation debris head loss tests completed, LANL report due in February 2004. Key findings are that debris bed formed by CalSil and fiber glass can result in head loss much higher than created by fiber glass alone.

Latent debris and downstream effect tests

- Latent debris characterisation and additional head loss tests are ongoing. LANL report is due in May 2004.
- The downstream effect tests – Screen penetration and HPSI throttle valve clogging tests will be started. LANL reports due in May 2004 for screen penetration and in December 2004 for combined final report.

Integrated chemical effect tests

- Concern: Post-LOCA chemical interactions in PWR containment between ECCS/CSS water and exposed materials may produce additional debris.
- Issue was raised by ACRS in February 2003, cited evidence was “gelatinous” debris found in TMI after 1979 accident.
- A limited-scope study was conducted to assess potential for chemically induced corrosion products to impede performance of ECCS recirculation after a LOCA.
- No integrated tests were performed to demonstrate complete progression of chemical interactions from metal corrosion to the ultimate formation of precipitation products.
- Separate-effects tests were conducted for each potential stage of the progression.
- Precipitation was artificially induced in head loss flow tests by addition of metallic salts to the fluid.
- To assess formation potential and formation rate of corrosion precipitants (e.g. gelatinous material) caused by chemical interaction between ECCS/CSS water discharge and exposed materials in PWR containment under post-LOCA conditions.
- To characterise corrosion precipitants if formed.
- To assess transportation and collection of corrosion precipitants to collection screen.
- To measure effects of most important chemical variables on formation rate of corrosion precipitants and collection.
- NRC to consider integrated tests with cooperation from industry (EPRI):
 - staff participation from RES and NRR;
 - scaled tests;
 - realistic/prototypical;
 - timeliness;
 - industry involvement;
 - communicate with stakeholders.

EPRI OEM coatings study

- Study being conducted by EPRI and scheduled for completion mid-2004.
- Identify types of OEM unqualified coatings typically found in US PWR.
- Review EQ data/photographs depicting OEM coating performance during testing.
- Conduct DBA testing of selected OEM coating samples.

RESULTS OF TESTS WITH LARGE SACRIFICIAL AND SELF-CLEANING STRAINERS AND THE INSTALLATION AT RINGHALS 2

Mats E. Henriksson
Vattenfall Utveckling AB
SE-814 26 Älvkarleby
(Phone +46 26 83540, Fax +46 26 83670)
E-mail mats.henriksson@vattenfall.com

Abstract

The paper describes briefly activities performed by Vattenfall Utveckling AB at Älvkarleby Laboratory as part of the qualification programme for the new ECCS strainers at PWR plant Ringhals 2 based on the “robust solution” with large sacrificial strainers and a self-cleaning “wing-strainer” of same type as used for the five modified Swedish BWR plants.

With the new knowledge gained from several BWR strainer projects following the Barsebäck strainer incident in 1992, the functioning of ECCS strainers for PWR was re-evaluated. The upgrading at Ringhals 2, a 3-loop Westinghouse plant having fibreglass and mineral wool as insulation, was the result of a design study including a lot of experimental work mainly in 1993 and 1994. The new ECC system was installed in 5 days in the summer outage 1995.

In a first study in year 1993 in the large test tank at Älvkarleby Laboratory it was discovered that the earlier design basis for debris settlement was not fulfilled. Recirculating water falling from a large break will not only prevent settling of the fibrous insulation debris but also disintegrate wads and larger pieces to fibres and fines. It could no longer be assumed that the insulation would settle in front of the strainers. This discovery affected the further work within the project group and the work at Älvkarleby Laboratory.

It is presented some test data that have not been published before, e.g. combinations of fibres and particulate material. The test programme included also chemical treated fibrous insulation as well as combinations with carbon powder or oil. Also experiences from combinations of fibres and RMI debris were gained.

Some information from projects later performed for the US market are included. Also it is included some experience on deviations in results when tests are performed in different ways. At the end the modified strainer system for Ringhals 2 is presented.

1. Introduction

With the new knowledge gained from several BWR strainer projects [1, 2] following the Barsebäck strainer incident, the functioning of ECCS strainers for PWR was re-evaluated. The upgrading at Ringhals 2, a 3-loop Westinghouse plant having fibreglass and mineral wool as insulation, was the result of a design study including a lot of experimental work mainly in 1993 and 1994. The new ECC system was installed in the summer outage 1995.

The Ringhals 2 strainer upgrading project has been reported at the workshop in May 1999 and at the NEI Workshop, Baltimore July 2002 [3a, 3b] and has also earlier been described in two NEI articles [4a, 4b] A more general description of alternative designs developed by Vattenfall Utveckling AB was presented in another NEI article [4c].

This paper describes mainly activities performed by Vattenfall Utveckling AB at Älvkarleby Laboratory as part of the qualification programme for the new strainers at Ringhals 2.

Possible combination effects of oil and fibre in the water and effects of fibre and carbon powder in the recirculation water were studied in the small one-dimensional test rig.

CFD calculations of flow pattern in the bottom region of the containment were performed and revealed that quite high velocities could be present in areas close to the existing strainers.

Possible air ingestion caused by air pulling vortices was studied in a 1:3.5-scale model. The strainer system was found to perform satisfactorily at all operating conditions. The new ECCS system installed at Ringhals 2 in the summer outage 1995 is a self-cleaning wing strainer combined with horizontally mounted sacrificial strainers.

Self-cleaning is induced by short interruptions in the suction flow. The effectiveness of the cleaning was demonstrated in a full-scale test using fibrous insulation chemically treated to simulate a pressurised water reactor environment. Self-cleaning was also achieved for very thin layers of fibres having small pressure drops.

In Chapter 7 system aspects and information about the modification work of sump screens in Ringhals 2 are briefly covered.

2. Sedimentation, resuspension after disintegration and transport of fibreglass insulation

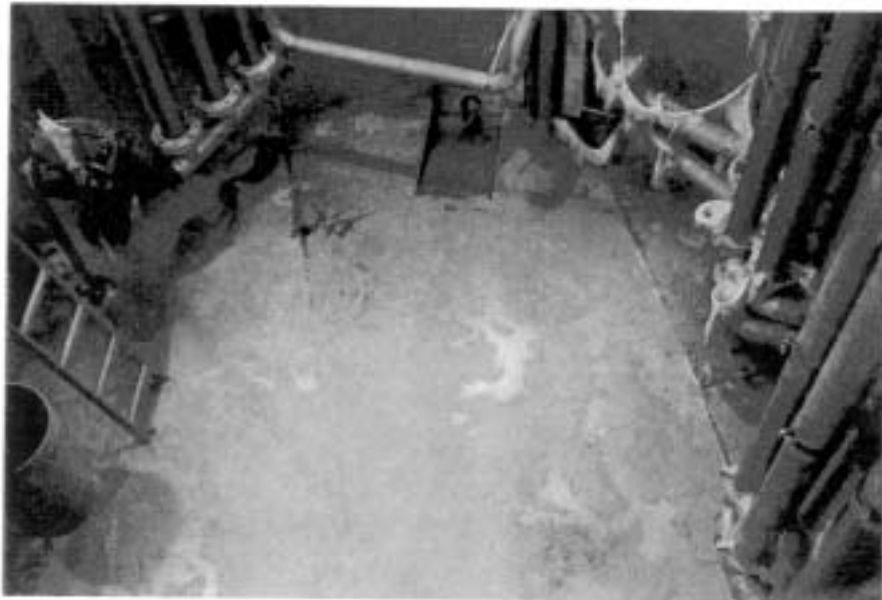
2.1 *The fill up phase*

An initial study [5] of the fill-up phase was performed in the 5 m diameter cylindrical stainless steel tank. Steam fragmented insulation (MIT NG2) from steam blasting in Karlshamn thermal power plant was used as well as insulation cut into pieces. A vertical pipe in the centre of the tank simulated a fall of 4.6 m. Figure A, shows first the start conditions of one test – large cut pieces and a water depth of 0.35 m. At a flow rate of 18.6 l/s the tank was filled up to 1.70 m of water during 26 minutes. The second picture, Figure B, shows the disintegrated insulation on the bottom when the tank was emptied.

Figure A. Cut insulation before recirculation fill-up started
(Tank diameter $D = 5.0$ m)



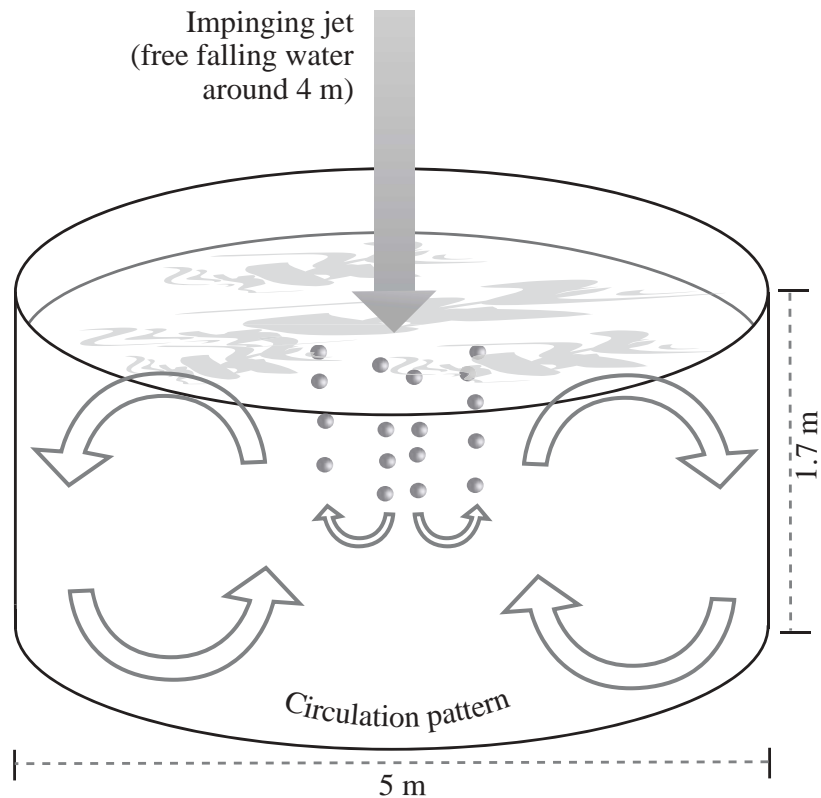
Figure B. After the test, when the tank was emptied
(Time $t = 26$ min, water depth $H = 1.7$ m when flow was stopped)



Most of the cubes had been disintegrated into tiny clusters and a lot of single fibres. Clusters fell to bottom within half an hour after the water flow was stopped but fibres remained suspended for hours.

The falling water entrains air and a circulation of the water is started, as shown on the Figure C. Pieces of the fibrous material will be moved up to the surface in the basin where the falling water is tearing apart larger pieces into smaller clusters, individual fibres and fines. This will continue as long as the plume of falling water remains.

Figure C. The falling water entrains air starting a circulation pattern, which will move fibrous insulation debris up to the surface in the basin where the falling water is tearing apart wads and clusters into fines and individual fibres
(Tank diameter $D = 5$ m, final water depth $H = 1.7$ m)



Individual fibres tend to be collected parallel to the strainer surface, i.e. perpendicular to the flow through the strainer.

The fibrous mat on the strainer will be very tight → high pressure drop.

A similar test using a plane weir, Figure D, elevated 4.6 m above pool bottom instead of a pipe created same type of disintegration. Circulation currents were weaker due to asymmetry and fragmentation was slower. But for long time operation in the circulation mode the final result of disintegration will be about the same. This is supported by results from the bed build up and head loss tests performed in the tank. (I would like to mention that in a high and narrow tank this phenomenon probably will be restrained.)

Figure D. Discharge over a horizontal edge (weir), simulating Ringhals 2



Ringhals reported [6] that half of the circulation flow will originate from plane plumes and the flow rate per unit width will be higher than tested. As the flow per surface area was representative of Ringhals 2 containment the test was expected to be very realistic and simulate conditions in the containment.

2.2 *Flat mesh strainer head loss test*

Steam-fragmented fiber insulation which had been further disintegrated by the falling plume was tested on a flat strainer 4 mm mesh and it caused very high pressure drops, see Figure E. Consequently these tests showed that it could no longer be assumed that the insulation would settle in front of the strainers and cause only minor head losses on the strainers. Also when settlements occur the finer parts will reach the strainers and the fibrous mat on the flat strainer mesh will be very tight.

Figure E. Debris layer on a flat strainer surface (mesh # 4 mm) using steam-fragmented fiber insulation



2.3 Containment pool circulation

The flow of water near the bottom of the containment during recirculation was also studied by 3D computations using CFD code Phoenix. A total flow rate of 800 kg/s was added in different ways and the same amount was withdrawn through the two existing strainers. The water was assumed to be free from impurities (such as insulation fibres). The results [7] indicated that the way water flows down in the containment towards its bottom is very important for the order of magnitude of the water velocities there. In Figure 6, Enclosure 3 results from a simulation of a uniformly distributed rain through the top of the computational domain (1.7 m above the bottom of the containment pool) are shown. Velocities on the order of several cm/s and upwards can be observed already here and according to the experimental results [5] a few cm/s is sufficient to impede sedimentation. In the calculations with concentrated water jets (water falls) flow velocities of the order 0.1 to 1 m/s were calculated in certain areas. Unfortunately a large postulated break location was close to the strainers also.

2.4 Debris bed build up on strainers and head loss increase

Head loss increase across the strainer over time is influenced by bed characteristics such as: debris sizes and distribution; porosity; compressibility; and filtration effects. To build up a debris bed with characteristics similar to actual plants, it is necessary to have not only the same flow velocities (flow per unit area) in the model as in the plants but also to have the correct concentration of material (debris) in the water that is approaching the strainer. Furthermore, for a complete simulation, it is important that the concentration over time is reduced in the same way as in an actual condensation pool. Thus, the turnover rate must be considered for each model.

Sedimentation also plays a roll in the removal of suspended debris from the suppression pool. The flow velocity profile and turbulence level of the pool together with the size, shape and density of the debris contribute to the sedimentation level. It should be noted that small amounts of fiber insulation in the water reaching the strainers combined with large concentrations of particulates (sludge) in the pool water can create a higher pressure drop than a large quantity of fiber on the strainers due to the “deep bed effect” in the latter case.

Also the sequence of the addition of the material to the test pool can be important. From e.g. the tests reported in reference 19 it was an experience that addition of particulate material (Minileit) after a fibrous bed (Rockwool) was formed created a much higher pressure drop compared to parallel addition or if the particulates were added first.

Thin layers of fibers plus particulates on a perforated plate can behave a bit unpredictable when holes close and open up, causing changes in the head loss as the strainer is loaded.

Sedimentation had earlier been studied in flume tests and a settling tank when sedimentation and “piling up” against the vertical, flat mesh strainers was considered an acceptable method. Typical settling velocities for chemical treated fibrous insulation in hot water was 3-14 cm/s and bottom transport started at approximately 5-6 cm/s for cut pieces, about 25 mm side length [22, 23].

Penetration of fibres from various fibrous insulations were studied in tests for Forsmark Sweden and TVO, Finland [18 and 24] and were reported in the “green book” [25]. Those early tests were performed with panel strainers having a hole size of 4 mm instead of 3 mm.

3. Head loss tests

3.1 *Strainer pressure drop from fibrous insulation*

The main tests for Ringhals 2 were performed in the large open tank and two types of tests were run, first a recirculation test with free falling water combined with the use of one half scale vertical wing strainer of Ringhals 1-type. This test showed that the head loss over the strainer was about the same as had been reached in earlier tests with steam fragmented fibreglass insulation at corresponding velocities.

The loading to reach a pressure drop of 2 m of water is in fact a little less (pint A) than the “pessimistic” curve F7 (Figure 1 in Attachment 1) used for computations of head loss development on BWR strainers using the computer code SILAR (version 1-4). In that code, it is assumed that the insulation material consists of fibres, pearls and fines. Flow through, growth of and pressure drop across the porous bed is computed to either Ergun’s or Leva’s equations. Details of the mathematical model are described in reference 20. Comparisons between results computed by SILAR and measurements in an experimental model of a 1:2 scale screen system (Ringhals 1) was presented in reference 1, see Figure 2 in Enclosure 3. (The upper two head loss curves in Figure 1 are for cut pieces of fibre glass nuclear grade, whereas the lower data fibre glass of same type). Figures 3 and 4 give some additional information from those early tests 1992-1993 and how it deviated from those earlier available head loss correlations, used in the original designs. The test also showed that the filter cake fell off as four discrete packages when the suction flow was reduced to zero [5].

The second type of tests in the tank was performed at dimensioning conditions for a 2 meter long segment of a horizontal full-scale strainer. Strainer surface area relative to floor area is same in model and plant. Recirculating flow was returned to the tank over a weir as described earlier.

A heat-treated mixture of rock wool and fibreglass insulation was added after a mechanical disintegration. One test run at half flow rate using half strainer area showed an increased pressure drop as a higher percentage of larger fragments are sedimenting and clusters and single fibres are building a more compact filter cake.

3.2 Combinations with particulate material

From our previous investigations for BWR plants it is also known that very thin layers with high concentration of particulate material in the debris bed can cause extremely high pressure drops. That was already reported in the OECD/NEA Workshop 1994 [1]. Thus, a situation where sedimentation of larger clusters occurs and disintegrated insulation (single fibres), in combination with particulates is suspended in the water body can cause the highest pressure drop, i.e. higher than in a “deep bed” situation, see Figure 5 in Enclosure 3 taken from reference 1, as Figure 4 E. This has later been confirmed by other tests, e.g. in US.

Work was early conducted mainly for Ringhals 1 but verification tests (scale 1:2) also were performed for the specific Barsebäck and Oskarshamn adaptations of the designs. Test of fibres in combination with particulates (calcium silicate) was part of a common programme for the three utilities Vattenfall, OKG and Sydkraft in 1992 and early 1993 before the large sacrificial and self-cleaning (wing-strainers) were installed in the five Swedish BWR's that had to be modified. Slabs of reinforced calcium silicate were water jet eroded to produce the particulates. One example from these tests is given in Figure F(a) and F(b) from reference 13 where the wing strainer was cleaned by back flushing when full suction flow was maintained from the sacrificial strainers.

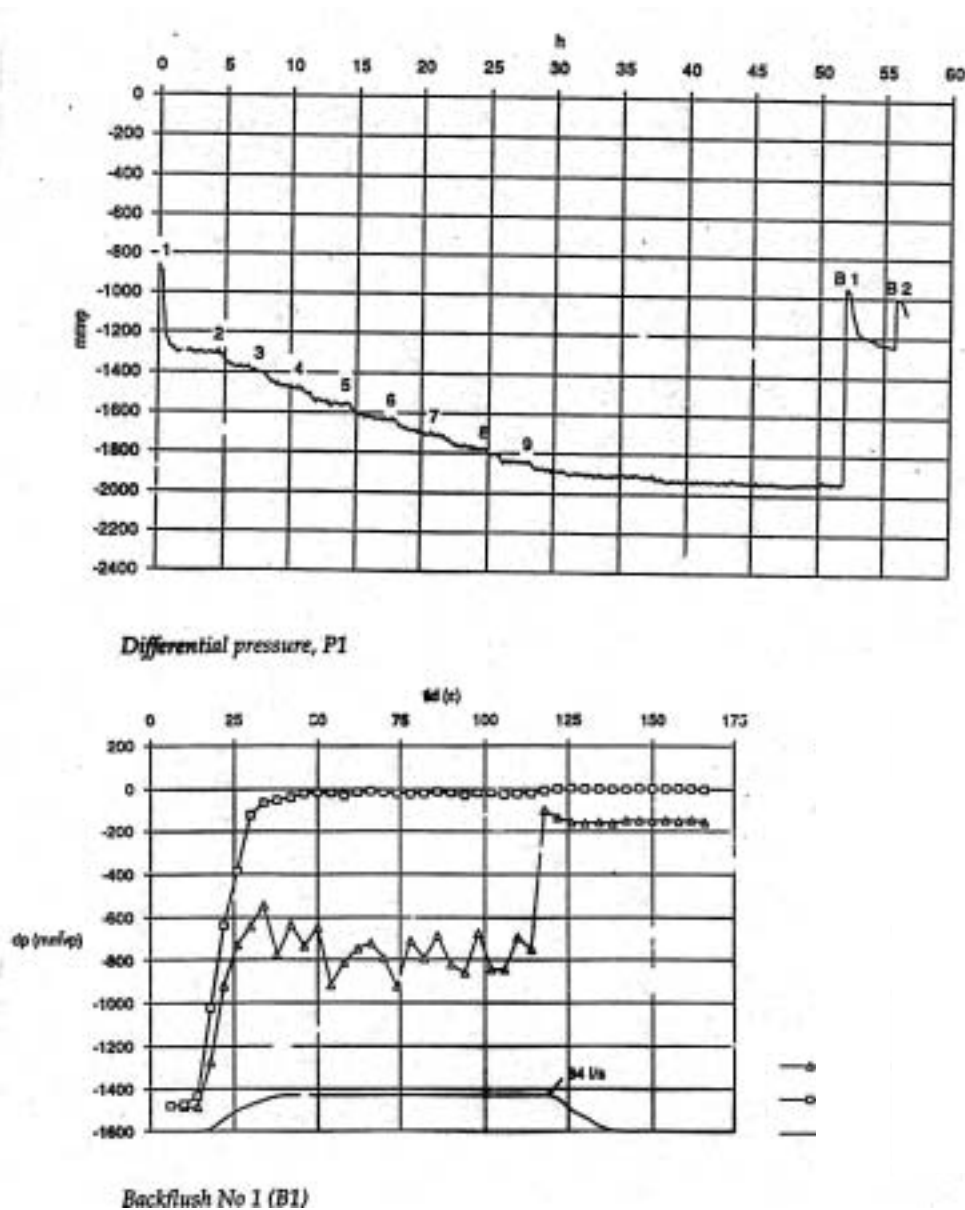
In a later test for Oskarshamn NPP Units 1 and 2 Transco fibre glass and Gullfiber 6212 was compared [21]. Aging and funmentation (hydrapulper) according to our standard procedure was again used to produce immaterial comparable to the steam fragmented insulation. A vertical wing strainer (D = 250, H = 475, hole size 2.5 mm, 20.2 percent) was used with a flow rate and tank volume was selected to give correct turn-over time compared to the pressure-suppression pool of the plant. The tests showed that head loss for Transco was close to the earlier used F4-curve in Figure 1. Gullfiber had a considerably higher head loss.

As part of the Proof of Principle (POP) testing programme on three designs a series of tests with one large wing-strainer (0.3 m diameter), located either vertically or horizontally, were performed in 1996 as a joint effort between ABB Atom AB, ABB Combustion Engineering and Vattenfall Utveckling AB, at the Vattenfall Utveckling test facility in Älvkarleby, Sweden.

Figure F(a). Ringhals 1 strainer system some time after cleaning of the wing strainer when a further build up of debris on the wing strainer has occurred



Figure F(b). Intake strainers for ECCS. Pressures recorded at model tests, scale 1:2. Test 4 in phase 2



This “passive, self-cleaning wing strainer” was tested with sludge, insulation and recipe material consistent with that requested by the BWR Owner’s Group (BWROG). The purpose of these tests was to record their operability under conditions consistent with tests of other strainers for US BWRs. The sludge, as requested, consisted of Grade 2008 and 9101-N-40 black iron oxide, presoaked according to a procedure.

Different loadings with different ratios particulate material and fibres were tested and can be used for more general head loss correlations. Debris per unit area for a certain approach velocity was simulated as the main parameter and the strainer was operated under specified flow rates in order to collect the debris on the strainer surface. The strainer performance was recorded for each debris type and combination tested. Some tests were run until all particulate material was collected on the strainer

– the black water was cleaned and it was checked by taking water samples. Some results are given in Figures G, H and I(a) and the photo in Figure I(b) taken from reference 14.

It was concluded that the test results can be used in the design of passive, self-cleaning wing strainers for conditions in the Reference Plant.

These tests also demonstrated that self-cleaning first occurred at zero flow. On horizontal strainers, fins are proposed to be located on the lower half of the strainer, preferably at 4:30 and 7:30 positions. This arrangement would allow for cleaning of one-quarter of the system. It is not necessary, and thus not the intention to clean the whole strainer area using this passive, self-cleaning system. Sacrificial areas on the strainer act to clean the pool water and bind the insulation on the strainers.

In the additional testing specified for Cooper NPP, Nebraska results showed that the method to calculate head losses presented in Utility Resolution Guidance (October 1996) gave considerably lower pressure drops than measured in the test [15].

Figure G. Passive self-cleaning wing strainer, altered wing position, segmented length (600, 600, 600 mm)

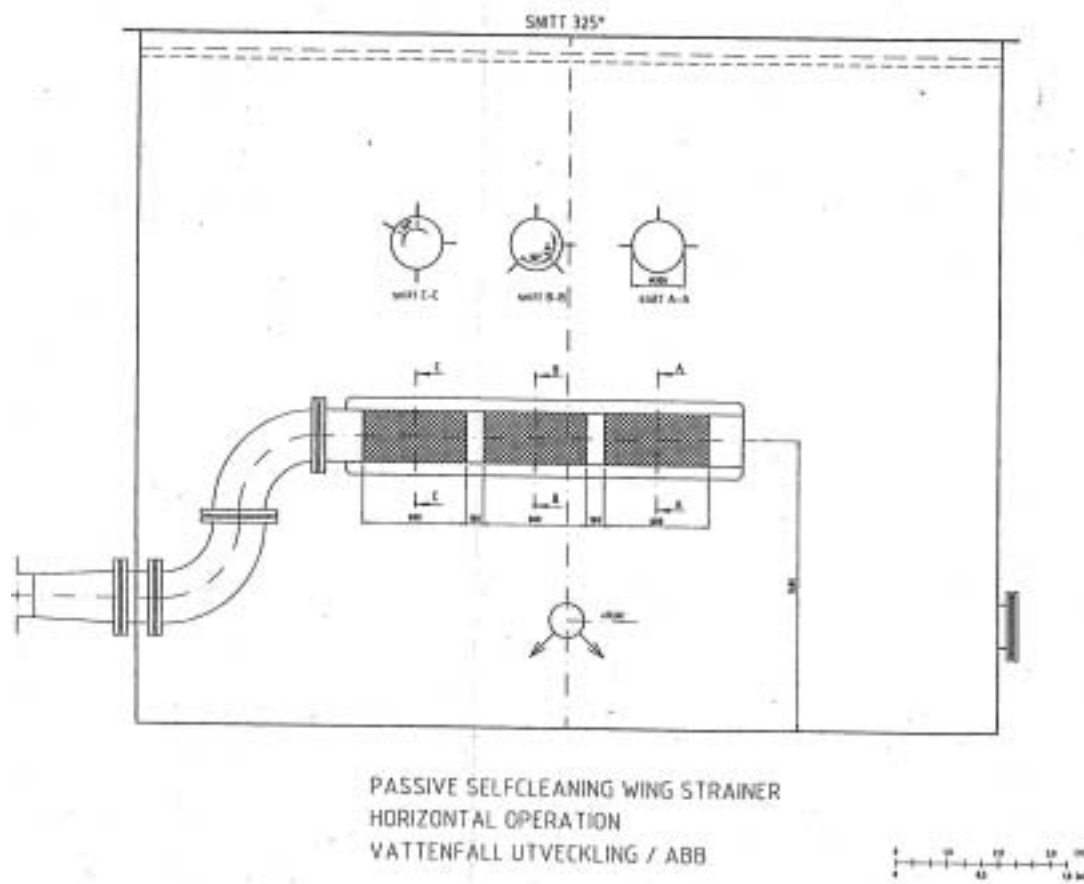


Figure H. Test W42H – Flow rate and pressure drop as a function of time

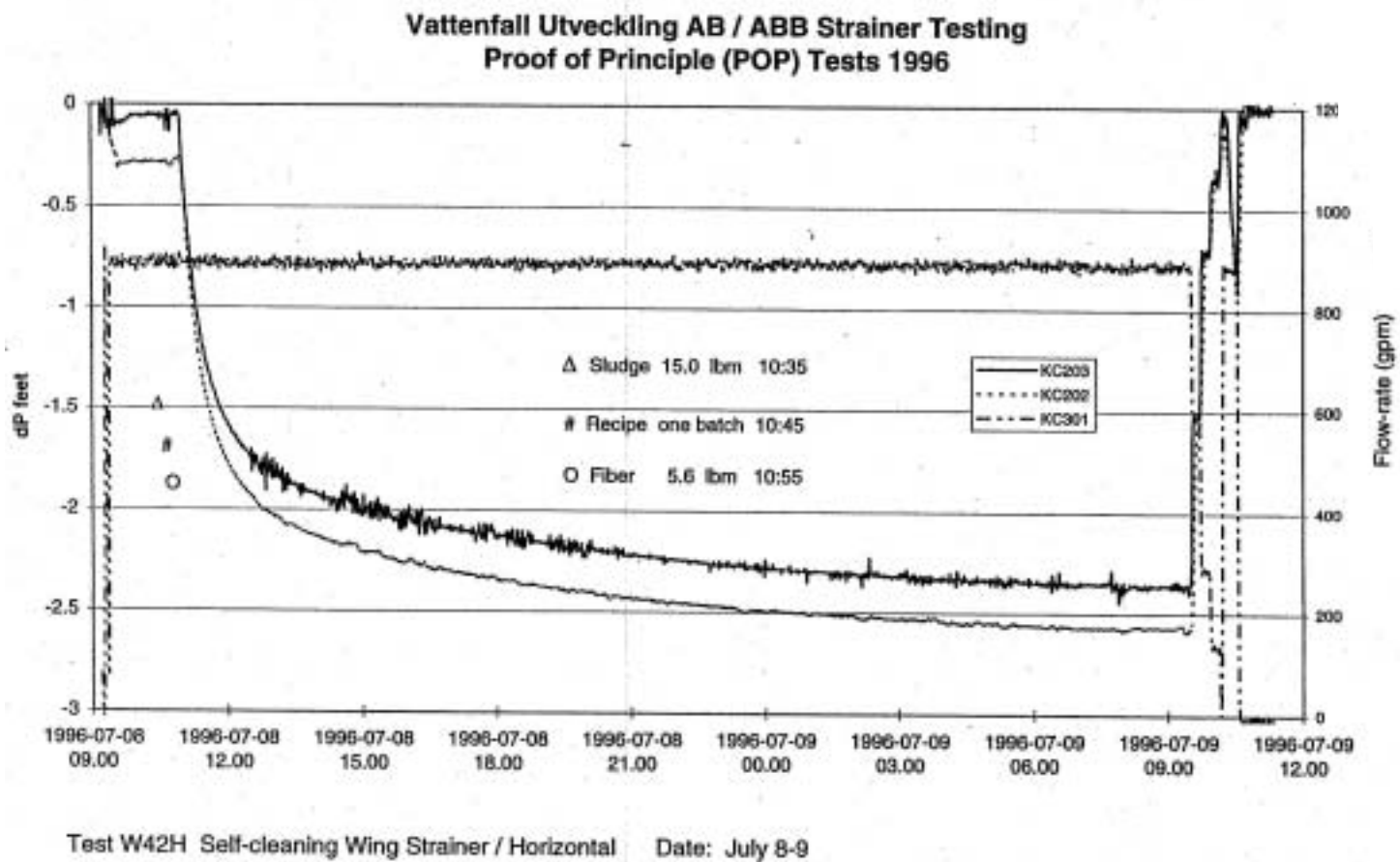
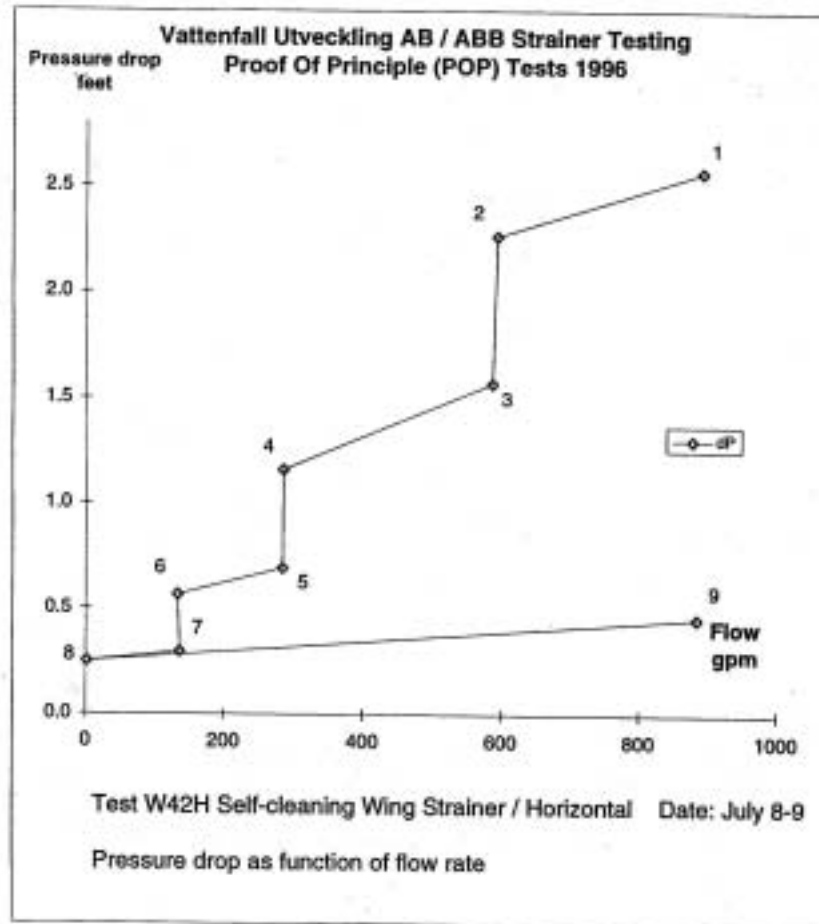
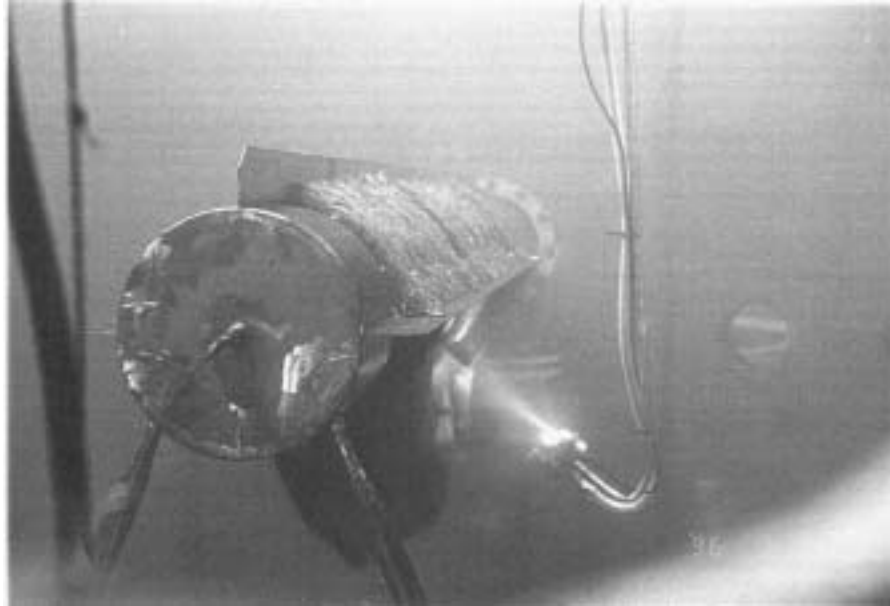


Figure I(a). Test W42H – Pressure drop as a function of flow rate



Point	Time	Flow-rate (%)	dP (ft)
1	09.29	100	2.57
2	09.33	67	2.27
3	09.42	66	1.57
4	09.46	32	1.16
5	09.55	32	0.69
6	09.58	15	0.57
7	10.08	15	0.30
8	10.10	0	0.25
9	10.24	99	0.46

**Figure I(b). POP test W62H
Cake is falling off after loading glass of fiber insulation (1.3 kg/m²)
sludge (3.6 kg/m²) recipe when flow rate is reduced to zero**



3.3 Possible effects of oil or carbon powder

These tests for Ringhals 2 were performed in a small one-dimensional model using water with temperature and chemistry representative for conditions at a LOCA. A filter bed of rock wool and fibreglass that had been heat-treated and disintegrated was formed before carbon or oil was added. No extra pressure drop was found for the small but typical concentrations that were tested [10].

3.4 Pressure drop increase during long time recirculation

Long time recirculation tests were carried out at Siemens laboratories in Erlangen as a part of the Steam Generator Replacement Project for Ringhals Unit 2. From these tests during post LOCA representative temperature and chemistry it was known that the pressure drop increased after 120 hours and more. There was no limit to the pressure drop increase.

The pressure drop increase over long time was explained by four factors:

1. The chemicals e.g. NaOH in PWR Post LOCA water is soaking SiO₂ from the glass fibres. Thus the kinematic viscosity of the water increases.
2. The glass fibres are being less resilient as a result of the chemical attack and therefore the filter is being packed denser.
3. Impurities captured by the filter migrate from upstream positions to downstream positions. The same is valid for fibres, when dislocated they always moves downstream, which result in a less porous filter.
4. The increasing pressure drop due to 1, 2 and 3 will create an increased load over the filter bed and this will cause further compression which will then give even higher pressure drop, etc.

3.5 Behaviour of reflective metallic insulation (RMI)

Same type of large tank tests for Ringhals 2 [8] performed with RMI and combinations of RMI and fibrous insulation showed that the RMI will stay at tank bottom and will not be transported to the strainers as the approach velocities are very low for this design. The fibrous insulation will have a minor effect on the movement of RMI and only a few very small metallic pieces were observed in the filter cake. This means that no extra head loss is likely to occur due to a combination of RMI and fibres. The material used was RMI from the high pressure blast tests at Karlstein, Germany.

The transport tests in a flume [8] showed that velocities above 0.09 m/s were needed for moving that material (7 classes). Approach velocities to the vertical strainers lower than 0.04 m/s never could hold any of the blasted pieces, and a more typical “holding value” was 0.1 m/s. Settling tests in a tank showed that all fragmented RMI (all classes) settled at a speed above 0.1 m/s. Hyvärinen (STUK) found sedimentation velocities about 0.04 to 0.08 m/s for the statlest descent mode of flat pieces [26].

The strainer loading and head loss tests for Ringhals 2 had very low approach velocities (0.01-0.02 m/s) to the strainer, but the tank was also stirred up by the falling water.

4. Test of self-cleaning of the wing strainer

4.1 Ringhals 2 design

The self-cleaning qualities of the wing strainer at Ringhals 2 were verified at full scale using one quadrant of the full-scale strainer. Also in this test serie water chemistry after a LOCA was simulated, but all the five tests were all run at room temperature. Two different mixtures of fibreglass and rock wool were tested and all tests were made for very thin layers with a low pressure drop. Self-cleaning was achieved when layer thickness was more than 12-25 mm. A sequence from the self-cleaning at zero flow is presented in the four photos on Figure J.

Figure J. Self-cleaning occur at PWR plant Ringhals 2 [9b]



4.2 BWR design

In the development work for BWR large sacrificial and self-cleaning strainers it was in numerous tests demonstrated that self-cleaning occur on the wing wtrainer [1, 3, 13, 14, 15 and 16]. Two examples of self-cleaning are already presented in Figures F and I(b) from tests with vertical wing strainer (Ringhals 1) and a horizontal one (from the POP-tests, [16]).

5. Gas accumulation prevention in the system

5.1 Possible air ingestion from vortices

Possible air ingestion caused by air pulling vortices was studied using a reduced scale 1:3.5 hydraulic model [11]. An appropriate area of the Ringhals 2 containment with major obstacles was included in the model.

This relatively large scale was selected for the test due to possible scale effects in modelling vortices. Experiences from similar testing were incorporated, especially those from extensive US studies for NRC concerning reactor containment recirculation sumps of the present PWR type. The sensitivity to extra distortions of the approach flow profiles was also tested as well as exaggerated flow rates (above correct Froude number).

At correct Froude number simulation surface dimples (vortex type 2, [27]) occurred frequently and in some cases also vortex type 3 occurred. At full scale (plant) velocities dye cores (type 3) occurred more frequently. At double plant velocities type 5 vortices (pulling air bubbles) were observed occasionally, before the main current “washed away” the vortex rather than promoted its build up. At extreme low water levels that circulation is stopped by the fins and only very local disturbances were noticed. Pictures from those tests are shown in Figure 7, Enclosure 3.

Main conclusions were that the proposed design of the new strainer system using long horizontal cylindrical strainers in combination with vertical self-cleaning strainers of Ringhals 1-type was found to perform satisfactorily for all operating conditions considered. The likeness of air ingestion from vortices would be small.

5.2 Boiling in the debris layer

As the water temperature could be close to 100°C at recirculation and Regulatory Guide 1.1 does not allow the use of containment overpressure in the NPSH calculations, the maximum head loss over the strainers must not be higher than the water column above the strainers. Otherwise there will be boiling in the debris layer. The Ringhals 2 strainers are designed to avoid boiling in the debris layer rather than investigating the effects of boiling, i.e. pressure drop over strainer is kept low and measured by the dp-system installed. The design of the recirculation water source i.e. the refuelling water storage tank is also of great importance.

6. Bi-stable wing strainer

This is a new, patented, self-cleaning strainer system, which can be cleaned without either changing the suction flow or back flushing.

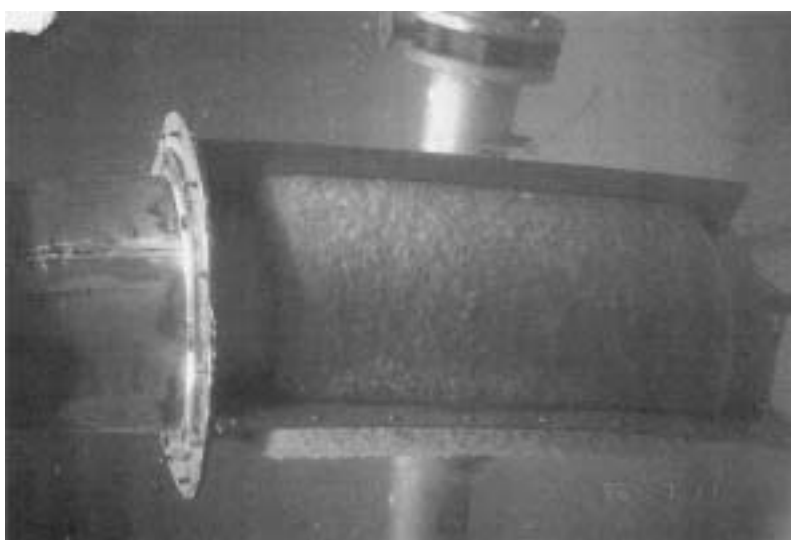
In this design a flexible bi-stable wall is installed inside the strainer. The free edge can be closed against either of two opposing arch-shaped walls in the strainer, or in the pipe. As the filter becomes clogged, the pressure difference between one side of strainer and the other increases. When a certain pressure difference is obtained, the bi-stable wall switches from one side of the strainer to the other. The pressure pulse, in combination with the fins, cleans one side, making it ready for when the other side is clogged and the next switch will take place. This strainer is easy to install because it can be mounted on an existing flange.

The principle of the bi-stable strainer (model data $D = 375$, $H = 600$ mm) was successfully demonstrated during the POP-tests [16, 17]. Figures K and L are from those tests.

Figure K. Bi-stable strainer during installation for testing at Vattenfall Utveckling AB, Älvkarleby Laboratory



Figure L. Bi-stable strainer during testing



It was also [16] concluded that further development work and testing will be required before the bi-stable strainer is ready to be installed in a plant. The flow rate and NPSH requirements will determine the actual size and spring force. However, the estimated size of the bi-stable strainer, based on a flow rate of 10 000 gpm (630 litres/s), is approximately 4 ft (1.2 m) in height and 2-2.5 ft (0.6-0.75 m) in diameter with 23% porosity.

Later it has been discussed to have the bi-stable wing strainer as a further back-up in the “Swedish robust solution”.

7. Plant modification at Ringhals 2. Large sacrificial and self-cleaning strainers – a robust system

7.1 Basic design requirements and defence in depth philosophy

The basic technical requirements for the ECCS strainers in the USA plants are essentially the same as for the Swedish plants. The strainers shall have capacity to separate from the recirculation flow the amount of debris that is determined by reasonably conservative plant specific analysis. Other basic design criteria such as low internal pressure drop and structural strength are also similar in Sweden and the USA.

The concept chosen for Ringhals 2 is based on a defence in depth philosophy and comprises:

- large passive strainer area;
- differential pressure measurement over the strainer;
- possibility to clean a part of the strainer area.

The large strainer area means that the thickness of the layer of impurities is reduced. It has been demonstrated that debris spreads evenly over the strainer area. The pressure drop over a layer of debris is a function of the thickness of the layer and the water velocity. Therefore the enlargement of the strainer area is the most straightforward way of increasing the strainer capacity. In strainer area should be large enough to. In the short term recirculation, strainer area should be large enough to capture all impurities within the limits of the maximum allowed pressure drop. By using a differential pressure measurement system the operators can get on line indication of differential pressure development.

In the long time recirculation mode, i.e. more than 100 h, the pressure drop is expected to increase. Small dislocations of particles and fibres are packing the debris layer denser on the strainer surface. Therefore a part of the strainer area should be possible to clean. With the chosen strainer design it is possible to clean a large enough area only by turning off the flow to normally no backflush system is needed. Should active backflushing system be preferred, such a concept can be added or a bi-stable strainer can be included.

7.2 General information about Ringhals 2

Ringhals 2 is a 3-loop Westinghouse PWR in operation since 1974. The architect engineer was Gibbs & Hill Inc. There are two 100% emergency core cooling (ECCS) and four 50% Containment Spray (CS) trains. The ECCS flow is 2*240 l/s and the CS flow is 4*125 l/s. In the original design the recirculation trains were taking suction from two cage type sump screens each having an area of 7 m². The screens were designed in conformance with NRC Regulatory Guide 1.82, published in June 1974.

At steam generator replacement in 1989 the steam generators were insulated with nuclear grade fibreglass insulation. Insulation tests were performed by Vattenfall and the insulation material supplier. It was found that the capacity of the strainers was insufficient. A new design was developed resulting in an installation of a wire fence type pre-strainers. In addition, an overflow was added to the original screens. This design was based on sinking debris.

The Ringhals 2 containment contains the following types and quantities of insulation materials.

Metal reflective foils	10 720 m ²	Polyurethane	4 m ³
Fiberglass	136 m ³	Reinforced cement (Linpac)	2 m ³
Mineral wool	85 m ³		

7.3 Design review of Ringhals 2 recirculation function in 1993

In light of the knowledge gained as a result of the Barsebäck strainer incident a design review of the Ringhals PWR's recirculation function was made in 1993. As described above, tests and CFD calculations performed at Älvkarleby Laboratory with new and aged insulation material in a containment model showed that insulation debris did not sediment at the bottom of containment during the recirculation phase as previously anticipated, mainly due to the stirring effect of the recirculation water falling down into the water pool. In addition the falling water broke up the insulation debris into finer particles, which would create a higher pressure drop over the strainers than previously anticipated. Thus the design review showed a necessity to improve the recirculation function. With the experience gained during the work with the strainers for the Swedish BWR's, namely the necessity to handle a variation of insulation materials and impurities, it was decided to improve the strainers rather than change insulation material.

7.4 Design basis

The Ringhals 2 requirements on a solution of the ECCS and CS problems were the following:

- The plant shall fulfil the FSAR requirement namely that the strainers shall be able to handle the effects of all the limiting events for the plant plus a single failure.
- The strainer should be able to handle the various combinations of debris.
- Man-machine aspects are important. The operating instructions should be easy and also give the operator's sufficient information and control over the recirculation function.
- The strainers should have a simple and robust design.
- The solution should as far as possible be verified by tests.
- The strainers should be possible to install during a normal refuelling shutdown.

7.5 Limiting events, physical separation and single failure, design- and service loadings

The FSAR safety analyses and probabilistic risk assessment showed that the two limiting events when strainers would be used are large and medium size loss of coolant accidents (LOCA).

The two sump cages were replaced by four pipe strainers one for each ECCS and one for each 2*50% CS train. The capacity of one ECCS plus one CS strainer should be sufficient to handle all debris even if it is assumed that the CS flow may be interrupted depending on the type of initiating event. Thus the design can handle a single active failure in one of the safety trains.

The strainers are designed to sustain the following loads:

Design pressure:	50 kPA (external and internal pressure).
Design temperature:	149°C without pressure loading. 100°C with pressure loading.
Seismic loads:	No. According to the plant limiting events, LOCA and earthquake do not occur in combination as the reactor coolant pressure boundary is seismically qualified.
Missiles and jets:	The strainers are not designed for direct missiles as they are only used after LOCA's and the complete reactor coolant pressure boundary is inside the missile barriers. They are however protected against smaller objects.

7.6 Strainer capacity for fibers, metal foils and impurities

Vattenfall's tests reported at the OECD/NEA Workshop in Stockholm showed that nuclear grade fiber insulation without jacketing could be fragmented at a distance of 35 pipe diameters from a pipe break. As Ringhals 2 has a limited amount of pipe restraints to keep the jet in a fixed position, the strainer capacity is based on fragmentation of all the insulation material inside one complete loop (missile barrier) plus some insulation material, on connecting piping outside the missile barrier such as main steam piping, in total 45 m³ of fiber glass and 12 m³ of mineral wool. In addition metal reflective insulation material as well as other debris is considered. To gain sufficient knowledge for this design review, water and steam jet tests of metal reflective insulation as well as transportation and head loss tests were performed.

Among the debris studied could be mentioned lubrication oil for the reactor coolant pumps and carbon from ventilation filters. The special qualities of PWR water resulting from the addition of boric acid and tri-sodium phosphate was also studied.

The head loss characteristics used for the combined effect of debris from mineral wool, fiber glass, metal foils, oil and other impurities was at that time expressed as:

$$\Delta p = 5\,500 * v^{1.5} * t^{1.5} * \nu / \nu_{20} \text{ mvp} \quad (\text{m.o.w})$$

where: v = velocity in m/s,

t = debris thickness in meters with as installed density,

ν = temperature dependent water viscosity (Δp is in metres of water pillar).

The design was based on the empirical experience that 2/3 of the insulation reaches the pool. Due to the stirring effect of the recirculation water falling down into the pool no sedimentation is assumed.

Tests of metal reflective insulation subjected to steam and water jets were performed in Karlstein. Steam jet tests of fiber insulation were performed in Karlshamn and Studsvik. The tests showed destruction of the insulation material at distances of 15 to 35 pipe diameters from the break. The fragmented material was used for head loss tests.

7.7 *Cleaning of the wing strainer*

Due to the difficulties of determining the strainer head loss for all combinations of debris during a long recirculation period and to make the design robust it was decided to equip a small part of the strainers with cleaning possibilities. Previous testing of the new Swedish BWR strainer systems supplemented by additional tests of Ringhals 2 strainers at Älvkarleby showed that wing strainers will be cleaned automatically when recirculation is reduced. Thus cleaning of Ringhals 2 strainers is achieved without backflushing or use of moving parts, see also sections 4.1 and 4.2 above.

7.8 *Limiting factors for the recirculation function*

In most cases the main limiting factors for the BWR recirculation function are the head losses over the suction strainers and the recirculation water level and temperature, which can create low available NPSH for the ECCS and CS pumps. In addition the recirculation pool water level and pool dynamic effects can create air ingestion into the pump suction – compare section 5.1 above. For Ringhals 2 the limiting factor for the recirculation function is the water level in the containment pool or rather the water level above the strainer debris layer. As the water temperature could be close to 100°C at recirculation and regulatory guide 1.1 does not allow the use of containment overpressure in the NPSH calculations the maximum head loss over the strainers must not be higher than the water column above the strainers otherwise there will be boiling in the debris layer. The Ringhals 2 strainers are designed to avoid boiling in the debris layer rather than investigating the effects of boiling.

The design of the recirculation water source i.e. the refuelling water storage tank is of great importance. The maximum allowed refuelling water temperature, maximum 50°C for the Ringhals PWR's, is a main contributor to the maximum recirculation water temperature and the volume of water gives the containment water pool level during recirculation. Another important parameter for the water level is the amount of water trapped in piping system, in compartments and on walls and floors. In Ringhals 2 the minimum water level is 1.6 m above floor level.

7.9 *Differential pressure measurement system*

A new system for measurement of the strainer differential pressure was tested for various containment water levels and pressure.

In order to give the operators information of the strainer status during recirculation the strainers were equipped with head loss measurement over the debris layer with indication and high pressure drop alarm in the control room. The head loss sensor is of a new patented design enabling a location of the sensor and transmitter in the reactor containment and avoiding sensitive capillaries.

8. Design of the strainer system – the robust solution

The solution is based on the same principle design as the strainers installed in the five Swedish BWR's that were stopped after the Barsebäck incident 1992. It was presented at the OECD/NEA Workshop on the Barsebäck Strainer Incident in Stockholm, 26-27 January 1994 [1], see Figure M.

The new robust strainer system (protected by patents) consists of a number of sacrificial cylindrical strainers connected in parallel to a common manifold pipe. A separate cylindrical strainer is attached to the suction line before it leaves the pool through the containment wall. Fins along the cylindrical, vertical strainer divide the fibre mat. When the strainer flow is reduced, fins split the debris into sections as the fibrous bed expands. The material falls off and remains on the pool bottom without requiring back-wash flow, see the four photos in Figure J.

The horizontal main strainers are shown in Enclosure 1. The area of the main ECCS strainers is $2 \times 50 \text{ m}^2$ and the area of the CS strainers is $2 \times 40 \text{ m}^2$. The self-cleaning strainers are shown in Enclosure 2. Each strainer has an area of about 1.8 m^2 . The strainer is protected from falling objects as shown in Figure O.

The hole in the strainer were chosen to have a diameter of 3 mm. Test at Älvkarleby [18] shows that this hole size together with a low approaching water velocity give a very small amount of impurities penetrating the strainers. This is required in order not to jeopardize the ECCS function but is not required for the CS function, which has been shown to be able to handle large amounts of debris.

Two photos from the installation at Ringhals 2 are presented in Figures N and O. The fins of the vertical, partly tapered cylindrical wing strainer can be seen. The sacrificial strainers are protected by a horizontal roof.

Figure M. Modified sump screens in Ringhals 2

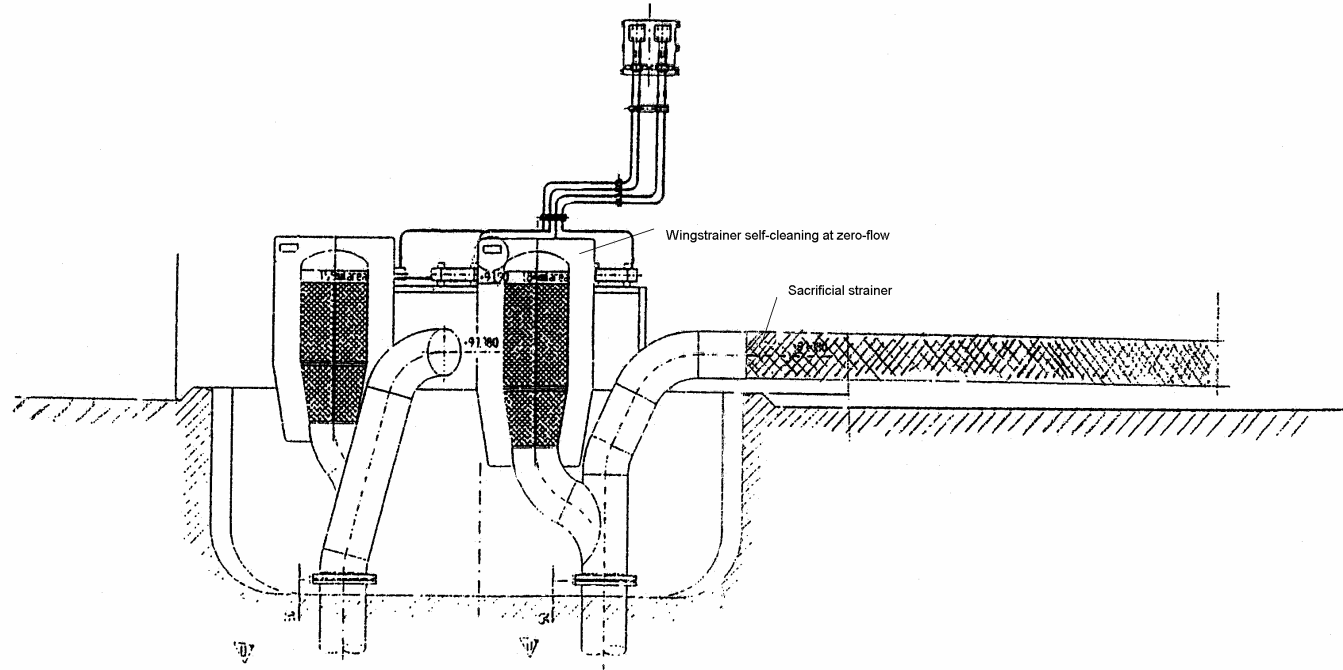


Figure N. Self-cleaning wing strainer at Ringhals 2 NPP



Figure O. The horizontal sacrificial strainers at Ringhals 2



6. Concluding remarks

The large sacrificial and self-cleaning strainers, often named the “Robust Swedish Solution” is a system that so far has proved to be able to handle “all bounding conditions” (the envelope). Although these systems are large, they are easily installed. The strainers are pre-fabricated and easy to transport into the containment. The new strainers at Ringhals 2 were installed in 5 days during the refuelling outage in 1995.

A short summary of the presentation (OH viewgraph picture) is given in Figure 8, Enclosure 3.

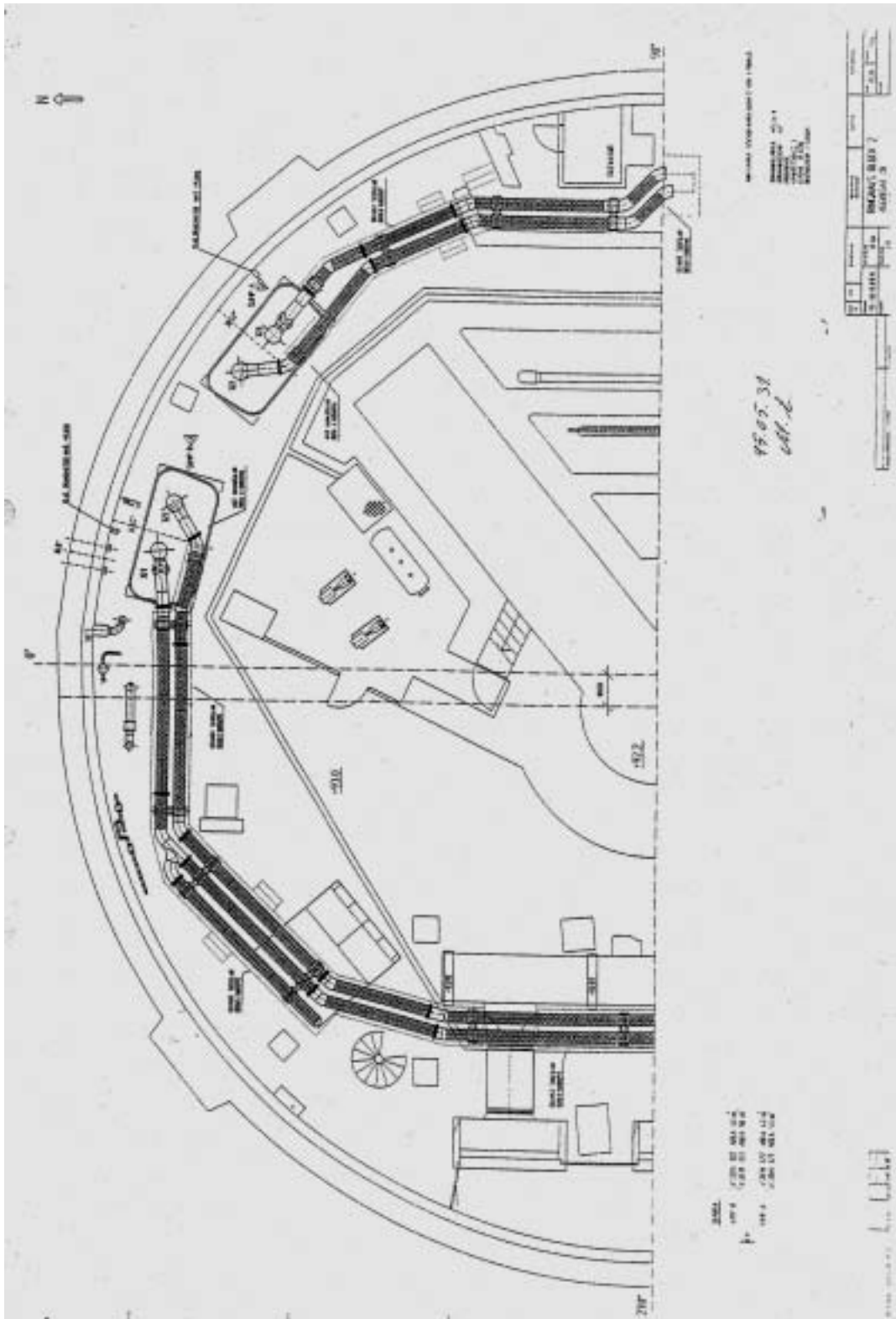
REFERENCES

- [1] Henriksson, M. (1994), "Research and experiment in support of the back-fitting measures at the Swedish BWR's", OECD/NEA Workshop on the Barsebäck Strainer Incident, Stockholm, 26-27 January 1994, Paris.
- [2] Bjerke, L.-E., "Ringhals 1 – Permanent solution", Ibid.
- [3a] Bjerke, L.-E., Henriksson M. (1999), "Modification of sump screens in Ringhals 2", International Working Group on Sump Screen Clogging, Stockholm, 10-11 May 1999.
- [3b] Henriksson M., "The Ringhals 2 Experience – The discovery of a strong debris disintegration mechanism", PWR Sump Performance Workshop, 30-31 July 2002, Baltimore, Maryland.
- [4a] Bjerke, L.-E., (1996), "Replacing strainers? – Look at plant design – basis events first", Nuclear Engineering International, February 1996.
- [4b] Trybom, J., "Upgrading strainers at Ringhals 2", Ibid.
- [4c] Henriksson, M., Schön, S. (1996), "New strainers build on Swedish Experience", Nuclear Engineering International, February.
- [5] Karlsson, R., Persson, J., Johansson, B., "Ringhals 2 – Prov avseende sedimentering, resuspension och transport av glasfiberisolering i reaktorinneslutningen" ("Tests of sedimentation, re-suspension and transport of fibrous insulation in the reactor containment"), Vattenfall Utveckling AB, report VU-S 94:B3 (restricted).
- [6] Myhrberg, B., "Uppskattning av vattenflöde till reaktorinneslutningens bottenplan vid en recirkulationssituation" ("Estimated flow rates to containment bottom in recirculation mode"), report Ringhals, OT/RBT Nr 0339/94, 97-03-21.
- [7] Alavyoon, F., "Ringhals – Beräkningar av strömningen i reaktorinneslutning med hjälp av beräkningsprogrammet PHOENICS" ("Flow pattern in the containment calculated by CFD code PHOENICS"), Vattenfall Utveckling AB, report VU-S 94:B 1994-05-05 (restricted).
- [8] Persson, J., "Ringhals 2 – Prov avseende sedimentering, resuspension och transport av metallisk isolering" ("Tests of sedimentation, resuspension and transport of metallic reflective insulation"), Vattenfall Utveckling AB, report VU-S 94:B13, 1994-06-17 (restricted).
- [9] Persson, J. "Ringhals 2. Funktion hos recirkulationssilar. Prov 3. Tryckfall vid dimensionerande förhållanden" ("Pressure drop at design conditions"), Vattenfall Utveckling AB, report US 95:9, 1995-05-14 Rev. 1 (restricted).
- [9b] Persson J., "Ringhals 2, Funktion hos recirkulationssilar. Prov 1, gräns för självrengöring. Vattenfall Utveckling AB", report US 95:8.

- [10] Persson, J., “Ringhals 2. Funktion hos recirkulationssilar. Prov 2. Inverkan av kolpulver och smörjolja” (“Influence of oil carbon powder on pressure drop”), Vattenfall Utveckling AB, report US 95:10, 1995-05-15 Rev. 2 (restricted).
- [11] Henriksson, M., Persson, J., “Ringhals 2 – Hydraulic model test of reactor containment recirculation sump with a new strainer system”, Vattenfall Utveckling AB, report US 95:11, 1995-05-14 Rev. 1 (restricted).
- [12] Henriksson, M., “Modification of sump screens in Ringhals 2. Comments on test performed”, OECD/NEA International Working Group Meeting in Washington DC, 28-29 October 1999.
- [13] Henriksson, M., Johanson, B., “Ringhals 1 – Head loss and back flush testing”, Vattenfall Utveckling AB, report VU-S 94:B9.
- [14] Henriksson, M., “Proof-Principle Strainer Testing – Passive, Self-cleaning Wing Design”, Vattenfall Utveckling AB, report UX 96:F4.
- [15] Henriksson, M., “Strainer testing additional testing for Cooper”, Vattenfall Utveckling AB, report UX 96:8.
- [16] Schön, S., “Vattenfall/ABB Proof-of-Principle Strainer Testing. Panel Strainer; Passive Self-cleaning Strainers; Bi-stable Strainer”, Report PAA 96-159.
- [17] Henriksson, M., “Proof-of-Principle Strainer Testing – Bi-stable Design”, Vattenfall Utveckling AB, report UX 96:F5.
- [18] Tinoco, H., “TVO 182-323-silens genomsläpplighet” (Penetration of fibres through strainers), Vattenfall Utveckling AB, report VU-S 93:B11.
- [19] Wiklund, B., Svensson L., “Oskarhamn 3, Silprov med Minileit” (Head loss tests using Minileit and Rockwool), Vattenfall Utveckling AB, report VU-S93:B22.
- [20] Persson, B., “Nedtransport och sedimentation av silmaterial samt dess uppbyggnad av tryckfall på sugsilarna”, OKG 1992, (Restricted, in Swedish).
- [21] Henriksson, M., “Oskarshamn 1-2. Återisolering med gullfiber. Jämförande silprov” (Comparisons between Transco and Gullfiber 6212 in test using a vertical wing strainer), Vattenfall Utveckling AB, Report UX 96:F1.
- [22] Karlsson, R., “Ringhals 2. Modellförsök avseende gränshastighet för transport av isolering samt funktion hos försil”, Vattenfall Älvkarlebylaboratoriet, Report UL-89:70 (In Swedish, restricted).
- [23] Karlsson, R., “Ringhals 2 – Modellförsök avseende sjunkhastighet och gränshastighet för transport av kemikaliebehandlad isolering”, Vattenfall Utveckling AB, Report VU-S 92:33 (In Swedish, restricted).
- [24] Wilhelmsson, G., Tinoco, H., “Forsmark 1 och 2 – silarsystem 322/323” (Test on Panel type strainers), Vattenfall Utveckling AB, Report VU-S 93:38 (In Swedish, restricted).

- [25] NEA (1996), “Knowledge Base for Emergency Core Cooling System Recirculation Reliability”, OECD/NEA/CSNI/R(95)11, February, Paris.
- [26] Hyvärinen, J., Hongisto, O. (1994), “Metallic insulation transport and strainer clogging tests”, STUK-YTO-TR73, Helsinki.
- [27] Serkiz, A.W. (1985), “Containment emergency sump performance”, US Nuclear Regulatory Commission, NUREG-0897, Rev. 1, October 1985.

Enclosure 1



Enclosure 3

Figure 1. Ringhals 1 Thermal insulation tests

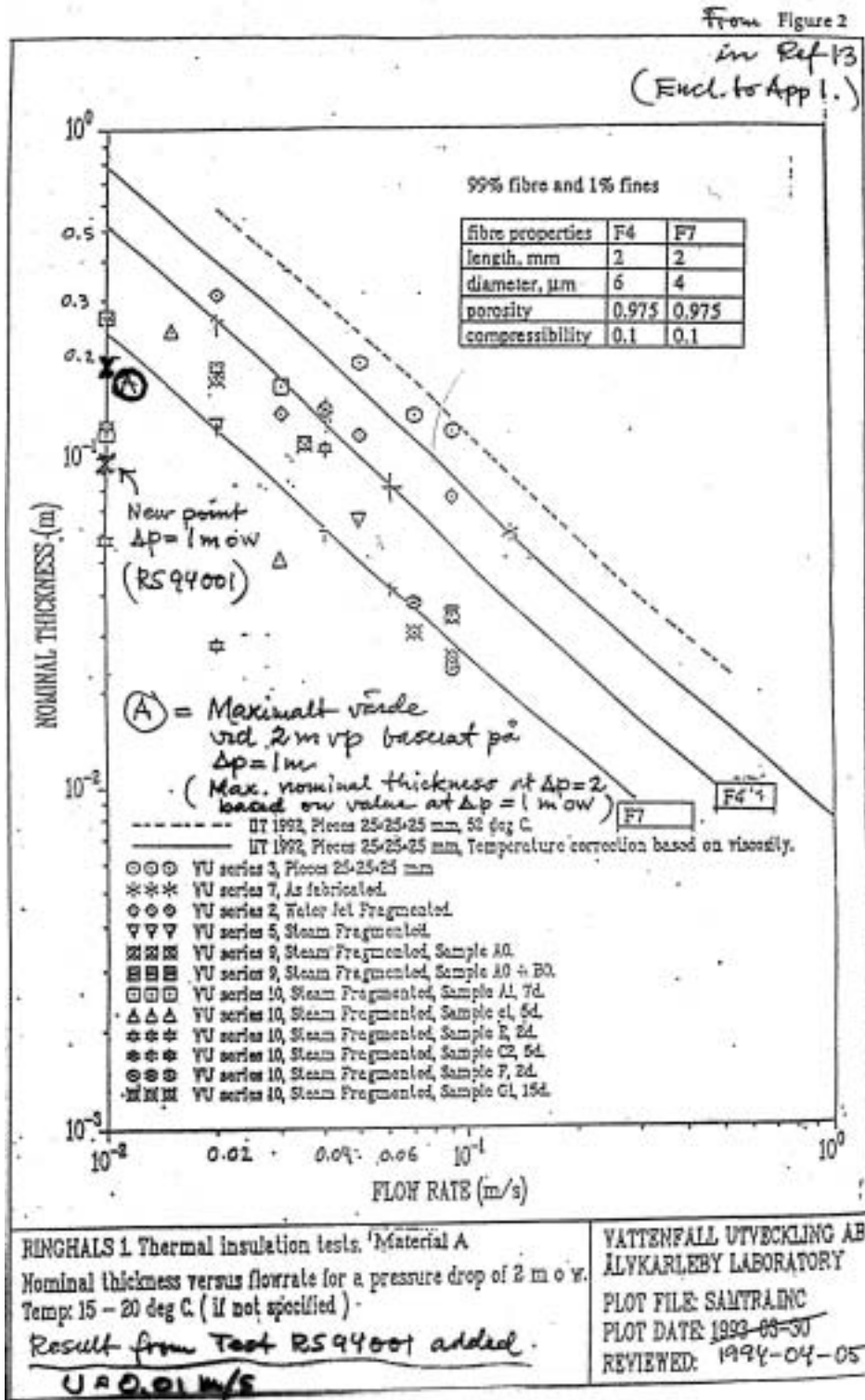


Figure 2. Ringhals 2. Thermal insulation tests

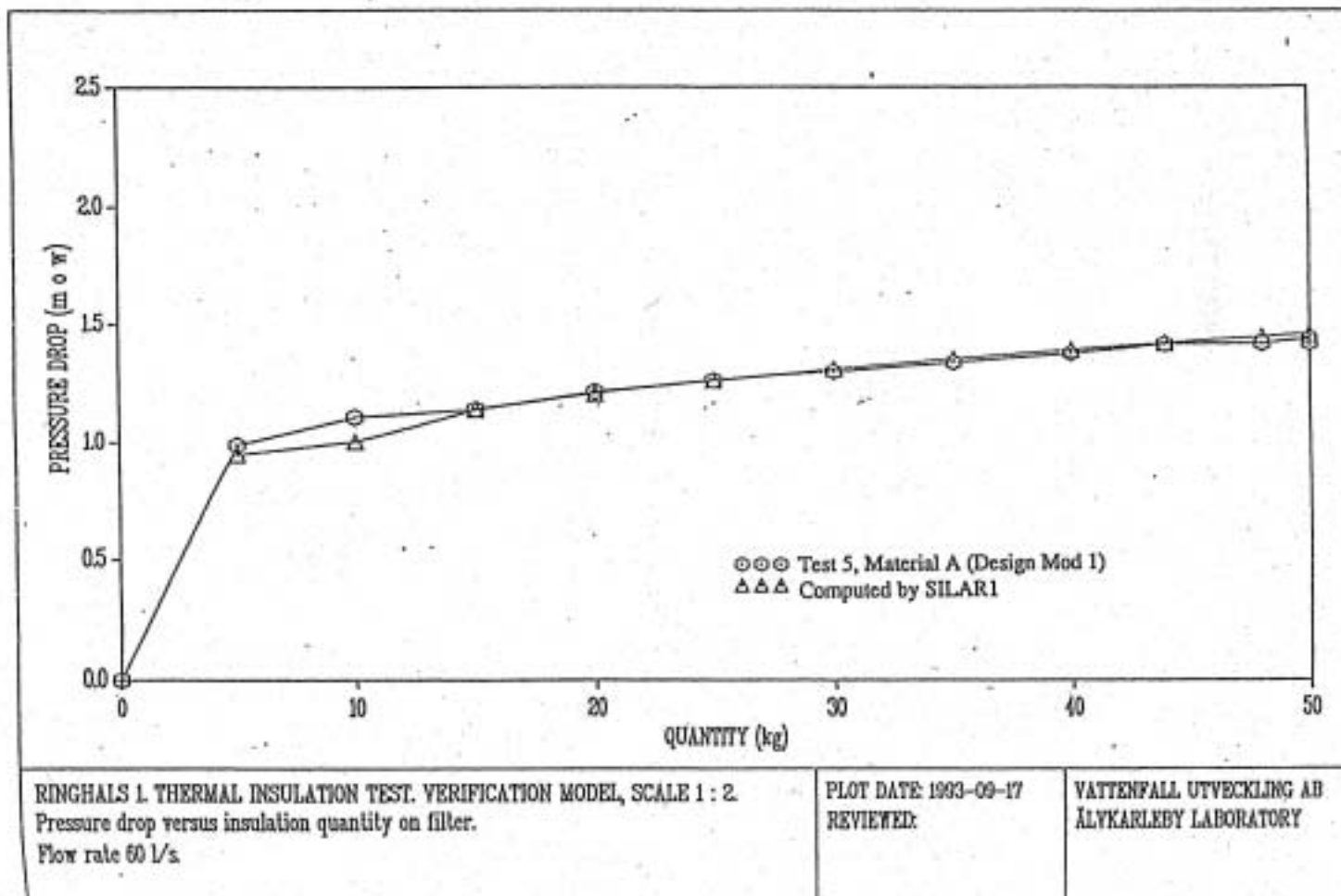


Figure 3. Ringhals 2. Thermal insulation tests

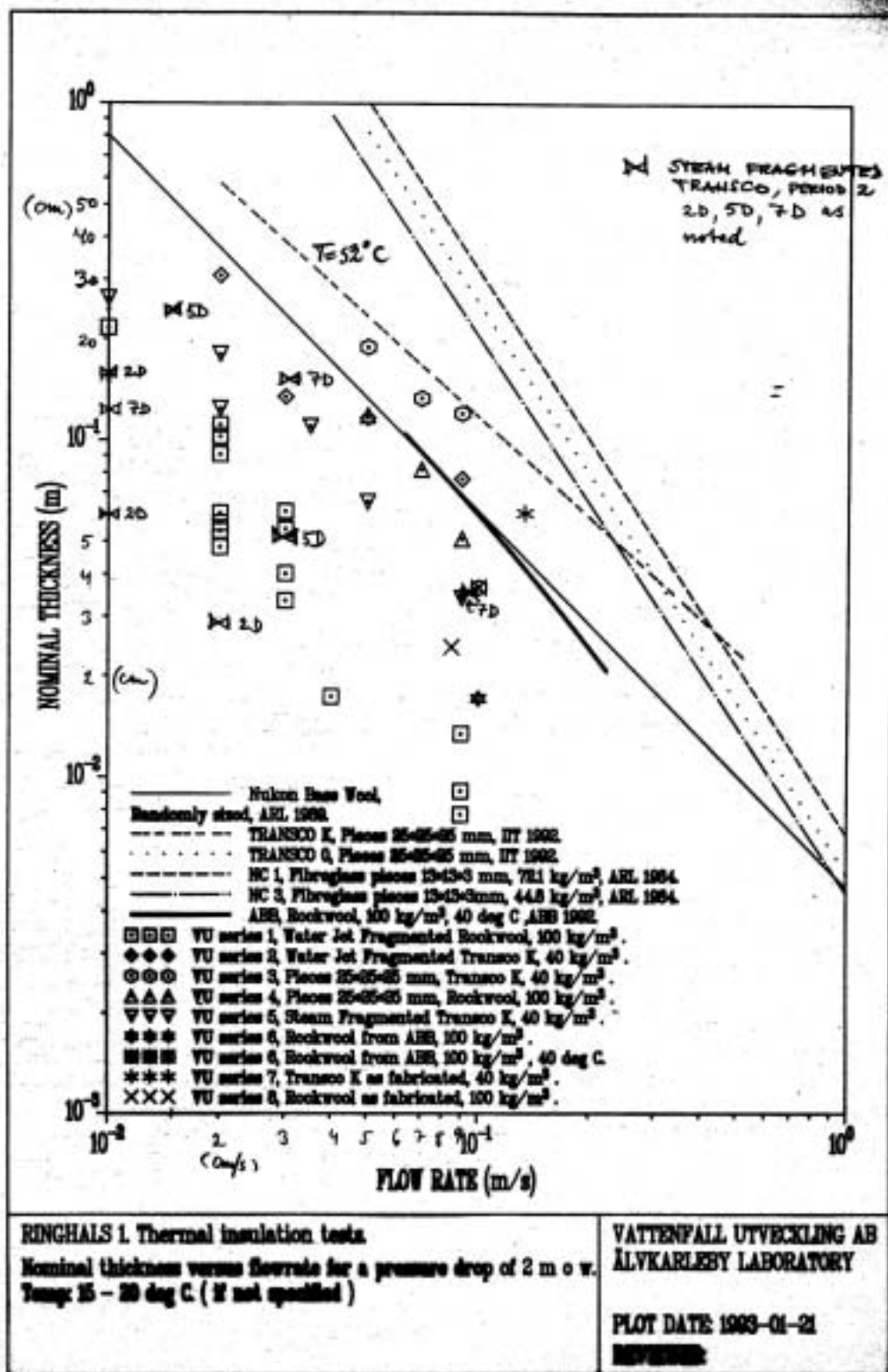


Figure 4. Forsmark 1 and 2

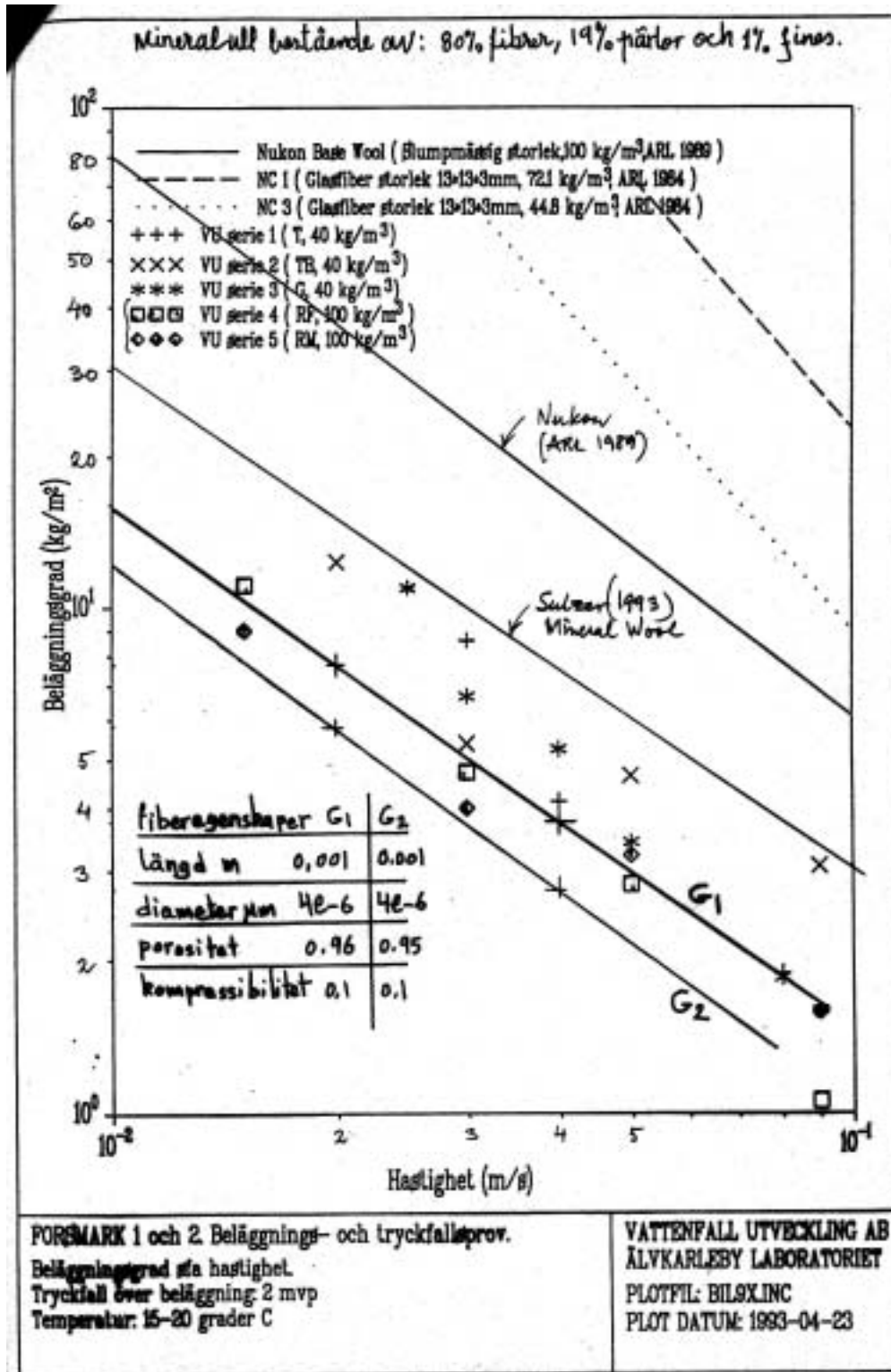


Figure 5. Final pressure drop for various combinations of fines (impurities) and fibres when all material is collected on the strainer (perforated plate). The amount of fines in the basin water is held constant (C kg) and the amount of fibres mixed in the water is varying

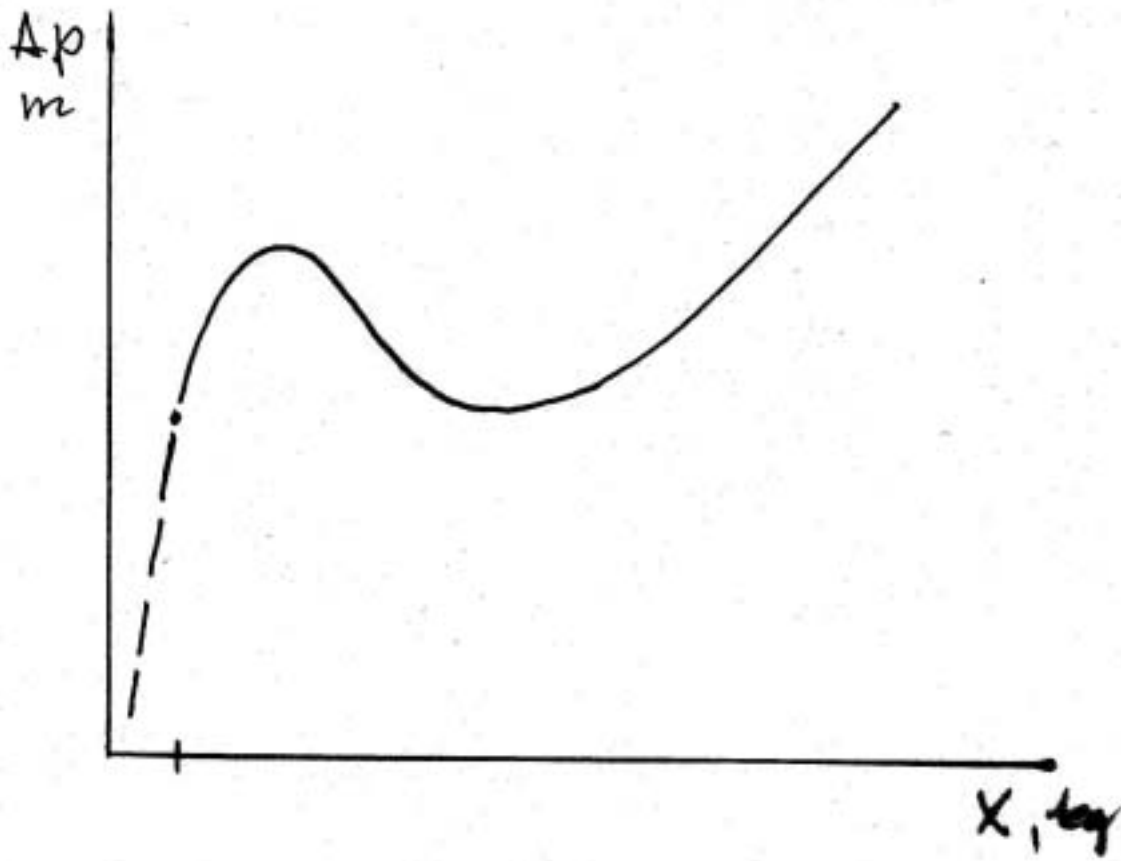


Figure 6. Ringhals 2. Vector plot of velocity

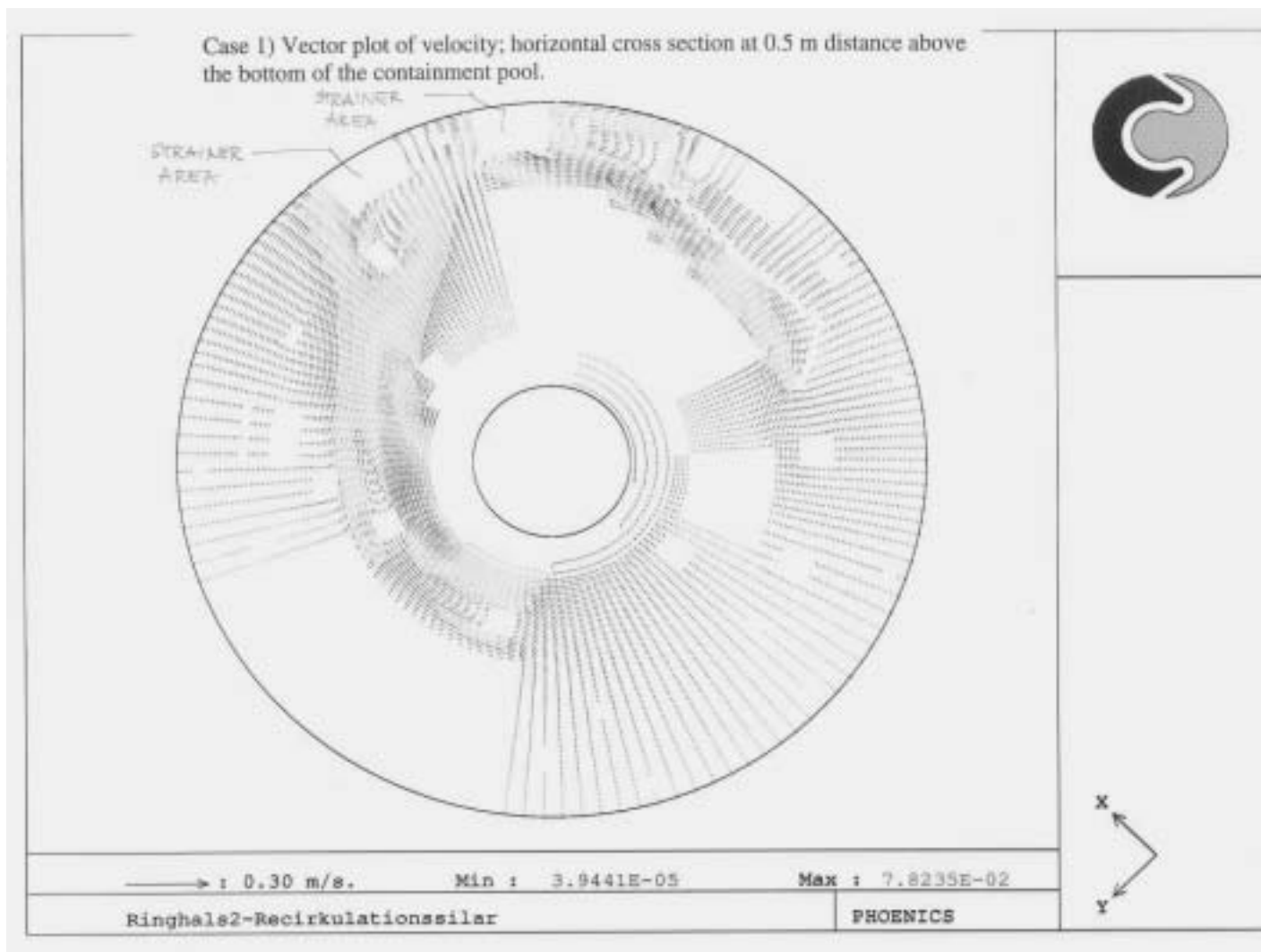


Figure 7(a). From dye studies in the sump area

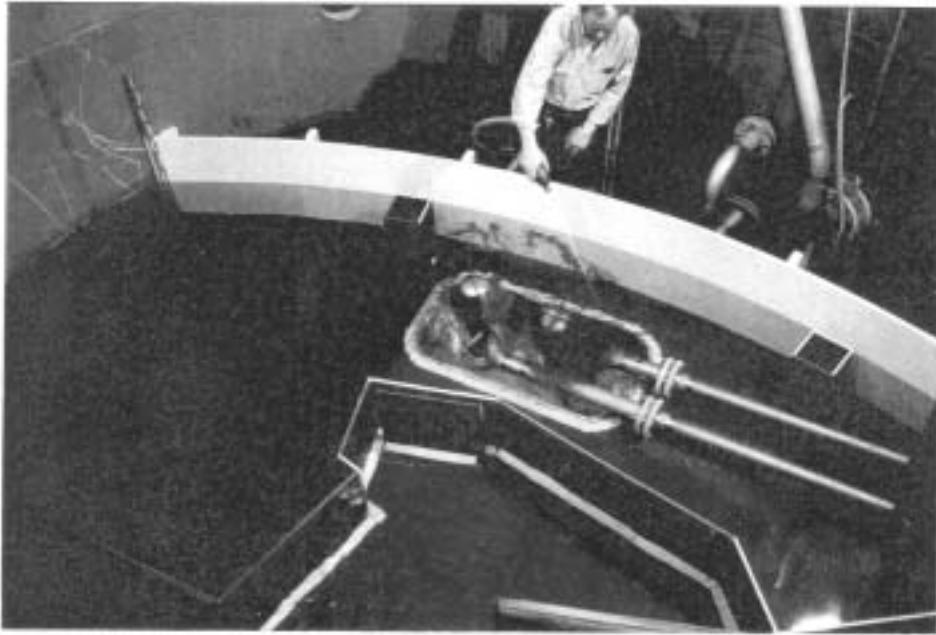


Figure 7(b). Circulating flow and vortex close to one of the vertical self-cleaning strainers

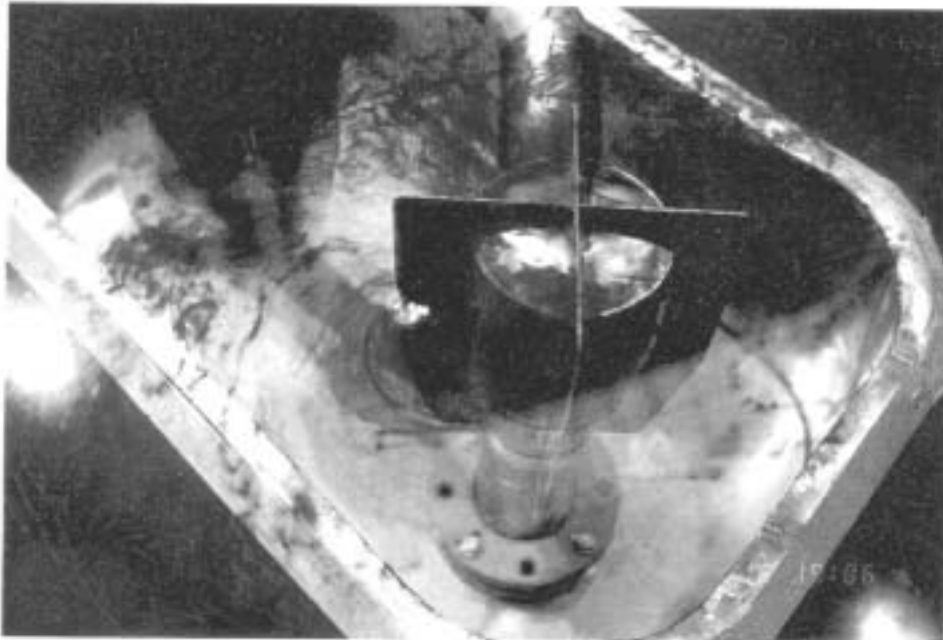
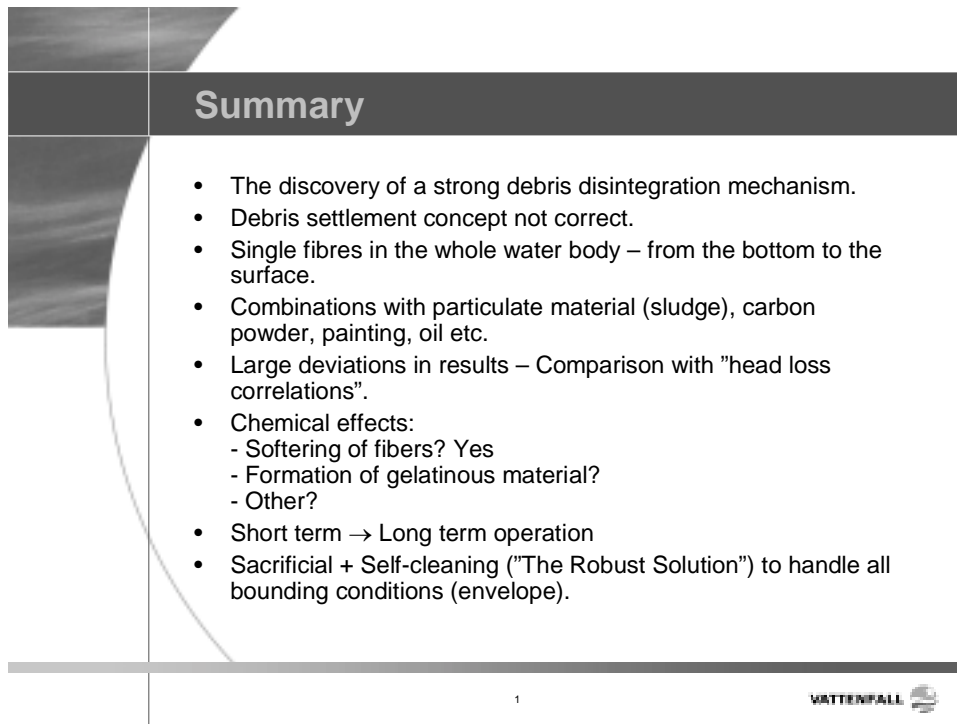


Figure 8. OH viewgraph picture



The image is a slide from an overhead projector. It features a dark grey header with the word "Summary" in white. Below the header is a list of bullet points. The slide has a decorative background on the left side consisting of a vertical line and a curved shape. At the bottom right, there is a small logo for "WATTENFALL" and a small globe icon.

Summary

- The discovery of a strong debris disintegration mechanism.
- Debris settlement concept not correct.
- Single fibres in the whole water body – from the bottom to the surface.
- Combinations with particulate material (sludge), carbon powder, painting, oil etc.
- Large deviations in results – Comparison with "head loss correlations".
- Chemical effects:
 - Softening of fibers? Yes
 - Formation of gelatinous material?
 - Other?
- Short term → Long term operation
- Sacrificial + Self-cleaning ("The Robust Solution") to handle all bounding conditions (envelope).

1

WATTENFALL 

SUMP PLUGGING RISK

Yves Armand, Jean Marie Mattei
IRSN, B.P. 17, 92262 Fontenay-aux-Roses, France

1. Introduction

The assessment of the operational characteristics of the filtration function used during the recirculation phase of safety injection system (SI) and containment spray system (SS), in the event of a primary system break in the containment, has been performed by the “Institut de radioprotection et de sûreté nucléaire” (IRSN) for the French pressurised reactors (58 reactors). Those one have been designed according with the RG 1.82 (rev. 1). The IRSN has focused in particular on the CPY series, 900 MWe 3 loops pressurised water reactors (28 reactors).

A general overview of the literature has been conducted between October 1999 and November 2000, which resulting in defining of an approach methodology and the writing of technical specifications. In this purpose, the “Institut de radioprotection et de sûreté nucléaire” has decided to perform an experimental program of studies on the sump plugging risk. Those studies have been carried out for the different sizes of primary breaks: large, intermediate and small LOCA. For each size of breaks, located on the welding between SG and hot leg, the different characteristics of generated debris, flows of SI and SS systems have been defined.

Methodology of event trees has been used to define the characteristics of the debris and their arrival point at the bottom of the containment using the results of the performed tests.

To estimate the risk involved in each case, the following points were studied:

- An inventory of debris generated. This consists of the following types:
 - glass wool thermal insulation fibers (spherical model: $L = 12.D$);
 - paints and particulates;
 - dusts present in the containment, in suspension or on the walls.
- vertical transfer of debris;
- structural modification of debris in the containment;
- horizontal transfer of debris at the bottom of the containment;
- filtration efficiency and modification of sump hydraulics/air and debris ingestion;
- operation of RIS and EAS circuit equipment with mud and air present.

The subjects giving rise to important questions have been collected and a corresponding full-scale experimental program concern:

- transfer of generated debris to the bottom of the containment, as it crosses the grating system and also under the action of chemical and thermal breakdown;
- settling and transport of generated debris at the bottom of the reactor building;
- the pressure drop value and the ingestion of air at the 4 filters of each suction inlet;
- the behaviour of the fiber bed under realistic conditions (temperature, pH, quality of the water, effects of different particulates).

2. Lessons

A full-scale approach was chosen in order to answer to questions raised from a preliminary study [6]. The following points were currently under experimental investigation:

- IVANA loop (VUEZ/SLOVAKIA): grinding of fibrous debris on the grating system (mechanical action of falling water);
- VITRA loop (EREC/RUSSIA): horizontal transfer speed of debris;
- MANON loop (VUEZ/SLOVAKIA): pressure drop and air and debris ingestion at the sump filters;
- ELISA loop (VUEZ/SLOVAKIA): breakdown of fibrous debris so-called efflorescence (chemical action of water, effect of temperature, establishment of different correlations).

An event tree has been developed and a sensitivity analysis performed. Those can be used as a tool of decision-making for new design [1].

It has been demonstrated the transport, vertical or horizontal, and the debris structural modifications do not lead more questions and can be seen as solved.

On the 12 June 2003, the standing group endorses the strong concern of IRSN [5] that Électricité de France has to perform the necessary actions to deal with the question of the efficiency of the filters of all the plants.

At the end of October (30 October 2003), French nuclear safety authority (DGSNR) has told Électricité de France to accelerate the study of the risk of sump strainer clogging in all 58 of its PWRs and to report by the end of the year.

The Électricité de France position has been presented at the end of 2003. Électricité de France considers that improvements are needed for all the French series to cope with primary breaks higher than 4”.

Two direct types of debris sources are considered:

- The latent debris. They correspond to any materials produced or left during normal operation, prior LOCA.
- The short term generated debris. They correspond to any materials destroyed by the shock wave and the jet effect, when the break appears (LOCA transients).

Those debris can be transported to the containment bottom by blow down/wash down. Otherwise, they are retained by any obstacles (gratings, equipment, etc.).

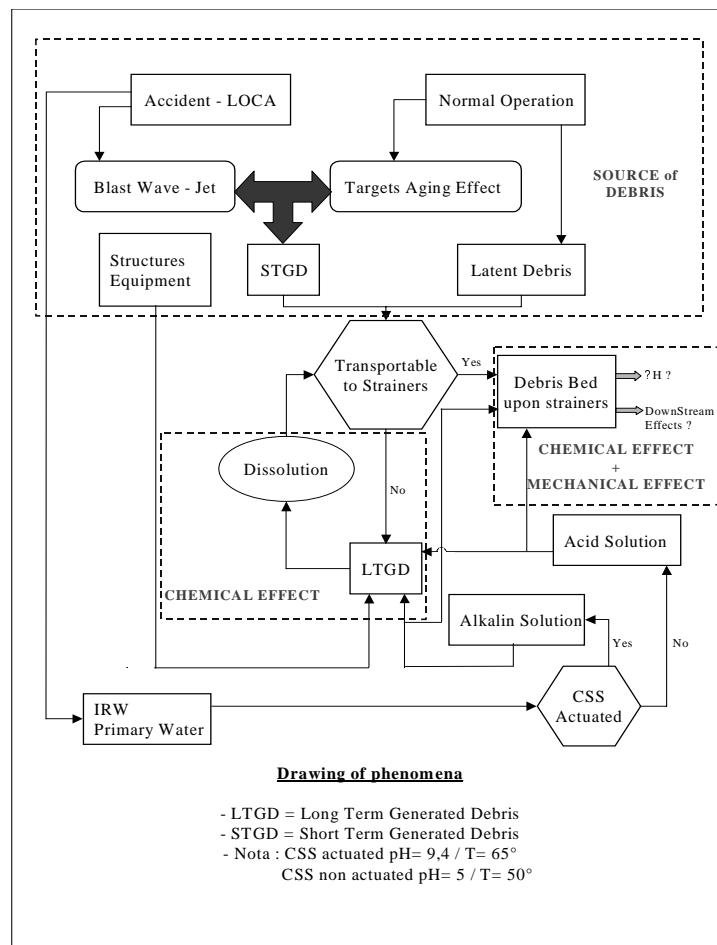
Finally, debris are transported in the containment bottom, both during the direct injection and during the recirculation phases. Otherwise, they settle.

In case of retaining or settling, several chemical phenomena appear and debris could be chemically disintegrated, giving new debris, then transportable.

The remaining opened questions to define approved safety requirements to define the new devices are related to:

- The phenomena of LOCA induced short term debris, so-called up to now “debris generation”.
- The phenomena of LOCA induced long term debris, as a combined temperature and chemical action of water, in correlation with the nature of the water (pH = 9,3). That phenomena involves any types of materials, direct debris or any equipment and structures inside the containment.

The following drawing presents the correlation between phenomena.



This drawing demonstrates the strong process time-dependence and its impact upon the debris bed across the strainers. The particulates and gelatinous debris could be non-homogeneously distributed in the thickness of the cake, increasing very strongly the head loss in comparison with the same amount of particulates, homogeneously distributed. **The right use of such relationship assuming a homogeneous distribution must be demonstrated before any calculations or new devices designs.**

Finally, a last class of phenomena and debris corresponds to the severe accidents induced debris. This one is mentioned below due to its interest in connection with future reactors designs.

3. LOCA induced short term debris

3.1 Concern

It concerns the break effects about destruction, in relation with the shock wave and the jet impact.

About that concern, the break is assumed to be located inside the steam generator box.

The primary circuit depressurisation depends on the type of pipe break considered. It is very short once the equivalent diameter is high (30 s) and longer when small break has to be interpreted, such that the primary and the secondary circuit pressures remain at similar values during several minutes.

3.1.1 Short term transients

The initial shock wave and the steam water jet effects must be considered in relation with the very limited volume inside the steam generator boxes due to the implementation of several equipment, or any other boxes, which leads to several effects of reflection and possible amplifications.

The debris repartition inside the containment before CSS operation fully depends on the overpressure mentioned above and that must be treated, instead to use the assumption of a well uniform debris distribution, which can underestimate the real amount of debris upon the strainers. The distance between the break location and the sumps has to be considered in relation with the blowdown effects.

This list below is not exhaustive. In particular, the “air jet” experiments are not presented. Also, the objective is to demonstrate only 2 facilities have worked at PWRs nominal pressure (*in italics*), **and none of experiments focused upon paint or concrete generation.**

TESTS	Pnom (Bar)	Tnom (°C)	Insulation	Paint	Concrete
KASHIRA	125	315	Yes	No	No
<i>KASHIRA</i>	<i>150</i>	<i>315</i>	Yes	No	No
OPG	100	300	Yes	No	No
<i>Batelle/KAEFER</i>	<i>140</i>	<i>300</i>	<i>Yes (cassette)</i>	No	No
Marviken (STEAM)			Yes	??	??
HDR	110	310	Yes	No	No
Karlsham	80	280	Yes	No	No

The BATELLE's facility (6 m³), now dismantling, provided results about degradation in relation with projection of debris (destroyed cassettes) upon other cassettes. **Also, that phenomena is similar with this one due to the projection of debris resulting from the degradation of I & C.**

The KASHIRA's facility is too much small (0,9 m³) to be used. More the water volume is small and less the steam/water jet impact appears, to be considered as negligible in comparison with the blast wave due to the opening.

This lack of data, both upon the reproduction of the destruction mechanism and the nature of targets used is stated.

The models are based upon calculations providing isobar curves, correlated with data obtained from the previous tests. A spherical zone of influence (ZOI) is widely used, in relation with the released energy amount. **Also, the problem is the sphere diameter, which is much higher than the free space between walls and break location.** Also, a part of the sphere, so the energy, is "virtually" lost. Typically, a steam generator box is 6 x 6 m² and a 12 inches break has a ZOI radius of 4 m.

Short-term transients are not well reproduced and the models widely used do not describe the reality. Models used up to now shall be justified.

3.1.2 Long term transients

Nothing exists about those long-term transients. No experiments have been performed and models used about short term transients are always applied in such case. Nevertheless, the phenomena could be very different.

Models used up to now shall be justified.

3.2 Issuance – ZOI inside debris

This question can be solved if the following conditions are together fulfilled:

1. Working at PWRs nominal parameters, 155 bar and 300°C.
2. Working with a large amount of water to reproduce the accidental transients with the real pipe breaks.
3. Working with targets at full scale.

Since April 2002, the I.R.S.N started to find a vessel responding to the conditions 1 and 2. Once found, a feasibility of studies including technical and cost/benefit aspects has been developed during the four last months of 2002 [3].

First at all, calculations using CATHARE and RELAP Computer codes have been performed at different diameters (Figures 1, 2 and 3).

Figure 1. Pressure (340 mm nozzle diameter). CATHARE

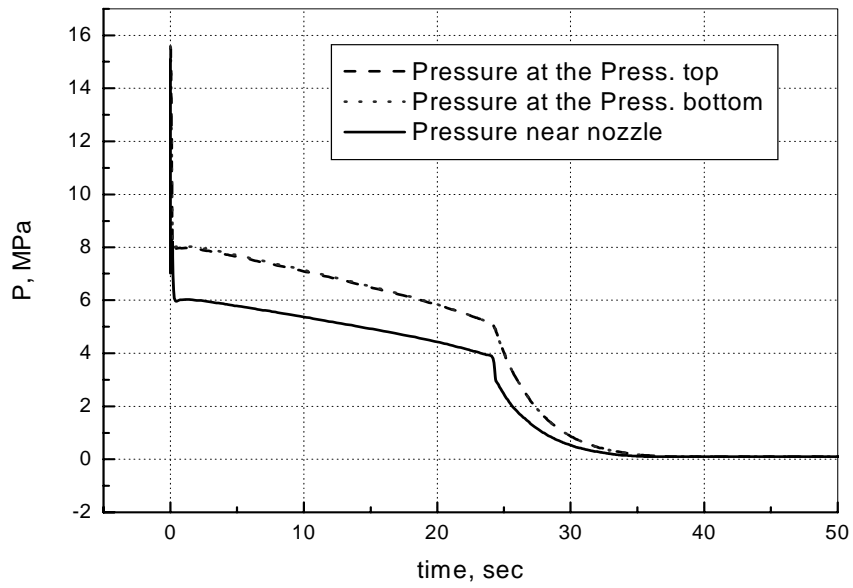


Figure 2. Pressure (340 mm nozzle diameter). RELAP

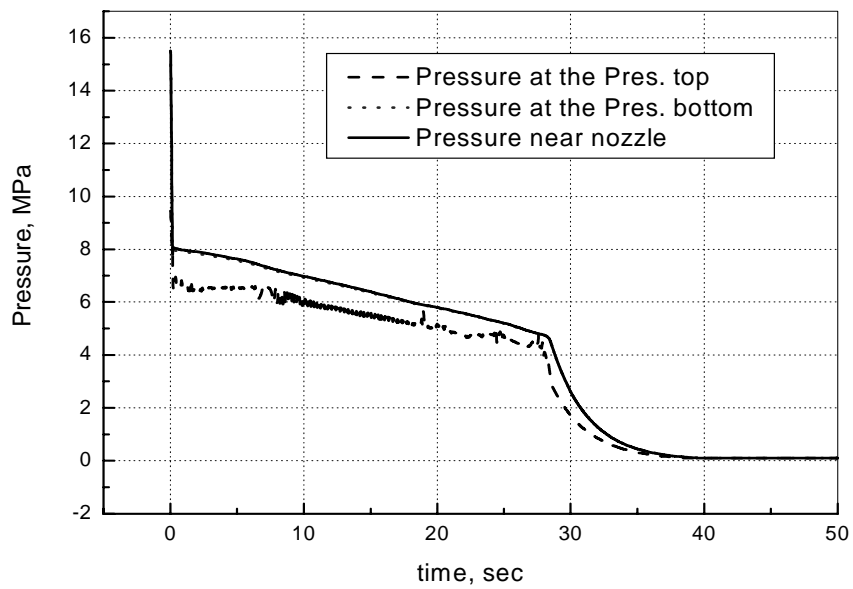
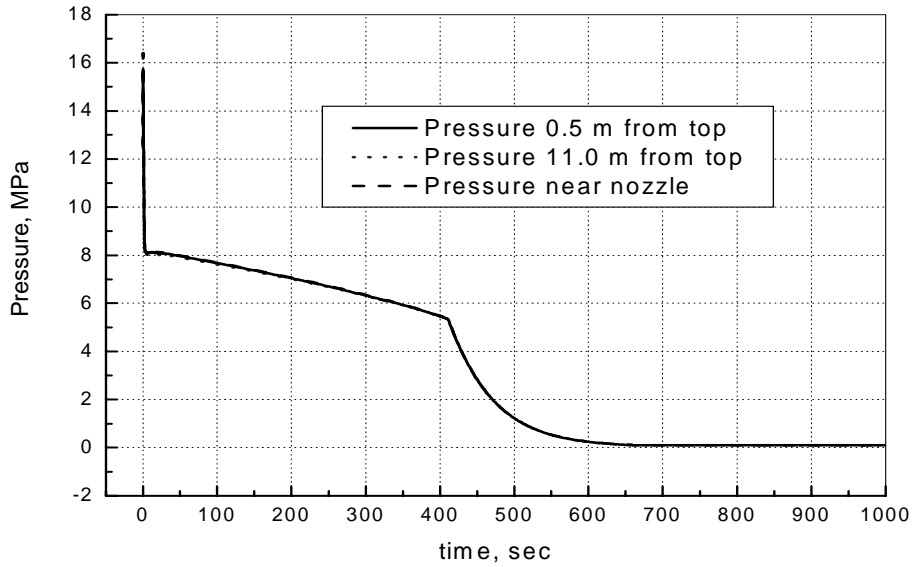


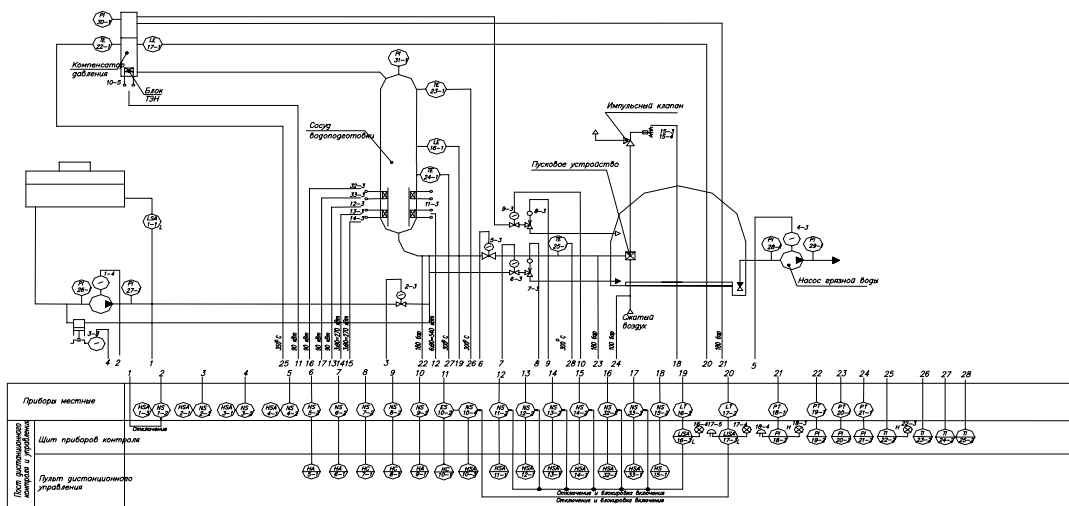
Figure 3. Pressure (76 mm Nozzle Diameter). CATHARE



Then, a basic design has been defined. From that work, an in-depth design has been performed and all required equipment have been identified (Figure 4).

In parallel, calculations have been performed to estimate the sound produced and its impact, in order to choose the best place to install that loop.

Figure 4. Instrumentation and control system of the test facility



The building-up has been described and cost established.

The tests have been delimited and targets selected (nature, shape, etc.). About steam generator or concrete, a supporting system has been thought to move it at different distances from the nozzle. The height corresponds to a ratio of 20 nozzle diameters, by assumption.

3.3 Issuance – ZOI outside debris

The two following actions have to be considered:

- A systematic review inside containments about those components able to be destroyed by the DBA conditions. Firstly all components in plastic have to be considered.
- In case of doubts about their integrity under those conditions, those components can be removed and new qualified components used.

4. LOCA induced long term debris

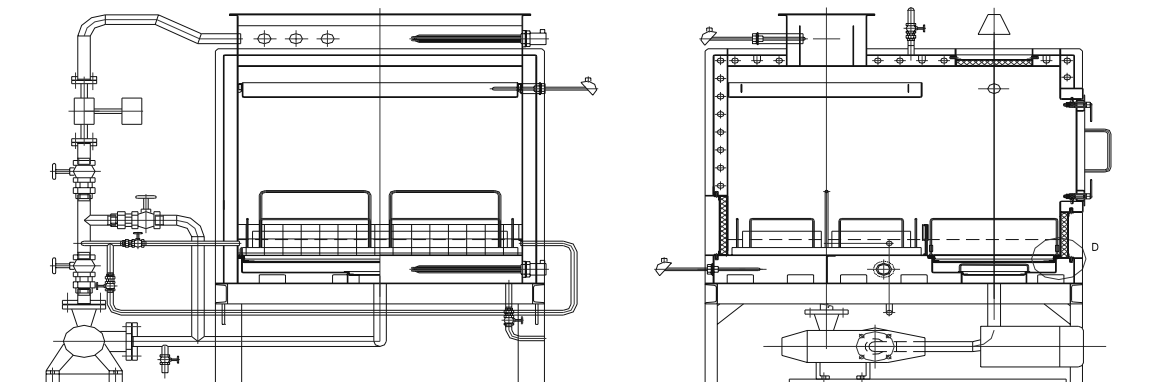
This terminology represents the materials transformations inside the containment due to the combined temperature and chemical impact. The LOCA induced long term debris includes the transformation of debris already on the strainers or in the containment.

Qualitative tests have been already performed to get information upon:

- the water hardness effects;
- the fiberglass leaching.

A study using the loop ELISA (Figure 5, [4]) is now engaged by IRSN to characterise the most important phenomenon.

Figure 5. Loop ELISA. Schematic aspect



The aim of the program will be the characterisation of the behaviour of the head loss of the fiber bed fixed on the filtering devices during accidental conditions flow recirculation and under precipitation effects.

Firstly, this program has to be focused on the design basis accidents of the existing units. The treatment of the severe accidents has to be investigated later.

Accidental conditions during recirculation phase are mainly linked with the following parameters: pH and temperature. The given pH of the sump solution (9,3) has a large effect on corrosion and precipitation reactions.

Concerning the temperature, the maximum expected sump temperature is 113°C and this temperature is achieved very quickly. Within long term, the temperature decreases to 70-60°C. The compounds and products are of a major interest under those thermo dynamical conditions, foreseen at the equilibrium.

The pressure is not considered as an important parameter. For French units, it has to be underlined that during recirculation phase, the sumps are always under water.

To be able to use the results of the program for different units with different quantities and varieties of debris, the program will be shared in two steps.

4.1 *First step*

The first step of this program is to determine the concentration of precipitates and gelatinous compounds which can be produced at long-term. It can be described with the following steps:

1. Determination of the *nature of the water involved*. The IRWST water and in addition the compounds, which are inside the primary circuit water have to be considered. Besides, the CSS is not in operation once the break size is less than 4". Also, it means the nature of water (NaOH content) is different considering the accidental events depending on the CSS activation, also there are two equilibriums.
2. Measurements of the *degradation kinetic rates* (dissolution/corrosion) for the main types of "material of interest" (latent debris and so-called short-term debris related with the debris generation due to the jet effects). Some of materials with their respective importance based on judgment expert are mentioned below:
 - Insulation generated by the jet – Important
 - Concrete generated by the jet – Important
 - Paint generated under the jet – Important for zinc oxides
 - Corrosion products existing before the accident – Lower importance
 - Corrosion products created during the accident – Lower importance
 - Seals carried by the flow – Lower importance
 - Cables washed by the water (copper, insulation) – Lower importance

- Dirt and dust washed by the water – Important
 - Others including:
 - any types of plastic materials – Lower importance
 - identification labels... – Lower importance
3. **Computer modelling of time evolution of complex system.** This step requires the use of computer codes like JCHESS (Geochemists' Workbench WEB site), ESP, etc. The objective is to calculate the nature and the quantity of complex at the equilibrium (pH = 9.3, T = 65°C for Large LOCA or acid pH = 4 and T = 25°C for Small LOCA), inside the containment.

At that step, the volume and the reacting surfaces of the simple debris are of a major interest about quantification.

In addition, modes will be realised to characterise the quality of the precipitation forms (gelatinous or crystallisation).

4.2 Second step

The second step, in case of significant amount of precipitates and gelatinous compounds, is to determine their effect on head loss of the fiber bed fixed on the filtering devices. It can be described with the following steps:

4. **Head loss tests.** The loop ELISA will be used and eventually the MANON loop. The goal of the tests will be to quantify the respective influence on the filter head loss of insulation leaching, of precipitation crystal forms and of precipitation gelatinous forms.

5. Severe accident debris

During severe accident progression, the temperature of the gas inside the primary circuit will increase significantly. Due to these very high temperatures, the insulation, for example glass wool, could not be able to withstand temperature higher than 500°C. In this case, the insulation could be damaged and could fall down at the bottom of their metallic coffering. Under effect of the spray system or under the effect of the containment heat removal system for the future reactors, this coffering could be damaged. Consequently, a large amount of additional debris could be transported to the sumps, in addition to those one generated by the core itself.

Besides, the water chemistry is very different from the DBA conditions.

Those issues have to be studied.

6. Conclusion

The new filtration devices, if required, cannot be designed without a complete understanding about the amount and the nature of both short and long term LOCA induced debris and a systematic review of latent debris.

Any kinds of in-depth safety analysis have to consider all those aspects to conclude about the operation of the safety injection system and the containment spray system. In this purpose, IRSN proposes an action plan [7].

REFERENCES

- [1] “Synthesis Report”, IRSN/DES/SERS/400, 14 October 2003.
- [2] “GOSNICAES Kashira Report”, 1996.
- [3] “Feasibility Studies Report – EREC”, OT FEAS 118 1.001-02, 30 November 2002.
- [4] “ELISA Reports – VUEZ SA”, TS/ODA/1301-1; TS/ODA/1301-2; TS/ODA/1302-1; TS/ODA/1302-2, 12 March 2002.
- [5] Armand, Y., J.M. Mattei, “Albuquerque Workshop (2004) – Issue on French PWR”, IRSN, France.
- [6] Armand, Y., J.M. Mattei, “Albuquerque Workshop (2004) – Experimental program”, IRSN, France.
- [7] Armand, Y., J.M. Mattei, “Albuquerque Workshop (2004) – Action plan proposal”, IRSN, France.

SESSION 2

EXPERIMENTAL WORK

Chairpersons: Dr. Y. Armand (IRSN) and Dr. B. Letellier (LANL)

HIGHLIGHTS

Seven papers were presented in Session 2.

Extensive investigation and tests on this issue were performed in Germany, and the conclusion was that no major backfitting was necessary on their Siemens PWRs. This was largely due to the use of strong cassette type insulation only on the primary system; special efforts to ensure break preclusion for the main coolant lines thus allowing application of reduced break sizes in their debris generation calculations; the fact that no containment spray systems exist in these plants; high water levels in the sump allowing increased sedimentation; and the enforcement of containment cleanliness after refuelling.

The general sense of the session was that because of the different containment designs and insulation materials used, more tests were needed for debris generation, debris transportation, head loss and downstream effects. Many tests were performed on this issue for the BWR plants, however, since PWR plant reactor coolant operates at higher pressure and temperature than those for the BWR plants, the debris generation test data (e.g. damage pressure, the L/D parameter, etc.) performed for BWR plants should not be blindly applied for the PWR plants. In addition, since these tests are very debris type specific, more tests will be needed for different debris types.

Regarding the head loss correlation presented in NUREG/CR-6224, some countries found it to be not suitable for their particular debris type and plants, and as a result they generated their own correlation instead. Since the head loss correlation presented in NUREG/CR-6224 is debris type specific, caution should be exercised in its use.

The IRSN representative presented the experimental program and results from the test loops (namely ELISA, MANON, IVANA, and VITRA) designed for the specific conditions of the plant type investigated and realised during the year 2001. Those results have been directly used to assess the risk of sump plugging in France.

The Canadian paper discussed the strainers implemented in the CANDU stations (between 64 and 1 200 m² of surface area). Those strainers have been designed and implemented such that other new modules can be added to those which are now in place. Considerable efforts have been expended to characterise and quantify debris (walk downs, etc.).

Other presenters discussed various experimental programs and results on latent debris inside containments, potential chemical reactions between the exposed material and post-LOCA containment environment, large scale tests of mineral wool insulation behaviour in German PWR plants, data to validate containment CDF models and head loss tests.

RISK OF SUMP PLUGGING EXPERIMENTAL PROGRAM

Yves Armand, Jean Marie Mattei
IRSN, B.P. 17, 92262 Fontenay-aux-Roses, France

J. Batalik, V. Gubco, J. Murani, I. Vicena
VUEZ, a. s. Levice, Sv. Michala 4, 934 80 Levice, Slovakia

V.N. Blinkov, M. Davydov, O.I. Melikhov
EREC, 6 Bezymyannaya Electrogorsk, 142530 Moscow Region, Russia

1. Introduction

Assessment of the operational characteristics of the filtration function used during the recirculation phase of safety injection system (ECCS) and containment spray system (CSS) in the event of a break of the primary system in the containment has been performed by the “Institut de radioprotection et de sûreté nucléaire” [1] for the French pressurised reactors (58 reactors) in particular the CPY series, 900 MWe pressurised water reactors (30 reactors) designed according Regulatory Guide 1.82 (Rev. 1).

To estimate the risk involved, the following points were studied:

- Inventory of debris generated of the following types:
 - glass wool thermal insulation fibers;
 - paints;
 - dust;
 - dust present in the containment, in suspension or on the walls.
- Vertical transfer of different debris.
- Structural modification of debris in the containment.
- Horizontal transfer of debris at the bottom of the containment.
- Filtration efficiency under realistic conditions (temperature, pH, quality of the water, effects of different particulates).
- Modification of sump hydraulics/air and debris ingestion.
- Operation of SI and SS circuit equipment with mud and air present.

The subjects giving rise to important questions have been collected.

For some of them, assumptions have been taken. They concern the insulation debris generation for which a spherical model of degradation has been adopted for double-ended break (NUREG 6762) with a ratio of $L/D = 12$ and the insulation debris repartition established on the basis of KASHIRA test results.

For the other ones, an experimental approach was chosen due in one hand to some lack of knowledge, in the other hand, to the difficulty to use generic results to assess the French units and their specificities.

The corresponding full-scale experimental program concern:

- IVANA loop (VUEZ/SLOVAKIA): transfer of generated debris to the bottom of the containment under mechanical action of falling water, as it crosses the grating system and also under the action of chemical and thermal breakdown [2].
- VITRA loop (EREC/RUSSIA): settling and transport of generated debris at the bottom of the reactor building [3].
- MANON loop (VUEZ/SLOVAKIA): pressure drop value and ingestion of air at the 4 filters of each suction inlet [4, 5].
- ELISA loop (VUEZ/SLOVAKIA): behaviour of the fiber bed under realistic conditions (temperature, pH, quality of the water, effects of particulates) [6, 7].

2. IVANA loop

2.1 Objectives and requirements

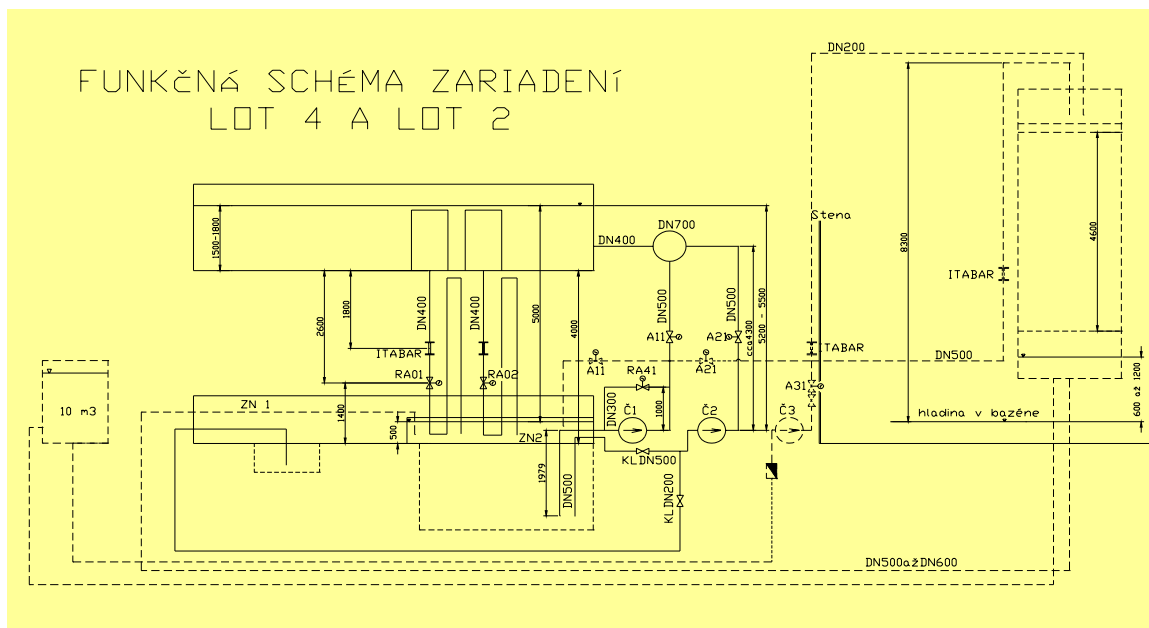
The objectives are to verify and to quantify the kinetics of disintegration of thermal insulation under the mechanical effects of falling water and evaluate the character of insulation debris (glass wool TELISOL or BOURRE) obtained after grinding.

2.2 Technical description of the loop IVANA

To meet the objectives defined above, the test equipment respects the following requirements and criteria:

- To enable fall by gravity of water with ambient temperature on insulation samples from a height of ~ 4.6 m.
- To assure a controlled water flow-rate (between 50 and 1 100 m^3/h) with the required cross-sectional area of the discharge opening (0.3 and 0.9 m^2).
- To enable the collection of ground and washed-out insulation debris on filters, filter removal and debris analysis during experimental testing.
- To satisfy the requirements imposed upon the measuring system and instrumentation.

Figure



2.3 Tests and procedure of evaluation

The parameters are flow rates, sizes of thermal insulation debris and area of discharge. The main test evaluation criteria are as follows:

- Time-dependent weight loss of tested samples.
- Time-dependent weight increase of insulation debris collected on individual filters.
- Time-dependent weight increase of insulation debris collected on filters in fractional distribution.
- Video-records of test processes, album of photos and insulation samples.

2.4 Results

The tests performed proved a substantial impact of mechanical effects of flowing water on thermal insulation degradation leading the samples to be transformed into simple fibers. Water discharge during the tests is limited to its free flow without any pressure or temperature effects.

Regarding the mechanical degradation, in a few minutes, 55% of the insulation initially installed on the gratings is destroyed under the effect of SS and become fibers with a mean length value of 0.5 mm and a maximal length of 7 mm before being transported at the bottom of the containment.

Additional tests were performed with the purpose to define the different effect on insulation grinding if the insulation is placed on a grate or falls to the grate with water from a height of 4.5 m.

For these additional tests (test 01 and test 02), insulation was placed at an elevation of 4.5 m and, together with water, it fell on a grate with mesh size 20 x 20 mm with a water flow-rate of 200 m³/h.

In the table below, obtained results are compared with tests 01-P and 02-P that were realised with insulation initially installed on gratings.

Test No:	01		01-P	
Type of insulation:	BOURRE		BOURRE	
Weight of inserted insulation:	3 500g		3 095g	
Weight of debris collected on filter A (2.5 x 2.5 mm):	3 135g	89.6%	1 550g	50.1%
Weight of debris collected on filter B (0.63 x 0.63 mm):	142g	4.1%	357g	11.5%
Weight of residual insulation remaining on the grating:	223g	6.4%	1 188g	38.4%
Test No:				
	02		02-P	
Type of insulation:	TELISOL		TELISOL	
Weight of inserted insulation:	3 100g		3 079g	
Weight of debris collected on filter A (2.5 x 2.5 mm):	2 411g	77.8%	1 873g	60.8%
Weight of debris collected on filter B (0.63 x 0.63 mm):	376g	12.1%	244g	7.9%
Weight of residual insulation remaining on the grating:	313g	10.1%	962g	31.2%

From the results, it follows that if insulation sample is placed at an elevation of 4.5 m, it passes through the grate with a mesh size 20 x 20 mm much more quickly than if it is located directly on the grate. This is caused by the fact that, when falling on the grate, the insulation sample is in the core of falling water stream and, as a result, it almost immediately passes through the grate with mesh size 20 x 20 mm.

3. VITRA facility

3.1 Objective and requirements

The objective was to identify, from a statistical point of view, the settling and transportation velocities of various samples as a function of the fluid velocity. The samples (2 thermal insulations, concrete, paint and oxides) are sized from 50 µm to 10 cm. Moreover, it was required to observe the effects of the concentration of debris, at 1.5 and 10% and on the corresponding velocities.

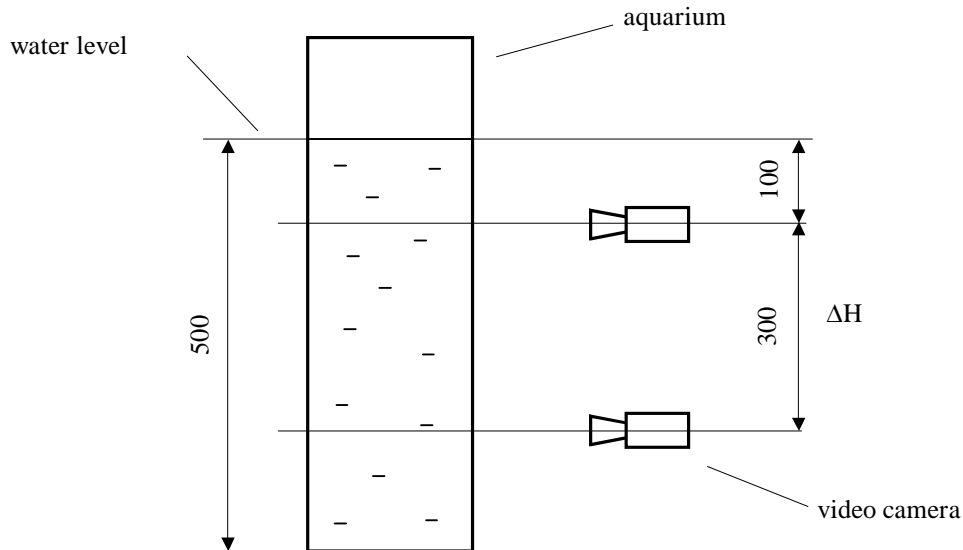
3.2 Tests and procedure of evaluation

All measurements are made with cameras. Their synchronisation is realised by special device (“quadrator”) and velocities are calculated after computer processing of images.

Special devices (optical fibers which have a few micrometers of diameters) are used to measure the fluid velocity in all points of importance. All other measurements are made according standard means.

3.3.1 *Settling*

Several aquariums of different dimensions to study sedimentation of debris are used. For example, the investigations of sample settling (sizes 1-10 mm) needed an aquarium with two video cameras (Figure below).



3.2.2 *Transportation*

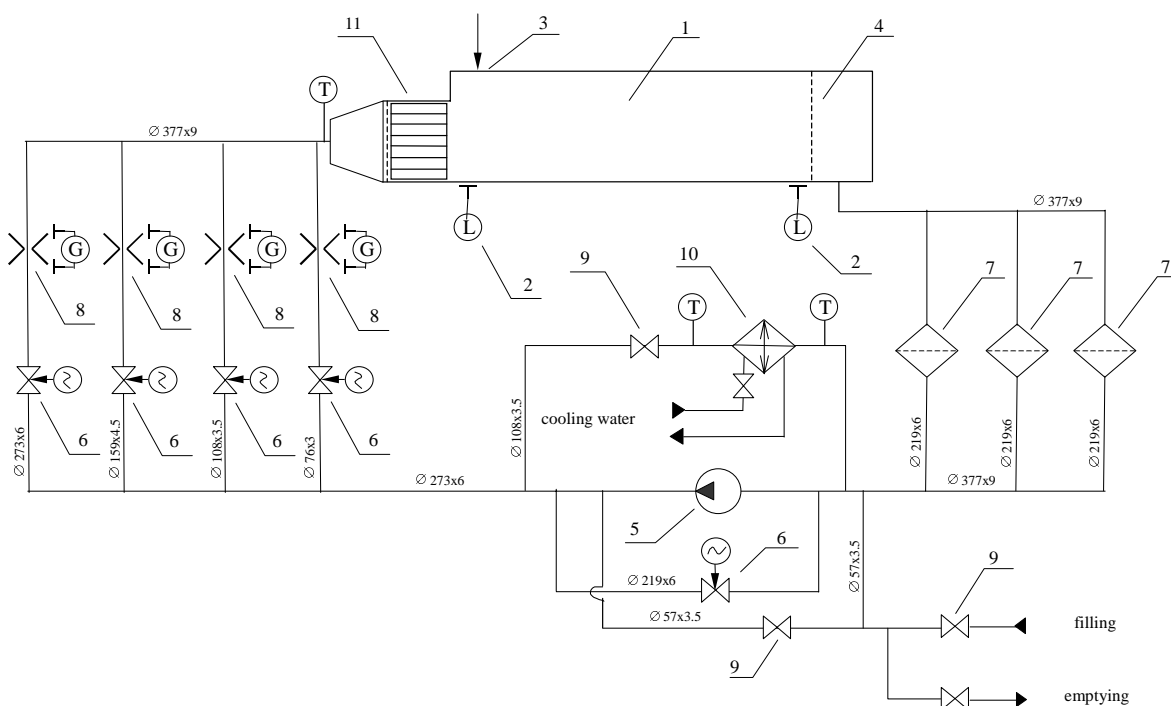
The test facility consists of a working zone (the hydraulic channel), a recirculation loop and several auxiliary systems.

The working zone is an open rectangular basin 0.513 m wide, 0.8 m high and 3.5 m long. One side wall of the working zone is in Plexiglas to allow video recording during the tests. The opposite wall and the steel basin bottom are painted white with black painted markings. The bottom of the working zone is covered with Plexiglas to reduce the coefficient of the samples rubbing on the bottom of the basin.

The recirculation loop consists of a pump, water supply and flow rate measurement system, a water filtering unit, temperature stabilization and pump load control circuits. The maximum pump flow was chosen to ensure an average water speed of 0.5 m/s in the working zone.

The water flow in the recirculation loop supply ducts in the facility is measured using concentrators and differential pressure sensors. Sensors of this type are also used to measure the differential pressure determining the water level in the basin. Special fiber optic speed sensors measure the water speed in the working zone. The displacement speed of the samples is measured using a video optic system based on video recordings with the images processed by computer.

The loop VITRA is presented below.



Note: 1. working zone; 2. level; 3. sample loading zone; 4. grid; 5. pump; 6. control valve; 7. filter; 8. flow meter; 9. stop valve; 10. heat exchanger; 11. water jet rectifier with grid.

3.3 Results

3.3.1 Settling

52 tests have been performed. A part of the results is presented below.

Material	Dimensions (mm)	Settling velocity (cm/s)
Glass wool	100 x 100 x 80	8.3 ± 1.5
Glass wool	50 x 50 x 50	7.6 ± 0.3
Glass wool	20 x 20 x 20	7.0 ± 0.6
Glass wool	10 x 10 x 10	4.7 ± 0.3
Paint	30 x 30 x 0.2	3.1 ± 0.5
Concrete	Ø 0.3	3.5 ± 0.2
Ferric oxide	Ø 0.04	0.26 ± 0.01

3.3.2 Transportation

51 tests have been performed. A part of results is presented below.

Material	Dimensions (mm)	Flow velocity for 95% of samples begins to move (cm/s)
Glass wool	100 x 100 x 80	4.4 ± 1.4
Glass wool	50 x 50 x 50	3.2 ± 0.6
Glass wool	20 x 20 x 20	3.9 ± 0.8
Glass wool	10 x 10 x 10	2.2 ± 0.7
Paint	30 x 30 x 0.2	13.4 ± 2.7
Concrete	Ø 0.3	7.1 ± 1.4
Ferric oxide	Ø 0.04	6.0 ± 1.2

Regarding horizontal transport, the observed velocities are 3 cm/s for 50% of the insulation debris and 4 cm/s for 95%. For the paints, the velocity for 95% (respectively 50%) of the particulates is 14 cm/s (respectively 11 cm/s).

4. MANON facility

4.1 Objectives and requirements

In order to meet the objectives, the test equipment is designed:

- to represent about ¼ of the full-size annular space;
- to represent filter the four filtering boxes and the three pre-filters in the scale 1:1; the corresponding filtering boxes and the pre-filters are movable;
- to avoid turbulences upstream the pre-filters;
- to have a volume of working fluid (150 m³) circulating through the filter boxes allowing 1 100 m³/h per each sump;
- to work at different values of pH;
- to simulate settling of debris during the IRWST injection;
- to control the different parameters from a control room and to follow in line their evolution;
- to adjust the flow rates of the four suction lines to simulate the real conditions of work of the ECCS and the SS pumps during different primary break sizes accidents;
- to stop, under specific conditions of head loss of the filtering boxes, different suction lines of the safety systems and to reconnect them if needed during the tests.

The volume of water is not heated.

The test facility is equipped:

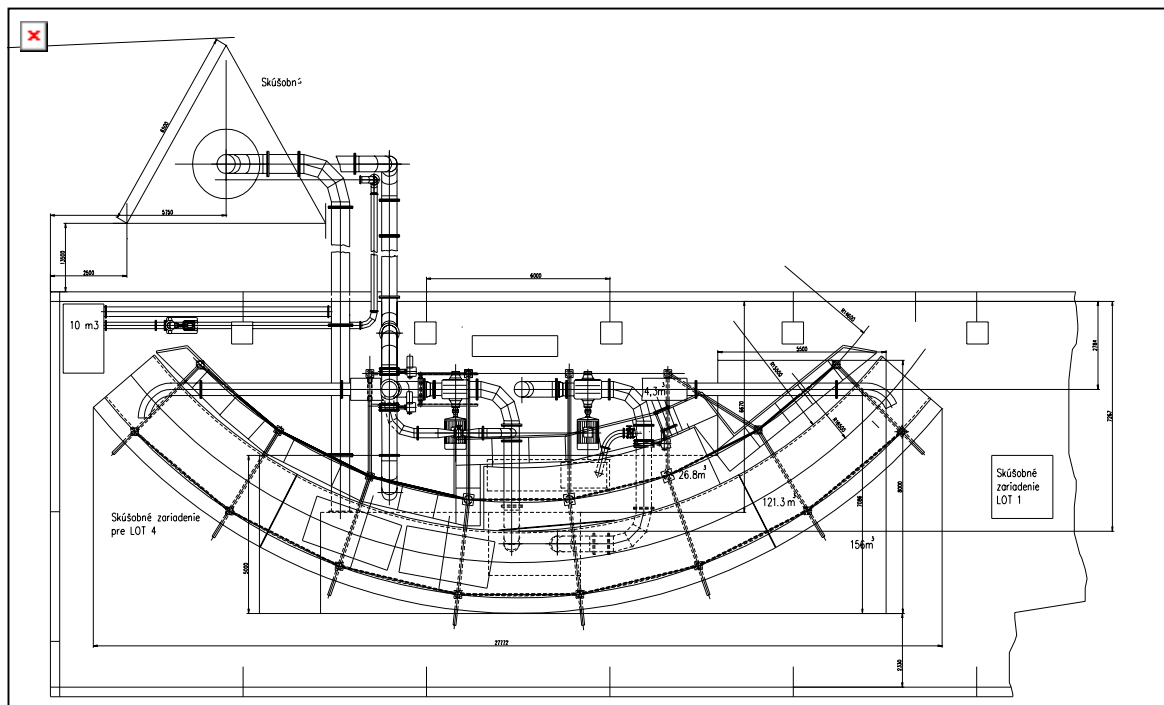
- to measure head loss of the different filter boxes and/or pre-filters under specified experimental conditions;
- to measure level of water inside the filtering boxes;
- to measure fluid flow velocity in selected locations;
- to measure air intake into the filter box discharge line;
- to assess the dependence of filter box and pre-filter head losses on the quantity of insulation fibres and particles and on the thickness of collected bed;
- to measure the other parameters of the flowing fluid that are necessary to define experimental conditions (temperature, pH, viscosity, density).

Moreover, the VUEZ Institute is equipped to assess the physical parameters of the bed fixed on the filtering boxes consisting of insulation fibres and/or a mixture of insulation fibres and dust particles (porosity, length of fibres collected on filter surfaces and dimensions of particles).

The obtained results on MANON loop are used with correlations established on ELISA loop to assess the corresponding conditions on the unit in case of occurrence of a primary break.

4.2 *Technical description of the loop MANON*

The figure below presents the loop MANON.



4.3 Tests and procedure of evaluation

The criteria are the followings:

- Weight of insulation and particles introduced into tank.
- Weight of bed removed from filter surfaces after test completion.
- Operating parameters of the test equipment (flow-rate, temperature, level, pH, head loss).
- Air intake.
- Thickness of beds formed on filter surfaces.
- Porosity of beds formed on filter surfaces.
- Dimensional analysis of fibers and particles (fractional composition).
- Collection of fibers and particles on filter surfaces and penetration through them.
- Laboratory analysis of pH.
- Composition and viscosity of test fluid.
- Video recording and taking photographs.
- Velocity field in tank.
- Level in tanks.
- Head loss of filter boxes and pre-filters.

Two types of seeding have been used:

- Pure fibers.
- Fibers and particulates (between 85 and 150 μm).

4.4 Results

The results of the last tests on MANON loop (see Table 1) demonstrate:

- The pre-filters are plugged very quickly. The tests performed proved a substantial impact of insulation materials on the pre-filters. In parallel, the level of water on the filters decreases. A large transient appears if the boxes are uncovered and air gets into them.
- The negative effect of the pre-filters. Three levels are created:
 - the first one before the pre-filters;
 - the second one around the filtering grids;
 - the third one inside the filtering grids.
- The criterion linked with air ingestion (anti-vortex plate on low level) is reached for small sizes of primary breaks when pre-filters are considered.
- A benefit due to removal of the pre-filters but not sufficient to cope with all the breaks considered in the design.
- The negligible effect of initial settling of the debris: 3% are always settled at the end.

- The important influence of the particles (depending of their sizes and instant of arrival). This significant influence leads to consider as critical size of breaks intermediate breaks and small breaks for which the quantity of damaged insulation is lower but the quantities of particulates could be greater due to the maintain of the jet at the location of the break.
- The important influence of the characteristics of the water (Ca, Mg, ...) on the behaviour of the fiber bed and consequently on the increase of its head loss during long term.
- The deposited debris on the first grids are put in suspension as soon as the internal grids of the filters are plugged.
- A significant increase of the head loss of a filter as soon as the nearby file is stopped due to migration of the fibers from the stopped file. This confirms that the compensatory measures consisting to stop a file are not really the best solution.

A correlation was defined to link the head loss obtained on the MANON loop with parameters such as ph or temperature. This correlation was established with the use of the ELISA loop.

Table 1

Tests/ results	Pre-filters	SG	LB	SB	SI	SS	Particulates	Criterion	Needed quantity (kg)	Correlated quantity (m ³) (T, pH)	Critical break size
Test 1	WITH	2	X		1 300 2 files	2 200	WITHOUT	Low level of AV plate on 2 files SS	43.8	2.3	4" or 3" if part.
Test 2 (1)	WITH	2	X		1 020 1 file	2 200	WITHOUT	Low level of AV plate on 1 IS	36.5	1.9	3" or 2" if part.
Test 3 (1)	WITHOUT	2	X		1 300 2 files	2 200	WITHOUT	Delta P max (1.5 m) on 2 files SS	204	10.7	12" or 8" if part.
Test 4 (1)	WITH	3	X		1 300 2 files	2 200	WITHOUT	Low level of AV plate on 2 IS	58	3.1	5" or 3.5" if part.
Test 5	WITH	2		X	900 1 file	0	WITHOUT	Not reached with pure insulation			
Test 6	WITH	2		X	430 1 file	0	WITHOUT	Not reached with pure insulation			
Test 7 (3) (with initial settling)	WITHOUT	2	X		1 300 2 files	2 200 2 files	WITHOUT	Delta P max (1.5 m) on 2 SS files	160 + 15 (1 st SS loss) + 35 (2 nd SS loss) = 210	11 (5.8 kg remain settled at the end of the test)	12"
Test 8 (3) (with initial settling)	WITHOUT	2	X		1 300 2 files	2 200 2 files	WITH (injection of insulation and of particulates is realised simultaneously)	Delta P max (1.5 m) on 2 SS files	135 (insulation) + 135 (particulates)	7.1	8"
Test 9 (12)	WITH	2	X		1 020 1 file	1 100 1 file	WITHOUT	Low level of AV plate on IS and SS	58.4	3.1	5" or 3.5" if part.
Test 10 (3)	WITHOUT	2	X		1 020 1 file	1 100 1 file	WITHOUT	Delta P max (1.5 m) on SS file	94.9	5	7" or 5" if part.
Test 11 (8) (with initial settling of insulation)	WITHOUT	2	X		1 300	2 200	WITH (particulate injection is realised after fiber bed creation)	Delta P max (1.5 m) on SS files	70 (insulation) + 20 (particulates)	5	6"

5. ELISA test

5.1 Objectives and requirements

The experimental program was carried out namely:

- to establish the relationships for Δp calculation depending on insulation and particle quantity for given boundary conditions as well as the dependence of Δp on temperature;
- to examine the effect of boric acid solution with a pH value equal to 9 on filter head loss;
- to examine the effect of water quality on filter head loss;
- to examine the effect of insulation and particle sample size and quality on head loss (sample size, way of sample preparation);
- to establish the way how the results obtained on ELISA test equipment will be applied to full-size equipment or to MANON conditions;
- to determine uncertainties of given results and to propose additional tests enabling to perform a complex analysis (to make modelling conditions as close as possible to real conditions).

The used vertical filter structure consists of two filters with a total area of $S = 0.1563 \text{ m}^2$. For the given surface area and flow velocity through the filter, the flow-rate of circulating fluid was determined. The flow-rate through the pump or filter was determined based on the calculation for real equipment ($Q = 1\ 100 \text{ m}^3/\text{h}$, $S = 9.55 \text{ m}^2$ – the surface are of the first row of filter in a filter box). The effect of variation the flow-rate on head loss was also studied.

The additional experimental program was carried out in the form of tests whose objective was to verify and quantify chemical and thermal effects of working fluid (hot water containing 2 000 ppm boron and treated with NaOH to pH 9) on defined samples, namely:

- effects of the working fluid on leaching the binding agent from insulation samples;
- degradation of insulation as a result of fibers coming lose and washed out and its time dependence.

To perform the experimental program on ELISA test equipment, the following insulation and particle samples were used:

- Insulation.

First, insulation mattress was cut lengthwise into 15 cm long pieces, then, by a second round of cutting, needed fraction was obtained.

- Particles:
 - Silica sand I (fine sand, non-ground).
 - Silica sand II (ground sand).
 - Fly ashes from an electric precipitator.

A uniform way of dosing was selected for all the tests: first, the sample was soaked in a small volume of water and fiberised by stirring and such a mixture was introduced in the test equipment. This procedure was applied also to the mixture of insulation and particles.

The test equipment respects the following requirements:

- to operate with hot water (up to 80°C) containing 2 000 ppm of boron acid and having a pH value of 9.3 (NaOH) without any effect on the test equipment base material;
- to perform tests under thermal equilibrium conditions;
- to assure a controlled flow-rate of the working fluid;
- to assure working fluid homogenisation by agitation;
- to enable monitoring of insulation behaviour during the tests and the quantification of insulation degradation under the chemical and thermal effects of the working fluid.

5.2 Tests and procedure of evaluation

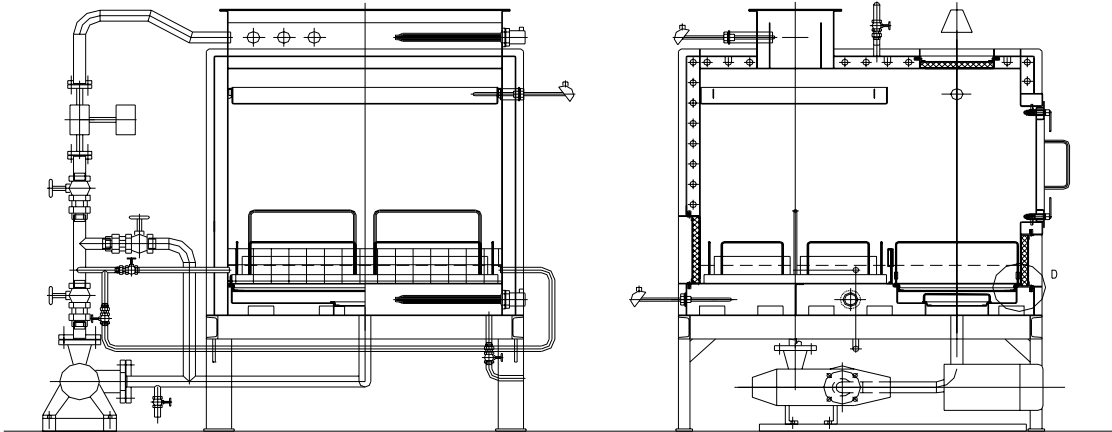
For the present experimental program, two types of thermal insulation were used:

- Type 1 – glass wool with resin as binding agent – trademark TELISOL.
- Type 2 – glass wool – trademark BOURRE.

Main test evaluation criteria were as follows:

- time-dependent weight loss of tested samples;
- time-dependent weight increase of insulation debris collected on individual filters;
- time behaviour of the chemical composition of working fluid (pH, density, viscosity);
- optical analysis of samples taken;
- definition of fiber length distribution-fractional composition of the initial sample and individual samples taken from filters;
- identification of globular particles encountered in the given sample.

Figure. ELISA tests



5.3 Results

5.3.1 Results of the ELISA tests

The main phenomena have been observed:

- a chemical effect appears when the temperature is more or equal to 40°C. 30% of the insulation mass is transformed after 96 hours;
- the size of the particulates is a critical parameter for the head loss of the fiber bed;
- when water used is not demineralised, a lot of precipitates appear, which increase strongly the head loss observed;
- these different parameters lead to an evolution of the head loss of fiber bed during time.

Some relationships are given below.

5.3.1.1 Relationships designed to determine Δp dependence on insulation and particle quantity and on temperature

The relationship for Δp calculation is as follows:

$$\Delta p = K \times \left[m_{TI} \times \left(1 + \frac{m_P}{m_{TI}} \right) \right]^a$$

Where: m_{TI} is the mass of insulation,
 m_P is the mass of particles.

The determined constants are applicable to a mixture of insulation and particles (fine non-ground sand I with an average fraction 125-250 μm). The above relationship with given constants is valid for a mixture of insulation and particles with an average size between 100 and 250 μm (i.e. more than 90% of particles belongs to the interval).

The experimental programme was performed using predominantly fine ground sand II with an average particle size between 100 and 200 μm .

To enable comparison of measurement results with Δp values calculated, values have been corrected in accordance with temperature dependence of Δp :

$$\Delta p = c \times t^b$$

The aforementioned relationships for Δp calculation depending on the amount of thermal insulation or a mixture consisting of thermal insulation and particles may be satisfactorily applied to the given type of insulation and particles and to the given boundary conditions.

The relationships are valid for the following fluids: demineralised water, hydrant (tap) water, H_3BO_3 solution in demineralised water with a pH value of 9.

The relationships cannot be used for a solution in mineralised (hydrant) water with a pH value of 9 due to substantial chemical effects and mutual interactions between the thermal insulation and the solution arising as early as after a few minutes or hours.

For the future, it will be necessary to determine limiting values for salts in water that is used to prepare solution under real conditions. This will enable to evaluate the effect of salts in terms of a macro-indicator on head loss behaviour.

5.3.1.2 Effect of boric acid solution, pH and water quality on head loss

To investigate the effect of boric acid solution, pH and water quality on Δp behaviour and value at different temperatures, some test results were realised. To compare test results in a maximum possible interval of insulation weight, namely from 0 to 1 650 g (the value of 1 650 g corresponds to a maximum insulation quantity for which a maximum Δp value was reached at a temperature of 70°C), Δp values were completed by linear regression.

From the results, the following conclusions may be drawn:

- The fluid temperature influences Head loss substantially.
- With the given insulation quantity and when using demineralised water with pH values of 7 or 9, head loss value almost does not change; this is proved by overlapping curves for the given temperature and selected parameters. No substantial chemical effect of thermal insulation and fluid on Δp was observed.
- Curve $\Delta p = f(M_{ti})$ for hydrant water with pH 7 and a temperature of 25°C is nearly identical with curves $\Delta p = f(M_{ti})$ for demineralised water pH 7, 25°C and demineralised water pH 9, 25°C. Mutual chemical interaction of thermal insulation and flowing fluid for the aforementioned fluids at a temperature of 25°C was not observed.

A detailed analysis of mutual chemical interaction of insulation fibres and boric acid solution (with different water quality) was performed by SAV office (Slovak Academy of Sciences) at Trencin University (Chapter 5.3.2). This analysis deals with the formation and identification of precipitate in the solution after adding some chemicals (boric acid, sodium hydroxide) and solution effect on insulation fibre degradation (formation of precipitates, formation of corrosion products, etc.).

5.3.1.3 Application of ELISA results to full-size equipment or to MANON conditions

Collected information was used to convert data measured on ELISA to MANON test equipment or to conditions of a pH 9 solution but for the time being without water that is normally used under real conditions, i.e. at NPPs (limiting values of salt content). Conclusions are valid merely for demineralised water or hydrant water and only up to 25°C. As an example, conversion of results for hydrant water with pH 7 and 25°C to demineralised water with pH 9 and 70°C can be used.

Table 2

Coefficient of chemical/temperature effect		
	Mti introduced	Mti collected
K_{ch,t}	= Mti_{pH 9}/Mti_{pH 7}	= Mti_{pH 9}/Mti_{pH 7}
E19/E 4 (15)	2.1	2.0
E19/E 4 (18)	2.2	2.1

Mti – mass of insulation

The above coefficient $k_{ch,t}$ can be used to convert the amount of insulation (Mti) introduced or collected for the temperature of 70°C and boric acid solution with pH 9, but when demineralised water is used. The coefficient may be used to convert the results within stated boundary and input conditions.

5.3.2 Results of the chemical effects

A specific study was performed on the main observed phenomena when water used is not demineralized. In this case, a lot of precipitates appear, which increase strongly the head loss observed.

5.3.2.1 Precipitate in alkaline solutions

During ELISA tests, it was observed that if tap water is used (initial pH of about 8 at 20°C), after adding 2g/l H₃BO₃ and NaOH to adjust pH of the solution to 9, precipitates are formed and after adding NaOH, circulating fluid change into a turbid suspension. These precipitates affect substantially the course of the experiment since they are collected in the insulation bed on filters and reduce thus permeability of the bed for circulating fluid which results in a substantial increase of head loss.

Consequently, a study was performed to define conditions necessary for the formation of calcium and magnesium precipitates in alkaline H₃BO₃ solutions, namely:

- Identification of limiting concentration for turbidity formation in solutions containing Ca²⁺ ions, optical investigation of temperature and time effects on turbidity formation.

- Identification of limiting concentration for turbidity formation in solutions containing Mg^{2+} ions, optical investigation of temperature and time effects on turbidity formation.
- Identification of limiting concentration for turbidity formation in solutions containing Ca^{2+} and Mg^{2+} ions, optical investigation of temperature and time effects on turbidity formation.

Formation of precipitates in systems prepared using tap water was plausibly attributed to the effect of changed pH value on the solubility of some salts. In tap water, calcium and partly also magnesium cations are encountered in the form of hydrogencarbonates (the so-called temporary hardness of water) and chlorides. This phenomenon can be explained based on a thermodynamic analysis of dissociation of dihydrogen carbonic acid in solutions with different pH.

At pH = 8 corresponding to the acidity of tap water used on ELISA loop, all the dissolved calcium salts occur in the form of hydrogencarbonates and chlorides. When pH increases to 9, the content of carbonate ions, CO_3^{2-} increases substantially and in such a way the product of calcium carbonate solubility [$K_s(CaCO_3) = 10^{-8.48}$] is exceeded which results in precipitate formation. The amount of precipitate depends on the content of calcium ions present in tap water in the form of hydrogencarbonates.

Precipitate may be formed not only as a result of an increased concentration of carbonate anions when pH value is increased but also as a result of reaction of soluble calcium and magnesium salts (e.g. chlorides) encountered in the system with trihydrogen boric acid. Taking into account a wide variety of borates and their hydrates that may arise in the system and taking into account the absence of relevant thermodynamic data (solubility products), additional investigations have been conducted to determine experimentally limiting concentrations of calcium and/or magnesium ions necessary for precipitate formation under various temperatures.

Turbidity or precipitate formation was evaluated using the following scale:

- CRO – clear solution.
- SZK – slight turbidity.
- SZR – slight precipitate.
- VZR – striking precipitate.

Results obtained for individual types of investigated systems are tabulated below:

Ca²⁺ concentration [mmol.dm⁻³]	Temperature				
	20°C	40°C	65°C	70°C	80°C
100.62	SZR	ČRO	ČRO	ČRO	ČRO
67.08	SZK	ČRO	ČRO	ČRO	ČRO
33.54	ČRO	ČRO	ČRO	ČRO	ČRO

Mg²⁺ concentration [mmol.dm⁻³]	Temperature				
	20°C	40°C	65°C	70°C	80°C
137.81	ČRO	ČRO	SZR	VZR	VZR
91.88	ČRO	ČRO	SZK	SZR	VZR
45.94	ČRO	ČRO	ČRO	ČRO	ČRO

Concentration		Temperature				
Ca ²⁺	Mg ²⁺	20°C	40°C	65°C	70°C	80°C
[mmol.dm ⁻³]						
67.08	91.88	ČRO	ČRO	ČRO	ČRO	VZR
33.54	45.94	ČRO	ČRO	ČRO	ČRO	SZR
16.77	22.97	ČRO	ČRO	ČRO	ČRO	ČRO

In case of calcium ions, the limiting concentration is somewhere between 33.5 mmol.dm⁻³ and 67.1 mmol.dm⁻³; in case of magnesium ions, it is limited by values 45.9 mmol.dm⁻³ and 91.9 mmol.dm⁻³.

In case of parallel occurrence of Mg²⁺ and Ca²⁺ ions, solutions with $n(\text{Mg}^{2+})/n(\text{Ca}^{2+})$ ratios of 1.37 were investigated. Precipitate formation was observed at concentrations lower than limiting concentrations specified for individual cations.

Crystalline magnesium hydrocarbonates, calcium carbonate and some chlorides were detected by a qualitative powder radiographic diffraction analysis of precipitates. They were formed in the precipitate from the liquor after precipitate dehumidification.

The most important seems to be the fact that a substantial content of amorphous phase was proved in the precipitate. This complies with the results of ELISA tests when the filter cake was very soon clogged with gel mass of precipitates and head loss increased dramatically as soon as in the initial phase of the experiment.

5.3.2.2 Leaching assessment

Exposure of glass to liquid media is accompanied with glass corrosion. It is a complex process consisting of several elementary phenomena including chemical reactions and diffusion. Glass corrosion results in gradual dissolution of glass accompanied in some cases also with formation of insoluble products that are formed on the surface of corroded glass and are dispersed mechanically throughout the liquid medium. When exposed to the effects of liquid media, chemical resistance of glass fibers depends on four essential factors:

- temperature;
- glass composition;
- leaching liquor composition;
- hydrodynamic conditions.

The simplest seems to be the qualitative assessment of temperature effects when temperature increase is always connected with an increased rate of fiber degradation. Glass composition together with leaching liquor composition can be considered as two decisive factors influencing the corrosion rate. Effects of some oxides on chemical resistance of glass (i.e. also on corrosion rate) are not always unambiguous. On the other hand, some oxides may be identified that positively increase chemical resistance of glass. They include particularly zirconium oxide and aluminium oxide. On the contrary, oxides of alkali metals reduce chemical resistance of glass.

A first study has been performed to investigate the kinetics of glass fiber dissolution:

- Definition of time behaviour of concentrations of selected dissolved components.
- Measurement of kinetics of glass fiber dissolution under different temperatures.
- Investigation of changed fiber morphology and precipitate formation on fiber surface during the leaching experiment using scanning electron microscope.

Composition of investigated glass was obtained by chemical analysis of glass fibers. Composition of leaching liquor was specified as aqueous solution of trihydrogen boric acid with pH value adjusted by adding sodium hydroxide to 9 at a laboratory temperature. In such an environment, there is no use to investigate qualitatively the amount of sodium cations released by leaching from glass fiber since it is of the order of magnitude lower than the amount of Na⁺ cations introduced in the leaching liquor when adjusting its pH value.

In order to assess the effect of chemical composition of leaching liquor on the kinetics of leaching, particularly in relation to potential passivation of glass surface by formation of insoluble precipitate films and in relation to a potential increase of driving force by reducing the concentration of leached glass components as a result of precipitation in alkaline borate environment (as concluded from its thermodynamic analysis presented in the previous part of the report, borate leaching liquor is in fact an alkaline buffer with a maximum buffering capacity), a series of tests was performed also with distilled water.

The morphology of the corroded glass fibers surface was studied after 8- and 48-hour exposure of fibers to borate corrosion liquor at a temperature of 80°C using scanning electron microscope.

In accordance with the results of chemical analysis of glass fibers, powdered glass batch was prepared using the different corresponding chemicals.

The results are characterised by time dependences by a parameter expressed in mg of glass per m² of glass surface for individual determined elements X (X = Na, K, Mg, Ca, Si).

Three hundreds chemical analyses (two parallel determinations plus one blank test per each point) have been realised. A more detailed investigation of leaching kinetics would require more parallel determinations, longer period of investigation (more than 8 hours) or, possibly, a thicker frequency of points on the time axis and a combination of static and flow leaching tests. In such a way, some stochastic effects expressed in oscillation behaviour or discrete behaviour of leaching curves would be eliminated.

Consequently, obtained results may be evaluated rather on a semi-quantitative level.

Leaching of crushed glass in distilled water

A substantial effect of temperature on leaching kinetics can be identified unambiguously. In case of silicon, sodium and potassium, temperature increase by 15°C resulted in a marked increase in leaching rate. On the other hand, in case of calcium and magnesium, no substantial effect of temperature was observed. This is caused by the fact that, after leaching from glass matrix, they form precipitates of calcium and magnesium hydroxides or alkaline borates and silicates in the alkaline environment.

Tests performed at a temperature of 40°C pointed out that leaching rate is very low and study of kinetics would require measuring of kinetic curves in the interval of days and not hours. In the interval of 8 hours at a temperature of 40°C, concentrations were obtained comparable with (only a slightly higher than) the blank test.

A typical characteristic of glass leaching in distilled water is a distinct change in pH resulting from increasing concentration of leached alkali (sodium hydroxide and potassium hydroxide) with practically zero buffering capacity of distilled water. Consequently, with the process of leaching, pH is increased and at the same times also the rate of dissolution of silicate net.

Leaching of crushed glass in alkaline solution of trihydrogen boric acid

Similarly to distilled water, also with trihydrogen boric acid a substantial effect of temperature on leaching kinetics was observed. In this case, owing to buffering capacity of trihydrogen boric acid solution, a substantial increase in concentration was observed also for magnesium and calcium. An interesting piece of information obtained is the non-uniformity of kinetic curve behaviour for silicon that corresponds to a combined effect of dissolution of silicate net, on the one hand, and formation of silicate and borate-silicate precipitates in leaching liquor, on the other.

Leaching of glass fibers in alkaline solution of trihydrogen boric acid

In case of BOURRE glass fiber, the important is that the fiber is not obtained by drawing but by fiberisation on a rotary disk. That is why it is very difficult to characterise the material (consisting of small fragments of fibers with a different thickness and length, glass droplets and particles) by specific surface. For the purpose of sample surface calculation, an infinite fiber was assumed with a representative radius of 10 µm. The situation is complicated also by a non-uniform behaviour of the kinetic curve. To clarify the substance of the observed difference, repeated measurements in longer time intervals would be needed.

6. Conclusion

IRSN has performed an experimental program, from 2000 until now, concluding on the potential sump screens plugging for the 58 existing French units. A lot of experimental data have already been obtained and conclusions drawn on this issue. At the present time, an agreement exists between all the French concerned organisations on the need to consider the problem and to implement improvements on all these units [8].

The knowledge evolution gained by IRSN could be internationally used. IRSN intends to provide it under the OECD's Auspice. Moreover, IRSN considers the current knowledge is not enough substantiated about a few main fields needed to precise design requirements to assess globally this issue. The pending problems are related to the debris generation and the water chemical effects on the fiber bed fixed on the filters [9].

An experimental program is proposed by IRSN to solve these two open questions in a short term. This program could be of interest for a great number of countries. Therefore, IRSN propose to perform it under the OECD's Auspice in compliance [10] with the following conditions:

- Concerning the debris generation, the proposal consists to realise the experimental program in EREC (RUSSIA), to share the global cost (EUR 1.8 million) between the interested partners and to include in this program their specific tests.

- Concerning the chemical effects on the fiber bed fixed on the filters, the proposal consists to realise the program in VUEZ (SLOVAKIA) under IRSN funds (EUR 0.44 million) and to allow the partners involved in the debris generation program to take benefit of the results and the models. If some partners want to perform focused tests, their cost will be in charge of these partners.

7. References

- [1] Synthesis report IRSN/DES/SERS/400, 14 October 2003.
- [2] IVANA report – VUEZ SA – TS-OTS-1318, May 2002.
- [3] VITRA report – EREC – MT DA 118 1.091-02, 2002.
- [4] MANON report – VUEZ SA – TS-OTS-1336, December 2002.
- [5] MANON report – VUEZ SA – TS-OTS-1398, October 2003.
- [6] ELISA report – VUEZ SA – ZZ-OTS-1331, August 2002.
- [7] ELISA report – VUEZ SA – TS-OTS-1397, October 2003.
- [8] Armand, Y., J.M. Mattei, Albuquerque Workshop – Issue on French PWR, IRSN (France), 2004.
- [9] Armand, Y., J.M. Mattei, Albuquerque Workshop – Opened questions, IRSN (France), 2004.
- [10] Armand, Y., J.M. Mattei, Albuquerque Workshop – Action plan proposal, IRSN (France), 2004.

EMERGENCY CORE COOLING STRAINERS – THE CANDU EXPERIENCE

A. Eyvindson and D. Rhodes
Atomic Energy of Canada Limited, Canada

P. Carson
New Brunswick Power, Canada

G. Makdessi
Ontario Power Generation, Canada

Summary

The Canadian nuclear industry, including Atomic Energy of Canada Limited (AECL) and the four nuclear utilities (New Brunswick Power, Hydro-Québec, Ontario Power Generation and Bruce Power) have been heavily involved in strainer clogging issues since the late 1990s. A substantial knowledge base has been obtained with support from various organisations, including the CANDU Owners Group (COG), AECL and the CANDU utilities. Work has included debris assessments at specific stations, debris characterisation, transport, head loss measurements across strainers, head loss models and investigations into paints and coatings. Much of this work was performed at AECL's Chalk River Laboratories and has been used to customise strainer solutions for several CANDU (PWR-type) stations. This paper summarises the CANDU experience, describing problems encountered and lessons learned from strainer implementation at stations.

Between 1999 and 2003, AECL supplied strainers to six different CANDU stations, representing 12 units with a total power output of approximately 8.2 GWe. Each station had unique needs with respect to layout, effective area, allowable head loss and installation schedule. Challenges at various sites included installation in a covered trench with single-point access, allowing for field adjustments to accommodate large variations in floor level and pump suction location, on-power installation, very high levels of particulate relative to fibrous debris, and relatively low allowable head loss.

The following are key points to consider during any station assessment or strainer implementation:

- a realistic testing model and method is essential for accurate predictions of head loss, and the limits of the model must be understood;
- assessment of station debris must be sufficiently conservative to overcome uncertainties in debris generation and transport models;
- appropriate and reliable data (e.g. flow rate, layout, size of test model, method of debris generation and deposition, test duration), with true representation of the various field conditions, is necessary to select the appropriate strainer solution;

- flexibility in the strainer design permits adaptability to different plant layouts and schedules, while maintaining basic design qualification;
- innovative header design can improve strainer efficiency;
- reducing the strainer footprint-to-surface area ratio is desired; and
- detailed review of specific station layout is critical prior to final design, fabrication and installation.

The experience attained in Canada shows that practical solutions for strainer issues can be developed to meet a wide range of needs. However, diligence is required to ensure that the solution has adequate (but not undue) conservatism to accommodate uncertainties, that station-specific design issues are properly addressed, and that the installation schedule for new strainers is suitable. Interaction with the regulator early in the project also helps to bring any outstanding issues to the forefront when there is still sufficient time to make adjustments, and to facilitate subsequent approval.

Background

Following the Barsebäck incident in Sweden, Canadian nuclear stations and Atomic Energy of Canada Limited (AECL) began assessing the current status of emergency core cooling (ECC) systems in Canadian and off-shore CANDU stations. Early on, it was recognised that the available information was inadequate to address CANDU needs, and a research programme was developed. This research, carried out primarily at AECL's Chalk River Laboratories, with various funding sources, focussed on characterising the head loss across a strainer as a function of a multitude of variables. These variables were selected to encompass CANDU station configurations and included type and quantity of fibrous and non-fibrous debris, water temperature, pH, flow rate, strainer configuration, debris generation and deposition, and test duration, among others. As the database expanded, the validity of an existing correlation was evaluated for its applicability to the conditions tested. When it was found not to provide acceptable agreement, a new correlation was developed for specific CANDU-type applications.

Concurrently, in consultation with the Canadian Nuclear Safety Commission (CNSC), the utilities began to evaluate the suitability of their existing ECC systems. These evaluations included debris assessments within the reactor building, and analyses of accident scenarios. In its role as reactor designer, AECL assisted off-shore CANDU stations in similar tasks. Eventually, stations were ready to proceed towards a solution that would satisfy the regulator (CNSC). Typically, the solution involved a combination of strainer replacement and some debris replacement. Interaction with the regulator continued throughout the process to ensure compliance. Most stations have now completed, or are near the end of, their strainer programmes and have satisfied the regulator that their ECC system configuration now meets safety requirements.

Testing

Considerable effort has been expended in Canada to characterise and quantify debris that may reach the ECC strainers. A large portion of this work was funded through the CANDU Owners Group (COG), a body representing CANDU station owners and developers. The results of walkdowns at stations were used as a starting point. Similar debris to what was found in the stations was obtained for the testing. Visual examination, including scanning electron microscope (SEM) imaging, was performed early on to provide a baseline. A variety of small-scale tests were then performed in several

different facilities at Chalk River Laboratories. These included measuring material strength and density, the deposition rate of particulate and fibrous debris, the effect of temperature on the material structure, and the effect of particulate size on generic clogging. In addition, several bench-top flow loops were set up to observe flow passage through a strainer. A significant amount of information was generated and served to direct future testing.

A medium-scale test facility was then built for more rigorous testing. This is a Jacuzzi-sized tank with piping to connect to a pump. A stirring device in the rig allows debris to mix, while a heater/chiller maintains the desired water temperature. The strainer surface filters the debris as the water flow passes through it. Any debris passing through the strainer can be caught in a downstream trap if desired, and a heat exchanger scaled to CANDU size can be piped in. The downstream components can be used to evaluate different hole sizes in the perforated metal in terms of plugging downstream components. The strainer surface area and orientation can be adjusted in the rig. The rig is fully instrumented and includes flow and temperature control. Over one hundred and fifty tests have been performed in this facility, ranging in duration from a less than an hour to three months. Figure 1 shows the medium-scale facility.

Figure 1. Medium-scale facility



A large-scale facility is also available. This facility was commissioned for development of AECL's *Finned Strainer*[®] product. It accommodates one complete *Finned Strainer* module, which, depending on the application typically has 20-33 m² available straining surface area. It consists of a large lined tank (approximately 1.5 m deep, 2.5 m wide and 5 m long) connected to a large piping system. Temperatures, pressure drop across the strainer, test duration and flow rate are monitored during testing. Figure 2 shows the large-scale facility.

Figure 2. Large-scale test facility



Development testing using the large-scale facility included testing fibrous and particulate debris, as well as the ability of the strainer to accommodate large debris such as rubber gloves, plastic bags, etc. Extensive vortex testing was also performed. In these tests, the flow rate, water level above the strainer, pressure drop and debris loading were all investigated to determine their effect on the formation of hollow-core vortices, which could result in air ingestion and pump damage.

The large-scale facility was also used to confirm the performance of each strainer supplied to a customer.

Finned Strainer[®] is a registered trademark of AECL.

Vortex testing

Of considerable concern for the CANDU utilities was the potential for the formation of hollow core vortices. With a large pressure drop across the strainer, stations needed assurance that air ingestion due to vortices was not possible. A number of tests were performed in which the submergence of the strainer (the distance between the water surface and the upper-most straining area) was fixed and the flow rate was varied to see if a vortex would form. This was done for several different submergence levels and debris loading conditions. Table 1 shows the results of one set of tests, which forced the flow through a much smaller section (~90 mm wide) of the strainer than would normally be expected. This test simulated the effect of the flow concentrating at the screen nearest the pump intake. This could only happen when there is no debris on the strainer; once debris builds up, the extra resistance distributes flow to the whole screen area, effectively reducing the likelihood of vortices.

Table 1. Vortex test results*

Flow (L/s)	Submergence (mm)	Pressure drop (kPa)	Hollow core vortex?
150	450	28 (some debris)	No
100	375	7 (clean)	No
75	375	3 (clean)	No
75	300	3 (clean)	Yes (3 mm dia core)
55	300	1 (clean)	No
55	225	1 (clean)	Yes (occasional, 3 mm diameter core)

* The strainer area was not identical for each test.

The results of the vortex tests were used to refine the strainer design for a given station, either by adjusting the submergence or the surface area to prevent flow concentration that could cause vortexing.

Head loss correlation

A head loss correlation available publicly was evaluated for use in CANDU applications. However, as the test database expanded, it became clear that this correlation was not suitable for CANDU. A new correlation was then developed, based on the tests performed. However, even this correlation was found to be limited in its range of applicability. For instance, a high particulate-to-fibre volume ratio was found to result in significantly higher head loss than predicted. The development of the correlation highlighted the uncertainties in many of the parameters (e.g. materials, order of deposition on the strainer) and the need to perform rigorous testing for each customer in a large-scale facility.

Debris

The debris types common to CANDU stations include fibrous debris (fibreglass), calcium silicate, marinite (a dense form of calcium silicate), rust, dust, dirt and paints (coatings). Samples of these were obtained from stations and from commercial suppliers, using the same suppliers as the stations where possible.

Fibrous debris was photographed using SEM imaging. Fibre diameters from different sources were compared. For head loss testing, a leaf shredder was used to break the fibrous debris into smaller

pieces. The fibrous debris was then soaked prior to insertion in the test tank, as the debris reaching the strainer in CANDU stations would also be wet.

Calcium silicate was broken up using an impact hammer. A variety of screen sizes could be used with the hammer mill to affect the resulting particulate size distribution. The effect of the different sizes was evaluated in the testing. Other experiments were performed to determine the rate of erosion of calcium silicate pieces exposed to flowing water. Of concern was whether significant debris could be generated by erosion of large pieces of material that fall into the flow during an accident but are not transported to the strainer. Significant erosion of large chunks of material could lead to delayed deposition of calcium silicate on the strainer, which could lead to different results than for a fully-mixed debris bed.

Iron oxide of two different particulate size distributions was purchased to represent rust.

Paint chips were prepared at Chalk River Laboratories and added to the debris mixture for the tests. In addition, a detailed test program was performed to evaluate the performance of paints and coatings typically used in CANDU stations under accident scenarios. The intent of this testing was to determine if, during an accident, the coatings would be likely to degrade to a degree that could impact strainer performance. This testing involved irradiation, exposure to high-temperature, high pressure transients, and long-term exposure to post-accident conditions. Tensile and adhesion tests were performed periodically.

Relevant accident scenarios for CANDU stations

CANDU stations are a subset of pressurised water reactors (PWRs). In these reactors, heat from the reactor is transported by means of high temperature, high pressure heavy water in the primary heat transport system (PHTS) to a steam generator. The energy is then transferred to light water in the steam generator for driving the turbine.

In the PHTS, the main coolant pumps force water into headers, from which multiple small feeder tubes (between 380 and 480, depending on the station) pass through the reactor core and regroup in another header on the other side (Figure 3). From here, the water passes through a steam generator before re-entering the PHTS pump. The feeders are located in an insulated “feeder cabinet”. A break in any of the PHTS piping is considered a loss of coolant accident (LOCA). In a CANDU 6 station, such an accident triggers a high-pressure injection system, in which pressurised water is injected into the PHTS, and a dousing system sprays cool water into containment to reduce the pressure. This is followed by medium-pressure injection, consisting of emptying a large tank of water, located in the reactor building ceiling, into the system. The water added during high- and medium-pressure injection eventually leaks out of the break in the PHTS and fills the reactor building sump to a level sufficient to initiate the low-pressure injection system. When this system is operating, the basement water is filtered through a strainer prior to passing through the ECC pumps, heat exchangers and back into the PHTS to provide continued cooling to the reactor core. The low-pressure injection mission period is typically three months. Figure 4 shows the high-, medium- and low-pressure injection systems for the CANDU 6 station.

Multiple-unit CANDU stations have a single “vacuum building” connected to all four units that prevents pressure build-up during a LOCA, instead of the dousing system used in CANDU 6 station. Water for high-pressure injection is contained in a large storage tank. Low-pressure injection is similar to that described above, except that for Darlington, all four units share the same strainer. Figure 5 shows a schematic of the system.

Figure 3. CANDU 6 header and feeder arrangement

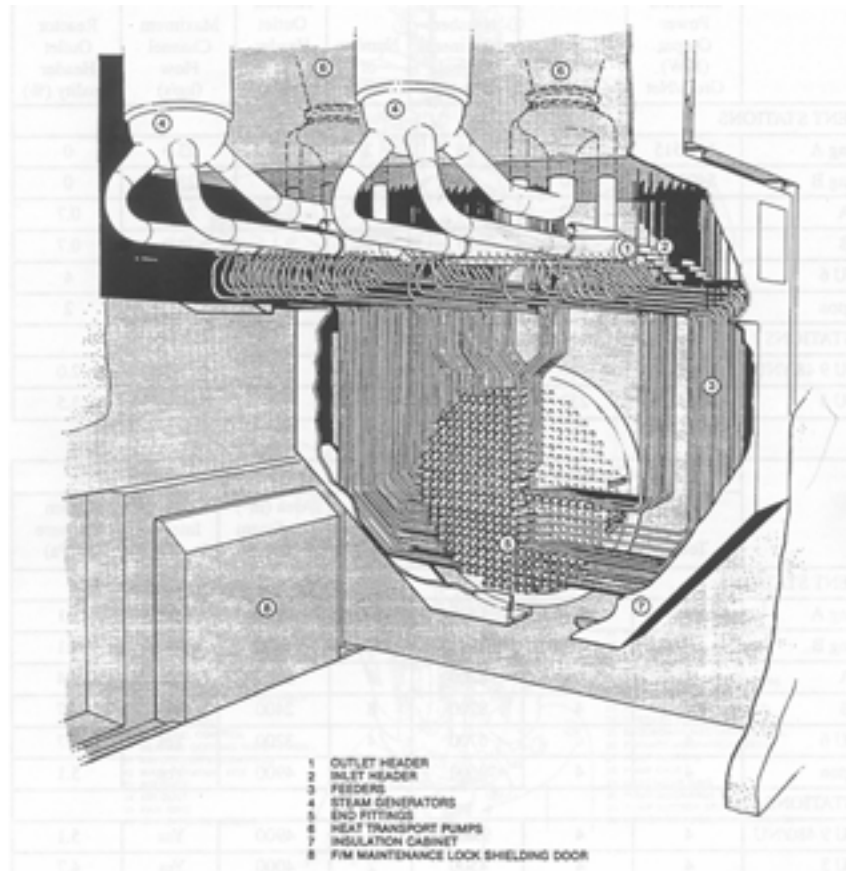


Figure 4. CANDU 6 emergency core cooling system

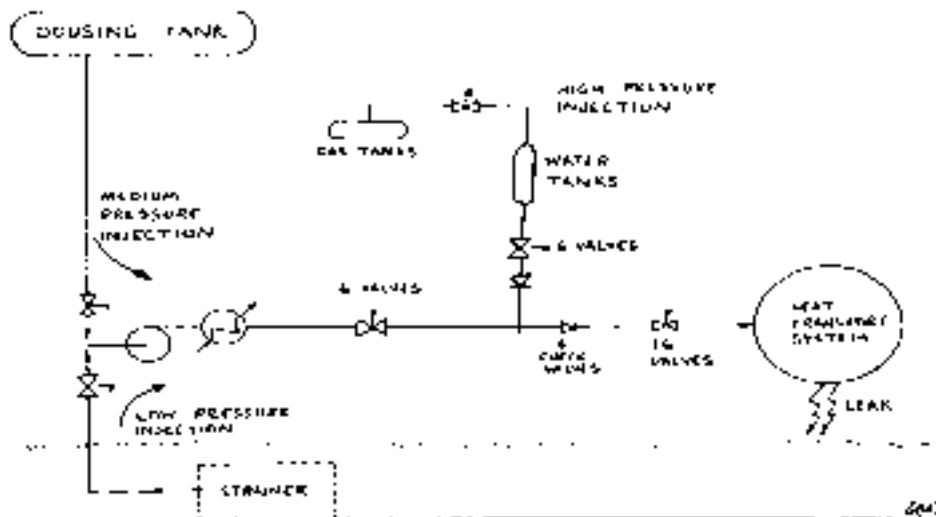
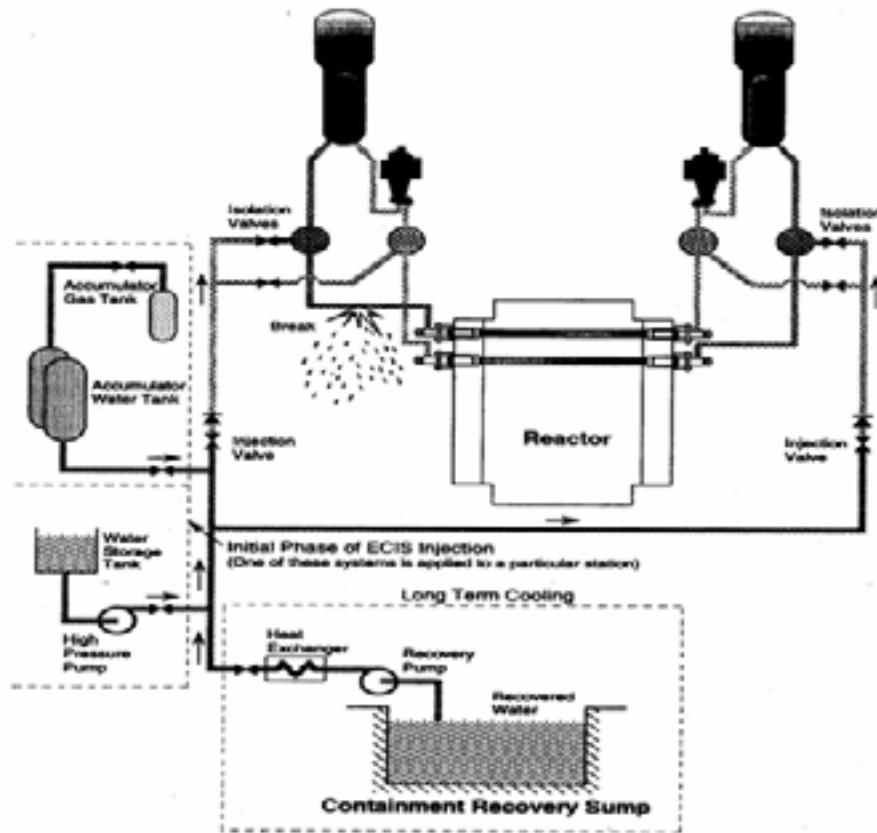


Figure 5. Typical multi-unit CANDU emergency core injection system



One of the main postulated sources of debris is from the feeder cabinet. A break in any of the feeders could result in a jet of high temperature, high pressure water impacting upon the insulation in the feeder cabinet, liberating large amounts of material which then could flow towards the sump. Other debris from this and other rooms along the way, such as fibreglass or calcium silicate insulation, dust, paint flakes, rust, or loose trash could also get transported to the sump. All this debris must be filtered by the strainer.

A break in the header or the large piping may occur in a variety of areas and sizes, each scenario liberating a different amount and type of material. Thus a multitude of possibilities must be assessed.

Failure of the strainer by clogging could cause the ECC pump(s) to cavitate, potentially leading to insufficient heat removal from the reactor core. Failure of the strainer by debris passage (e.g. due to large perforations or partial collapse) could result in damage to the ECC pumps, clogging of heat exchangers or clogging of pressure tubes in the reactor core. All of these could lead to unacceptable heat build-up in the reactor core.

Customer needs

While the background research was in progress, stations performed assessments of their ECC systems to determine requirements for any upgrades. A key part of this task was the debris assessment, in which every room in which water could flow during a LOCA was examined to determine the type and amount of debris that could become dislodged and could potentially travel to the ECC sump. Assessments were made for all applicable scenarios.

Based on the above assessment, strainer requirements were defined. The existing strainer(s) was then evaluated against these requirements. In most cases, deficiencies were noted and upgrading the strainer was initiated, based on the identified needs, available space and other restrictions.

The CANDU stations that have chosen to meet their regulatory requirements by upgrading their strainers are shown in Table 2.

Table 2. Upgraded strainers at CANDU stations

Station	Rated flow (L/s)	Old surface area (m ²)	New surface area (m ²)	Old footprint (m ²)	New footprint (m ²)	Number of ECC strainers per unit
Point Lepreau	606	6	79	1.1	12	2 ^a
Gentilly-2	606	6	100	1.1	14	2 ^a
Pickering A (four units)	340	~4	~64	~2	~7	2
Pickering B (four units)	707	4	110	~3	22	1
Embalse ^c	625	6	100	1.1	15	1 ^b
Cernavoda 1 ^d	625	6	79	1.1	12	2 ^a
Darlington (4 units)	2 190	~10	1 200	~6	70	1 ^e

^a One 100% capacity strainer per pump, only one pump is used at a time (two pumps total).

^b Two pumps connected to one 100% capacity strainer, only one pump typically operating at a time.

^c This station is located in Argentina.

^d This station is located in Romania.

^e Single strainer is connected to all four units.

For the CANDU stations listed above, models generally predict that approximately 10 m³ of fibrous debris and lesser quantities of other debris types may reach the strainer, although the amounts vary depending on the break size, location and the particular station's debris types. In some plants, the quantity of calcium silicate pipe insulation that could reach the strainers has been a concern, so measures are being taken to remove or protect some of this material, and to prevent its use in new plants.

The *Finned Strainer*[®] units designed and manufactured by Atomic Energy of Canada Limited for retrofit into these stations are very compact, allowing a large surface area for filtering to be installed in a small space, which allows them to fit into crowded plants. They are also modular, allowing flexibility in the layout and size.

Utility/supplier interactions

During the early testing period, a close working relationship was developed between the utilities and AECL. The utilities had a large input into the test programs and, in many cases, visited AECL to

view the test facilities. These close relationships were maintained during the commercial contracts, which overlapped the background test period. In fact, the schedule or even scope of the COG-funded background testing was sometimes revised to suit the utilities' immediate strainer retrofit issues, provided that all other COG members agreed to the change. In this way, the utilities gained confidence in AECL's capabilities, and AECL had the flexibility to address utility concerns quickly.

The high level of communication between supplier and client ensured a full understanding by AECL of the layout restrictions, installation schedule and operating sequence for each station. Detailed knowledge of layout restrictions was particularly important at Pickering B. In this four-unit station, the strainer was to be located in a covered trench, approximately 50 feet long, 4 feet deep and 4 feet wide, with a small opening at one end. The size of the trench limited the size of the strainer. Installation was also extremely challenging, due to the confined area and the necessity to work in plastics. Because the trench cover was permanent, the strainer had to be lowered in modules into one end of the trench. Typically, each module consisted of a section of header, several perforated fins (which provide the bulk of the straining area) and bracing. The strainer is shown in Figure 6. A "railroad track" was built on the bottom of the trench and each module was rolled on the track along the trench until it butted up against the preceding module. Modules were fastened together in order until the entire strainer had been assembled. A mock-up of the trench was fabricated at site to provide training for personnel prior to assembly in the real trench. This was an important means of preventing difficulties during on-site assembly.

All strainers supplied to the utilities were pre-assembled at AECL to test all hardware prior to arrival at site. Station personnel were invited to Chalk River Laboratories to witness strainer fabrication in the sheet metal shop and to become familiar with the equipment prior to installation at site. Not only was this an important training opportunity for station personnel, their feedback was needed to ensure that installation issues were resolved before the equipment arrived at site. This proved exceedingly valuable. The pre-assembly was also useful to verify the steps in the operating manual, and was key to the smooth assembly of each strainer at site. Figure 7 shows a typical CANDU 6 strainer installed at site.

The Darlington NGS strainer replacement project was also challenging. The first major issue was the large quantity of particulate debris (originating from calcium silicate insulation). This necessitated a very large strainer, shown in Figure 8, having over ten times the surface area at other CANDU plants. The other major issue was the desire to install the unit while at power. To achieve this, the strainer was installed on top of the existing sump grating, and used the existing grating as part of the structure of the new strainer. As it turned out, the installation was completed very smoothly and ahead of schedule, leaving all parties very pleased with the outcome.

Minimising the footprint for a given required strainer surface area was a key requirement for each station. At Embalse, this was complicated by the existence of a non-structural 'L'-shaped wall separating the two sump inlets. Although a single strainer joining both sumps was desired, removal of the wall would extend the outage time to an unacceptable duration. Eventually, a complete reconfiguration of the initially-accepted layout was proposed, in which the strainer snakes around the end of the wall and doubles back to connect to both suction pipes. This option was accepted and resulted in a much shorter installation time and reduced costs because the wall could be left as is. A further challenge for this project was to ensure that the design had sufficient flexibility to accommodate the measurement uncertainties in the location of the suction pipe inlets and in the elevation of the basement floor where the strainer was installed. A trip to the site to inspect the strainer area, clarify the requirements, and identify customer needs and wishes was key to the success of this project.

Figure 6. Pickering B *Finned Strainer* pre-assembled at AECL shop (top) and installed in covered trench at Pickering (bottom)



Figure 7. Typical CANDU 6 *Finned Strainer*



Figure 8. Darlington NGS *Finned Strainer*



Large-scale testing

Each strainer supplied by AECL was originally sized and configured based on the background test results. In addition, station-specific tests were conducted in the large-scale facility to confirm that the strainer met the head loss requirements stipulated by the customer. To qualify a strainer for its intended use, one full-scale module was placed in the tank and connected to the piping system. If the module represented 1/5th of the total strainer surface area to be supplied to the customer, then 1/5th of the full-scale debris was prepared for the test. As with the debris, the flow rate was scaled based on the ratio of full-scale surface area to test surface area in order to obtain the desired approach velocity. The temperature was set to the predicted station value. Once the tank was filled, the pump was started and debris was added. All relevant parameters were monitored throughout the test. The test report provided to the customer was later used by them to satisfy the regulator that the strainer was fully qualified.

Regulator interactions

For the Canadian utilities, acceptance of their proposed strainer solutions by the CNSC was required. This was facilitated because the CNSC had some previous exposure to the head loss testing being performed at AECL. By maintaining an open relationship with the regulator, AECL was able to understand their concerns and ensure that these were addressed in the strainer testing and design. Thus when final submissions to the CNSC were prepared by the stations, there were no last-minute issues to cause delays and concerns. In fact, Gentilly 2 asked AECL to attend their meeting with the regulator to make the presentation on their behalf.

Summary

A large body of knowledge relating to emergency core cooling strainers exists in Canada. This knowledge has been acquired through the co-operation of many parties, including utilities, strainer designers and COG. A great deal of cooperation and communication between utilities, designers and the regulator existed throughout the research, development and supply phases. This has permitted the knowledge to be utilised to provide effective solutions to CANDU ECC strainer issues. Stations are nearing the end of their ECC strainer programs and the industry is looking to move on to other challenges.

CHARACTERISATION OF LATENT DEBRIS FROM PRESSURISED WATER REACTOR CONTAINMENT BUILDINGS

Mei Ding, Amr Abdel-Fattah, Bruce Letellier, Paul Reimus, Stewart Fischer
Los Alamos National Laboratory (USA)

Tsun-Yung Chang
Nuclear Regulatory Commission (USA)

Executive summary

When accounting for the total amount of debris that may be present in a pressurised water reactor (PWR) containment pool during operation of the emergency core cooling system (ECCS), it is important to include a reasonable estimate of the latent dirt and foreign material that can be found in containment in addition to the debris generated by a high-pressure pipe rupture. Past and recent testing has shown that even small volumes of fibrous debris present on an ECCS sump screen can very effectively filter particulates that are present in the sump pool, leading to significant pressure losses across the composite debris bed. Debris present during routine operations that is subjected to containment spray and pool transport may contribute a significant source of particulate and perhaps fiber material. Because the PWR industry is working to estimate the quantity of latent debris present in containment, Los Alamos National Laboratory (LANL) is working, under the direction of the United States Nuclear Regulatory Commission (USNRC), to characterise the material composition and the hydraulic flow properties of actual plant debris samples. Beginning in August 2003 and ending in March 2004, this study is expected to quantify particulate and fiber debris parameters, such as the specific surface area and flow porosity that are critical to the proper application of the NUREG 6224¹ head-loss correlation. Microfiltering, optical microscopy, and organic dissolution chemistry tests are being used to fractionate the fibrous and particulate components. All tests are being performed at the geochemistry laboratory at the Isotope and Nuclear Chemistry Facility, Chemistry Division (C-INC), LANL, which has the necessary analytic equipment to make direct measurements of the hydraulic flow properties and to handle low-level radioactive PWR latent debris material. The success of this study is dependent on the participation and cooperation of the US PWR industry, the NRC, and LANL. Approximately six volunteer PWR plants are expected to contribute samples collected during their recent condition assessment surveys.

-
1. Zigler, G., J. Brideau, D.V. Rao, C. Shaffer, F. Souto and W. Thomas, "Parametric Study of the Potential for BWR ECCS Strainer Blockage Due to LOCA Generated Debris", United States Nuclear Regulatory Commission final report NUREG/CR-6224, Science and Engineering Associates, Inc., report SEA-93-554-06-A:1 (October 1995).

1. Introduction

This paper presents the results of a United States Nuclear Regulatory Commission (USNRC)-sponsored project focused on characterising debris resident in pressurised water reactor (PWR) containment buildings. Information is provided to establish the background and purpose for the work, as well as details associated with the experimental protocol being employed at Los Alamos National Laboratory (LANL) to collect the desired characterisation data. This paper presents preliminary results associated with this ongoing project. Much of the information that follows reflects the work-in-progress associated with this project.

2. Background and purpose

The USNRC is interested in evaluating accident scenarios at commercial PWR nuclear power plants in which “latent” debris is washed into reactor containment sumps during loss of coolant accidents (LOCAs). This “latent” or “pre-LOCA” debris potentially could clog screens upstream of pumps that supply cooling water to a reactor core that is experiencing a loss of cooling.^{2,3,4,5} “Latent” refers to debris that is already present and that resides inside the containment structure before the accident (as opposed to debris that is generated by the accident). Examples of latent debris include ordinary dust and dirt, insulation fibers, clothing fibers, paper fibers, chunks of plastic, metal filings, paint chips, human hair, or just about anything else that might end up on a floor or other surface inside an industrial building.

A primary safety concern related to long-term recirculation cooling following a LOCA is LOCA-generated and pre-LOCA debris material that is transported to debris interceptors (i.e. sump strainers or screens), which results in strainer blockage and degraded emergency core-cooling (ECC) pump performance. Draft Regulatory Guide DG-1107 “Water Sources for Long-Term Recirculation Cooling Following a Loss-of-Coolant Accident”^{6,7} suggests that the cleanliness of the reactor containment during plant operation (i.e. pre-LOCA or latent debris) be considered when estimating the amount and type of debris available to block the ECC sump screens. The potential for this material to impact the head loss across the ECC sump screens should be considered. This study focuses on characterising this latent debris material and assessing its potential to contribute to sump-strainer blockage.

-
2. Lochbaum, D., “Pressurized Water Reactor Containment Sump Failure”, Union of Concerned Scientists, internet issue brief (20 August 2003).
 3. Wald, M.L., “Safety Problem at Nuclear Plants is Cited”, *The New York Times* (8 September 2003).
 4. Rawlins, Wade, “Harris Plant Has Design Flaw”, *News Observer* (14 September 2003).
 5. Matthiessen A., and D. Lochbaum, Indian Point Energy Center, Petition Pursuant to 10 CFR 2.206, “PWR Containment Sump Failure”, letter to W.D. Travers, Executive Director for Operations, US Nuclear Regulatory Commission (8 September 2003).
 6. Draft Regulation Guide DG-1107, “Water Sources for Long-Term Recirculation Cooling Following a Loss-of-Coolant Accident”, United States Nuclear Regulatory Commission, Office of Nuclear Regulatory Research (February 2003).
 7. Bonaca, M.V., Draft final revision 3 to Regulatory Guide 1.82, “Water Sources for Long-Term Recirculation Cooling Following a Loss-of-Coolant Accident”, letter to N.J. Diaz, Chairman, United States Nuclear Regulatory Commission (30 September 2003).

Past and recent testing has shown that even small volumes of fibrous debris present on an ECC sump screen can very effectively filter particulates that are present in the sump pool, leading to significant pressure losses across the composite debris bed and resulting in degraded pump performance. Debris present during routine operations or pre-LOCA or resident debris that is subjected to containment spray (or wash-down from a coolant-pipe rupture) and pool transport may contribute a significant source of particulate and perhaps fiber material. The USNRC and its contractors are carefully studying pressure drop across “filter beds” as a function of the physical properties of the filter bed and the linear flow velocity through the bed.⁸ Semi-empirical equations have been developed to predict pressure drop across filter beds using a combination of fluid-flow theory and experimental results. Some of the most important parameters in these correlations are the density of the filter bed and the surface area per unit volume within the bed. The relative volume of “fibers” and “particles” in the bed is also important because the compressibility of the bed depends on this ratio.

This study, funded by the USNRC, focuses on characterising the pre-LOCA or latent debris resident in a PWR containment building. Specifically, the focus of this effort is to collect representative pre-LOCA debris from PWR containments and to characterise this debris consisting of dust and dirt samples; characterising will support the material property determination of the loosely dispersed resident debris constituents. The PWR industry has informally agreed to provide the samples of resident debris that are needed to complete this effort, and six PWR operators have agreed to provide samples. To date, three sets of samples have been received at LANL and are in various stages of characterisation. The material property data are needed to support the application of the NUREG/CR-6224¹ debris-bed head-loss correlation. In addition, the material property data to be collected for resident debris are expected to establish the basis for debris simulant for additional head-loss tests.

Previous work has focused on filter-bed materials that would be generated during an accident, not on debris that is already present in the containment structure. For this project, latent debris will be collected from within PWR containment buildings and shipped to LANL for physical characterisation. This characterisation will include, but not necessarily be limited to, qualitative separation of “fiber” and “particle” fractions from the rest of the latent debris, microphotographic classification of fibers, determination of average particle density of the debris measurement of the surface area per unit weight of the debris particles using the N₂-BET method, and possibly determination of filtration properties of the materials (pressure drop vs. flow rate) in small-scale experiments. LANL’s Geochemistry Laboratory is being enlisted for this work because the latent debris typically contains very low levels of radioactivity (primarily gamma-emitting activation products) and therefore must be handled in a radiological or nuclear facility.

3. Experimental protocol

Shipment of radioactive debris samples from candidate PWRs and the associated receipt and inspection at LANL required the establishment of a simple protocol to enable work to begin in the Geochemistry Laboratory. After the debris is collected at the plant site, its radionuclide content is determined by gamma spectroscopy to satisfy shipping requirements. This information must be provided to LANL so that a radioactive material receipt request can be filed through established LANL Geochemistry Laboratory protocols. To date, five PWRs have provided gamma spectra results of latent debris collected, and the results indicate that the debris contains radionuclide inventory less

⁸ United States Nuclear Regulatory Commission, “Transient ECCS Strainer Blockage Model, Appendix B”, NUREG/CR-6224 (October 1995).

than the “sum-of-fractions” barcode limit for a radionuclide inventory in the Geochemistry Laboratory. The quantities of latent debris received from these five PWRs vary from grams to kilograms. Thus, the total activity of debris samples expected from all six PWRs is unlikely to exceed the Hazard Category 3 nuclear facility limit.

When the material is received at the Geochemistry Laboratory site, it is taken first to the laboratory count room for gamma counting and spectral analysis before being unpackaged (the gamma spectroscopic report from the nuclear plant also is provided). The count room personnel will determine if they can detect any radionuclides to which national security programs in the building might be sensitive. To date, this has not been the case because the samples have not contained any debris from fuel elements (the radioactivity is generally attributable to activation products). Alpha and beta counting has not been conducted on the samples because the radioactivity in the samples is very heterogeneous (contained in only a few particles) and it is not possible to prepare the samples for alpha or beta counting without incurring greater risk of contamination than simply proceeding with the work after gamma counting.

Once the debris material has been received into the laboratory, experimental work can begin. The experimental scope is as follows:

1. determine qualitatively the composition of debris collected from each plant;
2. characterise particulate and fiber fractions using microscopic examination;
3. determine physical properties of particulate and fiber fractions; and
4. conduct small-scale filtration experiments.

The experimental debris characterisation proceeds as follows.

3.1 Removal of debris from its shipping container to laboratory containers

The debris from the first three plants arrived in two different types of containers. Two sets of samples consisted of small quantities (a few grams) of debris in double-contained baggies, e.g. Ziploc[®] bags. The debris either was loose in the bags or adhered to masolin cloth, paper “swipes”, or vacuum filters. Debris was removed from each bag and placed into a small Tupperware[®] tray. Filter/swipe papers were shaken gently to remove any loose debris. Wet filter/swipe papers are used to wash the debris adhered to the bags. Next, the swipes were gently agitated in a water bath to remove the debris. Another sample consisted of six HEPA filters with the quantity of debris ranging from 160 to 750 grams. Because of its greater quantity, transfer of this second debris sample to the Laboratory container was carried out in a glove bag to prevent potential spill and inhalation of the debris particles and fibers.

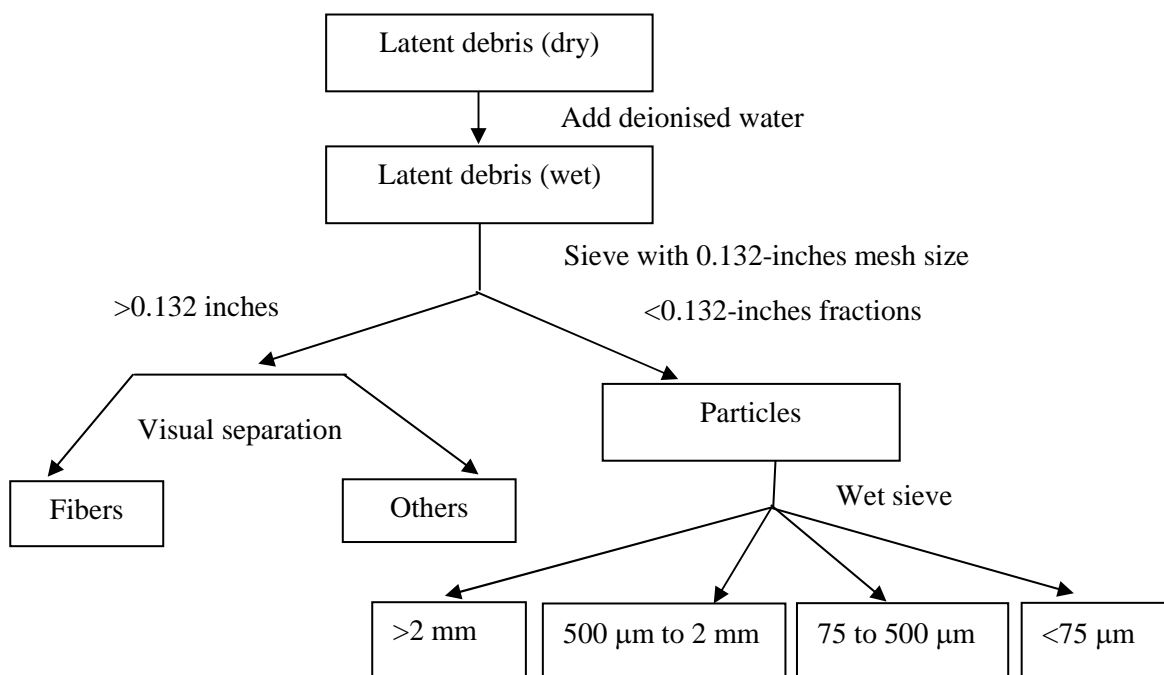
3.2 Separation of “fiber” and “particle” fractions from the remaining debris

Wet sieving was employed to separate “fiber” and “particle” fractions from the remainder of the debris by using a 0.132-in.-mesh-size sieve. The particle-size fraction less than 0.132 in. was further separated by wet sieving into four fractions, i.e. >2 mm; 500 µm to 2 mm; 75 µm to 500 µm, and <75 µm. Once acceptable separation was achieved, the water was allowed to evaporate in a hood overnight or over the weekend. Figure 1 demonstrates the wet separation scheme employed to segregate the latent debris.

3.3 Surface area and density measurement of particles

The surface areas of subtractions of the debris particles were measured by nitrogen adsorption. The subtractions were dried, weighed, and then loaded into a glass sample cell for measuring. The samples were loaded inside a hood to prevent spill and inhalation. The nitrogen adsorption BET surface area was measured using a Quantachrome Nova 1200 instrument. This technique also provided estimates of volume and thus densities of samples.

Figure 1. Latent debris qualitative separation flow scheme



3.4 Microphotographic classification of fibers

Fibrous debris varied in size and quantity for each sample. A metallurgical microscope with a 20X objective lens was used to identify the size/shape of the fibrous debris separated from the above procedures. The sample was loaded onto a microscope slide using glue.

3.5 Scanning electron microscope (SEM)/energy-dispersive spectroscopy characterisation (EDAX)

Fiber and particle sub samples that either appeared to be very representative or were of special interest because of an unusual characteristic (e.g. shape and colour) were selected for SEM/EDAX characterisation to show the surface topography and to qualitatively determine elemental composition.

3.6 Settling measurements

Settling measurements on different particle-size fractions were performed to provide information on settling velocities so that calculations could be conducted to determine fractions (or sizes) of particulate debris that would reach sump screens.

3.7 *Small-scale filtration experiments*

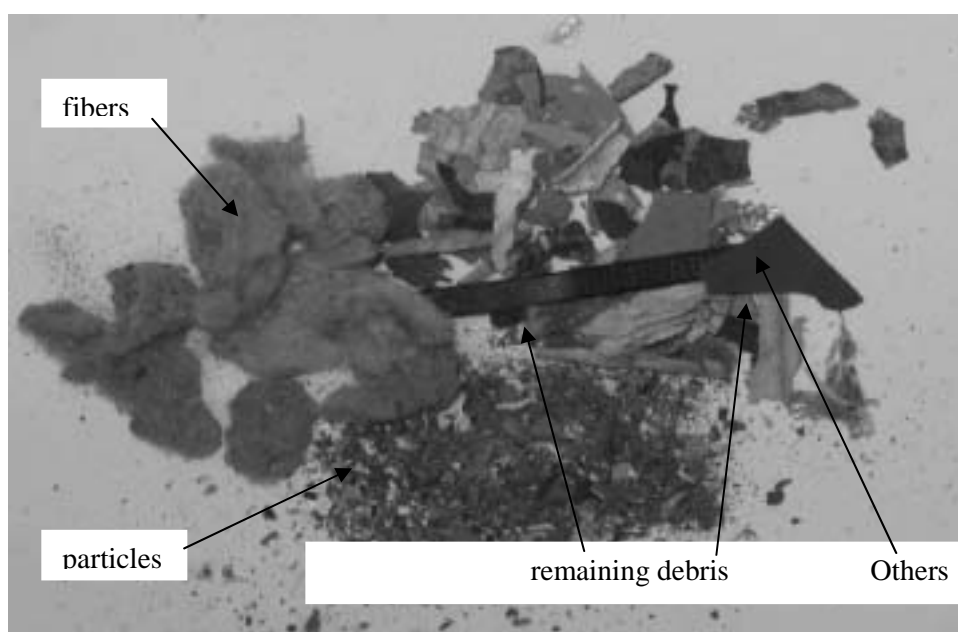
If sufficient quantities of material are available, bench-top experiments may be conducted to measure pressure drop as a function of filter-bed thickness, material mix (fiber vs. particle), and flow rate through the filter bed. Some of these experiments may be conducted in conjunction with the debris density measurements mentioned previously (density would be measured first, then water flow through the bed to measure pressure drop as a function of time and flow rate). All such experiments will be conducted with wet debris, and gravity will always be the preferred driving force for flow so that pressures will be relatively low. Double containment (spill trays) will be used to prevent the potential spread of contamination by leaks. Debris from settling measurements will be recovered and recombined with other debris to conduct filtration experiments. Linear flow velocities similar to those in nuclear plant sump strainers will be employed in a small test loop similar to the loop employed at the University of New Mexico. Meshes or screens of different sizes will be employed at the end of columns to initiate filter bed build-up. Once a filter bed has been built up, the bed density would be measured by measuring the length (and thus the volume) of the bed, weighing the column, and then removing and drying the material and column to get the dry weights of both the material and column. In addition to bed density, the filter-bed porosity also will be measured, which is another important parameter in the filter-bed head-loss correlations.

4. Results and discussion

4.1 *Composition of debris*

Debris samples from three PWRs, namely plants A, B, and C, have been received and have undergone characterisation. The quantity of debris received from these three plants is significantly different, varying from less than 10 grams to about a few hundred grams. In general, the debris consists of three major fractions, as illustrated in Figure 2.

Figure 2. Composition of debris (pictured from plant A debris)



Determining the composition of debris starts with the initial separation of debris into fibers, particles, and remaining debris, i.e. “other”. The weight percentage of each fraction of every sample is different, depending on where and how the sample was collected. Table 1 lists the initial separation results of debris from the three plants. At times, separation is difficult because very small particles adhere to the fibers and are nearly impossible to completely separate.

Table 1. Weight fraction of latent debris from plants A, B, and C

Plant A				Plant B				Plant C			
ID	Weight (g)			ID	Weight (g)			ID	Weight (g)		
	P ^a	F ^b	O ^c		P ^a	F ^b	O ^c		P ^a	F ^b	O ^c
1	0.32	0.02	0.02	B1	111	12	41	C1	4.42	0.05	0.66
2	0.45	0.06	0.12	B2	225	42	59	C2	NA ^d	0.30	NA
3	0.06	0.07	NA	B3	290	29	82	C3	0.77	<0.01	1.90
4	1.18	0.41	0.04	B4	267	23	51	C4	0.23	NA	0.13
5	0.15	NA	0.24	B5	474	24	255	C5	1.23	0.02	1.90
6	0.54	0.02	0.18	B6	74	40	121	C6	0.16	0.04	0.37
7	0.24	NA	0.06	Weight (wt %)			C7	4.20	0.35	7.59	
8	0.05	0.01	NA	B1	68	7	25	C8	3.76	NA	0.19
9	0.76	0.21	0.12	B2	69	13	18				
10	0.38	0.11	0.07	B3	72	7	20				
11	0.23	0.01	0.39	B4	78	7	16				
12	0.2	NA	NA	B5	63	3	34				
13	0.1	0.08	NA	B6	31	17	51				
14	0.4	0.04	0.01								
total	5.06	1.04	1.25					total	13.77	0.76	12.74
Weight (wt %)				Weight (wt %)				Weight (wt %)			
A	69	14	17					C	50.50	2.79	46.72

^a P = particles.

^b F = fibers.

^c O = others.

^d NA = not applicable.

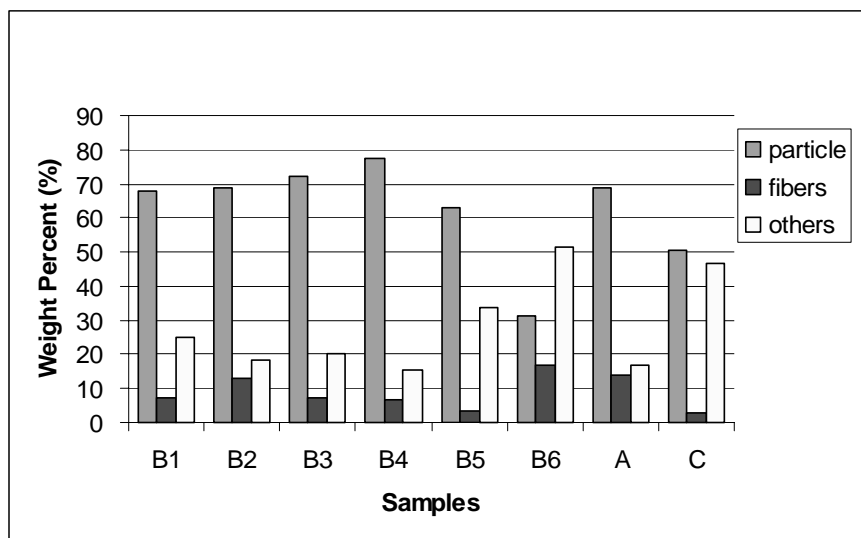
The quantity of debris in the individual debris samples from plant A was determined to be insufficient to conduct further characterisation tests. To enable further testing, all of the individual debris samples were combined to represent plant A.

In contrast to plant A, the quantities of debris in each sample from plant B were large enough to allow further characterisation.

Similar to plant A, the quantity of debris in the individual debris samples from plant C was not enough to conduct further characterisation tests for all samples. However, the character of each sample from plant C seemed quite different when compared with plants A and B. Individual sample characterisation will be completed on the samples with sufficient quantity.

Figure 3 summarises the results of the initial separation of debris for plants A, B, and C. In Figure 3, the six individual samples from plant B are shown, whereas the combined results for plants A and C are presented. The results are shown by weight percent; not surprisingly, particulate fractions significantly exceed fiber or “other” fractions for most samples.

Figure 3. Composition of latent debris from plants A, B, and C



To characterise the particulate in more detail, the debris sample particle fraction was further separated into four particle-size categories using sieves with mesh sizes >2 mm, $500\ \mu\text{m}$, and $75\ \mu\text{m}$. Table 2 lists the particle-size distribution results for plants A, B, and C.

Table 2. Particle-size distributions of plants A, B, and C debris

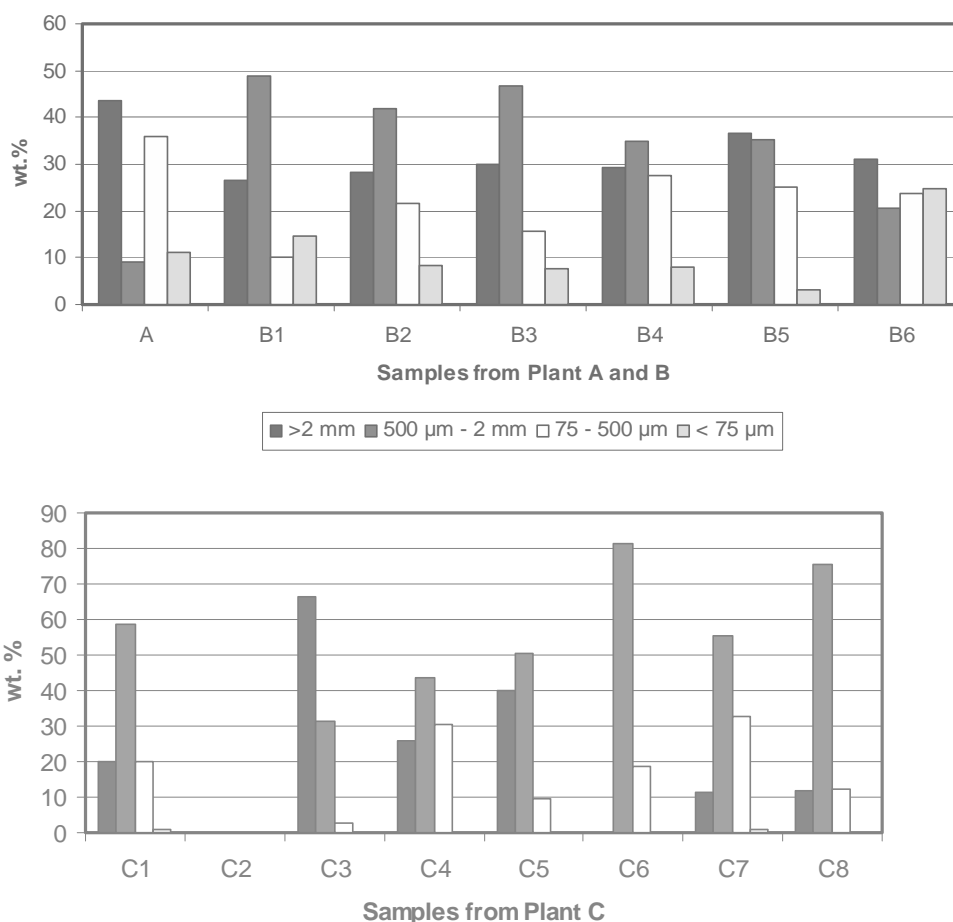
Sample ID	Particle size							
	>2 mm		$500\ \mu\text{m}$ to 2 mm		75 to $500\ \mu\text{m}$		$<75\ \mu\text{m}$	
	g	wt %	g	wt %	g	wt %	g	wt %
A	1.5	43.73	0.32	9.19	1.24	36.01	0.38	11.08
B1	26.03	26.49	48.04	48.88	9.97	10.14	14.24	14.50
B2	53.25	28.11	79.48	41.95	41.15	21.72	15.57	8.22
B3	77.76	29.95	121.03	46.62	40.15	15.60	20.30	7.82
B4	54.73	29.44	65.13	35.03	51.55	27.73	14.50	7.80
B5	134.51	36.49	130.44	35.39	92.23	25.02	11.44	3.10
B6	10.21	31.19	6.72	20.53	7.74	23.64	8.07	24.65
C1	0.69	20.18	2.01	58.77	0.69	20.18	0.03	0.88
C2	NA	NA	NA	NA	NA	NA	NA	NA
C3	0.51	66.23	0.24	31.17	0.02	2.6	NA	NA
C4	0.06	26.09	0.10	43.48	0.07	30.43	NA	NA
C5	0.49	39.84	0.62	50.41	0.12	9.77	NA	NA
C6	NA	NA	0.13	81.25	0.03	18.75	NA	NA
C7	0.47	11.19	2.33	55.48	1.37	32.62	0.03	0.71
C8	0.45	11.97	2.84	75.53	0.47	12.50	NA	NA

^a NA = not applicable.

Figure 4 presents the particle-size distribution results for plants A, B, and C. As indicated in Figure 4, particles with a size ranging between $500\ \mu\text{m}$ and 2 mm constitute the major fraction of the debris, followed by particles with a size range >2 mm. The quantity of particles with a size ranging

between 75 and 500 μm is also significant for almost all of the samples. Particles $<75 \mu\text{m}$ constitute the smallest fraction of almost all of the samples, especially in samples from plant C, in which the amount of particles $<75 \mu\text{m}$ is barely detectable. The fraction of very small particles, i.e. $<75 \mu\text{m}$, is highly dependent on the debris-collection method at each plant, which may help to explain the lack of very small particles in the plant C debris sample.

Figure 4. Particle-size distribution of plants A, B, and C debris



4.2 Classification of fibers

Several samples that were separated from the debris shipments from different plants were viewed under an optical microscope using a 20X objective lens. Figures 5, 6, and 7 show several selected microscopic images of “fibrous” samples from Plants A, B, and C, respectively. Because of the large variation in the fiber shapes and dimensions, these images are not necessarily fully representative of the original samples. This variation is not surprising considering the difference in sample collection locations within the plant, the dominant materials present in the plant at the time of sample collection, the methods used to collect the samples, and the techniques we used to separate the samples. However, several useful observations can be drawn from these images.

As these images depict, the fibers are between about 1 and 20 μm in diameter (or thickness), with the majority being closer to the upper range. The larger fibers ($\gg 5 \mu\text{m}$ in diameter or thickness) appear to be almost straight cylinders, single tortuous and flexible strands, or twisted, flat ribbon-like strips. Some of these strands appear to be interwoven to form larger clusters of multiple fibers attached at different points and have random orientations. The smaller fibers ($\ll 5 \mu\text{m}$ in diameter or thickness) appear to be interwoven together to form larger clumps. The size of these clumps ranges between a few microns to more than a millimetre (not shown in these images). The images also indicate that these clumps tend to attach (or clamp) to neighbouring fibers.

Another important observation from these images is that almost all of the fibers have particles attached to them. This attachment is apparently physiochemical rather than mechanical. The size of these particles is comparable to the diameter (or thickness) of the hosting fiber in most instances but can be much larger in other instances. However, because of the limited resolution of optical microscopy, it is not obvious whether these attached particles are single particles or clusters of smaller individual particles. These attached particles (or clusters) can have a significant effect on the overall transport behaviour of the debris, not only because they induce additional physical roughness to the fiber surfaces, but also because they can act as seeds that stimulate further attachment of other particles or further clustering of the fibers themselves.

Overall, the fiber characteristics qualitatively reflect the fiber-debris classification by shape, as summarised in Table B-3 of NUREG/CR-6224.⁸

Figure 5. Photo images of plant A fiber

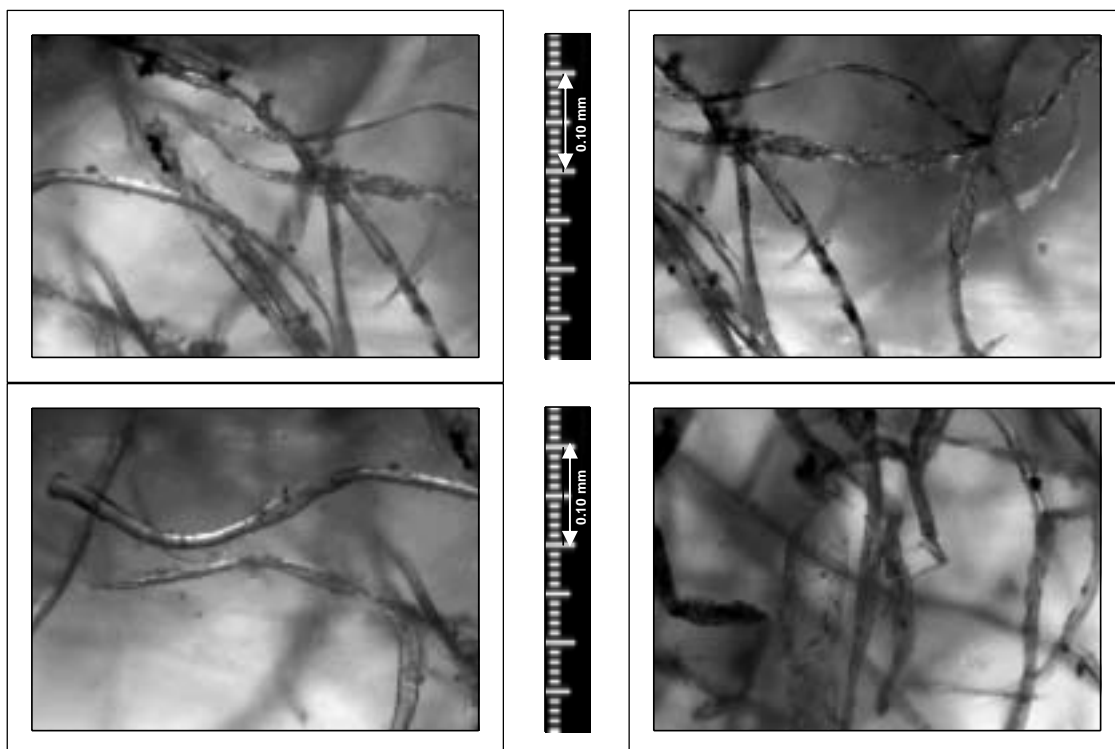


Figure 6. Photo images of plant B fiber

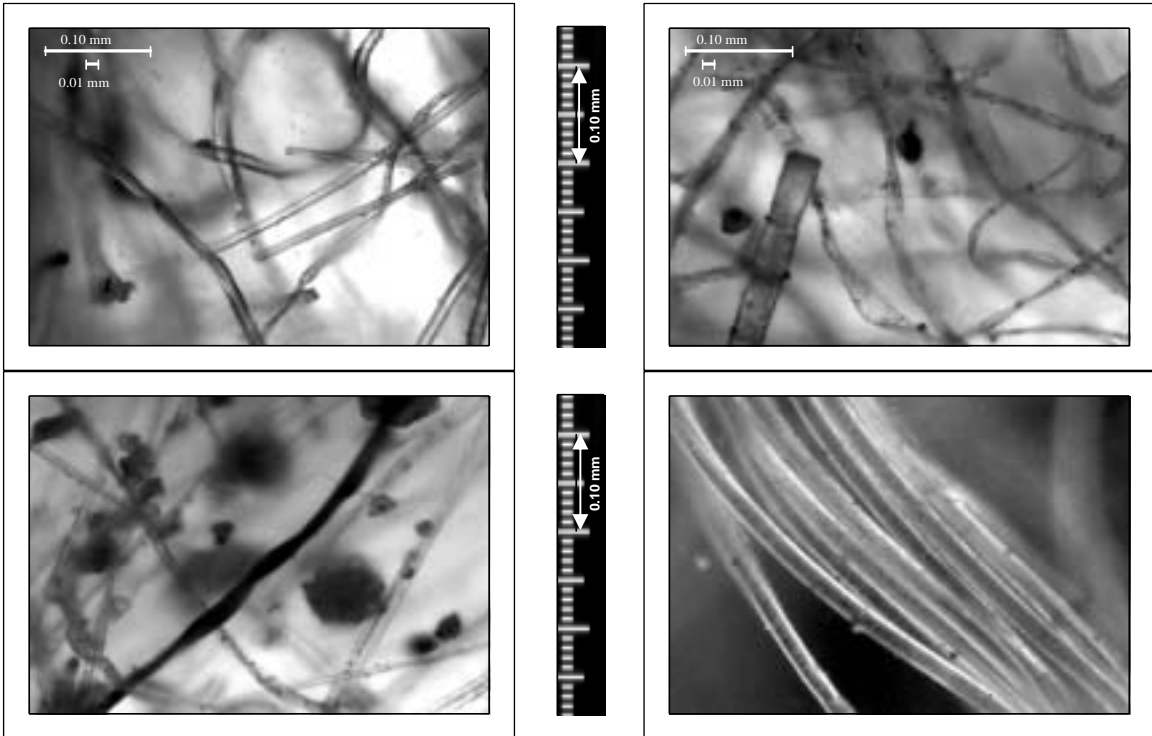
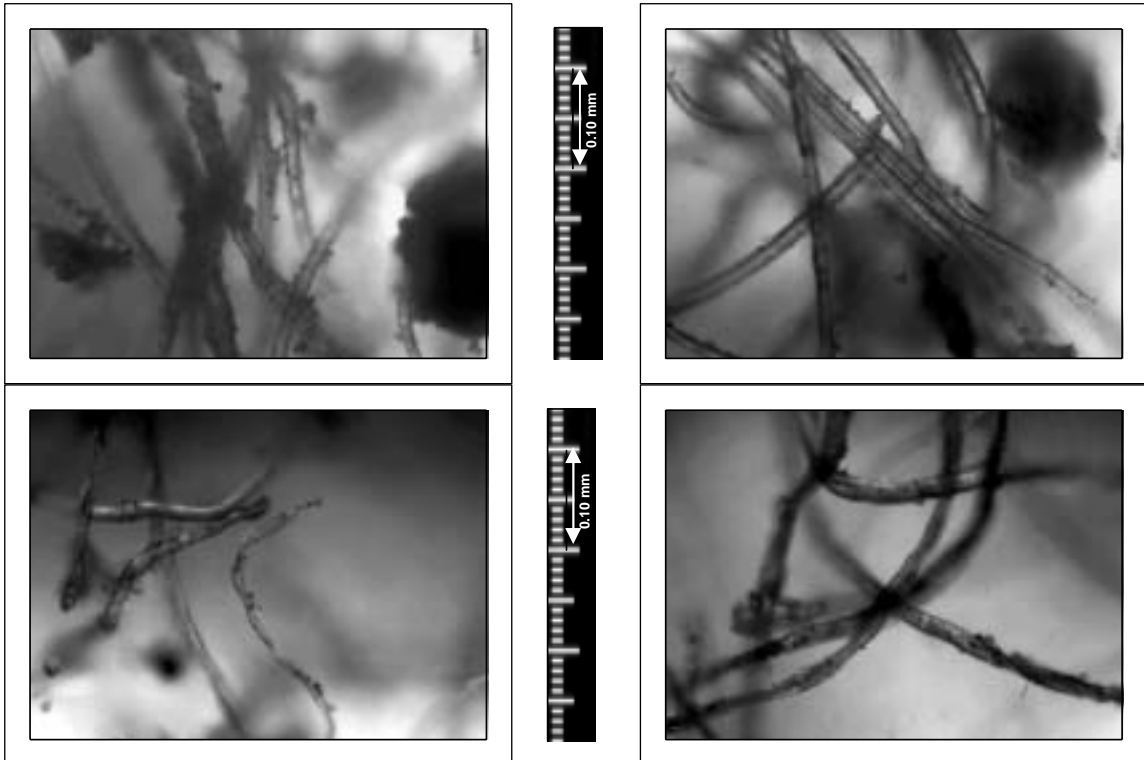


Figure 7. Photo images of plant C fiber



4.3 Specific surface area and density of particles in latent debris

According to the ECCS Strainer Blockage Model,⁸ the formation of a debris layer on the strainer surface results in pressure drops across a fibrous bed. The extent of the pressure drop depends largely on the character of the debris, including its specific surface area and density. To that end, one of the primary purposes of this study was to conduct specific surface-area measurements on various-sized particles of latent debris from plants A, B, and C. The average results of these measurements are listed in Table 3.

Table 3. Specific surface area and density of particles in debris from plants A, B, and C

Sample ID	<75 μm		75 to 500 μm		500 μm to 2 mm	
	Specific surface area (m^2/g)	Density (g/cm^3)	Specific surface area (m^2/g)	Density (g/cm^3)	Specific surface area (m^2/g)	Density (g/cm^3)
A	0.48	2.25	0.80	2.22	1.96	1.48
B1	0.66	2.80	0.11	2.51	0.05	2.69
B2	0.81	2.67	0.38	2.38	0.18	2.40
B3	0.68	2.88	0.43	2.87	0.99	2.10
B4	0.28	3.27	0.16	3.60	0.10	2.89
B6	0.42	3.31	0.29	2.65	0.89	2.46
C1	NA	NA	0.29	1.95	0.28	2.38
C8	NA	NA	0.01	3.04	0.02	2.95

The relationship between particle size, specific surface area (m^2/g), and density (g/cm^3) for all measurements completed to date is depicted in Figure 8; the densities of the particles in the debris range from 2 to 4 g/cm^3 . The plant A data point for particles sized between 500 μm and 2 mm is not shown in Figure 8. The densities for most of the samples, regardless of their particle-size and surface-area differences, range between 2.5 to 3.0 g/cm^3 . Interestingly, the surface areas of particles sized between 75 to 500 μm are generally smaller than the surface areas of particles sized <75 μm . Two ranges of surface areas appear for the large particle sizes shown in Figure 8. One set clusters around a low surface area of about 0.2 m^2/g , whereas the other clusters around a large surface area of about 1 m^2/g . Thus, it seems that the average density of debris does not depend on its particle size; however, the surface area of debris does seem to depend on its particle size. In general, the smaller the particle size of the debris, the larger the surface area. Exceptions do occur in which larger particles also have larger surface areas, thus reflecting the stochastic variability in the physical and chemical characters of the debris.

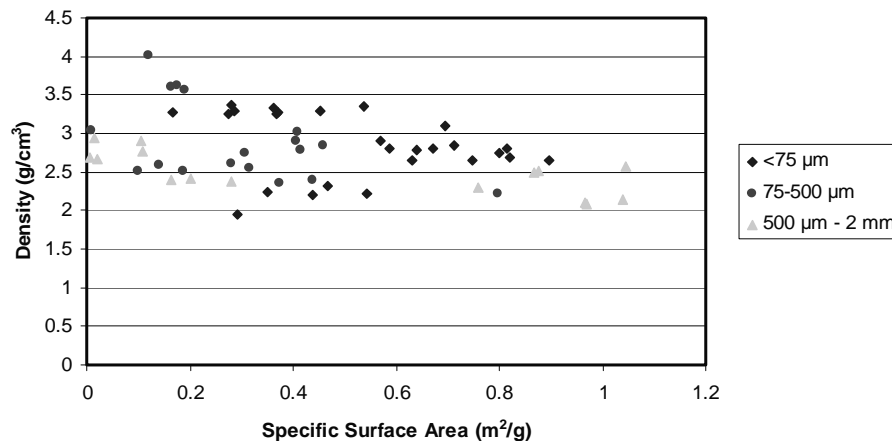
4.4 Characteristics of pores in latent debris

As discussed above, the surface area of particles depends not only on the particle size but also on the character of the porosity, the pore distributions, and the shape of the pores on the particles. Representative data for latent particle debris with the particle size of 75 to 500 μm were analysed using software AS1 Autosorb 1, provided by Quantachrome Instruments. The HK⁹ method was applied

9. Horvath, G. and K. Kawazoe (1983), "Method for the Calculation of Effective Pore Size Distribution in Molecular Sieve Carbon", *Journal of Chemical Engineering Japan* **16**:5, pp. 470-475.

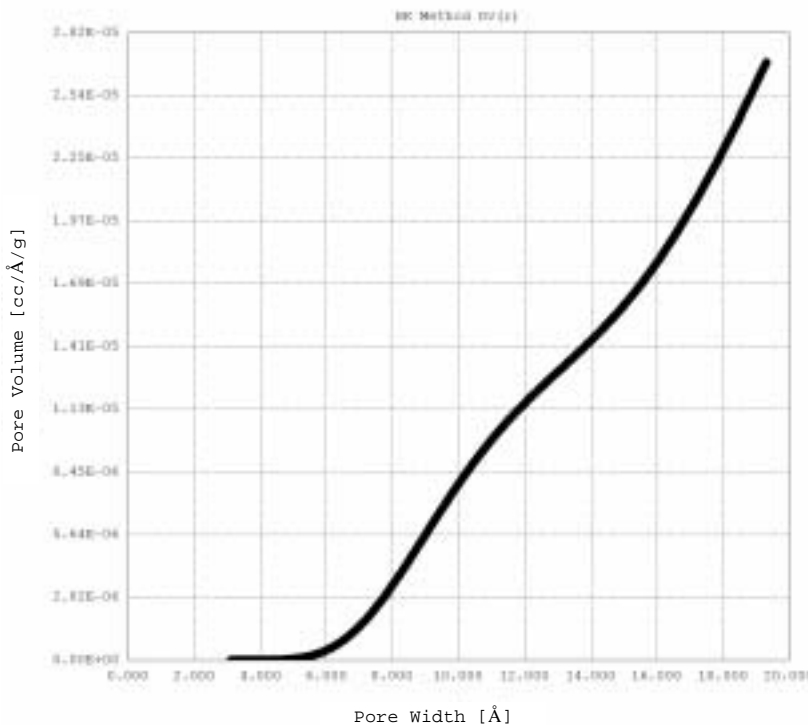
to the determination of pore distributions of micropores ($<20 \text{ \AA}$), whereas the BJH¹⁰ method was applied to the determination of pore distribution of mesopores (20 to 500 \AA).

Figure 8. Specific surface area and density of latent debris as function of its particle size.



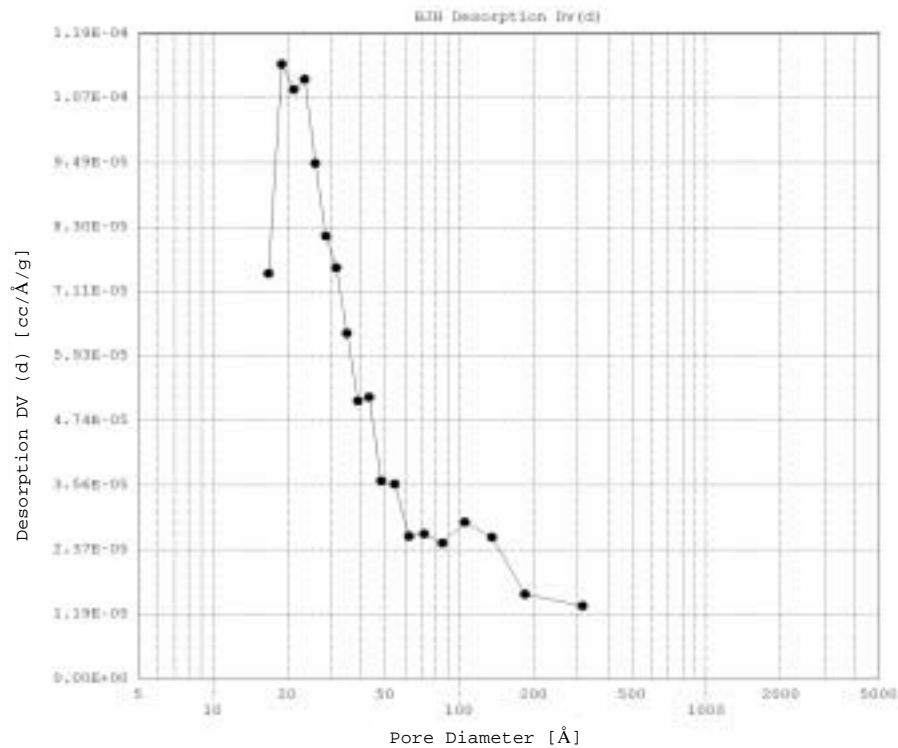
Figures 9 and 10 present the results of the HK and BJH methods when applied to determine the precise pore distribution of representative particle debris samples. These results are typical of the particle debris samples analysed to date. As shown in Figures 9 and 10, the pore diameters range from $10^{-3} \mu\text{m}$ to $3 \times 10^{-2} \mu\text{m}$ for particles in the range of 75 to 500 μm .

Figure 9. Micropore distributions in the representative particle debris



10. Barrett, E.P., L.G. Joyner and P.P. Halenda (1951), *Journal of the American Chemical Society* **73**:373.

Figure 10. Mesopore distributions in the representative particle debris



5. Conclusions

Latent debris from three PWRs has been characterised to date. Debris samples from the three plants show particle distributions ranging from 31 to 78 wt %, fiber distributions from 3 to 17 wt %, and other materials present in the debris from 16 to 51 wt %. The particle-size distribution appears to be highly dependent on the method used to collect debris samples within the plant; however, the results for the samples thus far analysed show the following distribution: >2mm, 11 to 66 wt %; 500 µm to 2 mm, 10 to 81 wt %; 75 to 500 µm, 3 to 36 wt %; and <75 µm, 1 to 25 wt %. Particle densities were observed to range from 1.5 to 4 g/cc, with a median density of about 2.7 g/cc. The specific surface areas of the debris particles ranged from 0.01 m²/g to 2.0 m²/g. Smaller diameter particles exhibited larger specific surface areas.

Qualitative photomicrograph observations of fibers show fiber diameters ranging from 1 to 20 µm, with shapes including straight cylinders, single tortuous flexible strands, and twisted flat ribbon-like strips. Some fibers appear to be interwoven, forming large clusters similar to the fibrous debris shape classification shown in NUREG/CR-6224.⁸ Most of the fibers, regardless of their shape and size, appear to have debris particles attached to them. The attached particle diameters range from about 1 µm to greater than 50 µm.

Additional work is needed to finish characterisation of the latent debris received at LANL to date. SEM/EDAX characterisation of the debris will provide information on surface topography and composition. Planned settling velocity measurements and small-scale filtration experiments will also provide further insight into the character of plant latent debris.

**DEBRIS ACCUMULATION AND HEAD-LOSS DATA FOR EVALUATING THE
PERFORMANCE OF VERTICAL PRESSURISED WATER REACTOR
RECIRCULATION SUMP SCREENS**

Clinton J. Shaffer
ARES Corporation (USA)

Mark T. Leonard
dycoda_{LLC} (USA)

Arup K. Maji and Ashok Ghosh
University of New Mexico (USA)

Bruce C. Letellier
Los Alamos National Laboratory (USA)

Tsun-Yung Chang
United States Nuclear Regulatory Commission (USA)

Abstract

Experimental and analytical results are summarised from experiments sponsored by the United States (US) Nuclear Regulatory Commission (NRC) and performed under the direction of Los Alamos National Laboratory (LANL) in facilities operated by the Civil Engineering Department at the University of New Mexico (UNM). The study generated data needed to support the resolution of Generic Safety Issue 191, which addresses debris accumulation on the pressurised water reactor (PWR) sump screen and the consequent loss of the emergency core cooling-system pump's net positive suction head. These experiments investigated: (1) the accumulation of debris on a screen typical of those found in the PWR plants; and (2) the subsequent head loss associated with debris from calcium silicate (CalSil) insulation. Both of these investigations are key elements in the resolution of the PWR sump-clogging issue and were needed to fill gaps in our knowledge base.

Debris-accumulation patterns on vertical screens that were placed in an open flume were recorded in photographs that provide qualitative insight into the accumulation processes. Head-loss testing was conducted in a closed-loop apparatus where the screen was positioned horizontally and the tests involved beds of mixed debris. The focus of the tests was on mixed beds of a low-density fiberglass insulation debris, and CalSil insulation debris, for which existing data strongly indicated that the associated head losses could be disproportionately higher than comparable quantities of other types of insulation debris. The objectives of the head-loss testing was to establish a technical basis for applying the NUREG/CR-6224 head-loss correlation to debris beds containing significant quantities of CalSil insulation and to generate head-loss data to support confirmatory evaluations of sump screen performance.

1. Introduction

The capability of estimating the accumulation of loss of coolant accident (LOCA) generated debris and the subsequent head loss associated with this debris on pressurised water reactor (PWR) recirculation sump screens is a key element in the resolution of the PWR sump-clogging issue. Jet impingement forces would dislodge thermal piping insulation and other materials (e.g. paint and concrete) in the vicinity of the break. The operation of containment sprays, as well as the break effluent flow, would transport a portion of debris and resident materials (e.g. dust and dirt) to the sump floor. There, a certain amount of debris would accumulate on the sump screen and cause a subsequent resistance to emergency core cooling system (ECCS) recirculation flow, thereby threatening long-term recirculation cooling.

Experiments sponsored by the United States (US) Nuclear Regulatory Commission (NRC) were performed under the direction of Los Alamos National Laboratory (LANL) in facilities operated by the Civil Engineering Department at the University of New Mexico (UNM) to generate data needed to support the resolution of Generic Safety Issue 191.¹ This issue addresses debris accumulation on the PWR sump screen and the consequent loss of the ECCS pump's net positive suction head. These experiments investigated (1) the accumulation of debris on a screen typical of those found in the PWR plants and (2) the subsequent head loss associated with debris from calcium silicate (CalSil) insulation. Both of these investigations were needed to fill gaps in our knowledge base.

When debris approaches a vertical (or slanted) screen, its pattern of accumulation depends on whether the debris is suspended in the water flow or has settled to the floor of the pool and whether the flow velocities are high enough to move debris vertically up on the screen once debris is deposited at the bottom. Debris that is accumulated uniformly on the screen will cause a higher head loss than the same quantity of debris accumulated in nonuniform patterns, such as skewed toward the bottom by gravitational settling. Accumulation data were needed for the range of insulation materials known to be used in US PWR plants. These materials include fiberglass insulations, microporous insulations, and reflective metallic insulations (RMI).

A substantial base of experimental head-loss data was amassed during the boiling water reactor (BWR) strainer-clogging resolution;² however, this base of knowledge did not include sufficient data to support credible predictions of head loss associated with microporous insulations, for which CalSil is perhaps the most notable member. However, existing data strongly indicated that the head losses associated with microporous insulation could be disproportionately higher than comparable quantities of other types of insulation debris. CalSil was chosen for testing with an objective of establishing the applicability of the NUREG/CR-6224³ correlation to debris beds that included CalSil, in particular,

-
1. Rao, D.V., M.T. Leonard, C.J. Shaffer, A.K. Maji, and A. Ghosh, "GSI-191: Experimental Studies of LOCA-Generated Debris Accumulation and Head Loss with Emphasis on the Effects of CalSil Insulation", prepared for the United States Nuclear Regulatory Commission, draft report LA-UR-03-0471 (February 2004).
 2. Rao, D.V., C.J. Shaffer, M.T. Leonard, and K.W. Ross, "Knowledge Base for the Effect of Debris on Pressurized Water Reactor Emergency Core Cooling Sump Performance", United States Nuclear Regulatory Commission report NUREG/CR-6808, Los Alamos National Laboratory report LA-UR-03-0880 (February 2003).
 3. Zigler, G., J. Brideau, D.V. Rao, C. Shaffer, F. Souto, and W. Thomas, "Parametric Study of the Potential for BWR ECCS Strainer Blockage Due to LOCA Generated Debris", United States Nuclear Regulatory Commission final report NUREG/CR-6224, Science and Engineering Associates, Inc. report SEA-93-554-06-A:1 (October 1995).

debris beds consisting of fiberglass and CalSil insulation debris where the CalSil acts as the particulate filtered from the flow by the fibers of the fiberglass insulation. NUKON[®] low-density fiberglass insulation was chosen for the tests because the NUREG/CR-6224³ correlation was validated for this insulation debris. Both the CalSil and the NUKON[®] insulation samples were obtained from Performance Contracting Inc. (PCI).

To accomplish the vertical-screen debris-accumulation objectives, vertical-screen experiments were conducted in an open-flume apparatus using a variety of insulation debris types, including NUKON[®], CalSil, and RMI debris. In addition, limited debris-accumulation data were taken in the integrated tank debris transport tests.⁴ To accomplish the head-loss objectives, experiments were conducted in a closed-loop test apparatus where the screen was positioned horizontally and the tests used mixed beds of NUKON[®], a dirt and concrete dust particulate, CalSil, and RMI debris.

2. Debris-accumulation patterns

Debris-accumulation data consist of qualitative insights recorded in photographs, which illustrate how debris was deposited on the vertical screen. Debris-accumulation patterns depend on whether the debris is suspended in the approaching flow and on screen-approach velocities. Uniformity increases the head loss associated with a specific quantity of debris. Accumulation uniformity is illustrated in the following three examples.

The photo in Figure 1 shows the build up of fine fibrous debris on a partially submerged vertical screen, which is caused primarily by suspended fibers. This photo was taken during the integrated debris transport testing, where the approach velocities generally ranged from ~0.1 to 0.2 ft/s. The pool depth in this photo was ~9 in. In this test, fibrous debris of any significant size settled to the bottom of the pool, where most of this debris failed to reach the screen. An exception was the free individual fibers that remained suspended in the pool, because of pool turbulence, until the fibers were filtered from the flow passing through the screen. This process resulted in a very uniform bed of fibrous debris across the submerged portion of the screen. A significant fraction of a destroyed fibrous insulation blanket would be present in the form of individual fibers or small groups of fibers, which would subsequently readily transport to the sump pool if the containment spray system were to operate; this type of debris accumulation is an important consideration. It was found that individual fibers remained in suspension, even at relatively low levels of turbulence.

The photo in Figure 2 shows an accumulation of NUKON[®] insulation debris, which was created by mechanically shredding the insulation. This photo was taken during a debris-accumulation test in the large open-channel linear flume operated by UNM. The channel test section was 1 feet wide and 4 feet high. The water level in the test section was operated several inches higher than the 1 feet high vertical test screen. Upstream of the test section, the flow was conditioned to remove inlet-generated turbulence and was straightened for flow uniformity. The screen approach velocity for the test shown in Figure 2 was ~0.9 ft/s, which was several times faster than the velocity needed to cause bulk tumbling along the flume floor, which occurs at ~0.16 ft/s.⁵ The debris was released at floor level, well

-
4. Rao, D.V., C.J. Shaffer, B.C. Letellier, A.K. Maji, and L. Bartlein, "GSI-191: Integrated Debris-Transport Tests in Water Using Simulated Containment Floor Geometries", United States Nuclear Regulatory Commission report NUREG/CR-6773, Los Alamos National Laboratory report LA-UR-02-6786 (December 2002).
 5. Rao, D.V., B.C. Letellier, A.K. Maji, and B. Marshall, "GSI-191: Separate-Effects Characterization of Debris Transport in Water", United States Nuclear Regulatory Commission report NUREG/CR-6882 (August 2002).

upstream of the test screen; however, the flow velocity was sufficiently high to entrain the debris into the flow and scatter it across the screen relatively uniformly but still slightly skewed by gravity toward the bottom of the screen. The extent to which the bed became skewed depended on the velocity of flow.

Figure 1. Typical build up of fine suspended fibrous debris



Figure 2. Typical build up of small pieces of fibrous debris



The photo in Figure 3 shows an accumulation of crumpled foils of stainless-steel (SS) RMI debris. The approach velocity was ~ 0.9 ft/s, which is three times the bulk tumbling velocity of ~ 0.3 ft/s for SS RMI debris. This debris travelled along the floor from the point of release until it encountered the base of the screen, forming a pile at the base. Over several minutes, pieces of debris climbed over the pile to cover debris-free portions of the screen. This accumulation pattern was highly skewed toward the bottom of the screen.

Figure 3. Typical build up of RMI debris



A realistic fiber debris bed could consist of fine fibers uniformly distributed over the screen, with larger pieces piled at the base. Predictions of head loss usually are performed assuming that the fibrous debris is distributed uniformly across the screen to ensure that the estimate is conservative. In addition, estimating head losses through a skewed bed of debris is complicated because the flow through the bed would not be distributed uniformly.

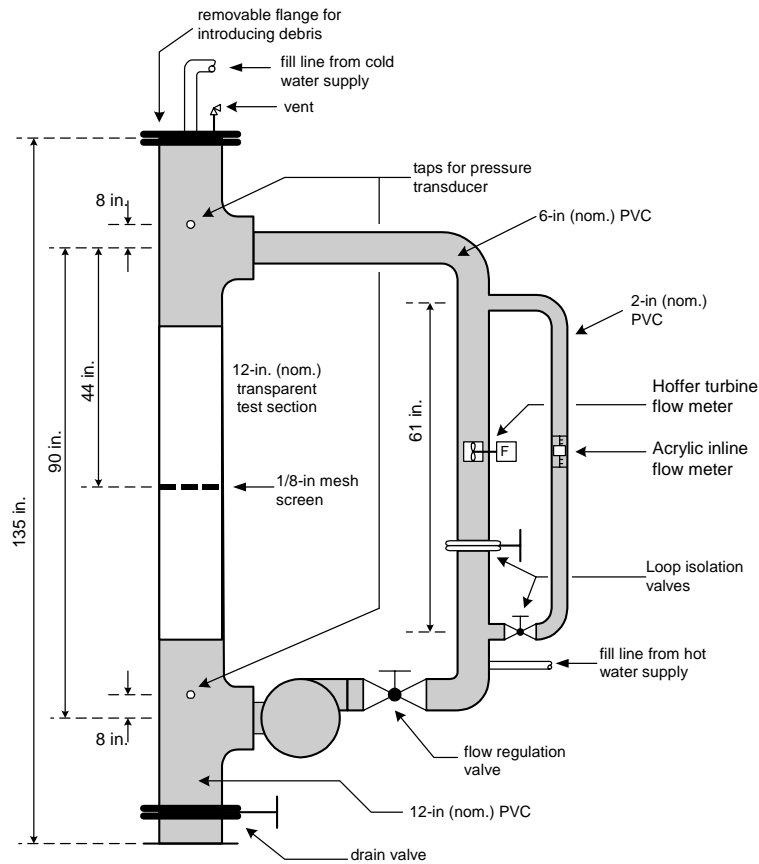
3. Head-loss testing

Head-loss testing was performed to establish a technical basis for applying the NUREG/CR-6224³ head-loss correlation to debris beds containing significant quantities of CalSil insulation debris (which also typically contains substantial quantities of fibrous debris) and to generate head-loss data to support confirmatory evaluations of sump-screen performance for plants with CalSil insulation. The head-loss testing, which is illustrated in Figure 4, was performed in the closed-loop apparatus operated by UNM. A horizontal debris-laden screen was located at about midheight in a transparent vertical 12-in.-dia (nominal) pipe. The screen was a 1/8-in. rectangular mesh similar to those used as PWR recirculation sump screens supported by a coarse steel grating. The loop included a pump, regulating flow valves, flow meters, a top access to introduce debris, and a lower drain. Pressure transducers measured the head loss across the debris bed. The test variables included the quantities and types of debris, the approach velocity, and the water temperature. The initial water temperature was either at nominal room temperature or heated to $\sim 125^{\circ}\text{F}$. Pump heating subsequently heated the water several degrees during the course of the test. The types of debris included NUKON[®] fiberglass insulation, CalSil insulation, and SS RMI crumpled foils.

NUREG/CR-6224³ head-loss correlation

The NUREG/CR-6224³ correlation is a semitheoretical head-loss correlation developed to predict the head loss for flow through porous media consisting of fibrous and particulate debris.

Figure 4. Schematic of closed-loop head-loss test apparatus



During the resolution of the BWR strainer blockage issue, this correlation was validated thoroughly for debris beds consisting of low-density fiberglass and iron oxide corrosion products. The correlation is valid for other combinations of fibers and particulates, as long as the appropriate input parameters are known for these materials. The input parameters are best determined by deducing the parameters from applicable head-loss test data through the application of the correlation to that data. The correlation is programmed into the NRC-developed BLOCKAGE code.⁶

The general equation, valid for laminar, transient, and turbulent flow regimes, is formulated as:

$$\frac{dH}{dL_o} = C \left[3.5 S_v^2 (1 - \epsilon_m)^{1.5} [1 + 57(1 - \epsilon_m)^3] \mu U + 0.66 S_v \frac{(1 - \epsilon_m)}{\epsilon_m} \rho_w U^2 \right] \left(\frac{dL_m}{dL_o} \right)$$

6. Shaffer, C., W. Bernahl, J. Brideau, and D.V. Rao, "BLOCKAGE 2.5 Reference Manual", United States Nuclear Regulatory Commission report NUREG/CR-6371, Science and Engineering Associates Inc., report SEA96-3104-A:4 (December 1996).

where

$$C = 4.1528 \times 10^{-5} \text{ (ft-H}_2\text{O/in.)}/(\text{lb}_m/\text{ft}^2\text{-s}^2) \text{ (units conversion constant),}$$

$$S_v = \text{specific surface area (ft}^2/\text{ft}^3\text{),}$$

$$\mu = \text{dynamic viscosity (lb}_m/\text{s-ft),}$$

$$U = \text{velocity (ft/s),}$$

$$dH = \text{head loss (ft-H}_2\text{O),}$$

$$\rho_w = \text{water density (lb}_m/\text{ft}^3\text{),}$$

$$dL_o = \text{fiber bed theoretical thickness (in.), and}$$

$$dL_m = \text{actual bed thickness (in.).}$$

The mixture porosity, ε_m , is given as:

$$\varepsilon_m = 1 - \left(1 + \frac{\rho_f}{\rho_p} \eta\right) (1 - \varepsilon_o) \frac{dL_o}{dL_m}$$

where

$$\rho_f = \text{density of an individual fiber (lb}_m/\text{ft}^3\text{),}$$

$$\rho_p = \text{density of each individual particle (lb}_m/\text{ft}^3\text{),}$$

$$\eta = \text{ratio of the mass of particulate to mass of fiber in the bed, and}$$

$$\varepsilon_o = \text{theoretical fiber bed porosity.}$$

Values for ε_o and dL_m can be calculated as:

$$\varepsilon_o = 1 - \frac{c_o}{\rho_f}$$

$$dL_m = \frac{c_o}{c} dL_o$$

where

$$c_o = \text{the "as-fabricated" density (lb}_m/\text{ft}^3\text{) and}$$

$$c = \text{actual bed density (lb}_m/\text{ft}^3\text{).}$$

The following correlation is used to estimate the compressibility of the debris bed:

$$c = \alpha c_o \left(\frac{dH}{dL_o} \right)^\gamma$$

where

$$\alpha = 1.3 \text{ and}$$

$$\gamma = 0.38.$$

The homogeneous specific surface area of the bed is determined from the specific surface areas of the individual components. A debris bed likely will consist of multiple types of fibers and particulates, each with their respective specific surface area. The homogeneous bed specific surface area for a bed consisting of one type of fiber and one type of particulate is given by:

$$S_v = S_{vf} \left[\frac{1 + \frac{\rho_f}{\rho_p} \eta \frac{S_{vp}}{S_{vf}}}{1 + \frac{\rho_f}{\rho_p} \eta} \right]$$

where

S_{vf} = the fiber specific surface area (ft²/ft³), and

S_{vp} = the particulate specific surface area (ft²/ft³).

The solution of the general NUREG/CR-6224³ correlation and its supporting equations requires an iterative solution. In addition, a practical limit to the fiber bed compression exists whenever significant particulate is embedded in the fiber matrix. The particulate cannot be compressed beyond its granular packing density (also referred to as the “sludge density”) (e.g. ~65 lbm/ft³ for BWR suppression pool iron oxide corrosion products). Therefore, whenever the bed density reaches the limit expressed in the next equation, further compression ceases.

$$dL_m = dL_o \frac{c_o}{c_{sludge}} (\eta + 1)$$

where

c_{sludge} = the granular packing or sludge density.

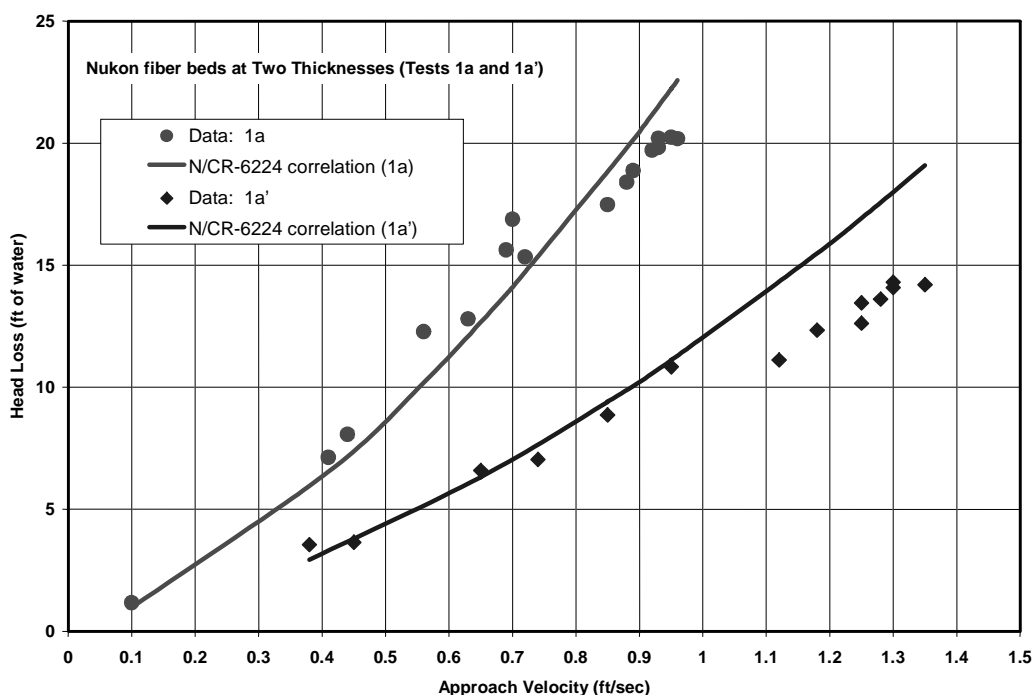
The NUREG/CR-6224³ correlation provides a method of analytically predicting the head loss associated with a bed of debris that has accumulated on a strainer or sump screen. Another way to think of the correlation is that it provides a method of extrapolating limited test data to the types of debris beds expected for postulated accident scenarios. When the correlation is applied to appropriate test data, the correlation input parameters can be determined experimentally for specific types of debris. The head-loss parameters that require experimental determination are the specific surface area and the granular packing density specific to each type of debris and to the size distribution of the particles and perhaps the fibers. The density of the individual particles usually can be estimated from the material composition. It should be emphasized that the specific surface area, if not the granular packing density, is very dependent on the particle size distribution.

In the development of the NUREG/CR-6224³ correlation, it was assumed that the debris bed would be uniform in thickness so that the velocity of flow through the bed would be constant across the bed. The correlation applies to flat screens or to screens or strainers that have been shown to be approximated as flat screens, such as truncated cone-shaped strainers. It also was assumed that the bed is homogeneous, and thus, the composition and head-loss properties would not depend on the location within the bed. In reality, a debris bed could be skewed to one side or formed lumpy so that it is not uniform in thickness. A nonuniform bed will not create as high of a head loss as will an ideally uniform bed. All test results inherently have some degree of nonuniformity, and the tests reported herein have varying degrees of nonuniformity. However, the head-loss parameters should be determined from relatively uniform beds of debris.

Qualification testing

The UNM head-loss test apparatus was qualified by testing with NUKON[®] insulation debris as the only debris because the NUREG/CR-6224³ correlation was already validated for this insulation, i.e. the correlation was found to predict head loss for this debris with reasonable accuracy. Tests were conducted at two debris-bed thicknesses and at two water temperatures; the resulting test data were compared with correlation predictions. Figure 5 shows the comparison of the correlation with the two debris-bed thicknesses of 0.86 and 1.72 in. (based on the as-fabricated density). The NUKON[®] only test data were in good agreement with the correlation predictions.

Figure 5. Comparison of fiber tests with correlation for two bed thicknesses

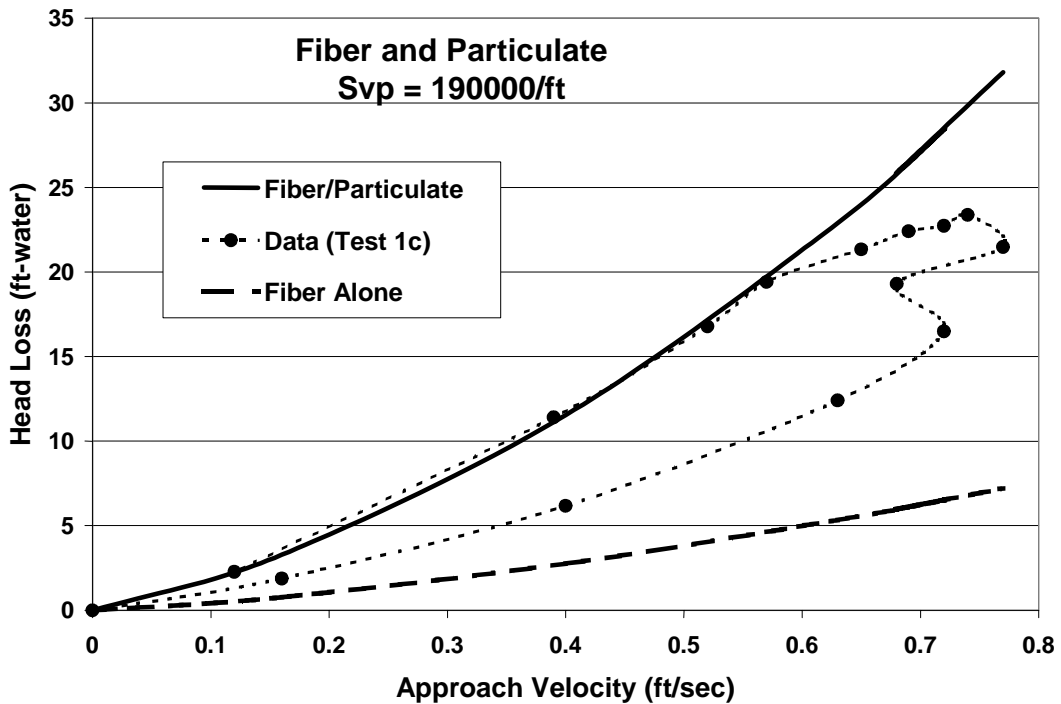


A second set of qualification tests involved the addition of a dirt and concrete dust particulate to the fibrous debris bed. Concrete dust is one possible form of particulate in a PWR plant. The data from these tests were used to demonstrate the deduction process whereby the specific surface area for this particulate was determined. The correlation prediction for Test 1c is compared with the data in Figure 6, where 190 000/ft² and 162 lbm/ft³ were assumed for the particulate's specific surface area and the particle's density, respectively.

During this test, the flow velocity was increased incrementally after the debris was introduced into the loop and the debris bed was formed. With each increase in velocity, a new head loss was recorded; thus, the bed head loss was measured as a function of bed approach velocity. When the head losses approached the limits of the test loop, the flow velocities were then subsequently decreased incrementally. The higher head losses were associated with the decreasing velocities. A likely reason for this behaviour is that a portion of the particulate remained in solution during the ramp-up portion of the test, with the smaller particles passing through the bed. At higher velocities, the bed porosity decreased substantially because of bed compression, with a corresponding increase in the particle filtration efficiency. Once the particulate was effectively embedded, it tended to remain in the bed as the velocity decreased. A hysteresis effect typically has been encountered with fibrous beds because

the bed does not expand as easily with velocity reduction as it compresses with a velocity increase; however, the effect shown in Figure 6 is more substantial than the hysteresis effect seen before. Near the top of the velocity increase, one data point dropped back in velocity due to a relatively rapid increase in debris-bed head loss (i.e. as more of the particulate was filtered from the flow, the head loss increased and the pump flow decreased too rapidly for the experimenters to counter by opening the flow control valve to compensate for the increased head loss). These types of test problems were encountered again and to a greater extent during tests with CalSil.

Figure 6. Comparison of fiber dirt and concrete dust particulate tests with correlation



For a test data point to qualify as a valid head-loss measurement, the debris bed must be relatively uniform, nearly all of the particulate must be filtered from the flow, the head-loss measurements must be relatively stable (after accounting for normal fluctuations), and the flow must be relatively free of air entrainment. The use of the correlation required uniformity. If a portion of the particulate is still in solution, then the quantity in the bed is an unknown. If the indicated head loss is not stable, then the loop is still in a transient condition. Achieving all of these conditions simultaneously was not always possible, particularly when it came to filtering the entire quantity of very fine CalSil from the flow.

CalSil test data

The CalSil insulation obtained from PCI was manufactured primarily from diatomaceous earth (DE) and lime in roughly equal portions (approximately 90% of the total mixture). The DE is mostly silica and the lime is primarily calcium carbonate, but miscellaneous compounds such as iron oxide were present in the DE and lime. Small quantities of fiberglass fibers and a binder were added for strength. The components were mixed, shaped, and baked, whereby the DE and lime reacted to form the CalSil in a porous crystal lattice structure that provided good insulation properties.

Forces from a LOCA jet would pulverise substantial portions of the CalSil insulation in its path. The impact of containment sprays, the subsequent drainage, and sump pool turbulence would further break down CalSil debris into fine particulates that would readily transport to the sump screens. Two methods of debris preparation were tried during the CalSil insulation debris testing. During the earlier testing, the CalSil insulation was fragmented into small pieces that also resulted in a portion of fine particulate. During the final testing, the CalSil was pulverised prior to introduction into the test loop. When the CalSil debris was introduced as small pieces, these pieces subsequently underwent dissolution during testing because of the constant flow of water, and the dissolution rate increased with water temperature. Thus, the CalSil dissolution introduced a transient nature to the debris bed. The most stable and uniform debris beds were formed using finely destroyed NUKON[®] debris and pulverised CalSil that approached the test screen in a uniformly dispersed manner; an example is shown in Figure 7.

Figure 7. Well-formed uniform bed of NUKON[®] and CalSil debris



The unknown properties of the CalSil that are required input to the NUREG/CR-6224 correlation include the particle density, the sludge density, and the specific surface area. The effective particle density for the particles and the fibers in the CalSil debris was estimated by introducing a measured mass of CalSil debris into a beaker of water and then measuring the water displacement after sufficient time elapsed for trapped air to escape. This density was $\sim 115 \text{ lbm/ft}^3$. Note that when applying the NUREG/CR-6224 correlation to debris beds containing CalSil, both the particle and fiber components of the CalSil have been treated as particulate on the basis that the very fine fibers integrated into the manufacture of CalSil insulation are generally substantially smaller than the NUKON[®] fibers and therefore would not contribute significantly to the fiber behaviour of the bed. In the same property test, the volume of CalSil debris that settled in the bottom of the beaker provided a rough estimate of the sludge density ($\sim 12 \text{ lbm/ft}^3$) when the debris was not subjected to the pressures of flow. It was anticipated that the sludge density would increase significantly under the force of flow, but this number would have to be deduced from the test data. The density of the CalSil insulation, as manufactured, was estimated by the manufacturer as $\sim 14.5 \text{ lbm/ft}^3$.

The efficiency at which the NUKON[®] fibers filtered the CalSil from the flow stream is an issue when testing with a fine particulate such as CalSil. The filtration efficiency was found to be a function of the compression of the fibrous bed, which affects the interfiber spacing. At low flow rates, the water generally appeared cloudy due to CalSil that continuously passed through the bed, but at higher velocities the water clarity improved immensely. During the final series of tests, water samples were taken to measure turbidity, which provides concentration estimates of the CalSil in solution. The idea was to estimate the CalSil actually in the debris bed as the difference between the quantity of CalSil added to the test loop and the quantity circulating through the loop. However, this approach was problematic because the CalSil that tended to remain in solution was the very finest of the particles, which happen to contribute more to the total specific surface area on a unit mass basis than did the larger particles in the debris bed. For example, if 10% of the CalSil remained in solution, substantially more than 10% of the total specific surface area remained in solution. Note that at the lower velocities where substantial CalSil mass remained in solution, the NUREG/CR-6224 correlation tended to predict head losses proportional to the square of the specific surface area. The turbidity measurements correction to the input of the head-loss prediction of the test data was of limited use, but the turbidity data facilitated the understanding of the filtration process.

The quality of each head-loss measurement depended on a number of parameters, including the uniformity and stability of the debris bed, the completeness of the particulate filtration, the stability of the flow, the stability of the head-loss measurement, and the minimisation of air entrainment. The quality of several tests was compromised by skewed debris beds, incomplete filtration, debris beds disturbed by flow fluctuations, and debris-bed deformation due to relatively high pressure differentials. High pressure differentials have formed bore holes through the debris bed, allowing portions of the flow to bypass the debris; in a thin-bed test, the debris bed became totally disrupted. Data from the highest quality tests were used to determine the appropriate parameters for the NUREG/CR-6224 correlation, and it was assured that those parameters also conservatively predicted the test results where some aspect of the test compromised the quality of the data.

The CalSil test results reported herein represent a sampling of the more pertinent tests available and the application of the correlation to those results. Because testing had not concluded at this writing, the LANL test report should be consulted for final recommendations regarding simulating CalSil head loss.

Figure 8 shows the head-loss results for Test 6C. In this test, the debris bed was formed with 12 g of NUKON[®] and 6 g of CalSil (particle-to-fiber ratio of 0.5 and a screen area of 0.706 ft²). The nominal bed thickness (assuming the as-manufactured density of 2.4 lbm/ft³) was 0.19-inch. The debris bed in this test illustrates the concept of a thin-bed formed using CalSil.

The experimental head loss shown in Figure 8 starts out increasing slowly until the flow velocity was increased beyond ~0.5 ft/s; then the head loss increased rapidly before resuming a more gradual rate of increase. This behaviour is attributed to the filtration efficiency at which the NUKON[®] fibers filtered the CalSil from solution. The higher pressures of flow at higher velocities compressed the fiber, reduced the interfiber spacing, and increased the particulate filtration efficiency. Apparently, when the velocity was increased beyond 0.5 ft/s, the filtration process filtered more of the very fine CalSil particles from the flow, subsequently rapidly increasing the resistance to flow; the actual increase in mass filtered from the flow was much less significant.

The filtration process also is illustrated by the turbidity measurements (a measure of water clarity) as shown in Figure 9, where the turbidity in nephelometric turbidity units (NTU) is compared with the bed compression ratio predicted using the NUREG/CR-6224 correlation. According to the NUREG/CR-6224 correlation, when a debris bed is compressed to the limit determined by the

granular packing density, further compression ceases. In Figure 9, the turbidity is shown to drop significantly at that point (a bed compression ratio of ~ 0.22), signalling a sharp increase in the particulate filtration, which, at this level of turbidity, means the very small particles. Note again that the specific surface area is substantially higher for smaller particles than larger particles (i.e. roughly proportional to 1 divided by the diameter of the particle). This is a strong indicator that the relative high head losses associated with CalSil can be attributed to the fineness of the particulate.

Figure 8. Head-loss data from thin-bed Test 6C

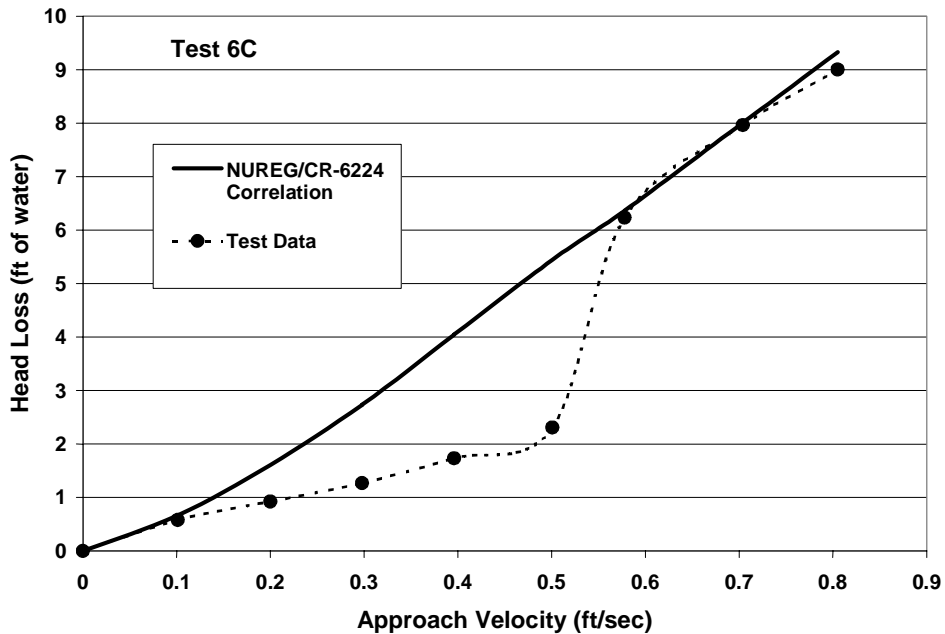
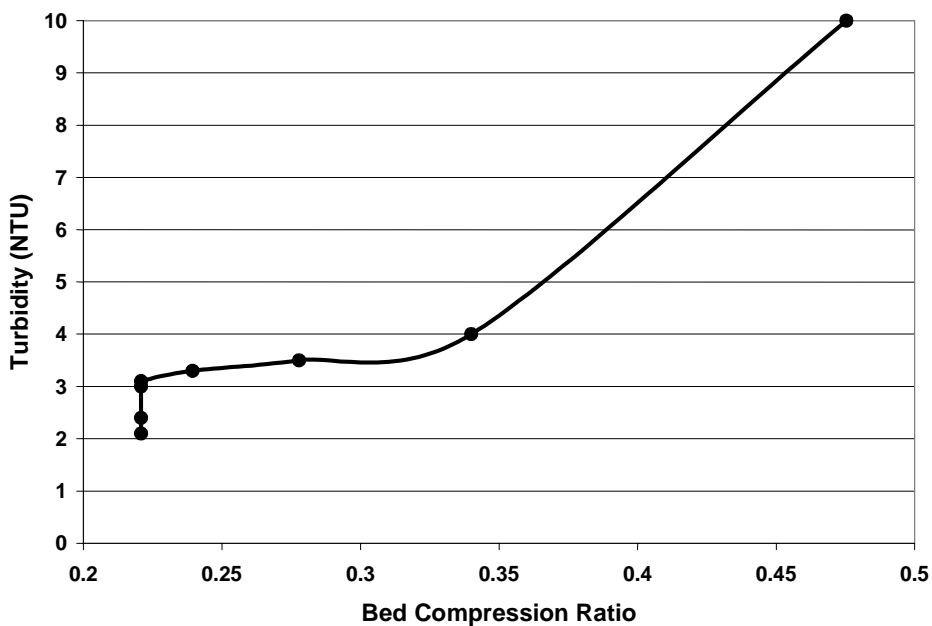


Figure 9. Turbidity measurements for Test 6C relative to debris-bed compression



Because Test 6C passed the compressible phase into the compression limited phase, this data was used to estimate the sludge or granular packing density for the CalSil using the NUREG/CR-6224. That is, the packing density was varied in the correlation until the data point at ~0.5 ft/s was not limited but the data point at ~0.6 ft/s was limited. The sludge packing density was estimated at 16.3 lbm/ft³ (~12% more dense than the fabricated density). In the same analytical process, the specific surface area for the CalSil was varied until the NUREG/CR-6224 correlation predicted the overall test results with reasonable accuracy, as shown in Figure 8. Note that the correlation does not account for incomplete filtration. The specific surface area estimated from the Test 6C results was 550 000 ft²/ft³.

The head-loss results for Tests 6F and 6B are shown in Figures 10 and 11, respectively. In both of these tests, the NUREG/CR-6224 correlation, using the parameters estimated from the analysis of Test 6C, did a reasonable job of predicting the test data. A hysteresis effect is shown for both of these tests, where the head loss upon flow reversal remained higher than when the flows were increasing, i.e. the bed decompressed at a much slower rate as the velocities slowed than when the velocities increased. A majority of the CalSil (by mass) was filtered from the flow upon bed formation, but the water still appeared cloudy because of fine debris in suspension. The water tended to clear substantially by the time the flow velocity was increased to ~0.2 ft/s. As the velocities decreased, some of the CalSil was released from the bed; however, most of it remained trapped in the fibers.

The debris bed in Test 6B was formed uniformly enough (shown in Figure 7) that the thickness of the bed was measured as a function of the approach velocity. The nominal as-fabricated bed thickness was 1.56-in. The measured bed thickness is compared with the NUREG/CR-6224 predicted bed thickness in Figure 12. The predicted thicknesses are within the uncertainty of the measured thicknesses. This comparison further validates the NUREG/CR-6224 correlation regarding its ability to predict the behaviour of NUKON[®].

Figure 10. Head-loss data from Test 6F

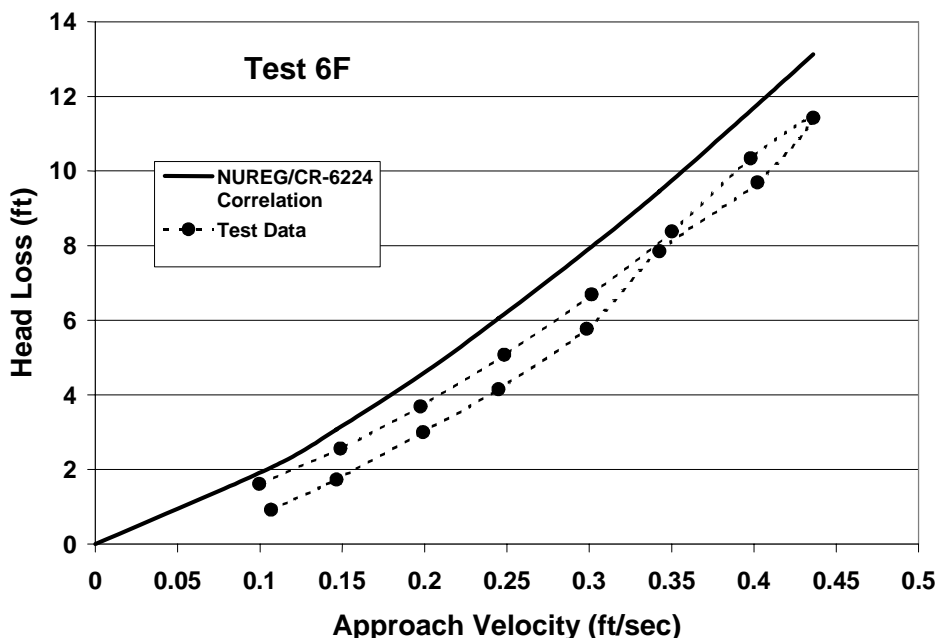


Figure 11. Head-loss data from Test 6B

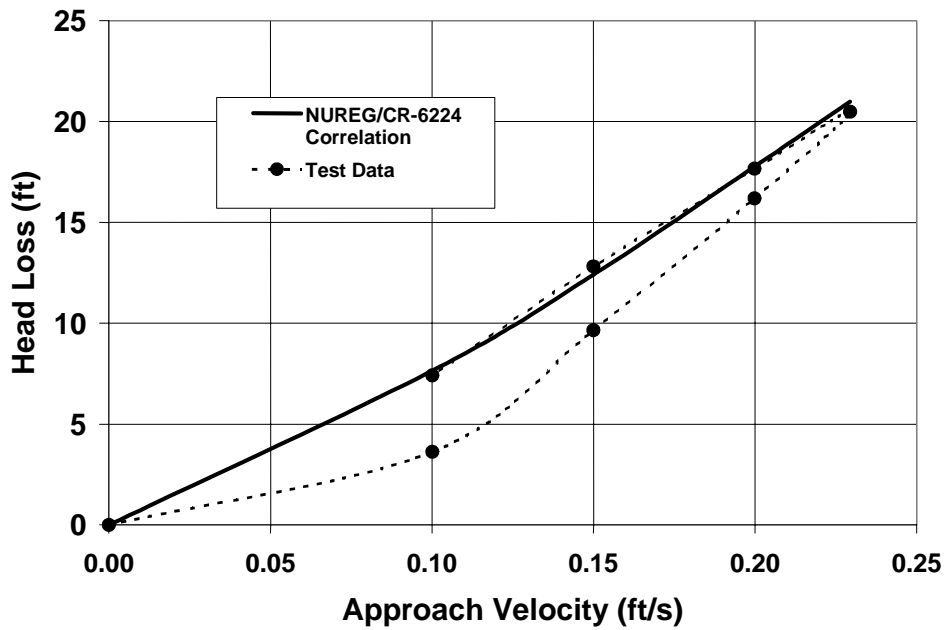
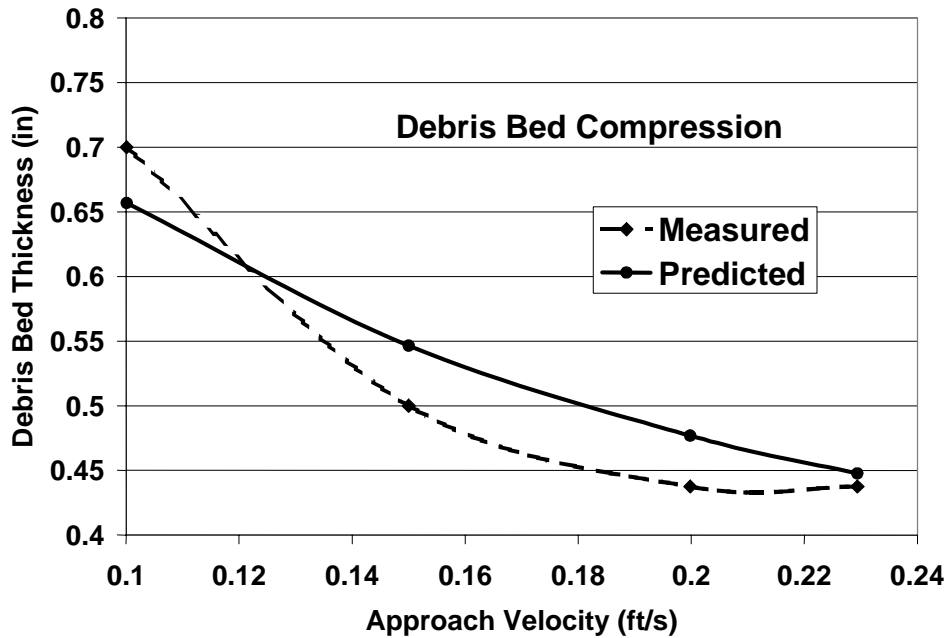


Figure 12. Comparison of debris-bed compression from Test 6B with correlation



The NUREG/CR-6224 correlation, using the parameters estimated from the analysis of Test 6C, also was compared with the data for other test results, with either good agreement or conservative prediction of the data. The quality of several of the tests was compromised by the testing difficulties discussed above, resulting in lesser head losses than would have occurred had the test been trouble free. In such cases, the correlation would be expected to overpredict the data, as was the case.

4. Conclusions

Debris-accumulation data, consisting of qualitative insights recorded in photographs, illustrated how debris deposits on a vertical screen. The accumulation of fine fibrous debris that remains suspended in the sump pool, even at relatively low levels of turbulence, will form a very uniform bed of fibrous debris across the submerged portion of the recirculation sump screen. Larger debris in suspension, due to high flow velocities and associated turbulence, also will accumulate relatively uniformly but may be gravitationally skewed toward the bottom of the screen, depending on the velocity of flow. Debris that travels along the floor as it approaches the screen tends to form a pile at the base of the screen; however, if flow velocities are sufficient, pieces of debris then may climb the screen to cover previously debris-free portions of the screen. A realistic fiber debris bed could consist of fine fibers uniformly distributed over the screen, with larger pieces piled at the base.

The capability of the NUREG/CR-6224 correlation to predict the head losses associated with CalSil insulation debris has been demonstrated. For CalSil and other types of debris, an appropriate set of debris-specific input parameters must be determined. The tests demonstrate that the principal reason CalSil insulation debris causes disproportionately higher head losses than comparable quantities of other types of insulation debris is the relative fineness of the particulate. The more fine the particulate, the higher the specific surface area and the higher the head losses. A difficulty in testing CalSil has been the incompleteness of the filtration of the particulate from the flow stream, which depends on the compaction of the debris bed. When a thin bed forms that has a granular layer of CalSil debris, the filtration efficiency increases substantially so that the very fine particles that might normally pass through the bed are filtered. The addition of the very fine particles to the debris bed, along with the corresponding high specific surface areas, contributes greatly to the disproportionately high head losses.

The input parameters for the NUKON[®] and calcium insulations, as tested and as applied to the tests reported herein, are:

Parameter	PCI NUKON [®]	PCI CalSil
Effective particle density (lbm/ft ³)	175	115
Granular packing density (lbm/ft ³)	N/A	16.3
Specific surface area (ft ² /ft ³)	171 000	550 000

Cautions regarding the use of these CalSil parameters include:

- The LANL test report, LA-UR-03-0471, should be consulted for final recommendations.
- These properties pertain to the PCI CalSil insulation tested herein, and the properties for CalSil manufactured using different materials or mixtures or processes may differ significantly.
- These properties should be conservatively enhanced for safety analyses.

**EXPERIMENTAL INVESTIGATIONS FOR FRAGMENTATION AND INSULATION
PARTICLE TRANSPORT PHENOMENA IN WATER FLOW**

S. Alt, R. Hampel, W. Kaestner, A. Seeliger
University of Applied Sciences Zittau/Goerlitz (Germany)

Abstract

The paper includes the description of separate effect test facilities used for investigations with regard to the fragmentation and the transport behaviour of different insulation materials in multi-dimensional aqueous flow. The instrumentation of the rigs is specified, in particular modern digital image processing technologies. First experimental results are shown and discussed generated at three acrylic glass test facilities. The experimental data could use for CFD-modelling and validation.

1. Introduction

The investigations for debris generation and transport gain in importance regarding the reactor safety research for PWR and BWR considering all types of LOCA as well as short and long term behaviour of emergency core coolant systems. As a result of LOCA's solid particles such as insulation materials can be released in the coolant circuit. In this scenarios core safety should be provided. Therefore investigations of methods (analytical and experimental) and tools (simulation codes, models) are necessary, which allows two and three dimensional simulations for stationary and dynamic behaviour of coolant flow with solid particles. A gist within these investigations is the development of 3-D-models simulating two-phase flow of water and insulation particles in large geometries. The background of experimental investigations consists of the generation of a wide data base developing and validating such CFD-models (computational fluid dynamics) for the description of insulation particle transport phenomena in flow (e.g. drift, subsidence) under various geometric and fluidic boundary conditions, as well as sedimentation, resuspension, agglomeration, clogging and increasing of differential pressure at hold-up devices. Separate effect experiments regarding these processes were carried out at three acrylic glass test facilities (Column quasi 1/2-D, Ring Channel 2-D, Tank 3-D) using modern flow measurement and digital image processing technologies.

2. Test rig "Fragmentation"

Blast experiments were carried out at the rig "Fragmentation" (Figure 1) to simulate LOCA and to fragment different insulation materials under real accident conditions, e.g. with saturated steam up to 7 MPa (BWR-LOCA). The facility was also designed for experiments with saturated water up to 11 MPa (simulation of PWR-LOCA).

As a result of these experiments fragmented insulation materials were produced. The debris of each experiment was stored in aqueous solution to apply this debris solution at the various separate effect acrylic glass test facilities.

Figure 1. Scheme of the test rig Fragmentation

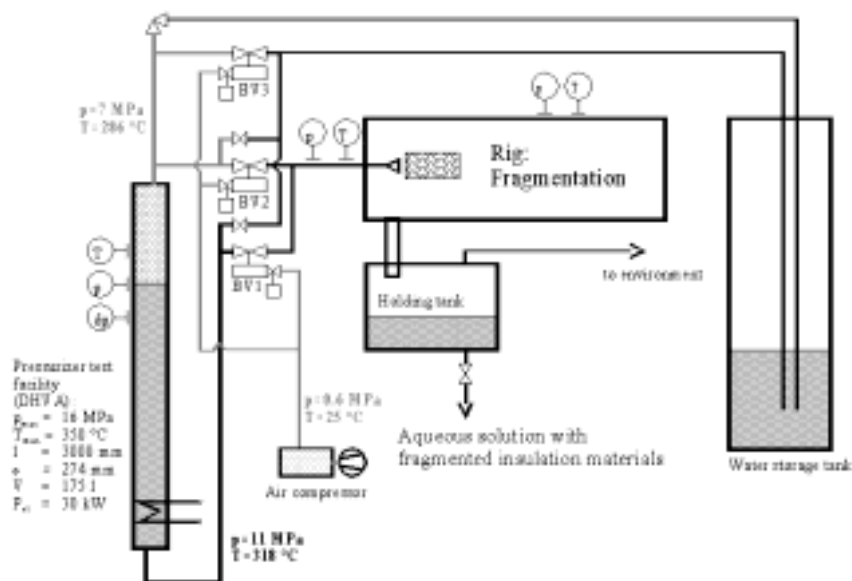
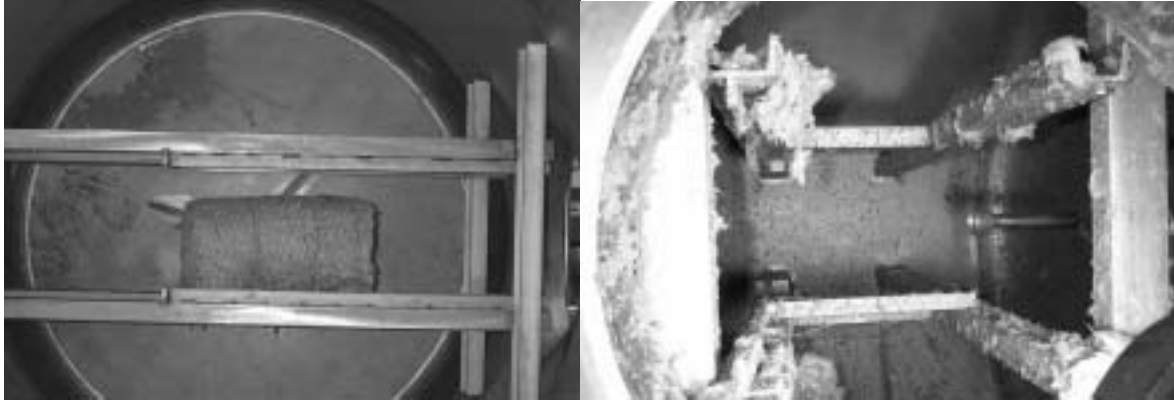


Figure 1. a) Mineral fibre (MD2, 1999) test body

b) Fragments after rupture simulation (7.0 MPa; 285°C)

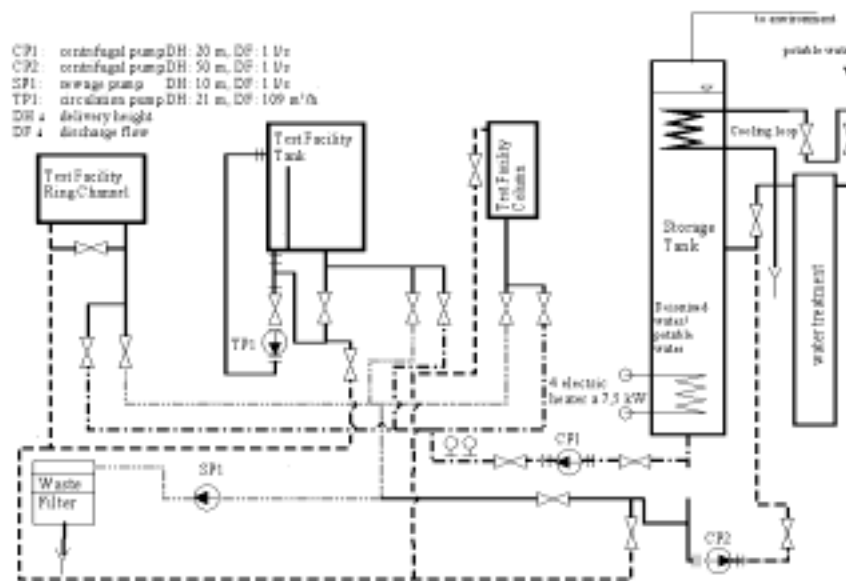


3. Acrylic glass test facilities

3.1 General survey

An overview about the arrangement of several acrylic glass test facilities, the water supply and waste water disposal and the auxiliary components (ball valves, pumps, heaters) are shown in Figure 3. It is possible to feed the facilities with potable water or with deionised water or a mixture of both. A degassing of water can be realised with the electric heaters in the storage water tank. The three acrylic rigs work under atmospheric pressure conditions. The temperatures can vary between 20°C and 80°C.

Figure 3. Scheme of the water system for three acrylic glass facilities “Column”, “Ring Channel” and “Tank”



3.2 “Column” test rig

The behaviour of gravitating insulation particles in aqueous solution and sedimentation processes were observed at the test facility “Column” in 1/2D-geometry without enforced water flow using an image processing system. The facility consists of a rectangular acrylic glass column with the following dimensions:

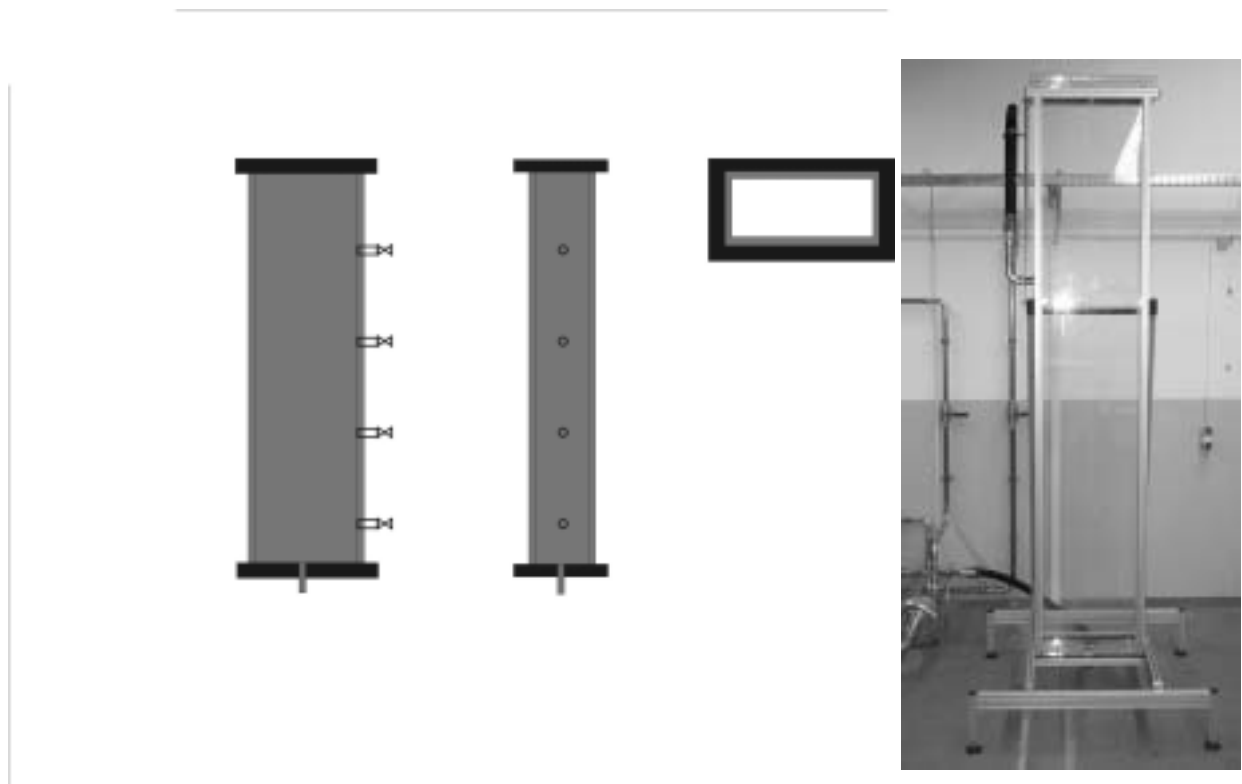
- inner length: 0.50 m;
- inner width: 0.10 m;
- inner height: 3.00 m.

The thickness of the acrylic glass amounts 25 mm.

The mean measured values are:

- x-y-paths of sinking particles;
- sink rates or settling velocities of the insulation particles;
- geometric properties and light densities of the single particles; and
- distribution of particle concentration.

Figure 4. Scheme of the “Column” rig



3.3 “Ring Channel” test facility

The “Ring Channel” was designed as an oval acrylic glass flow channel. The channel consists of two straight sections with a length of 5 m, separated into single segments with a length of 1 m, and two semi-circular segments (Figures 5 and 6). The facility dimensions reads as follows:

- length: 6.20 m;
- width: 1.20 m;
- height: 1.20 m;
- flow width: 0.10 m;
- stretched length of the channel: 13.31 m;
- length of straight channel segments: 5.00 m;
- maximal flow velocity : 0.85 m/s;
- volume (1 m filling height): approx. 1.40 m³.

Figure 5. Scheme of the facility “Ring Channel”

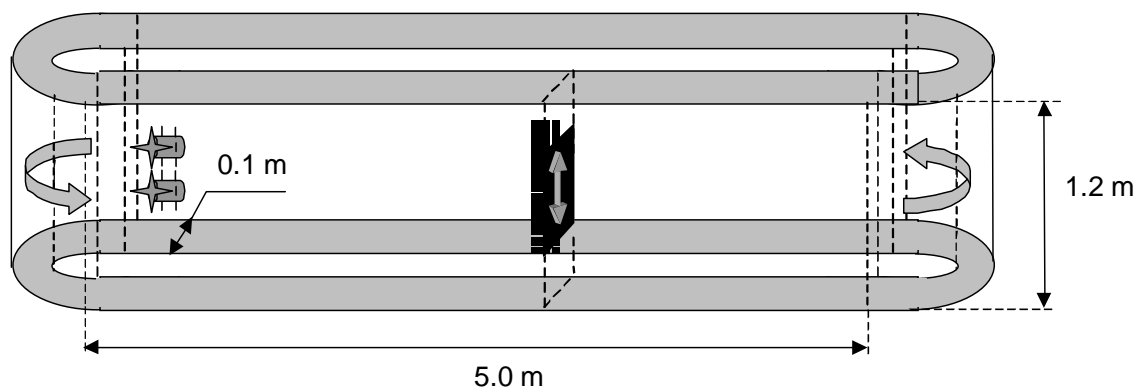
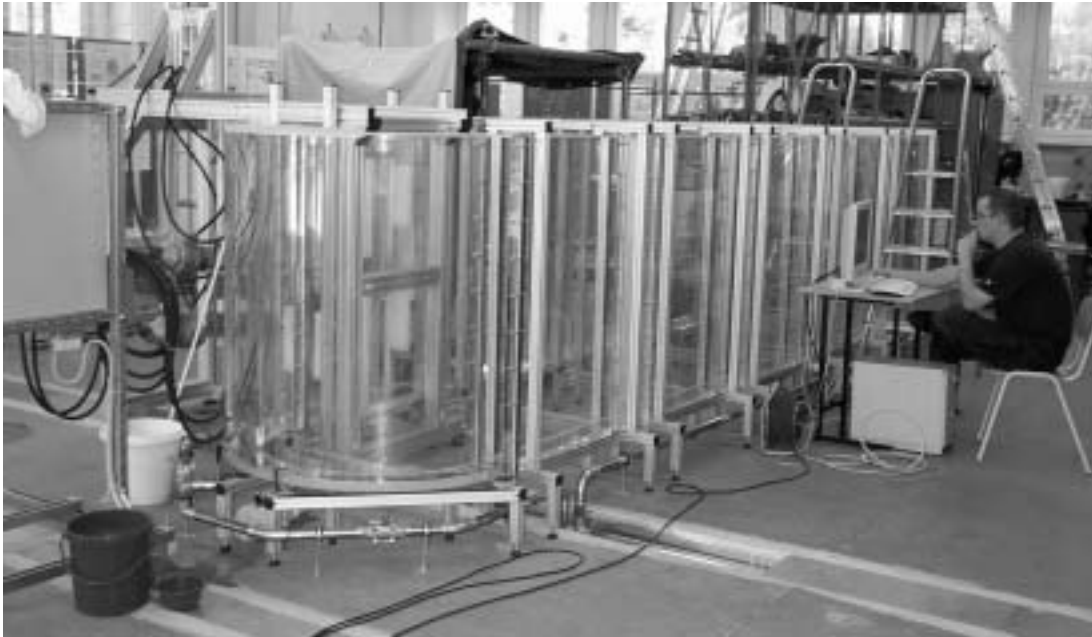
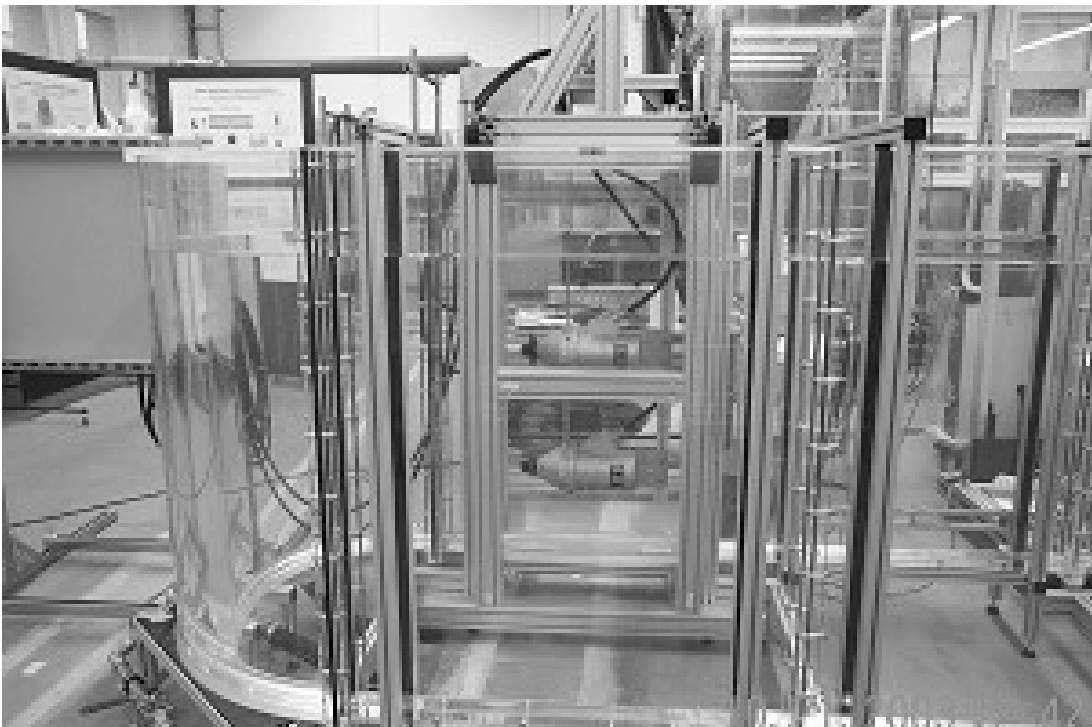


Figure 6. Facility “Ring Channel”



The segments of the facility are designed in form of a rectangular cross section with a wide of 100 mm and a height of 1 200 mm. To generate a defined flow regime two impellers are installed, which have the advantage of a reduced influence on the isolation material (Figure 7). The vertical position of the impellers can be changed. The impeller rotation frequencies can be varied continuously within a range of 0 to 50 rpm.

Figure 7. Acrylic glass segment with impellers (background)

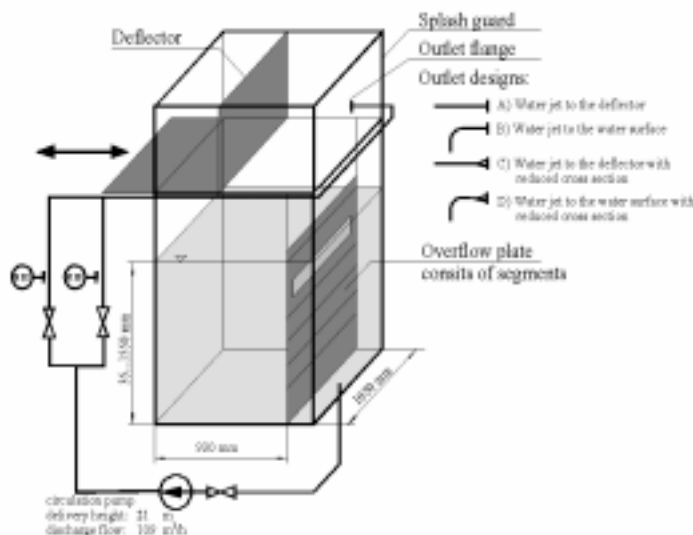


Experiments for the determination of 2D-transport behaviour of different particle sizes in horizontal carrier flow were realised at facility “Ring Channel”. Experimental results were generated with constant cross section area along the whole channel length as well as with barriers and varied cross section areas (e.g. stairs).

3.4 Test rig “Tank”

Experiments performed at the test facility “Tank” included the investigations regarding waterfall effects on a two phase mixture of insulation particles and water under consideration of turbulences in a 3D-flow field. It was taken into account three types of water fall jets (free jet, line jet, area jet).

Figure 8. Configuration of the “Tank” facility

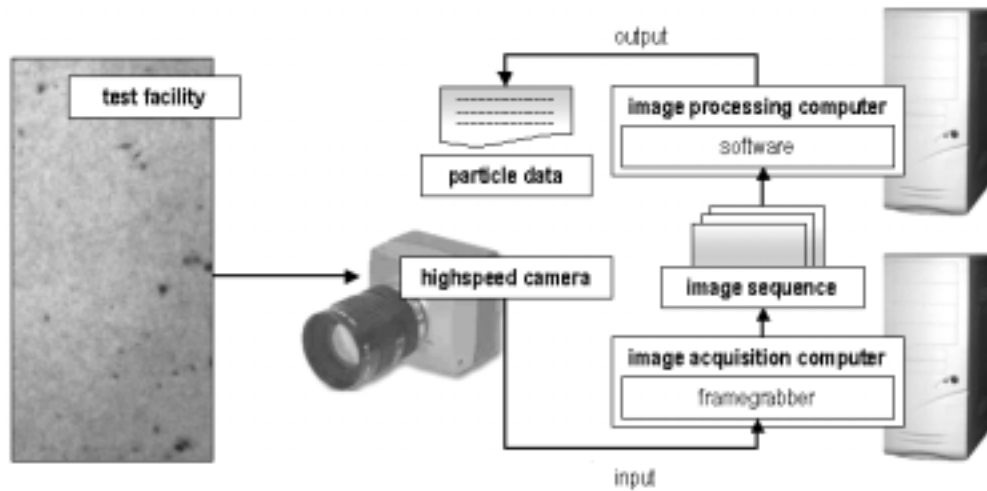


3.5 Instrumentation

The generation of a qualified data basis for CFD-Code model development needs detailed data of the water basis flow and the relative movement of particles in this flow. The velocity profiles of the water basis flow were measured with LDV-technology (Laser Doppler Velocimetry) as well as with a PIV-system (Particle Image Velocimetry). Laser measurement technology also allows the investigation of the intensity of turbulence. Furthermore, the average velocity was measured at different heights with an ultrasonic system in the facility “Ring Channel” using the difference elapsed time method. The total mass flow of the circulation in the “Tank” test rig was detected with MID (magnetic inductive detectors).

Modern digital image processing technologies were applied to measure particle geometries, particle movements and particle velocities using digital highspeed CMOS-cameras. The used image processing system is displayed in Figure 9. It consists of altogether two highspeed cameras, which allow the taking of pictures with a resolution up to 1 280 x 1 024 pixel. Because of random programmability of window size, position (region of interest) and clock frequency, the resolution and the frame rate can be adapted to any specific need. Both cameras can be triggered simultaneously.

Figure 9. Configuration of the image processing system

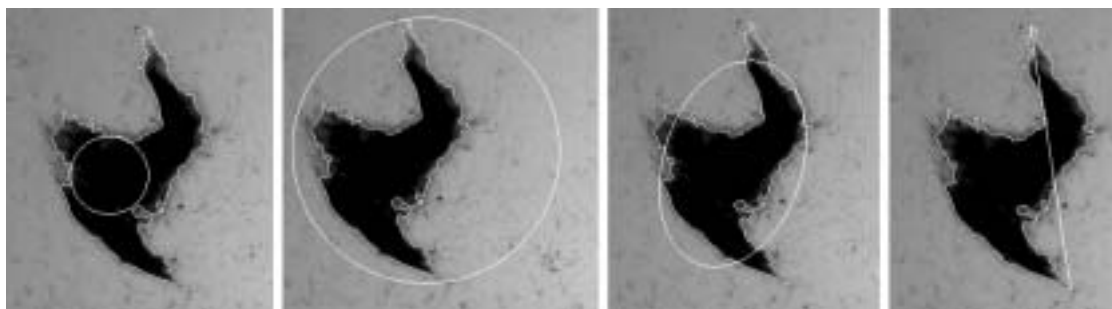


The resulting images underwent a preprocessing for improving attributes like contrast and brightness. Radial distortion effects, caused by optical components of the system, were compensated. In the following operation the objects of interest and the image background were segmented by using several image processing methods like background subtraction and the region growing algorithm.

As a result the unique particle regions of an image were specified. Significant characteristics of the particle objects can be calculated, e.g. contour length, surface area, grey value volume, centre of gravity for area and grey value, position in x and y directions of the world coordinate system (for 2-D geometries), volume, position in x, y and z directions of the world coordinate system (in 3-D geometries).

In addition to these properties several shape factors can be figured out, e.g. circularity, compactness, convexity, largest inner circle of the particle region, maximal distance between two contour points, parameters of the equivalent ellipse and smallest surrounding circle.

Figure 10. Graphical representation of a subset of shape factors
(inner circle, outer circle, equivalent ellipse, maximal distance between contour points)



Applied to a whole sequence, it was possible to trace particles image by image. The velocity of the observed objects could be calculated taken into account the recording time of the sequence. Furthermore, it was also possible to detect a whole range of specific phenomena like particle collision, overlap, splitting and merge.

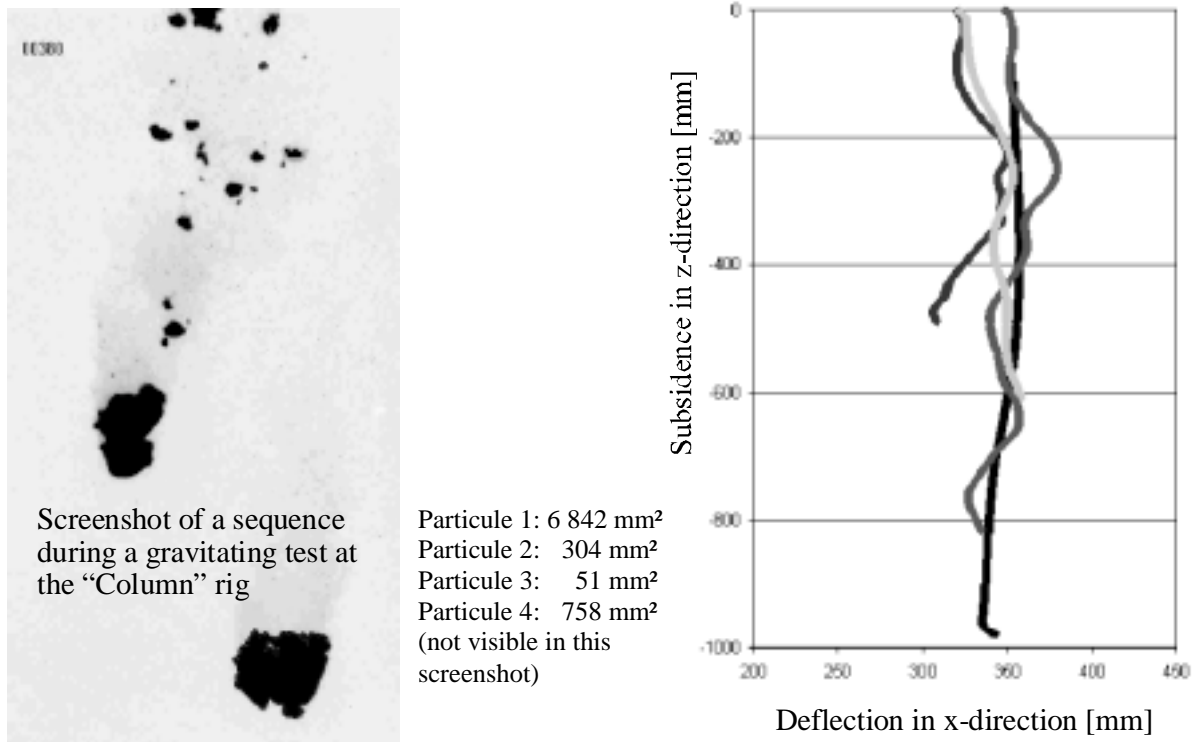
Statistical analyses permitted a classification of flow relevant parameters in clusters which depended on typical geometrical dimensions and on shape factors of different particle sizes.

4. Experimental results

4.1 Results of sinking experiments at facility “Column”

Sinking experiments were carried out with single particle fragments as well as with particle mixtures. Figure 11 shows a screenshot of the detected high speed sequence during a sinking experiment with MD2 insulation material. Analysis algorithms of image processing methods admit the detection of each particle, their properties and motions. On the right side of Figure 11 the movement of the grey value centre is illustrated for four particles with different cross sections.

Figure 11. Example of a sinking experiment



Taken into account the image system parameters it is possible to determine the time depended motion of the particles and the vectorial velocities, how it is shown in Figures 12 and 13.

Figure 12. Time dependent motion of gravitating particles in z-direction

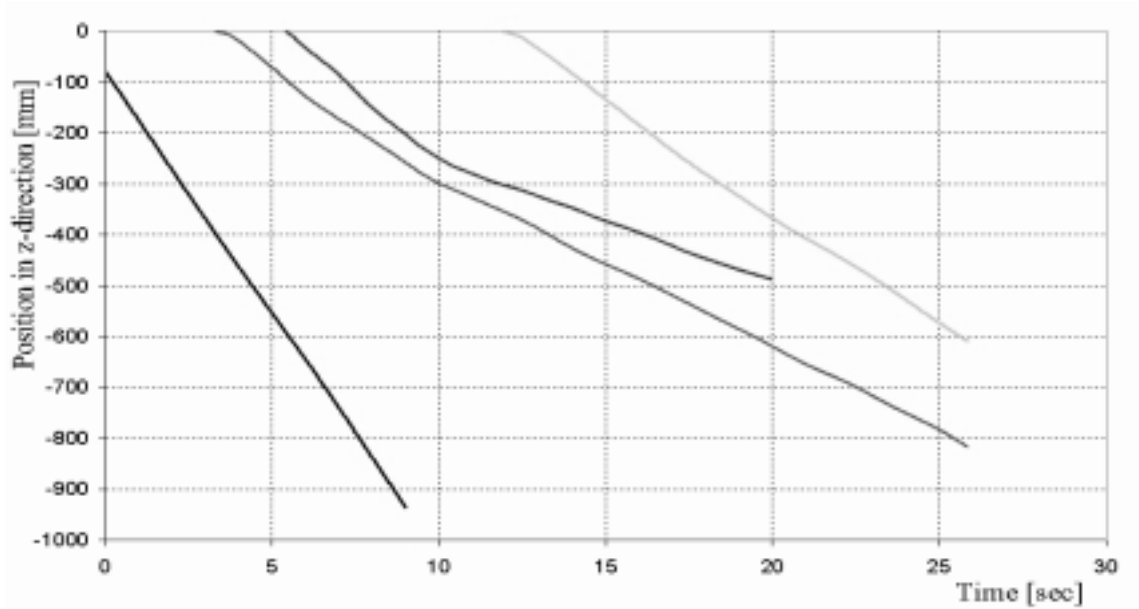
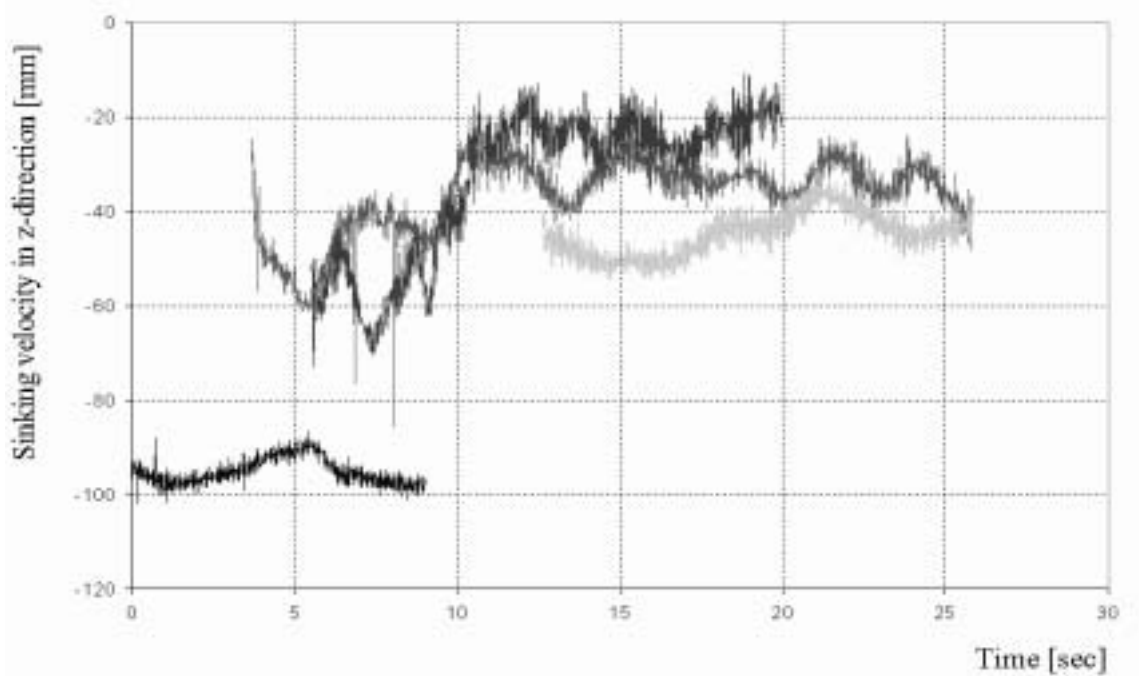
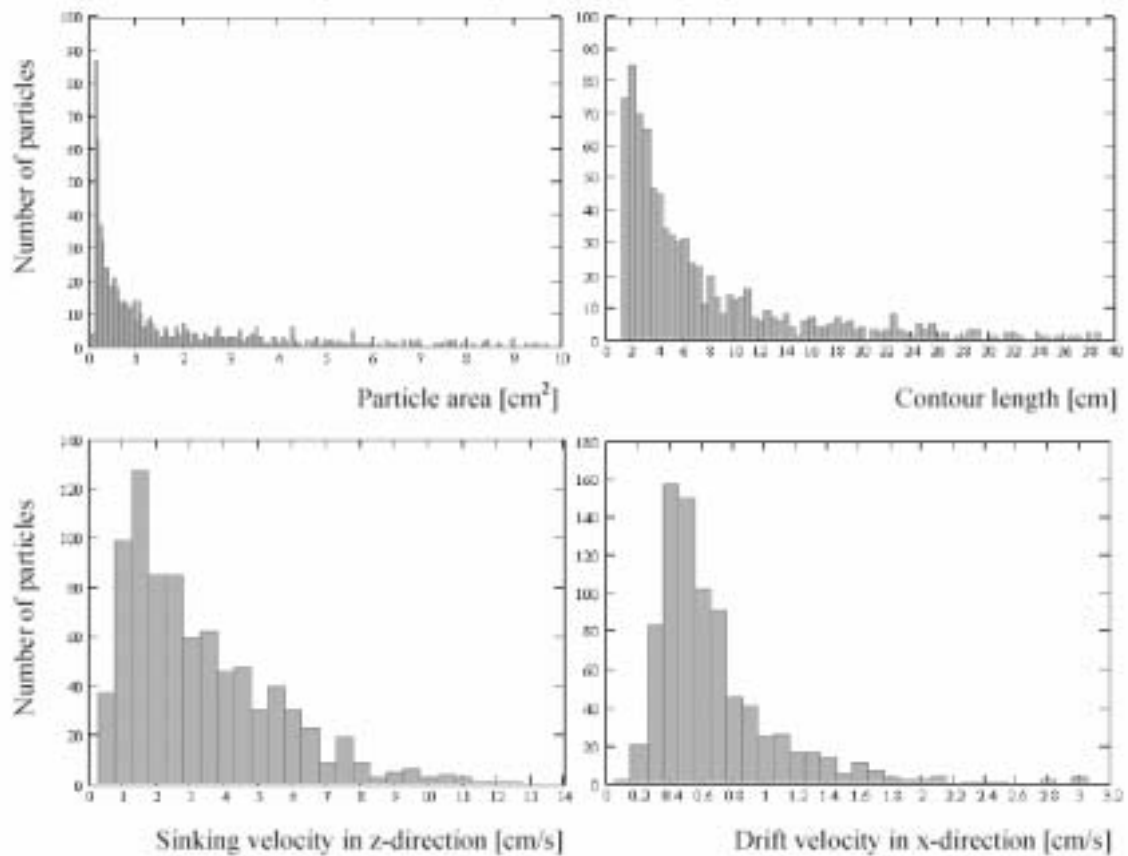


Figure 13. Vectorial velocity in z-direction



A lot of sinking experiments were realised. The vectorial velocities of several hundreds particles were determined. The histograms for particle areas, contour lengths and vectorial velocities of first MD2-sinking experiments at the “Column”-rig are shown below in Figure 14. Next steps of data evaluation will include the data interpretation with methods of cluster analyses to generate dependencies of vectorial velocities on the detected parameters.

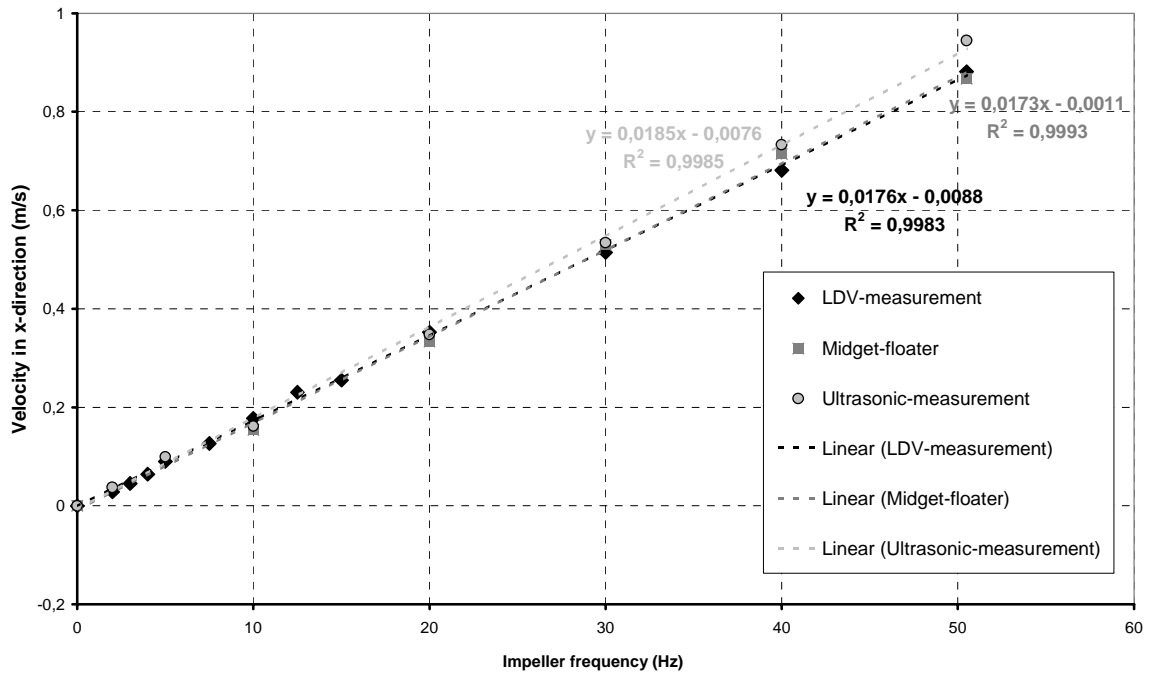
Figure 14. Histograms for sinking experiments



4.2 Water basis flow and particle movement at facility “Ring Channel”

At first it was necessary to detect the dependence between impeller rotation speeds and average water basis flow velocities. The characteristic curves which were measured by different measuring systems are very closed, how it is shown in Figure 15. However, it is possible to control the average water velocities in the “Ring Channel” between 0 and 0.90 m/s.

Figure 15. Characteristic diagram of average water velocity over impeller frequency



Secondly the vertical and horizontal profiles of the water basis flow were determined in the segments. Figure 16 includes the vertical profile of the average velocity in segment 3 measured by the ultrasonic system. This segment 3 is arranged two segments in direction to the impeller segment. The impellers were positioned in 250 mm and 625 mm height and rotated with equal frequencies. Characteristic vertical velocity profiles with two maxima at 100 mm and 500 mm height were observed up a speed of 5 cm/s. Quite uniform profiles could be determined for lower impeller rotation speeds. The profiles have been approved by local LDV-measuring. The LDV measured data are shown in Figure 17. The absolute LDV values are larger than the ultrasonic data because the LDV data were determined in the centre of the “Ring Channel’s” breadth and the US data represents average velocities.

Horizontal profiles at different elevations are shown in Figure 18 with the lowest impeller rotation speed at 2 Hz. The results clarify quite good turbulent profiles. So, it was possible to accept that the image measurement system could observe a 2D-flow behaviour of insulation particles.

Figure 16. Vertical average velocity profile of the basis water flow in segment 3

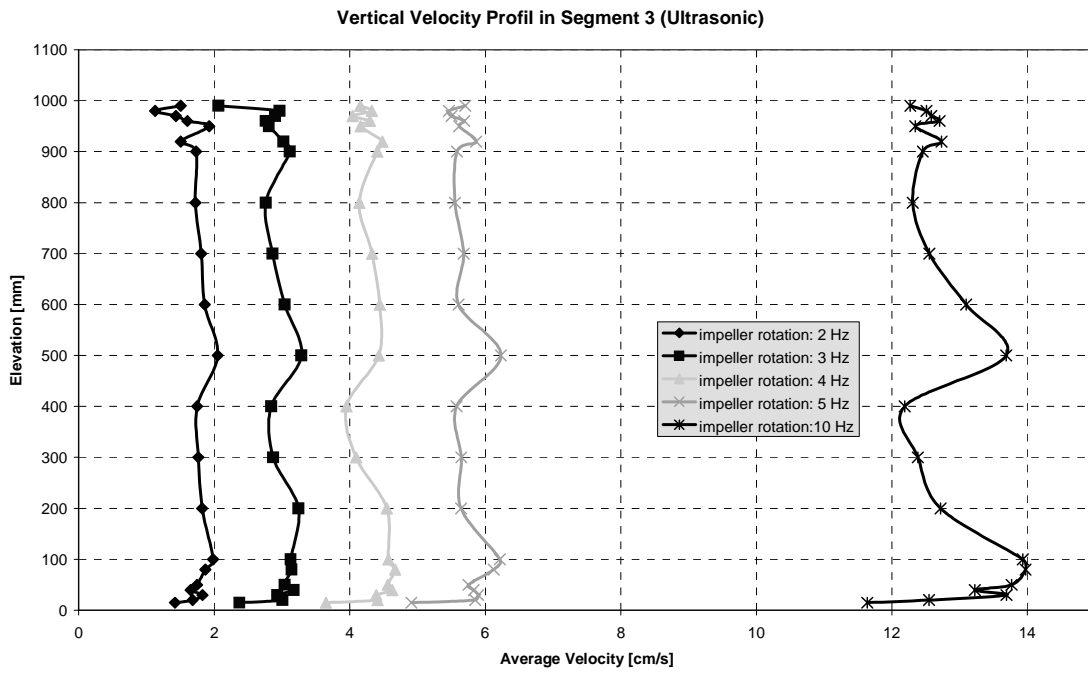


Figure 17. Vertical local velocity profile of the basis water flow in the centre of segment 3

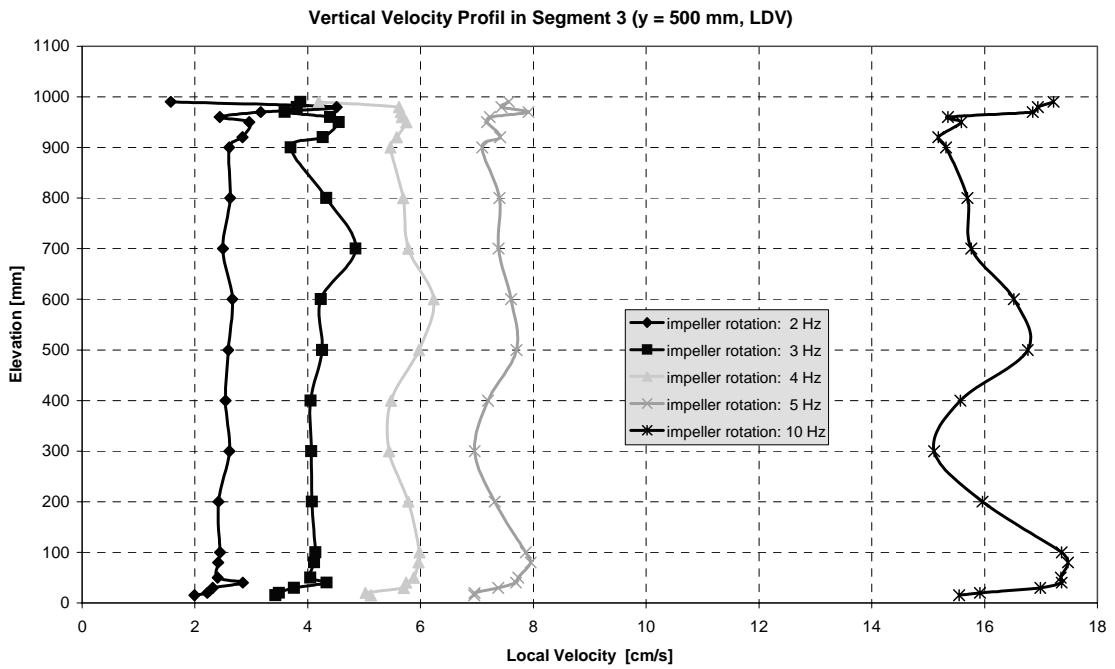
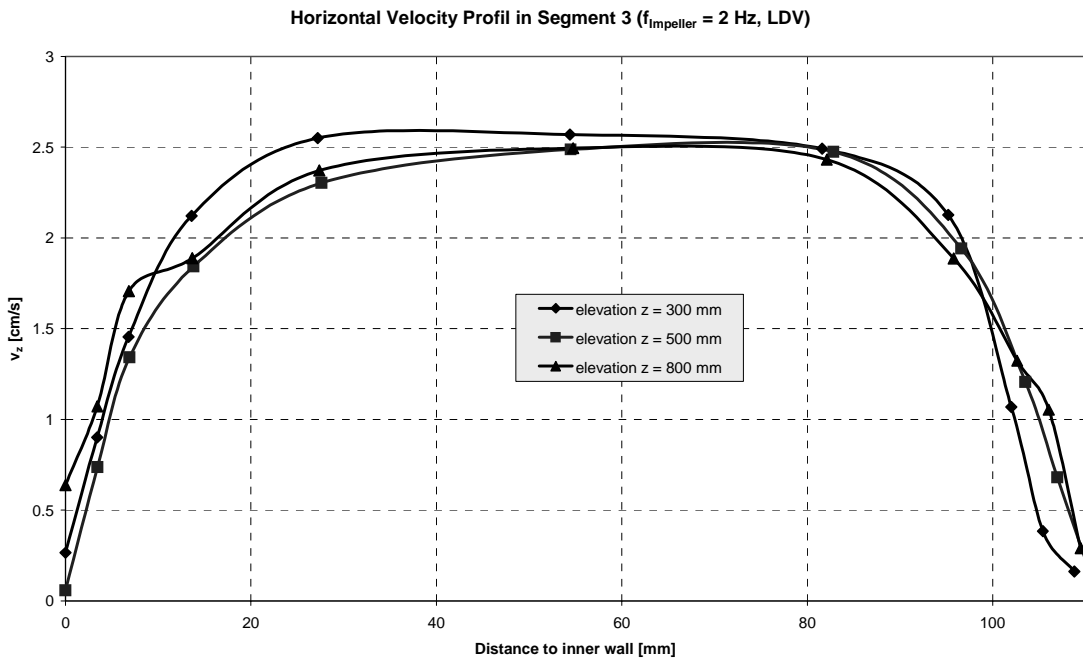


Figure 18. Horizontal velocity profiles of the basis water flow in segment 3



After the determination of the basis water flow, experiments with particle fragments were realised.

Figure 19 shows a screenshot of a sequence generated at segment 3 with a MD3 insulation particle solution and impeller frequencies of 5 Hz.

The coloured lines of each particle illustrate the trajectories. The blue lines surround the ambient dimension of the particles. This is a size for the cross section area of the particles. So, it is possible to determine some important parameters for CFD-modelling, how the velocity vectors of each particle, the drift in the 2D-water basis flow field, the 2D-area (3D-volume) fraction of solid-water flow, the sedimentation rate, etc.

The next steps will include statistic analyses of the very large data basis for 2D-solid-water flow. The experiments will be going on with different insulation materials as well as with barriers, grids and varied cross section areas (e.g. stairs) inside the “Ring Channel” test facility.

Figure 19. Screenshot of a sequence observed with the image measurement system at segment 3



5. Outlook

Statistic analyses will permit a classification of flow relevant parameters in clusters which depend on typical optical parameters, geometrical dimensions and on shape factors of different particle sizes. The analyses also allow the formulation of general rules concerning the behaviour of insulation particles under various ancillary conditions.

The data basis for CFD-Code will be extended by additional data to the 2D-flow concerning the behaviour of insulation particles in a 3D-flow field under consideration of turbulences. According experiments will be realised at the test facility "Tank". It permits the observation of any influences of waterfall effects on a two-phase mixture of insulation particles and water.

Furthermore, the developed modelling for CFD-Codes will be validated by supplemental experiments on large scaled integral test facilities.

Acknowledgements

The investigations described in this paper have been financed by the German Federal Ministry of Economy and Labour.

EFFECTS OF DEBRIS GENERATED BY CHEMICAL REACTIONS ON HEAD LOSS THROUGH EMERGENCY CORE COOLING SYSTEM STRAINERS

Kerry Howe and Arup K. Maji

University of New Mexico, Albuquerque, New Mexico, USA

Ashok Ghosh

New Mexico Institute of Mining and Technology, Socorro, New Mexico, USA

Bruce C. Letellier and Russ Johns

Los Alamos National Laboratory, Los Alamos, New Mexico, USA

Tsun-Yung Chang

Nuclear Regulatory Commission, Washington, DC, USA

The effect of debris generated during a loss of coolant accident (LOCA) on the emergency core cooling system (ECCS) strainers has been studied via numerous avenues over the last several years. The research described in this manuscript examines the generation and effect of secondary materials – not debris generated in the LOCA itself, but materials created by chemical reactions between exposed surfaces/debris and cooling system water. The secondary materials studied in the research were corrosion products from exposed metallic surfaces and paint chips that may precipitate out of solution, with a focus on the corrosion products of aluminium, iron, and zinc. The processes of corrosion and leaching of metals with subsequent precipitation is important because: (1) the surface area of exposed metal inside containment represents a large potential source term, even for slow chemical reactions; (2) the chemical composition of the cooling system water (boric acid, lithium, etc.) may affect corrosion or precipitation in ways that have not been studied thoroughly in the past; and (3) an eyewitness report of the presence of gelatinous material in the Three Mile Island containment pool after the 1979 accident suggests the formation of a secondary material that has not been examined under the generic safety issue (GSI)-191 research program.

This research was limited in scope and consisted only of small-scale tests. Several key questions were investigated: (1) do credible corrosion mechanisms exist for leaching metal ions from bulk solid surfaces or from zinc-based paint chips, and if so, what are the typical rate constants? (2) can corrosion products accumulate in the containment pool water to the extent that they might precipitate as new chemical species at pH and temperatures levels that are relevant to the LOCA accident sequence? and (3) how do chemical precipitants affect the head loss across an existing fibrous debris bed? A full report of the research is available.¹

1. Johns, R.C., B.C. Letellier, K.J. Howe, and A.K. Ghosh, “Small-Scale Experiments: Effects of Chemical Reactions on Debris-Bed Head Loss”, Los Alamos National Laboratory report LA-UR-03-6415 (November 2003).

Experimental setup and methods

The research consisted of two components: (1) corrosion rate experiments conducted in batch reactors, and (2) head-loss experiments conducted in a closed-loop recirculating hydraulic test system.

Zinc corrosion tests

Corrosion tests were conducted in 1-liter containers. The candidate metal for the corrosion tests was zinc, and the tests were performed with zinc granules, zinc coupons, and crumbled inorganic zinc paint primer. The experimental variables were pH, temperature, immersion duration, and immersion solution. Corrosion rates were determined using the weight loss method; i.e. a quantity of material with a known surface area was immersed in a solution for a known duration, and the change in weight due to corrosion was measured. Samples ranging from about 1 g to 10 g were used, and the weight loss was determined by measuring the weight of the sample before and after immersion using procedures in Standard Method 2540-D.² Weight was measured with an analytical balance that had a resolution of 0.0001 g. In addition, the zinc concentration in solution after immersion was measured to provide a second, and independent, measurement of the mass of zinc lost.

The immersion solution for most experiments was a prepared solution containing 3.3×10^{-2} M boric acid (H_3BO_3) and 2.0×10^{-4} M lithium hydroxide (LiOH) in deionised water, to simulate the solution chemistry in the containment pool. The pH of the immersion solution was adjusted using HCl or NaOH, with the target pH typically being either pH = 7.0 or pH = 9.0. Some tests selected as a control group used only deionised water as the immersion solution. The first several sets of experiments used glass containers as the immersion vessel and the final set used polypropylene containers.

The target values for the immersion temperature were room temperature, 40°C, and 80°C. The room temperature experiments were conducted by leaving the immersion vessels on a laboratory countertop; the room temperature in the laboratory ranged from 22°C to 25°C during these experiments. The higher temperature experiments were conducted by placing the immersion vessels in a constant temperature laboratory oven capable of maintaining the desired temperature. The immersion duration ranged from 1 to 11.75 days. Many of the experiments were conducted in triplicate.

Head-loss tests

Head-loss flow tests were conducted in a small-scale (10-liter), vertical, closed-loop circulation, hydraulic test system built for measuring the head loss across a fiber-laden screen in a chemical environment typical of that found in the ECCS recirculation sump. Calibration tests were first performed to confirm that head losses induced by a debris bed in the small test system were consistent with previous experiments and with standard correlations documented in NUREG/CR-6224.³ Subsequent tests examined the additional head loss incurred by the precipitation of dissolved

-
2. *Standard Methods for the Examination of Water and Wastewater*, prepared and published jointly by the American Public Health Association, American Water Works Association, and Water Environment Federation, Washington, DC (1999).
 3. Zigler, G., J. Bridaue, D.V. Rao, C. Shaffer, F. Souto, and W. Thomas, "Parametric Study of the Potential for BWR ECCS Strainer Blockage due to LOCA Generated Debris", United States Nuclear Regulatory Commission report NUREG/CR-6224, Science and Engineering Associates, Inc. Report No. 93-554-06-A:1 (January 1994).

metals within the closed circulation loop. These tests were performed with a solution chemistry of 3.3×10^{-2} M H_3BO_3 and 2.0×10^{-4} M Li^+ in deionised water, with pH adjusted to either pH = 7.0 or pH = 9.0 by the addition of HCl or NaOH.

Each test was started by filling the system with the recirculation fluid. The recirculation pump was started and adjusted to a low velocity. Shredded NUKON[®] fibrous insulation was slowly added and allowed to settle against the screen. Once the fibrous debris bed was in place and the head loss was determined to be similar to that predicted by NUREG/CR-6224, the recirculation velocity was adjusted to the predetermined value for that experiment. At that point, precipitation was artificially induced by adding a metal nitrate salt solution to the recirculation loop water. The metal ion concentration in the recirculation loop was significantly above the solubility limit, and precipitates formed almost immediately. The metal ion addition ranged from 5.0×10^{-5} M to 1.0×10^{-2} M. The first tests incorporated the simultaneous precipitation of aluminum, iron, and zinc metals. Head loss across a pre-established fiber mat was observed using pressure transducers located above and below the fiber mat. Temperature and pH were monitored continuously using in-line instruments. The tests were typically an hour in duration, although some longer tests were also conducted.

Results and discussion

Zinc corrosion tests

Six groups of tests were conducted, resulting in 62 separate experiments conducted under a variety of conditions. Each group of tests examined a specific set of independent variables, such as the effect of temperature and pH, the effect of material configuration, or the effect of immersion duration.

The experimental procedures were refined with each set of experiments and, as a result, the final set of experiments produced the most consistent corrosion rate measurements. Weight loss data from the final set of experiments is reproduced in Table 1. For this group of experiments, the material was zinc coupons and the solution chemistry was 3.3×10^{-2} M H_3BO_3 , 2.0×10^{-4} M Li^+ , and pH = 7, and each test condition was done in triplicate.

At room temperature, the coupons lost an average of 9.9 mg after 2 days and 17.1 mg after 4 days. These weight loss measurements correspond to a corrosion rate of $0.055 \text{ g/m}^2\cdot\text{h}$ averaged over 2 days and $0.046 \text{ g/m}^2\cdot\text{h}$ averaged over 4 days. The continued loss of weight between the second and fourth days suggests that the solution had not reached a saturated condition and that the corrosion rates measured by weight loss were representative of the true corrosion rates present under these experimental conditions. These corrosion rates were somewhat higher than those observed in earlier tests but are consistent with the observation that the time-averaged corrosion rate decreased as the zinc concentration increased in solution (in the first group of tests and at the same experimental conditions, the corrosion rate was $0.017 \text{ g/m}^2\cdot\text{h}$ averaged over 11.75 days).

Similar corrosion rates were initially observed for the coupons immersed at 40°C. These coupons lost an average of 10.4 mg after 2 days, corresponding to a corrosion rate of $0.057 \text{ g/m}^2\cdot\text{h}$. After 4 days, however, the average weight loss had increased only marginally to 10.9 mg, causing the time-averaged corrosion rate to drop to $0.030 \text{ g/m}^2\cdot\text{h}$. Since the coupons did not continue to lose weight between the second and fourth days, it appears that the solution had reached saturated conditions, which prevented further corrosion of zinc without the formation of corrosion products.

For this group of tests, the measured zinc concentrations in solution were consistent with the measured weight lost from the zinc coupons, providing two independent sets of measurements that result in similar corrosion rates.

Tests conducted at higher temperature and higher pH conditions were less successful at producing quantifiable corrosion rates, but were nonetheless successful at producing qualitative indications of corrosion. Many of the tests at these conditions resulted in a weight gain over the test duration, thus indicating the formation of a corrosion product with a higher molecular weight than the original material. In addition, many of these tests resulted in the formation of a black coating on the zinc granules and coupons, which could be scraped off. The black coating and the increase in weight indicate the formation of a corrosion product and are qualitative indicators of corrosion.

Table 1. Weight-loss measurements and corrosion rates for the sixth group of zinc corrosion experiments

Test no.	Temp (°C)	Time (h)	Beginning weight (g)	Final weight (g)	Weight change (g)	Corrosion rate (g/m²·h)
6-1	40	48	3.4539	3.4403	-0.0136	0.0769
6-2	40	48	3.4752	3.4679	-0.0073	0.0410
6-3	40	48	3.8883	3.8780	-0.0103	0.0518
				Average:	-0.0104	0.0566
				Std. dev:	0.0032	0.0184
6-4	40	96	3.4306	3.4190	-0.0116	0.0330
6-5	40	96	3.4963	3.4880	-0.0083	0.0232
6-6	40	96	3.8794	3.8666	-0.0128	0.0322
				Average:	-0.0109	0.0295
				Std. dev:	0.0023	0.0055
6-7	22	48	3.4408	3.4298	-0.0110	0.0625
6-8	22	48	3.4763	3.4666	-0.0097	0.0545
6-9	22	48	3.7284	3.7194	-0.0090	0.0472
				Average:	-0.0099	0.0547
				Std. dev:	0.0010	0.0077
6-10	22	96	3.4526	3.4348	-0.0178	0.0504
6-11	22	96	3.7159	3.6979	-0.0180	0.0473
6-12	22	96	3.9052	3.8897	-0.0155	0.0388
				Average:	-0.0171	0.0455
				Std. dev:	0.0014	0.0060

The results from these experiments were compared to previous research conducted under similar conditions. Piippo *et al.*⁴ measured zinc and aluminium corrosion rates using electrical resistance measurements with several test solutions. The solutions included: (1) distilled water that had been adjusted to pH values of 8.0 and 10.0 using LiOH and maintained in either aerated or de-aerated conditions and (2) a 0.1-M H₃BO₃ solution buffered at pH 9.2. For purposes of comparison, the test conditions in the current experiments are most closely comparable with the H₃BO₃ solution used by Piippo. In that solution, Piippo measured zinc corrosion rates of 0.05 g/m²·h at 50°C, 0.03 g/m²·h at 70°C, and 0.04 g/m²·h at 90°C. Piippo *et al.* noted that their measured corrosion rates were consistent with previous results reported by van Rooyen⁵ and Loyola and Womelsduff⁶, which also experimentally measured corrosion rates of zinc in water containing H₃BO₃. The results of the current study, with corrosion rates of 0.055 g/m²·h at 22°C and 0.057 g/m²·h at 40°C, are consistent with rates measured in previous studies.

Piippo measured higher zinc corrosion rates under other experimental conditions. For most aqueous solutions, the corrosion rate increased by at least an order of magnitude when the temperature increased above the normal boiling point of water. In the H₃BO₃ solution, Piippo measured a zinc corrosion rate of 4.45 g/m²·h at 110°C and 1.26 g/m²·h at 130°C. However, the highest measured zinc corrosion rate in the Piippo report was a value of 11.27 g/m²·h, which was measured in deaerated deionised water at 170°C, after the test materials had been exposed to hot steam at 300°C.

Several attempts were made to identify chemical and physical characteristics of the corrosion products. Visualisation with a light microscope demonstrated a change in appearance after immersion, with the zinc granules exhibiting a shiny, light-grey appearance before immersion and either a dull light-grey or dull black appearance after immersion. Scanning electron microscope (SEM) imaging identified the formation of a platelet structure, which was not characteristic of the original zinc material. Elemental composition by energy-dispersive spectrometry (EDS) and zinc content by mass balance both suggested that the corrosion product was about 60 percent zinc. Chemical composition by x-ray diffraction suggested the presence of zinc oxide but could not conclusively identify other zinc compounds. EDS identified the other elements present as oxygen (18 to 20 percent), silica (10 to 12 percent), carbon (6 to 10 percent), and aluminium (trace). No evidence of the presence of boron or lithium was observed. One of the species predicted to precipitate by water-chemistry modelling is Zn₅(CO₃)₂(OH)₆, which has an elemental composition of 60 percent zinc, 35 percent oxygen, 4 percent carbon, and 1 percent hydrogen. It is possible that the EDS analysis detected a combination of Zn₅(CO₃)₂(OH)₆, background metallic zinc, and other compounds that formed on the granules, including some silica-containing compounds.

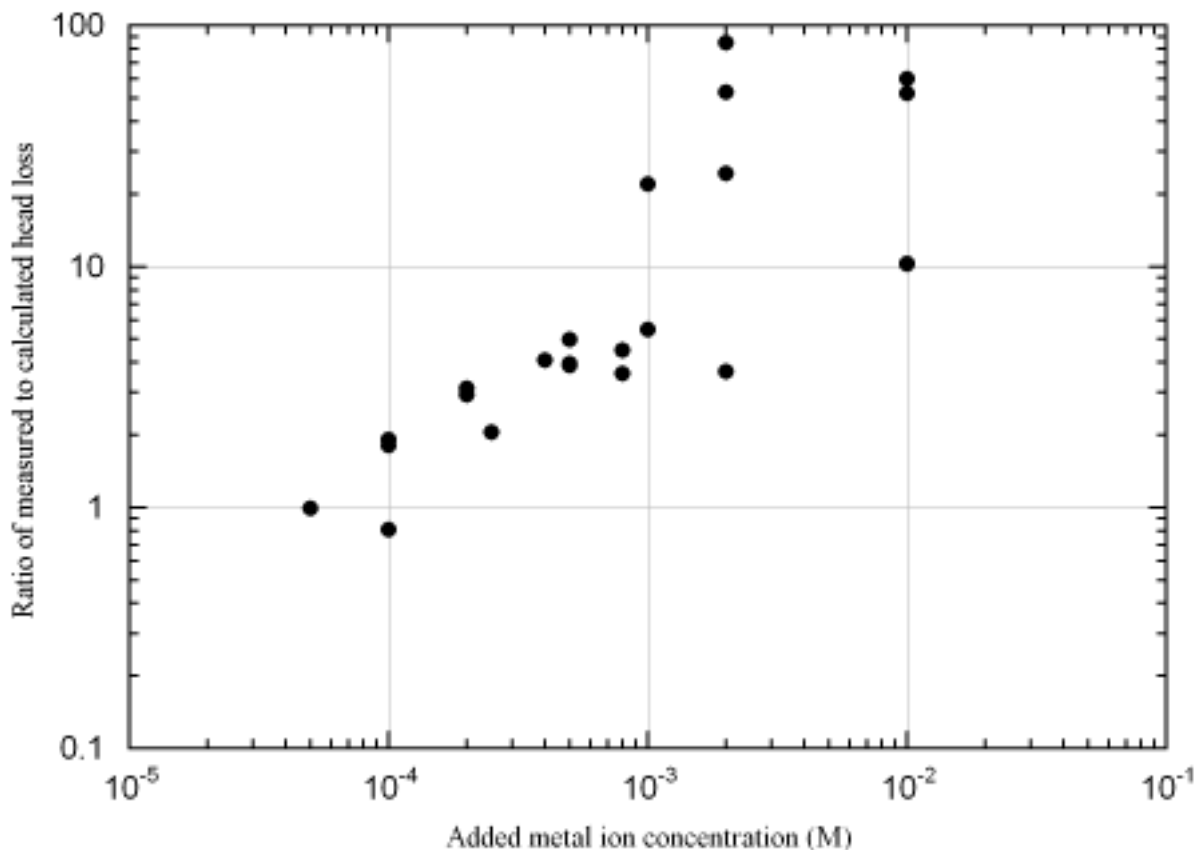
-
4. Piippo, J., T. Laitinen, and P. Sirkiä, "Corrosion Behaviour of Zinc and Aluminium in Simulated Nuclear Accident Environments", Finnish Center for Radiation and Nuclear Safety report STUK-YTO-TR 123, (February 1997).
 5. van Rooyen, D. "Hydrogen Release Rates from Corrosion of Zinc and Aluminum", BNL-NUREG-24532 informal report, pp. 1-37 (May 1973).
 6. Loyola, V.M. and J.E. Womelsduff, "The Relative Importance of Temperature, pH, and Boric Acid Concentration on Rates of H₂ Production from Galvanized Steel Corrosion", Sandia National Laboratories report SAND82-1179, United States Nuclear Regulatory Commission report NUREG/CR-2812 (November 1983).

Head-loss tests

Previous experimentation has established a correlation for head loss through ECCS strainers caused by a bed of fibrous debris composed of NUKON[®] insulation. This correlation was documented in NUREG/CR-6224.³ The primary focus of the current experiments was on the additional head loss due to the capture of insoluble corrosion products that may precipitate after the corrosion of metals in the containment structure, assuming a fibrous debris bed has already formed on the ECCS strainers. The first tests incorporated the simultaneous precipitation of calcium, aluminium, iron, and zinc compounds, which were each added at a concentration of 1.0×10^{-2} M. High head loss was observed almost immediately, and the test had to be terminated within 15 min because the head loss had exceeded 15 ft and the recirculation flow rate had dropped to almost zero. Subsequent tests were conducted with only one metal precipitate at a time.

In all, more than 20 experiments were conducted with various concentrations of metal precipitates. The head loss caused by a combined bed of fibrous debris and precipitated metals was compared to the head loss by a fiber-only debris bed. This comparison was made by calculating the fiber-only head loss with the NUREG/CR-6224 correlation using the NUKON[®] quantity and actual measured temperature and velocity at the end of each test. A ratio of head loss with and without precipitated metals was then calculated, and is presented in Figure 1 for each of the tests.

Figure 1. Ratio of head loss through a fibrous debris bed with and without chemical precipitates



The ability of a precipitate to cause additional head loss appeared at an added metal ion concentration of about 1.0×10^{-4} M (equal to a concentration of 6.5 mg/L of zinc or 2.7 mg/L of aluminium). These concentrations correspond to less than 100 lb of metal dissolved into 1 million gallons of water. The quantity of NUKON[®] used for preparation of the fibrous bed was 4.4 g ($\sim 1.5 \text{ cm}^3/\text{cm}^2$); therefore, the precipitate-to-fiber mass ratio at which additional head loss appeared was 0.015 for zinc. These results are significant because previous studies have reported that the sludge-to-fiber mass ratio at which additional head loss appears was 0.1 or higher.³ Additional head loss from precipitates of corrosion products may be significant at mass ratios on an order of magnitude lower than reported for incompressible particulate debris.

The results were reasonably consistent and repetitions of tests under identical test conditions produced repeatable results despite the potential for wide variations resulting from test conditions that were difficult to control, such as the uniformity of the formation of the initial fibrous debris bed. Higher quantities of metal precipitate consistently led to higher head loss. The head loss through a mixed bed of precipitate and fibers was about an order of magnitude higher than that through a fiber-only bed when the added metal concentration reached about 2.0×10^{-3} M. Greater variability in the ratio of head loss with and without precipitates developed above an added metal concentration of about 1.0×10^{-3} M. Above this value, the measured head loss through the debris bed was substantial and taxed the ability of the recirculation pump in early experiments (the pumping system was modified in later experiments, leading to an improved ability to maintain a uniform velocity throughout the test). The greater variability in this ratio at low flow conditions suggests that the head loss caused by the precipitated material does not have the same dependence on velocity as other materials that have been studied. This different dependence on velocity may be due to the compressibility of the material, since other debris that has been studied has been incompressible.

Physical examination of the beds after the tests revealed the presence of a sticky, gelatinous coating on the entire surface of the bed. This continuous gelatinous layer appeared to cause more physical resistance to water flow than mixed beds containing fibers and discrete particles. Examination of the beds by SEM showed that material adhered to individual fibers, although the gelatinous materials were desiccated by the high vacuum in the SEM. This gelatinous coating may be compressible and may exhibit a significantly different head-loss relationship than that described in NUREG/CR-6224.

Conclusions

Leaching tests to evaluate the corrosion of metal materials were conducted at ambient and elevated temperatures and at two pH values (pH = 7 and 9) in the presence of an aqueous solution containing boric acid and lithium. The ability of metals to corrode under these conditions was observed. Evidence for corrosion included weight loss of the metal materials and accumulation of soluble metal ions in the water. The measured corrosion rates were similar to literature values from previous studies with similar chemical conditions.

High-temperature corrosion tests attempted in this study were clearly confounded by exceeding the solubility limits of zinc in solution. Because the immersion vessels were quiescent, it is possible that only the local concentration near the sample surface, and not the bulk concentration, exceeded saturation when crystallisation was initiated. This condition would not be expected in a system with flowing water, such as in the containment pool.

Chemical solubility relationships predict that chemical precipitation can occur at relatively low concentrations of dissolved metal; precipitation at low metal concentrations was confirmed in

laboratory testing. Chemical solubility relationships suggest that the precipitants are metal oxides and hydroxides, which can have flocculent characteristics, thus causing them to aggregate into amorphous masses that can plug a fibrous debris bed more efficiently than dust or dirt that may be present on the containment floor. Preliminary tests reveal that these metal precipitants can have a significant effect on the head loss through a fibrous debris bed on an ECCS strainer. Precipitation (noted as a rapid milky white change in water clarity) and measurable head loss have been observed for concentrations as low as 1.0×10^{-4} M. Higher metal concentrations caused head loss that was substantially greater than the head loss occurring through a fibrous debris bed without chemical precipitants. As a result, these tests suggest that secondary debris generation may be a significant issue that should be addressed with further research.

Referring to the three questions posed at the beginning of this manuscript, the following conclusions can be drawn from this research:

1. Credible evidence of a corrosion mechanism for zinc in conditions characteristic of the containment pool after a LOCA were observed. The measured corrosion rate was $0.055 \text{ g/m}^2\cdot\text{h}$ at 22°C .
2. Theoretically, corrosion products could accumulate in the containment pool water to the extent that they might precipitate as new chemical species at pH and temperatures levels that are relevant to the LOCA accident sequence. The solubility of metal oxides and hydroxides is very low and the surface area of exposed metals within containment is substantial.
3. If precipitation occurs, the chemical precipitants could have a substantial negative effect on the head loss across an existing fibrous debris bed. Additional head loss was observed at added metal ion concentrations as low as 1.0×10^{-4} M, and the head loss increased by about an order of magnitude above that without metal precipitants when the added metal ion concentrations reached 2.0×10^{-3} M.

This investigation provided credible evidence for a sequence of events that could lead to excessive head loss across the ECCS sump strainers following a large LOCA. It should be noted, however, that the complete progression of events necessary to produce excessive head loss was not studied in an integrated manner. The scope of the experiments was limited to an analysis of the individual steps in the progression scenario; i.e. corrosion/leaching tests in a batch reactor and head-loss tests with artificially induced precipitation. Integrated testing of the complete progression of events is being explored as a follow-on activity.

**RESULTS OF LATEST LARGE-SCALE REALISTIC EXPERIMENTS INVESTIGATING
THE POST-LOCA BEHAVIOUR OF MINERAL WOOL DEBRIS IN PWRs
(fragmentation, transport, deposition on sump strainers, slip through strainers, pressure losses)**

U. Waas, G.-J. Seeberger
Framatome ANP GmbH

Abstract

Several series of experiments investigating the post-LOCA behaviour of fragmented insulant material (mineral wool) were carried out and evaluated in the period between 2001 and 2003.

The experiments concentrated on:

- Fragmentation of mineral wool under as realistic conditions as possible; this was performed by exposing stainless steel-clad mineral wool panels as used in German nuclear power plants to a jet of saturated water (DN 200, approx. 290°C, approx. 110 bar).
- As realistic as possible investigation of transport and sedimentation of finely fragmented insulant material in the containment sump; the sump geometry of German PWRs was modelled on a scale of approx. 1:4 by volume.
- Deposition on the sump strainers of the fine debris component transported in sump recirculation mode under as realistic conditions as possible (flow velocities, thickness of layer on strainers;
- Effects of different mineral wool types on pressure loss correlations.
- Effects of different mesh sizes on slippage and pressure losses.

The following main insights were gained:

- The stainless sheet steel-clad insulant panels featured significant resistance to jet impingement loadings. At favourable impacted locations, i.e. on the surface of the panels remote from edges, the panels were only indented without releasing insulant material, even in areas near the break.
- If mineral wool is released and fragmented by the jet, fragmentation in the area near the break is extensive, i.e. the fine component is large.
- The fine and very fine components are crucial to the transport, deposition on sump strainers, and slippage of fragmented insulant in sump recirculation mode and, in particular, to the resulting pressure losses (millibar per kg/m²); this has consequences for the selection of mesh size in order to achieve sufficient sump strainer retention efficiency.

- Even under highly conservative test conditions representative of German PWRs, approximately 75% of the mineral wool debris are deposited before reaching the sump strainers.
- The pressure losses across the sump strainers with deposited insulant debris are essentially determined by the deposited mineral wool – the strainer mesh size is of secondary importance.
- With a sump strainer mesh size of 3 x 3 mm slippage through the strainer is limited such that coolant flow through the fuel assemblies in the reactor core is not unacceptably degraded even under adverse conditions.
- Considerable differences in pressure losses exist for the same mass depositions on the strainers depending on the type of mineral wool (by factors of as much as 2 and more).

1. Introduction

During loss-of-coolant accidents in power plants fragments of the material which is used to insulate the ruptured pipe and is located in the jet impingement area of the blow down flow are released into the reactor containment. Depending on the position of the break and the direction of the jet, the insulation on nearby pipes and components may also be affected. The amount of insulant released depends on the type of material and on the break size and location. Moreover, the transportation of fragmented insulant, particularly in the sump region, its sedimentation or deposition on the sump strainers and slip through the sump strainers all depend on a range of technical plant features which can result in considerable differences between the various PWR types. This dependence on plant-specific boundary conditions, together with important correlations, for example, has been described in “Knowledge Base for Emergency Core Cooling System Recirculation Reliability”, prepared by US NRC for OECD.¹

Analysis of the main findings has shown that integrated experimental studies should simulate specific plant boundary conditions as realistically as possible. The decision was therefore taken to conduct large-scale integrated experiments whose boundary conditions reflect the actual situation in Siemens PWRs in order to validate and expand on findings obtained from earlier, small-scale experiments. The main focus was as follows (see Figure 1):

- 1) Use of representative insulant material.
- 2) Definition of boundary conditions in the test facility representative for Siemens PWRs.
- 3) Determination of insulant particle size distribution in fragmentation experiments under realistic conditions similar to those in plant operation.
- 4) Determination of sedimentation behaviour in the containment sump, deposition processes on the sump screens and resulting pressure losses across the sump screens.
- 5) Determination of amount of insulant entrained into the reactor core, investigation of deposition behaviour in the reactor core and resulting increase in pressure losses.

In 2001, preliminary experiments to ascertain representative insulant as well as three series of main experiments were performed under contract to VGB Power Tech Service GmbH as part of the “Assured Sump Suction Function” research and development project. The main test series comprised fragmentation experiments, transport experiments and fuel assembly experiments.² In 2003, supplementary tests were performed on a small-scaled test rig to investigate separate effects like the influence of changing the mesh size on head loss and slip for various kinds of mineral wool.

2. Selection and provision of representative insulant material

Mineral wool materials from various vendors (mostly Isover MD2 and Rockwool RTD2) are used in German nuclear power plants. The different mineral wools were investigated in preliminary

-
1. NEA/CSNI/R(95)11, *Knowledge Base for Emergency Core Cooling System Recirculation Reliability*, prepared by U.S. NRC for OECD, CSNI PWG 1, February 1996.
 2. Seeberger, *Experimental Verification of the Secured Sump Recirculation Following LOCA in KWU Pressurized Water Reactors*, Framatome ANP, Erlangen, Technical Report NGES1/2002/de/0210, 2002.

experiments (before the main test series) to ascertain their response to wetting and their pressure loss behaviour.^{3,4} The purpose of these investigations was to select representative insulating material for the main experiments. Mineral wool from components and piping of PWR and BWR plants, which had generally experienced lengthy exposure to high temperatures (> 250°C), was provided to reflect realistic thermal aging of the insulant.

Wetting tests

The wetting tests were carried out with demineralised water at room temperature and at 90°C. They were used to determine the degree of aging of the mineral wools taken from the power plants and to quantify possible effects on pressure losses. The most important results are:

- 1) The type of insulating wool (Isover MD2 or Rockwool RTD2) had no observable effect on response to wetting.
- 2) The effect of water temperature on the material's response to wetting was negligible compared with the effect of material aging.

Pressure loss tests

These tests were designed to ascertain how thermal aging, different mineral wool types and production-related differences between mineral wools affect increased pressure loss when such materials are deposited on screens (mesh size 1.5 mm x 1.5 mm). The amount of insulant material deposited on the test screen was 6.4 kg/m² in all experiments. As far as possible, extraction of the mineral wool from the panels provided, fragmentation of the extracted mineral wool by subjecting it to a high-pressure jet of water for a previously specified time, and deposition of the sample material on the test stand screen, were performed in an identical manner for every experiment so as to guarantee comparable results. This was confirmed on the basis of corresponding repeat tests.

Testing was performed at room temperature using demineralised water conditioned with boron (2 200 ppm) and lithium (3 ppm).

Summary of results from the preliminary experiments

- 1) Mineral wool that is used in the relevant areas (reactor coolant system and connecting pipes) is exposed to extensive aging. Only a small fraction of the material (corresponding to < 1/8 of the original layer thickness) still contains water-repellent bonding agents or similar constituents.
- 2) New, artificially aged material behaves no differently in response to wetting than material that has aged under real operating conditions. Its response to wetting and sedimentation behaviour are almost exclusively a function of the degree of thermal aging.

3. *Ibid.*

4. Seeberger, *et al.*, *Characterization of Insulating Materials as a Basis for Selection of Representative Materials for Use in Experiments*, Framatome ANP, Erlangen, Work Report FANP NDS4/2001/1005, 9 February 2001.

- 3) The mineral wools used in power plants can be classified in two different groups (manufacturers). The main distinguishing feature for material types within the respective groups is the year of manufacture (see Figure 2).

The material Rockwool RTD2 produced in year 2000 is responsible for the highest pressure losses. The 1983 product shows pressure losses only marginally lower than are, however, higher than all pressure loss figures obtained for the material Isover MD2. Of the six different specimens of Isover MD2, the sample from the year 2000 also exhibits the highest pressure loss reading although this is lower than the RTD2 result by a factor of 0.6. Pressure loss values for MD2 from the 1983 production run represent the mean for this material.

- 4) The pressure loss correlation between the different mineral wool types obtained from the preliminary experiments can be used in the subsequent transport and fuel assembly experiments to extrapolate the results obtained for the mineral wool type featured in the main experiments to the other types of mineral wool used in power plants.

3. Fragmentation experiments

The fragmentation experiments were designed to ascertain the size of the mineral wool particles following destruction of the insulating panels in the area $L/D < 3$ (zone of influence 1 of the NUREG-Three-region two-phase conical-jet ZOI model [6]) and to provide mineral wool fragmented under realistic conditions for the subsequent transport and fuel assembly experiments. It was not the primary purpose of the fragmentation tests to ascertain the degree of fragmentation of panels and insulating material in the various zones of influence (ZOIs) of the NUREG-Three-region two-phase conical-jet ZOI model or to verify the NUREG-Three-region two-phase conical-jet ZOI model. In total, 5 experiments were performed under PWR conditions (blow down of high-temperature hot water) and these are also documented in detail in individual reports.⁵

Test rig and experimental setup

The fragmentation experiments were carried out on the large valve test rig GAP at FANP in Karlstein. This test rig basically consists of an accumulator with a cubic capacity of 125 m³. Operating pressure and temperature are 110 bar and 310°C. A pipe with DN 250 leads from the accumulator to the blow down pool (Figure 3). The pipe opens directly in front of the mounting support for the insulant panels.

To trap the released fragments of mineral wool a collecting chamber was partitioned off inside the blow down pool using a sturdy framework structure (Figure 4a). The collecting chamber is 9.8 m long, 5 m wide and 3.9 m high. The top and one side panel of the chamber were covered with perforated plates (2 mm diameter holes) or wire mesh with a mesh size of 2 mm. Compressive forces during the blow down process were transferred to the framework structure by means of gratings. Figure 4b is an external view of the collecting chamber showing the side panel.

5. Rödel, *Fragmentation Experiment for Verification of Secured Sump Recirculation Following LOCA – Experiment FV1_1: High-Temperature Hot Water Experiment with G+H Insulant Panels with Isover MD2 Mineral Wool*, Framatome ANP, Erlangen, Technical Report NT34/2001/055, 5 November 2001.

Positioning of insulant panels

The half pipe panels (internal diameter 750 mm) were mounted on the support pipe and fastened together using the snap closures on the panel edges. One course of panels (= two half shells) was positioned such that the jet was directed straight at the joint between the two half panels, i.e. with one half panel to the left and one to the right of the jet (Figure 5). In the following experiments with four panels, an identical arrangement was used for the upper and lower courses of panels so that the jet was directed at the intersection between the abutting panel joints.

The distance between the front panel or the panel joint and the opening of the blow down line was 40 cm. Jet centre pressure p_i was about 13 bar with this distance and with a pressure of 100 bar at the rupture disk and a temperature of 285°C. It therefore corresponds to the jet centre pressure in an actual plant over the distance of 3 x DN from a break ($p_i = 12.7$ bar).

With this experimental setup, the front parts of the panels were located in ZOI 1 of the NUREG-Three-region two-phase conical-jet ZOI model and the rear parts in ZOI 2.

Test performance

At the start of testing the accumulator contained approx. 40 m³ of water heated to the specified values for pressure and temperature. Testing was started by depressurising the space between the two in-line rupture disks. The blow down phase in the different experiments varied from 4.6 s to 8.7 s. Depending on test duration, the volume of blow down water was between 4 Mg and 7 Mg. Approximately 40% of the blow down water evaporated on depressurisation to ambient conditions. Due to the forming of steam it was impossible to observe or photograph the fragmentation process. At the end of the experiment the test pool contained several centimetres of water.

In total five experiments were performed with high-temperature hot water; the conditions specified for these experiments are summarised in Seeberger's Siemens Work Report.⁶

The first experiment was performed with 4 panels manufactured by G+H Montage.

The water jet dislodged the top two panels from the mounting support and damaged them. All of their mineral wool content was released. Panel positioning and degree of damage sustained by these two panels are shown in Figure 6. The lower panel which was oriented toward the jet was dented but not destroyed. The lower panel which was oriented away from the jet was unimpaired. Only two of the six snap closures which held the two bottom panels together had opened.

Since the purpose of the fragmentation experiments was to produce as much realistically fragmented mineral wool as possible for subsequent test series, panels were arranged with their abutting edges facing the jet in all further experiments.

In the second experiment only two panels from G+H Montage were used. The two panels were torn from the mounting support and totally destroyed. Their entire mineral wool content was released.

6. Seeberger, *Specification for Transport Experiments Using Insulating Material for Verification of Secured Sump Suction Piping following LOCA*, Framatome ANP, Erlangen, Siemens Work Report SNP NDS4/2001/1004, 17 January 2001.

In the third experiment, four panels from the supplier Kaefer were used. All four panels were torn from the mounting support and destroyed. Two of these panels still contained considerable amounts of mineral wool after the experiment (Panel KKK 2/1 16.7 kg of an original 23.5 kg, Panel KKK 3/2 8.2 kg of an original 19 kg; see Figure 7). These two panels were evidently dislodged from the support before their mineral wool content was expelled by the jet. If the panels are positioned just outside the direct jet impingement area considerable amounts of mineral wool can be retained, due also to the wire mesh inside the panels.

In the remaining experiments also, individual panels remained intact despite adverse positioning.

Test results

1) Distribution of mineral wool in the collecting chamber

All PWR experiments showed that the released and fragmented mineral wool was distributed over the entire collecting chamber. At the end of the experiment, less material was found on the walls and top panel than in the water inventory in the bottom of the chamber. (Most of the material deposited on walls and top panel apparently dropped off at the end of blow down.) Larger amounts were found deposited on fields 7 and 8 of the partition wall, i.e. at the far end of the collecting chamber viewed in the direction of jet impingement (Figure 8). The fact that the remaining fields were entirely free from deposits shows that the main flow path from the discharge valve was initially in the direction of the opposite wall (i.e. practically straight on) before exiting the collecting chamber through the last two fields (7 and 8).

2) Expulsion of mineral wool from the collecting chamber

Figure 9 shows the amounts of mineral wool expelled from the collecting chamber for every experiment as a function of blow down time. The mass of material expelled from the collecting chamber reduces with shorter blow down times. Figure 10 shows the mass of material expelled from the collecting chamber as a function of the total mass expelled in each of the experiments. There is no particular correlation between the mass expelled from the collecting chamber and the total mass expelled in each case. It can be concluded from this that the mineral wool was expelled during the initial test phase during which mineral wool debris was also deposited on fields 7 and 8. Once these preferred blow down areas had been extensively or completely covered further expulsion of mineral wool virtually ended or was at least significantly reduced. In the final experiment (using Rockwool RTD2), during which only slightly more than 20 kg was released, a total of 15.8 kg was expelled from the collecting chamber; only 5.4 kg remained inside the collecting chamber.

3) Determination of particle size distribution of fragmented mineral wool

It was impossible to ascertain any quantifiable size distribution of fragments on the partition wall and in the water inventory. Sorting of mineral wool fragments by size was therefore superfluous.

The size of Isover MD2 and Rockwool RTD2 particles deposited on the wire mesh is shown in Figures 11 and 12 respectively. As this comparison shows, RTD2 was considerably more finely fragmented than Isover MD2.

4) Release of insulating material

If insulant panels are positioned in ZOI 1 of the NUREG-Three-region two-phase conical-jet ZOI model but the jet strikes only the outer panel edges, the panel generally is not destroyed and no

insulant material is released. If the jet is directed at the abutting edges of a course of panels the panels are partially destroyed with corresponding release of mineral wool. This observation suggests that application of the NUREG-Three-region two-phase conical-jet ZOI model is conservative, at least for panels of the style used in German PWRs.

In the case of panels that are dislodged from the support (or the component) before being stripped of their mineral wool content, a considerable quantity of mineral wool is likely to be retained in the panel, e.g. due to the internal wire mesh.

No measurable difference in terms of panel integrity was found between the two panel types.

Evaluation of the use of the mineral wool in subsequent transportation tests

The panels were located in ZOI 1 and the near part of ZOI 2 of the NUREG Three-region two-phase conical-jet ZOI model. Since in a real power plant situation mineral wool is released and fragmented from insulant material located in ZOI 1 through 3, the experimental fragmentation of the mineral wool can be seen as representative or slightly conservative.

The mass balances in the fragmentation experiments showed that a component of the released mineral wool passed through the cover plates of the test chamber. This will mostly have been very fine component that the fine wire gratings and perforated plates were unable to retain. This should be evaluated as follows: The very fine component passing through the cover plates has evidently been transported in the steam flow. In a real plant, in which the break area is not surrounded by a very fine wire mesh, there would be even more efficient transport of material out of the break area. This very fine component, carried in steam, would be uniformly distributed throughout the containment, deposited at locations distant from the break location and therefore have very little probability of being flushed into the sump, particularly if there is no containment spray system. The mineral wool fragments collected from the test pool therefore represent a mixture of coarser and finer components with a significantly higher proportion of fine component than would realistically be found in the sump. The collection and use of such fragmented mineral wool in subsequent transport tests is therefore conservative with regard to (low) sedimentation and (high) pressure losses.

4. Transport experiments

The purpose of these tests was to determine the transportation, deposition and pressure loss behaviour of realistically fragmented mineral wool under conditions as similar as possible to those in actual plant operation.

4.1 Modelling

Representative reactor sump and model sump

To define the geometry and dimensions of the model sump, data on the reactor sump, suction chambers and sump screens were collected from all Siemens PWRs. This information was then used to define a representative, enveloping reactor sump in the context of the test objectives. "Representative" means that geometric data are used that are as far as possible representative of mean values obtained from the full range of plant data, taking their frequency into consideration. "Enveloping" means that

these mean values were biased to the point where the experimental results can be considered to be enveloping. Enveloping sump data were selected on the following basis:

- Small sump volume impedes sedimentation.
- A low water level at the time of changeover to sump suction raises the momentum increment by the blow down flow and increases the formation of fine component.
- High delivery rates from the residual heat removal pumps cause higher speeds upstream of the sump screens, transportation of more mineral wool onto the screens and high differential pressures across the screens.

In order to minimise the scaling effects encountered with previous small-scale test stands the model sump was designed on a scale of 1:4 (Figure 13) apart from its height dimension, which corresponded to the original dimension of the representative reactor sump.⁷ This ensured correct simulation of the momentum increment by the leakage flow. Also retained were the original values for the time taken to transport the mineral wool from the break location to the sump screen, for sump level on changeover to sump suction, for the height of the intake chambers and for the height of the sump screens. The sump screen surfaces were variable so as to envelop all PWRs as far as possible. An additional conservative factor was given by the fact that low water temperatures (25°C) were used in the tests compared to approx. 90°C at the start of recirculation, i.e. the higher viscosity in the tests resulted in decreased sedimentation and increased resuspension. Five experiments were performed in total. The Isover MD2 mineral wool released in the earlier fragmentation experiments was used in all of these experiments.

Leakage flow

A 0.1A (small) break at a weld in the reactor coolant line is indicative of cracks which lead to diffuse blow down and leakage flows. The momentum increment by leakage flow into the reactor sump is small. A break in a connecting line, however, produces a bundled leakage flow. For the purpose of the experiments, therefore, a rupture of the surge line was simulated since the largest amount of mineral wool is released with a break in this location. To achieve this, the jet must be directed at the pressuriser, for example, as this is the only way for correspondingly large amounts of mineral wool to be released. In the test stand an impingement plate was arranged approx. 2.50 m from the pipe outlet (corresponding to $L/D = 7$) to simulate flow impingement on the pressuriser. The jet was directed in a slight downward direction through a nozzle (10°). The flow velocity of the jet with 2 low-pressure pumps in recirculation mode was 15 m/s or 25 m/s with 4 low-pressure pumps in recirculation mode. The nozzle was located 10 m above the floor of the model sump corresponding to the height of the reactor coolant line above the sump floor.

With a 2A break of the reactor coolant line the jet is still directed at components but these can be considerably further away from the break location ($L = 5$ m for $L/D = 7$). Since the flow rate is significantly diminished after the pressure relief phase the jet from certain break locations can then flow into the sump without first impinging on components. The impingement plate was therefore removed for this experiment (Figure 14). The height of the nozzle remained unaltered at 10 m above the sump floor.

7. *Ibid.*

Break location in the model sump

With the equipment described it was possible to simulate breaks with a leakage flow straight into the sump (break above the grating). This break location is enveloping with regard to the momentum increment of the flow into the sump and the ensuing production of fine component.

If a break occurs above the concrete slab, parts of the mineral wool lying on the slab are washed into the sump with the flow. Given the small drop from the concrete slab to the sump floor (approx. 2 m), the reactor building sump fills up far less turbulently than if the jet is assumed to be in the form of water cascading into the sump from a height of 10 m. The momentum increment is many times smaller, also with the result that correspondingly less fine component is produced. Breaks above the concrete slab are therefore enveloped by the tests involving a break above the grating as far as the transportation and production of fine component are concerned. (Important: Possible break locations in Siemens PWRs would mostly be above the concrete slab.)

Test performance

The transportation experiments were performed at the GKSS Research Center in Geesthacht with mains water at ambient temperature (23°C-27°C) (Table 1).⁸

The leakage flow was affected as shown in Figure 15. Switchover to suction from the model sump occurred when the level reached 2.60 m with simulation of 2 residual heat removal pumps and 3.50 m with simulation of 4 residual heat removal pumps in operation, both events timed at approximately 1 100 s.

The mineral wool was entrained straight onto the grating in the jet (or flow of falling water). The fragmented flakes were mostly flushed straight through the grating and into the sump. With the jet or water cascading from a height of approx. 10 m the sump filling process was very turbulent in the initial phase while the level was still low. The fine component became separated from the mineral wool in this phase as was evident from the extreme turbidity of the water. These tests are therefore representative for breaks with leakage flow direct into the sump via the grating.

Transport and sedimentation of the mineral wool

Due to severe turbulence in the filling phase the mineral wool suspended in the water was distributed over virtually the entire model sump. Even during the filling phase, i.e. before changeover to sump suction, fine component was transported through the sump screens (coarse and fine screens) into the suction chambers. Turbulence in the lower part of the model sump declined with increasing sump level, allowing sedimentation of mineral wool flakes. Circulation flows which could have disturbed these sedimented flakes of mineral wool were not observed in any of the experiments with a full sump. Just 0.5 m to 1 m beneath the water surface no further turbulence was observed.

Changeover to sump suction took place as soon as the specified sump level was reached.

The test pool was emptied after each experiment. The amount of mineral wool deposited on the sump floor was determined area by area. Mineral wool was found in nearly all areas of the model

8. Seeberger, *Experimental Verification of the Secured Sump Recirculation Following LOCA in KWU Pressurized Water Reactors*, Framatome ANP, Erlangen, Technical Report NGES1/2002/de/0210/, 2002.

sump, including between the two partition walls and in the passive suction chamber. The largest mineral wool deposits were found close to the point of entry (fields 2 and 3 in Figure 16).

Screen deposits

Following shutdown of the recirculation pumps in experiments 2, 3 and 4 (or on initiation of sump screen back flushing in experiment 4), the mats of mineral wool stuck to the screens partially detached themselves (observed in situ or on video recordings). In some cases whole mats became detached with the screen pattern visible on their reverse sides. These mineral wool deposits on the upstream side of the screens had to be clearly classified during the determination of material deposited on the screens. Smaller quantities detached themselves from the screen as flakes. According to information from the experimenters, these quantities were assigned to the floor area upstream of the screen. When evaluating the results, therefore, it should be considered that the quantities of mineral wool deposited on the screens in the experiment were possibly slightly larger than specified in the original test reports. The following description of results therefore specifies a range of screen deposits which includes the mineral wool collected upstream of the fine screens. Unless otherwise indicated, the values given in the original report are used in evaluating the experiments and for comparison with other experimental results.⁹

4.3 Results of the transport experiments

The transport experiments for the enveloping break location with leakage flow through the grating into the reactor sump were performed using the mineral wool Isover MD2 from general production in the period 1980/82 and are therefore representative for this material only. The properties of other materials should be duly considered for determination of differential pressures. An approximate conversion is possible using the factors ascertained during the preliminary experiments.¹⁰

The transport experiments were carried out using 9 mm x 9 mm screens. The results are therefore representative for screens with this mesh size only. For screens with other mesh sizes it may be necessary to perform suitable small-scale experiments to ensure transferability of the transport experiments.

The results of the transport experiments (Table 2) can be summarised as follows:

- 1) The mobilised mass is the amount of mineral wool or the amount of a mixture of mineral wool and other insulant materials in the sump that is transported up to the sump screens. It comprises the material deposited on the sump screens and the material that passes through the fine screens. Figure 17 shows the mobilised mass as a function of the mass in the sump. In transport experiments 1 to 4 the mobilised mass was between 19% and 24% (possibly 30% if some of the detached debris is taken into account) of the mineral wool mass in the sump.

In experiment 5 (mineral wool with an 11% Minileit component) the mobilised mass was considerably higher at 37%. This is due, at least in part, to the fact that mineral wool from

9. *Ibid.*

10. Seeberger, *et al.*, *Characterization of Insulating Materials as a Basis for Selection of Representative Materials for Use in Experiments*, Framatome ANP, Erlangen, Work Report FANP NDS4/2001/1005, 9 February 2001.

transport experiment 2 was reutilised and exposed to further fragmentation. Experiment 5 is therefore not representative as far as the mobilised mass in the sump is concerned.

- 2) The amount of mineral wool retained by the fine screens is essentially a function of the mineral wool entrained into the model sump (or the mobilised mass), velocity at the screen and screen size. The amounts retained are shown in Figure 18 as a function of the mobilised mass in the sump.

In experiments 1 and 2 (with screen areas of 1.67 m² and 1.5 m²), differential pressure across the micro-screen reached a quasi-steady-state final value before this occurred with the fine screen (Figure 19). This indicates that hardly any further fine component passed through the fine screen, in other words that the fine screen became fully covered with debris with correspondingly good filtration effect. In experiments 3 and 4 (with screen areas of 11 m² and 3 m²) differential pressure across the micro-screens carried on increasing even after differential pressure across the fine screens had reached its quasi-steady-state final value. This indicates that parts of the fine component suspended in the water were still passing through the fine screens and that covering of the fine screen was therefore incomplete. The retention efficiency of the fine screens must therefore be classified according to these two phenomenologically distinct areas, one with complete screen covering (amount of debris deposited > 0.7 kg/m²) and one with incomplete screen covering (amount of debris deposited < 0.7 kg/m²). Figure 18 shows that the quantities retained in both areas increase with decreasing screen size.

- 3) The differential pressures across the fine screens are essentially a function of fine screen covering (mass of mineral wool deposited per screen area) and flow velocity upstream of the fine screens. In experiments 2 and 4 flow velocity was varied once the screens had become fully covered. The amount of debris on the screens differs by a factor of 2 due to the different screen areas. For both experiments, a near linear correlation between flow velocity and differential pressure is observed (Figure 20).

In Figure 21 the differential pressures recorded in experiments 1, 2, 3 and 4 are plotted converted linearly to a flow velocity of 10 cm/s. The graph shows that the differential pressures from experiments 1, 3, and 4 can be described well as a linear relationship.

On variation of the flow velocities, no compression/decompression of the filter bed on the fine screens or associated change in differential pressures was observed. [Note: This phenomenon had been observed in the preliminary experiments with horizontal screen arrangement.¹¹] As far as the present experiments are concerned, this can be attributed to the fact that the material deposited on the screens was almost exclusively made up of fine and very fine component which cannot be compressed to any appreciable extent through the flow velocities occurring here. An effect of this type involving raised differential pressure is therefore unlikely to occur even in long-term sump recirculation mode.

A very high level of screen deposits was determined in transport experiment 2 (4.1 kg/m²) with a differential pressure reading of only 183 mbar. This result is incompatible with those of transport experiments 1, 3 and 4 because extrapolation of the latter results with a screen deposits of 4.1 kg/m² yields a differential pressure of approx. 400 mbar. Experiments 1, 3, and 4 differ from experiment 2 in the amount of mineral wool introduced and the initial volumetric flow which was nearly twice as high in experiment 2 as in experiments 1 and 4.

11. *Ibid.*

Differential pressure behaved similarly in the fuel assembly experiments described in Chapter 5. Two test series were performed; the initial volumetric flow in Series 1 was 6 m³/h, and 12 m³/h in Series 2. Despite otherwise identical boundary conditions, the differential pressures recorded in Series 2 are significantly lower than those of Series 1 which had the lower initial volumetric flow. This suggests that the result from transport experiment 2 is not based on a spurious measurement. Since all FA experiments involving the material MD2 used only mineral wool from transport experiment 1, the effect of “pre-treatment” in the transport experiments must also be ruled out. So it seems that the initial volumetric flow in the transport experiments might affect deposition behaviour and consequently pressure loss behaviour. It was not possible to come to a definite conclusion on this phenomenon with the test data to hand. For enveloping analyses, therefore, determination of differential pressures across the sump screens should be based on the values obtained from transport experiments 1, 3 and 4.

- 4) Slip through the fine screens is the component of the mobilised mass that is not retained by the fine screen. It is calculated as the difference between the mobilised mass and the amount deposited on the fine screen. Slip must therefore also be classified in the two phenomenological areas “complete” and “incomplete” screen covering. Slip through the fine screens is shown as a function of the screen area in Figure 22.

Maximum slip was recorded in experiment 3 (maximum screen area and lowest deposit on the screen) with 88% of the mobilised mass, i.e. 17.1% of the amount entrained into the sump.

In all experiments mineral wool was observed to settle downstream of the fine screens; therefore, it is not part of the component entrained into the primary system. The amount collected from the floor area between the fine screens and the micro-screens is between 1.14 kg/m² and 1.82 kg/m² in all experiments. In experiments 1 and 2 the floor area between fine screen and micro-screen was 13 m². In experiments 3 and 4 with additional use of coarse strainers, the floor area between the fine screens and the micro-screens was 5.2 m² and 2.6 m² respectively. The amounts collected from the floor area are shown in Figure 23.

The amount of material deposited on the micro-screens can be taken as the postulated amount entrained into the primary system. The maximum amount on the micro-screens (which therefore counts as the enveloping amount entrained into the primary system) was 12.7% of the amount in the sump in experiment 3.

Evaluation of range of screen deposits

In the sections on the individual transport experiments a theoretical range was specified for fine screen deposits because of the point that the amount deposited on the fine screens was possibly greater than stated. Determination of the amount deposited on the screens was complicated by the general tendency of the mineral wool mats to detach themselves from the screens when the recirculation pumps were switched off or when the test pool was drained. The bandwidth was determined based on the amounts of deposited material and the additional quantities that had been collected from the floor upstream of the fine screens.

The fuel assembly experiments are described in Chapter 5 below. The mineral wool introduced into the test stand was mostly deposited on the fuel assembly bottom end piece and/or on the first

spacer. Under otherwise identical conditions, no difference in pressure losses could be detected whether the debris was deposited on the fuel assembly bottom end piece or on the spacer. Nor is there any indication that pressure loss behaviour differs whether mineral wool is deposited in a fuel assembly or on a vertical sump screen. The probable amount of debris deposited on the sump screens can therefore be deduced by comparing differential pressures as a function of screen deposits. This is a sensible approach because less uncertainty was involved in determining the amounts of material deposited in the FA experiments.

Figure 24 shows the differential pressures recorded in the transport and fuel assembly experiments as a function of screen deposits (continuous and dotted lines). These values apply to a flow rate of 10 cm/s, unborated water, a water temperature of 20°C and mineral wool Isover MD2. The theoretical range for the amounts of material deposited is plotted for transport experiments 1 and 4. An increase of the screen deposits, which is still in the region of measurement uncertainty, would agree well with the fuel assembly experiments.

- 5) Brief shutdown of the recirculation pumps or initiation of backflow conditions causes large pieces of the deposited material to fall off the fine screens. This results in a significant decrease (e.g. halving) of differential pressure across the sump screens when the recirculation pumps are switched on again. There is no consequent increased slippage of mineral wool through the fine screens.
- 6) Coarse screens (30 mm x 30 mm) have no appreciable effect on the amount of mineral wool retained.

In all, the results of this experiment can be considered conservatively enveloping when transferred to actual plants for the following reasons:

- a) The mineral wool used in the transport experiments was the material released in earlier fragmentation experiments from insulant panels located in ZOI 1 and the adjacent part of ZOI 2 of the NUREG-Three-region two-phase conical-jet ZOI model. In an actual plant situation, a considerable part of the mineral wool fragmented would be from more distant areas resulting in larger debris size. The fragments produced experimentally therefore contain a higher proportion of fine component than would be the case in an actual plant.

In the fragmentation experiments the fragmented mineral wool was retained by perforated sheet metal covers and fine-gauge wire meshes. In an actual plant situation fine and very fine components are particularly likely to be distributed throughout the entire containment in the steam flow with very little chance of being flushed into the sump. The retention devices in the test setup, which are not present in an actual plant, increase the amount of experimentally produced fine component in the fragmented mineral wool.

More fine component produces a larger mobilised mass in the sump (see also transport experiment 5), therefore leading to larger screen deposits and higher differential pressures across the sump screens.

- b) All of the mineral wool was entrained in the jet (or cascading water) directly upstream of the active suction chamber. The entrained fragments of mineral wool were consequently exposed to the momentum increment of the leakage mass flow, particularly in the turbulent filling phase; this caused further fragmentation of the mineral wool. In an actual plant situation, the fragmented mineral wool is (as already mentioned) widely distributed throughout the containment with the result that only an extremely small component is

found in the immediate location of the suction chambers. Moreover, only in a very small proportion of break locations is the jet aimed directly toward the sump suction chamber.

Entrainment of the entire mineral wool component directly into the leakage jet produces a conservatively large fine component.

Entrainment of the mineral wool in the immediate vicinity of the active suction chamber in each case causes more mineral wool to be transported into this suction chamber (the difference can be seen from experiment 3 with two operating suction chambers).

In all, these boundary conditions result in a greater accumulation of fine and very fine component at the sump screens; this is conservative with regard to pressure losses across the sump screens and slippage.

5. Fuel assembly experiments

The fuel assembly experiments were conducted to ascertain the deposition and pressure loss behaviour of mineral wool entrained into the core and deposited there under realistic experimental conditions similar to those encountered in an actual plant.

5.1 Test setup and performance

The test stand consists of a plexiglas housing with a square internal cross-section of 225 mm x 225 mm which corresponds to the external dimensions of an 18 x 18 fuel assembly (Figure 25). The approx. 1.75 m high test stand was large enough to hold a dummy fuel assembly reduced in length to 1.65 m including fuel assembly bottom and top end pieces. This reduced-length FA had three spacers. The experiment involved measuring and recording differential pressures across the FA bottom end piece, across the individual spacers and across the FA as a whole.

The test stand was filled either with mains water (experiments 1-3) or with 2 200 ppm borated demineralised water (experiments 4-7). The test temperature was then set with the recirculation pump in operation. Once the initial conditions had been set the experiment started with timed additions of mineral wool.

The amount of mineral wool to be added was calculated from the amount of material deposited on the microscreens as a function of time in the transport experiments. In transport experiment 1 (0.1A break simulation) 2.8 kg of the total 27.5 kg of mineral wool entrained was deposited on the microscreens. Based on the 1:4 scaling used in the transport experiments, the amount of mineral wool required for the FA experiments is 58.6 g. This quantity represents the amount of mineral wool entrained into one of 193 fuel assemblies, if one assumes that all debris entrained into the primary system would be deposited in the core. Since the residual heat removal pumps inject into both the cold and the hot legs, this is the total amount of mineral wool entrained as a result of cold and hot-leg injection. It was impossible to simulate combined injection in the FA test stand because the multi-dimensional flow conditions in the upper plenum and the reactor core cannot be modelled on the basis of a single fuel assembly. In order to obtain enveloping measured data, the total mass (58.6 g) was introduced for one flow direction.

5.2 Results of the FA experiments

The fuel assembly experiments follow the fragmentation and transport experiments consistently. The same conservative assumptions regarding material treatment used in the former experiments apply to the fuel assembly experiments.

The fuel assembly experiments are directly transferable to the deposition behaviour of the mineral wool Isover MD2 from the production period 1980-1982 in a reactor core with fuel assemblies with IDF (integrated debris filter) or standard bottom end piece. The test results obtained with Rockwool RTD2 are only conditionally transferable because this material had not previously been used in a transport experiment. With regard to other materials, due consideration should be given to their material properties in determining whether the results obtained can be transferred to an actual plant situation. If necessary, other comparative tests must be performed based on the preliminary experiments.

The results of the fuel assembly experiments can be summarised as follows:

- 1) Two fuel assembly bottom end plates of different design were used in the FA experiments. These two items are compared in Figure 26. The experiments show that all of the Isover MD2 is retained by the IDF bottom end plate (Figure 27), whereas only 70% of Rockwool RTD2 is retained. The standard bottom end piece does not retain any fine component of the mineral wool Isover MD2. On this basis it can be assumed that Rockwool RTD2 is not retained either. The mat of mineral wool deposited on the FA bottom end piece drops off as soon as the pump is switched off.

Only one spacer type, the HTP (high thermal performance) spacer, was used in this test series. Spacers are, however, very similar in terms of free flow cross-sections and therefore their ability to retain fine component of mineral wool. The fuel assembly experiments showed that with reduced retention at the FA bottom end piece virtually all of the mineral wool is retained by the first spacer. This result is enveloping for other analyses because if one assumes that other spacer types would have a smaller retention capacity this would produce more favourable flow and consequently more favourable cooling conditions in the fuel assembly because of the temperature dependence of differential pressures.

- 2) With identical amounts of material deposited (per area) and identical flow velocity, differential pressures are not dependent upon the location of debris deposition in the FA (i.e. bottom end piece or spacer, Figure 28).

Differential pressures increase in direct proportion to the amount of material deposited (Figure 29); in this case, the increase is a function of the material. Figure 30 compares the differential pressures obtained with MD2 from experiments 5 and 7 with those obtained for RTD2 from experiment 6. For this purpose, differential pressures were converted linearly to a deposition amount of 1 kg/m². By dividing the values obtained for RTD2 by 1.4 the results for RTD2 agree well with those for MD2.

Differential pressures are nearly proportional to flow velocity.

Differential pressures decrease with increasing water temperature, roughly on a line corresponding to the dynamic viscosity of the water (Figure 31).

Mains water was used in experiments 1 to 3. The following 4 experiments were performed using demineralised water with a boron content of 2 200 ppm. Comparison of the test results from experiments 3 and 4 lead to the assumption that boric acid has the effect of increasing pressure loss. It is unclear, however, what physical mechanism is involved here so further studies are needed to investigate whether some other effect is implicated in the increased pressure loss.

Under the same boundary conditions (deposition amount, flow velocity, unborated water, temperature and mineral wool type) differential pressures in the fuel assembly compare well with those recorded in the transport experiments, and similarly with those used in previous analyses up to a velocity of 5 cm/s (Figure 32).

To verify the previously determined quantitative effect of the individual parameters on differential pressures, all FA test results were compared (apart from test 2 results). To do this, differential pressures were converted to the following parameters: temperature 30°C, deposition amount 1 kg/m², material MD2. The results are given in Figure 33. This diagram shows that differential pressures follow two distinct trends. The converted test readings for experiments 1 to 4 are in the upper results range, those for experiments 5 to 7 in the lower range. As far as these differences are concerned, the test series can be classified in two categories. In tests 1 to 4, with a volumetric flow rate of approx. 6 m³/h, 58.6 g of mineral wool was entrained into the test stand, in experiments 5 to 7, 127 g was entrained with an initial volumetric flow rate of 12 m³/h. Differential pressures in the tests with an initial volumetric flow rate of 6 m³/h and otherwise identical conditions are approx. 1.6 times higher than in the tests with the higher initial volumetric flow rate. Since all other influencing parameters were uniquely quantifiable independently of the initial volumetric flow rate, these differences could be attributed to the initial volumetric flow rate and/or the material mass.

This phenomenon occurred in only one of the transport experiments so that these test results were initially presumed to be spurious. However, the FA test series seem to confirm this phenomenon. Another assumption that transport experiment 2 and the FA test series used the same material but one differing from that used in the other experiments could be ruled out based on confirmation provided by the experimenters that mineral wool deposited on the micro-screen in transport experiment 1 was used for all FA experiments.

The physical processes that lead to the lower differential pressures could not be explained satisfactorily, even with the results of the FA experiments. Therefore, when transferring differential pressures to actual plants the data obtained from the first measurement series involving the higher differential pressures should be used as the basis for enveloping analyses.

6. Results of supplementary tests on individual effects

The supplementary tests were performed on a horizontal ring main (Figure 34). They were designed to examine the following effects:

- Effect of screen mesh size on slip through the screens.
- Effect of screen mesh size on pressure loss.
- Examination of the pressure loss ratio of different types of mineral wool.

The main results obtained were as follows (Figures 35-39):

- The amount of slippage is a function of the type of mineral wool.
- For a mesh size of 9 x 9 mm slip increases significantly with increasing velocity at the screen but shows no clear relation to velocity for a mesh size of 3 x 3 mm.
- Reducing the mesh size from 9 x 9 mm to 3 x 3 mm decreases the slippage of mineral wool fragments in the velocity range from 4 to 10 cm/s by a factor of 5-10.
- Screen mesh size has no considerable effect on pressure loss across a deposited layer of mineral wool fragments. The observed change was in the order of measurement uncertainty.
- The amount of pressure loss across a layer of mineral wool fragments is significantly affected by the type of mineral wool.

7. Important results with application to Siemens PWRs

Insulation material used in Germany:

- Predominantly mineral wool, in some locations (e.g. narrow gaps) a kind of calcium silicate (RMI only in RPV cavity, not relevant for sump clogging issue).
- Insulation material predominantly enclosed within stainless steel sheet panels.
- Basically two suppliers for mineral wool, material from general production in the period 1980-2002.

Due to range of different mineral wools a test series was performed to identify representative mineral wool; result:

- Pressure losses can vary by a factor of up to 4 depending on the supplier and year of production (all other conditions identical).

Large scale fragmentation tests (break diameter 200 mm, 100 bar, 285°C); results:

- Even in ZOI (Zone of Influence) 1 only part of the stainless steel sheet panels is broken (damaged such that mineral wool is released).
- Mineral wool released in ZOI 1 or the adjacent part in ZOI 2 is greatly fragmented, i.e. the fine component is large.
- Transport of the fine component by steam flow is very effective, i.e. the fine component produced during blow down would be distributed inside the containment proportional to the steam flow.

Large scale transportation tests; results:

- Under conditions comparable with sump pool geometries and post-LOCA water flows and velocities in Siemens PWRs, a large part of the mineral wool debris is deposited on the pool floor before reaching the strainers.
- For reference mineral wool tested, the resulting pressure loss is approximately 100 mbar for deposition of 1 kg/m², water velocity 10 cm/s and 25°C. Combination with particulates can cause higher pressure losses.

- Pressure losses over the deposited mineral wool show a near linear correlation to the thickness of the mat, the water velocity and the temperature dependant viscosity of the water.
- With a mesh size 9 x 9 mm² the slippage through the strainers is > 50% and can reach > 90%, depending on velocity, amount of deposition and type of mineral wool.
- If the fibrous mat on the strainers, generated during recirculation, reaches a thickness of approx. ½ cm or more, shut down of the recirculation pumps will cause the mat to fall off the vertical strainers.

Fuel Assembly tests; results:

- All of the mineral wool debris that passed the 9 x 9 mm² strainers and was entrained into the core was deposited in the debris filter, or in the debris filter and the first spacer of the fuel assembly.
- Pressure loss correlations for FAs were comparable to those of the strainers.

Open question: Effect of Boration of coolant on head losses?

Open question: Effect of flow velocity on debris bed structure and head losses?

Additional small scale tests (differences between 9 x 9mm² and 3 x 3mm² mesh sizes); results:

- Slippage through strainers is reduced by one order of magnitude (slippage increasing with the flow velocity, decreasing with the amount of deposition).
- Pressure loss is determined by the fibrous mat. Mesh size has only small influence in case of fibrous mats.

The application of the test results to Siemens PWRs is conservative for the following reasons:

- The tests were performed with a content of fine debris in the fragmented mineral wool that was increased in comparison to the real situation in a plant (see results of debris generation tests).
- The conditions for flow velocities and turbulences were chosen conservatively for a real plant.
- In the FA-tests only a one-directional flow current was used, i.e. local reversal of flow due to fluctuations was not taken into account.

Specific features of Siemens PWRs compared with other PWRs:

- Great effort put into break preclusion (above and beyond LBB!)
 - Less insulation material debris.
- Extensive use of stainless steel jacketed insulation panels
 - Less insulation material debris.
- Large full-pressure containment/large areas for sedimentation
 - Less entrainment into sump.

- No containment spray system
 - Less entrainment into sump by wash down, no momentum input stirring up the sump water.
- Higher water level in sump, most break locations not above sump compartment
 - Less momentum input stirring up the sump water, sedimentation on sump floor/in “dead flow zones” very effective.
- Large sump suction chambers, low flow velocities
 - Sedimentation effective even in sump suction chambers.
- No significant amounts of exposed ferritic surfaces
 - No release of rust particles.
- No use of glass wool, no use of NaOH
 - No chemical reactions with emergency coolant which, in the long term, would result in considerable increases in pressure losses across sump screens with deposits;
 - Sump water with low acidity, no significant zinc corrosion (also comparatively small exposed surfaces).
- Controlled cleanliness after refuelling
 - Hardly any particles other than fragmented insulation material.
- Coatings qualified for LOCA conditions
 - Hardly any particles other than fragmented insulation material.
- Cold- and hot-leg injection by emergency core cooling system
 - Better coolant injection into core.
- Low pressure recirculation pumps insensitive to small mineral wool debris (no usage of sump water for lubrication of bearings), high pressure injection pumps not used for recirculation
 - Long term recirculation ensured.

BIBLIOGRAPHY

Bordihn, *et al.*, *Evaluation of Tests on the Influence of Various Kinds of Mineral Wool and Mesh Sizes on Head Loss and Slip through Screens* (Auswertung von Versuchen zum Einfluss unterschiedlicher Isoliermaterialien und Siebmaschenweiten auf Druckverluste und Schlupf), Framatome ANP, Erlangen, Work Report NGPS4/2003/de/0190/, 30 October 2003.

NEA/CSNI/R(95)11, *Knowledge Base for Emergency Core Cooling System Recirculation Reliability*, prepared by the U.S. NRC for OECD, CSNI PWG 1, February 1996.

NUREG/CR-6808, *Knowledge Base for the Effect of Debris on Pressurized Water Reactor Emergency Core Cooling Sump Performance*, February 2003.

Rödel, *Fragmentation Experiment for Verification of Secured Sump Recirculation Following LOCA – Experiment FV1_1: High-Temperature Hot Water Experiment with G+H Insulant Panels with Isover MD2 Mineral Wool* (Fragmentierungsversuch für den Nachweis der gesicherten Sumpfansaugung nach einem Kühlmittelverluststörfall – Versuch FV1_1: Heißwasserversuch mit G+H Isolierkassetten mit Isover MD2 Isolierwolle), Framatome ANP, Erlangen, Technical Report NT34/2001/055, 5 November 2001.

Seeberger, G.-J., *et al.*, *Characterization of Insulating Materials as a Basis for Selection of Representative Materials for Use in Experiments* (Charakterisierung von Isoliermaterialien als Basis für die Auswahl repräsentativen Materials für Versuche), Framatome ANP, Erlangen, Work Report FANP NDS4/2001/1005, 9 February 2001.

Seeberger, G.-J. *Experimental Verification of the Secured Sump Recirculation Following LOCA in KWU Pressurized Water Reactors* (Experimenteller Nachweis der gesicherten Sumpfansaugung nach einem Kühlmittelverluststörfall bei KWU-Druckwasserreaktoren), Framatome ANP, Erlangen, Technical Report NGES1/2002/de/0210, 2002.

Seeberger, G.-J. *Specification for Transport Experiments Using Insulating Material for Verification of Secured Sump Suction Piping following LOCA* (Spezifikation für Transportversuche mit Isoliermaterial zum Nachweis der gesicherten Sumpfansaugung nach einem Kühlmittelverluststörfall), Framatome ANP, Erlangen, Siemens Work Report SNP NDS4/2001/1004, 17 January 2001.

Table 1. Transport experiments performed and experimental parameters used

Exp.	Type and size of break	Mineral wool entrainment into sump	Minileit	Active intake chambers	Area of fine screens	Coarse strainers upstream of fine screens	Recirculating flow	Corresponds to recirculation mode with
1	0.1 A	27.5 kg	No	1	1.67 m ²	No	570 m ³ /h (158 l/s)	2 LP pumps
2*	2 A	62.5 kg	No	1	1.5 m ²	No	1 000 m ³ /h (278 l/s)*	4 LP pumps
							500 m ³ /h (139 l/s)	2 LP pumps
3	0.1 A	27.5 kg	No	2	2 x 5.5 m ²	Yes	2 x 500 m ³ /h (2 x 139 l/s)	4 LP pumps
4	0.1 A	27.5 kg	No	1	3 m ²	Yes	580 m ³ /h (161 l/s)	2 LP pumps
5 ⁺	0.1 A	27.5 kg	3.5 kg	1	1.67 m ²	No	580 m ³ /h (161 l/s) ⁺	2 LP pumps
							137 m ³ /h (38 l/s)	

* Experiment 2: Volumetric flow reduced because design differential pressure exceeded at the fine screen of the test rig.

+ Experiment 5: Volumetric flow reduced because design differential pressure exceeded at the micro-screen of the test rig.

Table 2. Results of the transport experiments

Exp.	In sump	At fine screen		Strainer area	Amount deposited on fine screen	Velocity upstream of fine screen	Differential pressure across fine screen	Slip through fine screen		At micro-screen		Mobilised component	Relative slip***
		kg	%					kg	%	kg	%		
1	27.5 kg	2.44 kg	8.9%	1.67 m ²	1.46 kg/m ²	9.5 cm/s	138 mbar	4.16 kg	15.0%	2.80 kg	10.2%	24.0%	63%
2	60.1 kg	6.14 kg	10.2%	1.50 m ²	4.09 kg/m ²	18.6/9.3 cm/s	183 mbar	7.52 kg	12.5%	6.10 kg	10.1%	22.7%	55%
3-1	26.1 kg	0.22 kg	0.8%	5.50 m ²	0.04 kg/m ²	2.5 cm/s	< 4 mbar	1.30 kg	5.0%	0.94 kg	3.6%	19.5%	88%
3-2		0.40 kg	1.6%	5.50 m ²	0.07 kg/m ²	2.5 cm/s	< 4 mbar	3.16 kg	12.1%	2.38 kg	9.1%		
4	27.3 kg	1.32 kg	4.8%	3.00 m ²	0.44 kg/m ²	5.4 cm/s	23 mbar	4.30 kg	15.8%	2.50 kg	9.2%	20.6%	77%
5*	30.8 kg	2.84 kg	9.2%	1.67 m ²	1.70 kg/m ²	2.2 cm/s	60 mbar	8.60 kg	27.9%	6.80 kg	22.1%	37.1**	75%

* Experiment involving admixture of 11% pulverised Minileit.

** Mineral wool fragments already used previously in one transport experiment.

*** In percent of mobilised component.

Figure 1. Concept of the large scale VGB tests 2001

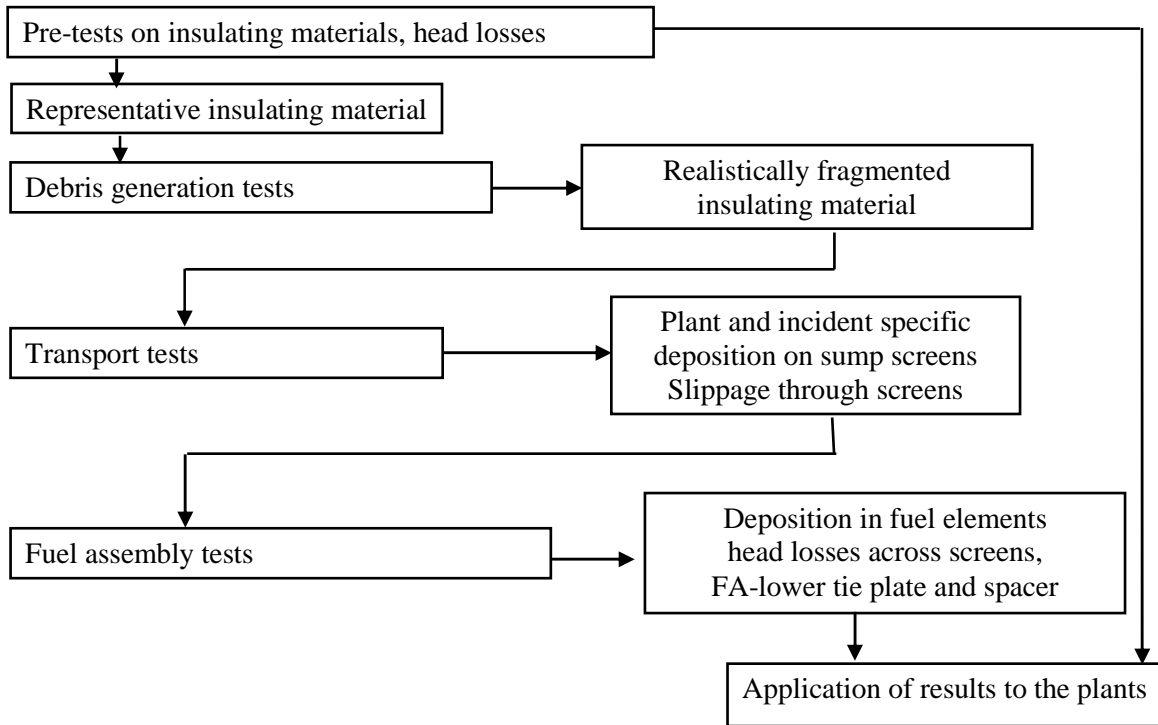


Figure 2. Pressure losses recorded in the preliminary experiments as a function of flow velocity for all mineral wools studied

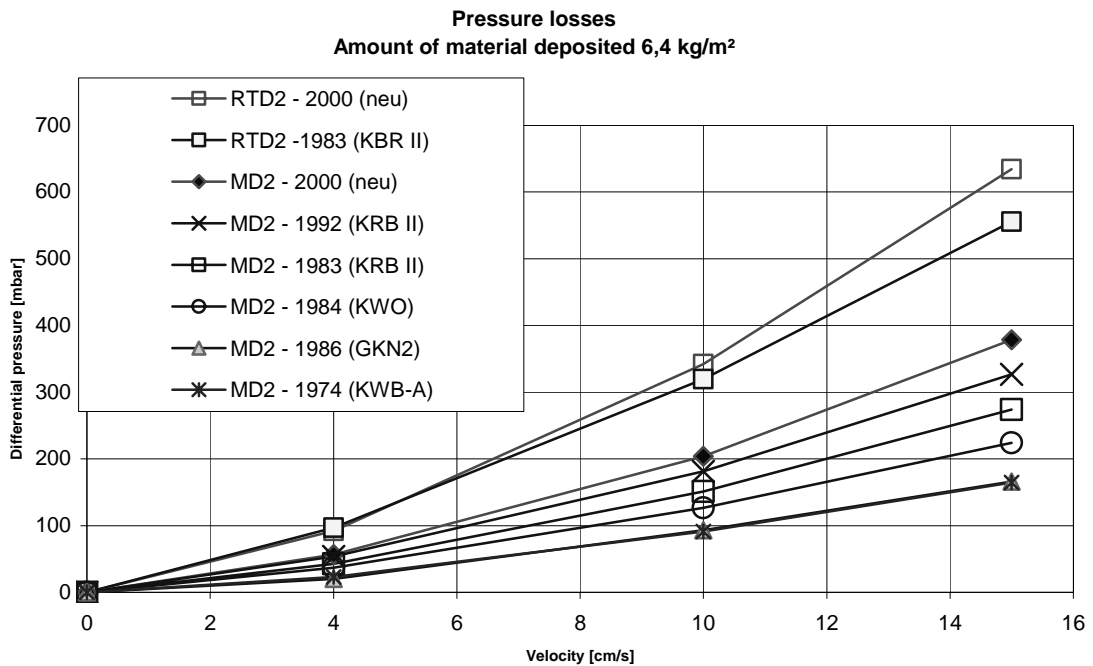


Figure 4b. External view of collecting chamber looking toward the side partition panel



Figure 5. A course of insulating panels positioned with the joint facing the jet



Figure 6. Position of the top two panels G+H II/1 (foreground) and G+H II/2 (background)



Figure 7. Insulating panel KKK 2/1 with residual content



Figure 8. Mineral wool deposited on Fields 7 and 8 of the partition panel



Figure 9. Amount of mineral wool expelled from the collecting chamber as a function of blow down time

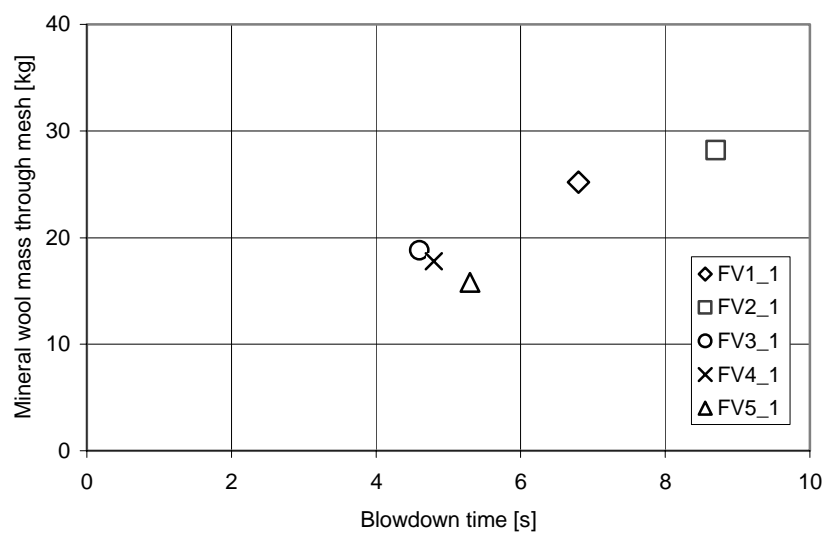


Figure 10. Amounts expelled from the collecting chamber as a function of the total amounts released

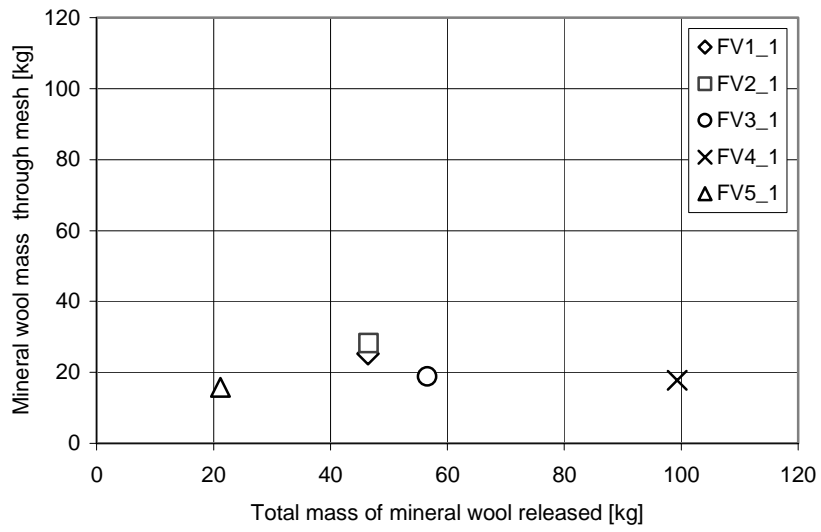


Figure 11. Mineral wool MD2 on the wire mesh

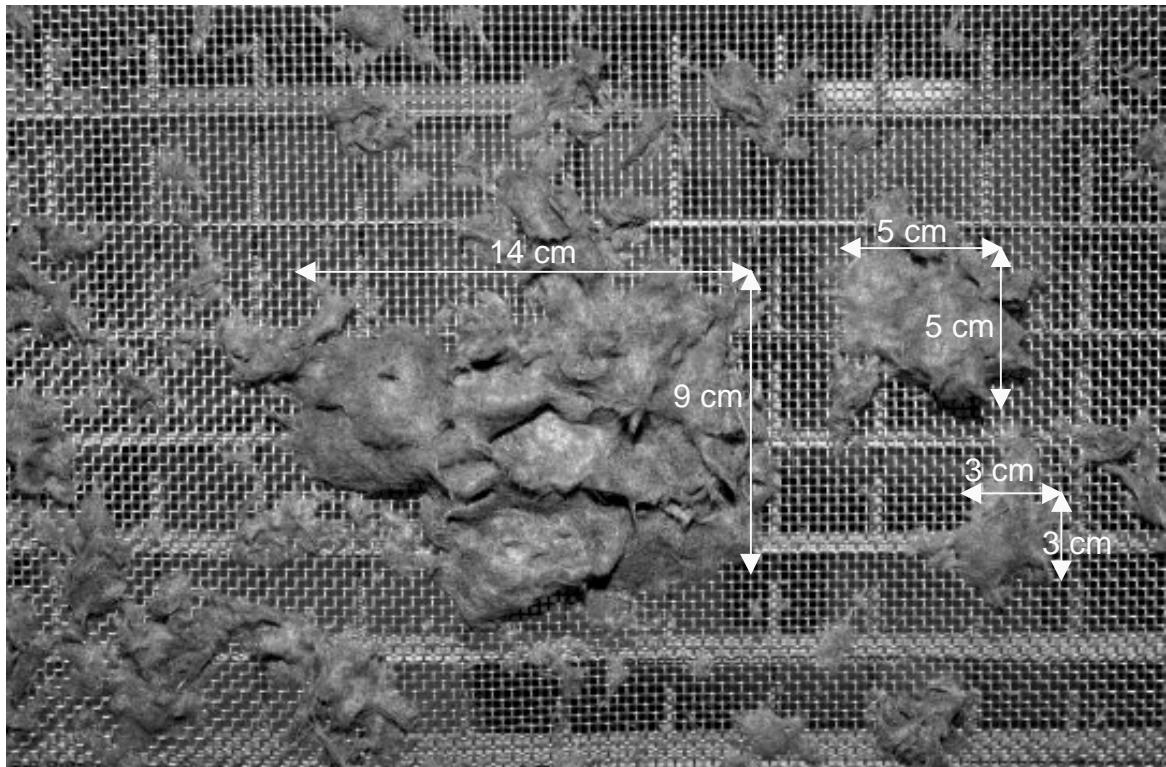


Figure 12. Mineral wool RTD2 on the perforated plate

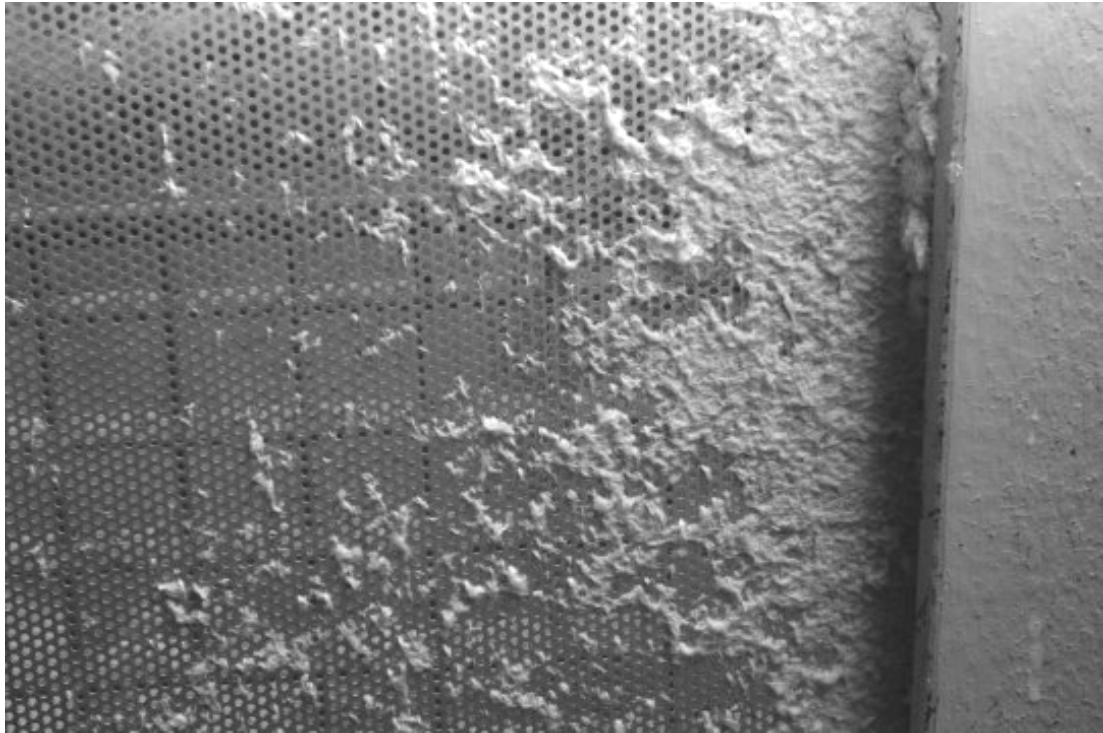


Figure 13. Enveloping reactor sump and model sump

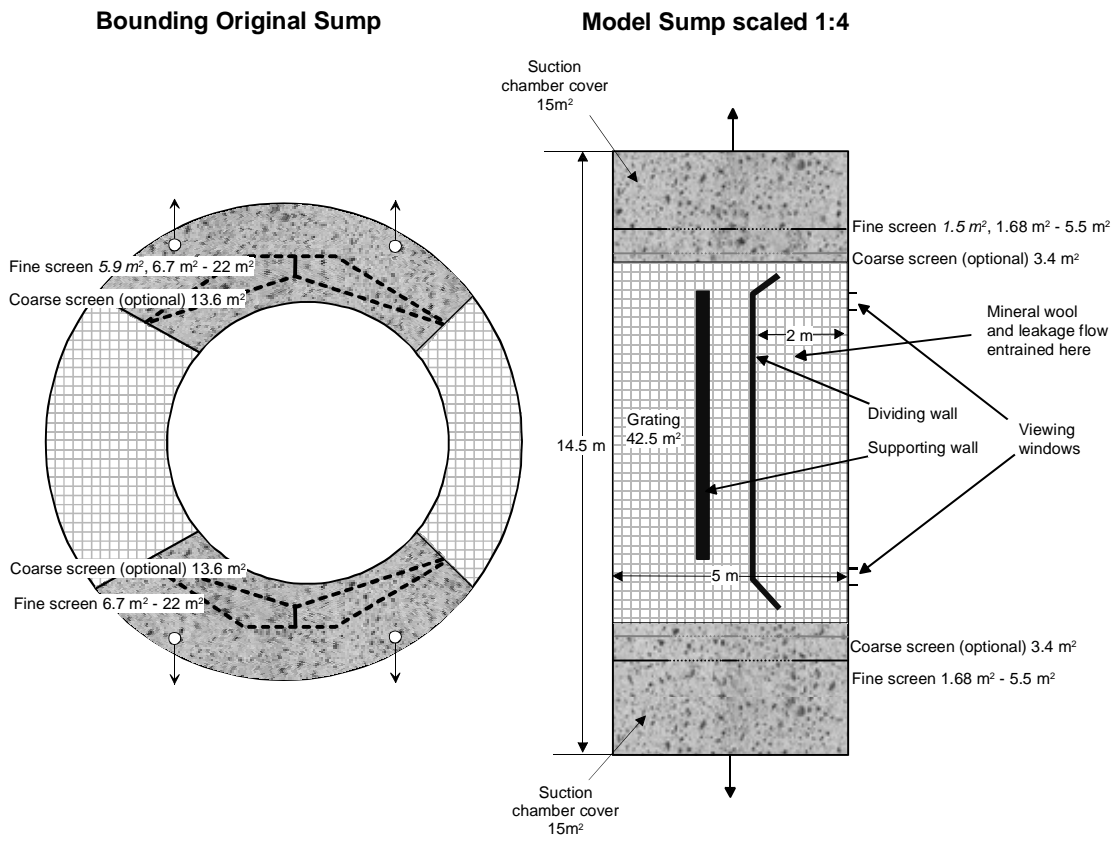


Figure 14. Blow down configuration for 2 A break simulation



Figure 15. Specified water level profile in the model sump with simulation of 2 and 4 residual heat removal pumps

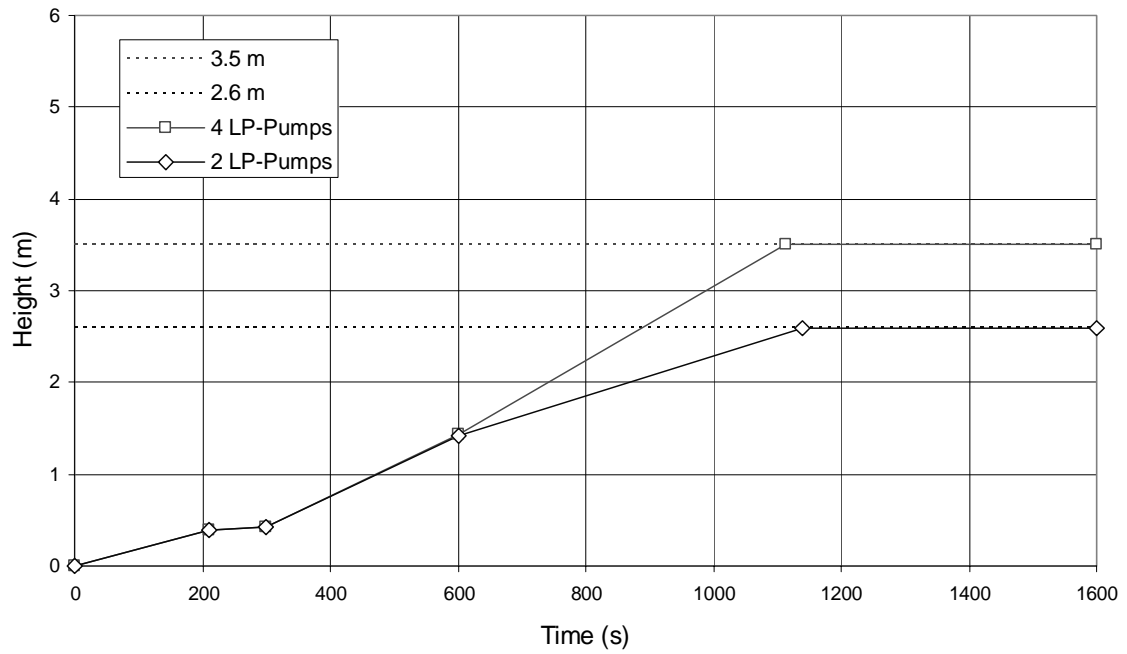


Figure 16. Model sump split into areas for determination of mass distribution of mineral wool sediments and mineral wool deposited on screens

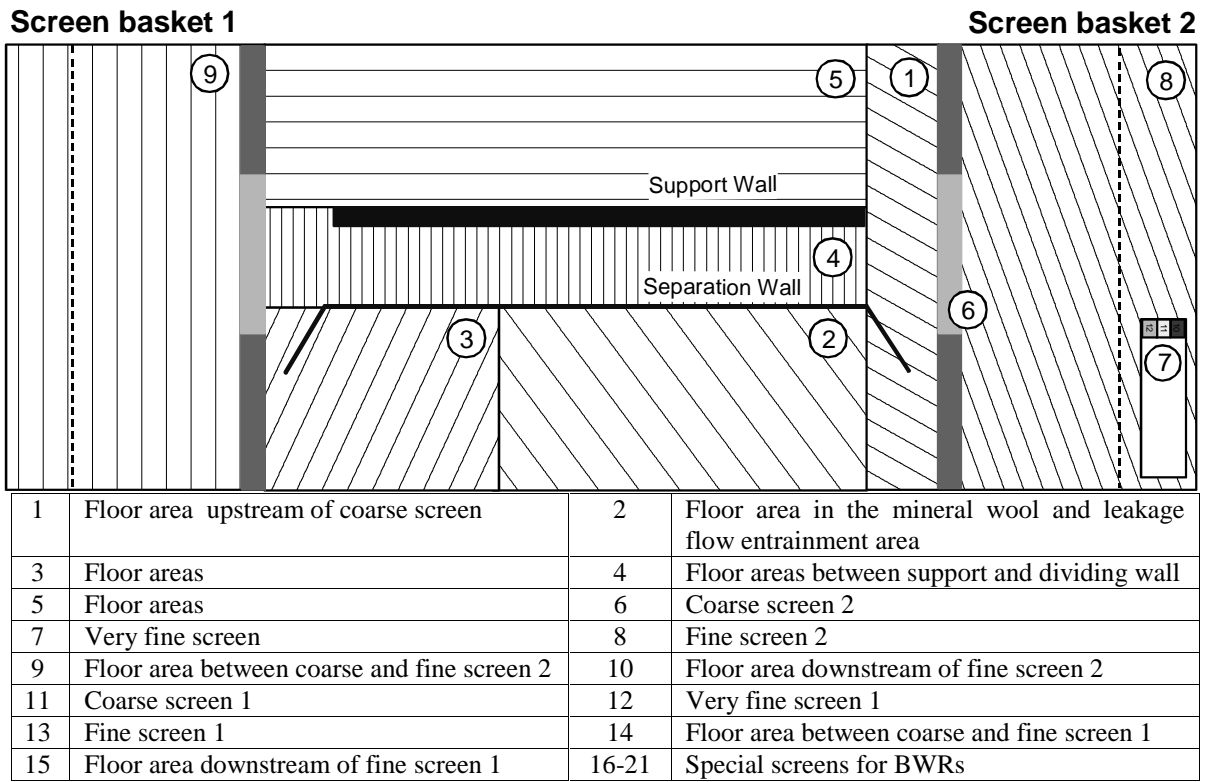


Figure 17. Mobilised mass as a percentage of the amount in the sump

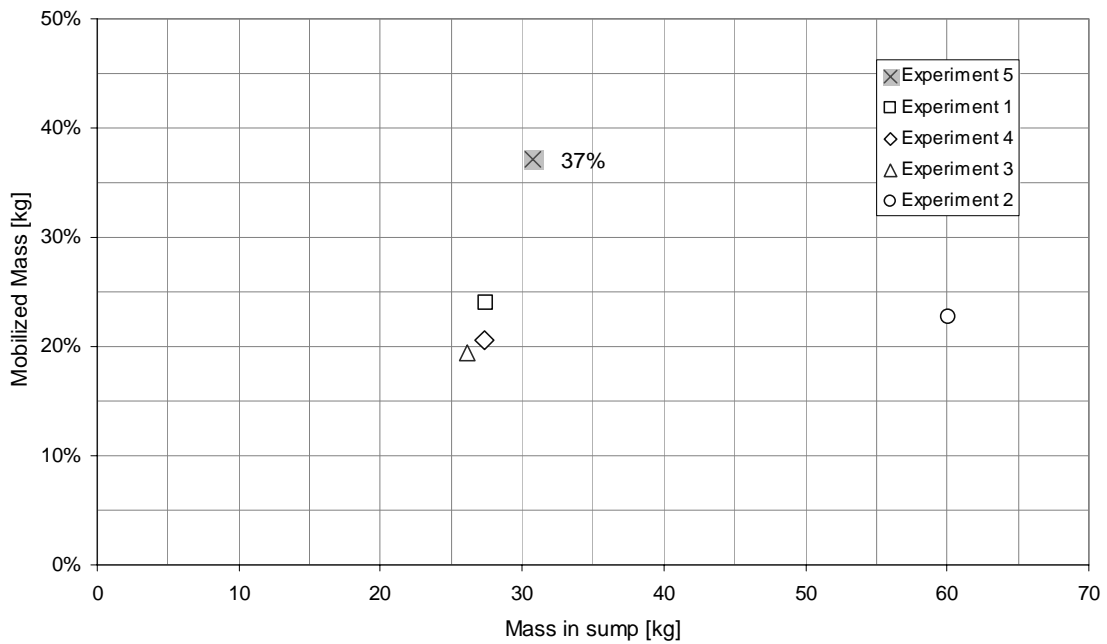


Figure 18. Comparison of the mineral wool amounts deposited on the fine screens as a percentage of the mobilised mass

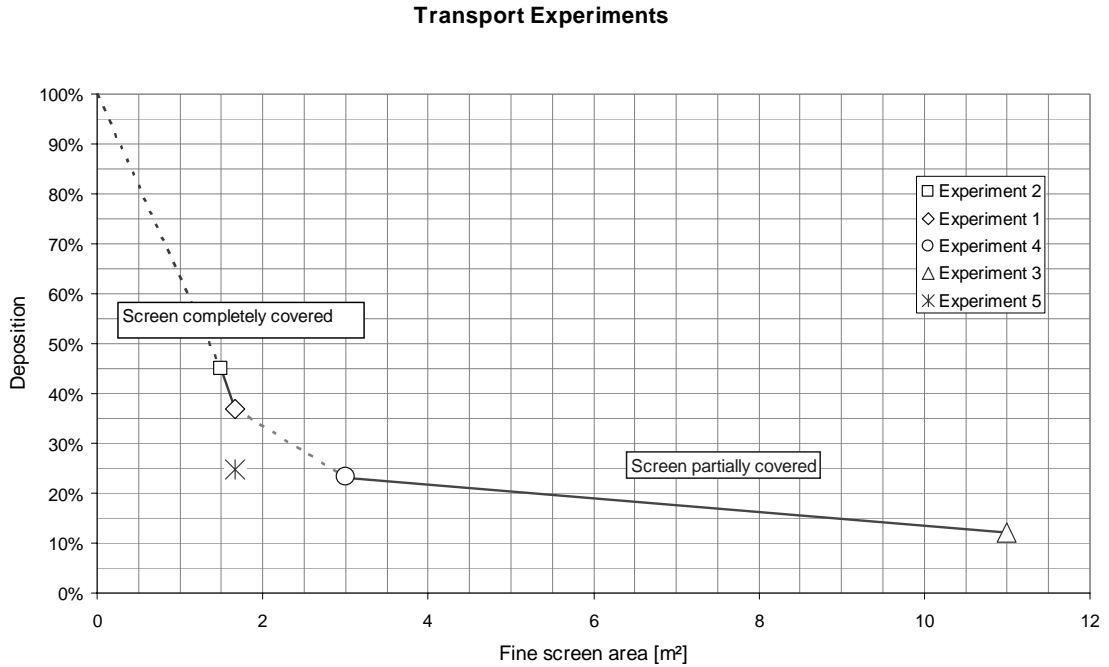


Figure 19. Differential pressures across the fine screen and the micro-screen in transport experiment 1

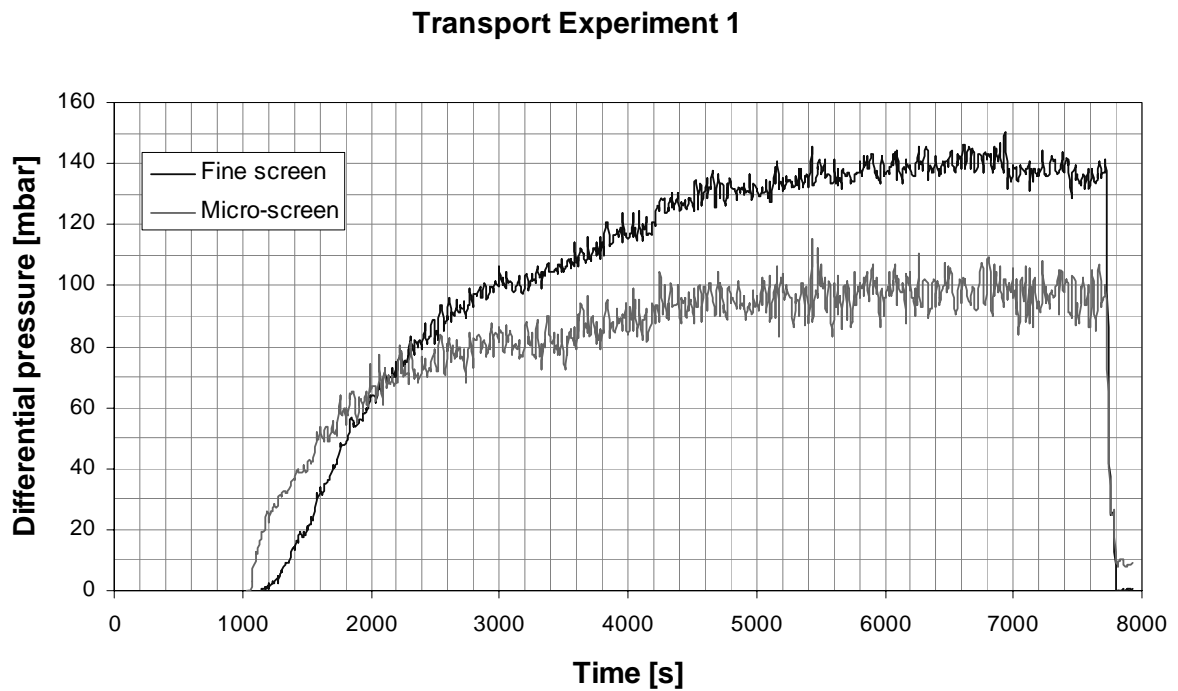


Figure 20. Differential pressure across the fine screen for various flow velocities in transport experiment 2

Transport Experiment 2 (Material Deposited on Screen 4.1 kg/m²)

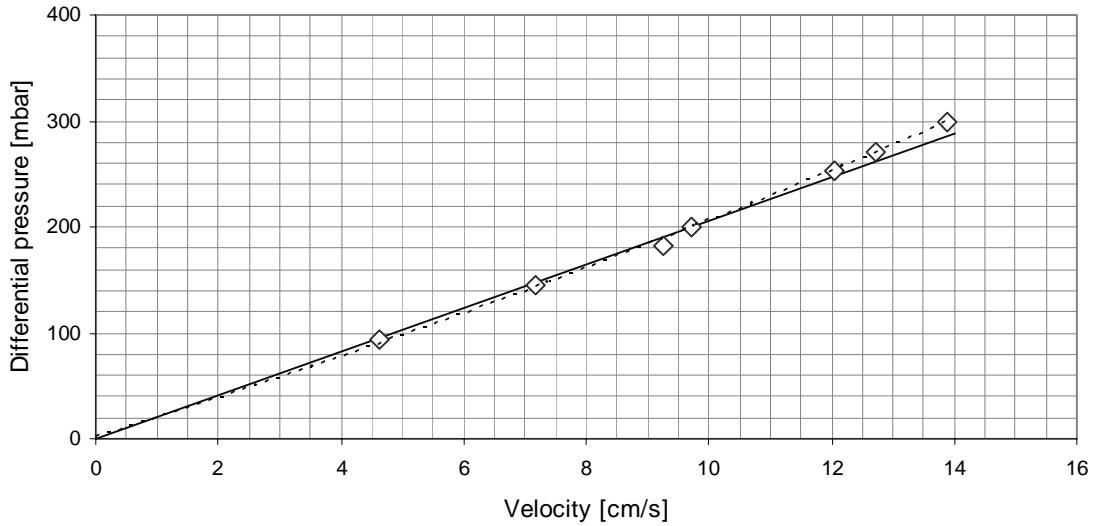


Figure 21. Differential pressures from transport experiments 1 to 4 after linear conversion to a flow velocity of 10 cm/s as a function of screen deposits

Transport Experiments 1, 2, 3 and 4 (~25°C 10 cm/s 0 ppm)

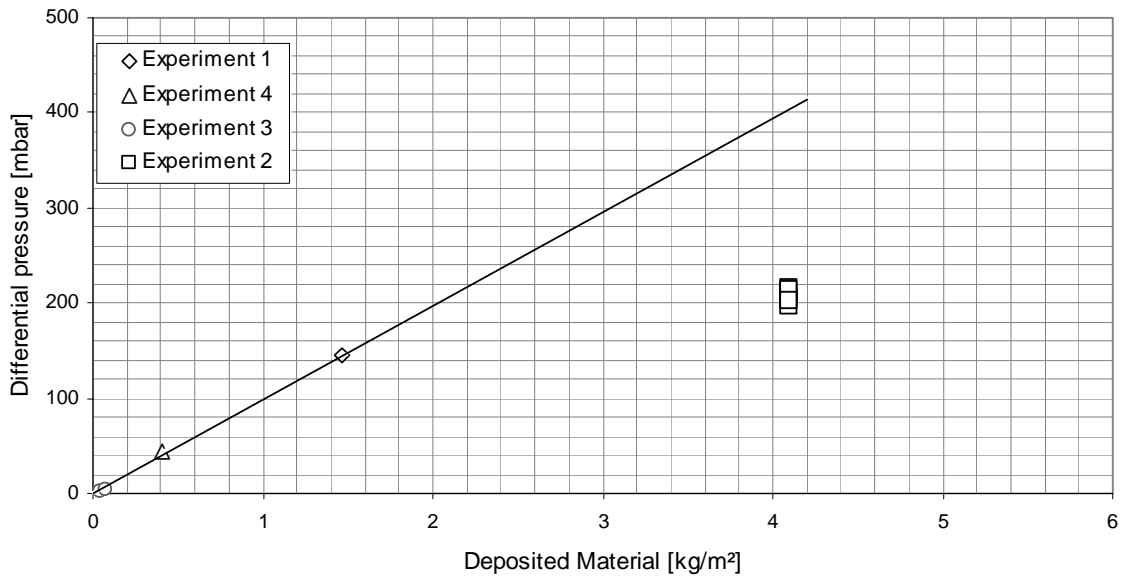


Figure 22. Slip through the fine screens as a function of fine screen area

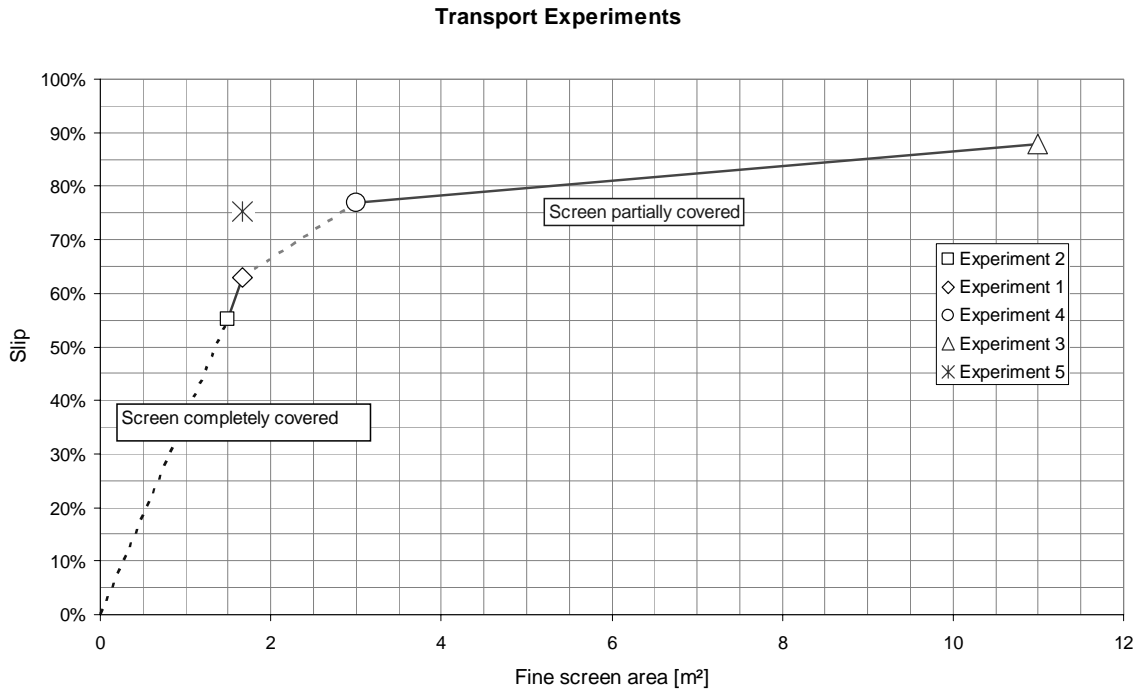


Figure 23. Amounts of sediment between fine screen and micro-screen and amounts deposited on the micro-screen in the transport experiments as a percentage of the mobilised mass

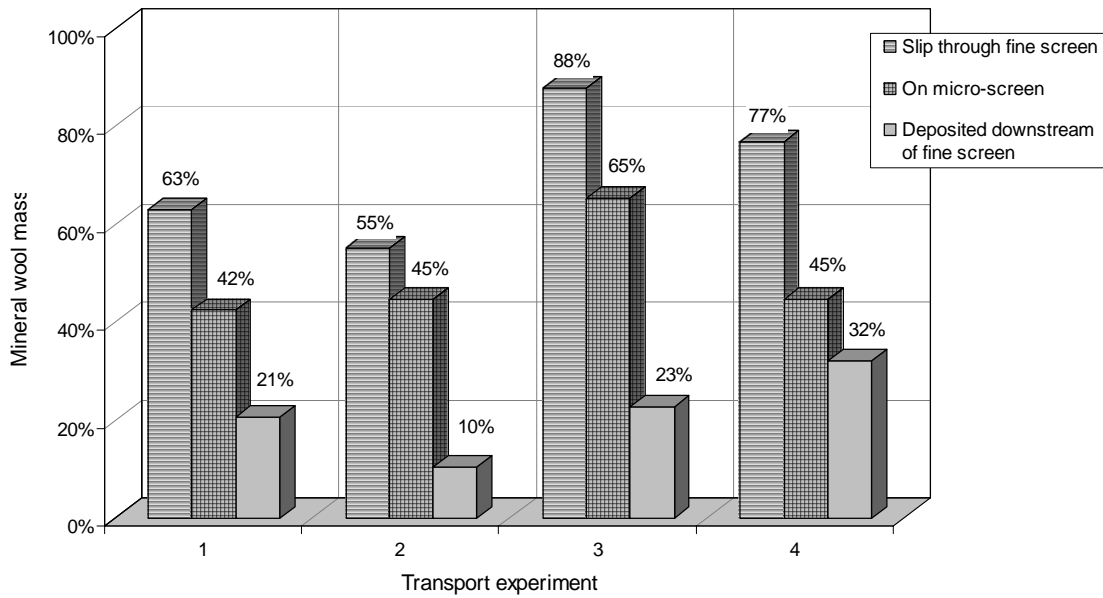


Figure 24. Comparison of differential pressures with mineral wool deposited on the sump strainers and in the fuel assembly

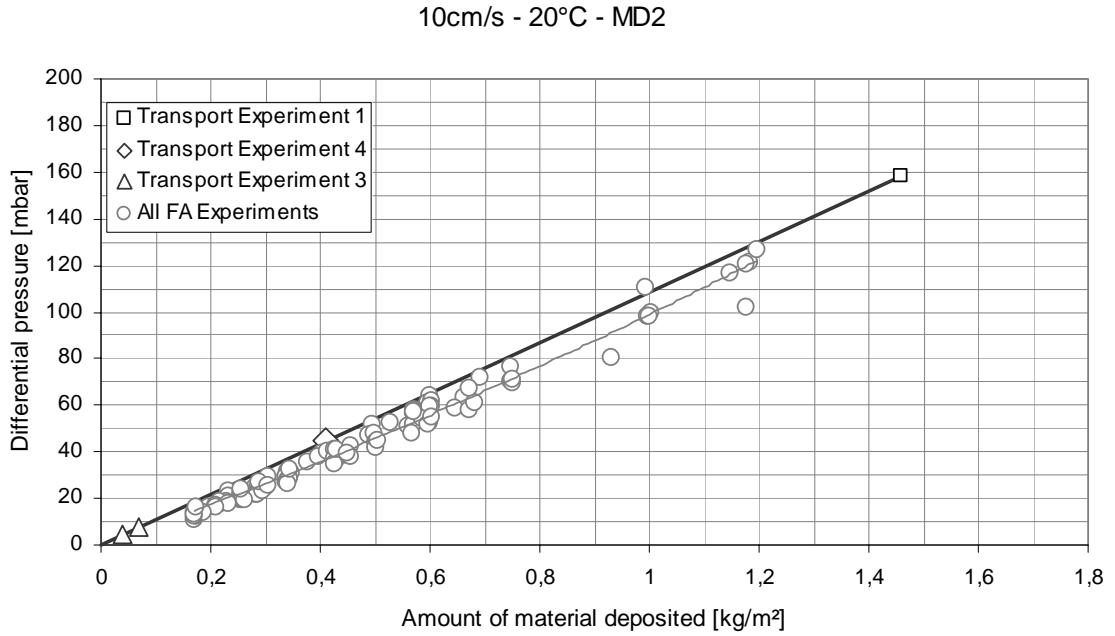


Figure 25. Schematic diagram of the fuel assembly test rig

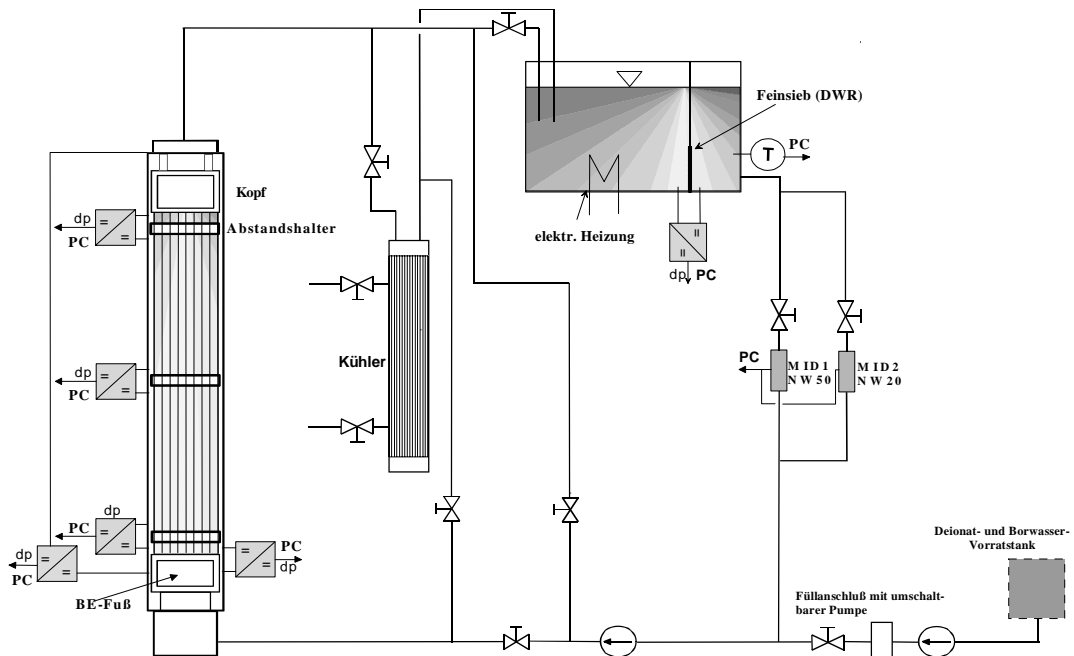


Figure 26. Top view of IDF and standard bottom end piece

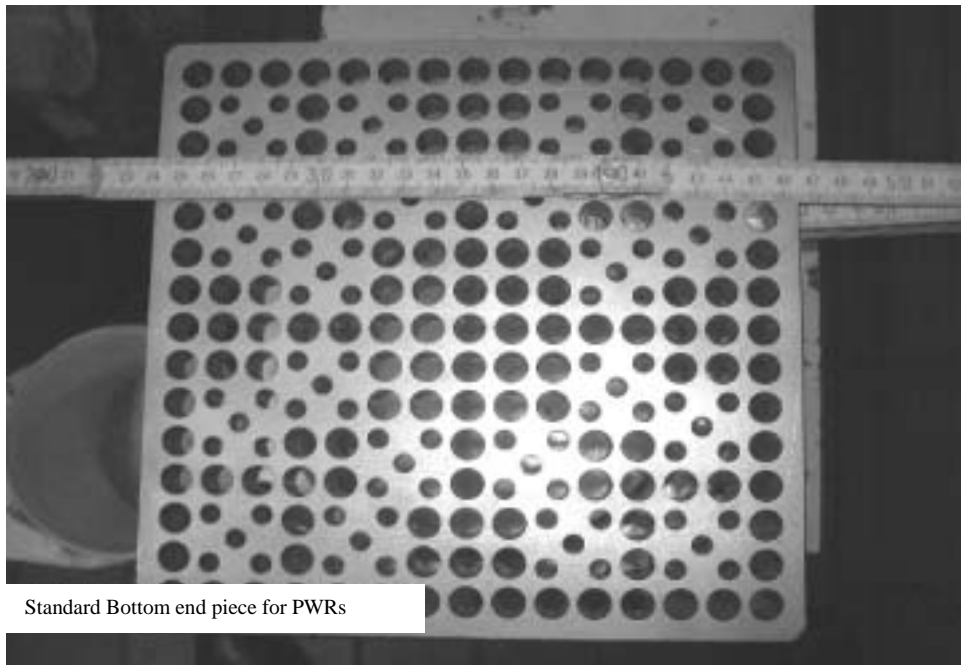
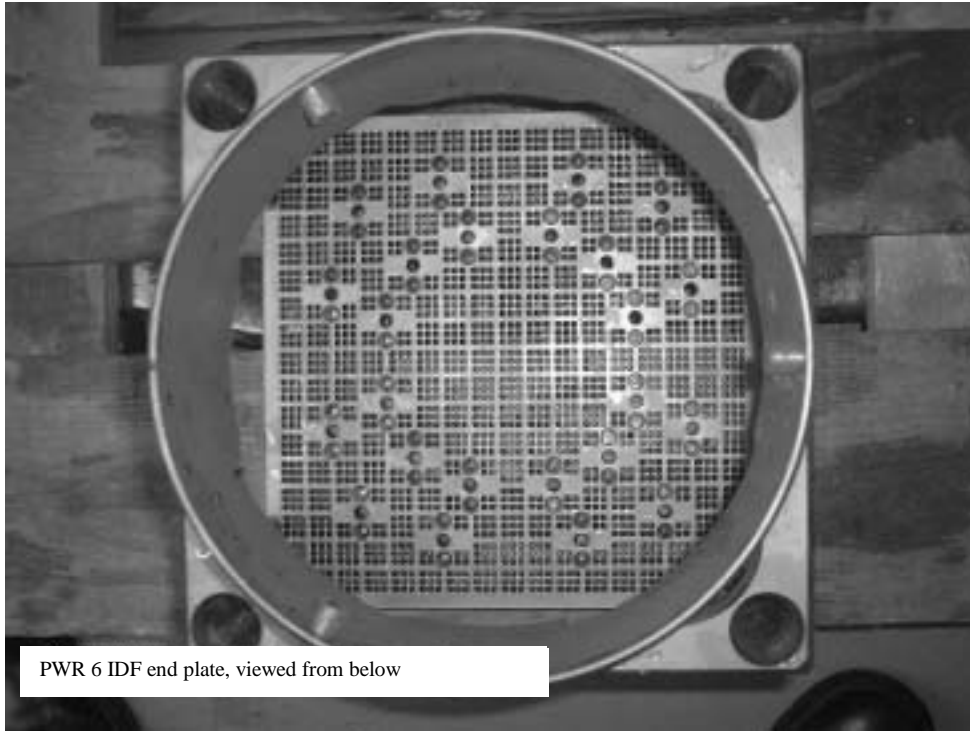


Figure 27. Mineral wool deposits on IDF bottom end piece during experiment 3

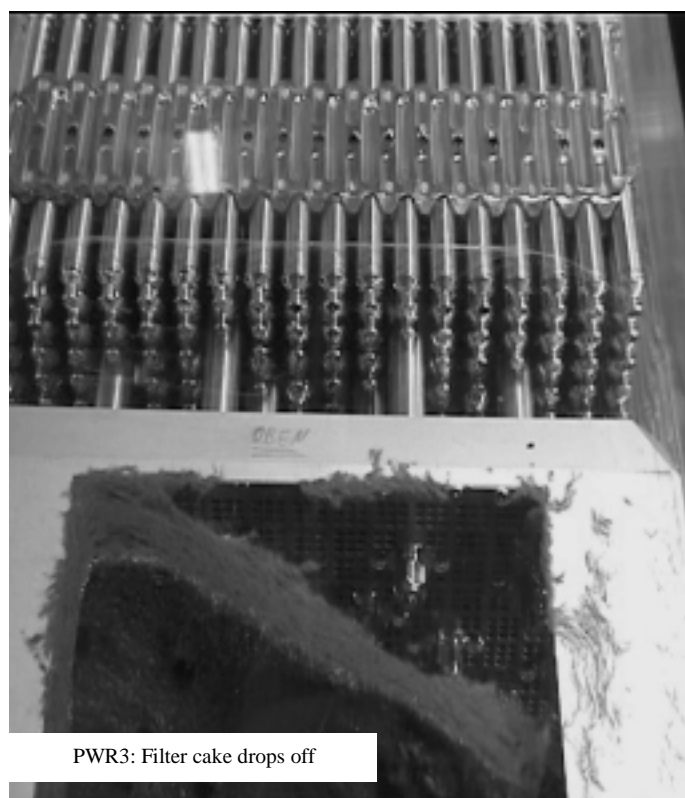
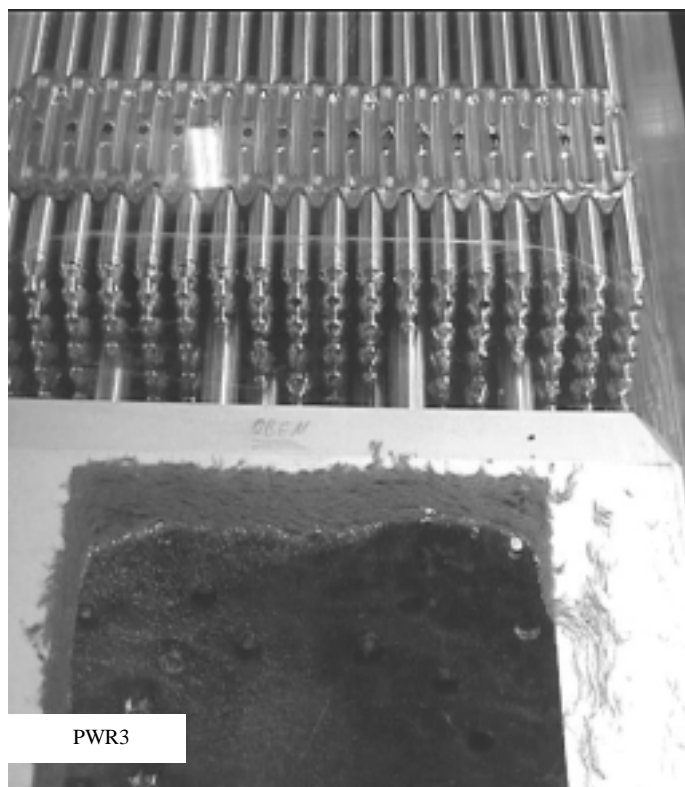


Figure 28. Comparison of differential pressure with mineral wool deposits on the fuel assembly bottom end piece and on the spacer

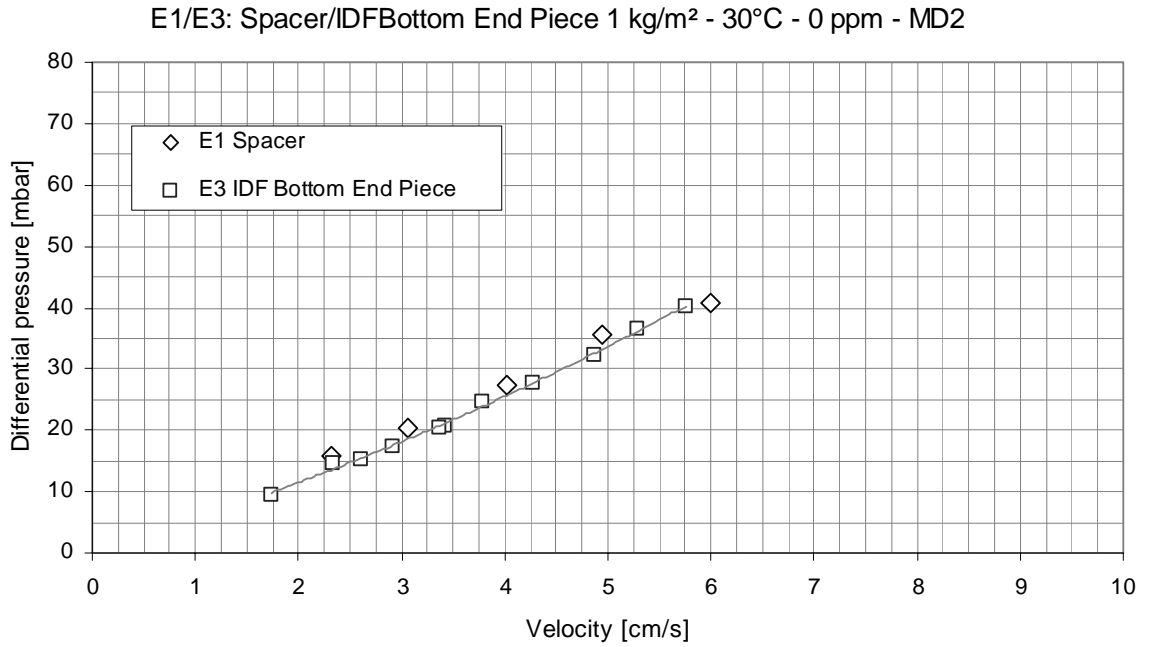


Figure 29. Differential pressure across spacer as a function of deposited mass

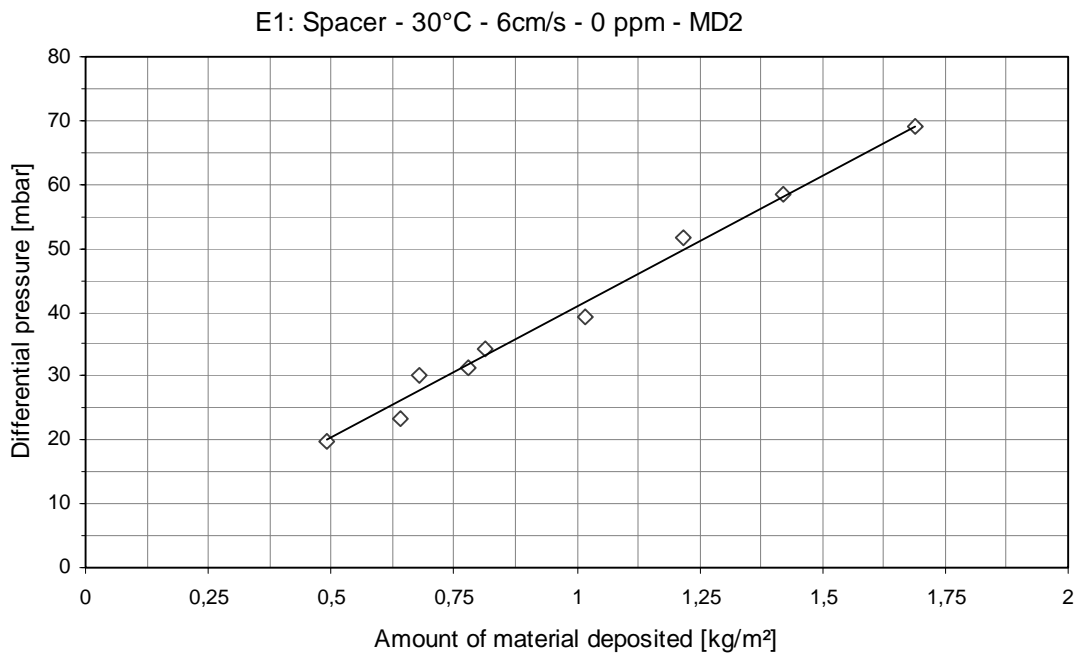


Figure 30. Comparison of differential pressures with different types of mineral wool at 50°C

E6 / E7: 1kg/m² - 80°C - 2200ppm - RTD2 / MD2

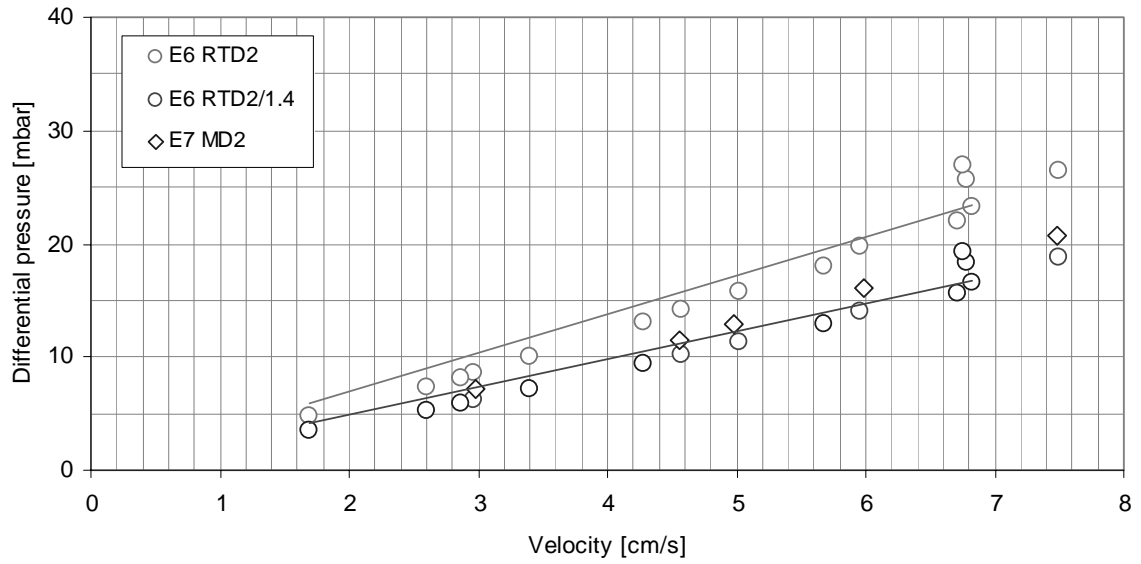


Figure 31. Differential pressures as a function of water temperature

1kg/m² - 5cm/s - 0ppm

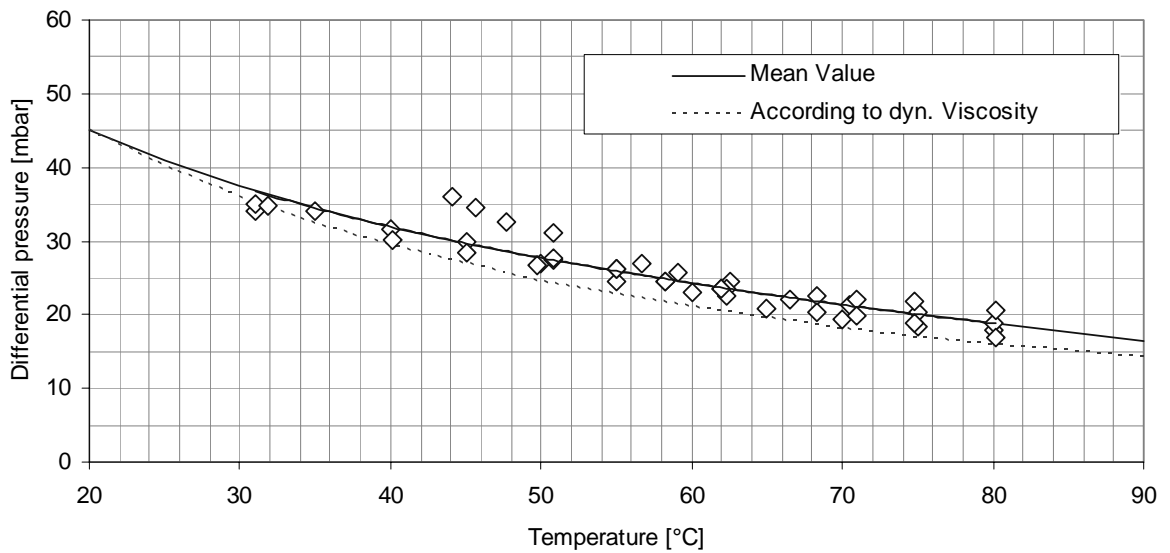


Figure 32. Comparison of normalised differential pressures from transport and FA experiments and previously used assumptions [11]

All Experiments: 1 kg/m² - 20°C - 0ppm /2200ppm- MD2

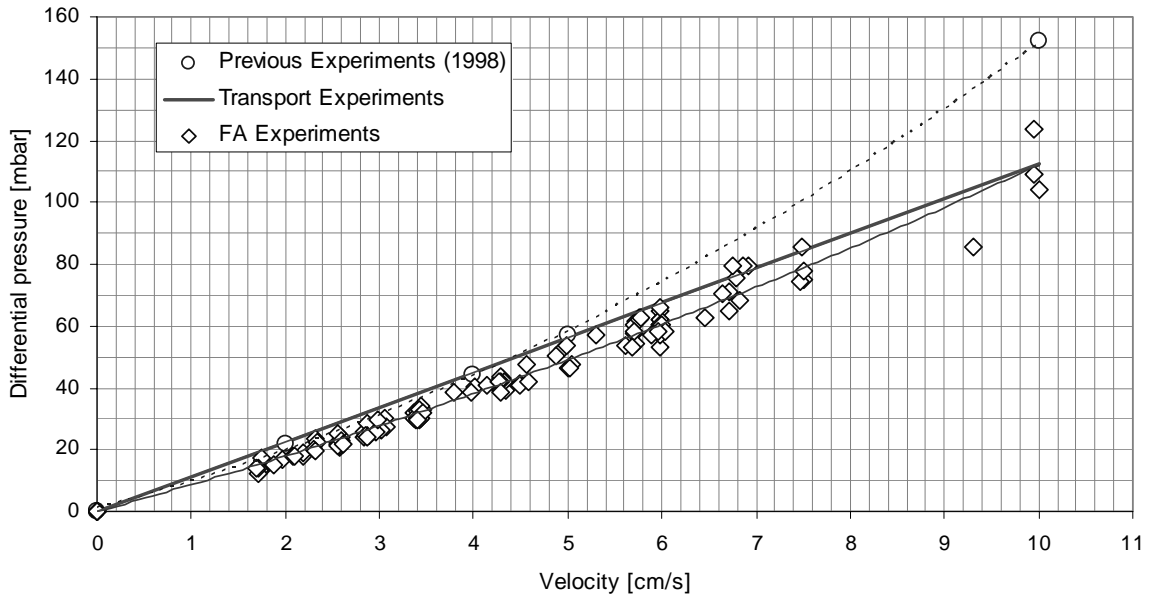


Figure 33. Comparison of normalised differential pressures as a function of velocity in the case of material deposited with high and low volumetric flows

All FA Experiments: 1 kg/m² - 30°C - MD2

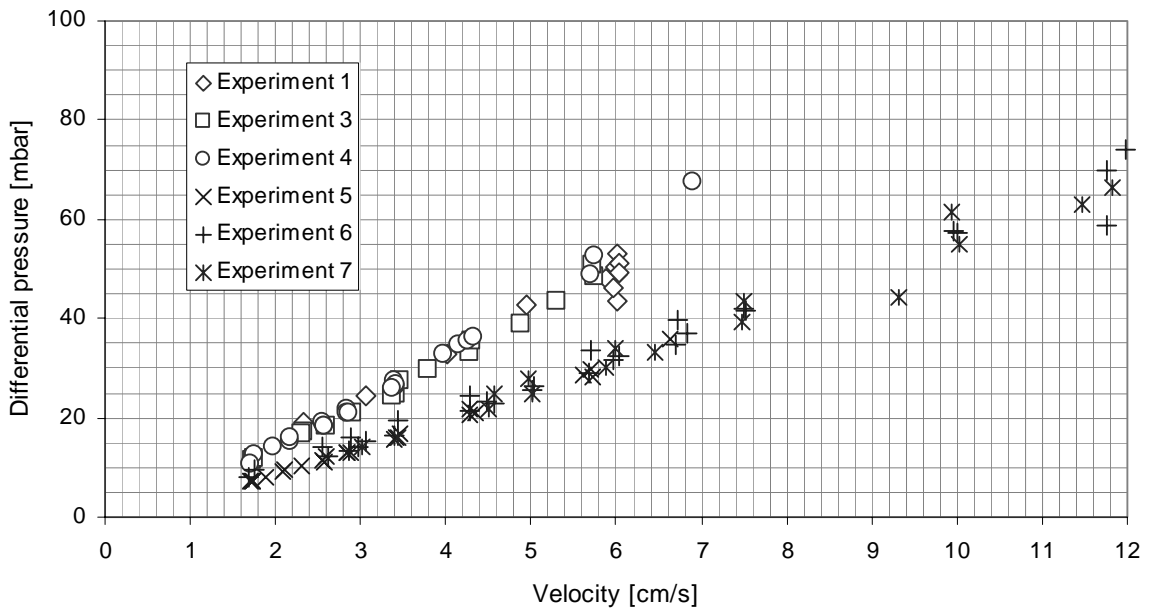


Figure 34. Schematic diagram of the “ring main” test rig

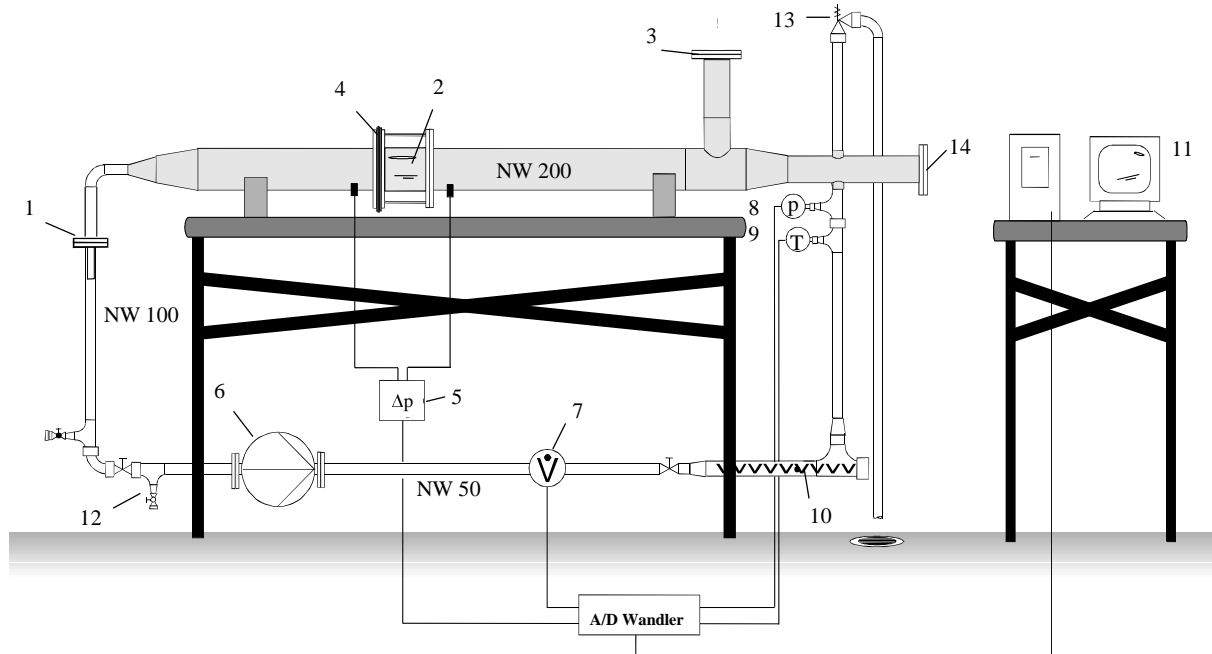


Figure 35. Relative slip as a function of velocity, 9 x 9 mm grating

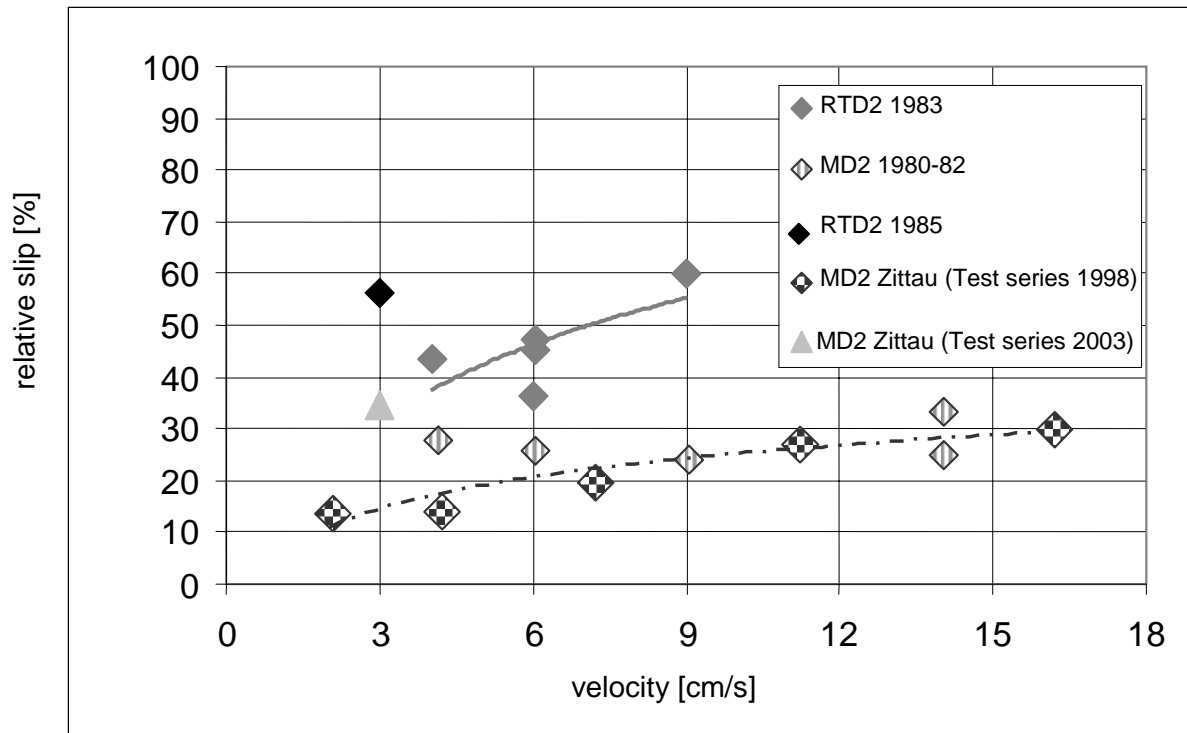


Figure 36. Relative slip as a function of velocity, 3 x 3 mm grating

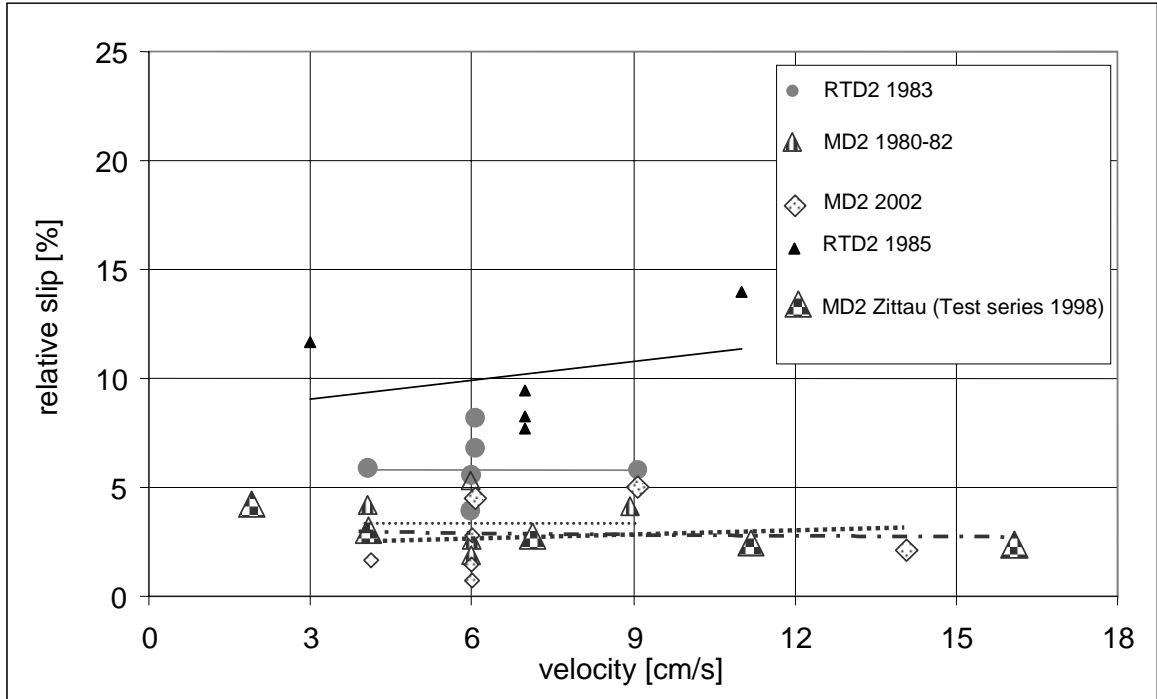


Figure 37. Slip ratio as a function velocity (MD2)

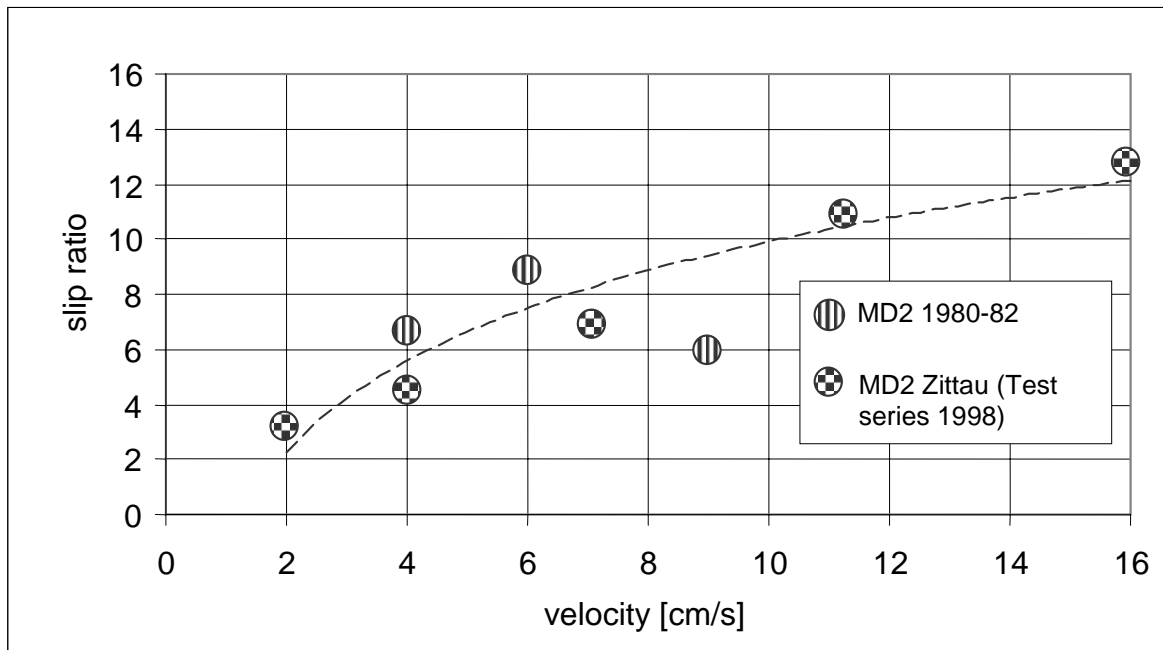


Figure 38. Slip ratio as a function velocity (RTD2)

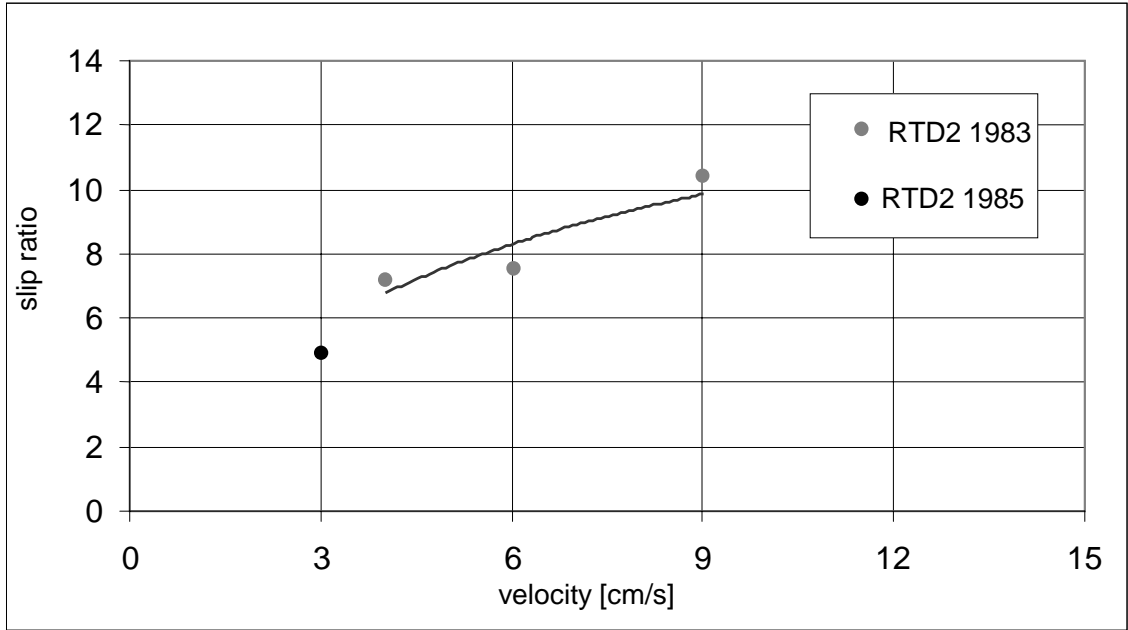
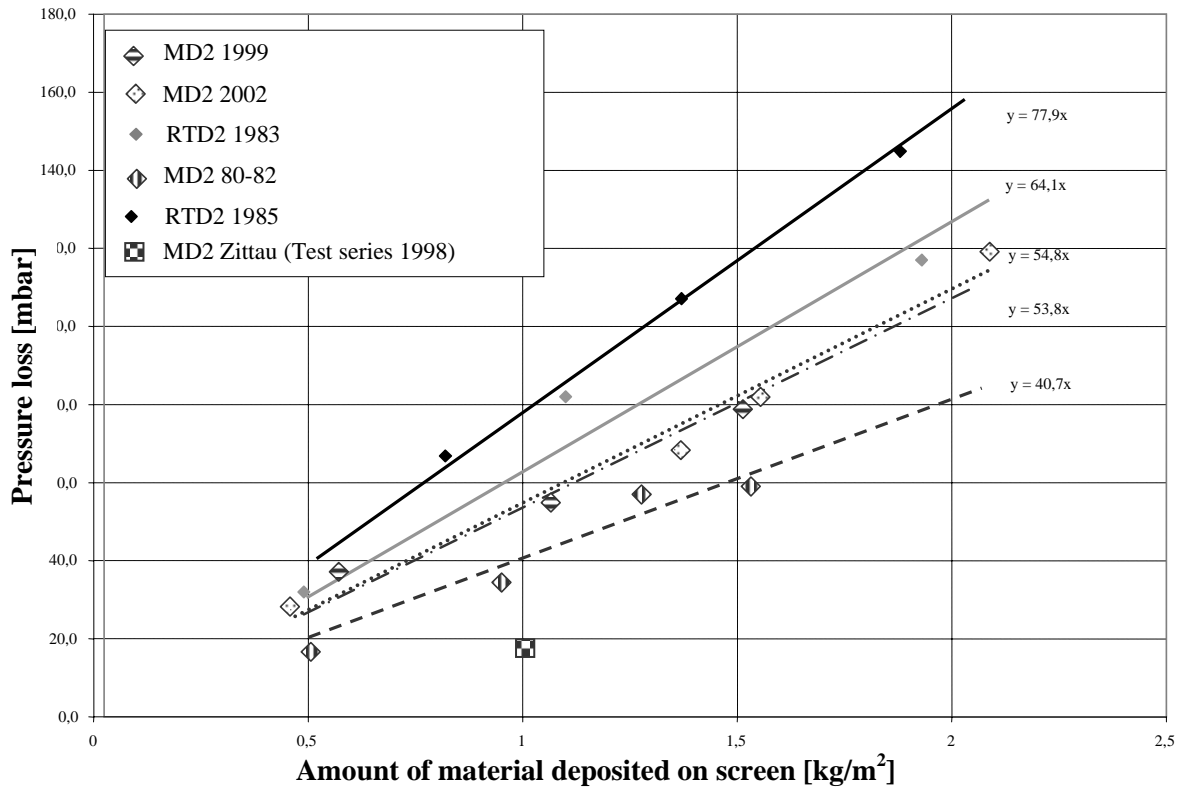


Figure 39. Comparison of pressure losses across a 3 x 3 mm grating at 6 cm/s



Parameters for rule of thumb analysis in Siemens-PWRs

Parameter	Realistic	Conservative	Comments
Leak postulate	0.1 F/ Breach*	0.1 F/ Breach*	* 0.1 F elimination of leaks
Debris generation model	NUREG- Cone	NUREG- Cone	
Sump entrainment ¹			
Break location over ... Grating	15% 10%	50% 25%	
Concrete slab			
Transported portion in the sump ²	24%	27%	
Screen precipitate ²			For reference mineral wool
9 x 9	16%	27%	
3 x 3	24%	27%	
Slip ²			
9 x 9	15%	17%	
3 x 3	2%	3%	
Core precipitate ³	40%	50%	
Head loss correlation	100 mbar for 1 kg/m ²	100 mbar for 1 kg/m ²	Deposition of reference mineral wool at 25°C and flow of 10 cm/s
Head loss scaling	0.6 ... 2.4	0.6 ... 2.4	For different mineral wools
Boron coefficient	1	1	
Coefficient	< 1.25	< 1.25	
9 x 9 → 3 x 3			
Coefficient for particulate	< 2	< 2	Values apply for particulate- portion ≤ ca. 10 w/o

1. Based on disposal.

2. Based on sump entrainment.

3. Based on slip

SESSION 3

ANALYTICAL WORK

Chairpersons: Dr. M. Maqua (GRS) and Dr. T.Y. Chang (USNRC)

HIGHLIGHTS

Session 3 comprised six papers; four of them were presented in the workshop. The main topics dealt with the debris transport in water, the debris impact on pump performance, and break characterisation (break size and location) of pipes using fracture mechanics methods to determine the debris source term.

The approaches to investigate water-borne debris transport were the following: calculate debris generation from the break location by using basic hydraulic equations, use computational fluid dynamics (CFD) to determine the flow field in the sump region and particle transport, and open channel flow modelling. Significant efforts had been made and were still ongoing to validate the CFD calculations by special effect tests. Some of these experiments were discussed in Session 2.

The main goal of computing the flow field in the sump region was to identify locations where the flow velocities exceed the tumbling or lifting velocities of the anticipated debris types. This knowledge supported the estimation of the potential transport fraction of debris from the sump to the sump suction strainers. In addition, the effect of barriers could be assessed in changing the flow field and trapping debris in locations of low flow velocities.

First attempts have been made to include particle motion in CFD calculations. The results from simple test geometries indicated that the Eulerian-Eulerian approach in describing particle motion were successful. It will take at least another year for first calculations on real reactor sump conditions.

Analytical work on impact of debris passing the strainer is a difficult challenge. The first approach is to assess the debris impact on pumps, valves, heat exchangers and spray nozzles by screening existing operating experiences on components which are operating in fluid conditions that comprise particle loads. Thus pump failure rates such as those for pumps in raw water systems can be used to estimate the increase of failure rates of safety system pumps of similar design if operating under post-LOCA conditions including debris loads. The discussion showed that increased failure rates for post-LOCA operation with debris loads seem likely for multi-stage pumps, throttle valves and some heat exchanger designs. Thus, it seems to be highly safety significant to reduce the amount of debris penetrating the sump strainers.

SIMPLE EVALUATION MODEL FOR LONG TERM DEBRIS TRANSPORT VELOCITY IN THE TORUS OF A MARK I CONTAINMENT

Jens-Uwe Klügel¹

Kernkraftwerk Gösgen-Däniken, Switzerland

Introduction

After the Barsebäck 2 strainer clogging incident from 28 July 1992, a first review of the design features of a Mark I containment and the thermal insulation typically employed revealed a potential for the transportation of larger amounts of insulation into the wetwell (torus) of the containment during a LOCA. Although Switzerland took a quick decision to increase the strainers of all BWRs till the end of 1993 (as it was performed by the Swiss Utilities) for the meantime it was necessary to develop tools for assessing the effectivity of accident management actions proposed by the utilities for the existing (old strainer) design. Among others tools a simple evaluation model for assessing the transport velocity of insulation debris caused by the suction of operating strainers was developed, which was applied for a BWR with a Mark I containment and can as well be applied for sump pool conditions of a PWR (submerged sump strainers).

Model description

Basic modelling assumptions

Based on a review of the containment design features and the allocation of the torus strainers in relation to the possible entry paths of insulation it was concluded, that the following assumptions for long term operation of emergency core cooling systems can be applied to develop the model:

1. The flow in the torus can be modelled as a multidimensional steady state potential flow with distributed flow sinks (strainers).
2. The distance between the strainers is large enough to neglect the effects of superposition of the flow fields in the immediate surrounding of the strainers.
3. The flow sinks are modelled to have point shape and are located at the elevation of the strainers. The water below the strainers does not take part in the water exchange between the different torus layers.

1. The work presented was performed while the author was working with the Swiss Nuclear Safety Inspectorate.

Basic equations

The model developed based on the assumptions above can be solved analytically for the spatial velocity distribution of water in the torus. The corresponding equations (in polar coordinates) for the velocities in radial and vertical directions are given below. Q is the volumetric flow of the system taking suction from the strainer of interest.

$$C_r = \frac{Q}{(2 \cdot \pi \cdot z \cdot r)} \quad (1)$$

$$C_z = C_{\text{strainer}} \cdot \frac{A_{\text{strainer}}}{A_{\text{torus}}(z)} \quad (2)$$

Goals and object of the investigation

The model was used to estimate the transport velocities of insulation material (rockwool) floating in the torus of a BWR with Mark I containment. The main goal of the investigation consisted in the evaluation of the success chances of accident management measures like:

- throttling of suction flow;
- temporarily transferring ECCS injection to the cold condensate storage tank interrupting suction from the torus;
- restarting suction from torus after drain of cold condensate tank assuming settlement of insulation material.

Figure 1 shows a cross section of the plant containment.

In the original design (meanwhile the strainers were replaced) the plant possessed three small suction strainers spatially separated from the blowdown lines in different segments of the torus. The plant of concern has 6 different trains of ECCS systems:

- TCS – torus cooling system – 2 trains.
- CS – core spray system – 2 trains.
- ALPS – alternate low pressure system – 2 trains.

The total suction flow in case of operation of all trains consists of $0.43 \text{ m}^3/\text{s}$. The minimal suction flow in case of operation of one train of the torus cooling system and one train of ALPS consists of $0.085 \text{ m}^3/\text{h}$. All strainers are connected to a common ring line below the torus area subdivided to the different system trains. The free flow area of one strainer was 0.206 m^2 . The distance between the strainers and the next blowdown line into the torus is 8.1 m in horizontal direction and 1.71 m in vertical direction. The strainer surface was allocated 3.58 m below the normal torus water surface.

The suction strainer thus was well separated from the possible entry points of insulation with the blowdown flow.

Results and conclusions

A large set of calculations for different operating conditions of emergency core cooling systems was performed. Table 1 gives an overview of the conditions considered.

Table 1. Operational conditions investigated

ECCS suction flow	Number of strainers in operation	Comment
0.430 m ³ /s	3	Maximum suction flow with all strainers in operation
0.430 m ³ /s	1	Maximum suction flow with 2 strainers clogged
0.085 m ³ /s	3	Minimum suction flow with all strainers in operation
0.085 m ³ /s	1	Minimum suction flow with 2 strainers clogged

Figures 2-7 show the velocity distribution in the surroundings of a suction strainer for different operating conditions. Based on a comparison with typical settlement velocities of thermal insulation debris (mainly rockwool of different age) it was demonstrated, that the flow suction from the strainers has only minor effect on the settlement velocity of the debris. The suction effect in radial direction is also very limited, once stabilised flow conditions are achieved in the torus. On the other hand this means, that material which is able to float (old insulation material) can keep floating for a very long period of time not being directed to the strainers. Only material transported close to the strainer position is expected to participate in a potential strainer clogging. Spatial separation of strainers from the blowdown lines gives some reasonable protection against strainer clogging. The largest uncertainty remained was the distribution of thermal insulation during and immediately after the blowdown phase of the accident.

With regard to accident management actions it was concluded:

- that flow reduction for operating emergency core cooling systems is an effective measure to reduce the risk of strainer clogging;
- that it is unlikely, that once settled debris, for example after an interruption of ECCS operation or back flushing will relocate to the strainers;
- that the accident management actions implemented by the utility as an intermediate measure:
 - Injection from an alternate water source (cold condensate storage tank) allowing to stop suction from the torus.
 - Back flushing of strainers from cold condensate system is efficient to limit the consequences of a LOCA accident within the regulatory safety limits.

On the other hand, it was concluded that human interaction may be necessary within the first 30 minutes after an accident to avoid partial clogging and to circumvent the uncertainty related to the initial insulation distribution in the torus. This situation was not in compliance with the deterministic 30 min-rule (Swiss Regulation R-101), requiring that design basis accidents shall be governed mainly by automatic means not allowing for not safety directed human interactions (like throttling or turning off ECCS-systems) during the first 30 minutes of an accident.

That's why in 1993 the effective strainer surface of all BWRs in Switzerland was enlarged substantially.

Figure 1. Mark I containment

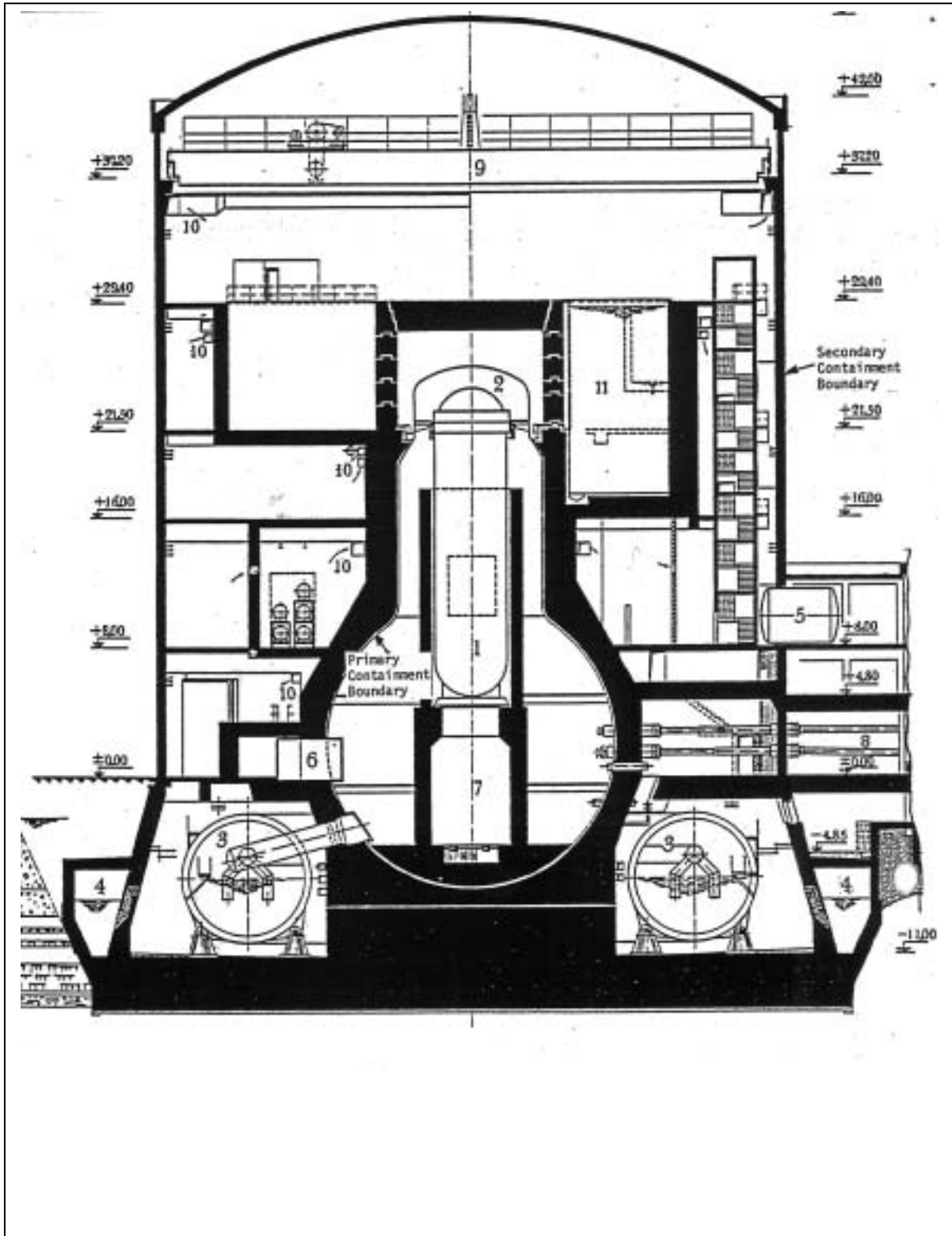


Figure 2. Radial velocity distribution, $Q = Q_{max}$, 1 operating strainer

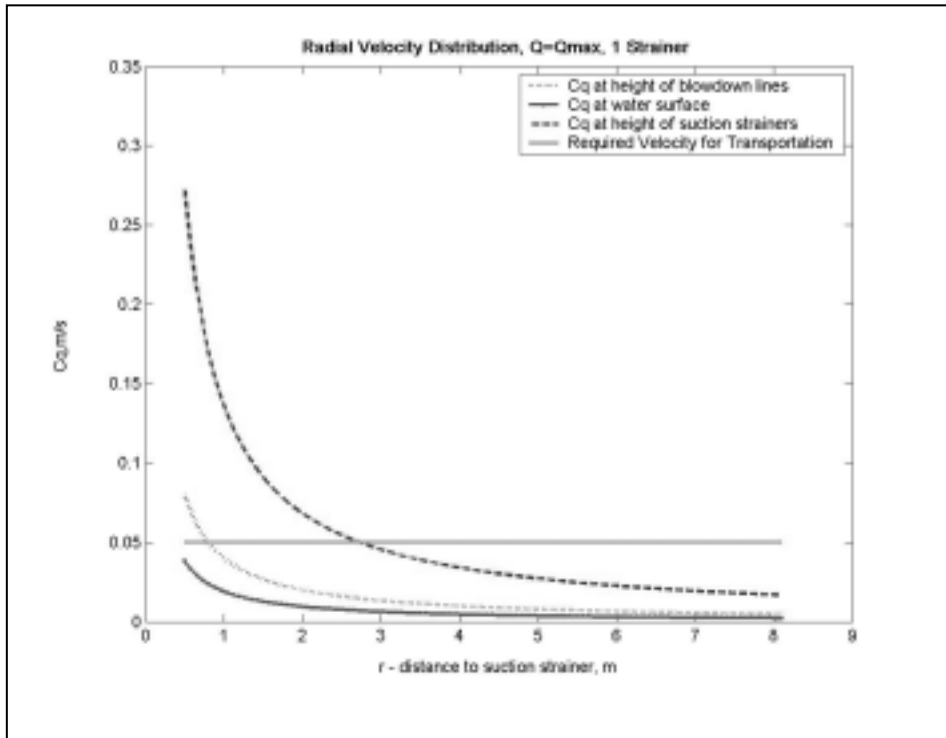


Figure 3. Radial velocity distribution, $Q = Q_{max}$, 1 operating strainer – Surface plot

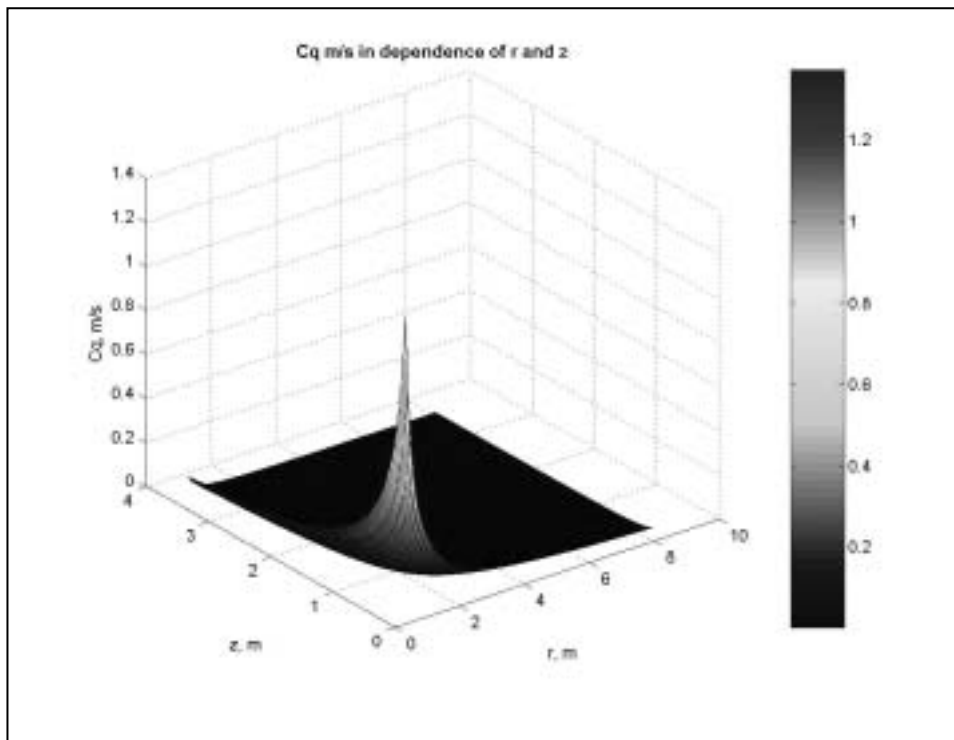


Figure 4. Axial velocity distribution, $Q = Q_{max}$, 1 operating strainer – Surface plot

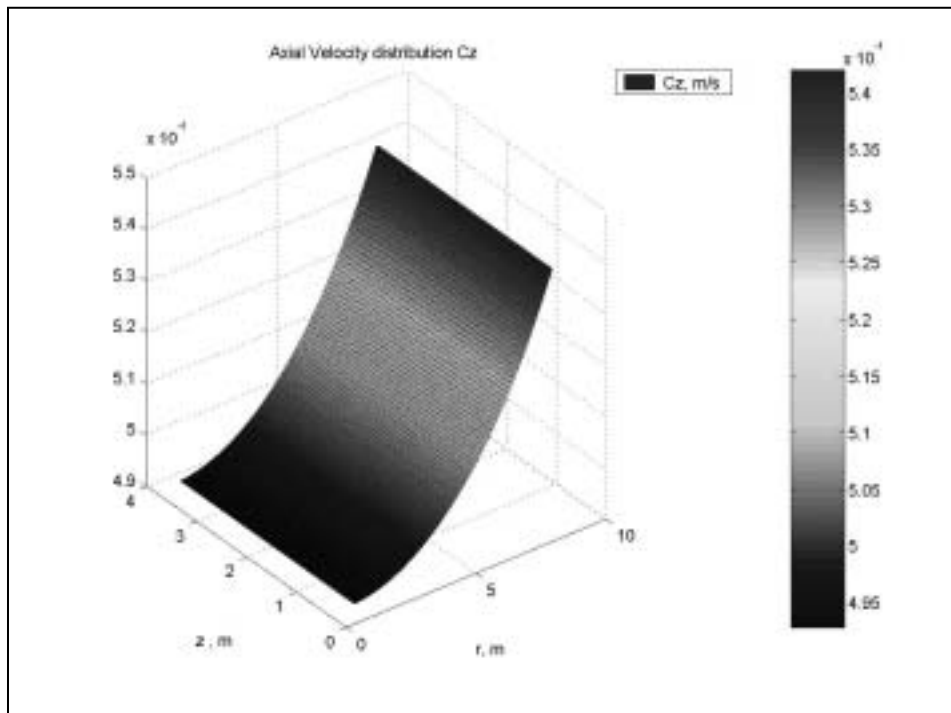


Figure 5. Radial velocity distribution, $Q = Q_{max}$, 3 operating strainers

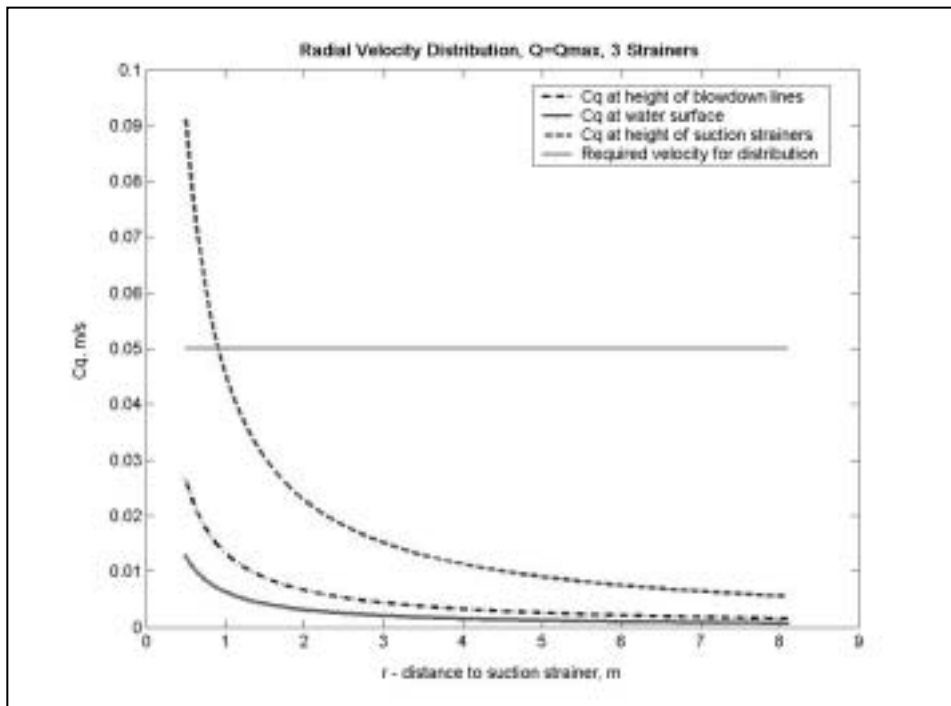


Figure 6. Radial velocity distribution, $Q = Q_{min}$, 1 strainer

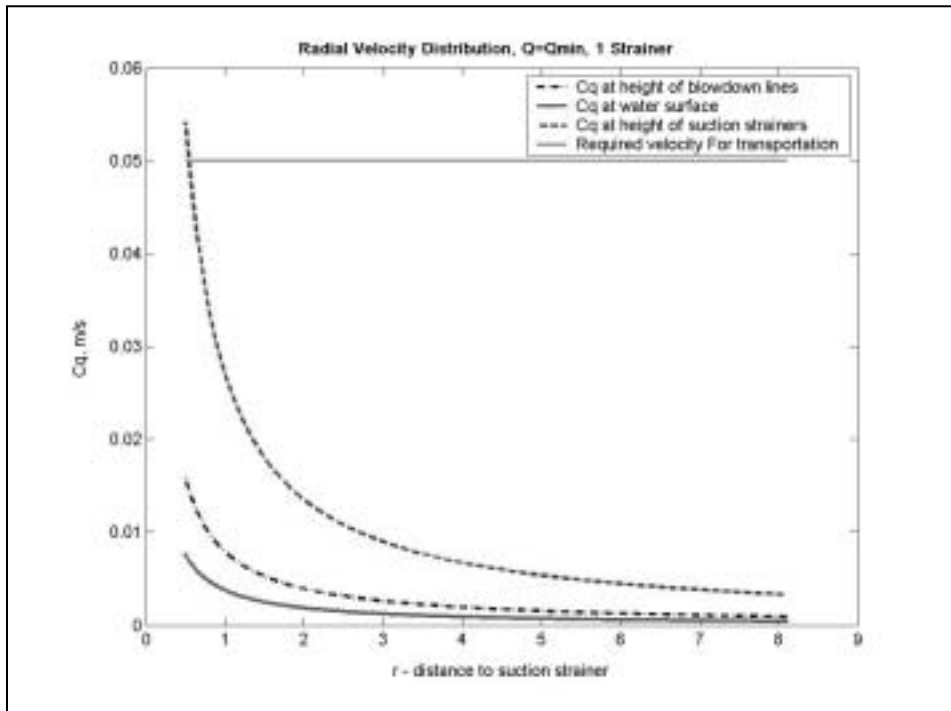
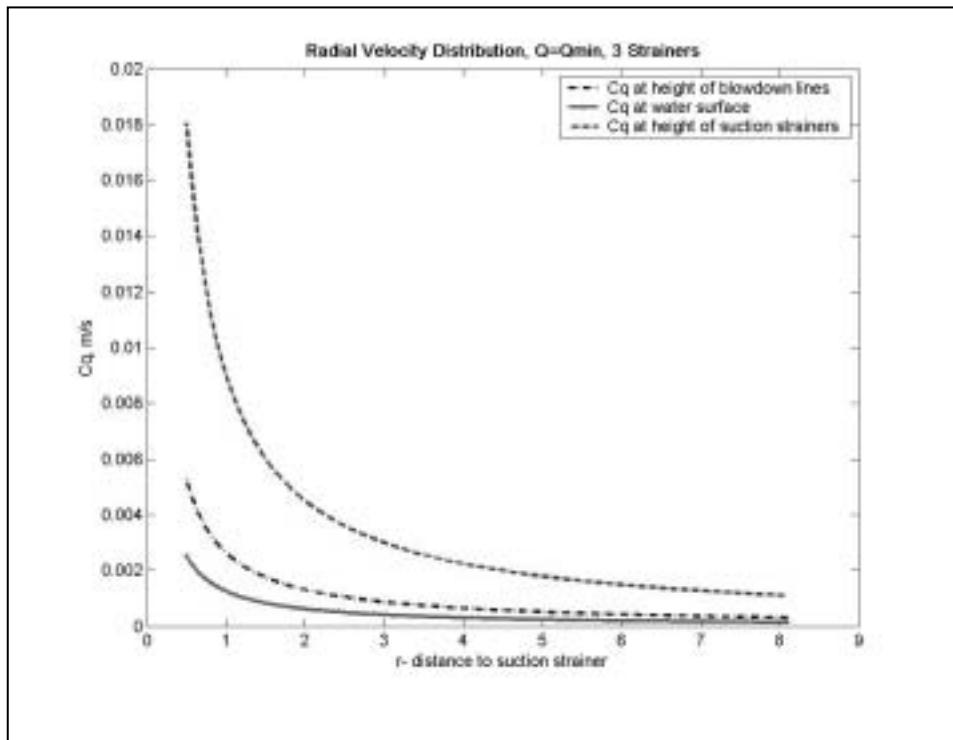


Figure 7. Radial velocity distribution, $Q = Q_{min}$, 3 strainers



NUMERICAL INVESTIGATIONS OF INSULATION DEBRIS TRANSPORT PHENOMENA IN WATER FLOW

Eckhard Krepper, Alexander Grahn

Forschungszentrum Rossendorf e.V., Institute of Safety Research
D-01314 Dresden, POB 510119, Germany

1. Introduction

The investigation of insulation debris generation, transport and sedimentation gains importance regarding the reactor safety research for PWR and BWR considering the long term behaviour of emergency core coolant systems during all types of LOCA. The insulation debris released near the break during LOCA consists of a mixture of very different particles concerning size, shape, consistence and other properties. Some fraction of the released insulation debris will be transported into the reactor sump where it may affect emergency core cooling. Open questions of generic interest are e.g. the sedimentation of the insulation debris in a water pool, possible resuspension, transport in the sump water flow and particle load on sieves.

A common research project in cooperation with IPM-Zittau deals with the experimental investigation and the development of CFD models for the description of particle transport phenomena in coolant flow (see Alt, *et. al.*). While experiments are performed at the IPM-Zittau, theoretical work is concentrated at Forschungszentrum Rossendorf.

In the present paper the basic concepts for CFD modelling are described and first feasibility studies are shown. During the ongoing work further results are expected.

2. Basic CFD concepts

3D computational fluid dynamics (CFD) codes describe a fluid flow based on the solution of the conservation equations for mass, momentum and energy. CFD methods are distinguished by different solution strategies of the basic equations and physical models for the closure laws. For the actual problem, basically two different approaches are possible: The application of the Euler/Lagrangian or the Euler/Euler approach.

The first approach relies on the solution of the Navier Stokes equations for the continuous fluid phase and on the solution of the Lagrangian equations for single particles. The single particles are modelled having a certain mass. The flow field acts on each particle and influences the particle path. The particles themselves take effect on the turbulence quantities of the fluid. The advantage of this approach is, at the end to know the path of each modelled particle, i.e. to get more information about the reason for a certain flow behaviour.

The Euler/Euler approach assumes at least two fluids continuously penetrating each other. The volume fraction of the fluids in each cell sums to unity. For each fluid the full set of conservation

equations is solved. That means, each fluid has a different velocity field. The mechanisms of interaction of the fluids are the flow resistance modelled by momentum transfer, phase change modelled by mass transfer and heat conduction modelled by energy transfer. Whereas the two latter interactions in the present problem are not relevant, the flow resistance is essential for the description of debris transport. The advantage of the concept is to easily calculate mass balances, as will be shown later. In our investigations the Euler/Euler approach was preferred for insulation debris transport modelling.

3. Modelling of insulation debris transport

3.1 Drag forces

The particle transport in the Euler/Euler approach is described by the momentum exchange between the two phases. In the case of dispersed spherical gas bubbles or spherical particles moving in a continuous fluid, the interacting forces have in principle the form:

$$F_{Drag} = \frac{1}{2} n \rho A C_D |U| U$$

with the particle number density n , the liquid density ρ , the cross sectional area of the particle in flow direction A , the relative velocity between the phases U and the drag coefficient C_D . The drag coefficient depends on the Reynolds Number, which is defined as

$$Re = \frac{\rho |U| d}{\mu}$$

with μ as the dynamic liquid viscosity.

For low velocities and Reynolds Numbers $\ll 1$ the viscosity effects are dominating. The regime is designated as Stokes-Regime and we find:

$$C_D = 24 / Re$$

For high velocities ($1\,000 < Re < 1.2 \cdot 10^5$) the inertia effects are dominating and we have:

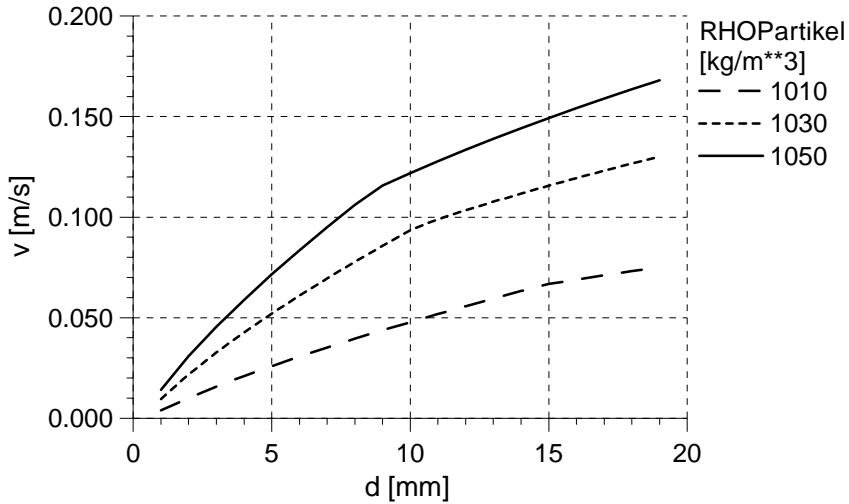
$$C_D = 0.44$$

In the transition region ($0.1 < Re < 1\,000$), where both effects are of the same order of magnitude, we find:

$$C_D = \max \left[\frac{24}{Re} (1 + 0.15 Re^{0.687}), 0.44 \right]$$

The last equation is known as the Schiller/Naumann correlation.

Figure 2. Dependency of the sinking velocity on the particle diameter d and the particle density calculating the drag coefficient according to Schiller/Naumann



The sinking experiments were modelled using the CFD code CFX applying the Euler/Euler approach. Assuming a drag force according to Schiller/Naumann, the terminal sinking velocity V_{sink} can be calculated with the gravity acceleration g , the particle respective water density ρ , a particle diameter d and a drag coefficient C_D :

$$V_{sink} = \frac{4}{3} g \frac{\rho_{particle} - \rho_{water}}{\rho_{water}} d \frac{1}{C_D} \frac{1}{V_{sink}}$$

Figure 2 shows the dependency of the terminal sinking velocity V_{sink} on the particle density $\rho_{particle}$ and the particle diameter d , when the drag coefficient C_D is calculated according to the Schiller/Naumann correlation. With a water density of $1\,000\text{ kg/m}^3$, a terminal sinking velocity of 0.05 m/s is obtained when the particle diameter amounts of 5 mm and the particle density of $1\,030\text{ kg/m}^3$. Therefore in this respect these parameters particle diameter and particle density are “virtual parameters” related to the flow behaviour of the particles.

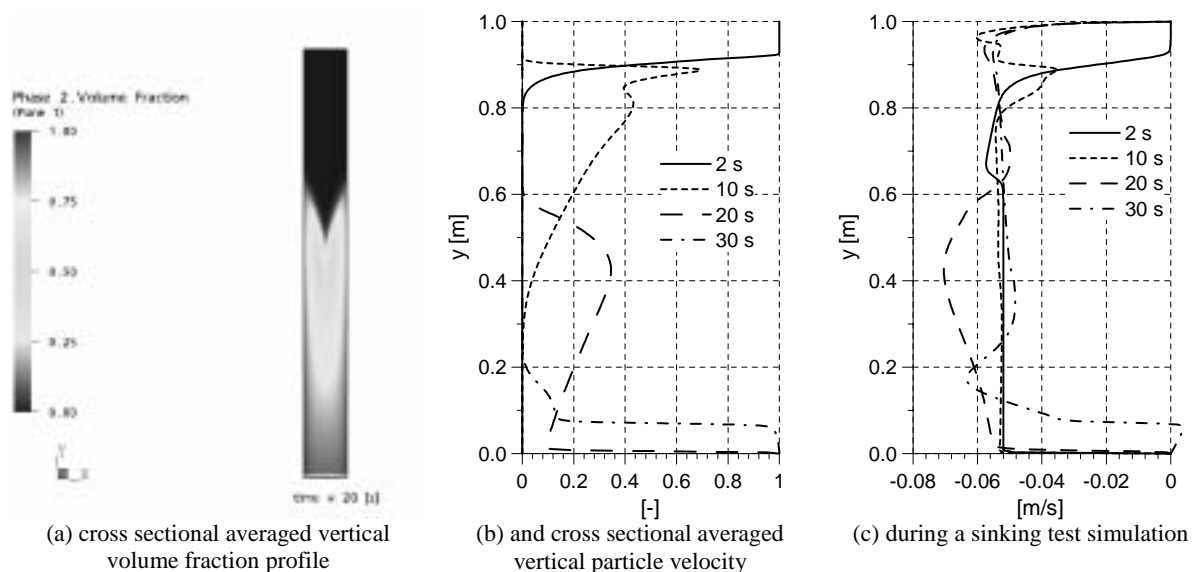
3.3 Application of the model

Using the CFD code CFX, different situations were simulated, to check the capability of the Euler/Euler approach. A water density of $1\,000\text{ kg/m}^3$, a particle density of $1\,030\text{ kg/m}^3$ and a particle size of 5 mm were assumed.

3.3.1 Simulation of the experiments at the test rig “column”

In a column of a height of 1.0 m a mixture of water and particles was investigated during a transient simulation. At the beginning of the transient all particles are assumed to be in the upper 0.1 m of the column, i.e. at a height from 0.0 to 0.9 the volume fraction of the “particle phase” was set to 0 and from 0.9 to 1.0 m was set to 1.0 . Considering gravity, within 40 seconds the particle phase is moved downwards. Figure 3 shows: (a) the volume fraction distribution after 20 seconds; (b) the cross averaged (xz-plane) vertical volume fraction distributions; and (c) the cross averaged vertical particle velocities. Figure 3c shows indeed during most of the time the particle sinking velocity to be 0.05 m/s .

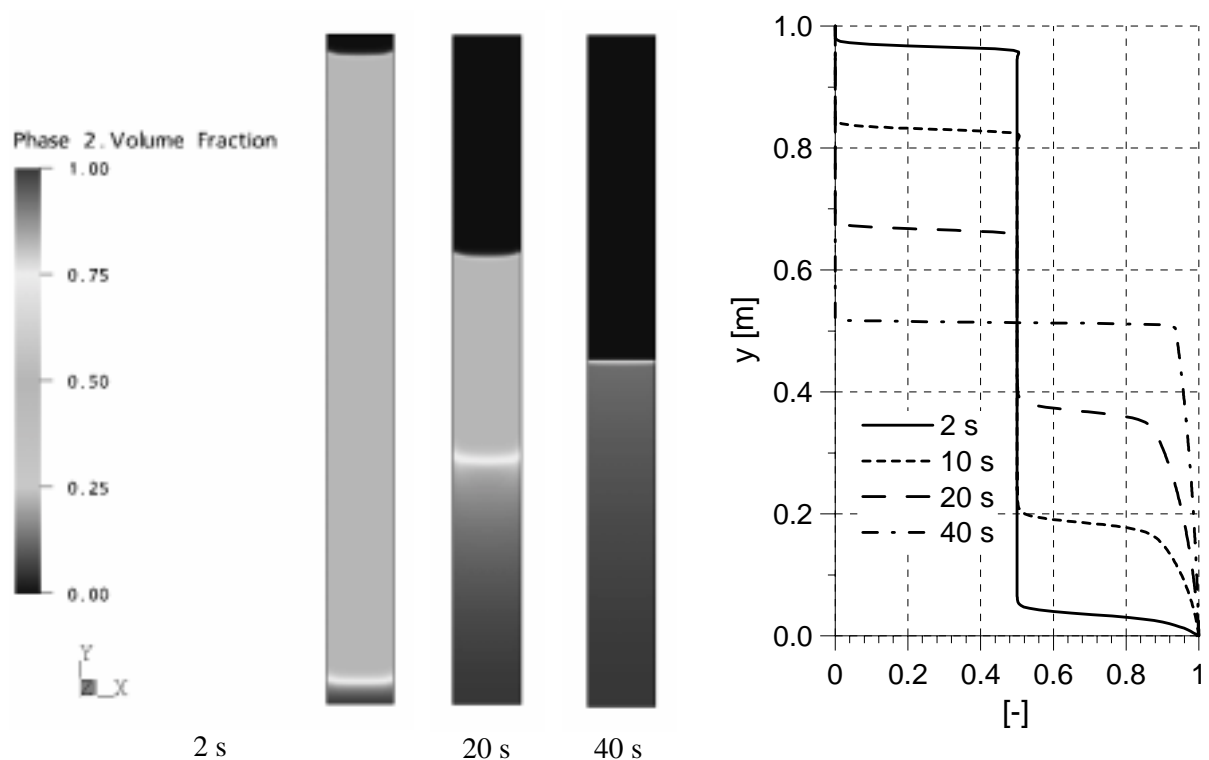
Figure 3. Volume fraction distribution after 20 s



3.3.2 Segregation test

During a further numerical test of a column, an initial volume fraction distribution of 0.5 over the whole height was assumed. After about 40 seconds the phases are completely segregated under the influence of gravity (see Figure 4). The test shows, that the code CFX is from the numerical point of view able to model these phenomena.

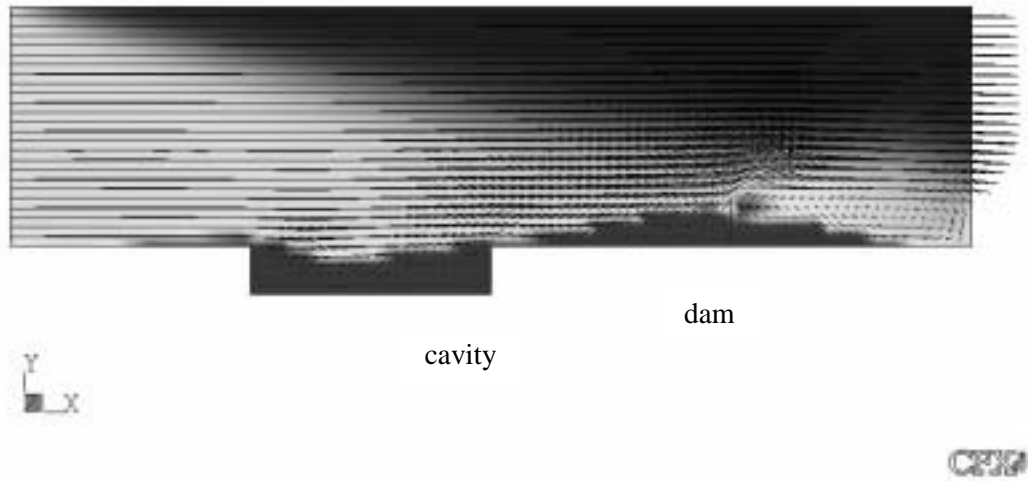
Figure 4. Volume fraction distribution and vertical volume fraction profile during the numerical segregation test



3.3.3 Flow in a channel with obstacles

In a further simulation, the flow in a horizontal channel equipped with steps, hollows and a dam is modelled (see Figure 5). The situation corresponds to phenomena which are expected in the test facility rig “channel” at IPM Zittau. The facility is designed to investigate the flow behaviour of the insulation debris. The figure shows, the particles are especially deposited in areas with lower fluid velocity, i.e. behind a step or behind a dam.

Figure 5. Flow and volume fraction distribution in a horizontal channel with obstacles



4. Modelling of debris sedimentation and resuspension

To simulate debris suspension and resuspension the viscosity was modelled depending on other parameters. Figures 6 to 8 show the effect of viscosity depending on particle volume fraction r . While in Section 3.3.3. the dynamic viscosity was assumed to be constant $\mu_r = \mu_{\text{water}}$ (case a), in the actual example (case b) the viscosity was modelled for volume fraction $r > 0.6$ as $\mu = \mu_{\text{water}} [1 + 1.0 \cdot 10^4 (r - 0.6)^3]$ (see Figure 6). Figure 7 shows the integral mass of the particle in the cavity. Figure 8 shows the particle volume fraction distribution and the velocity field for the case (b) [compare Figure 5 for case (a)]. The dependency $\mu = \mu(r)$ was used here only for demonstration of the applicability of this approach to model this phenomenon. A more realistic function will be received by fitting the relation to experiments.

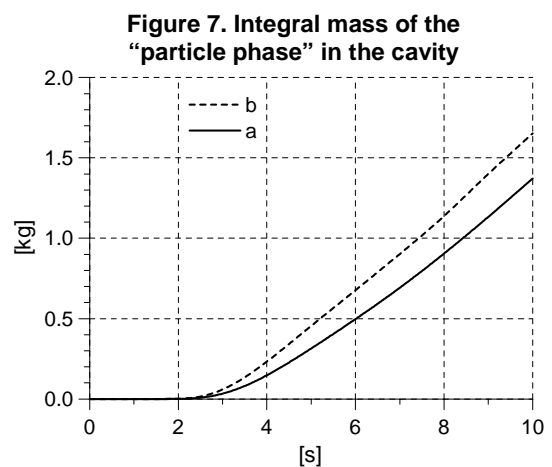
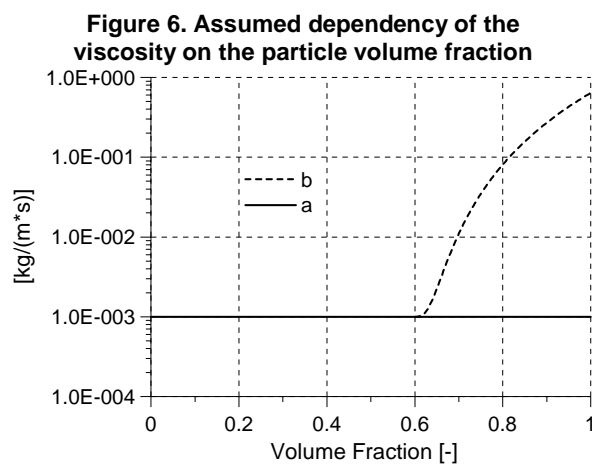
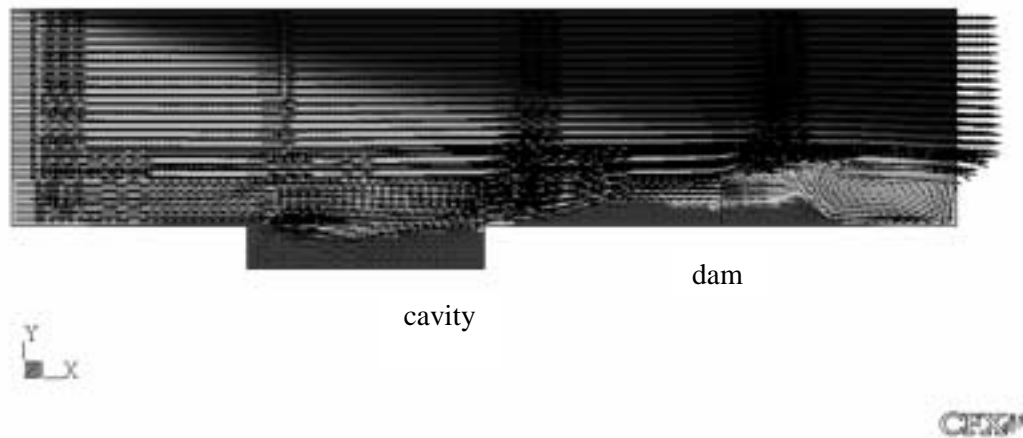


Figure 8. Flow and volume fraction distribution in a horizontal channel with assumed dependency of the viscosity on the particle volume fraction (compare Figure 5)



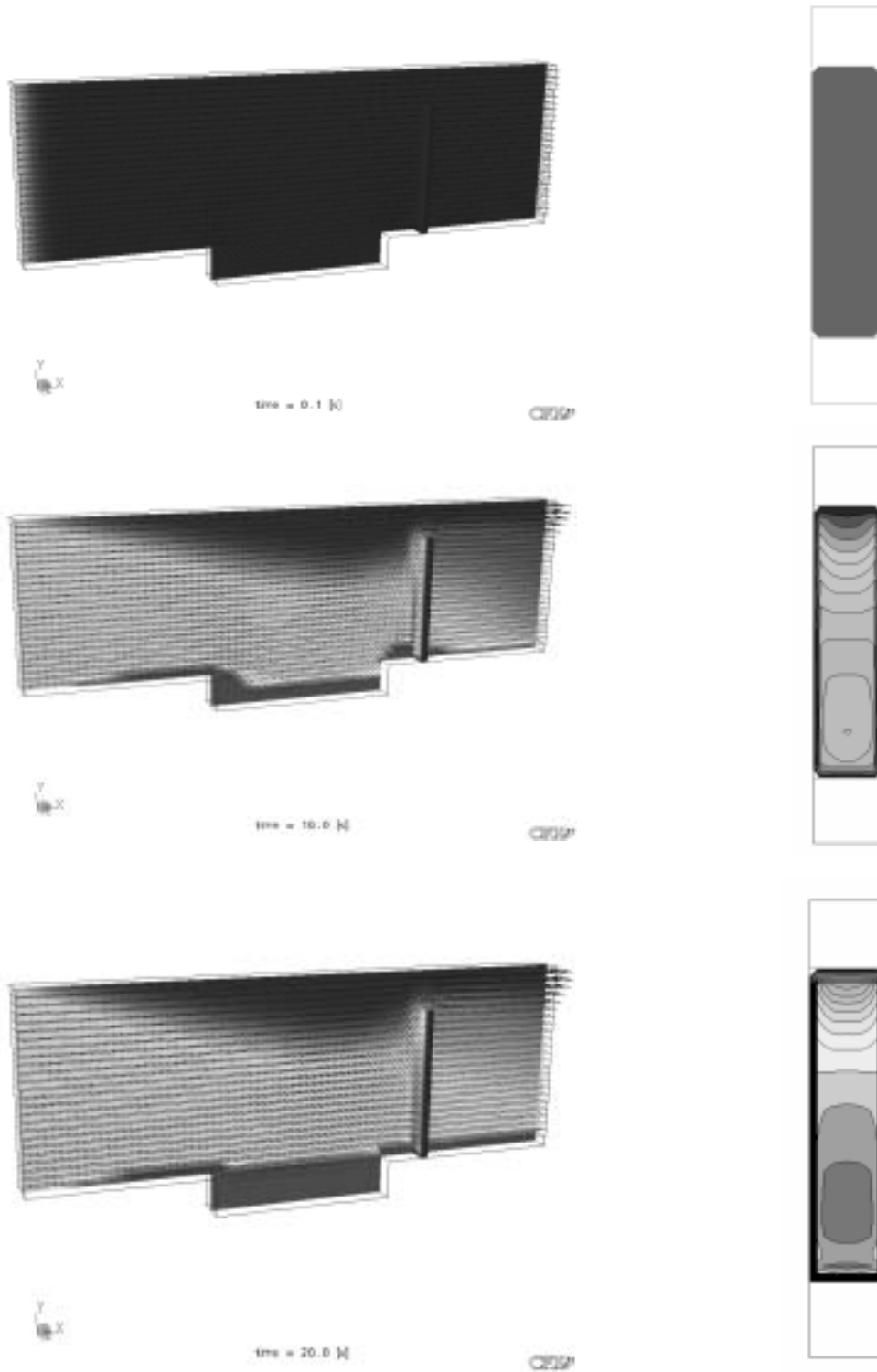
5. Modelling of strainers

A model of a gradually blocked strainer was developed and tested using CFX. The model of a porous body was used for the strainer. The model comprises the partial obstruction of the flow and the flow resistance caused by the porous media. The integral mass flow of the “particle phase” was calculated in each cell of the strainer. The increasing flow resistance of the strainer was simulated by an increasing sink term in the momentum equations depending on the integral mass flow of the “particle phase”. In this way, the model can be used to simulate the effect of a strainer with beginning local blockage.

Figure 9 shows the volume fraction distribution and the velocity field in the channel. In the right side of the figure the increasing sink term simulating a gradual blockage of the strainer is shown. In the geometry of the test channel above the strainer a small gap was left. Initially the flow is almost equally distributed. Near the end of the transient when the strainer is gradually blocked most of the fluid flows through the gap above the strainer (see Figure 9c).

Before applying the model to the solution of practical problems the adjustment of the dependency of flow resistance on integral mass flow of the particle phase using experiments is necessary.

Figure 9. Transient development of a flow field with gradually blocked strainer
Strainer blockage (right side)



6. Summary and next steps

The basic concepts for CFD simulation of insulation material transport and for suspension and resuspension are described. A model for the simulation of a strainer is presented. A careful check of the models and a careful tuning of the model parameters and model functions to adapt them to experimental results is the next task. The planned experimental activities at IPM-Zittau are very well suited, to do this work.

Acknowledgements

The reported investigations are funded by the German Federal Ministry of Economy and Trade under contract No. 1501270.

References

Alt, S., R. Hampel, W. Kaestner, A. Seeliger, “Experimental Investigations for Fragmentation and Insulation Particle Transport Phenomena in Water Flow”, see this workshop.

REASSESSMENT OF DEBRIS-INGESTION EFFECTS ON EMERGENCY CORE COOLING SYSTEM PUMP PERFORMANCE

Frank W. Sciacca

Omicron Safety and Risk Technologies, Inc., USA

D.V. Rao

Los Alamos National Laboratory, USA

1. Introduction

A study sponsored by the United States (US) Nuclear Regulatory Commission (NRC) was performed to reassess the effects of ingesting loss of coolant accident (LOCA) generated materials into emergency core cooling system (ECCS) pumps and the subsequent impact of this debris on the pumps' ability to provide long-term cooling to the reactor core.¹ ECCS intake systems have been designed to screen out large post-LOCA debris materials. However, small-sized debris can penetrate these intake strainers or screens and reach critical pump components. Prior NRC-sponsored evaluations of possible debris and gas ingestion into ECCS pumps and attendant impacts on pump performance were performed in the early 1980s.² The earlier study focused primarily on pressurised water reactor (PWR) ECCS pumps. This issue was revisited both to factor in our improved knowledge of LOCA generated debris and to address specifically both boiling water reactor (BWR) and PWR ECCS pumps.

This study discusses the potential effects of ingested debris on pump seals, bearing assemblies, cyclone debris separators, and seal cooling water subsystems. This assessment included both near-term (less than one hour) and long-term (greater than one hour) effects introduced by the postulated LOCA.

The work reported herein was performed during 1996-1997.

1.1 *Methodology and scope*

The overall steps in the methodology used in this study are as follows:

1. The debris likely to be ingested by ECCS pumps was evaluated using all available information regarding the types and quantities of debris available for possible pump ingestion. Analyses were performed to develop time-dependent profiles of fluid-stream debris types and concentrations. Separate evaluations were performed for BWRs and PWRs.

-
1. Sciacca, F., J. Brideau, D.V. Rao, and W. Thomas (Science and Engineering Associates, Inc.), and J. Simonis and A. Rogers (Southwest Research Institute), "Reassessment of Debris Ingestion Effects on Emergency Core Cooling System Pump Performance", SEA 97-3102-A:1, prepared for the USNRC, 31 July 1997.
 2. Kamath, P.S, T.J. Tantillo, and W.L. Swift, "An Assessment of Residual Heat Removal and Containment Spray Pump Performance Under Air and Debris Ingesting Conditions", NUREG/CR-2792, CREARE TM-825, September 1982.

2. Important design features and characteristics of ECCS pumps currently installed in operating commercial nuclear power plants (NPPs) were reviewed to help identify susceptibility to debris-related damage. A failure modes effects analysis (FMEA) approach was used to systematically identify possible pump failures resulting from ingestion of small debris for a reference pump design. A generic pump design was used for the FMEA. Failure modes judged as “likely to occur” were evaluated further using analytical techniques.
3. A thorough review was made of NPP ECCS pump failures reported during the 20-year period prior to this study. Failure data for other NPP pumps were also evaluated for applicability to the ECCS pumps and for insights as to pump behaviour with debris-laden fluid streams.
4. Insights and conclusions of the likelihood of particular ECCS pump-failure modes then were developed. These insights were based on the qualitative FMEA, as supported by analytical calculations, pump-failure data, and engineering judgment.

This paper is organised according to the above steps. The projected ECCS pump-suction conditions following a LOCA are reviewed for both BWRs and PWRs; debris types, sizes, and concentrations are estimated. Pump features and characteristics that could be adversely impacted by the presence of debris in the fluid stream are reviewed. The results of the FMEA are discussed briefly. Pump-failure data is reviewed, including a comparison of failure data for pumps operating with debris-laden fluid streams vs. those operating with clean fluids. Finally, estimates are provided of the likelihood of ECCS pump failure during the post-LOCA period of required operation.

1.2 Assumptions and basis

The debris considered in this study included fibrous insulation debris, sludge (in BWRs), paint chips, concrete dust, rust particles, and reflective metallic insulation shards small enough to pass through the holes of a BWR pump-suction strainer (typically 1/8 inches diameter) or a PWR containment sump screen (typically 1/4 inches \times 1/4 inches openings). The study focused on the effects of small fibrous and particulate debris on the pump system components downstream of the pump-suction strainer or screen. The effect of debris on ECCS system components downstream of the pumps was not included.

A time-varying strainer filtration model was developed to estimate the amount of debris passing through the strainers or screens over time. Separate models were prepared for BWRs and PWRs. These models include the filtering effects of fibrous debris-bed buildup on strainers and screens that serve to trap particulate materials. Also, the important differences in filtering characteristics between fibrous insulation debris materials and reflective mirror insulation (RMI) debris were factored into the models, as was the precipitation of hydroxides in PWR systems as an additional source of particulate debris.

The suppression pool strainers present in BWRs were assumed large enough that a thin (about 1/8 inches) debris bed would be formed on the surface of the strainer. For PWRs, typical sump screen sizes were assumed.

There is enough design variability among the installed pumps at nuclear power plants that a typical or generic pump could not be defined adequately. A reference pump design was used in the FMEA evaluation. However, alternative pump features were evaluated for potential debris-related degradation.

The focus of this effort was on low-pressure pumps because of their likelihood to be subjected to debris ingestion following a LOCA. However, under certain conditions, high-pressure safety injection pumps may be used in a recirculation mode, whereby they would draw from the suppression pool in BWRs or from the containment sump in PWRs [piggybacked onto the residual heat removal (RHR) pumps]. The high-pressure pumps are assumed more susceptible to debris-related degradation than are the low-pressure pumps.

1.3 Limitations

At the time of the study, there were no data regarding either short- or long-term ECCS pump performance or reliability under actual post-LOCA conditions. Therefore, this study was based on analysis and interpretation of available information; it did not have the benefit of a dedicated experimental program that might have resolved issues related to ECCS pump performance.

Relatively little NPP data were available for pumps operating with significant debris in the fluid streams.

Vendors that have supplied ECCS pumps to operating NPPs were contacted to determine if they had information on pump performance with debris-laden fluid streams; however, they were unwilling to share this type of information.

The pump-failure data reviewed for this study sometimes were limited in the description of the failure modes and root causes of the failure. Some failures appeared to be debris-related, even though debris was not mentioned specifically in the failure report. Thus, there was considerable uncertainty in interpreting much of the available data.

The work reported herein was performed during 1996-1997 and was based on the data, plant characteristics, and analytical methods available at that time. The study results have not been updated to reflect information that is more recent, ECCS improvements, or any improvements in our knowledge of debris-related impacts.

2. ECCS pump debris-ingestion conditions following a LOCA

2.1 LOCA-generated debris characteristics

Assessments were performed of the types, quantity, and characteristics of the post-LOCA debris likely to be ingested by ECCS pumps. The quantity of debris is characterized in terms of volume concentration, which is defined as “the ratio of the solid volume of the debris in the pumped fluid to the volume of the pumped fluid”. Debris conditions will be different between BWRs and PWRs because of factors such as the quantity of debris generated by LOCA forces, the size of the openings in containment sump screens or suppression pool strainers, and the volume of water that the debris mixes with and that acts as the ECCS-pump water source. Debris generation models developed as part of the USI A-43 study³ and the BWR ECCS Strainer Blockage Study⁴ were used to develop estimates of debris types and quantities.

3. Serkiz, A.W. “Containment Emergency Sump Performance”, NUREG-0897, Rev. 1, 1995.

2.2 Anticipated conditions for BWRs

The types of debris expected to reach the BWR suppression pool following a LOCA include insulation debris, paint chips, concrete dust, suppression pool sludge, and miscellaneous rust particles. The postulated LOCA was assumed to occur on a 24 inches diameter, high-energy line that suffered a double-ended guillotine break (DEGB) in the most congested part of a Mark I containment. The insulation on about 1 000 ft² of primary piping and other components was estimated as damaged or destroyed. For conservatism, a drywell transport factor of 1.0 was used, i.e. all debris generated was transported to the suppression pool.

Surveys of operating BWR plants indicated that most of the primary insulation employed is either low-density fiberglass (NUKONTM) or RMI.⁵ Some plants employ both types; however, for the purposes of this study, individual plants were assumed to employ either 100% NUKONTM or 100% RMI. Table 1 lists the types and quantities of debris in the BWR suppression pool modelled for this analysis. The suppression-pool water volume was assumed to be 58 900 ft³, the smallest suppression pool volume employed by any US BWR.

Table 1. Quantity and characteristics of debris reaching BWR suppression pools

Debris type	Mass (lbm)	Mass conc. (lbm/ft ³)	Debris characteristics			Volume conc. (%)
			Size range	% by Mass	Density (lbm/ft ³)	
NUKON TM fiberglass ^a	600	0.00640	100 to 1 800µm ≥ 0.5 in	5 95	180 ^b 2.4 ^c	0.000282 0.403200
RMI ^a	10 605	0.18000	0-1/8 in 1/8 to 1/4 in 1/4 to 1/2 in > 1/2 in	0.50 3.75 20.25 75.51	488	0.000183 0.001395 0.007460 0.027700
Paint chips	85	0.00090	0 to 800µm 800 to 3 000µm	50 50	131	0.001100
Dirt, dust, concrete	150	0.00160	0 to 50µm 50 to 150µm 150 to 2 000µm	25 50 25	156	0.001620
Sludge (iron oxide)	450	0.00480	0 to 5µm 5 to 10µm 10 to 75µm	81 14 5	324	0.002360
Rust particles (iron oxide)	50	0.00053	0 to 100µm 100 to 800µm 800 to 3 000µm	10 50 40	324	0.000260

a Either NUKONTM or RMI present, but not both.

b Density of individual glass fibers.

c Density of fiberglass blanket.

-
4. Zigler, G., J. Brideau, D.V. Rao, C. Shaffer, F. Souto, and W. Thomas, "Parametric Study of the Potential for BWR ECCS Strainer Blockage Due to LOCA Generated Debris", NUREG/CR-6224, SEA No. 93-554-06-A:1, 15 September 1995.
 5. Green, T., "BWR Owner's Group Response to NRC Comments and Questions Regarding the Utility Resolution Guidance for ECCS Suction Strainer Blockage", letter transmittal, OG97-044-161, January 1997.

The projected time-related variation in the debris concentration entrained in the flow to the example BWR ECCS pump is illustrated in Figure 1. Figures are shown based on plants with either 100% NUKON™ or 100% RMI insulation types. The NUKON™-type insulation is expected to form a debris bed on the ECCS suction strainer surface, which will filter out substantial amounts of particulate and fibrous debris during the first hour of ECCS operation. RMI-type insulation does not serve as an effective filter medium. Particulate-debris concentrations in the ECCS flow to the pumps for RMI-insulated plants are expected to remain relatively unchanged throughout the period of ECCS operation.

Conservative assumptions were used in developing the trends shown in Figure 1. The suppression pool ECCS suction screens were assumed to be large enough that a thin bed ($\leq 1/8$ inches) would form on the surface of the screen (NUKON™-type insulation).⁶ Small-sized debris, unless filtered out by the debris bed on the surface of the ECCS screen, was assumed to remain in suspension. The ECCS suction screen openings were assumed to be 1/8 inches in diameter.

2.3 Anticipated conditions for PWRs

The debris types and concentrations in PWR ECCS fluid streams will be different than those expected for BWRs because of differences in the quantities of materials impacted by high-energy line breaks and differences in plant design features. Table 2 presents the debris types and quantities assumed for the PWR ECCS pump evaluations.^{7,8} The quantities involved are considerably larger than those for the BWR, shown in Table 1.

The sump water volume used to derive the concentrations shown in Table 2 was 56 000 ft³, which occurs after the refuelling water storage tank (RWST) water volume has been pumped into the reactor coolant system and has drained through the break into the sump. This RWST volume is reasonably typical of that of many PWRs.

When this study was performed, containment sump screens in PWRs typically were characterised by openings on the order of 1/4 inches \times 1/4 inches. The analysis assumed that all debris smaller than 1/4 inches would remain in suspension. Some filtration of particulate and fibrous material would occur on the surface of the sump screen for the case with fibrous insulation.

Figure 2 shows the estimated debris concentration approaching the low-pressure safety injection (LPSI) and containment spray pumps as a function of time. PWR ECCSs initially take suction from the RWST, which provides clean water to the ECCS pumps until switchover to suction from the containment sump occurs. The rise in the debris volume concentration starting at about 10 h for the 100% NUKON™ case is due to boron precipitation, which is assumed to occur during one 24-h period. The effect of boron precipitation is less obvious for the 100% RMI case because more of the other particulate debris also remains in suspension. Note also that the concentration scales on the NUKON™ and RMI plots are different.

6. Zigler, G., J. Brideau, D.V. Rao, C. Shaffer, F. Souto, and W. Thomas, "Parametric Study of the Potential for BWR ECCS Strainer Blockage Due to LOCA Generated Debris", NUREG/CR-6224, SEA No. 93-554-06-A:1, 15 September 1995.

7. Kamath, P.S, T.J. Tantillo, and W.L. Swift, "An Assessment of Residual Heat Removal and Containment Spray Pump Performance Under Air and Debris Ingesting Conditions", NUREG/CR-2792, CREARE TM-825, September 1982.

8. Andreycheck, T.S., "Evaluating Effects of Debris Transport within a PWR Reactor Coolant System during Operation in the Recirculation Mode", Westinghouse Power Company, 1844.

Figure 1. Time-dependent volume concentration of debris in BWR ECCS flow to the pump

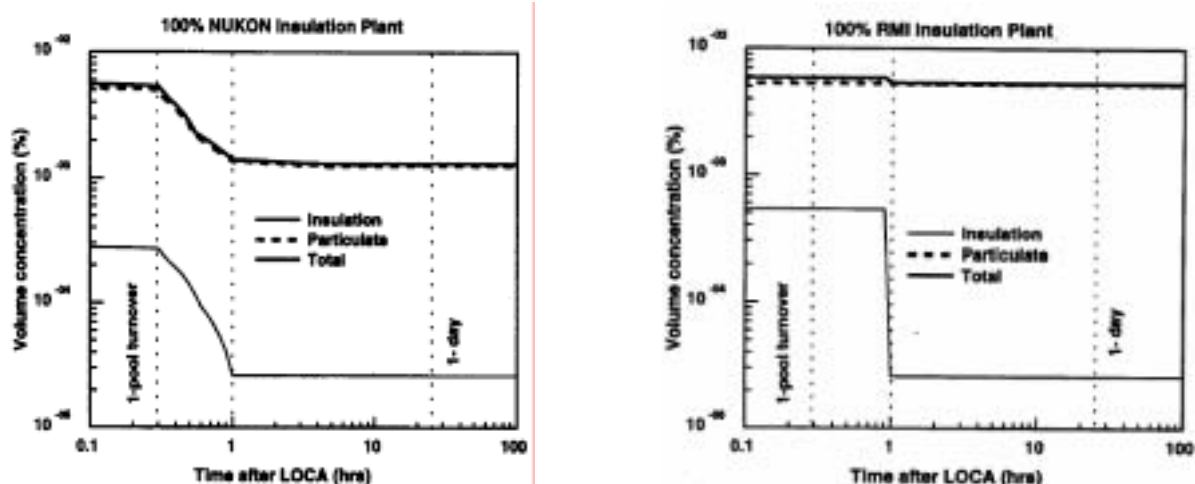


Table 2. Quantity and characteristics of debris reaching PWR ECCS sumps

Debris type	Mass (lbm)	Mass conc. (lbm/ft ³)	Debris characteristics			Volume conc. (%)
			Size range	% by Mass	Density (lbm/ft ³)	
NUKON TM fiberglass ^a	2 880	0.0179	100 to 1 800µm	5	180 ^b	0.000496
			≥ 0.5 in	95	2.4 ^c	0.709300
RMI ^a	50 574	0.9000	0-1/8 in	0.50	488	0.000323
			1/8 to 1/4 in	3.75		0.002420
			1/4 to 1/2 in	20.25		0.013070
			> 1/2 in	75.51		0.048800
Paint chips	4 250	0.0759	0 to 800µm	2.9	131	0.057900
			800 to 3 000µm	3.1		
			≥ 3 000µm	94.0		
Dirt, dust, concrete	150	0.0016	0 to 50µm	25	156	0.017200
			50 to 150µm	50		
			150 to 2 000µm	25		
Hydroxide precipitates	5 000	0.0893	0 to 10µm	100	187	0.047800

a Either NUKONTM or RMI present, but not both.

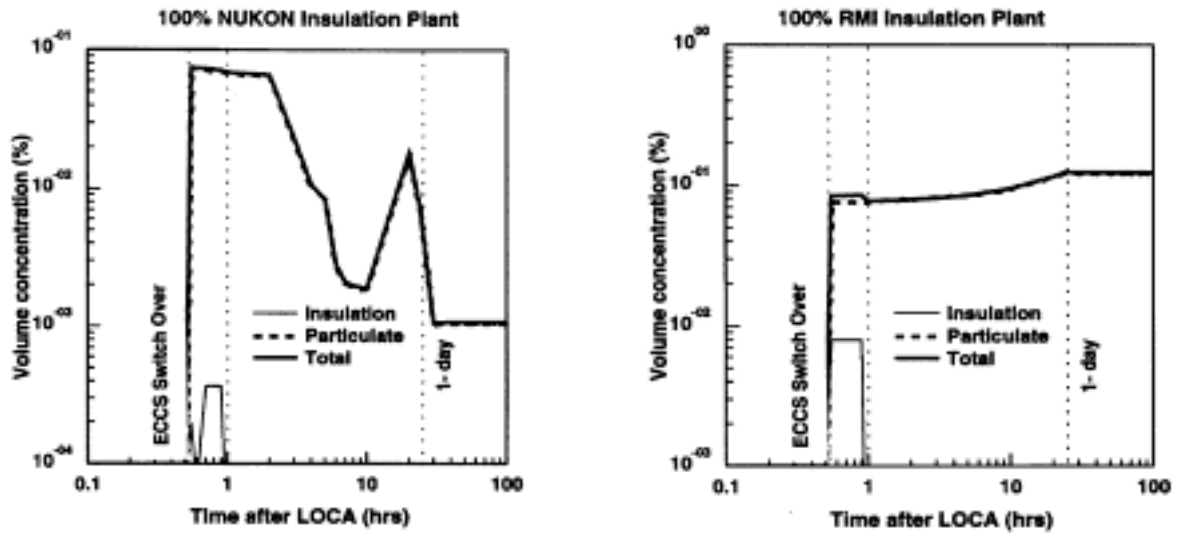
b Density of individual glass fibers.

c Density of fiberglass blanket.

A comparison of Figures 1 and 2 suggests the following:

- Volume concentrations of debris reaching ECCS pumps following a LOCA are potentially higher in PWRs compared with BWRs.
- In both PWRs and BWRs, the concentrations are higher for 100% RMI plants compared with 100% NUKONTM plants. Also, for fiberglass plants, debris concentration falls about an order of magnitude after about one day, whereas for the RMI plant, fairly uniform concentrations may be maintained for several days.

Figure 2. Time-dependent volume concentration of debris in PWR ECCS flow to the pump



- The volume concentration estimates were developed based on very conservative assumptions related to debris generation and transport. Despite the conservatism, the estimated debris concentrations are well below 1%.

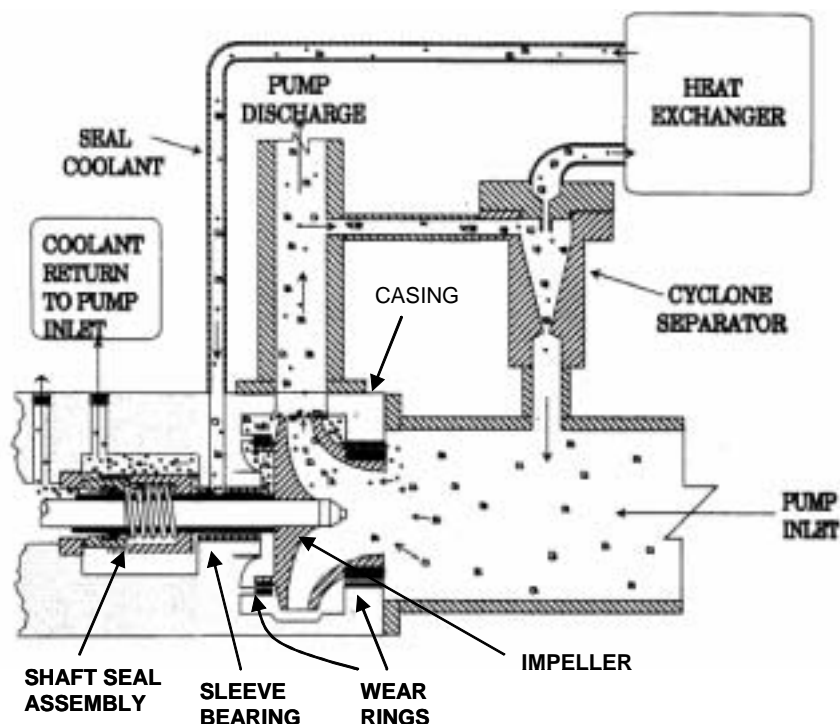
3. ECCS pump characteristics of concern

The ECCS pumps of primary interest to this study were the RHR and containment spray (CS) pumps. With few exceptions, practically all RHR and CS pumps installed in US NPPs are single- or multiple-stage centrifugal pumps. Multiple manufacturers have supplied these pumps, and there is considerable variation in particular design features from one pump to another. Nevertheless, essentially all of these pump designs have particular features that may be susceptible to debris-related degradation.

Figure 3 schematically illustrates key components typical of NPP ECCS RHR and CS pumps. A debris-laden fluid stream is depicted. Many ECCS pumps employ a cyclone separator and a heat exchanger to condition the water supplied to the shaft seals. The heat exchanger reduces the temperature of the filtered fluid and improves the fluid's effectiveness in cooling the seals and pump elements in the seal cavity. The heat removal decreases the operating temperatures of the seal cavity components.

The fluid that contains the debris flows from the pump inlet through the impeller and out of the pump discharge. Within each of the internal pump regions, the fluid and the debris may be circulated through small passages designed to provide water to pump components and other pump cavities, including the cavities formed between the impeller structure and the pump casing, the upper wear-ring support structure, and the lower wear-ring support structure. As illustrated in Figure 3, as the fluid and debris exit the pump, a small quantity of fluid and debris is drawn into the seal piping system. It then flows into the cyclone separator, where some of the debris is removed. The filtered fluid then passes through the heat exchanger, into the seal cavity, and then returns to the pump inlet.

Figure 3. Typical RHR and CS pump arrangement



The key pump components that could be adversely affected by debris during post-LOCA operation include the pump shaft seals, bearings exposed to the fluid stream, hydrostatic and hydrodynamic bearings, wear rings, cyclone separators, and heat exchangers. These components typically are designed with small passages or small clearances that could be blocked by debris. In addition, the components' critical clearances could be impacted adversely by debris in the fluid stream.

3.1 Concerns for individual pump components

Wear rings. Wear rings, or clearance rings, are incorporated into pumps to reduce the leakage of the pumped fluid from the discharge to the suction sides of the impeller. They provide tight clearances between the stationary pump housing and the rotating impeller. The gap between the stationary and rotating wear rings typically varies with ring diameter. Wear-ring diametral clearances for ECCS pumps likely are to be about 0.01 to 0.02 inches. Entrained debris with the appropriate geometric form will find its way into the gap between the stationary wear ring and the impeller. As the particles pass through this gap, they are expected to cause surface damage and wear. The wear and other attributes of the surface damage caused by the debris will enlarge the gap and reduce the effectiveness of the hydrodynamic film that serves to minimise the metal-to-metal contact between the rotating and stationary wear-ring surfaces. In addition, as this gap increases, the impeller will become more susceptible to wobble, which is manifested as increased vibration of the pump and increased loads on the bearings.

Some wear-ring designs employ weep holes, which help to control: (1) the flow of fluid between the rotating and stationary rings; and (2) the hydraulic forces acting on these components. Fluid and debris may be drawn into the cavity in the wear-ring support structure and then will exit through the weep holes in the wear ring.

If the debris alters the flow of water through the weep holes, the hydrodynamic support provided by the water between the wear ring and the impeller is reduced. Vibration and wobble of the rotating components can result, and metal-to-metal contact between the rotating and stationary components may occur. Any such imbalance increases the forces and stresses on bearings and support structures. Further, frictional heating caused by the rubbing of the impeller and wear ring may increase if the water flow is degraded. This reduced water flow may cause excessive thermal expansion of the wear ring and impeller structure, thus leading to actual seizure of the wear ring and impeller. Failures of this type have been observed for centrifugal pumps used in commercial applications. For some similar failures, the wear-ring retaining pins were sheared and the wear ring rotated in its support housing. Loose retaining pins also can pose direct hazards to continued pump operation because they can become wedged between the rotating and stationary pump components. Pump failures due to ingestion of objects such as retaining pins have been noted for ECCS pumps.

The wear-ring failure modes induced by excessive wear and abrasion would degrade the pump performance over the long term and could result in complete pump failure. Failures resulting from weep-hole blockage, which then induces imbalance, wobble, and/or vibrations, could occur any time debris is present. Such failures could occur early or late, depending on when a blockage might occur and the significance of any associated hydraulic imbalance effects.

Bearing assemblies. The pump shaft and attached impeller are supported on bearings that are either within the pump housing or external to the housing. Bearings located within the pump housing are typically sleeve or journal bearings. Bearings external to the housing are typically ball or roller bearings lubricated by an oil bath. These external bearings normally are not exposed to debris-laden pumped fluid. Some pump designs also employ hydrostatic bearings internal to the pump casing to stabilise the rotating components and to provide a low-friction arrangement. Metal-to-metal contact between the rotating and stationary components is minimised in such designs by the hydrostatic pressure of the pumped fluid. Thus, journal and hydrostatic bearings are of primary concern when considering the deleterious effects of debris ingestion in ECCS pumps.

In some designs, journal bearings are cooled and lubricated by the pumped fluid. Wear is expected on these components, and they are designed to be replaceable. RHR and CS pumps employing journal bearings of this type may be designed with internal passages that provide pumped fluid to the bearings.

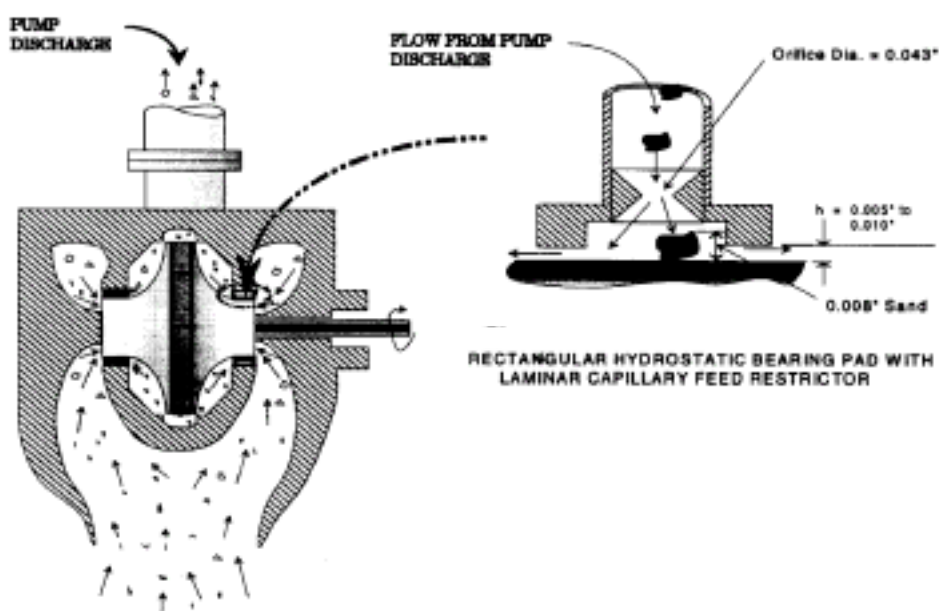
Some journal bearing designs are self-lubricating and do not rely on the pumped fluid for lubrication. Self-lubricating bearings for water-pump applications are carbon or graphite based and may contain metals or resins to achieve the desired structural and low-friction characteristics. These types of bearings do not require external sources of lubrication, but their performance is enhanced significantly by the presence of a liquid film between the sliding surfaces (the coefficient of friction is reduced about an order of magnitude compared with “dry” conditions). These self-lubricated bearings do not require internal coolant passages that direct coolant to the bearings. The pumped fluid acts to remove the frictional heat generated in the bearings. Also, these types of bearings are not subject to galling or seizure.

An illustration of a hydrostatic bearing of the type used in some RHR pumps is provided in Figure 4. This type of bearing is used to keep the impeller centred and rotationally stabilised within the pump housing by way of hydraulic-pressure control between the bearing pad and the rotating impeller. As indicated, hydraulic pressure is provided by diverting a small portion of the pump discharge flow to the bearing pad. Flow control is provided by orifices located at each bearing pad (the orifices are referred to as the “laminar capillary feed restrictors”). Several bearing pads are located around the circumference of the hydrostatic bearing. The dimensions of the orifice and the clearance between the

bearing pad and the impeller shown in Figure 4 typify those that exist in CS and RHR pump designs. For comparison purposes, the size of a grain of sand also is illustrated.

Hydrostatic bearings may also be susceptible to debris-induced problems. Because the fluid for hydraulic control of the hydrostatic bearing is obtained from the pump discharge media containing debris, the debris will pass through the bearing flow-control orifice to the bearing pad. To illustrate the potential for debris to become trapped within the bearing pad, note in Figure 4 the size of a typical grain of sand (0.008 inches) in comparison to that of the bearing pad clearance (0.005 to 0.010 inches). This illustration demonstrates the potential for hydrostatic bearing failure because of: (1) debris accumulating within the bearing pad, resulting in friction that can cause the impeller to overheat and possibly seize; and (2) debris restricting flow through the bearing flow-control orifices, causing loss of hydraulic-pressure control. Loss of hydraulic-pressure control will cause the impeller to become vibrationally unstable. Thus, this is one mode of debris-induced pump degradation that could cause early, significant, and possibly total failure of the affected ECCS pump.

Figure 4. Hydrostatic bearing configuration



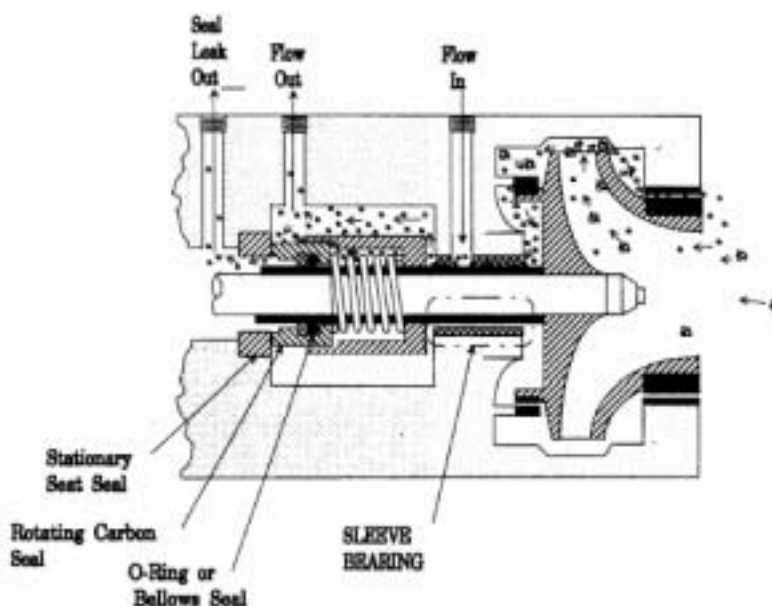
Sleeve bearings may be susceptible to debris-induced failures, depending on the bearing design and the materials used. As illustrated in Figure 5, debris will migrate from the high-pressure region of the impeller to the low-pressure region of the sleeve bearing and on to even a lower fluid pressure of the bearing seal cavity. The sleeve bearings may or may not be fed by internal passages that direct coolant to the bearing. Clearances between the bearing and the rotating pump shaft are typically about 0.005 to 0.020 inches. These clearances are such that paint chips, dirt, dust, concrete particles, sludge, and rust particles could enter the bearing. As the debris traverses the close-tolerance clearance between the pump shaft and the sleeve bearing, the debris is likely to be caught by the reduced clearances because of any nonconcentric operation of the pump shaft. Abrasion, galling, and frictional heating of the shaft and bearing surfaces can occur because of the presence of the debris. In the extreme case, the interactions with the debris can cause high-temperature effects and shaft bowing or seizure due to binding between the rotating and stationary members.

Graphite-based sleeve bearings may be less susceptible to debris-related damage in that these bearings are reportedly highly resistant to galling and seizure. The presence of debris undoubtedly

would result in accelerated wear and erosion of the bearings. This degradation mode would serve to increase clearances between the pump shaft and the bearing surfaces, which in turn would allow more vibration and wobble of the rotating components. Some loss of pump performance would be expected. Loss of pump function due to graphite-based bearing wear is not deemed very likely, at least not during the early period of RHR pump operation following a LOCA.

Note that sleeve bearings made of materials such as babbitt metal or bronze are typically dependent on the presence of a liquid film for lubrication and cooling. These materials are more susceptible to galling and seizure if the liquid film is lost or degraded than are the graphite-based bearings.

Figure 5. Typical pump shaft seal and sleeve bearing designs



Seal coolant piping, heat exchangers, and cyclone separators. These components typically have orifices or flow restrictors on the order of 0.12 to 0.20 inches in diameter. These restrictors could become blocked by large pieces of debris or by the buildup of small pieces of debris. Cyclone separators are relatively effective for removing debris larger than about 0.008 inches in size but are less effective with smaller debris. Thus, small-sized debris will be sent on to the shaft seal even if the separator is functioning properly.

Partial or complete blockage of the orifices and flow restrictors in these components will reduce the coolant flow to the shaft seals.

Pump seals. Many types of devices are used to prevent the egress of fluid around a rotating pump shaft. Labyrinth seals, stuffing boxes, lip seals, spiral groove seals, and mechanical seals are used for sealing rotating shafts. From the available data and the review of pump designs, the escape of fluid from the RHR and CS pumps in both BWR and PWR NPPs usually is prevented by mechanical face seals. Face-seal designs used in ECCS pumps normally are configured so that the leakage is radial between plane surfaces (face seal) rather than axial between cylindrical surfaces (bushing seal). One seal member is attached to the pump housing and remains stationary. Other seal members are attached to the pump shaft and rotate with the shaft. Most designs employ a spring with the floating member to

maintain a reasonably constant force between the seal faces. Several of these face seal features are illustrated in Figure 5.

A key failure mode for ECCS pump shaft seals is overheating of the seal faces due to loss of cooling flow to the seals. Flow obstructions at several points in the upstream flow path may be caused by debris accumulations or by single large pieces of debris. When coolant flow to the seals is reduced significantly or stopped, the frictional heating between the rotating and stationary seal face members will be sufficient to cause the liquid film to boil and vaporise. With the liquid film gone, the lubrication between the faces will be degraded considerably. The seal faces can be worn down rapidly, overheated, warped, or otherwise damaged.

Once the fluid and debris enter the seal cavity, the debris will be distributed throughout by the action of the pressure gradients present and by the rotating parts of the seal. Debris will impact the edges of the primary and secondary seals, will be drawn into the gap between the seal faces, and may accumulate in regions of low fluid flow. The fluid flowing into the seal cavity also will enter the cavity between the seal compression spring and the spring collar shown in Figure 5. Eventually, the accumulated debris can affect the functionality of the spring and other moveable parts. Operating plants have experienced the failure of ECCS pump seal springs to function properly because of debris accumulation, resulting in seal leakage.^{9,10}

Debris that enters the area between the seal faces will scar and abrade the seal surfaces. Extensive wear can result in complete failure of the seal. Moderate to extensive leakage from the pump will result. Many pumps are believed to be equipped with backup or disaster bushings that limit the extent of leakage from a damaged or destroyed seal. The leakage beyond the disaster bushings is reported to be limited to about 80 gal./h. Without these bushings, the leakage from a damaged or destroyed seal could be considerably greater than 80 gal./h. Reported ECCS pump seal failure incidents indicate seal leak rates of about 300 gal./h. with the pump stopped (low-pressure differential across the seal), further suggesting that not all ECCS pumps have disaster bushings.

3.2 Typical internal clearances in ECCS pumps

Table 3 presents a compilation of internal clearances and gaps characteristic of some ECCS pump designs. The values shown are judged to be reasonably representative of a range of ECCS pumps. The clearances noted in Table 3 are derived from multi-stage designs with internal journal or sleeve bearings. The values shown were obtained from pump maintenance manuals for operating NPPs, as this type of information was not forthcoming from ECCS pump manufacturers.

The pump-shaft-to-bearing clearances appear to be in the range of 0.005 to 0.023 inches. Essentially all of the debris types have characteristic dimensions small enough that the debris could enter into these shaft-to-bearing clearances. Materials such as paint chips and pieces of RMI foils are sufficiently thin that they also could enter these clearance spaces even though other dimensions of the debris pieces may be considerably larger than 0.02 inches.

-
9. NPRD Report, "Nuclear Plant Reliability Data System-Failure Master Report", NPRGO6AA, Job No. 3170.
 10. Stanton, R.H., "A Characterization Update of Pump and Pump Motor Degradation and Failure Experience in the Nuclear Power Industry (1994-1995)", ORNL/NRC/LTR/96-32, draft letter report, October 1996.

The clearances between the pump impellers and the wear rings are somewhat larger than those between the internal bearings. Here again, most of the debris that would be ingested by the pumps is sufficiently small that the debris pieces could enter the impeller-to-wear-ring gap.

Coolant flow passages feeding the pump shaft seals are estimated to be in the range of 0.1 to 0.2 inches in diameter. Most debris would pass through these passages; however, larger debris such as paint chips, clumps of fibrous debris, RMI pieces, and rust chips are large enough to obstruct or block the flow in these passages.

The shaft-face seals have clearances between the faces that are characterised by the face roughness. This roughness is very small, about a few micro-inches. Small dirt, dust, and concrete particles, as well as some of the smaller sludge particles, may be small enough to enter the spaces between the seal faces. Larger debris particles can enter the space between the seal faces if the faces are not held tightly together by the seal springs and the pressure in the seal cavity or if the seal faces are not parallel.

Table 3. Typical pump internal clearances

Characteristic pump clearances		
Components	Minimum (inches)	Maximum (inches)
Pump-shaft-to-bearing assembly, suction bell	0.005	0.02
Pump-shaft-to-bearing assembly, first stage	0.005	0.023
First-stage impeller to wear ring	0.02	0.039
Second-stage impeller to wear-ring eye	0.02	0.039
Third-stage impeller to wear-ring back	0.02	0.039
Pump shaft to bearing	0.01	0.023
Pump shaft to bushing	0.02	0.033
Shaft-seal coolant passages*	0.1	0.2
Shaft-seal face roughness	0.000005	0.00001
Cyclone separator orifices	0.125*	0.2

* Estimated values.

The clearances between the pump impellers and the wear rings are somewhat larger than those for the internal bearings. Again, most of the debris that would be ingested by the pumps is sufficiently small that the debris pieces could enter the impeller-to-wear-ring gap.

The cyclone separator passages appear to be reasonably large in comparison with the pump clearances. Most of the debris types could pass readily through the separator. The exceptions are long pieces of fibrous insulation (or clumps of fibers), large paint chips, large rust particles, and large pieces of RMI foil. Some plants have orifices located in the piping upstream of the cyclone separator. These orifices are used to control the flow rate. The examples found employed orifice diameters of 0.13 inches, just marginally larger than the 1/8 inches hole sizes found in most BWR suction strainers, but smaller than the 1/4 inches openings in PWR sump screens. These orifices would be susceptible to blockage by the larger pieces of debris ingested by the ECCS pumps or by blockage from accumulations of smaller pieces of debris.

3.3 *Note on slurry pumps*

Centrifugal pumps designed for pumping water can be used for pumping slurries and sludge, but experience has shown that pump reliability, in general, is poor and that the pumps experience excessive wear.¹¹ The slurry and sludge cause seal leakage and degradation of pump internal components.

Commercial pumps available for handling slurries and sludge are specially designed to accommodate the abrasive and corrosive nature of the pumped materials. Slurry pumps generally have larger internal clearances, specialised seal designs, and components built of durable materials. For example, shaft seals designed for abrasive environments employ sealing elements with two hard surfaces, whereas general centrifugal pump applications usually employ one hard surface and one relatively soft surface. In addition, seal cavities for slurry pumps generally are supplied with clean coolant, while normal pumps may or may not filter the coolant supplied to the seal cavity. Other special features may include the use of special wear- and corrosion-resistant materials and replaceable wear liners that extend the life of the pump by decreasing the need to completely replace hardened parts within the pump. Slurry pump designs often include features that enhance servicing and component replacement. To our knowledge, ECCS pumps do not include these special design features.

4. Failure modes and effects analysis

4.1 *Failure modes effects analysis basis*

Failure modes and effects analyses were performed on a generic pump design. The assumed design features tend to make the overall analysis somewhat conservative. As such, the individual failure modes covered in the FMEAs may not be applicable to ECCS pump designs that do not employ a feature susceptible to particular failure modes. The key alternative design features are as follows (the underlined features indicate those considered in the FMEAs):

- Bearings – *internal sleeve or journal bearings* (with and without internal passages or grooves to promote coolant flow to the bearings), *internal hydrostatic or hydrodynamic bearings*, *external ball or roller bearings*;
- Wear rings – *wear rings with and without weep holes*;
- Cyclone separators – shaft-seal coolant supply systems *with and without cyclone separators*;
- Disaster bushings – pump *with and without bushings used to limit the amount of leakage flow from a failed shaft seal*.

The analysis assumed that the largest debris ingested by ECCS pumps in PWRs could have characteristic dimensions up to ¼ inches, whereas the corresponding debris for BWR ECCS pumps could have dimensions up to 1/8 inches. These dimensions are based on the ECCS suction screen or strainer opening sizes prevalent in the NPP population at the time of the study.

11. Lebeck, A.O., “Principles and Design of Mechanical Face Seals”, Wiley, 1991.

Differences between BWRs and PWRs also were addressed in the FMEA. The key differences that could impact ECCS pump debris ingestion and the deleterious effects on the pumps are as follows:

- PWR ECCS pumps initially supply coolant to the reactor system by taking suction from the RWST; only after depletion of the RWST would the pumps be put in a recirculation mode where they draw from the containment sump. Because the water in the RWST is essentially clean, pump degradation from ingested debris normally cannot occur early (about the first 30 min following a LOCA) for PWRs, whereas early degradation of BWR ECCS pumps is possible from debris-ingestion effects.
- PWR sump screens have larger holes than BWR suppression pool strainers. Therefore, larger debris sizes can be ingested by the ECCS pumps in a PWR compared with a BWR.
- The most limiting breaks for a PWR will produce more insulation debris, paint chips, concrete dust, etc. than is expected for the most limiting breaks in a BWR. Therefore, the debris concentrations reaching the PWR ECCS pumps are higher than those expected in BWRs. For materials such as dirt, dust, and concrete, the PWR concentrations are an order of magnitude higher than for a BWR.
- BWR debris available for possible ingestion by the ECCS pumps includes sludge and rust particles, whereas little of these materials are expected to be present for PWRs. However, the PWRs have hydroxide precipitates in relatively high concentrations, which is not the case for BWRs.

The analysis also was based on the assumption that features of ECCS pumps that are susceptible to debris-related damage are the same in pumps employed in PWRs and BWRs; i.e. the assumed pump designs are identical for the two reactor types.

The mission time for ECCS pumps following a large LOCA is assumed to be 100 days. The further assumption was made that all ECCS pumps would be in continuous operation for this period of time; options such as alternating pump operation or pump throttling after a few days or weeks were not factored into the FMEAs.

4.2 Failure modes effects analysis results

The FMEA results indicated that the pump components judged most susceptible to significant debris-related damage, such that total pump failure might occur during the 100-day period of required operation following a large LOCA, are wear rings (particularly with weep holes) and internal bearings. Only those bearings that have significant loads and that require a liquid film for adequate lubrication are of concern in this circumstance. Pumps that rely on small internal passages or grooves in the bearings to supply coolant to the bearings are especially susceptible to debris-induced failure modes. Pumps without these features are less likely to incur degradation or failure than those with these features. However, note that pumps with external bearings are susceptible to debris blockage of coolant flow to the bearing oil coolers if the cooling is provided by the pumped fluid.

Essentially all ECCS pumps supply cooling water flow to the shaft seal by drawing from the pump outlet. Cyclone separators and heat exchangers may or may not be used to remove debris and cool this supply to the seals. Therefore, the shaft-seal failure modes and rankings developed in the FMEA apply to essentially all ECCS pumps, whereas the wear-ring and bearing failures may apply only to a subset of the ECCS-pump population. The FMEA identified that debris has a significant

potential to cause seal damage or failure. Note that seal failure would not necessarily disable the pump.

A greater number of “significant early” failures were assigned for cases with RMI insulation than with fibrous insulation. This outcome results from the judgments that: (1) RMI debris pieces can be relatively large and can block important passages readily; (2) the particles are hard and will induce more wear and abrasion; and (3) the minimal filtering qualities of RMI result in the circulation of more particulates through the ECCS pumps for a longer period of time than would be expected of fibrous debris.

5. Review of pump-failure data

An evaluation was performed to estimate the likelihood that RHR and other ECCS pumps would fail due to debris ingestion during their required period of operation following a LOCA. This evaluation combined a review and analysis of pump-failure data with engineering insights and knowledge gained from the pump-failure modes analysis. The review and analysis of pump-failure data were based on ECCS pump events contained in the INPO Nuclear Plant Reliability Data System (NPRDS).¹² Oak Ridge National Laboratory (ORNL) had analyzed the NPRDS information for all types of safety-related centrifugal pumps during 1990 through 1995, inclusive.¹³ The ORNL findings were supplemented by a separate, independent review of two sets of NPRDS data containing pump-failure events from 1976 to 1994-1995. One of these NPRDS data sets contained failure events for BWR RHR/low-pressure coolant injection (LPCI) pumps, while the other data set contained failure events for PWR RHR/low-pressure safety injection (LPSI) pumps and PWR containment spray pumps.

The ORNL reports noted the type and severity of the failures in the database. “Significant” failures were those likely to result in degradation such that the pump no longer could perform its function.

No significant data is available on ECCS pump operation with debris-laden fluid such as is anticipated following a LOCA. Debris-related ECCS pump failures have occurred, but the debris source and type was often associated with debris left in the system or component following manufacturing or maintenance/repair activities. ECCS pumps are normally in standby mode. RHR pumps provide shutdown cooling for extended periods, but in mode, they are circulating clean reactor coolant. BWR ECCS pumps are tested periodically by drawing suction from the suppression pool, which contains sludge and rust particles. These particles are quite small and are likely to pass through the pump without clogging internal passageways.

To get improved insights into the effects of debris on pump performance and reliability, a comparison was made between pump-performance data for systems pumping clean water and pump-performance data for systems pumping potentially contaminated or dirty water. The systems compared were essential service water (ESW) and component cooling water (CCW). Both of these systems have accumulated many thousands of hours of operation because they are normally operating when the plants are operating. ESW handles raw water (sometimes debris-laden river water), whereas CCW

-
12. NPRD Report, “Nuclear Plant Reliability Data System-Failure Master Report”, NPRGO6AA, Job No. 3170.
 13. Stanton, R.H., “A Characterization Update of Pump and Pump Motor Degradation and Failure Experience in the Nuclear Power Industry (1994-1995)”, ORNL/NRC/LTR/96-32, draft letter report, October 1996.

handles clean water. The data review indicated that relatively few plants (three of each type) were responsible for about 40% of all of the corresponding PWR and BWR significant pump failures.

Table 4 presents a summary of the data review results. Data for pump-failure rates are presented based on both the entire NPP population of each reactor type and for a few plants where the ESW pumps had relatively high failure rates and took suction from debris-laden sources. Failure rates are shown for all types of failures and for “significant” failures.

The data for all plants suggests that water quality plays a role in pump-failure rates. ESW pump “significant” failures were 3 to 5 times higher than those for CCW pumps. For the plants with high ESW failure rates and which included plants whose ESW systems took suction from silt-laden river water, the “significant” ESW pump-failure rates were about 25 times higher than typical CCW significant failure rates. Similarly, “all” failures for debris-ingesting ESW pumps were about 8 times higher than those for CCW pumps.

Table 4. Comparison of ESW and CCW pump-failure rates

System	Data for all plants		Data for plants with highest ESW failure rates	
	“All” pump failures	“Significant” pump failures	“All” pump failures	“Significant” pump failures
BWR pump-failure rates				
ESW	0.13	0.05	0.50	0.25
CCW	0.07	0.01	0.07	0.01
Ratio of ESW/CCW failure data	~2	~5	7	25
PWR pump-failure rates				
ESW	0.18	0.08	1.30	0.80
CCW	0.14	0.03	0.14	0.03
Ratio of ESW/CCW failure data	~1.3	~3	9	25

1. Failure data are expressed in failures/pump-yr.
2. CCW pump-failure rates for “all plants” are assumed representative of CCW pump-failure rates for plants with high ESW failure rates.

6. Likelihood of RHR/ECCS pump failure during the post-LOCA period of required operation

The data and insights discussed previously were used to support the derivation of estimates for RHR pump performance and reliability under post-LOCA conditions. In an attempt to bound these performance/reliability estimates, two scenarios were considered: (1) a baseline scenario in which RHR pump reliability essentially is unaffected by debris ingestion; and (2) a more pessimistic (and possibly worst case) scenario in which RHR pump reliability is degraded significantly by debris ingestion. Both scenarios are based on a post-LOCA operating interval of 100 days.

Baseline predictions of post-LOCA BWR-RHR/LPCI and PWR-RHR/LPSI pump performance were based on typical pump reliability data used in probabilistic risk assessments (PRAs) and Individual Plant Examination (IPE) studies. Pump reliability data contained in PRAs and IPEs are believed to represent baseline predictions of post-LOCA pump performance because: (1) failure data

used in these analyses typically are based on actual plant experience; and (2) most of the plant experience related to RHR pumps involves relatively clean pump-suction water. The following data indicate typical RHR failure rates used in PRAs and IPEs:

- Failure to start: 3E-03/demand.
- Failure to run: 3E-05/h.

Assuming that a particular RHR pump is continuously operated during a 100-day period (2 400 hours), the pump’s failure probability would be calculated by combining: (1) the pump “start” failure probability; and (2) the pump per-hour “run” failure rate multiplied by the exposure period of 2 400 hours. For both BWRs and PWRs, the baseline post-LOCA failure probability of an individual RHR pump would therefore be about 7E-02 (for significant failures).

A more pessimistic (and possibly worst case) prediction of RHR pump performance was generated by increasing the PRA/IPE “run” failure data above by a factor of 25 for “significant” failures. This factor is based on a comparison of ESW and CCW failures at the plants having the highest ESW failure rates. These higher failure rates were experienced by pumps operating with debris-laden water.

Table 5 summarises the probability of significant ECCS pump failure during the post-LOCA 100-day mission time.

Table 5. Post-LOCA estimated ECCS pump-failure rates

Post-LOCA run period (days)	Pump-failure probability (“Significant” failures)	
	Baseline scenario ^a	Pessimistic scenario ^b
1	0.004	0.02
5	0.007	0.09
10	0.010	0.20
38	0.020	0.50
100	0.070	0.80

a Based on typical IPE failure-to-run rate of 3E-05/h.

b Based on typical IPE failure-to-run rate of 3E-05/h × factor of 25 for dirty vs. clean fluid.

The factor of 25, which is used to generate the pessimistic failure probabilities in Table 5, is the ratio of the significant failure rates for ESW pumps experiencing “dirty” operating conditions to the failure rates for pumps whose pumped fluid is clean. The high failure rate is based on the experience of a few pumps known to be operating with debris-laden suction conditions. The concentrations and types of debris present in the pumped fluid for these pumps were not characterised in the reports used to derive the failure estimates. The debris may or may not bear any resemblance to the debris ingested by ECCS pumps following a LOCA. The expectation is that a significant fraction of the debris was composed of silt and sand; these materials are hard and abrasive, as are the sludge materials found in BWR suppression pools and PWR containment sumps. In addition, the ESW pumps experiencing the high failure rates are not identical in design to ECCS pumps. ESW pumps are believed to be totally submerged designs where all of the pump components, including some shaft bearings, are submerged. The pumps are connected to the electric drive motors by long shafts. The pump seals and internal bearings may or may not have been fed by clean water sources rather than from the pumped fluid. However, it does appear that the debris ingested by the ESW pumps contributed significantly to their failure.

As noted above, the precise types and concentrations of debris ingested by the ESW pumps experiencing the high failure rates are not known. However, the overall concentrations in the river water sources can be estimated. One or more of the plants experiencing the high ESW pump-failure rates is located along a river with “average” soil/silt/sand concentrations of about 0.15% to 0.25% (volume concentrations). These river-water debris concentrations are higher than those estimated for ECCS pumps by at least an order of magnitude for most debris types for BWRs and are somewhat higher than the debris concentrations estimated for PWRs.

Note that the failure rates displayed in Table 5 apply to significant pump failures, i.e. those failures that could render a pump inoperable and unable to fulfil its function. Less severe failures, such as seal failure, are more likely to occur, but would not necessarily disable the pump.

7. Conclusions

The evaluations performed and the results developed indicated the existence of several key factors and considerations that are important in assessing the effects of debris ingestion on ECCS pumps, including the following:

- **Debris types, characteristics, and concentrations.** Debris likely to be generated and transported following a LOCA includes insulation debris, sludge in BWRs, paint chips from containment coatings, rust particles, and concrete dust. Fibrous insulation and paint chips are “soft” materials, while the remaining debris types are considered “hard”. Actual data regarding the behaviour of these combinations of materials as it may affect ECCS pump operation were not available at the time of the study, and thus, large uncertainties remained as to potential ECCS pump problems caused by these combinations of materials. Debris concentrations are estimated to be higher in PWRs than in BWRs, and the concentrations are expected to remain at relatively high levels for longer periods of time in plants insulated with RMI than in plants insulated with fibrous materials.
- **ECCS suction strainer or screen characteristics.** At the time the study was performed, the hole sizes for suction strainers in BWRs were as large as about 1/8 inches, while the sump screens in PWRs had holes as large as the equivalent of about 1/4 inches in diameter. Thus, the debris sizes passing through the suction strainers in BWRs should not be larger than about 1/8 inches, and the debris ingested by PWR ECCS pumps should not be larger than 1/4 inches. Either of these debris sizes is deemed large enough to potentially cause blockage of small passages within ECCS pumps.
- **Time dependency effects and the accident progression.** The accident progression following a large LOCA is different between BWRs and PWRs. In BWRs, the ECCS pumps take suction almost immediately from the suppression pool, whereas in PWRs, these pumps initially take suction from the RWST (a source of “clean” water) for the first 20 or more minutes following a large LOCA. Pump suction in PWRs then is switched to the containment sump as the RWST inventory is depleted. Thus, PWR ECCS pumps should not experience any debris-related degradation when they are drawing from the RWST; whereas in BWRs, the pumps may be subjected to debris-laden suction conditions as soon as they are placed into operation.
- **Pump experience for operation under post-LOCA conditions.** Essentially no experience exists of ECCS pump operation under conditions of debris ingestion similar to those expected following a LOCA. Therefore, pump behaviour under these conditions has a large degree of uncertainty.

- **Pump features.** Particular pump features play a key role in determining the susceptibility of a given pump design to debris-related damage, including:
 - shaft seal design (with or without cyclone separators);
 - presence or absence of internal bearings;
 - internal flow passages that supply coolant to journal/sleeve bearings; and
 - features relied on to provide hydrodynamic or hydrostatic balance to the pump impeller and other rotating components.

The results of the evaluations indicate the following:

- Pump shaft seals have a relatively high potential for failing during the 100-day post-LOCA mission time. Seal failure should not disable the pump or degrade its performance to the point where the pump is considered failed, unless the leakage is very high. For many ECCS pumps, the leakage flow is limited by disaster bushings. If such bushings are not present, the leakage rates can be significant. The resulting loss of coolant for recirculation to the reactor core could impact the long-term effectiveness of the ECCS.
- Pump bearing assemblies, particularly those designs that depend on coolant availability to provide hydrodynamic or hydrostatic balance to the pump impeller and other rotating components, are susceptible to coolant-passage blockage by debris. Blockage of critical internal flow passages that feed hydrodynamic or hydrostatic bearings could lead to imbalance of the rotating components. The attendant wobble and vibrations can result in possible contact between rotating and stationary components (e.g. wear rings and pump housing). Pumps that rely on hydrostatic and hydrodynamic bearings are judged to have a significant potential for failure due to debris-related effects. Extensive use of such designs in ECCSs is not supported by the surveys and inquiries performed for this study.
- Any imbalance of pump rotating components, such as those induced by loss of hydrodynamic balance, imposes loads on the shaft bearings. This loading, coupled with the lack of coolant for heat removal and lubrication, can result in overheating and possible seizure of the internal sleeve/journal bearings. This scenario is particularly true for metallic bearings of this type. Failure of the bearings could disable the pumps completely. This type of debris-related pump failure can occur essentially any time during the required period of ECCS pump operation following a large LOCA. Note that graphite-based bearings are self-lubricating and are less vulnerable to this type of failure.

Cycling of pumps on and off or alternating the operation of individual ECCS pumps during periods of low core decay heat may not be benign. Evidence indicates that debris will settle into the gaps, clearances, and internal passages when the pumps are idled. The accumulated debris may interfere with the restart of the pump. These types of occurrences have been observed in available ECCS pump-failure data.

High-pressure pumps, such as those used in the HPCI or high-pressure core spray systems in BWRs or HPSI pumps in PWRs, may be used in a recirculation mode for certain types of accidents. Because they are typically multistage units with tight clearances, these pumps may be more susceptible to debris-related damage than the low-pressure ECCS pumps.

SEPARATE EFFECTS TESTS TO QUANTIFY DEBRIS TRANSPORT TO THE SUMP SCREEN

Arup K. Maji

Department of Civil Engineering, University of New Mexico, Albuquerque, NM 87131, USA

D.V. Rao, Bruce C. Letellier, Luke Bartlein

Los Alamos National Laboratory, Group D-5, Los Alamos, NM 87545, USA

Kyle Ross

Alion Science, Albuquerque, NM 87110, USA

Clint Shaffer

ARES Corporation, Albuquerque, NM 87131, USA

Abstract

In 1997 the United States Nuclear Regulatory Commission (NRC) initiated an investigation into the possibility of failure of the recirculation system in nuclear power plants (Generic Safety Issue GSI-191). If a loss of coolant accident (LOCA) were to occur within the containment of a pressurised water reactor, piping thermal insulation and other materials in the vicinity of the break would be dislodged by break jet impingement.^{1,2} Some of this debris could eventually be transported by the recirculating water and accumulate on the suction sump screens, clogging them and causing the cooling system to fail. The NRC initiated a test programme to investigate the amount of insulation debris that could transport to the sump screen.

It was not possible to conduct scale model experiments to determine if insulation debris generated at any location could be transported to the sump screen. This is because the fluid flow is scaled according to the Froude's number, whereas debris transport is a viscosity-driven phenomenon and thus scaled according to the Reynold's number. Therefore, a "separate-effects" test methodology was developed. The first step in the process was to determine independently the motion of insulation debris at different velocity and turbulence conditions using a 6 m (20 ft) long linear flume in the Hydraulics Laboratory of the University of New Mexico, USA.³ The second step in the process was to model the fluid flow on the containment floor using a computational fluid dynamics (CFD) code. A methodology was developed thereafter for predicting debris movement by combining the flow velocities determined by CFD and the linear-flume floor transport data. The methodology subsequently was proven by a series of tests conducted inside a 4 m (13 ft) diameter circular tank with in-built structures resembling the inside of a nuclear containment building. The methodology was verified using simulated debris (nylon spheres) and typical fibrous (NUKON[®]) and reflective metallic insulation debris. Many break locations were studied to increase the confidence in this approach further for different LOCA break locations.

1. NRC Bulletin 96-03, "Potential Plugging of ECCS Strainers by Debris in BWRs", May 1996.
2. Rao, D.V., *et al.*, "GSI-191: Parametric Evaluations for Pressurized Water Reactor Recirculation Sump Performance", Los Alamos National Laboratory report LA-UR-4083, Rev. 1 (August 2001).
3. Maji, A.K., *et al.*, "Transport Characteristics of Selected PWR LOCA Generated Debris", *Nuclear Technology Journal* **139** (August 2002), pp. 145-155.

Test facility

A steel tank was manufactured in four segments at the University of New Mexico. The fully assembled tank holds 11 200 L (2 970 gal.) and has a 4 m (13 ft) diameter x 0.76 m (2.5 ft) deep open top container fabricated from 12-gauge galvanised steel (Figure 1). The segments subsequently were bolted together in the laboratory. The tank then was filled with concrete and levelled to provide a smooth, flat surface. The surface was coated with a two-part epoxy paint formulated for use on galvanised metal. Once the basic tank was filled with concrete and painted, interior walls were modelled out of wood to mimic structures on a generic containment floor. The model walls were weighted down using cinder blocks to prevent floatation when the walls were immersed in water. Spray foam was used to seal the area under the wood, and caulk was spread around the bottom of each wall.

Figure 1. Test facility with simulated containment structure and break source



An 8.35 m³/min (2 200 gal./min) capacity pump was used to supply each testing area (flume or tank) with water via a 15 cm (6 inches) diameter polyvinyl chloride (PVC) pipe. The tank outflow was carried through two 20 cm (8 inches) diameter pipes that connected to the side of a box underneath the outflow screen. One of these pipes had a butterfly valve, and the other pipe had a 20 cm (8 inches) diameter gate slide valve. The butterfly valve was used to fine-tune the water level in the tank when required. A Hoffer flowmeter, model HIT-2-2-A-X-F, was used to monitor the flow rate in the main pipes. To reduce turbulence, a perforated bucket sometimes was used. Evaporative cooler pads were used to line the bucket and allow the water to exit through the pores of the pads.

Test procedure

Several test configurations were used in the setup described in the previous section. The primary objective of these tests was to observe the movement of debris in the three-dimensional (3D) tank.

Acrylic spheres, 1.9 cm (3/4 inches) in diameter, were used instead of the actual debris because the spheres had an incipient velocity in the same regime as NUKON® insulation debris tested in the linear flume, but with much less variability. The spheres did not transport if the water velocity was 0.061 m/s (0.20 ft/s), incipient movement was at 0.067 m/s (0.22 ft/s), and bulk movement was at 0.082 m/s (0.27 ft/s).

A series of tests was conducted with different break locations to observe the movement of the acrylic spheres under different flow conditions. For the sake of brevity, the only specific case discussed here is that of the break location at the opposite end of the tank (Figure 1). The height of the water was kept at 23 cm (9 inches) for each test. Once steady-state flow was reached by adjusting the outflow valves, a 2.5 cm (1 inch) diameter PVC pipe was used to drop each ball to the bottom of the tank into a desired position. The pipe then was removed slowly from the pool, leaving the nylon ball on the bottom of the tank. The sphere's movement and path were drawn by hand on a scale drawing of the tank. This process was repeated at several locations in the tank for each test. This method allowed the flow fields in the tank to be charted. A 30-s observation time was used in each instance. The black dots in Figure 2 designate the starting location. The movement of the spheres over the 30 s period is shown with the arrows. A black dot at the end implies that the sphere came to rest at that location. An arrow at the end designates that the sphere continued to roll at the end of the 30 s period.

Figure 2 shows the movement of acrylic balls under a flow rate of 150 gal./min. The volumetric flow was selected after some trial runs for best possible validation of the CFD results. At this flow it was possible to identify areas where the spheres do and do not move. At lower flow, very little movement was observed anywhere in the tank, and at higher flows, movement occurred almost everywhere along the annulus of the tank where the test was conducted. The flow velocities obtained from the CFD code are shown in Figure 3. The dark areas in the annulus are the only areas where the flow velocity is large enough to cause movement in the acrylic spheres. If we compare Figures 2 and 3, it is evident that floor transport of the spheres can be determined by looking at the CFD results.

Figure 2. Movement of acrylic spheres at 0.57 m³/min (150 gal./min) flow

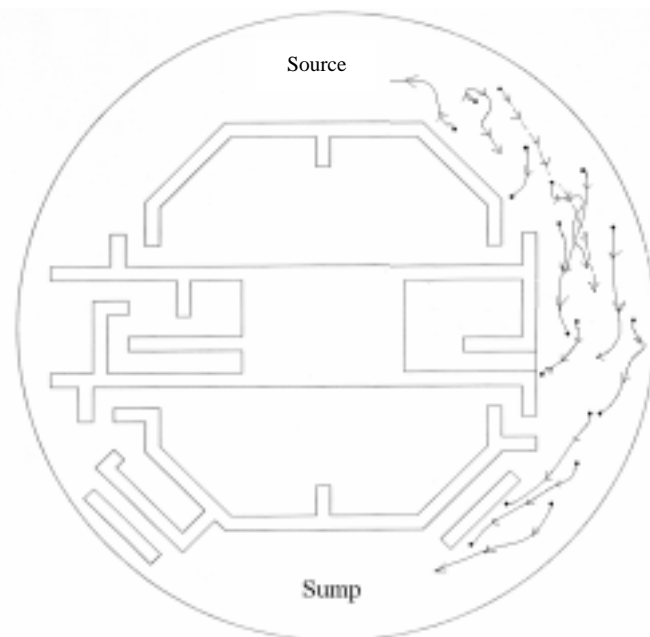
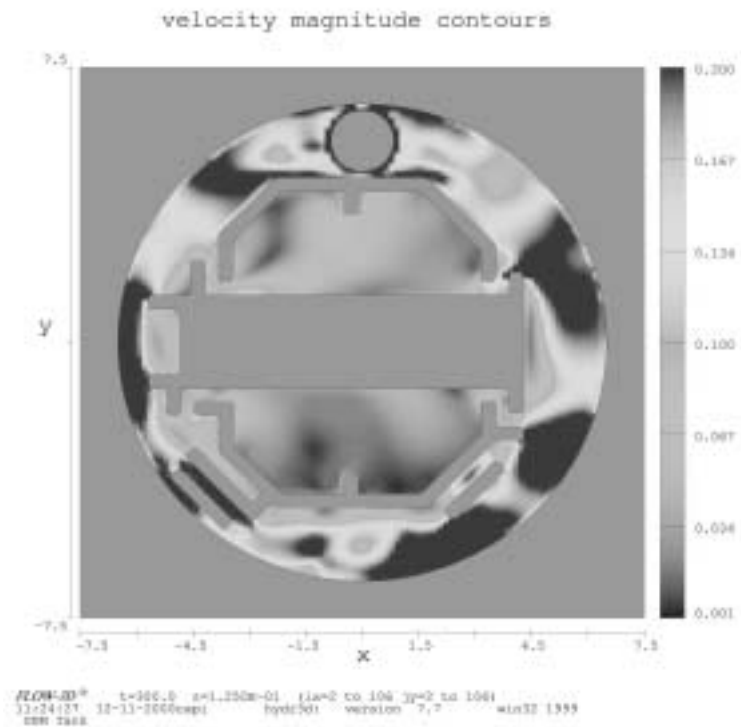


Figure 3. Velocity results from the CFD analyses



Fill-up phase studies

This set of tests was run to observe where debris is likely to transport during the fill-up phase (when the tank initially is filled up). The source was placed in the outer annulus region at the opposite end of the tank from the sump. Ninety 1.9 cm (3/4 inches) diameter spheres were randomly distributed in the tank, 30 in each of the outer “annulus” regions (Figure 4) and 15 in each of the closed “inside” regions. The rectangular boxes in Figure 4 show the total number of spheres initially placed in each region. The pump was started with a flow of 0.49 m³/min (130 gal./min), with the outlet valve completely open. The location of the balls after a steady state had been reached (4 min from the start) was noted. The numbers in the circles indicate the approximate location of the balls at the end of the 4 min. It is evident that because of the high flow velocity during the fill-up phase, most of the debris (39 spheres out of 90) will be swept to the screen in this configuration. Some of the spheres will be trapped in the inside regions and be unlikely to move later, regardless of the flow volume, when the outflow valve is opened later.

The fill-up phase test was repeated with aluminium reflective metallic insulation (RMI) (Figure 5). The numbers in the boxes represent the initial distribution of RMI, with 40% of RMI distributed randomly in each of the outer annulus regions and 10% distributed randomly in each of the inside regions. None of the material initially was placed within 1 m of the outflow screen. The valve for the outflowing water control was closed for these tests, and the tank was allowed to fill up to 23 cm (9 inches). At the start of flow, the flow rate was 0.27 m³/min (72 gal./min); after the water level reached 23 cm, the flow rate reduced to 0.09 m³/min (23 gal./min). The circled numbers represent positioning of RMI after the water level reached 23 cm. Once again, about 30% of the RMI ended up at the screen, as compared with the fraction of nylon spheres that reached the screen, as seen in Figure 4.

Figure 4. Fill-up phase tests with calibrated spheres

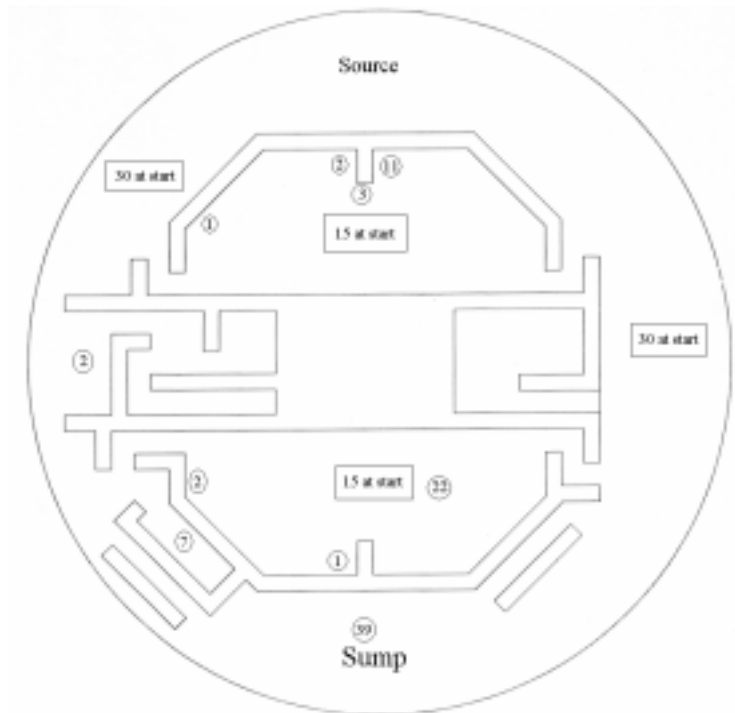
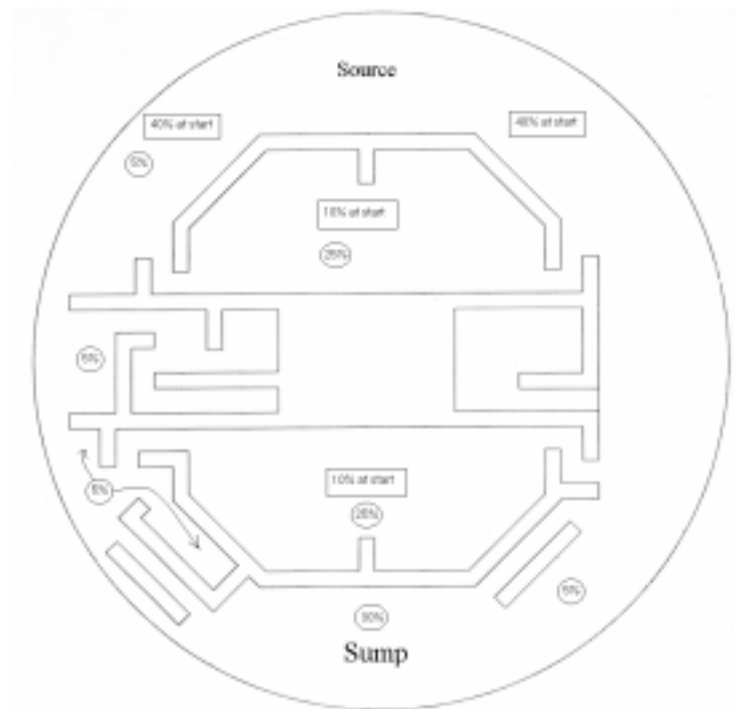
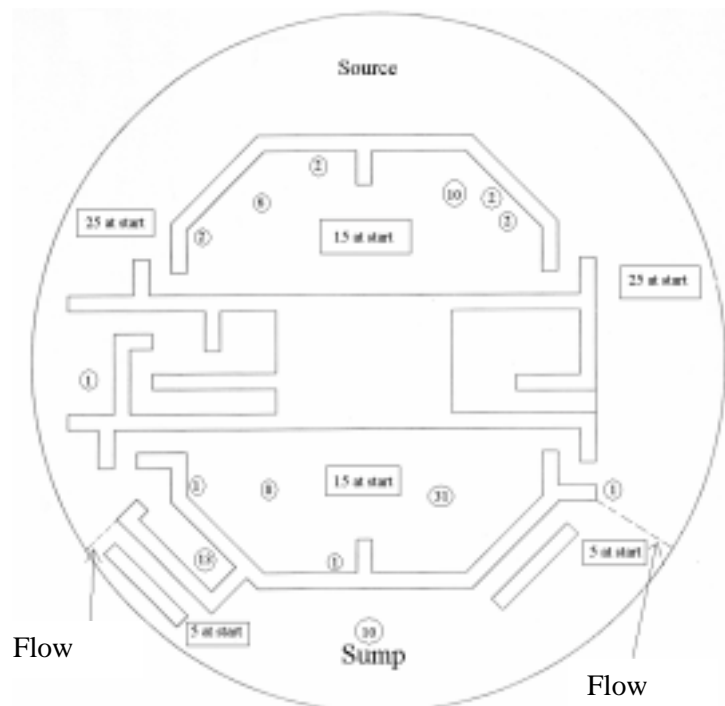


Figure 5. Fill-up phase tests with aluminium RMI



To explore a simple remedy that reduces the transport fraction to the screen under such circumstances, we ran a second set of tests with two pieces of 5 cm high x 10 cm wide wood blocks obstructing the flow at locations shown by the dashed lines in Figure 6. For this test, 25 spheres were placed in each of the outer annulus regions and 15 spheres were placed in each of the inside regions. In spite of the test being run at a lower $0.32 \text{ m}^3/\text{min}$ (85 gal./min) flow, only 10 nylon spheres reached the outlet screen. These 10 spheres were initially between the 2 x 4 blocks and the outlet screen. All the other spheres were diverted to the inside regions. This test demonstrates that even though the fill-up phase may lead to a very high transport fraction, it may be possible to implement simple design changes to the plant configuration in the form of flow barriers on the floor to eliminate this problem.

Figure 6. Fill-up phase tests with obstructions to divert flow



Conclusions

A combination of CFD analyses and incipient transport velocity of different types of LOCA debris can be used to estimate the fraction of debris that would end up on the sump screen.

Regardless of the flow rate, a significant amount of the debris can be transported during the fill-up phase because of the high water velocities. However, simple barriers at specific locations can remedy this problem.

Acknowledgements

This research was sponsored by the Division of Nuclear Technology, Office of Nuclear Regulatory Research, US Nuclear Regulatory Commission. The project was managed by Michael L. Marshall and Bhagwat P. Jain.

BREAK CHARACTERISTIC MODELLING FOR DEBRIS GENERATION FOLLOWING A DESIGN BASIS LOSS OF COOLANT ACCIDENT

**Timothy S. Andreychek, Bradley F. Maurer, Dulal C. Bhomick
Joseph F. Petsche, John Ghergurovich, David J. Ayres**
Westinghouse Electric Company, LLC, USA

Ashok Nana
Framatome-ANP, USA

John C. Butler
Nuclear Energy Institute, USA

Introduction

An important safety concern regarding long-term recirculation cooling following a loss of coolant accident (LOCA) is the transport of debris materials to interceptors (i.e. trash racks, debris screens, suction strainers) inside containment and the potential for debris accumulation to result in adverse blockage effects. Debris resulting from a LOCA, together with pre-existing debris, could block the emergency core cooling system (ECCS) debris interceptors and result in degradation or loss of recirculation flow margin. Potential debris sources can be divided into three categories: (1) debris that is generated by the LOCA and is transported by blowdown forces (e.g. insulation, paint); (2) debris that is generated or transported by washdown; and (3) other debris that existed before a LOCA (dust, sand, etc.). Each debris source is separately evaluated to estimate the quantity and other characteristics necessary to assess the fraction that could be transported to the containment recirculation sump and its combined effect on recirculation flow.

An initial step in evaluating post-accident sump performance is the determination of the amount of debris generated from a postulated breach in the piping system. Current regulatory guidance calls for determination of the quantity and characteristics of debris generated by a postulated LOCA covering a range of break sizes, break locations, and other properties, in a manner that provides assurance that the most severe postulated LOCAs are calculated. Methods for determining debris generation typically utilise a bounding combination of deterministic and mechanistic methods to provide a conservative representation of the destructive behaviour of a postulated break. These methods provide a conservative estimation of debris generation based upon models that are not representative of the expected behaviour of pipe breaks.

This paper presents a model for use by pressurised water reactor (PWR) plants that provides a more realistic representation of one aspect of debris generation modelling (break size) while maintaining an overall conservative representation of the debris generation potential of postulated breaks. The proposed model utilises fracture mechanics as the basis for determining a break size that is realistically conservative. This break size is then used in determining the quantity of debris that would be generated from identified break locations.

The fracture mechanics techniques described in this paper are the same techniques that have been used successfully in the support of leak before break (LBB) and the application of LBB to

postulated leakage cracks in large reactor coolant piping in PWRs. These leakage cracks have leak rates well above the demonstrated PWR leak detection capabilities (typically 10 gpm); while at the same time have been shown to remain stable under all normal and off-normal plant operating conditions.

While the proposed treatment method and LBB applications utilise the same technical basis, the method proposed in support of debris generation differs substantially from an LBB application. LBB applications¹ typically use fracture mechanics to demonstrate that the probability of fluid system piping rupture is extremely low, and using this basis, local dynamic effects are excluded. The proposed fracture mechanic approach continues to include the local dynamic effects (e.g. debris generation) but uses fracture mechanics as a basis for determining the amount of debris that is generated by the postulated break via identification of an effective break area. Therefore, this method credits the demonstrated toughness of PWR piping, yet defines a conservative design input for sump performance evaluations.

The proposed model will be one of the options available for use by PWR licensees as a step in the overall analysis effort necessary to demonstrate compliance with regulatory requirements governing operation of the ECC and containment spray systems (CSS).

2. Summary of current guidance and need for revised approach

Upon initiation of a break in the reactor coolant system of a PWR, the forces released by the break have the potential to dislodge piping thermal insulation and other materials in the vicinity of the break. A portion of this material will be transported to the containment floor by the break flow and by containment sprays. Upon initiation of recirculation flow from the containment sump to the reactor coolant system, some of the debris in the lower containment elevations will be transported to and accumulate on the containment sump screens. The resultant increase in resistance to the flow by the debris accumulating on the containment sump screen has the potential to challenge the capability of the ECCS to provide long-term cooling to the reactor core. In order to calculate plant response to a postulated event and the potential for significant blockage of the containment sump screens, it is necessary to take into account a wide range of phenomena and processes. These phenomena and processes are highly dependent upon plant design and operation as well as the specifics of the postulated LOCA event. The complexity and multivariate nature of the event progression, coupled with the absence of a comprehensive database addressing the full range of encountered phenomena inevitably leads to a calculation process that accounts for the resulting uncertainties in a conservative manner.

Typically the analyses investigating ECCS operation during the recirculation phase divide the process into three separate phases: (1) debris generation; (2) debris transport; and (3) debris accumulation and head loss. Each phase of the calculation process, while interdependent, involves its own set of phenomena and uncertainties. Known limitations in the knowledge base of these phenomena and associated calculation methods are typically accounted for in a bounding fashion during each phase of the process. The combined effect of these bounding calculations is a pessimistic prediction of ECCS recirculation performance that, while conservative, provides little insight into the realistically expected performance during a design basis event. An additional complicating factor is the realisation that, unlike most design basis calculations, there is no unique set of conditions that can

1. Applications utilising the provisions of General Design Criterion 4 contained in Appendix A to 10CFR Part 50, that allow the exclusion of local dynamic effects from the design basis for qualified piping systems.

be repeatedly shown to represent the worst case for recirculation performance. This necessitates either a full scope set of calculations looking at an effectively boundless set of possible permutations and combinations of conditions, or a more limited set of calculations that combines conditions in a bounding and often unrepresentative manner.

While it is not the intent of this paper to address the full set of calculations necessary to assess ECCS and CSS operation in the recirculation mode, it is informative to discuss current guidance and practices for the debris generation phase of the calculations.

2.1 Break size and location

Because the size and location of the break have a key influence on a number of key parameters that are specific to each plant's design and operation (e.g. debris generation quantities, debris transport capability, containment flood-up level and timing), it is not possible to predetermine the limiting break size or its location. The current practice is to analyse a full range of break sizes, ranging from the smallest break that has the potential to lead to ECCS recirculation operation to a full double-ended guillotine break of the largest reactor coolant system pipe. This full range of break sizes is postulated for a wide range of potential break locations to address factors such as variations in insulation materials on and around postulated break locations and proximity to the recirculation sump and its influence on debris transport.

Current guidance calls for debris generation to be calculated for a number of postulated LOCAs of different sizes, locations, and other properties sufficient to provide assurance that the most severe postulated LOCAs are calculated. Proposed revision 3 to Regulatory Guide 1.82 [1] calls for the following postulated break sizes and locations to be considered:

1. Breaks in the hot leg, cold leg, intermediate leg, and, depending on the plant licensing basis, main steam and main feedwater lines with the largest amount of potential debris within the postulated zone of influence;
2. Large breaks with two or more different types of debris, including the breaks with the most variety of debris, within the expected zone of influence;
3. Breaks in areas with the most direct path to the sump;
4. Medium and large breaks with the largest potential particulate debris to insulation ratio by weight; and
5. Breaks that generate an amount of fibrous debris that, after its transport to the sump screen, creates a minimum uniform thin bed (1/8 inch layer of fiber) to filter particulate debris.²

This process is applied in a deterministic fashion without consideration of the probability of a limiting size break occurring at the limiting location on the RCS. This can lead to a condition where the limiting break is controlled by a unique combination of break size, location and transport assumptions. This factor, in conjunction with other, more traditional, design basis assumptions (e.g. limiting single failure, maximum uncertainties on setpoints, timings, and flow rates) can easily lead to one or more extremely low probability events dominating calculation results.

-
2. Screen blockage experiments have determined that a 1/8 inch layer of fiber combined with particulate debris can result in significant head loss. Fiber layers thicker than 1/8 inch result in lower head loss, while layers less than 1/8 inch are unstable and tend toward self destruction as head loss increases. The uniqueness of the set of conditions that result in a stable "thin-bed" of fiber and particulate is not addressed in current guidance.

2.2 Debris generation

Given a postulated break size and location, the next step is to calculate (or estimate) the quantity and size distribution of debris that could be generated as a direct consequence of the break. The debris generation capability of a break is dependent on a number of factors including break size, break opening characteristics and break orientation, as well as characteristics of materials and structures surrounding the break. While a number of tests have been performed to investigate the mechanics of debris generation, these tests are limited in scope and both the tests and the resultant interpretation of test data have incorporated simplifying/bounding assumptions to address variability in key parameters.

One important simplifying assumption used in both debris generation tests and subsequent modelling of the tests is that the break opening time is instantaneous.³ This is a carry-over assumption from thermal hydraulic analyses of reactor coolant system response performed in accordance with Appendix K to 10CFR Part 50.⁴ A consequence of this assumption for debris generation is the generation of an acoustic shock wave. This pressure wave is believed to be a major contributor to debris generation surrounding the break. Component insulation is destroyed initially by the blast effects of a shock wave that expands away from the break. This destruction is continued by the two-phase jet of fluid emanating from the break. Experiments show that the shock wave may cause substantial damage to even the most heavily reinforced insulating constructions (e.g. steel-jacketed RMI or fiber) if they are located sufficiently close to the break.

In order for a shock wave to occur, the break opening time (BOT) must be on the same order as the acoustic propagation time across the piping. If the BOT is long relative to the acoustic propagation time then a shock wave will not occur and debris generation will be predominated by jet impact and displacement forces. As part of its evaluation of the potential for shock waves following a double-ended guillotine break General Electric [2] estimated that a shock wave will not be generated for large bore piping break opening times greater than approximately 10 milliseconds. Realistic estimates of break opening times for a full double-ended rupture derived from mechanical response analyses show that the quickest opening time for large bore PWR piping is on the order of 100 milliseconds. However, the presumption of an instantaneous break opening time and resultant shock wave remains in regulatory guidance applicable to debris generation. Regulatory guidance contained in Revision 3 (proposed) to RG 1.82 states:

- The shock wave generated during postulated pipe break and the subsequent jet should be the basis for estimating the amount of debris generated and the size or size distribution of the debris generated within the zone of influence.

The assumption of an instantaneous opening of the break is an unwarranted conservatism, and leads to a significant overestimation of the debris generation potential for a postulated break.

Determination of the amount of debris that is generated for a given break is also complicated by the complexity in modelling a three-dimensional jet of two-phase fluid expanding into a region

3. Instantaneous break opening is simulated in debris generation tests through the use of fast opening rupture disks designed to open in a time span of approximately one millisecond.

4. Appendix K to 10CFR Part 50 covers required and acceptable features of ECCS evaluation models designed to address core response and ECCS cooling performance following a design basis LOCA event. These analyses are performed to demonstrate compliance with 10CFR50.46 performance criteria addressing peak cladding temperature, maximum cladding oxidation and core coolability (flow channel blockage resulting from fuel rod ballooning). Separate analyses, using other “non Appendix K” models are used to demonstrate compliance with 10CFR50.46 criteria not addressed by Appendix K.

composed of a multitude of materials in widely varying geometric configurations. A number of conservative simplifications of the problem have been proposed and used. One method for estimating the amount of debris generated by a postulated LOCA is to define a spherical zone of influence. The size of the zone of influence is dependent of the size of the break and on the materials considered within the zone. Once the zone of influence is defined, all materials within the zone are assumed to be damaged. The simplicity of these models inevitably results in an overestimation of the quantity of debris generated by a postulated break.

The quantity of debris that can be generated by a break based on assumptions and conservatism cited above can be seen in results presented in NUREG/CR-6762 [3]. The reported results of debris-generation simulations show debris volumes of 1 700 ft³ for a large LOCA (> 6 inch diameter), compared to 40 ft³ for a medium LOCA (4 to 6 inch diameter) and 25 ft³ for a small LOCA (2 to 4 inch diameter).

In summary, current guidance calls for ECCS performance to be assessed in response to the most limiting set of conditions. One of the main controlling factors in calculations to assess ECCS recirculation performance is debris generation. The set of assumptions called for by current regulatory guidance result in ECCS performance being assessed in response to a spectrum of break sizes and locations. The probability of the limiting size break(s) occurring at specific locations is not accounted for in these calculations. The debris generation occurring at this limiting break size/location is then conservatively estimated based on models that are constructed from:

1. Unrealistic break characteristic assumptions (introducing phenomena that would not be expected to occur); and
2. A conservative expansion of limited test data, necessitated by the wide variety of materials and configurations involved and the large uncertainties associated with expansion of small scale experiments to PWR conditions.

The inevitable consequence of the current analysis methodology is an ECCS recirculation design that is based (focused) upon an extremely low probability event scenario.

In response to the large debris generation values resulting from the current approach, licensees may find it necessary to proactively reduce the debris generation potential in ways that may be detrimental to operation. Utilities may conclude that the only practical way to reduce the debris generation source term to a manageable size is to limit break size by installing (reinstalling) guard pipes, piping restraints, or other similar devices. The irony of such a change is that the justification for removal of such devices from plant designs originally was, in part, the low frequency of the same postulated breaks that would now be responsible for their return. The end result of such action is that the reactor coolant piping would be less accessible than was the case prior to these modifications. The modifications will result in less accessibility inside containment. This, in turn, will result in making the performance of some inspections no longer practical, cause other inspections to take longer, and result in plant personnel receiving increased doses for routine maintenance and inspection procedures.

Physical modification of the containment sump screen as a means to address GSI-191 concerns will likely be considered by many licensees. While an increase in sump screen area is an appropriate and perhaps necessary means to address GSI-191, large increases in sump screen area can have unintended consequences and every means should be taken to ensure that the size of the screen is appropriate for the issue. The large debris loadings resulting from non-mechanistic modelling of breaks could dominate the sizing requirements for containment sumps which, in turn, could lead to screen area requirements that lead to modifications that compromise other aspects of plant design and operation. Depending on the location of the containment sump, a large increase in screen area could

result in an encroachment on reactor coolant piping. This may require additional plant modifications, such as the addition of piping restraints to preclude damage to the enlarged sump screen. Large increases in sump screen flow areas are also likely to greatly impede access inside containment. This would make maintenance and inspection activities more difficult, and potentially impractical.

3. Description of proposed approach

As discussed in Section 2, current guidance calls for ECCS and CSS recirculation performance to be evaluated for a full range of break sizes across a full range of break locations. These calculations are performed to demonstrate that the ECCS can meet requirements for long-term cooling per 10CFR50.46(b)(5). In order to determine the quantity of debris that is generated as a direct consequence of the break it is necessary to specify the characteristics of the postulated break.

The following section summarises the break characteristic models currently used to meet ECCS performance requirement specified in 10CFR50.46. This is followed by a summary of the proposed approach for debris generation modelling.

3.1 Break characteristic models currently used to meet 10CFR50.46

There are currently two general methods for assigning the break characteristics for use in meeting requirements of 10CFR50.46. These are:

1. Models for in-core thermal hydraulic response and mass/energy release (Appendix K models); and
2. Models for in-core structural response (LOCA forces models).

Appendix K to 10CFR Part 50 covers required and acceptable features of ECCS evaluation models designed to address core response and ECCS cooling performance following a design basis LOCA event. These analyses are performed to demonstrate compliance with 10CFR50.46 performance criteria addressing peak cladding temperature [10CFR50.46(b)(1)], maximum cladding oxidation [10CFR50.46(b)(2)] and core coolability⁵ [10CFR50.46(b)(4)]. Separate analyses are performed to demonstrate compliance with the core coolability criterion of 10CFR50.46 by calculating the impact of break forces on vessel internals (e.g. fuel assemblies).

3.1.1 Model for in-core thermal hydraulic response and mass/energy release

For the purpose of demonstrating compliance with 10CFR50.46(b)(1) and (b)(2) (peak cladding temperature and maximum cladding oxidation) and for determining mass and energy release for containment response calculations, the postulated break is assumed to be an instantaneous double-ended opening of a pipe up to and including the largest piping in the reactor coolant system. These calculations are deterministic in that they do not take into consideration the frequency of piping rupture of a given size. The calculations are also non-mechanistic since no known failure mechanism can lead to an instantaneous pipe rupture.⁶ The assumption of an instantaneous break opening versus a

5. Appendix K analyses address core coolability primarily from the impact of flow channel blockage resulting from clad ballooning.

6. For this discussion, instantaneous can be considered to be a break opening time less than ~.01 seconds, i.e. the break opening interval necessary to generate a shock wave.

more defensible opening time (e.g. 100 milliseconds), has little impact on the associated in-core thermal hydraulic calculations.

The assumption of an instantaneous break opening time does have a significant impact on calculations performed for the purpose of meeting other 10CFR50.46 requirements.

3.1.2 Model for in-core structural response

Calculations performed to demonstrate compliance with 10CFR50.46(b)(4) (coolable geometry) typically incorporate the likelihood of various break locations in accordance with the provisions of GDC-4, using “leak before break” analysis techniques. Such consideration allows the elimination from the design basis of the dynamic effects of pipe rupture in piping systems so qualified. For piping systems that have not been qualified for “LBB exclusion” the analyses determine the effective break area resulting from the postulated break and determine, based upon the break forces, existing structures and restraints, the piping displacement. The effective break area, taking into account limited displacement, results in an effective break area that is, in most cases, significantly less than the full pipe diameter. Further, in select applications, the calculations apply a realistic break opening time (BOT) based on the consideration of fracture mechanics and dynamic system structural analyses. Realistic BOT’s are typically calculated using finite element dynamic analysis methods based on the assumption that the crack is developed instantaneously. Although testing and analysis results indicate a finite crack propagation time, this is conservatively neglected in the BOT determination. While BOT has relatively little effect in the long term on the blowdown transient, a realistic time for the break to develop to its full break area can have a considerable effect in the initial stages of the blowdown.

3.2 Application of current models to local debris generation

For the purposes of demonstrating compliance with 10CFR50.46(b)(5) (long-term cooling), either of the above two approaches for defining break characteristics could be considered, but each has noted limitations. The modelling characteristics used for in-core thermal hydraulic analyses (e.g. instantaneous break opening time) should not be considered appropriate for use in debris generation calculations because they are unrepresentative of break opening behaviour and lead to an overly conservative estimation of debris quantities. The methods utilised for in-core structural analyses to demonstrate compliance with 10CFR50.46(b)(4) are considered more appropriate for debris generation calculations, however, full application is constrained since experiments that have been conducted to determine debris generation have typically modelled instantaneous break openings using fast opening rupture disks. As such there is little experimental data available to support the debris generation that would occur for realistic break opening times.

The exclusion from consideration of LBB qualified piping that is currently applied in structural analyses for 10CFR50.46(b)(4) could be considered in debris generation calculations and was proposed by NEI in a letter to NRC dated 4 October 2002 [4]. As of the date this paper is prepared, the NRC has not provided a written response to the NEI request to utilise this approach; either accepting it as an appropriate method or by identifying the basis for its denial. Therefore, use of LBB piping exclusions remains a potential method for use in debris generation calculations.

However, the uncertainty associated with the schedule for NRC staff response on the proposed use of LBB exclusions led to the development of an alternative proposal that incorporates attributes of the two currently accepted pipe break characterisation models.

3.3 Proposed break characteristic model for debris generation

The proposed model utilises fracture mechanics considerations to establish a maximum credible flaw size in qualified piping. The area associated with this flaw size is then increased by three orders of magnitude to determine the break size (area) to be used in debris generation calculations. The calculation of the debris quantities generated from these pipe break areas have as a basis a conservative estimate of the actual behaviour of the piping material under normal and off-normal conditions.

The proposed model for determining the size of the pipe breach will utilise stable yet detectable leakage cracks already calculated for PWR primary coolant piping as a key input parameter. Compilations of stable leakage cracks that have been calculated for a number of PWR plants are presented in Table 1, along with the crack opening area for each crack. As seen from the listings presented in this table, the crack opening areas of the stable leakage cracks are quite small and would have little debris generating capability.

For the purposes of conservatively calculating debris generation for a postulated through-wall flaw, the breach area associated with the stable leakage crack is increased by a factor of 1 000. Use of a pipe breach area that is three orders of magnitude larger than the calculated area of the associated stable leakage crack results in maximum pipe breach areas for use in evaluating debris generation as follows:

- For B&W/Framatome plants 83 inch²
- For Combustion Engineering plants 40 inch²
- For Westinghouse plants 40 inch²

Using a circular hole for the break geometry, the equivalent hole diameters for the break areas identified above are calculated as:

- For B&W/Framatome plants 10.28 inch diameter
- For Combustion Engineering plants 7.10 inch diameter
- For Westinghouse plants 7.10 inch diameter

The geometry of the circular hole is assumed to be in the pipe centered at the midpoint of the through-wall crack or flaw. The proposed model could be applied to piping segments for which fracture mechanics analysis results are available for determining stable leakage crack areas. Piping segments for which the calculation of stable leakage cracks do not exist will assume the full cross sectional area of the inside diameter of the pipe for the purposes of debris generation.

The factor of 1 000 was not chosen arbitrarily. Rather, applying the factor of 1 000 results in a hole size that is representative of, and generally larger than, piping attached to the RCS. Thus, the factor of 1 000 provides for a conservatively realistic postulated breach in the RCS.

It is also important to note that the proposed break model is used only for the determination of dynamic effects impacting local debris generation. All other phenomena affecting long-term cooling, such as break flow, global effects within containment, debris transport, and screen blockage, will utilise a full range of break sizes and locations (up to full double-ended guillotine rupture of largest pipe).

3.4 Comparison of current and proposed break characteristic models

Table 2 provides a comparison of key attributes of current break modelling used to demonstrate compliance to 10CFR50.46 and break modelling proposed for use in calculating debris generation potential for postulated breaks.

4. Technical bases for proposed break characteristic model for debris generation

Significant testing and analyses have been performed to characterise the behaviour and response of flaws that may be present in reactor coolant piping. These efforts have provided a comprehensive and realistic basis for defining stable through-wall cracks in large PWR reactor coolant piping. The fracture mechanics analytical techniques, applied reactor coolant system loadings, actual material properties, and installed leak detection capabilities are discussed below. Combined in a comprehensive plant-specific analysis, these techniques demonstrate that a conservatively postulated through-wall crack would be large enough to be detected by plant leak detection systems, yet remain stable in the full power operating environment, including faulted loading conditions [5, 6, and 7].

The following discussion is applicable to and includes both stainless steel and carbon steel piping with stainless steel clad.

4.1 Piping system loading conditions

The loads resulting from both normal operating conditions and faulted plant conditions are applied in the evaluation of both the stability and leakage of through-wall cracks or flaws. These conditions conservatively bound other loading conditions on the piping systems of interest. The components for normal loads are pressure, dead weight and thermal expansion.

Normal condition loads are used in the leak rate calculations. For a given length crack or flaw, the application of normal operating condition loads determines the flow area and leakage rate.

For the faulted condition loading, loads associated with the safe shutdown earthquake (SSE) are considered in addition to the normal loads. This load combination is used in the demonstration of crack stability.

4.2 Material characterisation

Material properties for the fracture mechanics evaluations are taken from the certified material test reports (CMTRs). Properties are determined both at room temperature and/or at operating temperature. Forged and cast stainless steels both typically have high fracture toughness values. However, cast stainless steels are subject to thermal aging during service. This thermal aging causes an elevation in the yield strength of the material and a degradation of the fracture toughness. Detailed fracture toughness testing has been performed for cast stainless steel, the results of which are used to establish the end-of-service life (40 or 60 years, as determined by the plant) fracture toughness values for specific materials. Detailed fracture toughness testing has also been performed for the low alloy ferritic steel pipe materials and associated weldments.

4.3 PWR primary loop piping leak rate determination

The determination of leakage crack size is based on the leak detection capability of the plant leak detection systems.

Leak detection

Early detection of leakage in components of the reactor coolant pressure boundary (RCPB) system is necessary to identify deteriorating or failed components and minimise the release of fission products. Regulatory Guide (RG) 1.45 [8] describes acceptable methods to select leakage detection systems for the RCPB.

RG 1.45 specifies that at least three different detection methods should be employed. Plant sump level monitoring and airborne particulate radioactivity monitoring are specifically recommended. A third method can be either monitoring of condensate flow rate from air coolers or monitoring of airborne gaseous activity.

RG 1.45 also recommends that flow rates from identified and unidentified sources should be monitored separately, the former to an accuracy of 10 gpm and the latter to an accuracy of 1 gpm. (Note that plants with coolant activity levels sufficiently low as to suggest radiation monitoring will not detect leakage with an accuracy of 1 gpm have implemented alternate leakage monitoring methods.) Indicators and alarms for leak detection should be provided in the main control room. The sensitivity and response time for each leakage detection system used should be such that each is capable of detecting 1 gpm or less in one hour.

All US PWRs meet or exceed the leak detection guidance of the preceding paragraph. Specific leak detection capabilities of a plant are identified in its technical specifications.

Leak rate calculations

The first step for calculating the leak rates is to determine the crack opening area when the pipe containing a postulated through-wall flaw is subjected to normal operating loads. Using the crack opening area, leak rate calculations are performed for the two-phase choked flow condition. From the actual pipe stress analysis, deadweight, normal 100% power thermal expansion and normal operating pressure loads are used in the calculation of the crack opening area and hence the leak rate. All loads are combined by the algebraic summation method.

It is noted that a through-wall circumferential flaw is postulated in the piping that would yield a leak rate of 10 gpm. A flaw that results in a 10 gpm flow rate is used to assure a factor of 10 in margin between the calculated leak rate compared to the leak detection capability of the plant.

4.4 Fracture mechanics evaluation

The stability of a calculated leakage crack or flaw is demonstrated based on material properties and faulted applied load conditions. Based on extensive analyses, significant margins on crack stability have been demonstrated for the calculated leakage cracks.

4.4.1 *Local failure mechanism*

The local mechanism of failure is primarily dominated by the crack tip behaviour in terms of crack-tip blunting, initiation, extension and finally crack instability. Local stability will be assumed if the crack does not initiate at all. It has been accepted [9] that the initiation toughness measured in terms of J_{IC} from a J-integral resistance curve is a key material parameter defining crack initiation. If, for a given load, the applied J-integral value is shown to be less than the J_{IC} of the material, then the crack will not initiate [9].

If the initiation criterion is not met, then stability is said to exist when the applied tearing modulus value is less than the material tearing modulus value, and the applied J-integral value is less than the J_{MAX} value of the material.

4.4.2 *Global failure mechanism*

Determination of the conditions which lead to failure in stainless steel is done with plastic fracture methodology because of the large amount of deformation accompanying fracture. One accepted method for predicting the failure of ductile material is the plastic instability method, based on traditional plastic limit load concepts, but accounting for strain hardening and taking into account the presence of a flaw. The flawed pipe is predicted to fail when the remaining net section reaches a stress level at which a plastic hinge is formed. The stress level at which this occurs is termed as the flow stress. The flow stress is generally taken as the average of the yield and ultimate tensile strength of the material at the temperature of interest. This methodology has been shown to be applicable to ductile piping through a large number of experiments [9].

5. Compliance with applicable regulations

5.1 *Regulatory requirements*

Title 10, Section 50.46 of the Code of Federal Regulations (10CFR50.46) requires that licensees design their ECCS systems to meet five criteria, one of which is to provide the capability for long-term cooling. Following successful system initiation, the ECCS shall be able to provide cooling for a sufficient duration that the core temperature is maintained at an acceptably low value. In addition, the ECCS shall be able to continue decay heat removal for the extended period of time required by the long-lived radioactivity remaining in the core. The requirements of 10CFR50.46 are in addition to the general ECCS cooling performance design requirements found elsewhere in 10CFR Part 50, in particular the system safety function requirements in General Design Criterion (GDC) 35 of Appendix A to 10CFR Part 50.

The Containment Spray System is required to meet, in part, GDC 38 and GDC 40 of Appendix A to 10CFR Part 50. These criteria specify requirements regarding heat removal from the reactor containment following any loss-of-coolant accident and to control fission products that may be released into the reactor containment.

5.2 *Current regulatory guidance*

The regulations are not specific as to the manner in which ECCS “capability for long-term cooling” is to be demonstrated. The regulations are also not specific as to whether or how debris

generation, as a direct result of a design basis LOCA, is to be determined. Methods that are acceptable to the NRC for determining whether designs maintain a “capability for long-term cooling” and that meet regulatory requirements are currently specified in regulatory guidance. The applicable regulatory guide for this purpose is Regulatory Guide 1.82, *Water Sources for Long-Term Recirculation Cooling Following a Loss-of-Coolant Accident*, Revision 3.

This regulatory guide has undergone significant revision since its initial release in 1974, reflecting new insights and results of ongoing research. The revisions also reflect significant changes in the regulatory treatment of debris generation. As is discussed in the following section, the regulatory treatment has progressed from a fully non-mechanistic treatment (Rev. 0) which only accounts for the effect of debris generation on containment sump performance, to a mechanistic treatment that allows for consideration of the probability of pipe rupture (Rev. 1), to a mechanistic treatment with no allowance for consideration of the probability of pipe rupture (Rev. 2 & Rev. 3).

A summary of the evolution of regulatory guidance addressing debris generation following a LOCA event is given in the following paragraphs.

Regulatory Guide 1.82, Revision 0

The containment recirculation portions of the ECCS and CSS for US PWRs were originally designed and licensed in conformance with Regulatory Guide 1.82 Revision 0⁷ or predecessor guidance. In accordance with guidance contained in Revision 0 to RG 1.82, the “capability for long-term cooling” was demonstrated in a non-mechanistic fashion, by assuming 50% of the containment sump screen area was unavailable for flow due to blockage.

Debris Generation Guidance 1974-1985

- Applicable guidance contained in Regulatory Guide 1.82, Revision 0
- Non-mechanistic treatment
- Assume accident debris results in 50% blockage of containment sump screen(s)

Regulatory Guide 1.82, Revision 1

Regulatory Guide 1.82 was revised in November 1985 as part of the resolution to Unresolved Safety Issue (USI) A-43, “Containment Emergency Sump Performance”. The staff concluded at that time that no new requirements would be imposed on licensees; however, the staff did recommend that Revision 1 to RG 1.82 be used as guidance for the conduct of 10CFR50.59 reviews dealing with change out and/or modification of thermal insulation installed on primary coolant system piping and components. As part of this revision, guidance was added that called for “*evaluation or confirmation of ...debris effects (e.g. debris transport, interceptor blockage, and head loss) ...to ensure that long-term recirculation cooling can be accomplished*”.

For the purpose of defining break or rupture locations, Revision 1 to RG 1.82 refers the user to Standard Review Plan (SRP) Section 3.6.2⁸, which provides guidance for selecting the number,

-
7. Regulatory Guide 1.82, *Sumps for Emergency Core Cooling and Containment Spray Systems*, Revision 0, June 1974.
 8. Standard Review Plan, Section 3.6.2, “*Determination of Rupture Locations and Dynamic Effects Associated with the Postulated Rupture of Piping*”.

orientation, and location of postulated ruptures within a containment. SRP 3.6.2 provides instruction and guidance to NRC staff reviewers regarding break and crack location criteria and methods of analysis for evaluating the dynamic effects associated with postulated breaks and cracks in high- and moderate-energy fluid system piping. SRP 3.6.2 is the primary review guidance for ensuring that a design meets the requirements of General Design Criterion (GDC) 4. GDC 4 requires that structures, systems, and components important to safety shall be designed to accommodate the effects of postulated accidents, including appropriate protection against the dynamic and environmental effects of postulated pipe ruptures.

Compliance with GDC 4 requires that nuclear power plant structures, systems, and components important to safety be designed to accommodate the effects of, and be compatible with, environmental conditions associated with normal operation, maintenance, testing, and postulated accidents, including loss-of-coolant accidents. These structures, systems, and components are to be protected against pipe-whip and discharging fluids. GDC-4 allows such dynamic effects to be excluded from the design basis if the probability of pipe rupture is shown to be extremely low.

For determination of debris generation from identified break locations, RG 1.82 Rev. 1 identifies a multiple region insulation debris model developed in NUREG-0897 as an acceptable model.

Debris Generation Guidance 1985-1996

- Applicable guidance contained in Regulatory Guide 1.82, Revision 1
- Available for use, however, PWR licensees not required to adopt and revise design basis
- Break locations determined per guidance contained in SRP 3.6.2 and Branch Technical Position EMEB 3-1
- SRP 3.6.2 provides guidance for exclusion of dynamic effects of break locations (in accordance with GDC-4) based on low probability of piping rupture under design basis conditions
- Debris generation from identified break locations determined using experimentally developed multi-region insulation destruction model

Regulatory Guide 1.82, Revision 2

Regulatory Guide 1.82 was revised again in May 1996 to alter the debris blockage evaluation guidance for boiling water reactors. While the Introduction section notes that only the section concerning boiling water reactors (BWRs) were changed from Revision 1, a noted change to sections applicable to PWRs is the deletion of any reference to SRP section 3.6.2 for use in determining break locations.

Debris Generation Guidance 1996-2003

- Applicable guidance contained in Regulatory Guide 1.82, Revision 2
- Available for use, however, PWR licensees not required to adopt and revise design basis
- Removed allowance for consideration of extremely low probability of rupture per SRP 3.6.2, BTP EMEB 3-1 and GDC-4
- No specific guidance on break locations or break sizes for PWRs. BWR guidance revised to include consideration of debris generation from a range of break sizes, locations and other properties to provide assurance that most severe postulated LOCAs are calculated
- Debris generation from identified break locations determined using experimentally developed insulation destruction models

Regulatory Guide 1.82, Revision 3

Revision 3 to RG 1.82 was released to provide more detailed guidance for PWRs. Consistent with Revision 2, the guidance calls for determination of debris generation for a range of break sizes, break locations, and other properties to provide assurance that the most severe postulated LOCAs are calculated.

Debris Generation Guidance 2004 and Forward

- Proposed revision 3 to Regulatory Guide 1.82
- Consistent with Revision 2, no allowance for consideration of extremely low probability of rupture per SRP 3.6.2, BTP EMEB 3-1 and GDC-4
- PWR guidance revised to include consideration of debris generation from a range of break sizes, locations and other properties to provide assurance that most severe postulated LOCAs are calculated
- Debris generation from identified break locations determined using experimentally developed insulation destruction models

5.3 Precedence for consideration of fracture mechanics in meeting 10CFR50.46 criteria

5.3.1 GDC-4 – leak before break

In October 1987, General Design Criterion (GDC) 4 in Appendix A to 10CFR Part 50 was revised to allow the use of fracture mechanics to exclude dynamic effects from the design basis of qualified piping (i.e. piping for which the probability of rupture can be demonstrated to be extremely low). Specifically:

“Criterion 4 – Environmental and dynamic effects design bases. Structures, systems, and components important to safety shall be designed to accommodate the effects of and to be compatible with the environmental conditions associated with normal operation, maintenance, testing, and postulated accidents, including loss-of-coolant accidents. These structures, systems and components shall be appropriately protected against dynamic effects, including the effects of missiles, pipe whipping, and discharging fluids, that may result from equipment failures and from events and conditions outside the nuclear power unit. However, dynamic effects associated with postulated pipe ruptures in nuclear power units may be excluded from the design basis when analyses reviewed and approved by the Commission demonstrate that the probability of fluid system piping rupture is extremely low under conditions consistent with the design basis for the piping.” *[Emphasis added]*

The broad-scope rule introduced an acknowledged inconsistency in the design basis by excluding the dynamic effects of postulated pipe ruptures while retaining non-mechanistic pipe rupture for containments, ECCS, and environmental qualification (EQ) of safety-related electrical and mechanical equipment.

The NRC staff subsequently clarified its intended treatment of the containment, ECCS, and EQ in the context of LBB applications in a request for public comment on this issue that was published on 6 April 1988 (53FR11311). In its clarification the staff stated that the effects resulting from postulated pipe breaks can be generally divided into local dynamic effects and global effects. Local dynamic effects of a pipe break are uniquely associated with that of a particular pipe break. These specific effects are not caused by any other source or even by a postulated pipe break at a different location. Examples of local dynamic effects are pipe whip, jet impingement, missiles, local pressurisation, pipe

break reaction forces, and decompression waves in the intact portions of that piping or communicating piping. Global effects of a pipe break need not be associated with a particular pipe break. Similar effects can be caused by failures from such sources as pump seals, leaking valve packings, flanged connections, bellows, manways, rupture disks, and ruptures of other piping. Examples of global effects are gross pressurisations, temperatures humidity, flooding, loss of fluid inventory, radiation, and chemical condition.

The application of LBB technology eliminates the local dynamic effects of postulated pipe breaks from the design basis. However, global effects may still be caused by something other than the postulated pipe break. Since the global effects from the postulated pipe break provide a reasonably conservative design envelope, the NRC staff continue to require the consideration of global effects for various aspects of the plant design , such as EQ, ECCS, and: the containment.

5.3.2 *Industry proposal to apply GDC-4 exclusion to local debris generation*

In a letter dated 4 October 2002 [4], NEI provided its view on the application of the LBB considerations of GDC-4 to local debris generation from a postulated break. NEI presented the position that debris generation, as a result of break jet expansion and impingement forces, is a dynamic effect uniquely associated with pipe rupture and, as such, is appropriately encompassed within the scope of the revised GDC-4.

In its letter, NEI made the following three points:

- Debris generation within the zone of influence of a break is a local dynamic effect covered by GDC-4

The dynamic effects addressed by GDC-4 are delineated in the Federal Register notice that modified GDC-4 (52FR41288): “Dynamic effects of pipe rupture covered by this rule are missile generation, pipe whipping, pipe break reaction forces, jet impingement forces, decompression waves within the ruptures pipe and dynamic or nonstatic pressurisation in cavities, sub compartments and compartments.” The initial blast wave exiting a DEGB and the ensuing break jet expansion and impingement forces are the dominant contributors to debris generation following a LOCA. Other contributors are pipe whip and pipe impact.

- Debris generation does not fall within the scope of functional and performance requirements for containment, ECCS and EQ that were retained in the GDC-4 revision

The rule change acknowledged inconsistencies in the design basis by excluding the dynamic effects of postulated pipe ruptures while retaining non-mechanistic pipe rupture for containments, ECCS, and environmental qualification (EQ) of safety-related electrical and mechanical equipment. As stated in 53FR11311, “...*local dynamic effects uniquely* associated with pipe rupture may be deleted from the design basis of containment systems, structures and boundaries, from the design basis of ECCS hardware (such as pumps, valves, accumulators, and instrumentation), and from the design bases of safety related electrical and mechanical equipment when leak-before-break is accepted”. (Emphasis added).

- For PWR licensees, LBB considerations for debris generation would be applied as part of a revision to design bases that specifically incorporates mechanistic processes addressing debris generation, debris transport and debris blockage

The ECCS recirculation designs for most PWR plants in the US are based on guidance provided in Revision 0 of Regulatory Guide 1.82, *Sumps for Emergency Core Cooling and Containment Spray Systems*. This guidance accounts for screen blockage in a non-mechanistic fashion by assuming that one-half of the vertical screen area of the sump is unavailable for recirculation flow. Since the impact of LOCA-generated debris on sump blockage is not addressed directly through this approach, consideration of leak-before-break for LOCA-generated debris would have no effect on ECCS designs that utilize this guidance in their design bases. Subsequent revisions to Regulatory Guide 1.82 (Revision 1 – November 1985, Revision 2 – May 1996, Revision 3 – draft) have incorporated a more mechanistic process that provides a more phenomenologically accurate, but conservative, estimate of the debris blockage that PWR sumps could experience following a LOCA.

In a letter to NRC dated 30 April 2003 [10], NEI recommended that Revision 3 to Regulatory Guide 1.82 incorporate language that acknowledges treatment of debris generation under the LBB provisions of GDC-4. Specifically, NEI recommended that the following paragraph be included in the proposed revision to Regulatory Guide 1.82:

“Consistent with the requirements of 10CFR50.46, debris generation should be calculated for a number of postulated LOCAs of different sizes, locations, and other properties sufficient to provide assurance that the most severe postulated LOCAs are addressed. In accordance with GDC-4, dynamic effects associated with postulated pipe ruptures (including local debris generation) may be excluded from the design basis when analyses reviewed and approved by the Commission demonstrate that the probability of fluid system piping rupture is extremely low under conditions consistent with the design basis for the piping.”

5.3.3 Status of NRC response to NEI proposal

As of this writing, NRC has not issued a written response to the NEI positions on use of GDC-4 to exclude local debris generation as a local dynamic effect for qualified piping. NRC staff has stated during public meetings that they believe that the requested exclusion of local debris generation is not in accordance with the requirements of 10CFR50.46. Specifically, 10CFR50.46(c)(1) which defines LOCAs as “*hypothetical accidents that would result from the loss of reactor coolant, at a rate in excess of the capability of the reactor coolant makeup system, from breaks in pipes in the reactor coolant pressure boundary up to and including a break equivalent in size to the double-ended rupture of the largest pipe in the reactor coolant system [emphasis added]*.” The preliminary staff position appears to preclude the use of GDC-4 in analyses performed to meet the “long-term cooling” requirements of 10CFR50.46 criteria. Although, it is noted that NRC has reviewed and approved break-size exclusions allowed by GDC-4 in analyses performed to meet the “coolable geometry” criterion of 10CFR50.46.

5.3.4 Use of fracture mechanics to meet 10CFR50.46 “coolable geometry” criterion

Subsection (b) of 10CFR50.46 specifies 5 criteria that must be met by the ECCS. They are:

1. Peak cladding temperature. The calculated maximum fuel element cladding temperature shall not exceed 2 200°F.
2. Maximum cladding oxidation. The calculated total oxidation of the cladding shall nowhere exceed 0.17 times the total cladding thickness before oxidation.
3. Maximum hydrogen generation. The calculated total amount of hydrogen generated from the chemical reaction of the cladding with water or steam shall not exceed 0.01 times the

hypothetical amount that would be generated if all of the metal in the cladding cylinders surrounding the fuel, excluding the cladding surrounding the plenum volume, were to react.

4. Coolable geometry. Calculated changes in core geometry shall be such that the core remains amenable to cooling.
5. Long-term cooling. After any calculated successful initial operation of the ECCS, the calculated core temperature shall be maintained at an acceptably low value and decay heat shall be removed for the extended period of time required by the long-lived radioactivity remaining in the core.

The first three criteria (peak cladding temperature, maximum cladding oxidation and maximum hydrogen generation) are met through the use of approved ECCS models that meet requirements of 10CFR50.46(a). These models meet either the requirements of Appendix K to 10 CFR50.46 or make use of NRC approved best estimate models. These “core response” models model the full range of break sizes (up to and including full double-ended guillotine break of the largest pipe in the reactor coolant system) in accordance with 10CFR50.46(c)(1). The assumptions on break opening time range from “instantaneous” (a requirement for all Appendix K models) to 1 millisecond (for some NRC approved Best Estimate LOCA models). Fracture mechanics considerations are not taken into account in either the Appendix K models or Best-estimate models.

The fourth criterion (coolable geometry) is demonstrated through the performance of dynamic analyses of the assembled reactor vessel, internals, and fuel and is performed for a range of postulated LOCAs in accordance with applicable regulatory guidance. The results of these analyses provide assurance that the forces resulting from the postulated LOCAs will not result in fuel assembly deformation to an extent that would lead to a loss of “coolable geometry.”

For most, if not all PWRs, the range of LOCAs that are considered is limited through application of leak before break considerations, supported by fracture mechanics. Using NRC approved guidance, forces resulting from breaks in LBB qualified piping are not included in the set of analyses performed to demonstrate compliance to 10CFR50.46(b)(4).

The proposed use of fracture mechanics to demonstrate compliance with the fifth criterion (long-term cooling) is significantly more conservative than the NRC approved methods used to demonstrate “coolable geometry”. In the modelling that will be used to demonstrate long-term cooling following a postulated LOCA, a full range of break sizes (up to full double-ended guillotine rupture of largest pipe) will continue to be addressed for all relevant phenomena with the exception of the dynamic effects which impact local debris generation. All other phenomena affecting long term cooling (e.g. break flow, global effects within containment, debris transport, screen blockage) will model a full range of break sizes and locations.

6. Retained safety margins

The determination of debris generation that results as a direct consequence of the local dynamic effects of a postulated pipe break is a single step in the larger effort necessary to assess the recirculation performance of the ECCS and CSS following a design basis LOCA.

In order to calculate plant response to a postulated pipe break event and the potential for significant blockage of the containment sump screens, it is necessary to take into account a wide range of phenomena and processes. Figure 1 illustrates some of the phenomena and processes that must be considered. These phenomena and processes are highly dependent upon plant design and operation as

well as the specifics of the postulated LOCA event. The complexity and multivariate nature of the event progression, coupled with the absence of a comprehensive database addressing the full range of encountered phenomena inevitably leads to a calculation process that accounts for the resulting uncertainties in a conservative manner.

As noted before, typically the analyses investigating ECCS operation during the recirculation phase divide the process into three separate phases: (1) debris generation; (2) debris transport; and (3) debris accumulation and head loss. Each phase of the calculation process, while interdependent, involves its own set of phenomena and uncertainties. Known limitations in the knowledge base of these phenomena and associated calculation methods are typically accounted for in a bounding fashion during each phase of the process. Thus, it is important to note that the more realistic treatment of the debris generation phase using the break characteristics model described in this paper, neither eliminates nor alters the conservative treatment of other phenomena and processes. As such, the overall results from the analyses will retain a significant degree of conservatism.

7. Summary

This paper outlines a method of using fracture mechanics analysis techniques to define pipe break areas for the evaluation of consequential debris generation for post-accident containment sump performance evaluation. The proposed break characterisation model is based on stable leakage crack sizes that generate detectable leaks and have already been calculated for PWR primary coolant piping and, in some cases, surge line piping. The debris generated from the proposed break characteristic model areas are meaningful with respect to sump performance and are based on the actual behaviour of the piping material under normal and off-normal conditions.

For added margin, the proposed break characteristic model incorporates a factor of 1 000 applied to the flow area of a stable through-wall flaw that produces a 10 gpm leakage rate. The geometry of the breach will be taken to be a circular hole in the pipe of interest.

Fracture mechanics analysis techniques have been used successfully, in conjunction with plant leak detection systems, to determine the size of stable cracks for PWR primary loop piping. The leakage flow of these stable cracks has been evaluated to be 10 gpm, or a factor of 10 above the leak detection capability of PWR plants.

It is therefore concluded that the proposed break characteristic model based on calculated stable leakage cracks using proven fracture mechanics techniques provides an acceptable, conservative, yet realistic approach for the evaluation of containment sump performance.

REFERENCES

- [1] Regulatory Guide 1.82, Revision 3, *Water Sources for Long-Term Recirculation Cooling Following a Loss-of-Coolant Accident*, November 2003.
- [2] Moody, F.J., T.A. Green, *Evaluation of Existence of Blast Waves Following Licensing Basis Double-Ended Guillotine Pipe Breaks*, DRF A74-00003, (Provided in Technical Support Documentation of NEDO-32686-A, Utility Resolution Guidance for ECCS Suction Strainer Blockage) August 1996.
- [3] NUREG/CR-6762, *GSI-191 Technical Assessment: Parametric Evaluations for Pressurized Water Reactor Recirculation Sump Performance*, Volume 1, August 2002.
- [4] Marion, Alex (NEI), *Application of Leak-Before-Break Technology to Pipe Break Debris Generation and Request for Public Comment Opportunity*, Letter to Gary Holahan (NRC), 4 October 2002.
- [5] WCAP-15131, Revision 1, *Technical Justification for Eliminating Large Primary Loop Pipe Rupture as the Structural Design Basis for the D. C. Cook Units 1 and 2 Nuclear Power Plants*, [Proprietary] (This topical report is representative of a large number of plant specific analyses performed for Westinghouse designed plants.).
- [6] CEN-367-A, Revision 000, *Leak-Before-Break Evaluation of Primary Coolant Loop Piping in Combustion Engineering Designed Nuclear Steam Supply Systems*.
- [7] BAW-1847, Revision 1, *The B&W Owners Group Leak-Before-Break Evaluation of Margins Against Full Break for RCS Primary Piping of B&W Designed NSS*, [Proprietary] (This topical report is representative of the evaluations performed for the B&W designed plants.), September 1985.
- [8] USNRC Regulatory Guide 1.45, *Reactor Coolant Pressure Boundary Leakage Detection Systems*, May 1973.
- [9] NUREG-1061, *Evaluation of Potential for Pipe Breaks*, Report of the US Nuclear Regulatory Commission Piping Review Committee, Vol. 3, November 1984.
- [10] Pietrangelo, Anthony (NEI), *Comments on Draft Regulatory Guide DG-1107, Water Sources for Long-Term Recirculation Cooling Following a Loss-of-Coolant Accident*, (68 Fed. Reg. 13338), Letter to NRC Rules and Directives Branch, 30 April 2003.

Table 1. Stable leakage crack sizes for PWR primary loop piping

Westinghouse designed plants

Pipe OD (in)	Pipe wall thickness (in)	Stable crack length¹ (in)	Crack opening area (in²)
32.12-37.75	2.21-3.27	2.5-8.55	0.030-0.040

CE designed plants

Case (Type of rack evaluated)	Pipe wall thickness (in)	Stable crack length¹ (in)	Crack opening area (in²)
Circumferential crack in pump discharge	3.0	7.0	0.040
Circumferential crack in hot leg	3.75	7.0	0.040
Axial slot in pump suction elbow	3.0	4.0	0.040
Circumferential crack in pump suction elbow	3.0	11.0	0.040
Circumferential crack in pump discharge	2.5	7.0	0.040

B&W designed plants

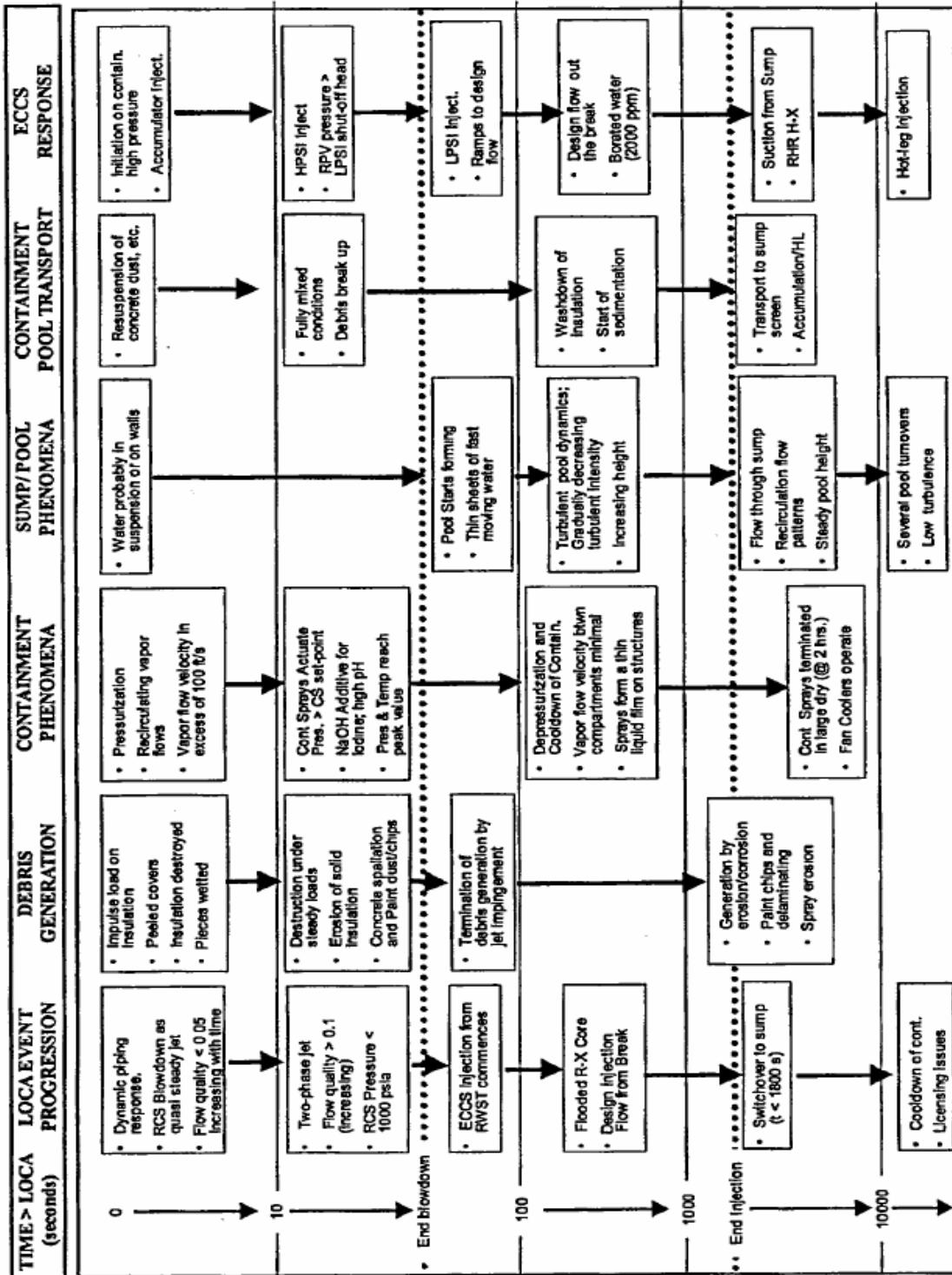
Applicable plants	Piping segment	Stable crack length¹ (in)	Crack opening area (in²)
Plants A, B, C, D, E, and F	Cold leg, straight	9.20	0.075
	Cold leg, elbow	9.00	0.075
	Hot leg, straight	8.00	0.068
	Hot leg, elbow	10.80	0.083
Plant G	Cold leg, straight	9.39	0.065
	Cold leg, elbow	9.41	0.074
	Hot leg, straight	11.39	0.074
	Hot leg, elbow	12.63	0.083

1. Stable crack length is based on a leak rate of 10 gpm.

Table 2. Comparison of break characteristic models for debris generation

Break characteristic models	(A) In-core T/H, M&E model	(B) In-core structural response model	(C) LBB application proposed in 10 April 2002 NEI letter	(D) Fracture mechanics approach
Current application	Used to support analyses that demonstrate compliance to 10CFR50.46(b)(1) and 10.46(b)(2)	Used to support analyses that demonstrate compliance to 10CFR50.46(b)(4)	Proposed for use in analyses that demonstrate compliance to 10CFR50.46(b)(5)	Proposed for use in analyses that demonstrate compliance to 10CFR50.46(b)(5)
Break opening time	Instantaneous	Varies by vendor. Ranges from instantaneous to value determined by fracture mechanics evaluation.	Instantaneous	Instantaneous
Break locations	All high-energy RCS piping (no exclusions)	All non-LBB qualified piping (LBB piping excluded per GDC-4)	All non-LBB qualified piping (debris generation from LBB piping excluded per GDC-4)	All high-energy RCS piping (no exclusions)
Break size	Up to full double-ended guillotine	Up to full double-ended guillotine	Up to full double-ended guillotine	Break size for debris generation determined using fracture mechanic
Similar applications	In-core T/H analyses performed to demonstrate compliance with 10CFR50.46(b)(1) and (2)	Structural calculations performed to demonstrate compliance with 10CFR50.46(b)(4)	Similar to In-core Structural Response model but conservatively retains modelling of instantaneous opening time for consistency with debris generation experimental database.	Similar to In-core T/H analysis model with exception of fracture mechanics based break size modelling in lieu of double-ended break

Figure 1. PWR large break LOCA progression for a large dry containment [1]



CONTAINMENT SUMP CHANNEL FLOW MODELLING

Timothy S. Andreychek

Westinghouse Electric Co., LLC, USA

Daniel J. McDermott

Westinghouse Electric Co., LLC, USA

1. Introduction

In the event of a loss of coolant accident (LOCA) within containment of a pressurised water reactor (PWR) there is the potential for the generation of debris with the attendant concern of containment sump screen blockage. The debris, consisting piping or equipment insulation, protective coatings or paints, concrete dust or general containment housekeeping materials, may be transported to the containment sump during the recirculation phase of emergency core cooling system (ECCS) and containment spray system (CSS) operations.

Unresolved Safety Issue (USI) A-43, "Containment emergency sump performance" had been previously evaluated and declared as resolved by the NRC in 1985. The NRC concluded from the results of research on boiling water reactor (BWR) ECCS suction strainer blockage that newly identified phenomena and failure modes were not considered in the resolution of Issue A-43. In addition, operating experience identified new contributors to debris and possible blockage of PWR sumps, such as degraded or failed containment paint coatings. NRC identified concerns regarding these new contributors to post accident sump performance as Generic Safety Issue (GSI)-191, "Assessment of Debris Accumulation on PWR Sump Performance" and initiated a research effort to address these new concerns.

The NRC subsequently issued Bulletin 2003-01, "Potential Impact of Debris Blockage on Emergency Sump Recirculation at Pressurized-Water Reactors", to address near-term interim measures. The purpose of the bulletin was to request information from the PWR licensees describing:

1. compliance with existing requirements; or
2. the implementation of interim compensatory measures.

The NRC has issued a Temporary Instruction with the primary purposes to:

1. ensure that licensee actions are consistent with bulletin responses and the bulletin's intent; and
2. verify PWR licensees are performing containment condition assessments to ensure that they are prepared to perform sump evaluations soon after guidance is issued.

Further, the NRC intends to issue a Generic Letter which will likely request the following information from licensees:

1. the guidance/methodology used to perform post-accident sump performance evaluation;
2. an implementation schedule for any modifications the evaluation demonstrates to be necessary;
3. a description of interim compensatory measures to be taken until necessary modifications can be performed;
4. a basis for concluding that the debris blockage concerns associated with GSI-191 do not adversely impact sump performance once any necessary modifications are complete; and
5. a description of any controls in place to ensure material brought into containment would not degrade sump performance.

The regulatory focus on this issue will ultimately require licensees to evaluate containment sump performance with a focus on the generation and transport of debris to the sump screens. The method presented here provides licensees with a method to analyse post accident fluid velocities on the containment floor without the complexity and manpower investment required to perform a computational fluid dynamics (CFD) calculation.

2. Analysis approaches

2.1 Computational fluid dynamics approach

Los Alamos National Lab (LANL) Nuclear Design and Risk Analysis Group developed a computational fluid dynamics (CFD) model of a volunteer plant. This volunteer plant provided the necessary information to LANL to develop a CFD model of their containment. The simulation model was formulated to evaluate fluid movement within the volunteer plant's flooded containment floor region following a loss of coolant accident.

The objective of the programme was to determine the expected water velocities in the containment pool following a postulated LOCA scenario and determine the potential for debris transport. The model developed and cases investigated utilised a commercial CFD code. Among the scenarios considered were a large break LOCA with maximum pool depths and safeguards flow rates. The model was used to perform a three dimensional steady state simulation of the fluid flow on the volunteer plant's containment floor and included nearly 500 000 cells. The boundary conditions were provide by the volunteer plant and included flow input points and magnitudes to the containment pool, safeguard pumped flow rates, the containment flood levels and the containment structural configuration. Much of the data provided to LANL had been previously developed by the volunteer plant to support other analyses related to sump debris issues at the plant.

2.2 Nodal Network approach

Westinghouse, under sponsorship of the Westinghouse Owners Group (WOG), undertook an effort approximate the results of the LANL CFD calculation results by utilising a conservative but less complex approach in an attempt to support evaluations by members of the WOG that are expected to be required to support closure of GSI-191. Specifically, the simplified approach taken was to consider the flow about the containment floor as a network of open channel flows.

An open channel flow network model was developed for the volunteer plant and evaluated with network analysis software tool. The results of the Nodal Network calculations were compared to the LANL CFD results. The results compared favourably with the LANL benchmark and are discussed in detail in Section 4.

3. Open channel flow network development

3.1 Purpose

It is fully expected that the licensees will be required to provide an analytical evaluation of the containment sump performance in light of the GSI-191 and the anticipated NRC Generic Letter. By necessity, an integral part of that evaluation will be the transport of event-generated and other debris to the containment sump to ascertain the potential for ECCS sump blockage. Deposition of that debris on the containment sump screen is a concern, as it may result in an unacceptable increase in differential pressure across the screen during operation of the ECCS and CSS as they recirculate fluid from the containment sump.

Integral to debris transport is the fluid velocity from the cooling water sources following the accident scenario to the containment sump. One method of evaluating fluid transport velocities is to develop a CFD model and simulate break and spray flows to determine local velocities. Although the CFD analysis provides a detailed prediction of local flow velocities and turbulence levels in the flow field, manpower requirements in generating the CFD model presents economic basis for pursuing other approaches. Under WOG sponsorship, Westinghouse undertook an effort to evaluate other potential means of predicting flow velocities within containment flooded regions. The efforts focused on a channel flow network analysis of the volunteer plant containment floor. The results of the CFD analysis assisted in developing an appreciation of containment channel flow and also served as a benchmark against which the analysis results could be compared.

3.2 Model inputs

The prerequisites for successful open channel flow network modelling of the post accident ECCS sump include the following inputs. For the Westinghouse effort, the inputs were provided by the identified sources.

3.2.1 Containment configuration

Floor plan and elevation configuration: It is essential that an accurate configuration of containment flooded region be well defined, including obstacles to flow. For the volunteer plant work, plant personnel provided structural and architectural drawings that gave the necessary depiction of the containment sump and flooded plane. Both plan and elevation views are required.

3.2.2 Containment water definition

Water sources: The sources of post accident water into the containment flood plane that were used as the boundary conditions for the LANL CFD analysis modelling were provided by volunteer plant personnel. A total of 24 water sources to the containment floor had been defined for previous containment debris analysis work. The water sources (magnitudes and physical locations) used in the

LANL CFD model were also used as inputs to the Westinghouse Nodal Network model to assure any comparison to the CFD results were valid.

Flood plane: The flooding level on the containment floor is an important parameter in addressing the potential for debris transport to the containment sump. The flooding level used in the Westinghouse Nodal Network calculations was based on the value used by LANL as supplied by volunteer plant personnel. This was done to provide a basis for consistent comparison of the Nodal Network calculations to the CFD calculations.

Post accident flow rates: The post accident containment sump flow rates (including ECCS and CSS flows) are necessary in the determination of velocities in the pool on the containment floor. To provide for a consistent basis of comparison between the Nodal Network calculations and the CFD calculations, the Nodal Network calculations used the same values as were used in the LANL CFD calculations. Flow rates were provided to LANL by volunteer plant personnel.

3.3 Model development

3.3.1 Channel definition

The open channel specification was based on identifying major flow areas from the various sources to the final destination, i.e. the sump. In the case of the volunteer plant containment, the basic channel model definition is a ring of channels around the containment floor with sources defined along the ring header and a destination of the containment sumps. Although most containments are expected to be a similar contiguous ring from sources to destinations, this feature is not essential to the modelling.

The boundaries of the individual channels are defined based on either major structural or flow changes. Essentially, at any point there is a significant change in flow area (increase or decrease) the channel should be terminated and new one defined until the next structural or flow change. The same approach is taken at points of significant flow input to the network. If less than major changes in flow are introduced along the defined channel it conservatively assumed to occur at the beginning of the channel.

Depiction of the volunteer plant channel network definition is illustrated in Figure 1.

Finally, the results of the LANL were used to enhance the understanding of fluid motion on the flooded containment floor and influence the definition of channel boundaries. The visual representation of the CFD results proved valuable in the understanding of flow movement. Figure 2 provides the channel definition superimposed over the velocity vector field.

3.3.2 Flow resistance calculations

Form and channel frictional losses were included in channel resistance to flow. Form losses were primarily based on the reduction or increase in flow areas and were calculated based on hydraulic diameters. K factors were taken from Crane Technical Paper 410 [1].

Frictional losses were calculated based on Altsul's Formula [2] and then verified with the Colebrook-White formula (also given in [2]).

Altsul's Formula:

$$f = 0.1 \left[1.46 \frac{k_s}{D_H} + \frac{100}{R_e} \right]^{\frac{1}{4}}$$

Colebrook-White Formula:

$$\frac{1}{\sqrt{f}} = -2.0 \log_{10} \left[\frac{k_s}{3.71 D_H} + \frac{2.51}{R_e \sqrt{f}} \right]$$

where:

f is the Darcy friction factor coefficient;

R_e is the Reynolds number;

D_h is the hydraulic diameter;

k_s is the roughness height.

Figure 1 provides schematic diagram of the Nodal Network channel definition developed for the Volunteer Plant. Included in the schematic are the calculated friction and form resistances, flow area and hydraulic diameter for each channel. Figure 2 then superimposes the channel network defined on the above basis onto a Cartesian plot of the LANL CFD model results. The figure is a composite of the results presented by LANL personnel at an NRC sponsored public meeting on GSI-191 on 5 March 2003 in Albuquerque, NM [3].

4. Evaluation of Nodal Network method results

4.1 Comparison of Nodal Network and CFD velocities

LANL provided electronic files containing the results of their CFD code simulation at a specific containment elevation. The data was reduced and used to calculate the channel flow velocities at locations corresponding to locations within the Nodal Network developed by Westinghouse. These velocity values were then compared to the velocity values calculated with the Nodal Network to ascertain the success in replicating the calculated flow results. Table 1 provides a tabulation of the comparison of the flow velocities calculated using the Nodal Network described above and those calculated at corresponding locations with the LANL CFD model. This comparison is for a large break LOCA in the lower left loop compartment with maximum ECCS and containment spray flow rates and a maximum flooding level.

The results compare very favourably with the network analysis providing slightly higher flow velocities. This result should be expected since typically the width of the channel is not the full width of the flow area but represents only the major flow area. The exception to the comparable comparison occurs in junction between nodes 10 to 7. At this junction, the calculated flow rate from the CFD data reduction appears to be inconsistent with the specified boundary condition of 1021 gpm flow out of the lower left compartment of the containment that contains the postulated RCS break. Using a revised

flow rate that is consistent with the calculated velocities from the loop compartment, the velocity comparison is more acceptable for all channels. This comparison of these revised calculated flow rates is shown in Table 2.

4.2 Discussion of advantages, limitations and cautions

The Nodal Network approach does have limitations with respect to the application of CFD. Two specific examples are:

- The Nodal Network approach does not allow for the calculation of local velocity effects, such as flow around objects in the flow stream.
- The Nodal Network approach does not calculate the turbulence level in the flow field.

In the first case, “dead zones” of stagnant fluid that are predicted by CFD models will not be predicted by Nodal Network models. In the second case, turbulence predicted by CFD models that might cause degradation of certain insulation and debris types is not predicted by Nodal Network models.

The Nodal Network approach may also have some benefits over the application of CFD. For example:

- Since Nodal Network approach is based on basic engineering principles, the model may be developed by plant engineering personnel. It follows that the model development may be accomplished more quickly, perhaps less expensively, and without specialised computer software (the equations may be solved by in a spreadsheet).
- Even with the limitations noted above, a Nodal Network may be used to gain quick insights to debris transport.
- Nodal Network results might indicate that a containment has sufficient amount of transportable debris that further refinement of flow calculations (use of CFD models) is not warranted.
- A Nodal Network may also be used parametrically to assess the sensitivity of various parameters, such as the amount of a type of debris in a specific location, on the amount of debris transported to the containment sump.

It is also noted that the Nodal Network and CFD approaches have similar data needs. Thus, much of the data to be identified and collected to develop a Nodal Network model is also needed to develop a CFD model. Thus, if the application a Nodal Network model suggests that the development of a CFD model is warranted, much of the data collection to support the Nodal Network is applicable to the development of the CFD model.

Table 1. Comparison of Nodal Network and CFD fluid velocities for volunteer plant, maximum flood level and maximum ECCS and CSS flow rates

Connected nodes		Nodal Network model fluid velocity	CFD model fluid velocity
From	To	(ft/sec)	(ft/sec)
2	3	0.042	0.057
3	4	0.135	0.120
4	5	0.381	0.296
5	6	0.449	0.400
6	7	0.594	0.457
8	9	0.053	0.034
9	10	0.158	0.084
10	7	0.315	0.660

Table 2. Comparison of Nodal Network and CFD fluid velocities for volunteer plant, revised flow rates for based on loop compartment velocities

Connected nodes		Nodal Network model fluid velocity	CFD model fluid velocity
From	To	(ft/sec)	(ft/sec)
2	3	0.084	0.057
3	4	0.165	0.120
4	5	0.438	0.296
5	6	0.490	0.400
6	7	0.642	0.457
8	9	0.015	0.034
9	10	0.080	0.084
10	7	0.682	0.660

5. Summary

5.1 Conclusions

Based on the comparison of channel flow Nodal Network calculations to CFD calculations presented in this paper, it is concluded that the Nodal Network technique may be applied to the determination of post-accident fluid velocities in the flooded containment regions. Given accurate input and boundary conditions, the network analysis approach can be used to provide reasonable, conservative fluid velocities in the fluid pool formed post-accident on the containment floor.

A Nodal Network tool, similar to the one described in this paper, may be developed, maintained and used by the plant engineering staff without specialised codes or training. Sensitivity calculations performed using a Nodal Network model may be used to identify when further, more detailed fluid analyses may not be warranted; that is, debris loading on the sump screens estimated from the Nodal Network model are sufficiently large such that additional refined analyses would not be beneficial. Furthermore, much of the effort to develop the input for a CFD model is common to that required for a Nodal Network model; both models use much of the same data.

Given the above, it is suggested that the use of a Nodal Network approach is a reasonable tool that may be used to evaluate both the bulk fluid movement and bulk debris movement in the containment pool post accident. Furthermore, a Nodal Network approach may also be used to support and guide the application of a more detailed CFD approach.

5.2 Guidance for future application

As a minimum, the following information and guidance is provided for the analyst to support the successful application of a Nodal Network approach. The model definition data is also considered necessary to support the successful application of a CFD approach.

Model definition data (see Section 3.2 for additional clarification):

- accurate physical configuration of containment flooded region;
- sources of post accident water flowing into the flood plane;
- definition of the flooding elevation;
- ECCS and containment sump flow rates.

Channel definition guidance:

- Channels should be defined at every major restriction and expansion of flow area.
- Significant portions of the containment floor are not active in the transport of debris (the construction of smooth velocity vectors assist in the definition major active flow paths and therefore channel definition).
- The velocity vector profiles provided by the LANL illustrate the active flow areas versus pooling regions.

REFERENCES

- [1] “Flow of Fluids Through Valves Fittings and Pipe”, Crane Technical Paper No. 410, 1981.
- [2] Montes, Segio, (1998) “Hydraulics of Open Channel Flow”, American Society of Civil Engineers.
- [3] DeCroix, David (Los Alamos National Laboratory), “Volunteer Plant Containment Pool Flow Analysis”, Nuclear Design and Risk Analysis Group, Presented at NRC Public Meeting, 5 March 2003.

Acknowledgments

Los Alamos National Laboratory personnel are acknowledged for their exhaustive work in generating the CFD analysis of the volunteer plant containment pool flow, and their willing support in providing data and guidance in the reduction of the CFD data.

The volunteer plant personnel are acknowledged for their support of this effort in providing the necessary containment architectural and structural drawings and assistance in understanding containment configuration as well as boundary condition data.

Figure 1. Schematic of Nodal Network for volunteer plant

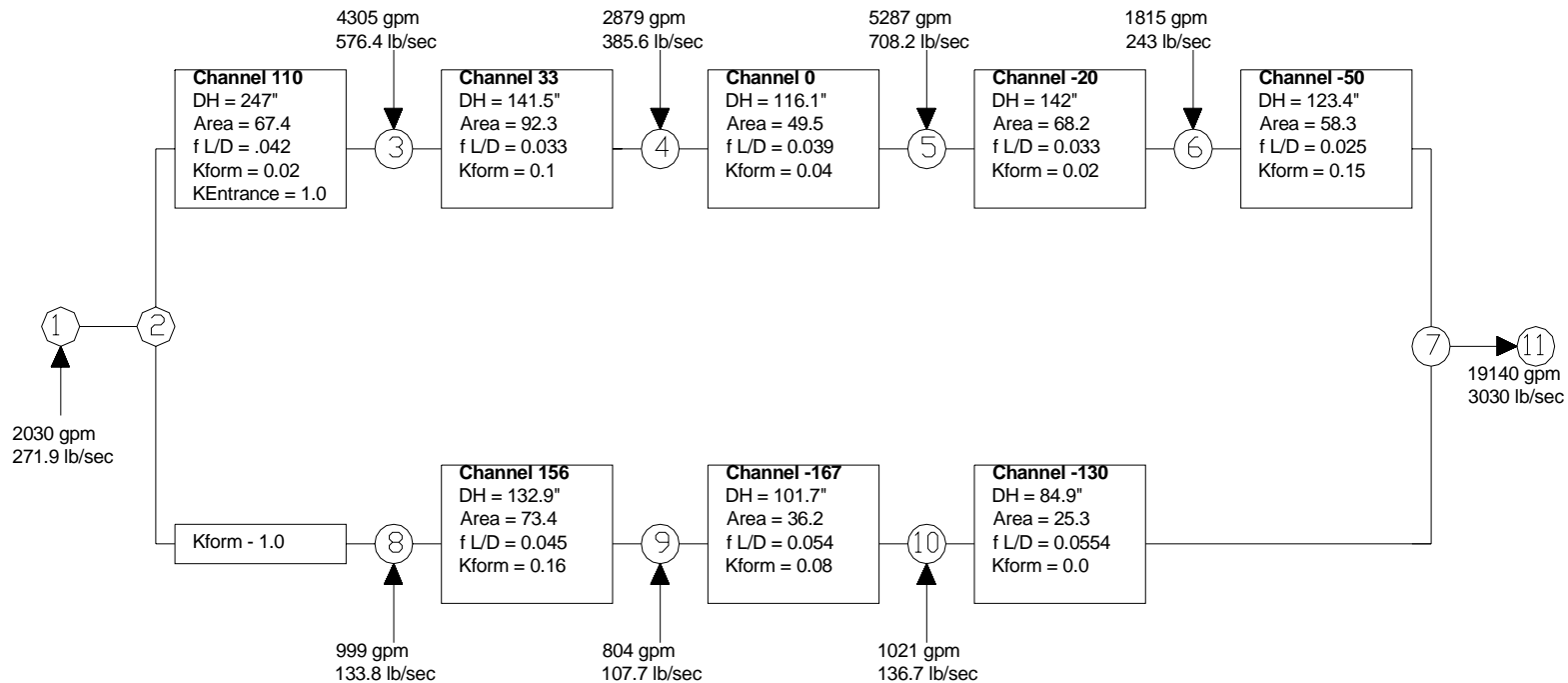
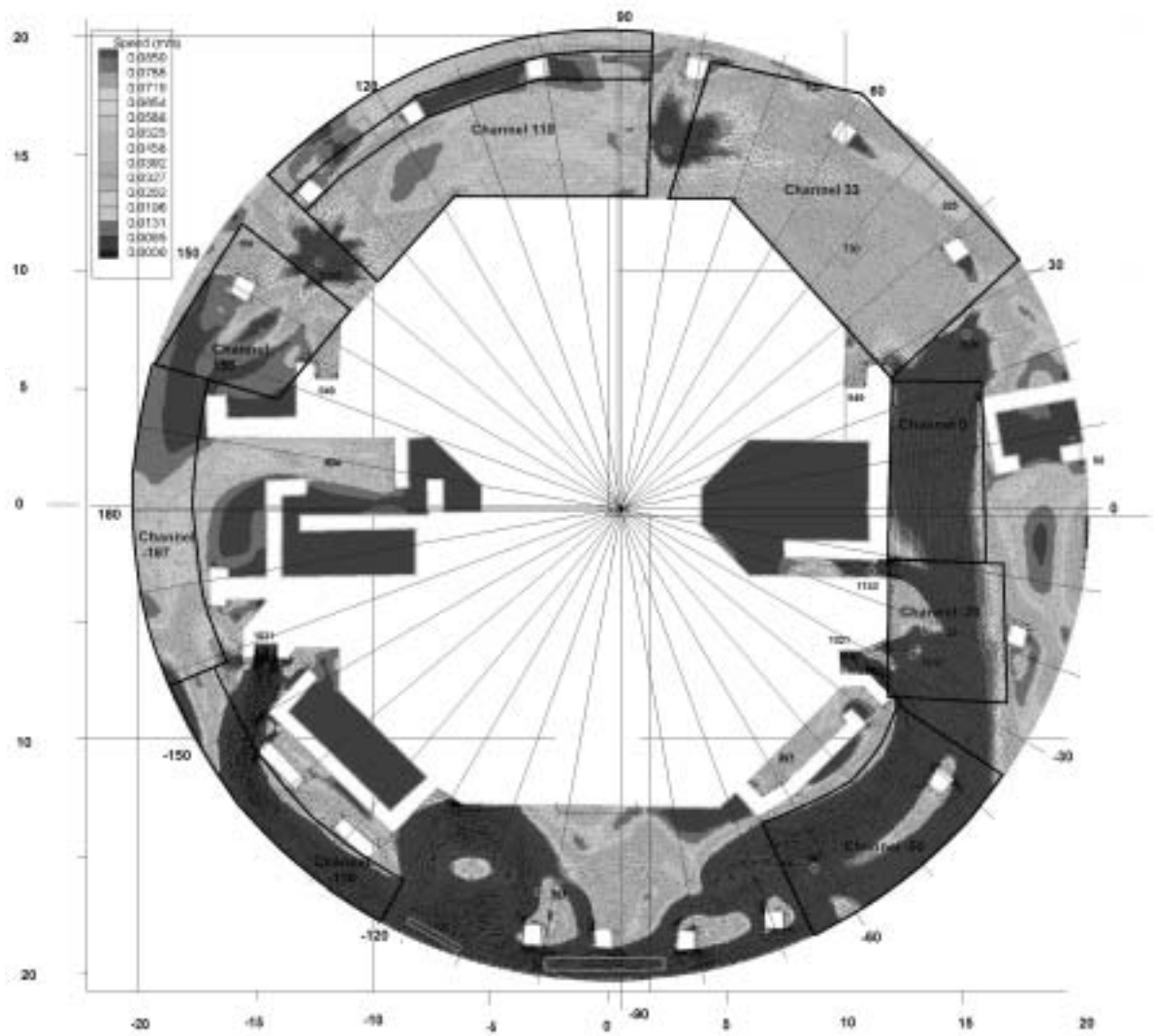


Figure 2. Nodal Network overlay onto CFD model of volunteer plant [3]



SESSION 4

INDUSTRY SOLUTIONS

Chairpersons: Mr. A. Vandewalle (AVN) and Mr. J. Butler (NEI)

HIGHLIGHTS

Five papers were presented in this session which described industry solutions for this issue in Belgium, Switzerland and the US. Two kinds of presentations were given. The first three presentations were from utilities or their engineering support that were studying the sump clogging issue, looking for solutions. The other two presentations concerned researches conducted by the industry, focusing on specific topics related to the debris source term (coatings and insulation materials).

1. Search for a solution

Most utilities seem to be convinced that the sump clogging is a real issue that must be addressed and solved. One part of the solution seems to be a significant increase of the strainer surface area. Another possibility to improve the situation is to modify the spray and/or on the recirculation flow rate, aiming to reduce the amount of debris generated and transported to the sump strainers. The impact of these actions on the safety studies and on the equipment was discussed.

Several utilities and designers presented that their specific designs are such that the sump clogging is not a significant safety concern for their plants if certain combinations of insulation materials are avoided or minimised. This is the case for German design PWRs. The associated debris impact assessment considered the use of strong cassette type insulation, the break preclusion concept, and the German PWR design which has no spray system with a sump geometry resulting in a low degree of turbulence at the sump floor. According to these specificities, the Germans and Swiss considered that the debris source term as well as the debris fraction transported to the strainers are relatively small and the sump should not be clogged during the recirculation phase.

Plant-specific ECCS blockage solutions anticipated to be used by US PWRs were reviewed by Framatome ANP of USA. These include solutions such as: reduction of ECCS flow rate or containment spray flow (for plants with excess decay heat removal margin) to reduce debris transported to the sump screen; enhancement of housekeeping efforts to reduce latent debris; installation of debris traps; use of enlarged passive strainers; use of active strainers, etc.

2. Industry research on specific topics (coatings and insulation materials)

As far as coating is concerned, especially no-DBA-qualified coatings, similar to insulation materials, it is important to determine the amount of generated debris and the behaviour of these with regard to the transportation and to the head losses on the strainers. The head losses due to insulation, including the effect of particles, seem to be well known. Detailed and validated correlations were developed in NUREG/CR-6224. The use of the NUREG/CR-6224 correlation to predict the head-losses for a specific case is a very difficult task that has to be performed only by experts.

EPRI and the Nuclear Utility Coating Council (NUCC) are conducting a research programme to investigate the actual effect of PWR post-LOCA environment on original equipment manufacturer's (OEM) protective coatings (paint) on components installed in US PWR containments.

ACTIONS TAKEN IN THE BELGIAN NUCLEAR POWER PLANTS FOR THE RESOLUTION OF THE GSI-191

Jean-Charles Delalleau
Electrabel, Brussels, Belgium

**Caroline Delveau, Guillaume du Bois d'Enghien,
Louis Vandermeeren and Jacques Pirson**
Suez Tractebel Engineering, Brussels, Belgium
jacques.pirson@tractebel.com
tel. +32/2/7738377 fax +32/2/7738900

Abstract

The emergency core cooling system (ECCS) of a nuclear power plant supplies cooling water to the reactor vessel in the case of a loss of coolant accident (LOCA). A LOCA generates debris by the force of coolant impinging upon pipe insulation and entraining a wide variety of particulate matter from the reactor building surfaces that the coolant flows over. During the recirculation phase following a LOCA, if a sufficient quantity of debris accumulates on the sump screens, the ECCS pumps' suction flow path can be reduced significantly, causing a drop in the available NPSH and, eventually, a loss of pump flow. If the ECCS flow is lost for a sufficiently long time, the core may become uncovered and overheat, causing severe damage to the fuel.

Since the Barsebäck strainer event (July 1992), studies and experiments are being undertaken all over the world to provide a better understanding of how the different types of debris are generated, distributed, transported, and how they accumulate on the sump screens.

All results of current experiments and research are not yet available. Nevertheless, a compensatory action plan was defined early last year to be applied to all Belgian units:

- Each nuclear power plant in Belgium has been inspected by a team of engineers who examined and documented their particular situations with respect to debris generation and potential sump blockage. During these inspections (called "walkdowns"), the physical configuration of the sumps, the type and state of thermal insulation and coatings are noted, along with any potential sources of debris and all information that may be useful for future assessment.
- Plant housekeeping procedures were analysed for any possible links to debris generation and adaptations were proposed when required.
- To reduce the risk of sump clogging, modifications of the post-accident operating procedures were analysed and mitigating actions were proposed.
- Solutions which have been applied at foreign power plants are being scrutinised. Lessons learned from a global study of the problem will yield a palette of possible solution elements which may be tailored to solve the problems encountered at any particular plant.

New information and regulating documents have been issued in 2003, in particular the revision 3 of the RG 1.82. and the draft of the Evaluation Methodology by the NEI. Based on the conclusions of plant inspections, on available results of experiments and research and on new regulation requirements, further actions are being defined in order to assess or improve the sump configuration and performance of Belgian nuclear power plants.

1. Sump configurations in the Belgian NPPs and reassessments

Seven PWR units are in operation in Belgium. These units are either of Westinghouse or Framatome design. Doel 1 & 2 are both 2-loop units. Doel 3 & 4 and Tihange 1-2-3 are all 3-loop units. See Table 1.

Table 1. The Belgian nuclear power plants

Units	Doel 1 & 2	Doel 3	Doel 4	Tihange 1	Tihange 2	Tihange 3
Type of reactor	PWR Twin units	PWR	PWR	PWR	PWR	PWR
NSSS Supplier	ACEC-Cockerill (Westinghouse licence)	FRAMACECO	ACECOWEN	A.C.L.F. Consortium	FRAMACECO	ACECOWEN
Commissioning year	1974-1975	1982	1985	1975	1983	1985
Electrical power (net) in MW	392.5 per unit	1 006	985	962	1 012	1 015
	FRAMACECO: Framatome + ACED + Cockerill ACECOWEN: ACEC + Cockerill + Westinghouse A.C.L.F.: ACEC + Cockerill + Creusot-Loire + Company "Société Franco-Américaine de Constructions Atomiques"					

The ECCS sumps at 5 of the 7 NPPs in Belgium were originally designed considering the US regulations and standards issued earlier. Nevertheless, the layout of the containments and the design of the sumps are different for all units.

At Doel 1 & 2, the oldest NPPs in Belgium and at Tihange 1, the sump screens were already modified in the late eighties, as part of the first decennial safety reassessments performed for these units. The requirements of NRC RG 1.82 Rev. 0 were taken into account.

The situation of the sumps was re-evaluated for all the units in the early nineties as part of the 10-year safety re-evaluations [1]. The RG 1.82 Rev. 1 and NUREG 897 Rev.1 were taken into account (see Table 2).

Table 2. ECCS and CSS Strainer characteristics of the Belgian plants

Unit	Doel 1	Doel 2	Doel 3 new SG	Doel 4 new SG	Tihange 1 new SG	Tihange 2	Tihange 3 new SG
ISBP flow rate (m ³ /h)	2 x 377	2 x 377	3 x 470	3 x 590	2 x 670	3 x 470	3 x 590
ISHP flow rate (m ³ /h)	–	–	3 x 250	3 x 290	–	3 x 250	3 x 290
CSS flow rate (m ³ /h)	–	–	3 x 550	3 x 650	ORC: 2 x 612 IRC: 2 x 504	3 x 520	3 x 555
Filtration surface (m ²)	26.5	23.5	3 x 23.3	24.1 + 24.4 + 24.9	ECCS/CSS ORC: 21.7+23.8 CSSIRC: 2 x 7.5	ECCS: 3 x 9.6 CSS: 3 x 7.5	ECCS: 3 x 12.7 CSS: 3 x 9.5
Mesh size (mm)	3 x 3	3 x 3	5 x 5	5 x 5	3.25 x 3.25	6 x 6	6 x 6
Insulation materials (1)	FG	FG	FG + MW	NU + FG + MW	NU + FG + MW	FG	NU + FG + MW
Insulation small debris (m ³)	13.7	13.7	25.0	21.3	20.3	25.0	22.9

1. FG = Fiberglass; MW = Mineral wool; NU = Nukon.

Considering the lessons learned from the Barsebäck strainer event, the regulatory requirements and performed analyses (inventory of the debris in case of a LOCA and possible blockage of the reactor pool evacuation system – no strainer experiment has been conducted in Belgium), the strainers at Doel 1 & 2 were subsequently enlarged in 1996. Since then, no strainer modification was carried out in any of the other Belgian units [2].

The models utilised for the calculations of the volume of debris generated were the double cone model for Doel 1 & 2, and the spherical model for all other units. Calculations showed however that the NPSH margin to ECCS and CSS pump cavitation at nominal recirculation flow rate is relatively small for some of the units. Furthermore, all of them are characterised by a very low approach velocity (less than 2 cm/s); this is very favourable for the sump clogging issue.

At that time, it was recognised that some phenomena should be considered in the sump screen assessments, but that insufficient data was available for this purpose; they are the following:

- structure modification of the material (devitrification);
- aging effect on material;
- filtration phenomenon of small particles (by insulation material);
- proportion of debris reaching the sump filters;
- sedimentation of debris;
- influence of pH;
- debris bed compaction (porosity, thickness) and combined debris beds;
- uncertainty.

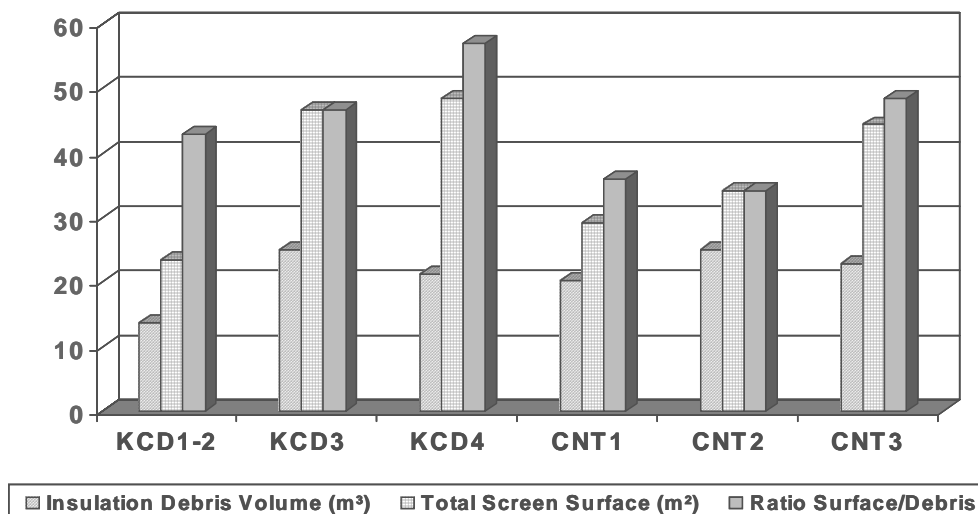
In the late nineties, the sump issue was still under discussion; in fact it was decided to follow the developments in other countries (mainly in the United States) in order to determine whether or not a new reassessment is necessary, but no tangible result has been reached and no corrective action has been decided. In the meantime, plant modifications with a positive impact on the sump issue were made:

- reduction of the ECCS recirculation flowrate in the Doel 1 & 2 units;
- possibility to back up the ECCS pumps by the CSS pumps (connection of the pump discharges – all units except Doel 1 & 2);
- interconnection of the 3 RWST tanks in Tihange 2 & 3;
- use of Nukon insulation for the replaced steam generators.

After the publication of the Los Alamos report in 2002, the Belgian Safety Authorities requested that initiatives be taken in order to define corrections if necessary for the Belgian plants.

An attempt was made to position the Belgian plants among the 60 US plants of the report; it didn't succeed as it would require the application of the models used for the classification of the US plants. Furthermore, the purpose of the Los Alamos report was not to classify the plants, but to show if sump screen clogging is an issue for the American PWR plants.

Figure 1 : Ratio Surface/Debris for plant comparison

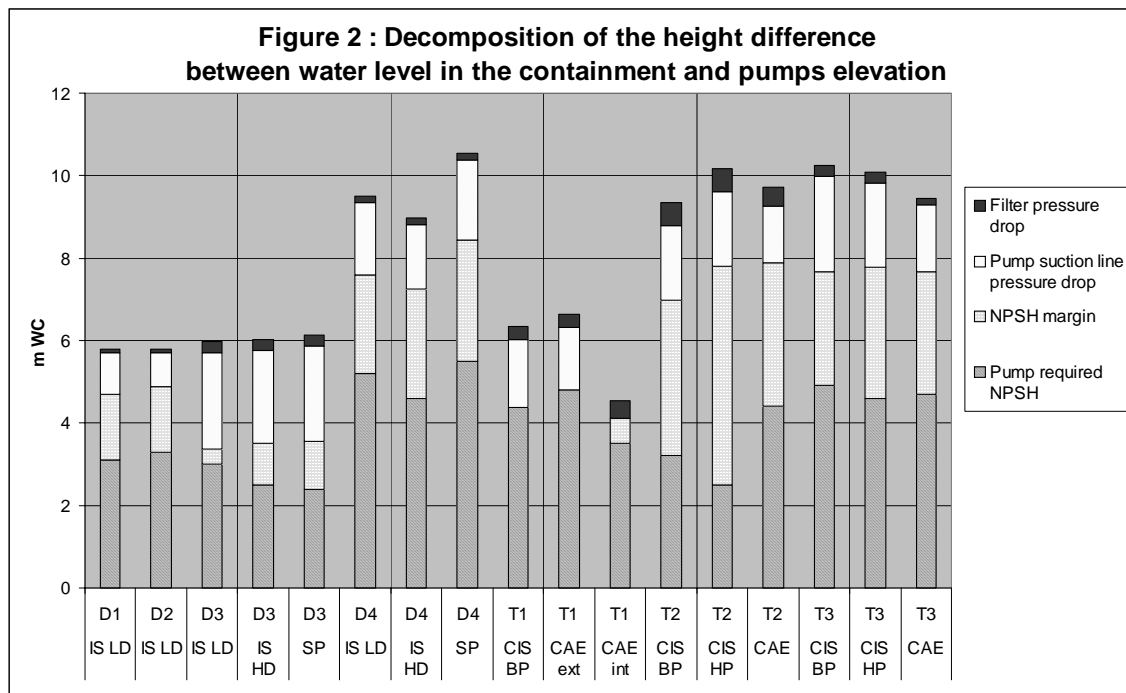


A rough comparison can be made between the plants comparing the screen surface with the debris volume; the higher the ratio surface/debris, the less sensitive to sump clogging the units are (see Figure 1). Doel 4 has the best ratio. However, this is insufficient to “quantify” the risk for the plants. Note that the units in Doel have a qualified ventilation system normally used to cool the containment atmosphere and allowing to shut down the containment spray system in the middle term after an accident. The units in Tihange have a strainer and suction line separated for the ECCS and CSS pumps.

Also, per NUREG-6808 [5], Figure 5-2, the settling velocity of insulation fibers occurs at a minimum rate of 1 mm/sec. Based on the recirculation actuation signal sump levels and on the water level in the containment, all of the insulation would have settled to the floor in almost all of the units (except Doel 1&2 and Tihange 3): enough time elapses for all of the insulation and coatings debris to settle onto the floor after the initial washdown phase is complete.

Furthermore, the approach velocity at the sump screen is very low for all plants (less than 2 cm/s) and even less than 1 cm/s (i.e. 0.04 ft/sec) for Doel 1-2; for these units, the velocity is thus less than the minimum screen retention velocity listed in NUREG-6808, Table 5-1.

2. Analysis of the last reassessment results



When examining the results of the sump assessment studies, some interesting conclusions can be drawn (based on the RG 1.82 Rev. 01). These results are summarised in the Figure 2 showing the decomposition of the available height resulting from the difference between the minimum water level in the reactor containment and the ECCS and CSS pumps level (in terms of pressure losses in the filters and in the pumps' suction lines, required NPSH and NPSH margin).

The following conclusions can be drawn:

- High margins for the Doel 4, Tihange 2 and Tihange 3 plants.
- NPSH margin may have different meanings; it is more important to have a sufficient margin in Doel 1-2 where LHSI pumps are the only pumps used in recirculation without backup. Respecting an absolute positive value is not a sufficient criterion.
- Substantial pressure losses in the pump suction lines. A more detailed model may reduce the conservatism.
- Limited impact of the screen surface increase on Δp in the filters in some cases.
- The impact of the insulation type depends on the initial Δp in the filters (e.g. consideration of Nukon insulation on the SGs has a higher impact in Tihange 2 than in Doel 3).

3. Action plan for Belgian NPPs [3]

A compensatory action plan to be applied to all Belgian units was defined and approved by the Belgian Safety Authorities early last year (2003). This plan is very similar to the interim compensatory measures that have been implemented or that will be implemented in the United States as requested by the US-NRC bulletin 2003-01.

3.1 Containment walkdowns and cleanliness controls

As first action of the plan, each nuclear power plant in Belgium (except one) has been inspected in 2003 by a team of engineers who examined and documented their particular situations with respect to debris generation and potential sump blockage. The NEI 02-01 guide [4] was used as basis to define the methodology for these walkdowns performed during the refuelling outages. One walkdown was attended by a NEI expert. The last walk down will be performed after the workshop (in March 2004), on the Tihange 1 unit.

During these inspections (called “walkdowns”), the physical configuration of the sumps, the type and state of thermal insulation and coatings are noted, along with any potential sources of debris and all information that may be useful for future assessment.

The list of needed repairs is transmitted every day to the plant maintenance services in order to schedule the interventions as much as possible during the outage.

Plant housekeeping procedures are analysed for any possible links to debris generation and adaptations are proposed when required.

3.1.1 Walkdowns objectives

The objectives are to identify and record:

- the potential debris generated by structural damages that could possibly occur in accidental conditions;
- the erection defaults or the significant damages to components and structures;
- the abnormal dust depositions on floors, gratings, components, etc. and the foreign materials likely to stay in the reactor building after start-up (foreign material exclusion);
- the possible flow paths and the recirculation water and/or debris holding spots;
- the state of the recirculation filters, the sumps and their structures.

The scope of the walkdowns was reduced compared to the NEI guide: it was decided not to perform the full mapping of the insulation material, but to make spot checks, concerning both thickness and used materials in order to correlate with the design documentation.

As the walkdowns progressed, the scope was increased on different bases:

- In the units where Calcium Silicates were found, a more detailed inspection was performed: the aim was to locate, identify and quantify the related materials throughout the whole building, including exposure considerations (exposed to spray or to a high/medium energy line break).
- The layout of the sumps and their structure was thoroughly checked, along with the available space left in the nearby areas (for potential surface increase). A complete set of photographs was taken to have a “complete 3-D model” of the sumps. Several system and equipment experts were invited to these inspections in order to have as much as possible feedback.
- An inventory of the panels and signs used in the different units was performed.

- As the findings were to be used by the Utility to organise repairs, clean-ups, ..., other information was also collected in order to plan these works (e.g. the need for scaffolding, harnesses, ladders ...).
- Samples of material for further analyses were also taken.

3.1.2 Organisation

The inspections, involving one system engineer, one layout expert and one insulation material expert, are performed with observation forms, and as many photographs as possible are taken in order to keep track of the comments (about 400 comments per walkdown). These comments are entered in a database which correlates the photographs, the location, the type of remark (insulation material, dust...), the comment itself, the need for scaffolding, the action/non action category of the comment, the questions raised and the status of these questions. Also, a set of layout drawings (5 to 6) of the different levels of the reactor buildings are brought together with the photographs in order to create maps allowing to recover the exact locations of the comments.

To allow the Utility to solve a maximum number of problems during the outage (erection defects, significant damages, foreign material presence, or areas to be cleaned), the comments are classified in action/ no action categories and passed on every day to the maintenance teams in order to allow if possible a repair or cleanup of the inspected areas during the outage.

The walk down period lasted between 4 and 6 full days, on a daily 7 to 8 hours of inspection basis. On top of that, 3 hours a day are needed for reporting (report and meeting). An extra inspection day was planned to state the general “as left” situation shortly before the start-up of the plant and to evaluate the working methodology of the maintenance teams.

The reports of the walkdowns were discussed with the Safety Authorities; the remarks were confronted with their own findings.

3.1.3 Lessons learned from the containment wal downs

As the situations and practices are different from plant to plant, it was tried to work out from the walkdowns the best practises in terms of:

- Housekeeping in general. Strong procedural requirements to keep containment clean and keep debris out of the sump must be included in the existing procedures;
- Materials and fasteners used for the signs and panels in the reactor buildings and for the protections installed to reduce the risks of injuries for the workers should be qualified;
- Housekeeping and cleaning-up of the sump areas on a regular basis (for evidence of structural distress, abnormal corrosion or any kind of damage) as well as the refuelling pool draining lines, the gutters that collect fluid leaks or clean-up waters on the floors (open-air drains);
- Check-up of the containment sump strainer to be performed by an ECCS System or Safety Engineer, or the scrutiny of foreign material in the lowest level of containment to be introduced in an adequate procedure (still to be discussed);
- State of the trash racks installed in front of the sump screens at the level of pipe penetrations (existence of large holes);
- Housekeeping of the plates protecting the vertical electrical racks when penetrating a floor;

- Regular inspection of the lamps (TL tubes) used all over the reactor buildings;
- Fire protection boxes, electrical cabinets or other empty boxes to be cleaned up;
- Use of “sealing” materials unqualified for the LOCA conditions like mastic, aluminium tape, silicone... to be prohibited;
- Periodical control of the paintings and coatings on the metallic liner, walls, supports and components inside the reactor building to be continued. Repair/replacement activities must assure that the amount of Service Level I coatings outside the zone of influence that could come loose from the substrate during a loss of coolant accident is minimised.

3.2 Operator support and training

How to prevent, delay and manage the cavitation and sump blockage risk after an accident? To reduce the risk of sump clogging, modifications of the post-accident operating procedures and mitigating actions are being analysed.

One of the interim compensatory measures of Bulletin 2003-01 involves procedure modifications to delay switch-over to sump recirculation operation by shutting off unnecessary pumps while in injection mode indeed. However, it was rapidly recognised that, if the shutting off an unnecessary train of pumps could provide a positive benefit by reducing the transport velocity to the sump strainer, thereby reducing debris transport to the sump, such an operator action can be harmful if performed too quickly after an accident. A new start of these pumps could fail. Therefore, it was suggested to await the conclusions of the Westinghouse Owners Group (WOG) on this topic before any modification of the Emergency Operating Procedures.

Also, the plant operators have identified flow path alignments to provide alternative water sources similar to those foreseen in the Severe Accident Management Guidelines: this could allow core and containment atmosphere cooling in the event that the sump is blocked. Obviously, water that can be injected in the containment must be compatible with the core criticality and containment structural analyses. These actions to provide alternative water sources have been compiled in one dedicated plant Emergency Operating Procedure.

One unit has already a procedure for high-flow backflushing of the sump strainers. It is not intended to develop such a procedure for the other units (not possible due to the presence of check valves or the flowrate being too low to permit efficient backflushing).

The appropriate staff and plant operating personnel have received training to be aware of the possibility of sump screen clogging, to improve the capabilities of the Control Room personnel to handle such symptoms and to take appropriate action such as reducing pump flow rates. It is possible that specific instrumentation should be installed.

3.3 Examination of technical solutions

Contacts have been taken with filter suppliers (not limited to the American approach – French, German and Swedish approaches are considered) in order to collect information about possible solutions.

Furthermore, solutions which have been applied in foreign power plants have been scrutinised. Lessons learned from a global study of the problem will yield a palette of possible solutions which may be tailored to solve the problems encountered at any particular plant.

We can also point to the solution studied several years ago for the Chooz A NPP, where a jet pump was installed in the sump recirculation suction line to solve the NPSH problems of the ECCS pumps, as part of the upgrading of the Safety Injection System performed in the mid 1980s for the SENA power plant (Chooz A unit). The driving fluid was taken at the outlet of the sump heat exchangers, part of the low pressure circuit of the recirculation system. The need for this modification was the discovery of a NPSH problem (as was the case for other plants of the same generation: e.g. Zorita, Beznau, Trino) for the high pressure safety injection pumps. This problem was linked to the application of the RG 1.1 requirement considering the boiling of the water in the sump in post LOCA recirculation.

This system was successfully tested and accepted by the French Safety Authorities.

3.4 Follow-up of the analytical developments for sump performance evaluation

The “theoretical” developments for an analytical approach supporting the emergency containment sump performance performed in the United States or in countries like France and Germany are followed up; in particular, the recent draft for a “PWR containment sump evaluation methodology” established by the NEI is being examined.

The needs and the methodology for a future assessment of an adequate NPSH available for the ECCS and containment spray pumps are still to be discussed with the Belgian Safety Authorities.

3.5 Belgian utility willingness to improve the plant safety level

Even if the regulatory framework and the new assessment methodology are not yet available and frozen, the Belgian utility has notified its intention to improve the situation of the Belgian plants.

Modifications to be realised in 2004 are being studied. The situation being very different from one unit to the other, each unit has its own problems or layout constraints. Increase of the screen surfaces in the same conditions as the present ones is the most probable modification which will be made.

The modification of the screen mesh in some units to make it compatible with the fuel assembly debris catchers is also being evaluated.

4. Summary of interim compensatory actions and conclusions

Belgian plants have implemented or are evaluating the following compensatory measures:

1. Operator training on indications of and responses to ECCS and CSS pump cavitation and sump clogging.
 - ✓ Enhancements to the operator training for these operating conditions (implementation planned in the late 2003 – early 2004).

- ✓ Procedure actions to delay switchover to containment sump recirculation being evaluated in the framework of the WOG project on this topic.
 - ✓ Identification of the alternative water sources for potential use in accident management guidelines.
2. Aggressive containment cleaning and foreign materials control. This includes in particular:
 - ✓ Ensure Containment drainage paths are unblocked.
 - ✓ Ensure Sump Screens are free of adverse gaps and breaches.
 3. Possible plant hardware improvements.

All these measures try to reduce the risk associated with potentially degraded containment sump recirculation functions for the immediate future. In parallel developments of methodologies to demonstrate that the containment sump strainers comply with the regulatory requirements are followed.

References

- [1] AVN, “The treatment of the sump screen clogging issue in Belgium”, OECD/NEA International Working Group on Sump Screen Clogging, Stockholm, May 1999.
- [2] Leblanc, O. (Tractebel Engineering) “Criteria for increasing sump screen area in the Belgian PWRs Doel 1 & 2”, OECD/NEA International Working Group on Sump Screen Clogging, Stockholm, May 1999.
- [3] Delalleau, J.C. (Electrabel) “*Étude générique « Barsebäck » – Proposition de plan d’action*”, EBL-TEE, rev. 3 dd., 23 January 2003.
- [4] NEI 02-01, “Condition Assessment Guidelines: Debris Sources inside PWR Containments”, Rev. 1, September 2002.
- [5] NUREG/CR-6808, LA-UR-03-0880, Rao, D.V., Clinton J. Shaffer, M.T. Leonard, “Knowledge Base for the Effect of Debris on Pressurized Water Reactor Emergency Core Cooling Sump Performance”, U.S. Nuclear Regulatory Commission, February 2003.
- [6] Regulatory Guide 1.82, “Water Sources for Long-Term Recirculation Cooling Following a Loss-of-Coolant Accident”, U.S. Nuclear Regulatory Commission, Revision 3, November 2003.
- [7] Note Tractebel Engineering GENERIC/4NT/10976/000/00, “The containment sump screen clogging issue: Situation of the Belgian units at end of year 2003”, January 2004.

SAFETY ANALYSIS PERFORMED IN SWITZERLAND FOR THE RESOLUTION OF THE STRAINER CLOGGING ISSUE

Jens-Uwe Klügel¹

Kernkraftwerk Gösgen-Däniken, Switzerland

1. Introduction

After the Barsebäck 2 strainer clogging incident from 28 July 1992, a short term and a long term action programme was initiated by the Swiss Federal Nuclear Safety Inspectorate to resolve the strainer clogging issue [1]. The issue was closed in 1994 based on implemented modifications of suction strainers (flow area largely increased by a factor of 7 to 30) for BWRs and the approval of the strainer design based on plant specific analysis for PWRs. The key parameters used in the plant specific analysis are still surveyed within the plant specific ageing programme. The work presented here was performed mainly between 1992 and 1994 for the resolution of the clogging issue.

2. Scope of safety analysis performed

The decision on the resolution of the issue was based on detailed plant specific analyses for all of the Swiss NPPs including:

- a review of the insulation types employed;
- an assessment of possible insulation damage during a LOCA;
- an analysis of possible transportation paths;
- an assessment of transportation velocities;
- an assessment of the fraction of insulation transported to strainers;
- an estimation of pressure losses on strainers and their effect on pump operation;
- the evaluation of alternative strategies for core cooling (accident management actions);
- the development of design requirements to new strainers;
- an evaluation of effects of alternative debris sources (coating paints).

This analysis was supported by some generic experimental work, for example:

- to develop head loss characteristics for new strainers;
- to assess settlement velocities of insulation debris.

1. The work presented was performed while the author was working with the Swiss Nuclear Safety Inspectorate.

3. Selected results

3.1 Insulation types and insulation damage

A survey of available insulation types and of the available experimental data (in 1992) on insulation damage showed that the most critical type is rockwool. In Swiss plants rockwool is frequently used but mostly in an encapsulated [Leibstadt and Gösgen (linked half shells)] or jacketed (Mühleberg) form. Beznau is mostly using RMI (stainless steel) or NUKON™ insulation. The insulation damage for all plants was calculated based on the most conservative interpretation of the 7D – criterion (3 region-model) for a spherical ZOI originated from NUREG 0897/Rev. 1. The following table summarises the calculated maximum values of insulation debris for BWRs and for the Nuclear Power Plant Gösgen. The critical break areas have been established during extended walkdowns and by analysis of plant documentation (see below).

Table 1. Calculated maximum amount of insulation debris for design basis accidents

Plant/Plant type	Maximum amount of debris, m³	Accident
Mühleberg/BWR-Mark I	1.8 (3.5 used as a conservative assumption for plant specific clogging analysis)	Break of a recirculation line pipe
Leibstadt/BWR	10	Break of a main steam line pipe inside containment
Gösgen/PWR (KWU-3-Loop)	1.65	Double ended break of main coolant pipe

Figure 1 illustrates the assessment process for the evaluation of insulation debris for the assumed double ended break of a main coolant line pipe for the Gösgen plant.

3.2 Debris transportation

3.2.1 Transportation paths

Based on a review of the design documentation and extended walkdowns (inspections) critical pipe break scenarios were derived based on the amount of insulation debris to be expected and the likelihood of successful transportation to the strainers. This approach was common for all plants. Figure 2 shows the relative location of the assumed critical break area in relation to the containment sumps for the Gösgen plant.

3.2.2 Transportation and settlement velocities

For the evaluation of long term water flow velocities in the wetwell of BWRs as well as for the sump design of one of the PWRs an evaluation model was developed [2]. The calculated velocities were compared with measured values for the settlement velocities and published experimental data on transportation velocities for different types of insulation. It was found that debris suction effects of strainers are short ranged. Settlement velocities for rockwool were found [3] to be in the area of:

- 20 mm/s for new rockwool (compact);
- 2 to 4 mm/s for fines;
- ca. 80 mm/s for aged rockwool (compact), 15 mm/s for single fines.

Similar results were also obtained in tests performed for the redesign of strainers of Swiss BWRs. Figure 3 shows the small scale test facility for the evaluation of settlement velocities and insulation retaining simulating the sump area of Gösgen. Based on the experiments retainment factors for the debris in the sump area were calculated for four different limiting scenarios. Table 2 shows the results of this combined experimental and analytical assessment. These calculations took into account that sump recirculation will start about 30 minutes after the break (thus determining the available time for sedimentation) according the design basis calculation for a double ended break of a main coolant pipe. As in the Barsebäck incident observed, it was assumed that about 20% of the insulation debris will be retained in the containment by condensation at structures. This assumption is justified due to the fact that Gösgen does not have a containment spray system which in other designs would contribute to the transportation of debris to the sump by washdown. Concerning the sedimentation processes it is also important to mention, that the effective pump suction is elevated above the floor of the sump area due to the specific geometrical conditions (spherical shape of the containment) forming a “dead” volume of water of a few m³ in the main sump pool area.

Although the calculated retainment factors are likely higher than 50%, it was assumed for the plant specific clogging analysis that no more than 50% of the debris can be retained outside the sump pool area. For the assessment of the clogging time the worst case assumption of a homogeneous distribution of debris in the sump/wetwell water was assumed not taking into account the possible debris settlement.

Table 2. Retainment factors for the Gösgen annulus and sump area

Case	Description	Condensation retainment	Sedimentation	Summary retainment
A	No retainment at containment grates, immediate transportation of all insulation to the pump sump	20%	80%	100%
B	As case A, but assuming that all insulation settled in an area of the sump with surge flow velocity > 3 cm/s will be sucked to the strainer (erosion zone)	20%	74%	94%
C	Continuous entry of insulation into the sump area until the start of the sump pumps, sedimentation starts then the water level achieves the grate plane above the sump, 50% retainment at the grate above the sump after the start of the pump	20%	17% + 31% (1 at sump grate)	68%
D	As case B but assuming that 50% of the already settled insulation debris will be detached and float in the sump pool water volume. 10% of the floating debris will be retained at the grate above the sump.	20%	37% + 4% (at sump grate)	61%

An insulation debris transport study performed for the Mühleberg plant came to the result that about 70% of the insulation debris can be retained in the drywell (10%) and in the torus (by sedimentation outside the strainers). Nevertheless for the design of the new strainers in Mühleberg retainment of insulation debris was not credited.

4. Head losses

4.1 Calculation of head losses

Head loss characteristics have been developed mainly for rockwool as the basis of the redesign of ECCS strainers of Swiss BWRs. Rockwool is also the main insulation material for the Gösigen plant. The developed characteristics took into account ageing effects, as well as different water temperatures. The head losses of rockwool in hot sump water of a PWR were found to be about a factor of 3 lower than for the cold water conditions. The evaluation of available NPSH and the redesign of the strainers were based on the most conservative calculation of pressure losses to achieve robust results. For this purpose a comparison of different empirical correlations with own experimental data was performed. Experiments included tests on horizontal sump screens about which was reported already in 1994 [1] as well as small scale tests on vertical sump screens using the facility shown in Figure 3. The experiments covered a wide range of rockwool conditions (new, old, shredded, etc.). Figures 4 and 5 show a comparison of measured pressure losses at a vertical screen with the NUREG 0897, Rev. 1 correlation results. The NUREG 897, Rev. 1 correlation had the following form:

$$\Delta P = 123 \cdot d^{1.36} \cdot V^{1.51} \quad (\text{EQ-1})$$

The pressure loss ΔP is in ft, d is in ft and the velocity V is in ft/s.

The calculated pressure losses for the NUREG correlation presented in Figures 4 and 5 are based on the velocity calculated on the basis of the gross sectional area of the strainer meshes used in the experiments.

The analysis of available data and correlations led to the conclusion that the NUREG 0897, Rev. 1 correlation for pressure losses is conservative if the velocity V is calculated based on the unblocked net cross sectional area (net velocity) of the sump strainer. Due to the lack of other experimental data at that time (1993) the decision was made to use the NUREG 0897, Rev. 1 correlation for the plant specific clogging analysis based on the net velocity. As a later comparison with experimental data obtained in Swiss experiments showed, the approach taken might be conservative for meshes with larger openings. The experimental data (Figure 6 shows the test facility) obtained for the design of the new strainers for the Leibstadt plant (BWR) would lead to the following correlation (net velocity):

$$\Delta P = 0.0137 \cdot d^{1.152} \cdot V^{1.146} \quad (\text{EQ-2})$$

Here the pressure loss ΔP is in m, d is in cm and V is in cm/s. It is obvious that the dependency on the velocity is less steep than in the NUREG correlation. The reason for this can be found in the test conditions. The sump mesh used was very fine (2.0 x 2.0 mm) and the range of test conditions covered relatively thick debris beds. For the validation of the design of the new strainers the Swiss Nuclear Safety Inspectorate requested to use the maximum pressure losses calculated by EQ-1 and EQ-2 to achieve a robust solution for the design of the new strainers.

An analysis of available experimental data for pressure losses on vertical screens with larger mesh openings led to the suggestion of the following correlation for head losses caused by rockwool debris:

$$\Delta P = 0.00497 \cdot d^{1.19} \cdot V^{1.21} \quad (\text{EQ-3})$$

This correlation is also based on the effective velocity at the strainer surface (based on the unblocked net cross sectional area), the same units apply as for (EQ-2). This correlation gives slightly lower pressure losses than the NUREG 0897, Rev. 1 correlation used with the net velocity. The correlation can be suggested for the following conditions:

- Mesh opening sizes (3-10) mm;
- Debris bed thickness (3-20) cm;
- Velocity at unblocked strainer surface (5-20) cm/s.

Experimental investigations in Switzerland as well as in other countries have shown that increasing sump water temperature leads to a decrease of the head losses at the sump screen. This effect can be described by the following empirical correlation for a temperature correction factor (multiplier to EQ-3):

$$K(T) = e^{-0.01682 \cdot (T-287.15)} \quad (\text{EQ-4})$$

The correlation is valid for rockwool and water temperatures between 14 and 85°C, T is in K.

4.2 Effect of coating paints

The effect of coating paints was found to be very plant specific. During the implementation phase of the plant specific ageing programmes the main material properties of coatings were established. Mixtures of insulation debris and coating paints [4] tend to settle much faster than debris from insulation (due to their compact form). Plant specific analysis for one of the PWRs indicated that debris- mixtures from ground coatings and insulation will settle before the sump strainer (at the curb threshold) with some low potential for clogging the lower part of the strainer, thus increasing the height of the threshold retaining other material from clogging the strainer.

4.3 Impact of head losses on pump performance

For one of the Swiss PWRs the effect of high pressure losses at sump screens on the RHR-capacity was analysed in detail. Based on flow/head characteristics provided by the pump vendor for cavitation mode of operation (obtained experimentally) it was shown, that 1 train of RHR is able to maintain the required heat removal in sump recirculation mode of operation even under assumed worst case cavitation conditions (average flow of the pump in this mode is less than 60% of nominal flow).

5. Plant specific strainer clogging analysis

Plant specific clogging analysis studies have been completed for all Swiss BWRs and for the Gösgen PWR by end of 1993. For Beznau a qualitative assessment of the situation and a detailed

comparison of the sump strainer design with RG 1.82, Rev. 1 showed that further detailed investigations were not necessary due to the insulation types installed, the large sump surface area and the low suction flows necessary for heat removal. The studies for BWRs resulted in the replacement of the suction strainers as has been reported during the OECD meeting in 1994 [1]. The analysis for the Gösgen plant based on very conservative assumptions:

- low retainment of debris in the containment (50%);
- use of the NUREG 0897, Rev. 1 correlation based on net velocity;
- no credit of temperature effects on strainer head losses;
- no credit for containment pressure during the LOCA;

showed sufficient NPSH-margin for the RHR pumps even for the case that only 2 of 4 (1 pump has 100% heat removal capacity) are available for sump recirculation. Figure 7 shows the available NPSH for the case of a double ended break. Nevertheless an accident management action was implemented for sump strainer back flushing from the internal fuel storage pool to mitigate the consequences of BDBA.

6. Risk assessment

Based on the obtained experimental and analytical results the impact of potential strainer clogging on the calculated values of core damage frequency for one PWR (Gösgen) was calculated. For this purpose two effects have been considered:

- the effect of debris transport on the plugging frequency of sump strainers;
- the effect of potential plugging on the success criteria of the PSA.

To consider the first effect a special plant specific data distribution for strainer clogging under LOCA conditions was developed. This distribution takes into account the frequency of strainer clogging by other sources (alien material) independent from the insulation debris impact as well as from the debris impact. Due to the appropriate design of the sump strainers at Gösgen the additional effect of insulation debris was established to be small.

Regarding the second effect it was conservatively assumed (see Figure 7) that pump cavitation is possible under conditions then at least two out of four pumps are failed for other reasons and the containment is not pressurised (loss of containment isolation) during a LOCA. It was assumed that pump cavitation would fail the pumps. Based on this assumption the model was modified requiring the availability of two pump trains in sump recirculation mode of operation instead of 1 pump as normally is required. The accident management action introduced at the Gösgen NPP for strainer back flushing was not taken into account. The analysis showed that the effect of strainer clogging on the plant specific core damage frequency can be neglected (risk increase below $1E-8/a$).

REFERENCES

- [1] Klügel, J.-U., R. Gilli, A. Voumard, “Measures performed in Swiss Nuclear Power Plants after the Barsebäck incident”, OECD/NEA workshop on the Barsebäck Strainer Incident in Stockholm, 26-27 January 1994.
- [2] Klügel, J.-U., “Simple Evaluation Model for Long Term Debris Transport Velocity in the Torus of a Mark I Containment”, to be presented at the open part of the Workshop, March 2004.
- [3] Attinger, R. “Nachrechnung der KKG-Sumpfsiebe gegen Verstopfung durch Isolationsmaterialien”, AN-Nr. 2973, 10.3.1994, Confidential.
- [4] Attinger, R. “Auswirkungen der Betonbeschichtungen auf die nukleare Sicherheit”, KKG, BER-M-2001-003, February 2001, Confidential.

Figure 3. Small scale test facility for sedimentation and pressure drops on vertical surfaces

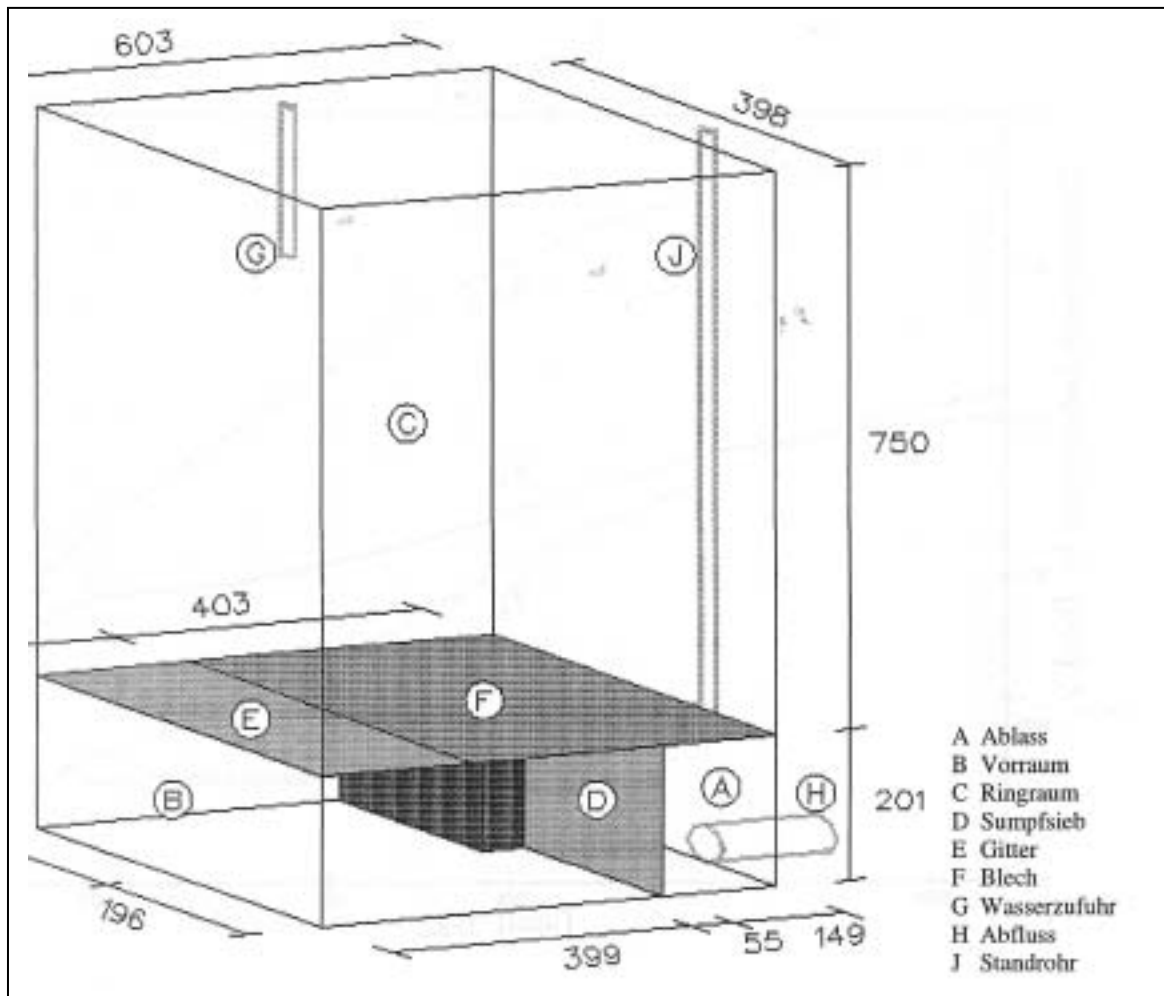


Figure 4. Measured pressure losses – Comparison with NUREG 0897 (gross flow area), Rev. 1, d = 6 cm

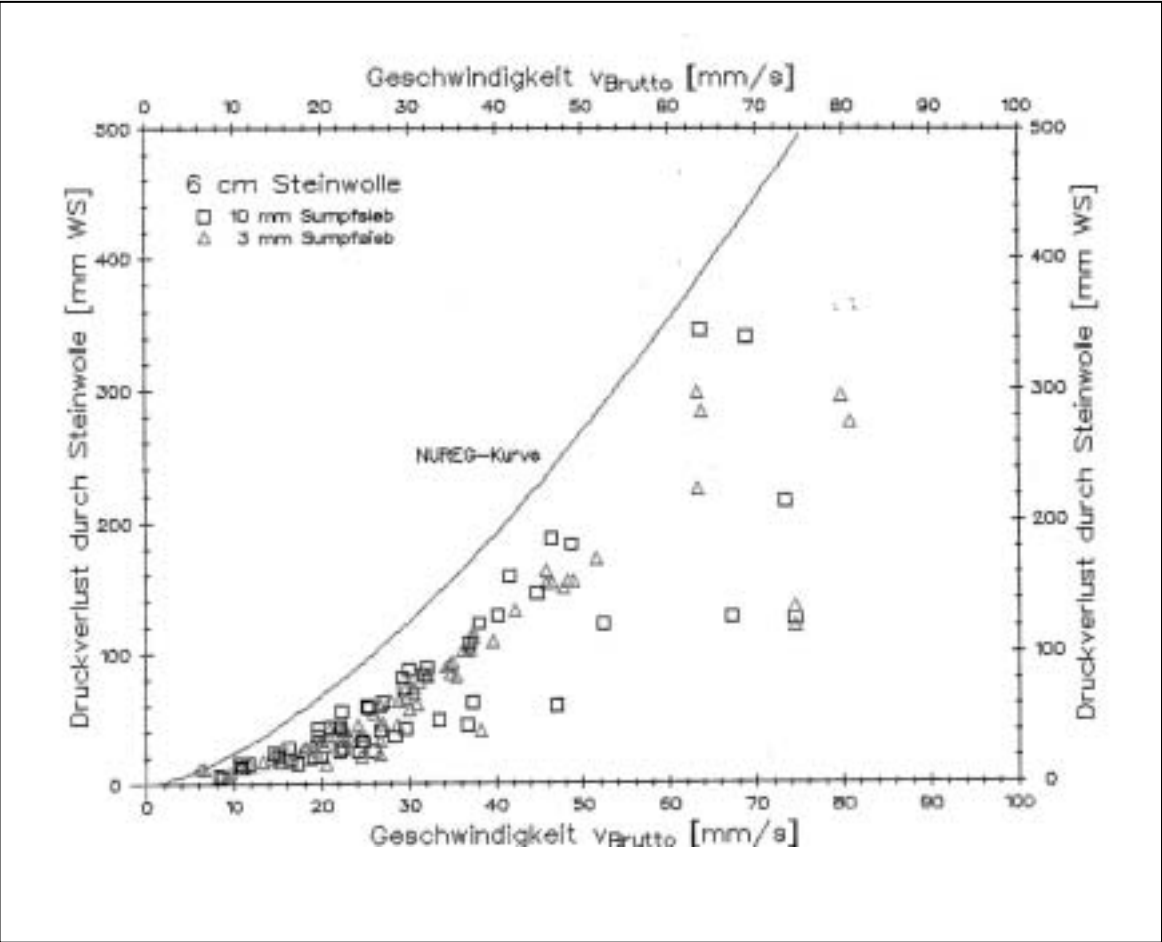


Figure 5. Measured pressure losses – Comparison with NUREG 0897, Rev. 1 (gross flow area), $d = 6$ cm

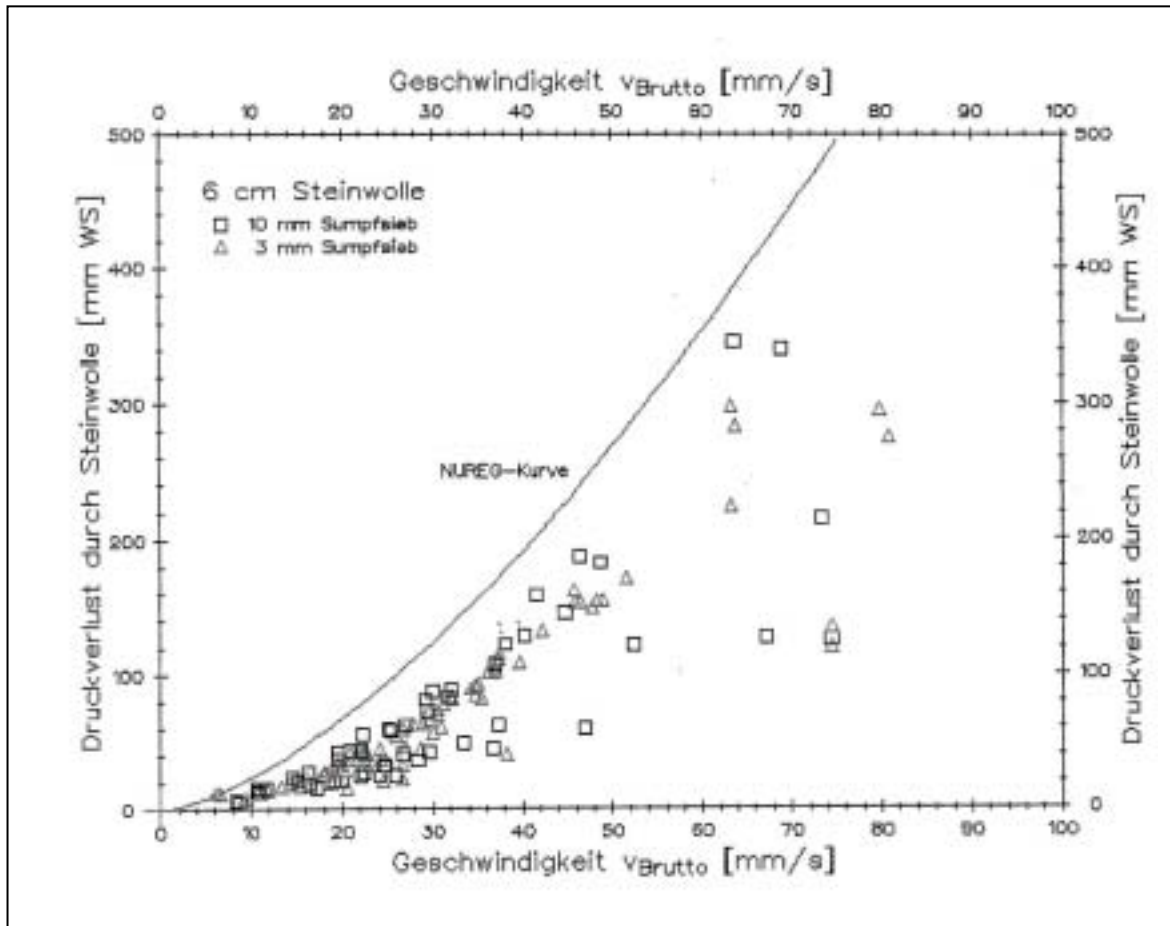


Figure 6. Test facility for the KKL strainer experiments performed by Sulzer

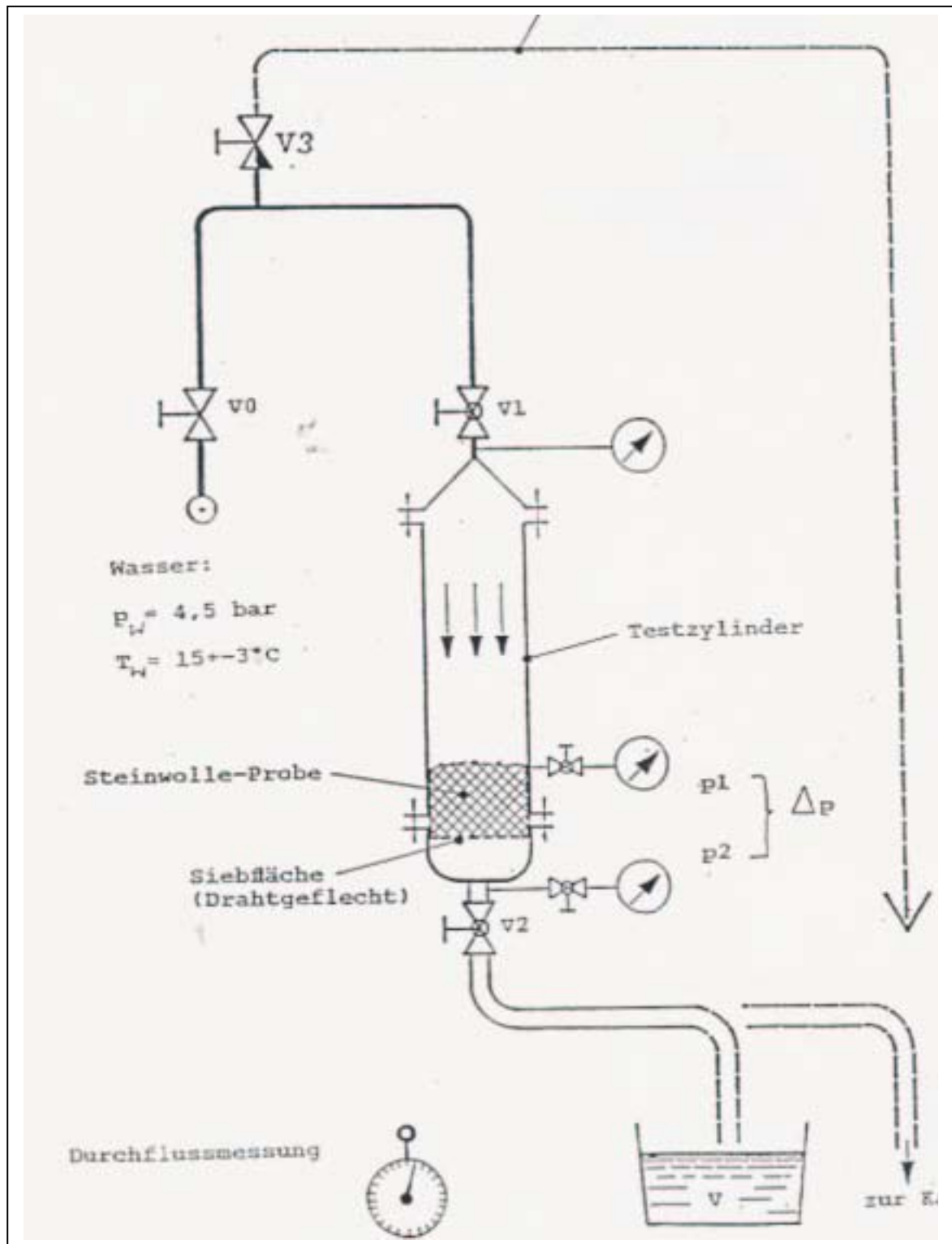
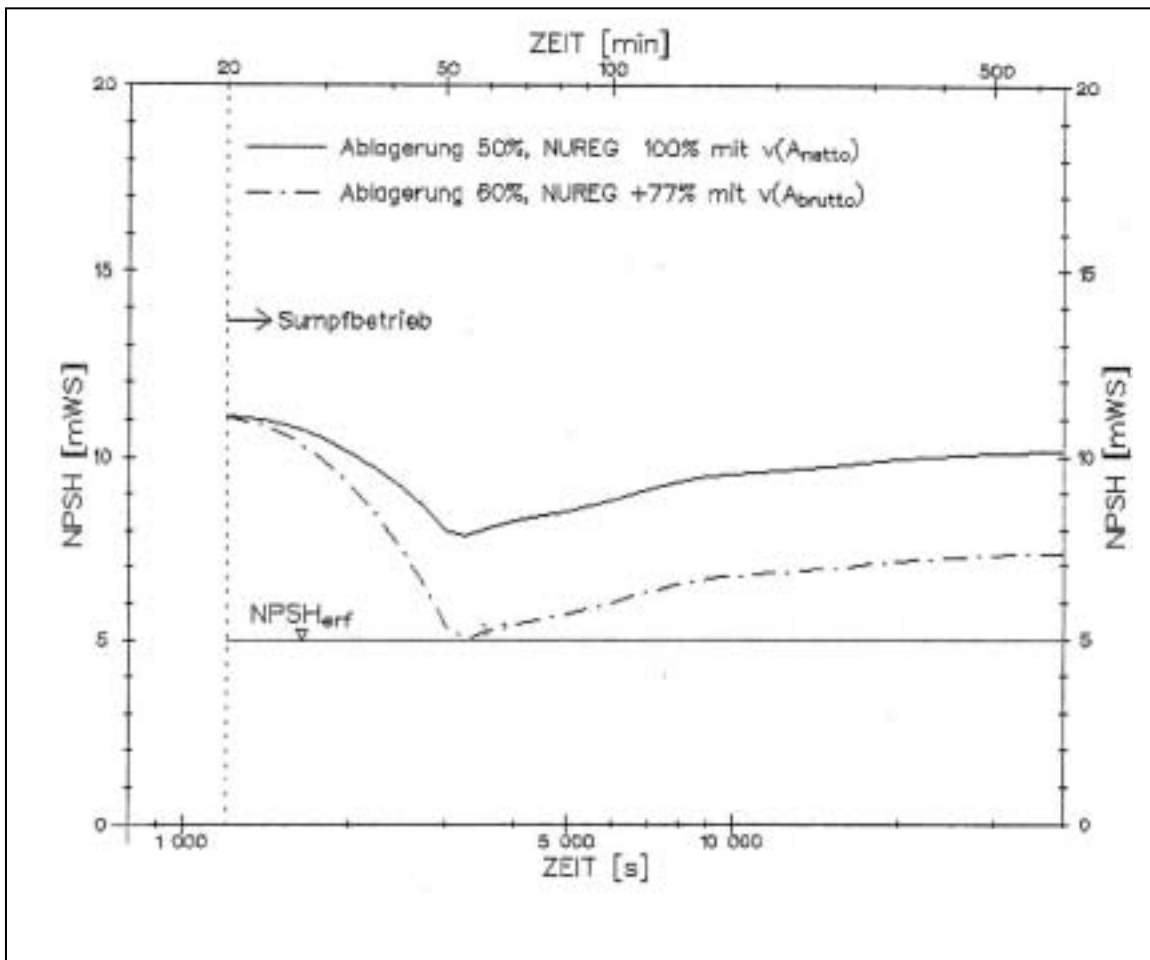


Figure 7. Available NPSH for RHR pumps in sump recirculation, 2 of 4 in operation



ORIGINAL EQUIPMENT MANUFACTURERS' (OEM) PROTECTIVE COATING DESIGN BASIS ACCIDENT TESTING

Jon R. Cavallo, PE

Corrosion Control Consultants and Labs, Inc. USA

Anthony Griffin

EPRI, USA

Introduction

The United States Nuclear Regulatory Commission (USNRC) currently holds the position that 100 percent of design basis accident (DBA) unqualified coating materials located within a pressurised water reactor (PWR) containment will fail (disbond) during a DBA (e.g. loss of coolant, main steam line break) and may contribute to the emergency core cooling system (ECCS) sump debris source term [1].

Electrical cabinets, small cranes, electric motors, pipe support components, and other miscellaneous equipment installed within US PWR containments are often coated by the original equipment manufacturers (OEM) using DBA unqualified coating materials (usually a standard shop oil based alkyd system). Little or no documented DBA test data currently exists concerning these OEM coatings.

In support of the US industry efforts to resolve Generic Safety Issue 191, EPRI International, PSE Division (EPRI PSE) and the Nuclear Utility Coating Council (NUCC) are jointly conducting research to investigate the actual effect of PWR DBA environmental exposure on OEM coatings applied to components installed in US PWR containments. This paper will present details concerning the study.

The EPRI/NUCC study, entitled, "Unqualified OEM Coatings Testing", will be conducted during 2004 in four major steps:

1. conduct an industry-wide survey to determine which components in US PWR containments are normally coated with DBA-unqualified OEM coatings;
2. determine which of the components identified in Step 1 have been previously EQ tested, and review available EQ test data to determine the performance of the OEM coatings when exposed to DBA environments;
3. determine which of the components identified in Step 1 have not been previously EQ tested, and perform DBA testing on samples cut from actual OEM components in accordance with ASTM D3911-03 and ASTM D4082-02; and
4. publish the results of Steps 2 and 3 in two separate reports.

The EPRI/NUCC study plan is described in this paper. Since the actual study will not be completed until mid-2004, updated information concerning the study progress will be presented at the February 2004 OECD conference.

Study plan

The EPRI/NUCC study will be conducted in seventeen discrete tasks during 2004 by EPRI PSE and its subcontractors, Corrosion Control Consultants and Labs, Inc., Keeler & Long PPG and University of Massachusetts at Lowell. A Task Group within NUCC will independently review the progress of the project and provide input as appropriate.

Task 1. Obtain OEM unqualified coating list from industry

Several US PWR plants and other nuclear industry sources will be contacted to identify the types of OEM unqualified coatings which are found in PWR plants. The type of information which will be collected includes:

1. What generic types of OEM equipment have unqualified coatings on them?
2. What types of OEM unqualified coatings are in containment?
3. What is the approximate square footage of each type of OEM unqualified coating in containment?

The information obtained from this preliminary survey will be used to develop the detailed survey described in task 3.

Task 2. Form EPRI/NUCC task group

An advisory task group will be formed by EPRI and NUCC to provide advisory input to the project effort as appropriate.

Task 3. OEM unqualified containment coating survey

An industry-wide survey will be developed to obtain information concerning the presence of OEM unqualified coatings in US PWR containments. The survey will request specific information, including:

1. What types of OEM unqualified coatings are inside a given containment?
2. What types of actual samples of OEM unqualified coatings can be obtained from a given containment?
3. When was the coated OEM equipment installed in containment?
4. When and by whom was the OEM equipment coated?
5. What type of surface preparation was performed prior to coating application?
6. Has the OEM equipment been EQ tested?
7. What OEM vendor contact information is available?

Task 4. *EPRI/NUCC task group meeting*

An EPEI/NUCC task group meeting will be held on 13 January 2004 to review the project progress.

Task 5. *Survey review and data consolidation*

The data obtained from the detailed survey described in task 3 will be reviewed and organised in three separate subtasks.

Subtask 5.1 – Organise the survey response data into an Excel spread sheet.

Subtask 5.2 – Organise the OEM unqualified coatings into two groups:

- A. OEM unqualified and not EQ tested
- B. OEM unqualified and EQ tested

Subtask 5.3 – Identify before and after testing photos available in the OEM unqualified and EQ tested group

Task 6. *Obtain before and after test photos from OEM EQ testing*

Before and after testing photos identified in subtask 5.3 above will be solicited from the various OEM vendors involved for review. These photos will be used to document the performance of OEM coatings on vendor-supplied equipment if possible, and may permit elimination of additional testing as described in tasks 12 and 14 below. Task 6 will be performed in two subtasks:

Subtask 6.1 – Collect and review photos at EPRI PSE

Subtask 6.2 – Review photos at vendors' facilities

Task 7. *Determine OEM coating types to be tested*

The various coating types identified in subtasks 5.2 and 5.3 above will be considered for laboratory testing. This selection will be performed in two steps:

Subtask 7.1. Review the quantities of each of the OEM unqualified and not EQ tested coatings identified in subtask 5.2 and select the coatings which are predominant in quantity for laboratory testing.

Subtask 7.2. Review the quantities of each of the OEM unqualified and EQ tested coatings identified in subtask 5.3, determine which of these coatings are not documented by before and after photos, and select the coatings which are predominant in quantity for laboratory testing.

Task 8. *Task group Web cast meeting*

After completion of task 7, a Task Force web cast meeting will be held to review the project results through task 7.

Task 9. Obtain in situ samples of OEM unqualified coatings for laboratory testing

Samples of OEM unqualified coated equipment to be laboratory tested as defined by task 7 will be obtained from PWR facilities and OEM's. Each sample will be documented on a chain-of-custody form and shipped to EPRI PSE for processing.

Task 10. Prepare samples for laboratory testing

Test samples will be cut from the OEM equipment samples by the EPRI PSE machine shop. These samples will be 2 in. by 4 in. in face dimension to fit into standard irradiation and autoclave testing fixtures.

Task 11. Obtain OEM coating sample information

EPRI will obtain vendor documentation will be obtained for the coating samples identified in tasks 6 and 9 above and tabulated. The types of vendor information which will be collected include:

1. surface preparation;
2. coating application procedures; and
3. coating material details (generic type, vendor brand name, etc.).

Task 12. Conduct radiation testing of OEM coating samples

Radiation testing of the prepared OEM coating samples will be performed in accordance with ASTM D4082 [2]. This testing will be performed at University of Massachusetts at Lowell's Radiation Laboratory. The samples will be visually examined and photographed before and after radiation exposure.

Task 13. Modify testing autoclave

A specially-engineered debris collection filtration system will be installed in the condensate recirculation system on the Keeler & Long PPG autoclave test system to collect any debris resulting from OEM unqualified coating failure during testing. The filtration system will include parallel filters so that filters can be changed out without interruption of testing. The spent filters will be retained for later analysis by others, if desired.

Task 14. Perform autoclave testing of OEM coating samples

Autoclave testing of the irradiated OEM unqualified coating samples will be performed at Keeler & Long PPG in Watertown, CT. Testing will be conducted in accordance with ASTM D 3911-03 [3]. Each coated sample will be photographed and documented before and after autoclave testing. A written report, including irradiation details, photographs and other documentation, will be prepared by Keeler & Long PPG upon the conclusion of autoclave testing.

Task 15. *Technical report on coatings not irradiated and autoclave tested*

Corrosion Control Consultants and Labs, Inc. will prepare a written report covering the OEM unqualified coatings not selected for irradiation and autoclave testing in tasks 12 and 14. This report will include available document and photographs.

Task 16. *EPRI report No. 1*

EPRI will publish a report including the information developed by Corrosion Control Consultants and Labs, Inc. in task 15.

Task 17. *EPRI report No. 2*

EPRI will publish a report including the information developed by Keeler & Long PPG in task 14.

Significance and use

The EPRI Reports prepared under tasks 16 and 17 above will contain documented technical data on all OEM unqualified coating evaluated under the EPRI/NUCC study, and will be made available to industry in accordance with EPRI publication policies. The two EPRI Reports will not contain conclusions concerning the significance and use of the data; this will be left to the users of the documents.

References

- [1] Generic Letter 98-04, “Potential for Degradation of the Emergency Core Cooling System and the Containment Spray System after a Loss-of-Coolant Accident Because of Construction and Protective Coating Deficiencies and Foreign Material in Containment”, USNRC, 14 July 1998.
- [2] ASTM D 4082-02, “Standard Test Method for Effects of Gamma Radiation on Coatings for Use in Light-Water Nuclear Power Plants”.
- [3] ASTM D 3911-03, “Standard Test Method for Evaluating Coatings Used in Light-Water Nuclear Power Plants at Simulated Design basis Accident (DBA) Conditions”.

OVERVIEW OF SITE SPECIFIC BLOCKAGE SOLUTIONS AT US PWRs

John W. Walker and H. Lee Williams
Framatome ANP, USA

The potential for LOCA-generated debris to degrade PWR ECCS performance during recirculation has gained international industry and regulatory attention. Many US PWR owners are still in the early stages of determining the significance of this issue for their particular plants. For a sizable number of these plants, resolution of the ECCS debris blockage issue will require a combination of analytical evaluation, changes to operating or maintenance protocols, and modifications or additions to some plant components. This paper provides an overview of site-specific ECCS debris blockage solutions anticipated to be used by US PWRs. The overview begins with a brief review of the variability in containment floor and ECCS sump configurations found in the US PWR fleet. With this variability in mind, discussion then focuses on the several different resolution modes that may be brought to bear on the ECCS debris blockage issue. Finally, a variety of factors that owners must consider in order to select an optimal means of resolution are surveyed.

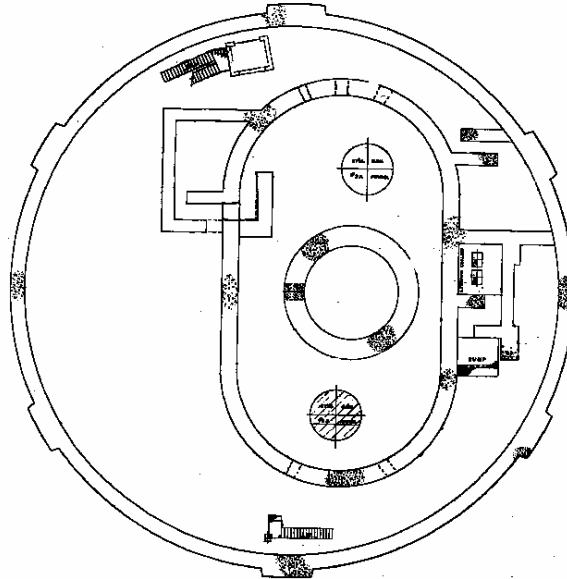
I. Wide variety of containment configurations and ECCS sump designs

The US PWR fleet employs a variety of structural configurations to meet general design requirements. These differing configurations are all intended to achieve several key functions – provide radiological shielding, provide missile hazard protection, provide structural support for plant equipment, and provide a barrier against release of radioactivity during or after a design basis accident. Terminology may differ from plant to plant; but all plants incorporate a relatively thick concrete bioshield around the reactor vessel. Reactor coolant loops, with steam generators and reactor coolant pumps, are generally located in separate areas, outside the primary bioshield but inside another, secondary bioshield. Other plant equipment, such as letdown heat exchangers, ECCS sumps, fan coolers, and service water manifolds, are generally located outside the secondary bioshield; main steam and feedwater piping also extend between their respective containment penetrations and steam generators.

The structural configuration of PWR containments determines the flow channels that will transport post-LOCA debris. Containment structural configuration, ECCS injection phase water volume stored in RWST/BWST, and containment pressure suppression method (ice condensers, containment spray, safety-related fan coolers) determines the containment pool depth – and thereby the NPSH available – during ECCS recirculation.

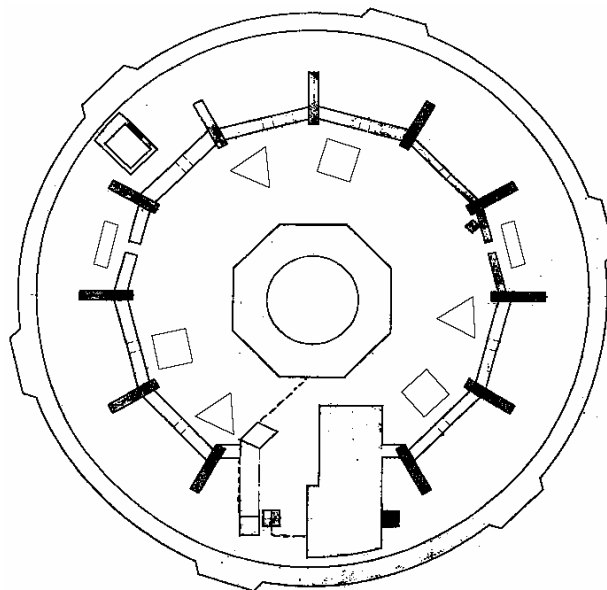
Some containment floor configurations have a relatively closed structure, as shown in Figure 1. The oval secondary bioshield encloses both loops. Four small scuppers are located near the floor in the curved sections of the secondary bioshield; the personnel access portal is the only other debris transport path through the secondary bioshield at the containment floor.

Figure 1



Another relatively closed containment floor configuration is shown in Figure 2. There are two personnel access portals, and several floor-level scuppers, breaching the secondary bioshield. Two square ECCS sumps are located outside the secondary bioshield, separated by the fuel transfer pool structure; part of the fuel transfer pool also overlies one of the ECCS sump pits.

Figure 2



Another containment floor configuration that will restrict debris transport paths is shown in Figure 3. The secondary shield wall features 19 vestibules, each with a small scupper, and three labyrinth personal access portals. Two ECCS sumps are located against the outer containment wall, 90° apart.

Figure 3

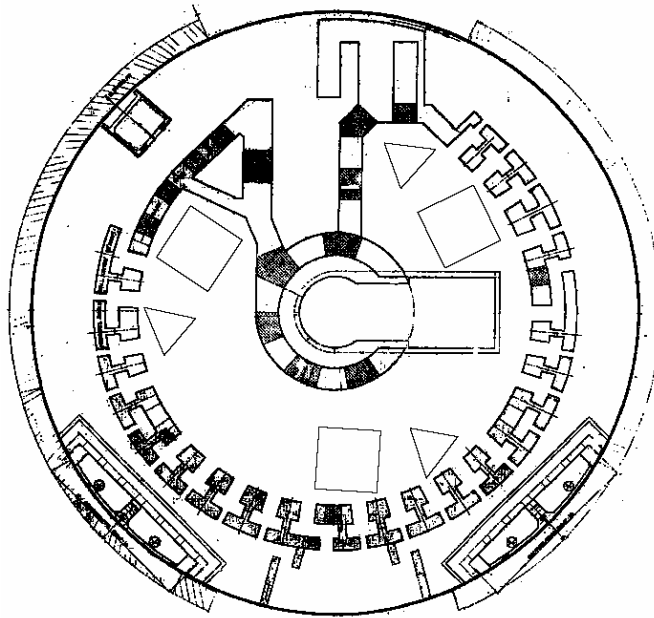
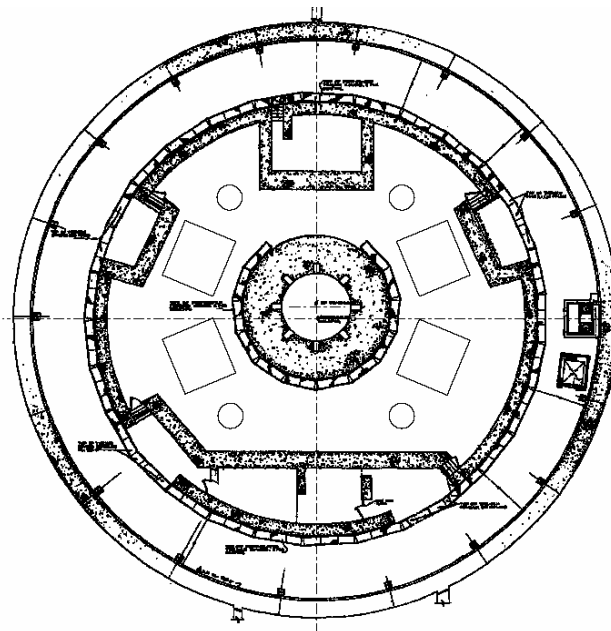


Figure 4 shows another relatively closed containment floor configuration. This configuration has four gated personnel access portals, and a relatively large area of screened floor drains that discharge to the ECCS sump.

Figure 4



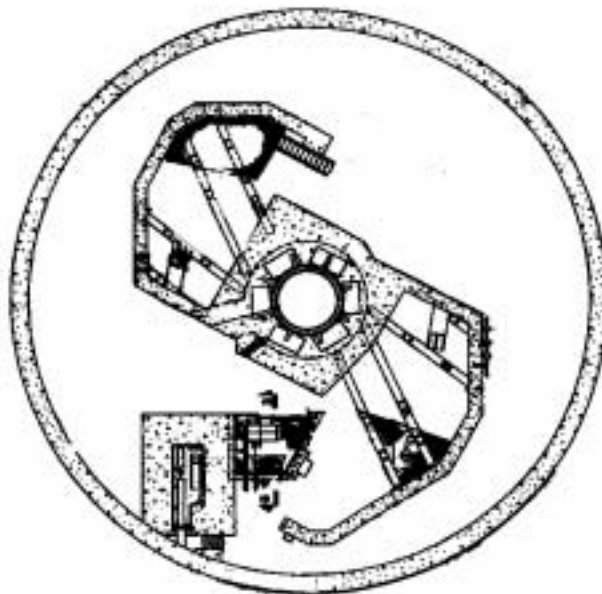
Other containment floor configurations present debris transport paths that are more open, as shown in Figure 5. The reactor coolant loops are completely enclosed in rectangular “loop cubicles” at elevations occupied by the loop piping and steam generators, but the loop cubicles are open to the rest of the containment both above and below those elevations. The ECCS suction is located close to the “portals” at the base of one of the two loop cubicles.

Figure 5



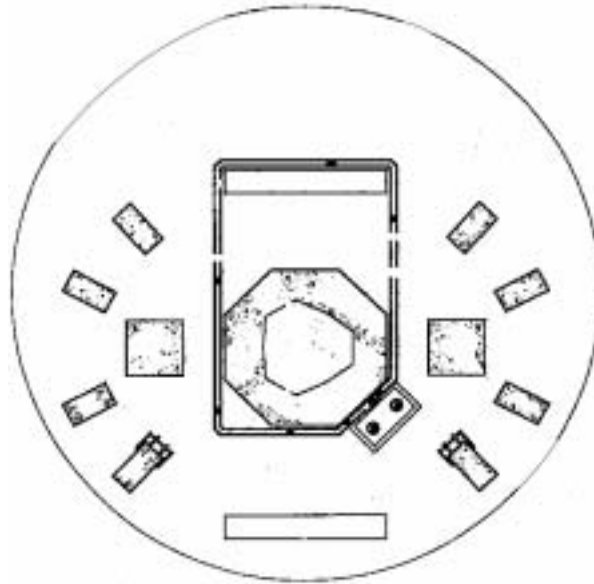
Some containment configurations are still more “open” with respect to debris transport. Figure 6 shows loops separated by secondary shield walls which radiate out from the primary bioshield and serve as missile barriers, but which are not “closed”. Direct debris transport paths to the ECCS suction screens exist, from loop piping as well as from pressuriser surge piping.

Figure 6



Other containment configurations are even more “open” with respect to debris transport. Figure 7 shows a lack of any structural barrier separating the loops at the containment floor; the sump is just outside the primary bioshield, but proximate to the loops.

Figure 7



Considerable variation also exists in the configuration of ECCS sumps in the US PWR fleet.

Figures 8 and 9 show cylindrical ECCS suction screens enclosed within a trash rack barrier mounted directly on the containment floor. The containment floor serves as the ECCS sump, with floor-mounted ECCS recirculation suction intakes.

Figure 8

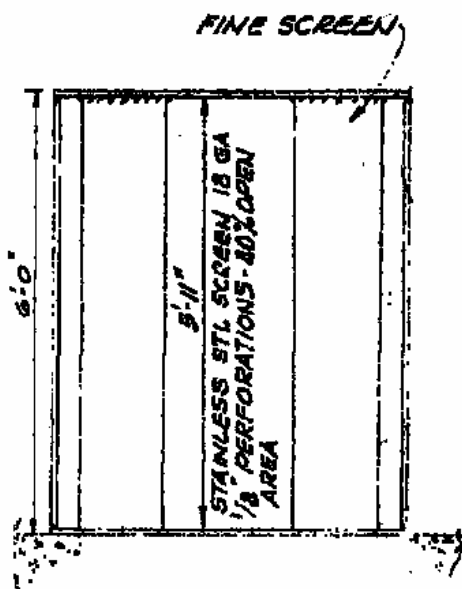


Figure 9

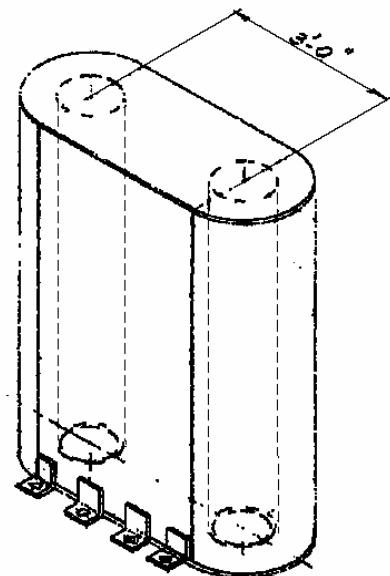
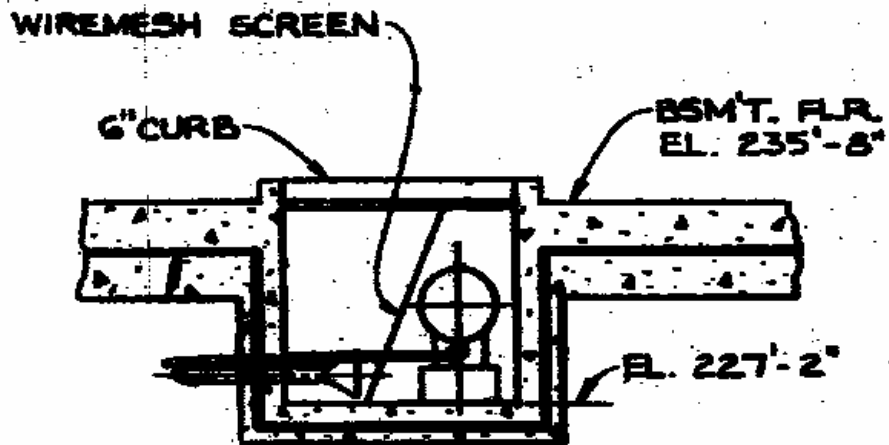


Figure 10 shows an ECCS recirculation sump that is a relatively shallow pit in the containment basement floor; with curbs, screen elements at the containment floor elevation, and the ECCS recirculation suction intakes set horizontally in the pit (left side of figure).

Figure 10



Figures 11 and 12 depict an ECCS recirculation sump design with a pit divided by an internal weir wall. Recirculation flow enters the sump through the curb mounted screen elements, and flows down one of the chambers formed by the internal wall into floor-mounted ECCS suction intakes. Containment floor drains are routed to the other side of the internal wall (left side of figure); any entrained debris settles to the floor, and water crosses through a fine screen above the wall to the recirculation chamber (right side of figure).

Figure 11

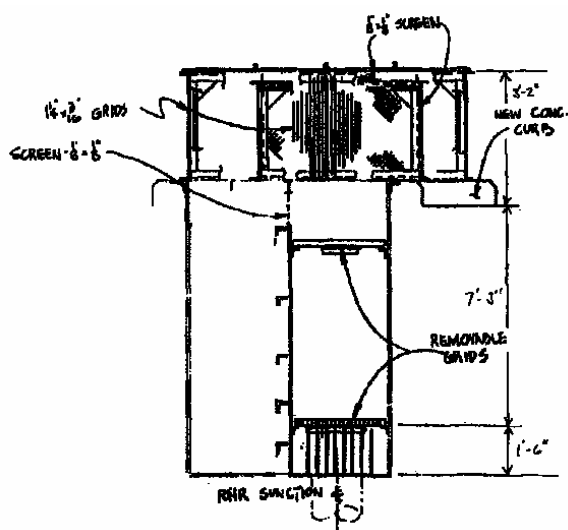


Figure 12

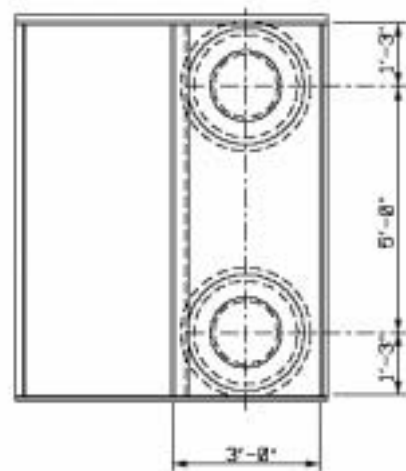
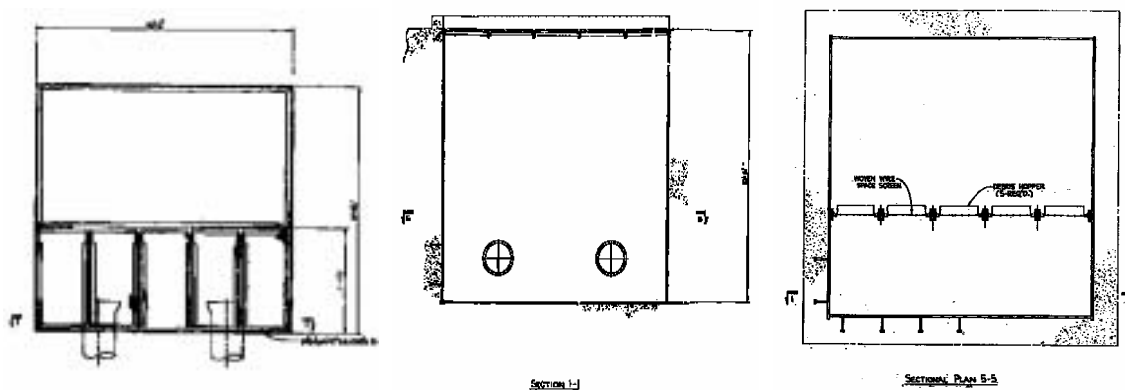


Figure 13 shows a variation on this theme. The ECCS recirculation sump is a deep pit divided by a set of internal screens. All floor drains empty to one side of the sump; recirculation flow must pass through the screens to the other side of the sump where the horizontally set ECCS recirculation suction intakes are located.

Figure 13



The variety of containment structural configurations and ECCS recirculation sump configurations complicates the selection of an optimum debris blockage solution for US PWRs. Further complications arise, for example, from the variety of pressure and temperature suppression methods which affect the quantity, timing, and entry path of the water volume that forms the containment pool.

II. Resolution modes

US PWR owners will consider several different resolution modes as they attempt to achieve a solution that is both technically sound and cost effective. These resolution modes include:

1. Analytical evaluation

All US PWRs will need to undertake an analytical evaluation to establish the limiting debris source terms for each particular plant. This will be necessary for a plant to successfully demonstrate that its existing ECCS suction screens will pass rated flow while retaining transported debris, and that the ECCS pumps will have adequate NPSH margin during recirculation. Since recirculation flow is a nuclear safety-related function of the ECCS systems in US PWRs, the analytical evaluations must be documented accordingly.

These analytical evaluations will encompass several activities:

- Walkdowns to validate the debris source inventory inside containment;
- Debris generation calculations to determine the limiting debris loads – including quantity and size distribution by debris source material – of debris generated by LOCA (and/or HELB) blast effects;
- Debris transport calculations to estimate the total quantity of debris of all types that will be transported to the ECCS suction as a result of LOCA (and/or HELB) blast effects; and

- Consideration of the limiting transported debris-load head loss at the ECCS suction screens in the NPSH margin for ECCS pump operation.

Studies such as the Los Alamos Report LA-UR-1-4083 “GSI-191: Parametric Evaluations for Pressurized Water Reactor Recirculation Sump Performance” suggest that, in the unlikely event of a large break LOCA, some US PWRs may be unable to demonstrate that they will retain adequate NPSH margin for a conservatively estimated debris load transported to their ECCS suction screens. Plants that find themselves in this group at the conclusion of their initial analytical evaluations will need to consider the following resolution modes.

2. *ECCS and containment spray operating protocol improvement*

The total quantity of debris transported to an ECCS suction screen is a function of the ECCS flow rate. Suspended debris will be drawn to the ECCS suction screen even at very low flow rates, but debris that settles on the containment floor will only move when the local fluid velocity exceeds the incipient bulk debris transport velocity for debris of that size and density. ECCS recirculation flow rate determines approach velocity near the suction screens, and affects net fluid velocity through the containment pool. A reduction in the required ECCS system flow rate would reduce the velocity field of the bulk fluid in the containment pool as well as the approach velocity near the screens. This, in turn, will reduce the total quantity of debris transported to the ECCS suction screen in several regards. First, reduced fluid velocities in the pool will reduce the quantity of debris that is transported along the containment floor – only debris small enough to be transported at the lower velocity will move. Second, reduced ECCS flow rate suggests a smaller portion of the containment pool in which the fluid velocity will be sufficient to transport settling debris. Reduced flow velocities also suggest a reduction in the amount of fines generated from the abrasion of larger debris pieces during recirculation. Finally, reduced flow field and screen approach velocities allow more time for settling to occur, further reducing the quantity of debris transported to the ECCS suction screens. Reduced screen approach velocities will also yield a lesser degree of debris bed compression at the ECCS screens, and reduced head loss across both the debris bed and the ECCS screens themselves.

Some plants may find that the ECCS system has excess margin for decay heat removal during the recirculation phase, so that they may be able to demonstrate adequate cooling flow through the core at a reduced ECCS recirculation flow rate. As the recirculation flow rate drops, the total quantity of debris transported to the ECCS suction screens will decrease, and the transported debris will skew towards smaller sizes and lower densities. It is conceivable that for some plants, the reduction in the total quantity of transported debris may be sufficient to reduce debris-loaded screen head loss, such that adequate NPSH margin is maintained at the reduced system flow rate. However, this approach will entail a broader analytical scope, including the revision of calculations supporting ECCS system design basis and plant design basis accident response during recirculation, as well as the revision of EOPs and the resetting of system control and alarm setpoints. This approach is also predicated on a safety analysis supporting the reduced ECCS recirculation flow rate, and regulatory approval of a corresponding change to the plant licensing basis, both of which would essentially tradeoff “thermal margin” during ECCS recirculation phase for assurance of adequate NPSH margin.

The design of containment spray systems at US PWRs utilizes the ECCS suction path to supply water for containment spray after the switchover to recirculation. Many plants continue containment spray flow through the early stages of ECCS recirculation. The reduction of containment spray flow during ECCS recirculation affords an additional opportunity to reduce overall ECCS flow rate, and debris transport to the ECCS suction screens. Indeed, many plants have already identified reduction to containment spray flow as one of the compensatory measures in response to NRC Bulletin 2003-01.

More recently, the role of containment spray in response to small break LOCAs (SBLOCA) has been questioned. The probability of a SBLOCA occurring is much greater than the probability of a LBLOCA occurring, and dominates the overall probability that a LOCA (of any size) will occur. However, in the event of a SBLOCA, the pressure/temperature excursion experienced inside containment is far more benign, and may remain within the capacity of the containment fan coolers normally used to control ambient temperature inside containment. Under these conditions, it may be counterproductive to require containment spray initiation, since it diverts some of the water flowing through the ECCS suction piping away from the core, and is not necessary to mitigate the ambient thermal transient inside containment. Moreover, the potential for fuel damage incident to the LOCA event is lower for a SBLOCA. Plant safety might better be served by raising the setpoints for automatic containment spray initiation to preclude operation during and after a SBLOCA. As with the changes to ECCS flow rate discussed above, implementation of changes to the CS operating protocols will expand the analysis scope as well as require revision to the licensing bases for a candidate plant.

Although LBLOCA frequency of occurrence is much lower than for SBLOCA, it remains a foreseeable event. As such, it is unlikely that regulatory relief will be given on requirements to assure ECCS recirculation capability in the aftermath of a LBLOCA.

3. *Debris source term reduction*

For plants in which the analytical evaluation indicates zero NPSH margin at either the maximum thin-bed head loss or the maximum debris load head loss for the debris-loaded ECCS suction screen, it may be possible to restore positive NPSH margin by removing or replacing some of the debris source materials that contribute to these head loss maxima.

With respect to the thin-bed case, it is unlikely that any plant will be able to guarantee that it will never have a fibrous debris load sufficient to form a thin bed. Even plants that rely entirely on reflective metallic insulation or entirely on granular insulation materials, which are predominantly made of particulate, will still need to account for a small quantity of miscellaneous fibers. These include fibers worn away from protective clothing, tool bags, and cleaning rags, or fiber-containing materials lost or discarded inside containment during construction or some time thereafter. One cubic foot of fibrous material is sufficient to yield a bed 1/8" (3 mm) thick on ~100 ft² (9.4 m²) of fine screens at the ECCS suction, enough to form a thin bed. The level of effort to support the assertion that insufficient fibrous debris exists inside containment to form a thin bed is prohibitive. Therefore, it becomes necessary to consider the particulate debris inside containment. For a given fibrous thin bed, the head loss is markedly affected by the quantity of particulates filtered out by the thin bed. Particulates arise from many sources, such as latent dirt and dust, unqualified coatings, and granular insulation materials, primarily calcium silicate, microporous, and asbestos insulation. Enhanced housekeeping efforts may justify a reduction to the latent debris source term for particulates from dirt and dust; inspection of debris generation analyses may identify specific sections of granular insulation that, if removed or replaced, might also yield a reduction to the particulates filtered by a thin bed of fibers collected on the ECCS suction screen.

With respect to the maximum debris-load case, debris load head loss is taken as the sum of the head loss contributions calculated for each of the various debris types. Again, inspection of the debris generation analyses for a particular plant may identify specific sections of thermal insulation that can be removed or replaced to yield a reduction in the overall quantity of transported debris or in the head loss generated by transported debris.

Since the maximum transported debris load scenario at most plants will likely involve debris generated by a break in the RCS, efforts to regain NPSH margin by the removal or replacement of deleterious insulation debris sources will incur a number of practical costs. These costs include ALARA, disposal of radioactive waste in the form of the removed insulation, procurement and installation of replacement insulation materials, and costs associated with removal of asbestos. Further costs may arise if the replacement thermal insulation material is a less efficient insulator, leading to an increased containment cooling load and hence an increased ambient temperature inside containment. In this case, additional costs may arise in the form of reduced process efficiency, required EQ program revisions, and/or increased rates of replacement required for EQ equipment.

4. *Debris trap installation*

The total quantity of debris transported to the ECCS suction screens is influenced by the channels available for recirculation flow. Obstacles in these flow channels will retain or divert some portion of debris in transport. If recirculation flow can only approach the ECCS suction screens through a few channels, then it may be possible to design and install debris traps in some or all of these channels to reduce the quantity of debris actually transported to the ECCS suction screens. Debris that transports along the containment floor may be stopped by a curb of adequate height; suspended debris may be intercepted by screens placed in the anticipated flow channels.

Plants that elect debris traps must consider designs that can be seismically qualified and withstand anticipated LOCA blast effects, including missile hazards; their design also must account for accessibility of personnel and equipment for maintenance purposes. The affect of a given debris trap design on both debris transport and ECCS recirculation flow must be evaluated, accounting for changes in flow through or around the debris trap as debris collects on the trap. Several iterations of debris transport and debris-loaded head loss calculations may be necessary to arrive at an optimal design and placement for a debris trap.

5. *Enhanced ECCS suction strainer installation*

The debris-loaded head loss across the ECCS suction screens is a function of a number of variables. Among these, screen area, recirculation flow rate, and the types and quantities of transported debris are key variables. Therefore, modifications to ECCS suction screens that increase available screen surface area will present a viable resolution option for some plants.

Passive strainers with enhanced screen surface area have been used previously in the US nuclear industry, mainly on the BWR side, and may be adapted to meet PWR requirements. A number of different designs have been developed, each seeking to maximise screen surface area. This minimises approach velocity, and also minimises the concentration of debris on the screen surface. As noted earlier, lower approach velocities provide greater opportunity for entrained debris to settle out of the containment pool prior to deposition on the ECCS screen, and reduce the extent of hydrodynamic compression on the debris bed as it forms. However, as ECCS suction screen size grows, some parts may be significantly more distant than others from the ECCS suction intake, and the effect of differential flow resistances once inside the device may result in differing approach velocities, differing debris accumulations, and differing debris-loaded head losses on the screen. Further, differences in plant structural configuration and equipment placement may impose limits on the overall size and orientation of passive strainers. Finally, minimum containment pool depth anticipated during ECCS recirculation also imposes a design constraint on the size and configuration of passive strainers.

Active strainers have been proposed as means of resolving ECCS suction screen blockage. A design currently available utilises a motor-driven rotating brush and plow assembly to clean the end disk of a strainer element. This design has not yet been tested with debris load quantities anticipated to be transported to the ECCS suction screen in PWRs. Because this design does not actually remove entrained debris from the sump, but simply pushes it off a strainer surface, qualification testing must demonstrate that debris removed from the end disk will not simply remain suspended in the pool and form a highly concentrated slurry around the strainer, eventually choking off recirculation flow. Relative to passive strainers, a workable active strainer offers a clear benefit in terms of allowing a relatively compact strainer element, but also imposes additional testing, operability, and maintenance requirements. Since the strainer serves a critical role in supporting the safety-related recirculation function of the ECCS system, an active strainer design will require a safety-related power supply and motor, and will need to undergo periodic operability testing to demonstrate that it remains functional. Evaluation of downstream effects must consider whether the operation of the active mechanism will contribute to debris throughput.

Active/passive strainer systems have also been proposed as a means of resolving ECCS suction screen blockage. Such a system was installed at Vattenfall's Ringhals Unit 2 in 1992. The active/passive strainer solution could utilise primary and secondary strainer elements separated by a normally closed valve. The primary strainer element would be a passive device with a large surface area directly connected to the ECCS suction piping. It acts as a "sacrificial" strainer element drawing most entrained or easily transportable debris when recirculation is initiated. After the debris bed has built up on this strainer element and NPSH margin has dropped to some threshold value, the valve is opened, allowing ECCS suction to draw water from the containment pool through the secondary strainer element. Debris already drawn to the primary strainer remains in place there, held by the slight differential pressure across the primary strainer element. One advantage of this concept is that the active element is protected within the strainer boundary, so is less likely to become jammed by debris. Disadvantages are that the physical size of an active/passive strainer will be large, and it will require careful accounting of debris quantities and transport rates to ensure that the debris bed deposited on the primary strainer is neither so great as to choke recirculation flow prematurely nor so slight as to allow the secondary strainer to become blocked.

6. Resolution combinations

Various combinations of the several resolution options may be combined to provide an integrated blockage solution for a plant. However, analytical demonstration that a particular resolution combination has the desired effect may involve iteration of debris transport and debris-loaded strainer head loss calculation drafts.

III. Factors affecting optimal selection of resolution means

Selection from among the foregoing resolution options will depend upon factors including established plant design, plant operations and maintenance protocols, type and variety of debris source materials in a specific plant, the extent to which plant structures restrict or channel ECCS recirculation flow to the sump, space limitations in the vicinity of the ECCS sump, sump accessibility, costs of engineering, fabrication, demolition and installation, ALARA, testing and maintenance.

1. *Established plant design features*

Established plant design features are those existing features which affect the relative vulnerability of the ECCS to debris blockage during recirculation. Plants which have relatively large ECCS suction screens – with total screen surface on the order of 1 000 ft² (~90+ m²) – are more likely to be able to accept the maximum debris load, and may also be relatively tolerant of a thin bed condition given homogeneous mixing of the latent and generated particulate debris. Plants which require relatively low ECCS recirculation flow rates – with ECCS suction screen approach velocities on the order of 0.1 fps or below – are more likely to see significant quantities of debris settle out rather than transport. Plants which have redundant ECCS suction trains that are physically separated by distance, barriers, or both are less likely to experience self-interference effects in which debris first transported to the operating ECCS suction train is re-transported to the stand-by ECCS suction train when operators shift recirculation from one train to the other. Plants designed to accommodate a deeper containment pool at the initiation of recirculation may tend to have greater NPSH margins than plants with more shallow containment pool depths, allowing greater tolerance for debris-loaded strainer head losses. Plants designed and equipped such that ECCS recirculation is not required in response to breaks in the main steam or main feedwater piping are somewhat easier to address analytically than plants which must consider debris generation from high energy line breaks on the secondary side.

2. *Type and variety of debris source materials*

The type and variety of debris source materials in a specific plant may affect the relative vulnerability of the ECCS to debris blockage during recirculation. Plants which have large quantities of granular (particulate-based) thermal insulation, such as calcium silicate and microporous, may find that it is more difficult to demonstrate assurance of ECCS function for a thin-bed debris condition, regardless of their housekeeping efforts to reduce latent debris particulates. On the other hand, plants in which all debris source materials are jacketed or encapsulated with stainless steel may take credit for the higher destruction pressures required to generate debris from these materials, which translates into a reduced quantity of debris generated relative to wrapped (“unjacketed”) debris source materials. Current analytical processes call for summing the head loss calculated for each individual type of debris, based on NRC-accepted correlations. Plants with four or five types of insulation materials as debris sources may need to include conservatism in their debris-loaded strainer head loss calculations that are more limiting than those required for plants with only one or two types of insulation materials, or for those with a greater degree of homogeneity to the mix of transported debris.

3. *Design basis analysis assumptions*

Design basis analysis assumptions will have an affect on the estimated quantity of transported debris, and thereby on the debris-loaded head loss. Most of the debris generation occurs during the initial LOCA blast, and the turbulence generated by the blast and subsequent blowdown has a major affect on the initial distribution of debris materials inside containment. However, there is little experimental data or actual experience available to facilitate assessment of blast/blowdown debris distribution. Engineering judgment, combined with reasonable, conservative assumptions and perhaps incorporated into logic trees, will necessarily govern the assessment of blast/blowdown debris distribution, taking into account the degree of compartmentalisation for a specific containment.

Another type of design basis analysis assumption arises from the tradeoff between rigor and conservatism associated with a specific methodology. For example, the debris transport “spectrum”

stretches from the basic – but conservative – assumption that 100% of generated debris is transported, through the simple – application of network nodal analysis yielding “one dimensional” average flow velocities, to the complex – application of computational fluid dynamics models to generate three-dimensional fluid velocity fields, accounting for a variety of boundary conditions and turbulence effects. Generally speaking, the more sophisticated the approach, the less conservatism will contribute to excessive estimates of debris transport.

Analysis assumptions also arise with respect to consideration of debris-loaded head loss for complex mixes of debris. Little data exists on the variation of debris bed head loss as a function of variations in the relative quantities of different types of debris materials present in the debris bed; this problem is exacerbated for complex debris beds involving a combination of several different debris materials, such as fiberglass, mineral wool, and particulates from dirt/dust, several types of coatings, and a granular insulation. Moreover, the assumption that the properties for a particular class of debris source materials do not vary as a function of manufacturing processes or treatments may not be valid.

The general tendency in the face of recognised design basis assumptions will be to build additional conservatisms into analyses; the resulting increase in transported debris and debris-loaded head loss will pressure plants to select more, and more varied, resolution methods to achieve a greater debris-load capacity than may actually be required. Depending on the resolution options deemed feasible for a specific plant, considerable time and effort may be expended to arrive at that excess capacity.

4. *Recirculation flow channel effects*

Recirculation flow channels imposed by the plant structures that configure the containment pool affect debris transport. All containments offer some flow paths to the ECCS sump, but some containment configurations implicitly present a more torturous flow path and greater opportunity to sequester debris in transport. Plants that have a “closed” bioshield or missile barrier architecture, with structural walls that restrict or channel recirculation flow located between the reactor coolant loops and the ECCS suction sump, may benefit from this effect. Other containment configurations may provide relatively open flow paths, but if there are only a few such paths, it may be feasible to utilise “choke points” in those paths to trap some debris in transport, reducing the debris load that ultimately accumulates at the ECCS suction.

5. *Plant operations and maintenance protocols*

Plant operations & maintenance protocols affect the quantity of latent debris available in containment. Current experience suggests that rigorous end-of-outage housekeeping efforts may be effective at limiting the quantity of latent dirt, dust and similar debris inside containment to under 150 lbs. of material. These debris materials may be generated during maintenance activities involving abrasion or grinding, may be carried into containment on tools, equipment, and protective clothing, or may arise from wear on active surfaces of moving components inside containment. Effective housekeeping efforts will strive to collect these debris materials as they are generated by maintenance activities, and will also strive to collect latent debris materials that collect on horizontal surfaces throughout containment. Another protocol, limiting the use of tape, adhesive labels, or other friable materials for identification markings inside containment, may serve to further reduce miscellaneous debris materials.

6. *Space limitations in vicinity of ECCS sump*

Space limitations in the vicinity of the ECCS sump may affect the choice of resolution options, or may force application of a combination of options. Some plant configurations have structures, such as the fuel transfer canal, overhanging the ECCS sump. Piping may run over or adjacent to the ECCS sump, and equipment may be located in close proximity to the ECCS sump. Where structures, piping, or equipment constrain the size and configuration of one resolution option, it may become necessary to consider a combination of several resolution options.

7. *ECCS sump accessibility*

ECCS sump accessibility considerations can affect design, installation and maintenance of replacement ECCS suction strainers. Some ECCS sumps are located inside high radiation areas. The approach to the ECCS sump area may be congested with piping and supports. Containment structures may overhang the ECCS sump. These present different obstacles to potential strainer resolutions. For sumps located in high radiation areas, the installation will entail higher ALARA costs and may require a larger installation team with frequent handoff of installation tasks. Active strainers and systems that require operability testing may impose recurring ALARA costs. Physically large passive strainers may be difficult to manoeuvre into place through a space that is congested with piping and supports. Overhanging structures may affect accessibility for installation as well as design configuration for both active and passive strainers

8. *Cost*

Costs of engineering, fabrication, demolition and installation, ALARA, testing and maintenance play into the selection of an optimal debris blockage resolution for a specific plant. Initial analytical evaluations are a common expense regardless of the resolution option selected. Reductions to ECCS or containment spray flow rate, if viable, will entail additional engineering analysis and licensing basis revision costs; they may also involve changes to operating procedures and operator training. Removal and replacement of small quantities of debris source insulation materials may be economically feasible; extensive insulation removal efforts will entail significant demolition and ALARA costs while insulation replacement will add fabrication, installation and ALARA costs. Installation of debris traps, if feasible, will require modest structural engineering, fabrication, installation and ALARA costs, and will impose a modest maintenance requirement.

Passive strainers will be considerably larger than active strainers, and therefore may cost more for material procurement and fabrication than active strainers even though the latter will also require motors and power connections. Installation costs will also be impacted by the costs of seismically qualified supports. Some passive strainer designs can be scaled to handle a given debris load without requiring further testing; other designs may require qualification testing to demonstrate that the actual debris-loaded head loss remains within the range that sustains a positive NPSH margin. Maintenance costs and in-service inspection (ISI) costs for passive strainers are anticipated to be low.

Active strainer installation costs will include routing power from a safety-related power supply to the motor. Since active strainers have not been tested under debris loads and pool conditions anticipated for PWRs, qualification testing with predicted debris quantities and types would be required in advance of installation. Although not pressure-retaining, active strainers will be required to operate to assure ECCS recirculation functionality, and thus will be subject to periodic testing to demonstrate operability. Maintenance, ISI, and in-service testing (IST) will impose recurring costs.

Failure of an active strainer to operate satisfactorily during a periodic test may have implications for plant operability; this is likely to impose additional costs, if only for procurement, storage, and maintenance of spare parts.

Active/passive strainer systems, like active strainers, will incur higher costs associated with impacts on plant design and licensing basis documentation. Use of either of these two solutions will also require revision of relevant post-LOCA operating procedures, both to confirm satisfactory system response, and to provide operators with alternative guidance in event that the active component fails to function.

9. *Coordination with other major plant modifications*

Coordination with other major plant modifications can affect timing, budget and resource availability for implementation of ECCS debris blockage resolutions. Alloy 600 resolution, reactor vessel head replacement, steam generator replacement, power uprate, and digital controls upgrades are all major initiatives that are competing with debris blockage for resources. Efforts to resolve Alloy 600 concerns are focused on reactor vessel penetrations (such as for CRDMs and/or BMIs), and may also be pertinent at some locations around the reactor coolant loops. In most plants, the ECCS sump is physically removed from these locations such that Alloy 600 work should not directly interfere with work to implement resolution of ECCS sump debris blockage. The same is generally true of reactor vessel head replacement and steam generator replacement work. However, when the incoming or outgoing component is being moved inside containment, personnel safety requirements may mandate that areas inside containment, including the areas in which the ECCS sumps are located, be cleared of personnel. Plants planning either reactor vessel head replacement or steam generator replacement during the same outage as debris blockage mitigation must schedule accordingly. In some cases, reactor vessel head replacement or steam generator replacement may require a temporary cut in the containment wall; it may be desirable to impose a heightened degree of FME inside containment to assure that dirt, dust, and other debris generated by the wall cut or allowed entry through the wall cut is not admitted into the ECCS sump or the recirculation suction piping. Power uprate projects may have implications for debris blockage resolution if they entail increases in the thermodynamic properties of the primary coolant (and, for plants that rely on ECCS recirculation for main steam or feedwater breaks, increases to thermodynamic properties of the secondary coolant). In other respects, power uprate projects normally will not interfere with debris blockage resolution. Digital controls upgrades are also unlikely to interfere with debris blockage resolution.

Plants that expect to carry out major upgrades in the areas discussed above during the same time frame in which they expect to implement ECCS debris blockage resolutions must plan, staff, schedule, and budget accordingly.

IV. Summary

In spite of having certain broad similarities in functional design, there is wide variation in both the structural configuration and ECCS sump pit configuration among the 69 US PWRs. These variations, together with plant-specific combinations and quantities of debris source insulation materials, strongly suggest that ECCS debris blockage resolution modes must be tailored to each specific plant. Broadly speaking, the available resolution modes include analytical evaluation, enhanced ECCS/Containment Spray operating protocols, removal and replacement of certain debris sources that cause high head loss, design and installation of debris traps in recirculation flow path choke points, design and installation of modified ECCS suction strainers using either a passive

strainer, an active strainer, or an active/passive system, and various combinations of two or more resolution modes. A number of factors must be considered in the process of identifying the optimum resolution mode for a specific plant configuration, debris source inventory, and limiting debris loads. Some of these relate to the physical features of a specific plant, some relate to design basis analysis assumptions, and some relate to either immediate or long-term implementation costs.

**LOCA INDUCED DEBRIS CHARACTERISTICS FOR USE IN ECCS SUMP SCREEN
DEBRIS BED PRESSURE DROP CALCULATIONS**

Gilbert Zigler

Alion Science and Technology, USA

Gordon Hart

ARTEK, Inc., USA

Jon Cavallo

Corrosion Control Consultants and Labs, Inc., USA

Abstract

Pressure drop calculations across a LOCA induced fibrous debris bed have been successfully demonstrated to be accurate using the NUREG/CR-6224 semi-theoretical head loss correlation. One of the critical parameters needed for the NURE/CR-6224 correlation to predict the pressure drop across a fibrous debris bed are the characteristics of the debris constituents (density and characteristic size). This paper provides a brief description of the NUREG/CR-6224 head loss correlation and presents suggested debris characteristics of typical sources of debris found in American nuclear power plants for use in the correlation.

Background

Following a hypothetical loss of coolant accident (LOCA) caused by a postulated pipe break in containment, nuclear power plants will inject water into the reactor vessel to control core temperatures via the emergency core cooling system (ECCS). For boiling water reactors (BWRs) the water from the suppression pool is used whereas for pressurised water reactors (PWRs) borated water from a storage tank is first introduced and when that water is exhausted, the ECSS recirculates the water from the containment pool. In both cases, some of the debris generated by the postulated break could be transported to either the suppression pool (BWRs) or the containment sump (PWRs). A screen is usually installed in the ECCS suction of the suppression pool or sump to ensure that LOCA induced debris will not be entrained and clog ECCS components such as containment spray nozzles. The LOCA induced debris transported to the suppression pool or containment sump could then form a debris bed on the ECCS suction screen. Some early investigation of the possibility of clogging the ECCS suction was performed in the early 1980s by the USNRC [1]. Since the Barsebäck incident in 1992 [2] the operators and regulators of nuclear power plants have become increasingly aware that a debris bed could be formed at the ECCS suction screen and cause potentially unacceptable pressure drops thereby challenging the post-LOCA operation of the ECCS. Several experiments have been conducted around the world [1, 2, 3, 4] with the aim of developing a correlation that could be used to predict the pressure drop (head loss) across a debris bed formed on the surface of the ECCS suction strainer or sump screen. In the USA the NUREG/CR-6224 head loss correlation developed by the USNRC for fibrous debris beds has been used to estimate the head loss in over 50% of the USA BWR strainers,¹ was used in the series of recently published NUREG/CR associated with Generic Issue 191 [6], and has been adopted by the industry for use in PWR sump screen performance assessments [7]. The NUREG/CR-6224 head loss correlation does not apply to debris bed formed by debris generated with the damage and destruction of reflective metallic insulation (RMI). RMI head loss correlations can be found in References 3, 4, and 9. This paper provides a brief description of the NUREG/CR-6224 fibrous head loss correlation and presents recommended values of debris characteristics to be use in estimating head loss across a debris bed when using the NUREG/CR-6224 correlation.

NUREG/CR-6224 head loss correlation

The NUREG/CR-6224 head loss correlation is described in detail in “Parametric Study of the Potential for BWR ECCS Strainer Blockage Due to LOCA Generated Debris”, Appendix B [5] and is a semi-theoretical head loss model. The correlation is based on the theoretical and experimental research for the pressure drops across a variety of fibrous porous media carried out since the 1940s. The NUREG/CR-6224 head loss model, proposed for laminar, transient and turbulent flow regimes through mixed debris beds (i.e. debris beds composed of fibrous and particulate matter) is given by:

$$\Delta H = \Lambda \left[3.5 S_v^2 \alpha_m^{1.5} (1+57 \alpha_m^3) \mu U + 0.66 S_v \frac{\alpha_m}{1-\alpha_m} \rho_w U^2 \right] \Delta L_m \quad (1)$$

1. The NUREG/CR-6224 was used to estimate the performance of the BWR ECCS stacked disk suction strainers developed by Performance Contracting Inc. installed as replacement strainers in US and Taiwanese BWRs.

where,

ΔH is the head loss,

S_v is the surface to volume ratio of the debris particle,

μ is the dynamic viscosity of water,

U is the approach velocity,

ρ is the density of water,

α_m is the mixed debris bed solidity,

ΔL_m is the mixed debris bed thickness, and

Λ is a unit conversion factor ($\Lambda = 1$ for SI units).

Each debris constituent has a surface-to-volume ratio associated with it based on the characteristic shape of that debris type. For typical debris types, we have

Cylindrically-shaped debris:

- fiber $S_v = 4/\text{diam}$
- lead-wool $S_v = 4/\text{diam}$

Spherically-shaped debris:

- sludge $S_v = 6/\text{diam}$
- dirt/dust $S_v = 6/\text{diam}$
- Cal-Sil $S_v = 6/\text{diam}$

Flakes (flat-plates):

- rust $S_v = 2/\text{thick}$
- paint chips $S_v = 2/\text{thick}$,

where “diam” is the diameter of the fiber or spherical particle, and “thick” is the thickness of the flake/chip. Other debris not listed above would have its surface-to-volume ratio calculated similarly based on one of the above characteristic shapes.

The mixed debris bed solidity is given by:

$$\alpha_m = \left(1 + \frac{\rho_f}{\rho_p} \eta \right) \alpha_o \frac{\Delta L_o}{\Delta L_m} \quad (2)$$

where,

α_o is the as-fabricated fiber bed solidity,

ΔL_o is the theoretical (or as-fabricated) fibrous debris bed thickness,

$\eta = m_p/m_f$ is the particulate to fiber mass ratio in the debris bed,

ρ_f is the fiber density, and

ρ_p is the particulate material density.

For N_p classes of particulate materials, m_p and ρ_p are defined by:

$$m_p = \sum_{i=1}^{N_p} m_i \quad (3)$$

and

$$\rho_p = \frac{\sum_{i=1}^{N_p} \rho_i V_i}{\sum_{i=1}^{N_p} V_i} \quad (4)$$

where m_i , ρ_i and V_i are the mass, density and volume of a particulate material i .

Compression of the fibrous bed due to the pressure gradient across the bed is also modelled. The relation that accounts for this effect, which must be satisfied in parallel to the previous equation for the head loss, is given by (valid for $(\Delta H/\Delta L_o) > 0.5$ ft-water/inch-insulation):

$$c = 1.3 c_o (\Delta H / \Delta L_o)^{0.38} \quad (5)$$

where,

c is the compressed debris bed density (in lb/ft^3),

c_o is the as-fabricated insulation density (in lb/ft^3), and

$\Delta H/\Delta L_o$ is the head loss in ft-water per inch of insulation.

The compression is limited such that a maximum solidity, α_{\max} , is not exceeded. In the NUREG/CR-6224 report, this maximum solidity is defined to be:

$$\alpha_{\max} = 65 \text{ lb}/\text{ft}^3 / \rho_p$$

which is equivalent to having a debris bed with a density of $65 \text{ lb}/\text{ft}^3$. Note that $65 \text{ lb}/\text{ft}^3$ is the macroscopic density of granular media such as sand, gravel or clay and is a reasonable value to use in case of iron oxide particles.

The NUREG/CR-6224 head loss correlation has been extensively validated for a variety of flow conditions and experimental facilities, types and quantities of fibrous insulation debris, and types and quantities of particulate matter debris. The test facilities include the Alden Research Laboratories (ARL) test loop [5], the Electric Power Research Institute (EPRI) facility, the five different experimental facilities used as part of the International Working Group (IWG) formed under the OECD Nuclear Energy Agency (NEA) [4], and the ARL chugging facility. The flow conditions have included approach velocities² from 0.06 ft/s (0.02 m/s) to 1.5 ft/s (0.5 m/s) and water temperatures from 50°F (10°C) to 130°F (55°C). The types of fibrous insulation material tested include NUKON™ and Temp-Mat®. The particulate matter debris tested includes iron oxide particles from 1 to 300 μm in characteristic size and paint chips. In all cases, the NUREG/CR-6224 head loss correlation results have bounded the experimental results.

The majority of these tests were performed with flat perforated plates [4]. Further, these tests involved a relatively uniform distribution of debris on the entire perforated plate. Consideration of a relatively uniform debris bed distribution on the strainers is appropriate and conservative. Furthermore, it can be shown [5] that assuming uniform distribution of debris results in higher head losses than for non-uniform distributions of debris.

In summary, the NUREG/CR-6224 head loss correlation is considered to be applicable to estimate the pressure drop due to mixtures of fibrous debris and particles. To implement this head loss algorithm for the estimating the head loss across a strainer or sump screen, the quantity and characteristics of the debris on each strainer and the temperature and velocity of the water flowing through the debris must be determined. Reference 8 is an example of the implementation of NUREG/CR-6224 by commercial organisation.

The few sections provide recommended debris characteristics for use in the NUREG/CR-6224 head loss correlation.

Debris characteristics

In a homogeneous debris bed, the densities and size characteristics of the individual constituents are necessary to determine the porosity of the debris bed. In general, the lower bound values for the characteristic sizes of the debris were adopted. This is conservative for head loss calculations because the specific surface is inversely proportional to the characteristic size of the debris particle. The smaller the characteristic size of the debris bed constituents the higher the pressure drop across the debris bed. The following tables provide a listing of the characteristics necessary for the head loss computations for debris originating from thermal insulation material, coatings, and miscellaneous debris.

Thermal insulation characteristics

Table 1 has characteristic values for thermal insulation materials which have been identified in American nuclear containments. Some are listed by trade names and others by generic names; some are listed as a system and some as simply an insulation material. The different types of mass insulation could be subdivided generically into fibrous, granular, and cellular insulation.

2. Approach velocity is defined is the total flow divided by the total screen area.

Fibrous insulation materials include fibrous glass wool such as Performance Contracting, Inc.'s NUKON®, Transco Products, Inc.'s Thermal Wrap®, preformed fiberglass pipe (made by Owens Corning, Knauf, and Johns Manville), and fiberglass pipe and tank wrap (from the same three manufacturers). The NRC refers to the insulation fillers in NUKON and Thermal Wrap as "Low Density Fiber Glass" (LDFG). There are also some glass fiber felt mat insulation materials and these include Temp-Mat® and Insulbatte® insulations, both made by JPS Corp., as well as some by other trade names such as Alpha Inc.'s AlphaMat®. Other fibrous materials include ceramic felt mat insulation, two of which are Thermal Ceramics Inc.'s Kaowool® and Cerawool®. Finally, there are mineral wool insulation products with a number of different trade names, forms, and densities. Major North American manufacturers are Rock Wool Manufacturing, Roxul, Fibrex, IIG, and Thermafiber. While mineral wool has been widely used in Europe in some nuclear containments and fibrous glass and glass fiber felt have not been widely used, mineral wool has limited use in North American nuclear containments. Mineral wool was the original drywell piping insulation, at the Barsebäck Plant, that was blown off by a lifted steam relief valve and which subsequently blocked a couple of ECCS strainers. In general, mineral wool is available in densities that are at least twice those of comparable fibrous glass wool insulations.

Granular insulation materials include calcium silicate and microporous. All the calcium silicate insulation in North America has been manufactured without the use of asbestos since about 1972. While it has been made by various manufacturers over the years, today all calcium silicate is manufactured by IIG, a joint venture between Calsilite Corp. and Johns-Manville Corp., at three factories. The only microporous insulation manufactured in North America is MinK®, manufactured by Thermal Ceramics, Inc. today but by Johns Manville for many years. Microtherm manufactured in the UK, is also available in North America.

The only cellular insulation on the above list is cellular glass. Most of what has been installed in US nuclear plants has been manufactured by Pittsburgh Corning Corporation and is known by its trade name, Foamglas®. This is an inorganic, rigid, and brittle cellular insulation typically used in containments on chilled water lines. However, for reference, there are numerous other types of cellular insulations available which are organic compounds; these include melamine, polystyrene, polyisocyanurate, phenolic, polyimide, polyolefin, flexible elastomeric, and polyurethane foams. There are numerous trade names by which these are known. The best known is Dow Chemical's Styrofoam, which is polystyrene foam insulation.

Failed coatings characteristics

Debris from failed coatings has been recognised as an important contributor to the particulate debris loading. Some of the earlier work in characterising coating debris can be found in [10]. The following types of coatings are commonly found within American PWR containments: inorganic zinc (IOZ), epoxy, epoxy phenolic and alkyd. Their characteristics for use in the NUREG/CR-6224 head loss correlation are shown in Table 2.

The specific gravity for IOZ is listed as 5.6. A specific gravity of 5.6 corresponds to a nominal density of 350 lbs/ft³. This value is lower than the 437 lbs/ft³ reported by carboline for the zinc dust used in the formulation of CarboZinc 11. As such, the nominal density value of 350 lbs/ft³ is conservative since lower density values imply higher volumes and thus higher head losses.

Coatings within the ZOI will be ablated by the break jets. In the absence of specific experimental details about the debris particle size distribution for IOZ, alkyds, epoxy and epoxy phenolic coating debris generated by high pressure water/steam jets in the ZOI, a diameter of 10 µm

has been selected as the characteristic size of coating debris generated within the ZOI. The 10 μm characteristic diameter is the nominal diameter of unbound zinc particles and also the alkyd pigment particles of failed coatings. Epoxy and epoxy phenolic coatings outside the ZOI will fail as chips. A typical lower bound for epoxy and epoxy phenolic coating chip thickness is 1 mil (25.4 μm). 10 μm diameters are shown as the characteristic size of IOZ and alkyd coating debris outside of the ZOI.

Table 1. Thermal insulation material characteristics

Debris name	Insulation material description	As-fabricated density (lbs/ft ³)	Material density (lbs/ft ³)	Characteristic size	
				µm	Inch
PCI's NUKON® blankets	Removable/reusable blankets with woven glass fiber cloth covering fibrous glass insulating board (referred to by the NRC as a "LDFG")	2.4	159	7.0 fiber diameter	28E-05
Fiberglass – preformed pipe	Knauf fibrous glass wool preformed into cylindrical shapes	4.0 +/- 10%	159	7.5 fiber diameter	30E-05
Fiberglass – preformed pipe	Owens Corning fibrous glass wool preformed into cylindrical shapes	3.5 to 5.5	159	8.25 fiber diameter	33E-03
Fiberglass – pipe and tank wrap	Fibrous glass wool wrap, using perpendicularly oriented fibers, adhered to an All Service Jacketing (ASJ) facing (made by Knauf, Owens Corning, & others)	3.0 +/- 10%	159	6.75 fiber diameter	27E-05
Transco's Thermal Wrap® Blankets	Removable/reusable blankets with woven glass fiber cloth covering fibrous glass insulant (Knauf ET Panel®) (referred to by the NRC as a "LDFG")	2.4	159	5.5 fiber diameter	22E-05
Temp-Mat® and Insulbatte®	Glass fibers needled into a felt mat; these are trade names of insulation products made by JPS Corp.	11.8	162	9.0 fiber diameter	36E-05 max.
Cellular Glass	Foamglas® is the trade name for this cellular glass product made by Pittsburgh Corning Corporation	6.1 to 9.8 (mean value of 7.5)	156	NA	0.05 to 0.08 pore size
Kaowool®	Needled insulation mat made from ceramic fibers; Kaowool is a trade name for a family of ceramic fiber products made by Thermal Ceramics, Inc.	3 to 12	160 to 161	2.7 to 3.0 fiber diameter	10.8 to 12.0E-05
Cerawool®	Needled insulation mat made from ceramic fibers; Cerawool is a trade name for a family of ceramic fiber products made by Thermal Ceramics, Inc.	3 to 12	156 to 158	3.2 to 3.5 fiber diameter	12.8 to 14.0E-05
Mineral Wool	Generic name for families of products made by Rock Wool Mfg., Roxul, Fibrex, IIG, and others	4, 6, 8, and 10 pcf are standard	90	5 to 7 fiber diameter	20 to 28 E-05
MinK®	Trade name of microporous insulation products made by Thermal Ceramics, Inc. from fumed silica, glass fibers, and quartz fibers	8 to 16 pcf	NA	< 0.1	< 4e-06
Calcium Silicate	Manufactured by IIG in three locations (2 use diatomaceous earth, 1 uses expanded perlite)	14.5	144	40 µm mean particle size (2 to 100 µm range)	1.60E-03

Table 2. Coating debris characteristics

Generic coating material	Material density (lbs/ft ³)	Characteristic size	
		µm	ft
Inorganic zinc (IOZ)	350	10 ³	3.28E-05
Epoxy and epoxy phenolic coating chip (outside ZOI)	94	25 ⁴	8.20E-05
Epoxy and epoxy phenolic coating particles (in ZOI)	94	10 ²	3.28E-05
Alkyd coating	98	10 ²	3.28E-05

Miscellaneous debris characteristics

Miscellaneous debris such as concrete debris, dust, dirt, other latent debris, rust, etc. all have to be considered if they are present inside the containment. Items such as equipment tags (paper or plastic) and things such as plastic sheeting or tarps also have to be evaluated. These latter ones are generally treated as a surface area reduction hence not included explicitly in the head loss calculations.

Rust flakes are considered as iron oxides with a microscopic density of 324 lb/ft³. Rust flakes have the same similar appearance as thick paint chips. As such it is reasonable to adopt the same lower bound value of epoxy paint chip thickness for rust flakes thickness. Hence an equivalent thickness of 1 mil (25.4 µm) was adopted for the characteristic size of rust flakes in this calculation.

In the absence of specific information, a microscopic density of 156 lb/ft³ is adopted for dirt/dust. Based on typical diameter of dust particles, a diameter of 10 µm was adopted.

Table 3. Miscellaneous debris characteristics

Debris material	Material density (lbs/ft ³)	Characteristic size	
		µm	ft
Rust	324 ⁵	25	8.2E-05
Dirt/Dust	156 ⁶	10	3.28E-05

-
3. Spherical Particle Diameter.
 4. Flat Plate Thickness.
 5. Flat Plate Thickness.
 6. Spherical Particle Diameter.

REFERENCES

- [1] Serkiz, A.W. "Containment Emergency Sump Performance", NUREG-0897, U.S. Nuclear Regulatory Commission, October 1985.
- [2] NEA, (1996) "Knowledge Base for Emergency Core Cooling System Recirculation Reliability", NEA/CSNI/R(95)11, Prepared by the U.S. Nuclear Regulatory Commission for the Nuclear Energy Agency (NEA) of the OECD, February 1996.
- [3] BWROG, "Utility Resolution Guidance for ECCS Suction Strainer Blockage", Boiling Water Owners' Group, NEDO-32686, Rev. 0, November 1996.
- [4] Rao, D.V., *et al.* "Knowledge Base for the Effect of Debris on Pressurized Water Reactor Emergency Core Cooling Sump Performance", NUREG/CR-6808, Los Alamos National Laboratory, February 2003.
- [5] Zigler, G., *et al.* "Parametric Study of the Potential for BWR ECCS Strainer Blockage Due to LOCA Generated Debris", US NRC Report NUREG/CR-6224, Science and Engineering Associates, October 1995.
- [6] Rao, D.V., *et al.* "GSI-191 Technical Assessment: Parametric Evaluations for Pressurized Water Recirculation Sump Performance", NUREG/CR-6762, Vol. 1. Los Alamos National Laboratory, August 2002.
- [7] Westinghouse Owner's Group/Nuclear Energy Institute, "PWR Containment Sump Evaluation Methodology", 30 October 2003.
- [8] Mast, Peter K. and Francisco J. Souto "HLOSS 1.0: A Code for the Prediction of ECCS Strainer Head Loss", ITS/ITS-97-01, ITS Corporation, 16 May 1997.
- [9] Zigler, G., *et al.* "Experimental Investigation of Head Loss and Sedimentation Characteristics of Reflective Metallic Insulation Debris", Science and Engineering Associates, Inc., Report No. SEA95-970-01-A:2, May 1996.
- [10] Bostelman, Jan and Gil Zigler, "Failed Coating Debris Characterization", BWROG Containment Coating Committee, 10 July 1998.

LIST OF PARTICIPANTS

BELGIUM

DELALLEAU, Jean-Charles (Mr.)
Nuclear Safety Engineer
Electrabel
Avenue De l'Industrie, 1
B-4500 Tihange

Phone: +32 8 524 39 66
Fax: +32 8 524 39 79
E-mail: jeancharles.delalleau@electrabel.com

DELVEAU, Caroline (Ms.)
Industrial Engineer
Tractebel Engineering
Avenue Ariane, 7
B-1200 Brussels

Phone: +32 2 773 97 24
Fax: +32 2 773 89 00
E-mail: caroline.delveau@tractebel.com

DU BOIS D'ENGHIEN, Guillaume
Tractebel Engineering
Avenue Ariane, 7
B-1200 Brussels

Phone: +32 2 773 08 47
Fax : +32 2 773 89 00
E-mail:
guillaume.duboisd'enghien@tractebel.com

GAUTHIER, Phillipe, (Mr.)
Westinghouse Energy Belgium S.A.
Rue de l'Industrie, 43
B-1400 Nivelles

Phone: +32 6 728 82 32
Fax: +32 6 728 83 32
E-mail: gauthier-ph@notes.westinghouse.com

TOMBUYSES, Beatrice (Dr.)
System Engineer
Association Vinçotte Nuclear (AVN)
Rue Walcourt, 148
B-1070 Brussels

Phone: +32 2 528 02 61
Fax: +32 2 528 01 02
E-mail: bto@avn.be

VANDEWALLE, André (Dr.)
Division Head
Inspections of Nuclear Installations
Association Vinçotte Nuclear (AVN)
Rue Walcourt, 148
B-1070 Brussels

Phone: +32 2 528 01 30
Fax: +32 2 528 01 01
E-mail: avw@avn.be

CANADA

EYVINDSON, Ailsa (Ms.)
R&D Engineer
Atomic Energy of Canada Limited
Chalk River Laboratories
Chalk River, Ontario, K0J 1J0

Phone: +1 613 584-8811 ext 4593
Fax : +1 613 584-8216
E-mail: eyvindsona@aecl.ca

RHODES, David (Mr.)
Manager,
Mechanical Equipment and Seal Development
Atomic Energy of Canada Limited
Chalk River Laboratories
Chalk River, Ontario, K0J 1J0

Phone: +1 613 584-8811 ext. 3733
Fax: +1 613 584-8216
E-mail: rhodesd@aecl.ca

CZECH REPUBLIC

KUJAL, Bohumir (Dr.)
Senior Consultant
Nuclear Research Institute Rez, plc
250 68 Rez

Phone: +420 266 173 657
Fax: +420 266 173 570
E-mail: kub@ujv.cz
bohumer.kujal@ujv.cz

VESELY, Jiri (Mr.)
Head of Local Inspectors, NPP Dukovany
State Office for Nuclear Safety
Senovazne nam.9 Prague

Phone: +420 568 815 552
Fax: +420 568 866 414
E-mail: jiri.vesely@sujb.cz

FINLAND

PAALANEN, Anssi (Mr.)
Nuclear Safety Engineer
Teollisuuden Voima Oy
FIN-27160 Olkiluoto

Phone: +358 2 8381 3233
Fax: +358 2 8381 3209
E-mail: anssi.paalanen@tvo.fi

SJOVALL, Heikki (Mr.)
Teollisuuden Voima Oy
FIN-27160 Olkiluoto

Phone: +358 2 8381 3222
Fax: +358 2 8381 3209
E-mail: Heikki.Sjovall@tvo.fi

FRANCE

ARMAND, Yves (Dr.)
Project Manager
Service d'Évaluation des Risques et des Systèmes
Département d'Évaluation de Sûreté
Institut de Radioprotection et de Sûreté Nucléaire
(IRSN), B.P. 17
F-92262 Fontenay-aux-Roses Cedex

Phone: +33 1 58 35 82 07
Fax: +33 1 58 35 89 89
E-mail: yves.armand@irsn.fr

BLOMART, Philippe (Mr.)
Senior Engineer
EDF
12-14 Avenue Dutrievoz
F-69628 Villeurbanne Cedex

Phone: +33 4 72 82 71 52
Fax: +33 4 72 82 77 02
E-mail: philippe.blomart@edf.fr

COLIN, Pierre (Mr.)
Fluid System Engineer
Framatome ANP
Tour Areva
F-92084 Paris La Défense

Phone: +33 1 47 96 32 94
Fax: +33 1 47 96 31 88
E-mail: pierre.colin@framatome-anp.com

DURIN, Michel (Dr.)
Deputy Head, Reactor Safety Direction
Institut de Radioprotection et de Sûreté Nucléaire
(IRSN), B.P. 17
F-92262 Fontenay-aux-Roses Cedex

Phone: +33 1 58 35 81 83
Fax : +33 1 46 54 32 64
E-mail: michel.durin@irsn.fr

DESCHILDRE, Olivier (Mr.)
Direction Générale de la Sûreté Nucléaire et de la
Radioprotection (DGSNR)
10 Route du Panorama
F-92266 Fontenay-aux-Roses Cedex

Phone: +33 1 43 19 70 60
Fax: +33 1 43 19 70 66
E-mail: olivier.deschildre@asn.minefi.gouv.fr

GORBATCHEV, Alexandre (Mr.)
Institut de Radioprotection et de Sûreté Nucléaire
(IRSN)
B.P. 17
F-92262 Fontenay-aux-Roses Cedex

Phone: +33 1 58 35 71 02
Fax: +33 1 58 35 86 54
E-mail: alexandre.gorbatchev@irsn.fr

MATTEI, Jean-Marie (Mr.)
Chef de Service
Service d'Évaluation des Risques et des Systèmes
Département d'Évaluation de Sûreté
Institut de Radioprotection et de Sûreté Nucléaire
(IRSN)
B.P. 17
F-92262 Fontenay-aux-Roses Cedex

Phone: +33 1 58 35 82 99
Fax: +33 1 58 35 89 89
E-mail: jean-marie.mattei@irsn.fr

PARADIS, Luc (Mr.)
Safety Projects Engineer
CEA
Commissariat à l'Énergie Atomique
Centre de Saclay
F-91191 Gif-sur-Yvette Cedex

Phone: +33 1 69 08 25 00
Fax: +33 1 69 08 58 70
E-mail: luc.paradis@cea.fr

ROYEN, Jacques (Mr.)
Nuclear Safety Division
OECD Nuclear Energy Agency
Le Seine Saint-Germain
12 Boulevard des Iles
F-92130 Issy-les-Moulineaux

Phone: +33 1 45 24 10 52
Fax: +33 1 45 24 11 29
E-mail: jacques.royen@oecd.org
royen@nea.fr

VIAL, Eric (Mr.)
Branch Manager
IRSN
77-83 avenue du Général-de-Gaulle
F-92140 Clamart

Phone: + 33-1-58-35-80-19
Fax: + 33-1-58-35-89-89
E-mail: eric.vial@irsn.fr

WALTER, Stephane (Mr.)
Engineer
ECCS
EDF-CIPN 140 Avenue VITON
F-13401 Marseille

Phone: +33 491 74 9283
Fax: +33 491 74 9538
E-mail: stephane.walter@edf.fr

GERMANY

ALT, Soeren (Mr.)
University of Applied Sciences Zittau/Goerlitz
Theodor-Koerner-Allee 16
D-02763 Zittau

Phone: +49 3583 611544
Fax: +49 3583 611288
E-mail: s.alt@hs-zigr.de

BRAUN, Gerhard (Mr.)
Hessian Ministry for Environment
Verbraucherschutz, Mainzer Strasse 80
D-65021 Wiesbaden

Phone: +01149 0611-815-1556
Fax: +01149 0611 815 1945
E-mail: g.braun@hmulv.hessen.de

HUBER, Josef (Mr.)
TÜV Süddeutschland Bau und Betrieb GmbH
Abteilung ETA 1
Westendstrasse 199
D-80686 München

Phone: +49 89 5791 1285
Fax: +49 89 5791 2696
E-mail: josef.huber@tuev-sued.de

KAESTNER, Wolfgang (Dr.)
Research Engineer
University of Applied Sc. Zittau/Goerlitz (FH)
Theodor-Koerner-Allee 16
D-02763 Zittau

Phone: +49 3583 611553
Fax: +49 3583 611288
E-mail: w.kaestner@hs-zigr.de

KNITT, Ulrich (Mr.)
Safety analysis
RWE Power AG
Huysenallee 2
D-45128 Essen

Phone: +49 201 122 2282
Fax: +49 201 122 1948
E-mail: Ulrich.knitt@rwe.com

KREPPER, Eckhard (Dr.)
Forschungszentrum Rossendorf e.V.
Institute of Safety Research
POB 510119
D-01314 Dresden

Phone: +49 351 260 2067
Fax: +49 351 260 2383
E-mail: e.krepper@fz-rossendorf.de

MAQUA, Michael (Dr.)
Assistant to the Scientific Director
Gesellschaft für Anlagen- und Reaktorsicherheit
(GRS) mbH
Schwertnergasse 1
D-50667 Köln

Phone: +49 221 2068 718
Fax: +49 221 2068 704
E-mail: maq@grs.de

OHLMEYER, Hermann (Mr.)
Head Section Reactor Safety
Hamburgische Electricitätswerke AG
Ueberseering 12
D-22297 Hamburg

Phone: +49 406 396 3701
Fax: +49 406 396 3004
E-mail: hermann.ohlmeyer@hew.de

PÜETTER, Bernhard (Dr.-Ing)
Group Leader, Accident Management
Thermal-Hydraulics & Process Eng. Div.
Gesellschaft für Anlagen- und Reaktorsicherheit
(GRS) mbH
Schwertnergasse 1,
D-50667 Köln

Phone: +49 221 2068 681
Fax: +49 221 2068 834
E-mail: pue@grs.de

SCHAFFRATH, Andreas (Dr.)
Section Head
Safety & Accident Analysis,
Technischer-Überwachungsverein Nord e.V.
Bereich Energie-und Systemtechnik
D-22525 Hamburg

Phone: +49 (40) 8557 2963
Fax: +49 (40) 8557 1901 7413
E-mail: aschaffrath@tuev-nord.de

SEEBERGER, Gerd Joachim (Mr.)
Senior Expert, Safety Engineering
Framatome ANP GmbH
POB 3220
D-91050 Erlangen

Phone: +49 9131 1892124
Fax: +49 9131 1894345
E-mail:

SEELIGER, Andre (Mr.)
University of Applied Sciences Zittau Goerlitz
Theodor-Koerner-Allee 16
D-02763 Zittau

Phone: +49 3583 6115 44
Fax: +49 3583 611288
E-mail: aseeliger@hs-zigr.de

TIETSCH, Wolfgang (Dr.)
Westinghouse Electric Germany
Dudenstrasse 44
D-68161 Mannheim

Phone: +49 621 388 2120
E-mail:
wolfgang.tietsch@de.westinghouse.com

WAAS, Ulrich (Mr.)
Senior Expert
c/o Framatome-ANP GmbH
NGPS
Postfach 3220
D-91050 Erlangen

Phone: +49 9131 1894 730
Fax: +49 9131 1894 787
E-mail: ulrich.waas@framatome-anp.com

WASSILEW-REUL, Christine (Ms.)
Referentin
Nuclear Safety
Robert-Schumann-Platz 3
D-53175 Bonn

Phone: +49 01888-305 2858
Fax: +49 01888-305 3963
E-mail: Christine.wassilew-reul@bmu.bund.de

JAPAN

ISHIKAWA, Masao (Mr.)
Senior Researcher & Senior Officer
Safety Information Analysis Group
Safety Intelligence Division
Japan Nuclear Energy Safety Org. (JNES)
Fujita Kanko Toranomom Bldg.
3-17-1, Toranomom, Minato-ku
Tokyo 105-0001

Phone: +81 3 4511-1932
Fax: +81 3 4511-1998
E-mail: ishikawa-masaaki@jnes.go.jp

MATSUOKA, Hiroshi (Mr.)
Mitsubishi Heavy Industries, Ltd.
1-1, Wadasaki-cho 1-chome, Hyogo-ku
Kobe, 652-8585

Phone: +81 78 672-3342
Fax: +81 78 672-3349
E-mail: hiroshi_matsuoka@mhi.co.jp

NAKAMURA, Hideo (Dr.)
Head of Laboratory
Japan Atomic Energy Research Inst. (JAERI)
2-4, Shirakata Shirane
Tokai-mura, Ibaraki-ken 319-1195

Phone: +81 29 282 5263
Fax: +81 29 282 6728
E-mail: nakam@lstf3.tokai.jaeri.go.jp

SHIRAYANAGI, Harunobu (Mr.)
Tokyo Electric Power
1-1-3, Uchisaiwai-cho, Chiyoda City
Tokyo Met.

Phone: +81 3 4216 4804
Fax : +81 3 596 8540
E-mail: shirayanagi.hal@tepcoco.jp

TANAKA, Toshihiko (Mr.) (Tosi)
Manager, Nuclear Engineer
Kansai Electric Power Co., Inc.
3-3-22 Nakanoshima Kita-ku
Osaka

Phone: +81 6 6441 8821
Fax: +81 6 6441 4277
E-mail: k410924@kepcoco.jp

MEXICO

MAMANI ALEGRIA, Yuri Raul (Mr.)
Technical Consultant
National Commission on Nuclear Safety and
Safeguards (CNSNS)
Dr. Barragan 779
03020 Distrito Federal

Phone: +52 55 5095 3235
Fax: +52 55 5095 3293
E-mail: yrmamani@cnsns.gob.mx

NETHERLANDS

HUIBREGTSE, Piet (Mr.)
Senior Engineer Evaluations
NV EPZ (NPP Borssele)
P.O. Box 130
NL-4380 AC Vlissingen

Phone: +31 113 356370
Fax: +31 113 352434
E-mail: p.huibregtse@epz.nl

ROOSEBOOM, Arend J. (Mr.)
Nuclear Safety Inspector
Nuclear Safety Dept (KFD), VROM Ministry
P.O. Box 16191
NL-2500 BD The Hague

Phone: +31 70 339 21 84
Fax: +31 70 339 18 87
E-mail: arend.rooseboom@minvrom.nl

SPAIN

ALONSO-ESCÓS, José R. (Mr.)
Division Manager (Nuclear Systems)
Consejo de Seguridad Nuclear (CSN)
Justo Dorado, 11
SP-28040 Madrid

Phone: +34 91 346 0207
Fax: +34 91 346 0216
E-mail: jrae@csn.es

ALONSO-LÓPEZ, Mónica (Ms.)
Nuclear System Specialist
Consejo de Seguridad Nuclear (CSN)
Justo Dorado, 11
SP-28040 Madrid

Phone: +34 91 346 0663
Fax: +34 91 346 0216
E-mail: mal@csn.es

SORIANO, Luis
Manager
Almara-Trillo NPP's
Carlos Trias Bertran, 7
SP-28020 Madrid

Phone: +34 619 748 134
Fax: +34 915 566 520
E-mail: l.soriano@cnat.es

TARRASA BLANES, Fernando (Mr.)
Systems Engineer, ANAV
Vandellos II Nuclear Power Plant
P.O. Box 27
SP-43890 L'Hospitalet de L'Infant

Phone: +34 977 81 87 00
Fax: +34 977 81 00 14
E-mail: ftarrasa@anacnv.com

VILLALBA-DOMINGUEZ, Cristina (Ms.)
Nuclear System Expert
Consejo de Seguridad Nuclear (CSN)
Justo Dorado, 11
SP-28040 Madrid

Phone: +34 91 346 0269
Fax: +34 91 346 0216
E-mail: cvd@csn.es

SLOVAK REPUBLIC

BATALIK, Jozef (Mr.)
Assistant to the Director
VUEZ a.s. Levice
Hviezdoslavova 35, P.O. Box 153
Levice

Phone: +421 366 35 5311
Fax: +421 366 35 5313
E-mail: batalik@vuez.sk

VICENA, Ivan (Mr.)
Senior designer
VUEZ a.s. Levice
Hviezdoslavova 35, P.O. Box 153
Levice

Phone: +421 366 355 336
Fax: +421 366 355 313
E-mail: vicena@vuez.sk

SLOVENIA

BASIC, Ivica (Mr.)
Lead Analysis Engineer
Nuclear Power Plant Krsko
NPP Krsko, Vrbina 12
8270 Krsko

Phone: +38 674 802 527
Fax: +38 674 921 528
E-mail: ivica.basic@nek.si

SWEDEN

HENRIKSSON, Mats E. (Mr.)
Vice-President
Corporate Senior Scientist
Vattenfall Utveckling AB
SE-814 26 Älvkarleby

Phone: +46 26 835 40
Fax: +46 26 836 70
Mobile: +46 70 520 95 30
E-mail: mats.henriksson@vattenfall.com

RINGDAHL, Kjell (Mr.)
Technical Support Ringhals Unit 3
Ringhals AB
SE-430 22 Väröbacka

Phone: +46 340 6685273
Fax: +46 340 667304
E-mail: kjell.ringdahl@ringhals.se

SANDERVAG, Oddbjörn (Mr.)
Reactor Safety Research Coordinator
Swedish Nuclear Power Inspectorate (SKI)
Klarabergsviadukten 90
SE-106 58 Stockholm

Phone: +46 8 698 84 63
Fax: +46 8 661 90 86
E-mail: oddbjorn.sandervag@ski.se

SIVULA, Mikael (Mr.)
Project Manager
Ringhals AB
SE-430 22 Väröbacka

Phone: +46 340 667585
Fax: +46 340 668851
E-mail: mikael.sivula@ringhals.se

SWITZERLAND

BLUMER, Urs Richard (Dr.)
Manager NS, Nuclear Engineering
CCI AG, IM Link 11
CH-8404 Winterthur

Phone: +41 52 264 9556
Fax: +41 52 264 9550
E-mail: urs.blumer@ccivalve.ch

ELVERT, Peter-Jens (Mr.)
Sales Engineer
CCI AG, IM Link 11
P.O. Box 65
CH-8404 Winterthur

Phone: + 41 52 264 9548
Fax: +41 52 264 9550
E-mail: peter-jens.elvert@ccivalve.ch

KLÜGEL, Jens-Uwe (Dr.)
Technical Adviser
Kernkraftwerk Goesgen
Kraftwerkstrasse
CH-4658 Daeniken

Phone: +41 62 288 2077
Fax: +41 62 288 2001
E-mail: jkluegel@kkg.ch

UNITED STATE OF AMERICA

ABDEL-FATTAH, Amr
Staff Member, Colloid & Containment Trans.
Los Alamos National Laboratory
PO Box 1663, MS J514
Los Alamos, NM 87545

Phone: +1 505 665-2339
Fax: +1 505 665-4955
E-mail: amr2450@lanl.gov

ANDREYCHEK, Timothy (Mr.)
Principal Engineer
Westinghouse Electric Company
4350 Northern Pike
Monroeville, PA

Phone: +1 412 374-6246
Fax: +1 412 374-5099
E-mail: andreysts@westinghouse.com

ARCHITZEL, Ralph (Mr.)
Senior Reactor Engineer
US Nuclear Regulatory Commission
Mail Stop One 11-A11
Washington, DC 20555-0001

Phone: +1 301 415-2804
Fax: +1 301 415-2300
E-mail: rea@nrc.gov

ASHBAUGH, Scott (Mr.)
Program Coordinator, Energy & Env. Progr.
Los Alamos National Laboratory
P.O. Box 1663, MS F606
Los Alamos, NM 87545

Phone: +1 505 664-0548
Fax: +1 505 665-5204
E-mail: sga@lanl.gov

BADEWITZ, Marty (Mr.)
Project Manager
Dominion Virginia Power
5000 Dominion Blvd.
Glen Allen, VA 23060

Phone: +1 804 273-2711
Fax: +1 804 273-3448
E-mail: marty_badewitz@dom.com

BAGNAL, Charles (Mr.)
Power Sales Manager, Nuclear Engineering
General Electric
3901 Castle Wayne Road
Wilmington, NC

Phone: +1 910 675-6785
Fax:
E-mail: charles.bagnal@gene.ge.com

BAHADUR, Sher (Dr.)
Deputy Director
Div. of Systems Analysis & Reg. Effectiveness
(DSARE), Office of Nuclear Reg. Research
US Nuclear Regulatory Commission
Mail Stop T-10 E29
Washington, DC 20555

Phone: +1 301 415-7499
Fax: +1 301 415-5160
E-mail: sxb@nrc.gov

BECK, Deane (Mr.)
Marketing Manager
Control Components, Inc.
22591 Avenida Empresa
Ranch Santa Margarita, CA 92688

Phone: +1 949 858-1878
Fax: +1 949 858-1878
E-mail: dbeck@ccivalve.com

BILANIN, Alan (Mr.)
Continuum Dynamics
34 Lexington Ave.
Ewing, NJ

Phone: +1 609 538-0444
Fax: +1 609 538-0464
E-mail: bilanin@continuum-dynamics.com

BLEIGH, James (Mr.)
Engineered Systems Manager
Performance Contracting, INC
4025 Bonner Industrial Drive
Shawnee, KS 66226

Phone: +1 913 441-0100
Fax: +1 913 441-0953
E-mail: jim.bleigh@pcg.com

BOSTELMAN, Janice (Ms)
Science Advisor
Alion Science & Technology
6000 Uptown Blvd., Suite 300
Albuquerque, NM

Phone: +1 505 872-1089
Fax: +1 505 872-0233
E-mail: jbstelman@alionscience.com

BRANDES, Matt (Mr.)
Design Engineer, Ameren UE
Callaway Plant
Jct CC & Hwy O
P.O. Box 620
Fulton, MO 65251

Phone: +1 573 676-8953
Fax: +1 573 676-4334
E-mail: mdbrandes@cal.ameren.com

BRYAN, Robert H. (Mr.)
Sr. Nuclear Specialist
Tennessee Valley Authority
1101 Market Street
Chattanooga, TN 37402

Phone: +1 423 751-8201
Fax: +1 423 751-7084
E-mail: rhbryan@tva.gov

BRYAN, Robert (Mr.)
Director, Atlanta Operations
Enercon Services, Inc.
500 Town Park Lane, Suite 275
Kennesaw, GA 30144

Phone: +1 770 919-1931, Ext. 222
Fax: +1 770 919-1932
E-mail: rbryan@enercon.com

BUTLER, John (Mr.)
Senior Project Manager
Nuclear Energy Institute
1776 I St. NW
Washington DC 20006

Phone: +1 202 739-8108
E-mail: jcb@nei.org

BUTNER, Nancy (Ms.)
Project Manager
Los Alamos National Laboratory
P.O. Box 1663, MS K557
Los Alamos, NM 87544

Phone: +1 505 667-8016
Fax: +1 505 667-5531
E-mail: nbutner@lanl.gov

CAIN, Stuart (Dr.)
Vice-President
Alden Research Laboratory, Inc.
30 Shrewsbury Street
Holden, MA 01520

Phone: +1 508 829-6000 ext. 439
Fax: +1 508 829-2795
E-mail: sacain@aldenlab.com

CARUSO, Ralph (Mr.)
Senior Staff Engineer
Advisory Committee on Reactor Safeguards
(ACRS)
US Nuclear Regulatory Commission
MS-T2E26
Washington, DC 20555-0001

Phone: +1 301 415-8065
Fax:
E-mail: rxc@nrc.gov

CAVALLO, Jon R. (Mr.)
Vice President
CCC & L, Inc.
P.O. Box 226
Eliot, ME 03903

Phone: +1 603 431-1919
Fax: +1 603 431-2540
E-mail: jrcpe@aol.com

CHANG, Tsun-Yung (Mr.)
Senior Project Manager
US Nuclear Regulatory Commission
11545 Rockville Pike
Rockville, MD 20852

Phone: +1 301 415-6450
Fax: +1 301 415-5074
E-mail : tyc@nrc.gov

<p>CHOROMOKOS, Robert (Mr.) Project Manager Alion Science & Technology 6000 Uptown Blvd. NE, Suite 300 Albuquerque, NM</p>	<p>Phone: +1 630 846-6787 Fax: E-mail: rchoromokos@alionscience.com</p>
<p>CORLEY, Clay (Mr.) System Engineer TXU Comanche Peak P.O. Box 1002 Glen Rose TX 76043</p>	<p>Phone: +1 254 897-5904 Fax: +1 254 897-0972 E-mail: claycorley@txu.com</p>
<p>CSONTOS, Aladar (Dr.) (Al) Materials Engineer US Nuclear Regulatory Commission Office of Nuclear Materials Safety & Safeguards MS T-7 F-3 Washington, DC 20555-0001</p>	<p>Phone: +1 301 415-6352 Fax: +1 301 415-5397 E-mail: aac@nrc.gov</p>
<p>CULLEN, Bill (Mr.) Sr. Materials Engineer US Nuclear Regulatory Commission MS T10 E-10 Washington, D.C. 20555</p>	<p>Phone: +1 301-415-7510 Fax: +1 301 415-5074 E-mail: whc@nrc.gov</p>
<p>DENNING, Richard S. (Rich) (Dr.) Sr. Research Leader Battelle 505 King Ave. Columbus, OH</p>	<p>Phone: +1 614 424-7412 Fax: +1 614 424-3404 E-mail: denning@battelle.org</p>
<p>DING, Mei (Dr.) TSM – Environmental Chemistry Los Alamos National Laboratory C-INC, MS J514 Los Alamos, NM 87545</p>	<p>Phone: +1 505 667-7051 Fax: +1 505 665-4955 E-mail: mding@lanl.gov</p>
<p>DRAKE, Andre (Mr.) Senior Engineer Constellation Energy Group Calvert Cliffs Nuclear Power Plant Lusby, MD 20657</p>	<p>Phone: +1 410 495-3932 Fax: +1 410 495-3944 E-mail: andre.s.drake@ceg.com</p>
<p>ELLIOTT, Robert (Mr.) (Rob) Technical Assistant US Nuclear Regulatory Commission MS 0-10A1 Washington, DC 20555</p>	<p>Phone: +1 301 415-1397 Fax: +1 301 415 3577 E-mail: rbe@nrc.gov</p>

EVANS, Michele (Ms.)
Branch Chief
US Nuclear Regulatory Commission
11545 Rockville Pike
Rockville, MD 20852-2738

Phone: +1 301 415-7210
Fax: +1 310 415-5074
E-mail: mge@nrc.gov

FEIST, Charles (Mr.)
Consulting Mechanical Engineer
TXU Energy
P.O. Box 1002
Glen Rose, TX 76043

Phone: +1 254 897-8605
Fax: +1 254 897-0530
E-mail: cfeist1@txu.com

FISCHER, Stewart (Dr.)
Team Leader/Nuclear Reactor Safety
Los Alamos National Laboratory
P.O. Box 1663 MS K557
Los Alamos, NM 87545

Phone: +1 505 665-3395
Fax: +1 505 667-5531
E-mail: sfischer@lanl.gov

FRIEDMAN, Michael (Mr.)
ECCS Strainer Project Manager
OPPD
Fort Calhoun Nuclear Station,
MS FC-2-4 ADM
Fort Calhoun, NE

Phone: +1 402 533-7341
Fax: +1 402 533-7390
E-mail: mjfriedman@oppd.com

GARCIA, Jeanette (Ms.)
Student Research Assistant
University of New Mexico
7905 Puritan Ct. NE
Albuquerque, NM 87109

Phone: +1 505 610-4410
Fax:
E-mail: janet_j_Garcia@yahoo.com

GARCIA-SERAFIN, Jose (Mr.)
Chief Nuclear Engineer
Florida Power & Light
700 Universe Boulevard
Juno Beach, FL

Phone: +1 561 694-3371
Fax: +1 561 694-4310
E-mail: jose_garcia@fpl.com

GARTLAND, Fariba (Ms.)
Project Manager, Plant Engineering
Framatome ANP
400 South Tyron St., Suite 2100
Charlotte NC 28285

Phone: +1 704 805-2288
Fax: +1 7-4 805-2650
E-mail: fariba.gartland@framatome-anp.com

GISCLON, John (Mr.)
Nuclear Engineering Consultant
EPRI
P.O. Box 1256
Ashland, OR 97520

Phone: +1 541 488-6928
Fax:
E-mail: jogisclo@epri.com

GOLLA, Joe (Mr.)
Systems Engineer, Plant Systems
US Nuclear Regulatory Commission
15555 Rockville Pike
Rockville, MD

Phone: +1 301 415-1002
Fax: +1 301 415-2300
E-mail: jag2@nrc.gov

HAMEL, Jeffrey (Mr.)
Product Manager
General Electric
175 Curtner Avenue
m/c 755
San Jose, California 95125

Phone: +1 408 925-2747
Fax: +1 408 925-5053
E-mail: jeffrey.hamel@gene.ge.com

HAMMER, Charles G. (Mr.)
Mechanical Engineer
US Nuclear Regulatory Commission
11545 Rockville Pike
Rockville, MD 20852-2738

Phone: +1 301 415-2791
Fax: +1 301 415-2444
E-mail: cgh@nrc.gov

HANNON, John (Mr.)
Branch Chief
DSSA/NRR
US Nuclear Regulatory Commission
MS O-11A11
Washington, DC 20555

Phone: +1 301-415-1992
Fax: +1 301 415-2300
E-mail: jnh@nrc.gov

HARRINGTON, Craig (Mr.)
Consulting Engineer
TXU Energy
P.O. Box 1002
Glen Rose, TX 76043

Phone: +1 254 897-6705
Fax: +1 254 897-0530
E-mail: charrin1@txu.com

HART, Gordon (Mr.)
Insulation Strainer Design
Performance Contracting, Inc.
11662 Fall Creek Road
Indianapolis, IN 46256

Phone: +1 317 578-3990
Fax: +1 317 578-2094
E-mail: Gordon.hart@pcg.com

HERMANN, Tim (Mr.)
Supervising Engineer
Ameren UE, Callaway Plant
Jct CC & Hwy O
P.O. Box 620
Fulton, MO 65251

Phone: +1 573 676-8494
Fax: +1 573 676-4334
E-mail: tdhermann@cal.ameren.com

HOLLOWAY, Ronald (Mr.)
Project Engineer
Wolf Creek Nuclear Operation Corporation
P.O. Box 411
Burlington, KS 66839

Phone: +1 620 364-4108
Fax: +1 620 364-4154
E-mail: rohollo@wcnoc.com

HOWE, Kerry J. (Dr.)
Department of Civil Engineering
MSC01 1070
University of New Mexico
Albuquerque, NM 87131-0001

Phone: +1 505 277-2702
Fax: +1 505 277-1988
E-mail: howe@unm.edu

HSIA, Anthony (Mr.)
Office of Nuclear Regulatory Research
US Nuclear Regulatory Commission
Washington, DC 20555-0001

Phone: +1 301 415-6933
Fax : +1 301 415-5074
E-mail: ahh@nrc.gov

JACKSON, Christopher (Mr.)
Technical Assistant
US Nuclear Regulatory Commission
One White Flint North
11555 Rockville, Maryland 20852 USA

Phone: +1 301 415-1750
Fax: +1 301 415-1757
E-mail: cpj@nrc.gov

JOHNSON, Michael (Mr.)
Deputy Division Director
System Safety & Analysis
US Nuclear Regulatory Commission
Mail Stop O-10A1
Washington, DC 20555

Phone: +1 301 415-3226
Fax: +1 301 415-3577
E-mail: MRJ1@nrc.gov

KEMPER, William (Mr.)
OIG Technical Advisor
US Nuclear Regulatory Commission
Mail Stop T5 D28
Washington, DC 20555-0001

Phone: +1 301 415-5974
E-mail: wek@nrc.gov

KHAN, Saif (Mr.)
Project Manager
Energy Operations, Inc.
1448 SR 333
Russellville, AR 72802-0967

Phone: +1 479 858-4941
E-mail: skhan@entergy.com

KISHIOKA, Kazuhiko (Mr.)
Japan Atomic Power Co. Representative
Japan Electric Power Info Center
1120 Connecticut Ave. NW Suite 1070
Washington, DC 20036

Phone: +1 202-955-5610
Fax: +1 202-955-5612
E-mail: genden@jepic.com

KOWAL, Mark (Mr.)
Reactor Systems Engineer
US Nuclear Regulatory Commission
11555 Rockville Pike
Rockville, MD 20852

Phone: +1 301 415-1663
E-mail: mxk7@nrc.gov

KRESS, Tom (Dr.)
ACRS Member
102B Newridge Road
Oak Ridge, Tennessee 37830

Phone: +1 865 483-7548
Fax: +1 865 482-7458
E-mail: tskress@aol.com

LAVRETTA, Maria Angeles (Ms.)
Reactor Systems Engineer
US Nuclear Regulatory Commission
Washington, DC 20555

Phone: +1 310 415-3285
Fax: +1 301 415-2300
E-mail: AXL3@nrc.gov

LEONARD, Mark (Mr.)
Dycoda, LLC
267 Los Lentos Rd.
Los Lunas, NM 87031

Phone: +1 505 866-4800
Fax: +1 505 866-4801
E-mail: mtl@dycoda.com

LETELLIER, Bruce C. (Dr.)
Los Alamos National Laboratory
D-5 Nuclear Design and Risk Analysis
P.O. Box 1663, Mail Stop K557
Los Alamos, NM 87545

Phone: +1 505 665-5188
Fax: +1 505 667-5531
E-mail: bcl@lanl.gov

LINCOLN, Donald (Mr.)
Director, Commercial Utility Programs
Alion Science and Technology
6000 Uptown Blvd. NE Suite 300
Albuquerque, NM

Phone: +1 505 872-1089
Fax: +1 505 872-0233
E-mail: dlincoln@alionscience.com

LUND, Louise (Ms.)
Section Chief
US Nuclear Regulatory Commission
MS 0-9H6
Washington, DC 20555-0001

Phone: +1 301-415-3248
Fax: +1 301 415-2444
E-mail: lxl@nrc.gov

MAJI, Arup (Prof.)
Department of Civil Engineering
MSC01-1070
University of New Mexico
Albuquerque, NM 87131

Phone: +1 505 277-1757
Fax:
E-mail: amaji@unm.edu

MATHUR, Kiran (Mr.)
Senior Engineer
Public Service Electric & Gas Co.
P.O. Box 236
Hancocks Bridge NJ 08038

Phone: +1 856-339-7215
Fax: +1 856-339-1218
E-mail: kiran.mathur@pseg.com

MCCLURE, Patrick R. (Mr.)
D-5 Group Leader, Nuclear Safety
Los Alamos National Laboratory
P.O. Box 1663, MS K557
Los Alamos, NM 87545

Phone: +1 505 667-9534
Fax: +1 505 665-2897
E-mail: pmcclure@lanl.gov

MCGOUN, Wes (Mr.)
Principal Engineer
Progress Energy
410 South Wilmington St., PEB-6
Raleigh, NC

Phone: +1 919 546-2040
Fax: +1 919 546-7854
E-mail: wes.mcgoun@pgnmail.com

MCNAMARA, Joseph (Mr.)
Engineering Supervisor
Civil-Structural Design
Nuclear Management Company
Point Beach Nuclear Power Plant
6610 Nuclear Road
Two Rivers, WI 54241

Phone: +1 920 755-7421
Fax: +1 920 755-7410
E-mail: joe.mcnamara@nmcco.com

MIDLIK, David W. (Mr.)
Senior Engineer
Southern Nuclear
P.O. Box 1295-031
Birmingham, Alabama 35201

Phone: +1 205 992-6860
Fax: +1 205 992-7149
E-mail: dwmidlik@southernco.com

MYER, Chalmer (Mr.)
Engineering Supervisor, Mechanical
Southern Nuclear
40 Inverness Parkway
Birmingham, Alabama 35242

Phone: +1 205 992-6335
Fax: +1 205 992-7149
E-mail: cmyer@southernco.com

PAGE, Joel D. (Mr.)
Mechanical Engineer
USNRC
MS T10-E10
Washington, DC 20555

Phone: +1 301 415-6784
Fax: +1 301 415-5074
E-mail: jdp2@nrc.gov

PARCZEWSKI, Krzysztof (Dr.)
Senior Chemical Engineer
US Nuclear Regulatory Commission
11555 Rockville Pike
Rockville, MD 20852-2738

Phone: +1 301 415-2705
Fax: +1 301 415-2444
E-mail: kip@nrc.gov

QUITORIANO, Gregory
Design Engineer
Pacific Gas & Electric
P.O. Box 56
Avila Beach, CA

Phone: +1 805 545-4948
Fax: +1 805 545-6605
E-mail: geq1@pge.com

RAO, Dasari V. (Dr.)
Los Alamos National Laboratory
P.O. Box 1663
Los Alamos, NM 87545

Phone: +1 505 667-4567
Fax: +1 505 665-5204
E-mail: nrcdvrao@lanl.gov

RINKACS, William (Mr.)
Westinghouse Electric Co., LLC
4350 Northern Pike
Monroeville, PA

Phone: +1 412 374-4545
Fax: +1 412 374-5099
E-mail: rinkacwj@westinghouse.com

RISLEY, Bryan (Mr.)
Product/Project Manager
Transco Products Inc.
1215 East, 12th Street
Streator, IL

Phone: +1 815 672-2197
Fax: +1 815 673-2432
E-mail: bryanrisley@transcoproducts.com

RISTE, Jerry O. (Mr.)
Licensing Supervisor
Nuclear Management Co., LLC
N490 Highway 42
Kewaunee, WI 54216

Phone: +1 920 845-5022
Fax: +1 920 388-8333
E-mail: Gerald.riste@nmcco.com

SCIACCA, Frank (Mr.)
Omicron Safety and Risk Technologies
P.O. Box 93065
Albuquerque, NM 87199-3065

Phone: +1 505 883-0553
Fax: +1 505 883-0588
E-mail: fsciacca@omicron.net

SETLUR, Achyut (Dr.)
President
Automated Engineering Services Corp (AES)
3060 Ogden Ave., Suite 205
Lisle, IL

Phone: +1 630 357-8880
Fax: +1 630 357-4445
E-mail: avsetlur@aesengineering.com

SETLUR, Shashi (Ms.)
Automated Engineering Services Corp. (AES)
3060 Ogden Ave., Suite 205
Lisle, IL

Phone: +1 630 357-8880
Fax: +1 630 357-4445
E-mail: sasetlur@aesengineering.com

SHAFFER, Clinton J. (Mr.)
Principal Engineer
ARES Corporation
851 University Boulevard, SE, Suite 100
Albuquerque, NM 87106

Phone: +1 505 272-7102
Fax: +1 505 272-7238
E-mail: cshaffer@arescorporation.com

SMITH, Aaron (Mr.)
Project Manager
Enercon Services
500 TownPark Lane, Suite 275
Kennesaw, GA 30144-5509

Phone: +1 770 919-1931 x 280
Fax: +1 770 919-1932
E-mail: asmith@enercon.com

SPRING, Nancy (Ms.)
UtiliPoint International, Inc.
6000 Uptown Blvd. NE, Suite 314
Albuquerque, NM 87110

Phone: +1 505 244-7600
Fax: +1 505 244-7658
E-mail: nspring@utilipoint.com

STROSNIDER, Jack Richard Jr. (Mr.)
Deputy Director, Office of Research
US Nuclear Regulatory Commission
TWFN 10F1
Washington, DC 20555-001

Phone: +1 301 415-6045
Fax: +1 301 415-5a53
E-mail: JRS2@nrc.gov

TWACHTMAN, Gregory (Mr.)
Editor
McGraw-Hill
1200 G St. NW, Suite 1000
Washington, DC

Phone: +1 202 383-2166
Fax: +1 202 383-2187
E-mail: Gregory_twachtman@platts.com

UNIKIEWICZ, Steven (Mr.)
Engineer
US Nuclear Regulatory Commission
Mail Stop 09-D3
Washington, DC 20555-0001

Phone: +1 301 415-3819
Fax: +1 301 415-2444
E-mail: smu@nrc.gov

WALKER, John (Mr.)
Manager
Framatome ANP
400 South Tryon Street, Suite 2100, WC26A
Charlotte, NC 28285

Phone: +1 704 805-2746
Fax: +1 704 805 2650
E-mail: john.walker@framatome-anp.com

WILLIAMS, H. Lee (Mr.)
Project Development Manager
Framatome ANP
400 South Tyrone Street, Suite 2100
Charlotte, NC 28285

Phone: +1 704 805-2065
Fax: +1 704 805-2675
E-mail: lee.Williams@framatome-anp.com

WINDHAM, Terrill (Mr.)
Project Manager
Entergy-ANO
1448 S.R. 333
Russellville, AR 72802

Phone: +1 479 858-4355
Fax: +1 479 858-4496
E-mail: twindha@entergy.com

WOLBERT, Edward (Mr.)
President
Transco Products Inc.
55 E. Jackson Boulevard, Suite 2100
Chicago, IL

Phone: +1 312 427-2818
Fax: +1 312 427-4975
E-mail: edwolbert@transcoproducts.com

ZIGLER, Gilbert (Mr.)
Senior Scientist/Engineer
Alion Science and Technology
6000 Uptown Blvd. NE Suite 300
Albuquerque, NM

Phone: +1 505 872-1089
Fax: +1 505 872-0233
E-mail: gzigler@alionscience.com

FRISBEE, Rebecca (Ms.)
Los Alamos National Laboratory
P.O. Box 1663, MS P366
Los Alamos, NM 87545

Phone: +1 505 667-5543
Fax: +1 505 667-7530
E-mail: rfrisbee@lanl.gov

WEAVER, Christine (Ms.)
Los Alamos National Laboratory
P.O. Box 1663, MS P366
Los Alamos, NM 87545

Phone: +1 505 667-9436
Fax: +1 505 667-7530
E-mail: cweaver@lanl.gov

ALSO AVAILABLE

NEA Publications of General Interest

NEA News

ISSN 1605-9581

Yearly subscription: € 49 US\$ 56 £ 31 ¥ 6 600

Nuclear Energy Today (2003)

ISBN 92-64-10328-7

Price: € 21 US\$ 24 £ 14 ¥ 2 700

Nuclear Safety and Regulation

Advanced Nuclear Reactor Safety Issues and Research Needs (2002)

Workshop Proceedings, Paris, France, 18-20 February 2002

ISBN 92-64-19781-8

Price: € 75 US\$ 65 £ 46 ¥ 8 700

Nuclear Fuel Safety Criteria Technical Review (2001)

ISBN 92-64-19687-0

Price: € 20 US\$ 19 £ 12 ¥ 1 900

Collective Statement Concerning Nuclear Safety Research (2004)

Capabilities and Expertise in Support of Efficient and Effective Regulation of Nuclear Power Plants

ISBN 92-64-02169-8

Free: paper or web.

Collective Statement Concerning Nuclear Safety Research (2003)

Good Practice and Closer Criteria

ISBN 92-64-02149-3

Free: paper or web.

Nuclear Regulatory Review of Licence Self-assessment (LSA) (2003)

ISBN 92-64-02132-9

Free: paper or web.

Regulator and Industry Co-operation on Nuclear Safety Research (2003)

Challenges and Opportunities

ISBN 92-64-02126-4

Free: paper or web.

Regulatory Challenges of Decommissioning Nuclear Reactors (The) (2003)

ISBN 92-64-02120-5

Free: paper or web.

CSNI Technical Opinion Papers

No.1: Fire Probabilistic Safety Assessment for Nuclear Power Plants (2002)

No.2: Seismic Probabilistic Safety Assessment for Nuclear Facilities (2002)

ISBN 92-64-18490-2

Free: paper or web.

No.3: Recurring Events (2003)

ISBN 92-64-02155-8

Free: paper or web.

No.4: Human Reliability Analysis in Probabilistic Safety Assessment for Nuclear Power Plants (2004)

ISBN 92-64-02157-4

Free: paper or web.

No.5: Managing and Regulating Organisational Change in Nuclear Installations (2004)

ISBN 92-64-02069-1

Free: paper or web.

Direct Indicators of Nuclear Energy Efficiency and Effectiveness (2004)

Pilot Projects Results

ISBN 92-64-02061-6

Free: paper or web.

Order form on reverse side.

Questionnaire on the quality of OECD publications

We would like to ensure that our publications meet your requirements in terms of presentation and editorial content. We would welcome your feedback and any comments you may have for improvement. Please take a few minutes to complete the following questionnaire. Answers should be given on a scale of 1 to 5 (1 = poor, 5 = excellent).

Fax or post your answer before 31 December 2004, and you will automatically be entered into the prize draw to **win a year's subscription to OECD's *Observer magazine***.*

A. Presentation and layout

1. What do you think about the presentation and layout in terms of the following:

	Poor	Adequate		Excellent	
Readability (font, typeface)	1	2	3	4	5
Organisation of the book	1	2	3	4	5
Statistical tables	1	2	3	4	5
Graphs	1	2	3	4	5

B. Printing and binding

2. What do you think about the quality of the printed edition in terms of the following:

Quality of the printing	1	2	3	4	5
Quality of the paper	1	2	3	4	5
Type of binding	1	2	3	4	5
Not relevant, I am using the e-book	<input type="checkbox"/>				

3. Which delivery format do you prefer for publications in general?

Print CD E-book (PDF) via Internet Combination of formats

C. Content

4. How accurate and up to date do you consider the content of this publication to be?

1 2 3 4 5

5. Are the chapter titles, headings and subheadings...

Clear Yes No
Meaningful Yes No

6. How do you rate the written style of the publication (e.g. language, syntax, grammar)?

1 2 3 4 5

D. General

7. Do you have any additional comments you would like to add about the publication?

.....
.....
.....

Tell us who you are:

Name: E-mail:

Fax:

Which of the following describes you?

IGO NGO Self-employed Student
Academic Government official Politician Private sector

Thank you for completing the questionnaire. Please fax your answers to:

(33-1) 49 10 42 81 or mail it to the following address:

Questionnaire qualité PAC/PROD, Division des publications de l'OCDE
23, rue du Dôme – 92100 Boulogne Billancourt – France.

Title: Debris impact on Emergency Coolant Recirculation

ISBN: 92-64-00666-4 **OECD Code (printed version):** 66 2004 15 1p

* Please note: This offer is not open to OECD staff.

OECD PUBLICATIONS, 2, rue André-Pascal, 75775 PARIS CEDEX 16

PRINTED IN FRANCE

(66 2004 15 1 P) ISBN 92-64-00666-4 No. 53751 2004

© OECD, 1999.

© Software: 1987-1996, Acrobat is a trademark of ADOBE.

All rights reserved. OECD grants you the right to use one copy of this Program for your personal use only. Unauthorised reproduction, lending, hiring, transmission or distribution of any data or software is prohibited. You must treat the Program and associated materials and any elements thereof like any other copyrighted material.

All requests should be made to:

Head of Publications Service,
OECD Publications Service,
2, rue André-Pascal, 75775 Paris
Cedex 16, France.

© OCDE, 1999

© Logiciel, 1987-1996, Acrobat, marque déposée d'ADOBE.

Tous droits du producteur et du propriétaire de ce produit sont réservés. L'OCDE autorise la reproduction d'un seul exemplaire de ce programme pour usage personnel et non commercial uniquement. Sauf autorisation, la duplication, la location, le prêt, l'utilisation de ce produit pour exécution publique sont interdits. Ce programme, les données y afférentes et d'autres éléments doivent donc être traités comme toute autre documentation sur laquelle s'exerce la protection par le droit d'auteur.

Les demandes sont à adresser au :

Chef du Service des Publications,
Service des Publications de l'OCDE,
2, rue André-Pascal,
75775 Paris Cedex 16, France.